Role of the chondrocyte cytoskeleton in health and disease

Rebecca Jane Shuttleworth

ProQuest LLC
789 East Eisenhower Parkway
P.O. Box 1346
Ann Arbor, MI 48106-1346

DECLARATION

This work has not previously been accepted in substance for any degree and is not concurrently submitted in candidature for any degree.

Signed ..... (candidate) Date 27:5:10

STATEMENT 1

This thesis is being submitted in partial fulfillment of the requirements for the degree of PhD.

Signed ..... (candidate) Date 27:5:10

STATEMENT 2

This thesis is the result of my own independent work/investigation, except where otherwise stated.
Other sources are acknowledged by explicit references.

Signed ..... (candidate) Date 27:5:10

STATEMENT 3

I hereby give consent for my thesis, if accepted, to be available for photocopying and for inter-library loan, and for the title and summary to be made available to outside organisations.

Signed ..... (candidate) Date 27:5:10

ACKNOWLEDGEMENTS

First and foremost I would like to thank my supervisors Dr Emma Blain, Professor Vic Duance and Dr John Wardale for their help and guidance over the course of my studies. Thank you for all of the support and time that you have given me. I could not have gotten through it without you. An extra special thanks to Emma and Vic, for all of the time spent reading drafts of my thesis and for their patience and encouragement through the process.

A very big thank you to all of the members of lab C 4.12 over the years for their time and patience in teaching me techniques and helping me 'find my feet'. Special thanks to go to Dr Emma Blain, Dr Sophie Gilbert, Karen Brakspear and Dr Siyuan Li for their friendship, for making the difficult days more bearable, and for putting up with my singing. Additional thanks go to Dr Tony Hayes for technical assistance with the confocal microscope.

For my time in AstraZeneca, thank you to John and Dr Nicky Le Good for their hospitality and to Leeane Elston for her help with the Taqman Arrays. Leeanne you made an initially daunting experience much more enjoyable. Thank you also to my fellow CASE student Louise Clough for her friendship.

My final thanks go to my family, for their love and support over the years and for helping me believe I could do this. Thank you to my wonderful husband Richard, who has suffered a lot of neglect these last few years and seen me through many difficult times.

It is very difficult to put years of gratitude into words. Thank you all from the bottom of my heart.

ABSTRACT

Introduction: Articular cartilage comprises a dense extracellular matrix (ECM) of primarily collagen, proteoglycans and water interspersed with the cartilage cell- the chondrocyte. Osteoarthritis (OA) is a disease characterised by articular cartilage degradation and a change in chondrocyte phenotype. Increased or abnormal joint loading is a risk factor for OA and can regulate chondrocyte phenotype. The chondrocyte cytoskeleton comprises actin microfilaments, tubulin microtubules and vimentin intermediate filaments and has been implicated in the propagation of physical signals to the chondrocyte nucleus, termed 'mechanotransduction'. In addition, the organisation of chondrocyte cytoskeletal networks has been observed to differ in both human OA and in a rat model of OA when compared with normal chondrocytes. We hypothesise that dysregulation of cytoskeletal networks prevents normal ECM-chondrocyte signalling and promotes a catabolic phenotype as in OA.

Results: When compared with normal human chondrocytes, OA chondrocytes exhibited differences in the gene expression of components of the cytoskeleton and in the spatial organisation and architecture of the cytoskeleton, both *in situ* and *in vitro*. In normal and OA human chondrocytes cultured in agarose hydrogels, disruption of each of the three main cytoskeletal elements resulted in gene expression changes in both normal and OA cells. A number of gene responses to cytoskeletal disruption were similar in normal and OA cells, such as *SOX9*, *MMP14*, *TGFB1*, *CASP3* and *PTGS2* (COX-2). Other genes responded differently to the same treatment in normal versus OA cells, including *ADAMTS5*, *COMP*, *FGFR3* and *NOS2A* (iNOS). Cyclic compression (15% strain, 0.5 Hz) for up to 40 minutes induced cytoskeletal reorganisation in normal and OA human chondrocytes and up-regulation of β-tubulin and destrin mRNA expression. Recovery in free swelling conditions for five hours post-load showed the chondrocyte phenotype was enhanced in OA chondrocytes. Cyclic compression in the presence of cytoskeletal disruption altered the transcriptional response of the actin depolymerising proteins cofilin and destrin in normal and OA chondrocytes, and the transcriptional response of *SOX9* and the actin sequestering protein thymosin β4 in OA chondrocytes.

Conclusions: Changes in the cytoskeleton of OA chondrocytes are not simply a result of the altered mechanical environment in OA articular cartilage. Changes in the cytoskeleton can affect chondrocyte phenotype and the response of chondrocytes to cyclic compression, therefore the observed differences in organisation and expression could result in the altered phenotype of OA chondrocytes. Differences between the effect of cyclic compression on normal and OA human chondrocytes support the existence of different or divergent mechanotransduction pathways that are mediated in part by elements of the chondrocyte cytoskeleton.

ABBREVIATIONS

Human gene names are denoted using capitals in italics and human proteins (where the name is the same as that of the gene) are in capitals.

ACT	Autologous chondrocyte transplantation
ADAMTS	A disintegrin and metalloproteinase with thrombospondin motifs
ADF	Actin depolymerisation factor
ADP	Adenosine diphosphate
APS	Ammonium persulphate
Arp2/3	Actin-related protein 2/3 complex
ATP	Adenosine triphosphate
AZ	AstraZeneca
Bbs	Bardet-Biedl syndrome
BCA	Bicinchoninic acid
BMF	Bcl2-modifying factor
bp	Base pairs
Calcein AM	Calcein acetoxymethyl ester
cDNA	Complementary deoxyribonucleic acid
CILP	Cartilage intermediate-layer protein
COMP	Cartilage oligomeric matrix protein
COX-2	Cyclooxygenase-2
Ct	Cycle threshold
CTGF	Connective tissue growth factor
CTX-II	C-terminal cross-linked telopeptide of type II collagen
dGEMRIC	Delayed gadolinium-enhanced magnetic resonance imaging of cartilage
DLC2	Dynein light chain 2
DMEM	Dulbecco's modified Eagle's medium
DMMB	Dimethylmethylene blue
DNA	Deoxyribonucleic acid
DNase	Deoxyribonuclease
dNTP	Deoxynucleotide triphosphate
DTT	Dithiothreitol

EBSS	Earle's balanced salt solution
ECL	Enhanced chemiluminescence
ECM	Extracellular matrix
EDTA	Ethylene diamine tetraacetic acid
EGTA	Ethylene glycol tetraacetic acid
ELISA	Enzyme-linked immunosorbent assay
ERK	Extracellular signal-regulated kinase
F-actin	Filamentous actin (ie. polymerised)
FAK	Focal adhesion kinase
FCS	Fetal calf serum (aka Fetal bovine serum)
FGF	Fibroblast growth factor
FGFR	Fibroblast growth factor receptor
FH1/2	Formin homology domain 1/2
FHL2	Four and a half LIM domains protein 2
FITC	Fluorescein isothiocyanate
G-actin	Globular actin (aka monomeric actin)
GADD45β	Growth arrest and DNA damage-inducible protein GADD45 β
GAG	Glycosaminoglycan
GAP	GTPase-activating protein
GDP	Guanosine diphosphate
GEF	Guanine nucleotide exchange factor
GTP	Guanosine triphosphate
HEPES	4-(2-hydroxyethyl)-1-piperazineethanesulfonic acid
HRP	Horseradish peroxidase
IGF	Insulin-like growth factor
IgG	Immunoglobulin
IHC	Immunohistochemistry
IL	Interleukin
iNOS	Inducible nitric oxide synthase
iPTG	Isopropyl β-D-1-thiogalactopyranoside
ITS	Insulin-transferrin-selenite
JNK	c-Jun amino-terminal kinase
LB	Luria-Bertani
LDH	Lactate dehydrogenase

LIMK	LIM domain kinase
MAPK	Mitogen-activated protein kinase
MES	2-(N-morpholino)ethanesulfonic acid
mHBSS	Modified Hank balanced salt solution
MMP	Matrix metalloproteinase
mRNA	Messenger ribonucleic acid
NEU	Normalised expression units
NITEGE	Asparagine-Isoleucine-Threonine-Glutamate-Glycine-Glutamate
NO	Nitric oxide
N-WASP	Neural Wiskott-Aldrich syndrome protein
OA	Osteoarthritis / Osteoarthritic
ORPK	Oak Ridge Polycystic Kidney
PAD	Peptidyl arginine deiminase
PAK	p21-activated kinase
PBS	Phosphate-buffered saline
PBST	Phosphate-buffered saline with 0.5% Tween-20
PCR	Polymerise chain reaction
PFA	Paraformaldehyde
PIP_2	Phosphoinositide 4,5-bisphosphate
PIPES	1,4-piperazinediethanesulfonic acid
PKA	Protein kinase A
PKC	Protein kinase C
PVDF	Polyvinylidene fluoride
RANKL	Receptor activator of nuclear factor κ-B ligand
REU	Relative expression units
RGD	Arginine-Glycine-Aspartate
RIPA	Radio-Immunoprecipitation Assay
RNA	Ribonucleic acid
RNase	Ribonuclease
ROCK	Rho kinase
RT	Reverse transcription
RT-PCR	Reverse transcription polymerise chain reaction
SDS PAGE	Sodium dodecyl sulphate polyacrylamide gel electrophoresis
SEM	Standard error mean

sGAG	Sulphated glycosaminoglycan
siRNA	Small interfering ribonucleic acid
SOX9	SRY (sex determining region-Y)-type high-mobility-group box transcription factor -9
TBST	Tris-buffered saline with 0.1% Tween-20
TGF	Transforming growth factor
TIMP	Tissue inhibitor of metalloproteinase
TNF	Tumour necrosis factor
TRITC	Tetramethylrhodamine isothiocyanate
VASP	Vasodilator-stimulated phosphoprotein
VEGF	Vascular endothelial growth factor
WASP	Wiskott-Aldrich syndrome protein

Genes included on the AstraZeneca Custom-designed Taqman® Array

Blank spaces and codes indicate genes required by AstraZeneca to be kept confidential

Scenario	Gene	Common name
adhesion	DPT	Dermatopontin
adhesion		A1
adhesion	ITGA2	Integrin alpha2
adhesion	ITGB5	Integrin alpha5
adhesion		A2
adhesion	VCAM1	vascular cell adhesion molecule 1
adipogen	ACADL	acyl-Coenzyme A dehydrogenase
angiogen		C1
angiogen	SDC2	Syndecan 2
angiogen	LECT1	Chondromodulin-1
angiogen		C2
angiogen	FLT1	VEGF receptor 1
angiogen	VEGF	Vascular endothelial growth factor
apoptosis	BMF	Bcl2 modifying factor
apoptosis	CASP3	caspase 3
apoptosis	GADD45B	GADD45 beta
apoptosis	HSPB1	HSP27
apoptosis		D2
apoptosis		D3
carbohydrate		E2
carbohydrate	SLC2A3	GLUT3
carbohydrate		E1
degradation	ADAMTS4	Aggrecanase 1
degradation	ADAMTS5	Aggrecanase 2
degradation		F1
degradation		F2
degradation		F3
degradation	MMP13	MMP13
degradation	MMP14	MMP14
degradation	MMP1	MMP1
degradation	MMP2	MMP2
degradation	MMP3	MMP3
degradation	TIMP1	TIMP1
degradation	TIMP2	TIMP2

degradation	TIMP3	TIMP3
differentiation	COL1A1	type I collagen
differentiation	COL9A1	type IX collagen
differentiation	SOX9	SOX9
growth factors	BMP2	BMP2
growth factors	CSF1	Colony stimulating factor 1
growth factors	FGF2	FGF2
growth factors	IGF1	IGF1
growth factors	LTBP1	TGF binding protein
growth factors	PDGFC	platelet derived growth factor C
growth factors	TGFBI	TGF beta1
hypertrophy	TGM2	Transglutaminase 2
hypertrophy	PTCH	Patched (Ihh target gene)
hypertrophy	RUNX2	RUNX2
hypertrophy	COL10A1	type X collagen
hypertrophy	COMP	COMP
hypertrophy	FGFR3	FGFR3
hypertrophy	FGF18	FGF18
hypertrophy		I1
hypertrophy		I2
Hypoxia/ph		J1
Hypoxia/ph		J2
Hypoxia/ph	TNC	Tenascin
inflammatory		K1
inflammatory	IL17	IL17
inflammatory	IL1a	IL1α
inflammatory	IL6	IL6
inflammatory	IL8	IL8
inflammatory	NOS2A	iNOS
inflammatory	PTGS2	Prostaglandin G/H synthase 2 (COX-2)
inflammatory	TNFSF11	RANK ligand
matrix	ACAN	Aggrecan
matrix	COL11A1	type XI collagen
matrix	COL15A1	type XV collagen
matrix	COL2A1	type II collagen
matrix	COL3A1	type III collagen
matrix	FBLN1	Fibulin 1
matrix	FN1	Fibronectin
matrix		L1
matrix	PRELP	proline/arginine-rich end leucine-rich repeat protein
metabolism		M2

metabolism		M1
neurogen		N2
neurogen		N1
neurogen	NGFR	NGF receptor
osmolality		O1
osteogen	SPP1	Osteopontin
osteogen		P2
osteogen	EXTL1	Exostoses 1
osteogen		P1
osteogen		P4
osteogen		P3
proliferation	B2M	β 2 macroglobulin
proliferation		Q1
transporter		R1
transporter		R2
Housekeeper	18S	
Housekeeper	ACTB	β-Actin
Housekeeper	GAPDH	GAPDH
Housekeeper	HPRT1	Hypoxanthine-guanine phosphoribosyltransferase
		S1 (PM marker gene)

Table of Contents

Table of Figures

Chapter 4

Chapter 5

Table of Tables

Chapter 6

Chapter 1: General Introduction

1. GENERAL INTRODUCTION

1.1 Articular Cartilage

Articular cartilage is an avascular and aneural tissue, located at the ends of the long bones in articulating joints. It functions to protect the ends of the bones during joint movement and does this by providing an almost frictionless surface to allow smooth articulation of the joint. Articular cartilage also protects the ends of the bones by dissipating any load experienced by the joint during movement.

1.1.1 Organisation of Articular Cartilage

The organisation of articular cartilage is not uniform throughout. The shape and spacing of chondrocytes and the orientation of collagen fibrils allows the cartilage to be split into zones, with the superficial zone beneath the articular surface, transitional (mid) zone, and radial (deep) zone above the calcified cartilage and subchondral bone (Fig 1.1). The superficial zone contains flattened chondrocytes orientated parallel to the articular surface. Collagen fibrils also run parallel to the surface and provide the superficial zone with high tensile strength, allowing it to resist and dissipate load applied to the tissue. The chondrocytes of the transitional zone possess a more rounded shape and collagen fibrils have an orientation intermediate to that of the superficial and deep zones, more randomly distributed but well-defined around chondrocytes (Pelletier et al., 1983b). In the radial (deep) zone, chondrocytes are spherical and arranged in columns with collagen fibres orientated perpendicular to the articular surface. The differences in the extracellular matrix (ECM) in these zones and the orientation of collagen fibrils lead to a difference in the mechanical properties of each zone.

In addition to the zonal variations within cartilage, the extracellular matrix can be divided into territories based on the matrix composition and its location with respect to the chondrocyte. Immediately surrounding a single chondrocyte is the pericellular matrix and together these make up the chondron [reviewed in (Poole, 1997)]. Surrounding chondrons are the 'territorial' matrices and these are separated from each other by the 'interterritorial' matrix, which makes up the largest portion of the ECM of cartilage.

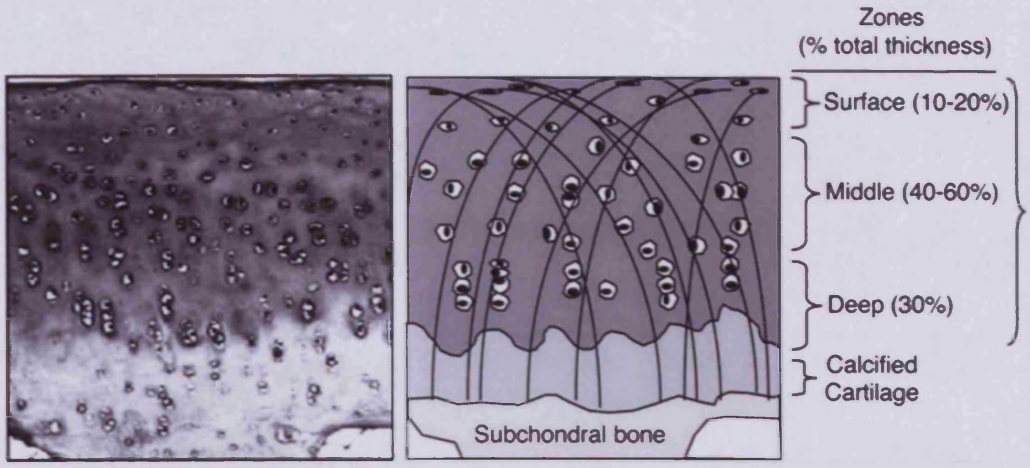

Figure 1.1:- Histologic micrograph and schematic diagram of the zonal organisation of human articular cartilage. Collagen fibrils are arranged parallel to the articular surface in the superficial zone and they become perpendicular to the surface in the deep zone; in the transitional zone fibrils have an intermediate orientation. Adapted from Griffin and Guilak (2005).

1.1.2 Composition of Articular Cartilage

The characteristic functions of articular cartilage can be related to its structure and composition. The four main components of articular cartilage are collagen, proteoglycan, water, and the cartilage cell- the chondrocyte.

1.1.2.1 Collagen

Articular cartilage contains a heterogeneous network of collagen, consisting predominantly of type II collagen (80-90% of the total collagen), with small amounts of types VI, IX and XI collagen. Type II collagen forms fibrils along with types IX and XI collagen. These vary in diameter, with thicker fibrils located in the interterritorial matrix and thinner fibrils in the pericellular matrix. Type IX collagen is associated predominantly with thin collagen fibrils (Fig 1.2) and displays a largely pericellular localisation in mature mammalian articular cartilage (Hagg et al., 1998). Type VI collagen is also localised to the pericellular matrix and is used as a marker of chondron microanatomy (Poole, 1997).

The collagen matrix provides the tissue with its mechanical strength, resisting mechanical stress and reducing the deformation of the tissue in response to these stresses. The tensile strength of the collagen matrix also functions to resist the swelling pressure of the proteoglycans (Maroudas, 1976), and thus provides cartilage with elasticity, allowing recovery after deformation in response to applied load.

1.1.2.2 Proteoglycan

Large aggregating proteoglycans ('aggrecan') represent the largest proportion of the proteoglycans present in articular cartilage. An aggrecan monomer consists of a multidomain protein core containing two globular domains towards the N-terminus (G1 and G2) and one at the C-terminus (G3) (Hardingham and Fosang, 1992). These are separated by chondroitin sulphate (CS) and keratan sulphate (KS) domains, to which the glycosaminoglycans CS or KS are attached. These glycosaminoglycans (GAGs) are highly negatively charged. Aggrecan monomers bind non-covalently, through their G1 domain and link protein, to hyaluronic acid, resulting in the formation of large anionic complexes which sequester water molecules (Fig 1.2).

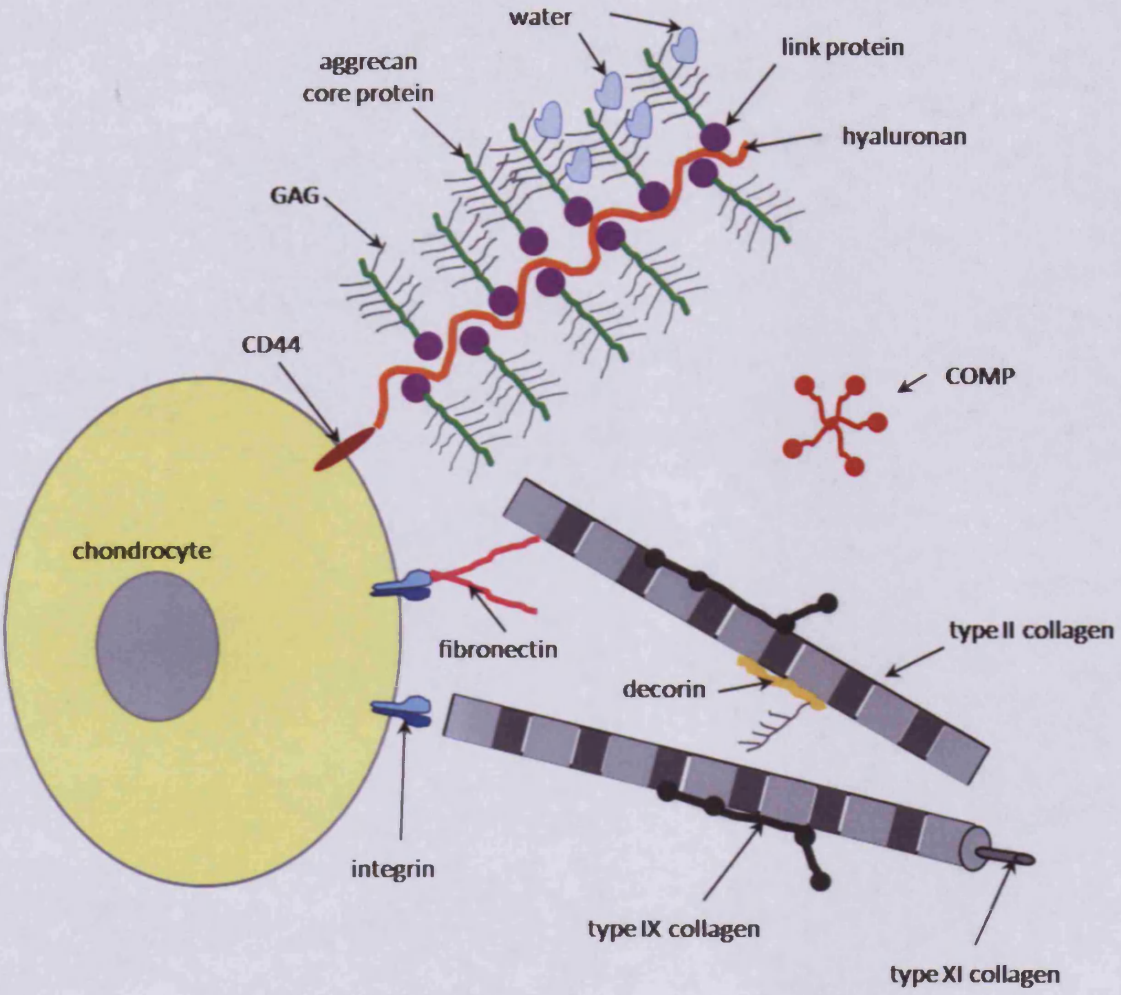

Figure 1.2:- A schematic diagram illustrating the interaction between the major components of articular cartilage. Type II collagen forms fibrils along with types IX and XI collagen. Aggrecan interacts with hyaluronan through link protein to form large aggregating proteoglycans which bind water molecules. Extracellular matrix receptors expressed by the chondrocytes, including integrins and CD44, bind to matrix molecules. COMP- cartilage oligomeric protein, GAG- glycosaminoglycan.

Adapted from (Silver and Glasgold, 1995)

Other proteoglycans present in articular cartilage include the small leucine-rich proteoglycans (SLRPs) decorin, biglycan and fibromodulin. These molecules bind to other matrix molecules and help stabilise the matrix. Biglycan has a pericellular distribution whilst fibromodulin is interterritorial and decorin is found associated with thick collagen fibrils in the interterritorial matrix of the superficial and deep zones (Hagg et al., 1998).

Proteoglycans provide the articular cartilage with its elastic properties. As the tissue is deformed under mechanical compression, water is forced out of the region under stress. Following removal of the stress, the hydrophilic proteoglycans attract water in to the deformed region and cause it to return to its original state.

1.1.2.3 Water

Water constitutes between 65–80% of the wet weight of healthy human articular cartilage and varies with age; from newborn to age 20, water content decreases from around 80% to 65–70% (Amado et al., 1976, Maroudas et al., 1973). Water is held in the articular cartilage tissue by proteoglycans and is an important component of articular cartilage. The movement of water molecules helps to dissipate any load applied to the cartilage and also enables the tissue to return to its original state following the removal of load; water is therefore essential to the mechanical properties and function of articular cartilage. Changes in water content, whether with age, loss of proteoglycans or disruption of collagen fibrils, would therefore affect the mechanical properties and function of cartilage. Increases in water content correlate with increases in tissue permeability and decreases in the equilibrium modulus (i.e. decreases in tissue matrix stiffness) in human articular cartilage (Armstrong and Mow, 1982). This is observed in osteoarthritic (OA) cartilage, which contains 6–9% more water than normal cartilage (Mankin and Thrasher, 1975, Maroudas et al., 1973).

1.1.2.4 Other Extracellular Components of Articular Cartilage

The remaining macromolecules of the articular cartilage ECM are the non-collagenous proteins and glycoproteins, including cartilage oligomeric protein (COMP), fibronectin, and tenascin C (Buckwalter and Mankin, 1998). COMP is a pentameric glycoprotein used as a systemic marker of OA, whilst tenascin C is an oligomeric glycoprotein, shown to be mechanically regulated in fibroblasts (Chiquet, 1999) and capable of interfering with the adhesion of cells to fibronectin. Fibronectin is localised to the

pericellular matrices of articular cartilage, interacting with type IX collagen and the cell surface of chondrocytes through the integrin cell surface receptors.

1.1.2.5 Extracellular Proteinases

The predominant proteinases present in articular cartilage are the matrixin sub-family of metalloproteinases known as the matrix metalloproteinases (MMPs). There are 23 different MMPs in humans (Table 1.1) and all are multidomain zinc metalloproteinases that exhibit sequence homology with the catalytic domain of MMP-1 (Murphy and Nagase, 2008). MMPs have historically been grouped based on their domain organisation and substrate preferences (Table 1.1); the gelatinases have three repeats of a fibronectin type II repeat inserted into their catalytic domain whilst the matrilysins lack a hemopexin domain (Figure 1.3). MMPs exhibit a zinc-dependant catalytic mechanism at the active site and are synthesised as pre-proenzymes. The signal peptide is removed during translation to generate proMMPs which are secreted in zymogen form. Activation of the latent forms of MMPs is proteolytic and can be performed by other MMPs or proteinases of the extracellular matrix, or by autocatalytic cleavage [reviewed in (Woessner, 1991)]. For example, all membrane-type MMPs (MT-MMPs) except MT4-MMP can activate proMMP-2 (Murphy and Nagase, 2008) and MT1-MMP (MMP-14) can also activate proMMP-13 (Knauper et al., 1996). MMPs have a role in ECM remodelling in both biological (e.g. wound healing) and pathological (e.g. cancer cell metastasis and arthritis) processes. The MMPs expressed in articular cartilage chondrocytes are indicated in table 1.1, as are any changes with osteoarthritis, which are discussed in more detail in section 1.3.1.1.2.

The natural inhibitors of MMPs, called tissue inhibitors of metalloproteinases (TIMPs), bind reversibly in a 1:1 complex to the MMPs [reviewed in (Nagase et al., 2006)]. There are four TIMPs that have currently been characterised and they each show a different specificity for the different MMPs. Expression of all four TIMPs has been detected in human articular cartilage (Kevorkian et al., 2004). In normal cartilage there is a balance between the levels of TIMPs and MMPs, with a small excess of inhibitor (Dean et al., 1989). The importance of this balance is indicated by the imbalance present in OA cartilage; an increase in MMPs is observed that is not sufficiently matched by an increase in TIMPs which ultimately results in ECM degradation and progression of OA. In human OA cartilage, levels of *TIMP3* mRNA are elevated whilst *TIMP1* and *TIMP4*

mRNA levels are decreased when compared with normal tissue; *TIMP2* mRNA levels are unchanged (Kevorkian et al., 2004).

Sub-group	MMP	Articular Cartilage Substrates	In Cartilage	Change with OA
Collagenases	MMP-1	types I, II, III & X collagen, FN	Yes[1]	▼[1]nc[2]
	MMP-8	types I, II & III collagen	No[1]	
	MMP-13	types I, II & III collagen, perlecan	Yes[1-3]	▲[1-3]
Gelatinases	MMP-2	types I, II, III, V, X & XI collagen, aggrecan, decorin, laminin	Yes[1]	▲[1]
	MMP-9	types V & XI collagen, denatured fibrillar collagens, aggrecan, FN	Yes[1]	▲[1]
Stromelysins	MMP-3	decorin, perlecan, FN, laminin, types III, IX & X collagen	Yes[1]	▼[1,2]
	MMP-10	FN, weakly types III & V collagen	Yes[1]	▼[1]
Matrilysins	MMP-7	decorin, FN		
	MMP-26	FN	Yes[1]	
	MMP-11		No[1]	
MT-MMPs *1) TM-type*	MMP-14	types I, II & III collagen[4], aggrecan, CD44, proMMP-2 & proMMP-13	Yes[1]	nc[1]
	MMP-15	laminin, FN, aggrecan, perlecan[5]		
	MMP-16	type III collagen, FN	Yes[1]	▲[1]
	MMP-24		Yes[1]	
2) GPI-anchored	MMP-17			
	MMP-25			
Other	MMP-12		Yes[6]	
	MMP-19	aggrecan, COMP, laminin, FN	Yes[1]	
	MMP-20	aggrecan, COMP	No[1]	
	MMP-21		Yes[1]	
	MMP-23		Yes[1]	
	MMP-27		Yes[1]	
	MMP-28		Yes[1]	▲[1]

Table 1.1:- Human matrix metalloproteinases (MMPs) and their substrates. Only substrates relevant to articular cartilage are included. MMPs whose expression has been detected in articular cartilage are indicated along with up- (▲) or down- (▼) regulation in osteoarthritic (OA) cartilage. COMP- cartilage oligomeric protein, FN- fibronectin, GPI- glycosylphosphatidylinositol, TM- transmembrane. [1](Kevorkian et al., 2004), [2](Bau et al., 2002), [3](Brew et al., 2010b), [4](Ohuchi et al., 1997), [5](d'Ortho et al., 1997), [6](Kerkela et al., 2001).

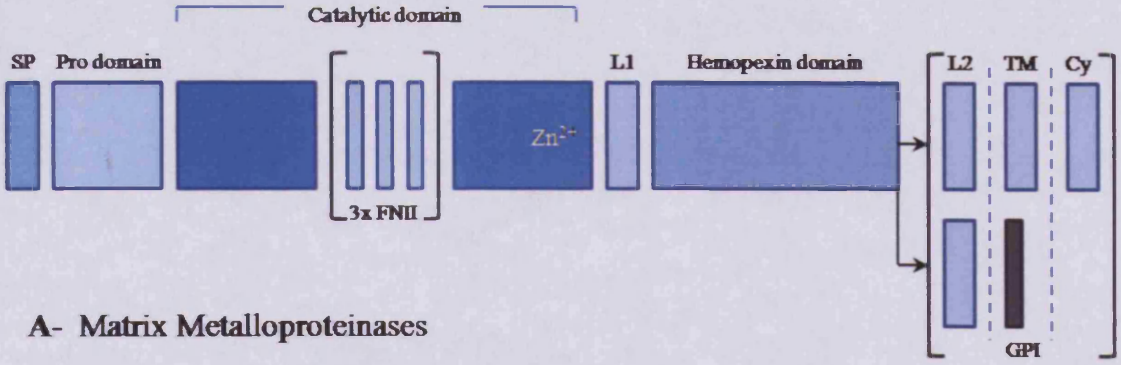

A- Matrix Metalloproteinases

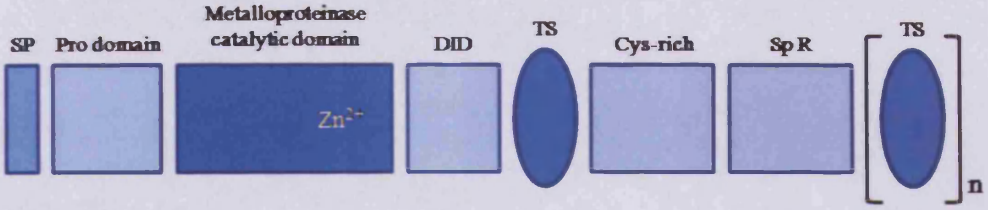

B- ADAMTS

Figure 1.3:- A schematic representation of the primary domain structure of matrix metalloproteinases (A) and ADAMTSs (B), adapted from Nagase *et al*, (2006) and Porter *et al*, (2005), respectively. Cy- cytoplasmic domain, Cys-rich- cysteine-rich domain, DID- disintegrin domain, FNII- fibronectin type II repeat, GPI- glycosylphosphatidylinositol anchor, L1/2- linker 1/2, SP- signal peptide, Sp R- spacer region, TM- transmembrane domain, TS- thrombospondin type I motif.

Other enzymes involved in matrix turnover have been characterised as belonging to the ADAMTS (A Disintegrin and Metalloproteinase with ThromboSpondin motifs) gene family. There are 19 ADAMTS genes in humans (Table 1.2) and all are expressed in human articular cartilage, with the exception of ADAMTS-7 and -8 (Kevorkian et al., 2004, Porter et al., 2005). As for MMPs, ADAMTSs are synthesised as inactive pre-proenzymes and the signal peptide removed during translation (Porter et al., 2005). The pro-domain is proteolytically cleaved from ADAMTSs by furin before secretion (Figure 1.3), although in the case of ADAMTS5, pro-domain processing occurs extracellularly (Longpre et al., 2009). The domain structure of ADAMTSs varies most at the C-terminus due to variations in the number of C-terminal thrombospondin type I motif (TS) repeats (Porter et al., 2005). The C-terminal TS repeats and spacer region are involved in ECM binding (Figure 1.3); for example, ADAMTS-7 and -12 bind COMP through their four C-terminal TS repeats (Liu et al., 2006a, Liu et al., 2006b) whilst ADAMTS4 binds to sulphated GAGs on aggrecan through its only TS motif and sites in the cysteine-rich and/or spacer region (Flannery et al., 2002). C-terminal processing of ADAMTSs can therefore alter ECM substrate binding and enzymatic activity. The 75 kD full-length active form of ADAMTS4 undergoes C-terminal processing to produce isoforms of 60 and 50 kD (Gao et al., 2002). This releases ADAMTS4 from the ECM, increases the number of substrates cleaved and changes the site in aggrecan cleaved by the protease (Kashiwagi et al., 2004). C-terminally truncated ADAMTS5 retains aggrecanase activity and the ability to bind to sulphated GAGs, but aggrecanase activity is significantly decreased with truncation before the first TS motif (Zeng et al., 2006). Enzyme activity can also be regulated by binding to other ECM molecules; for example fibronectin binds to the spacer region of ADAMTS4 and inhibits its aggrecanase activity (Hashimoto et al., 2004).

ADAMTS-4 and -5 are referred to as aggrecanase-1 and -2 respectively [reviewed in (Caterson et al., 2000)], but ADAMTS-1, -9 and -15 also exhibit aggrecanase activity (Porter et al., 2005). A number of the ADAMTSs are dysregulated in human OA cartilage (Table 1.2). However knockout or knockdown studies have shown that ADAMTS5 is the aggrecanase involved in OA and inflammatory arthritis progression in mice (Glasson et al., 2004, Glasson et al., 2005, Stanton et al., 2005, Majumdar et al., 2007) whereas both ADAMTS-4 and -5 mediate aggrecan degradation in human articular cartilage and human OA (Song et al., 2007); therefore only ADAMTS-4 and -5

are discussed further. In addition to C-terminal processing discussed above, the activity of ADAMTS-4 and -5 can be regulated by TIMP3, which binds to and inhibits the aggrecanases (Kashiwagi et al., 2001). At the transcriptional level, *ADAMTS4* expression is induced by pro-inflammatory cytokines in human chondrocytes, whilst *ADAMTS5* is constitutively expressed and is either modestly or unaffected by cytokines (Bau et al., 2002, Song et al., 2007, Fosang et al., 2008); work in our laboratory has demonstrated that *ADAMTS5* expression is up-regulated in response to IL-1 in combination with oncostatin M.

Also present in the ECM are the serine proteinases which function in the turnover of matrix molecules. In addition to extracellular proteinases, the aspartate and cysteine proteinases are involved in the turnover of the ECM, but function predominantly intracellularly. These proteinases are not covered by the present study but have been reviewed recently (Cawston and Wilson, 2006, Cawston and Young, 2010).

1.1.2.6 Chondrocyte

Chondrocytes are the cells embedded within the articular cartilage. In an aneural and avascular environment, they are responsible for the maintenance of the articular cartilage, synthesising and secreting collagen, proteoglycans and other ECM molecules. They also regulate the turnover of the matrix as they synthesise the proteinases which degrade the ECM components. The balance of synthesis and degradation of the matrix, as controlled by the chondrocyte, is essential in maintaining the function of articular cartilage. An imbalance and shift towards a catabolic phenotype, as occurs in OA [reviewed in (Goldring, 2000)], ultimately results in degradation of the articular cartilage and failure of the joint.

1.1.2.7 Extracellular Matrix Receptors

As discussed above, cartilage is an avascular and aneural tissue. This lack of 'input' from the outside environment means that the chondrocytes are responsible for tissue homeostasis. In normal cartilage each chondrocyte is surrounded by its pericellular matrix so there is no cell-cell contact. Cell-matrix interactions therefore provide the means of regulating chondrocyte metabolism and cartilage homeostasis. These interactions are through the cell adhesion receptors expressed by the articular cartilage chondrocytes, including both integrin and non-integrin transmembrane ECM receptors.

ADAMTS	Articular Cartilage Substrates	In Cartilage[1]	Change with OA[1]
ADAMTS-1	aggrecan	Yes	▼
ADAMTS-2	procollagen I, II & III N-propeptides	Yes	▲
ADAMTS-3	procollagen II N-propeptide	Yes	
ADAMTS-4	aggrecan, decorin, biglycan, fibromodulin	Yes	
ADAMTS-5	aggrecan, biglycan	Yes	▼
ADAMTS-6		Yes	
ADAMTS-7	COMP[2]	No	
ADAMTS-8		No	
ADAMTS-9	aggrecan	Yes	▼
ADAMTS-10		Yes	
ADAMTS-12	COMP[3]	Yes	▲
ADAMTS-13		Yes	
ADAMTS-14	procollagen I N-propeptide	Yes	▲
ADAMTS-15	aggrecan	Yes	▼
ADAMTS-16		Yes	▲
ADAMTS-17		Yes	
ADAMTS-18		Yes	
ADAMTS-19		Yes	
ADAMTS-20		Yes	

Table 1.2:- Human ADAMTSs (A Disintegrin and Metalloproteinase with ThromboSpondin motifs) and their substrates, adapted from Porter *et al*, (2005). Only substrates relevant to articular cartilage are included. ADAMTSs expressed in human articular cartilage are indicated along with up- (▲) or down- (▼) regulation in osteoarthritic (OA) cartilage. COMP- cartilage oligomeric protein. [1](Kevorkian et al., 2004), [2](Liu et al., 2006a), [3](Liu et al., 2006b).

1.1.2.7.1 Integrins

The integrins are a large family of cell adhesion molecules that are expressed on most cell types, including chondrocytes. They are heterodimeric transmembrane glycoproteins consisting of one α and one β subunit. There are eight genes encoding β integrin subunits and 18 encoding α integrin subunits in mammals, with 24 different αβ combinations identified at the protein level (Humphries et al., 2006).

Non-osteoarthritic human adult articular chondrocytes have been shown, by immunohistochemistry, to strongly express β1 and α5 integrin subunits and to weakly and occasionally express α1 and α3 integrins *in situ* (Salter et al., 1992). These results were supported by another group who also reported expression of the αVβ5 and αVβ3 heterodimers (Woods et al., 1994). Another study demonstrated expression of α1, α5, αV, β1, β5 and occasionally β4 integrin subunits by both normal and osteoarthritic articular chondrocytes *in situ* (Ostergaard et al., 1998). The αV integrin subunit was observed to vary between the different cartilage zones and was more highly expressed in the surface zone when compared with the deep zone (Woods et al., 1994, Ostergaard et al., 1998). Chondrocyte integrin expression may be altered by enzymatic isolation of cells from tissue and changes in the ECM, with the expression levels of integrins shown to increase with culture period (Woods et al., 1994, Knudson and Loeser, 2002). Foetal chondrocytes express α6β1 integrin (Salter et al., 1995) and chondrosarcoma and immortalised chondrocytes express higher levels of α2β1 integrin compared to adult chondrocytes (Holmvall et al., 1995, Loeser et al., 2000), indicating that integrin expression also alters with chondrocyte differentiation (Knudson and Loeser, 2002).

Integrin expression can also change with osteoarthritis. Osteoarthritic cartilage stained for α2 and occasionally α4 and β2 integrins and these were not detected in normal samples (Ostergaard et al., 1998), which suggests that the expression of certain integrins by chondrocytes may be altered by damage or loss of the ECM as occurs in OA. Expression levels of α1β1 and α5β1 integrins are elevated in OA cartilage when compared with normal tissue (Loeser, 2000). Furthermore, chondrocytes enzymatically isolated from human OA cartilage expressed α1, α2, α3, α4, α5, α6, αV and β1 integrin subunits, with the most frequently expressed of the α subunits being α1, followed by α3, α5 then α2 (Lapadula et al., 1997).

A common integrin-binding motif present in integrin ligands is the peptide sequence Arg-Gly-Asp (RGD). The extracellular domain of both α and β subunits are at the N-termini and both determine the specificity of the integrin. The ECM of articular cartilage contains a number of known integrin ligands (Table 1.3). Type VI collagen and fibronectin are bound by α1β1 and α5β1 integrins respectively- the primary chondrocyte receptors for these molecules (Loeser et al., 1995). Type II collagen is also a ligand of α1β1 integrin, as is matrilin-1 (Loeser et al., 1995, Knudson and Loeser, 2002). Another integrin receptor for type II collagen was identified as α10β1 integrin. Originally isolated from bovine chondrocytes, it has been shown to be expressed by human articular chondrocytes *in situ* by immunohistochemistry and to bind both type I and type II collagen, but not fibronectin (Camper et al., 1998).

Integrin	**Ligand**
α1β1	Collagen, Laminin
α5β1	(*RGD*) Fibronectin, COMP, Osteopontin
α10β1	Collagen, Laminin
αVβ1	(*RGD*) Fibronectin, Vitronectin, Osteopontin, BSP, LAP-TGFβ
αVβ3	(*RGD*) Fibronectin, COMP, Vitronectin, Tenascin, Osteopontin, BSP, MMP-2, LAP-TGFβ
αVβ5	(*RGD*) Vitronectin, Osteopontin, BSP
α3β1	Collagen, Fibronectin
α6β1	Laminin
α2β1	Collagen, Laminin
α4β1	Fibronectin, Osteopontin

Table 1.3:- Integrin heterodimers detected in articular chondrocytes and their extracellular ligands. Information is adapted from Loeser (2000) and Humphries *et al,* (2006) and only ligands relevant to cartilage and bone are included. Integrins that recognise the Arg-Gly-Asp (RGD) peptide sequence are indicated. BSP- bone sialoprotein, LAP-TGFβ- latency-associated peptide transforming growth factor β.

At the C-termini of α and β integrin subunits are the cytoplasmic domains. These cytoplasmic tails bind to signalling proteins and adaptor proteins. The 'adaptor proteins' are actin-binding proteins, making integrins a physical link between the ECM and the cytoskeleton. These cytoplasmic signalling complexes can be disrupted by catabolic mediators such as nitric oxide, which prevented the intracellular assembly of F-actin but did not affect clustering of α5β1 integrin in the presence of its ligand fibronectin (Clancy, 1999). The proteins associated with the cytoplasmic tails and actin-binding proteins provide integrins with 'bidirectional' signalling properties. Binding of ligand to the integrin extracellular domains signals to the cytoplasmic tails, likely through a conformational change, resulting in phosphorylation of proteins in the cytoplasmic integrin-associated protein complex and subsequent signalling events. This is termed 'outside-in' signalling, with extracellular changes transmitted to the cell. For example, chondrocyte binding of fibronectin by α5β1 integrin is required to support constitutive proteoglycan synthesis (Clancy, 1999). It is through 'outside-in' signalling that integrins function as mechanoreceptors, sensing mechanical forces applied to the ECM and transducing the signal to effector proteins inside the cell; the role of integrins in mechanotransduction is discussed in more detail in section 1.4.2.1.2.

Integrins are also capable of signalling in the other direction, transmitting changes within the cell to the extracellular matrix. 'Inside-out' signalling occurs through modulation of integrin-ligand binding by proteins in the cytoplasmic complex. This 'integrin activation' is mediated by the cytoplasmic domains and is required to increase the integrin affinity for a specific ligand (Longhurst and Jennings, 1998).

1.1.2.7.1.1 Cytoplasmic Integrin Complexes

Integrins do not have enzymatic or actin-binding properties themselves, therefore structural and signalling events are mediated by proteins associated with their cytoplasmic tails. Over 50 proteins have been identified in cytoplasmic focal adhesion complexes (Lo, 2006). Several are illustrated in figure 1.4, but only paxillin, talin, vinculin and focal adhesion kinase (FAK) are discussed here. One study of focal adhesion development in migrating endothelial cells demonstrated that newly formed focal complexes contained tyrosine phosphorylated β3 integrin at the leading edge (Zaidel-Bar et al., 2003). Talin and paxillin were incorporated next, followed by vinculin and FAK; all co-localised with phospho-tyrosine labelling. The application of

mechanical stress to integins, either externally through the ECM or internally through actin contractility, increases the recruitment of talin and vinculin to focal adhesions and results in FAK-dependent adhesion strengthening (Ziegler et al., 2006, Dumbauld et al., 2010).

Talin functions as an adaptor protein, binding to the cytoplasmic tails of β integrin subunits, actin microfilaments and other proteins such as vinculin and FAK (Critchley, 2009). The N-terminal head of talin contains one integrin binding site, one actin binding site and also binds FAK, whilst the rod domain contains a second integrin binding site and two more actin binding sites (Figure 1.4). Talin can exist in an auto-inhibited conformation in which regions in the N-terminal head domain interact with a region in the rod domain. Phosphoinositide 4,5-bisphosphate (PIP_2), the kinase Src and the integrin-activating small GTPase Rap-1A have been implicated in the activation of talin. Talin is unique amongst the adaptor proteins in that it can alter the affinity of the integrin extracellular domain for its ligand, thereby mediating 'inside-out' signalling; talin promotes the separation of the α and β cytoplasmic tails thought to be required for integrin activation (Critchley, 2009).

Paxillin is also classified as a molecular adaptor and contains discrete structural domains which mediate protein–protein interactions (Deakin and Turner, 2008). At the C-terminus there are four LIM domains, with LIM2 and LIM3 required for the targeting of paxillin to focal adhesions. Paxillin interacts with numerous proteins including β1 integrin, talin, FAK (Brown and Turner, 2004), vinculin (Turner et al., 1990) and tubulin (Deakin and Turner, 2008). Paxillin can be phosphorylated by kinases including p21-associated kinase (PAK), JNK, ERK and p38 MAPK, and phosphorylation of paxillin regulates its interaction with binding partners. Paxillin forms a scaffold for ERK activation as it binds the ERK kinase MEK and recruits inactive ERK, which associates with paxillin phosphorylated on Tyr118 (Ishibe et al., 2003). Although it does not bind F-actin directly, paxillin can regulate actin dynamics through the Rho GTPases (see section 1.2.1.1.6). Regulation of Rho GTPases is indirect, through recruitment of GTPase activating proteins (GAPs) and guanidine nucleotide exchange factors (GEFs); for example, tyrosine phosphorylation of paxillin at Tyr31 and Tyr118 indirectly activates Rac1 and inhibits RhoA (Deakin and Turner, 2008).

Vinculin is also present in focal adhesions (Geiger et al., 1980) and as discussed above, binds to both talin and paxillin (Figure 1.4). As an adaptor protein, vinculin binds to a number of other intracellular proteins including the actin-bundling protein α-actinin, the actin nucleating protein Arp2/3 (see section 1.2.1.1.2) and PKCα (Ziegler et al., 2006). Vinculin also binds F-actin through a region in its C-terminus and actin-binding promotes vinculin dimerisation, which in turn promotes actin cross-linking. As for talin, vinculin can exist in an auto-inhibited conformation as a result of interaction between its N- and C-termini. Vinculin is activated by binding of two or more of its binding partners.

A number of enzymatic proteins have been detected in focal adhesions (Lo, 2006) and one of these is FAK. FAK is phosphorylated by Src, which can be activated through a direct interaction with the cytoplasmic tail of β integrin (Arias-Salgado et al., 2003). The C-terminus of FAK targets it to focal adhesions, where it interacts indirectly with integrins through talin and paxillin (Figure 1.4)(Mitra et al., 2005). A number of tyrosine residues in FAK are subject to phosphorylation which regulates both its catalytic activity and interaction with other proteins. Tyrosine-phosphorylated FAK is present in focal adhesions and levels increase with increasing rigidity of the ECM (Wozniak et al., 2003). FAK and its phosphorylation is not required for focal adhesion formation but for their disassembly and turnover (Mitra et al., 2005). FAK also mediates cell signalling through binding or phosphorylation of downstream targets. The binding of α-actinin to actin is reduced following its phosphorylation by FAK, which therefore reduces actin bundling. FAK can also regulate actin microfilament dynamics through its association with GAPs and GEFs, which regulate the Rho GTPases. Phosphorylation of paxillin by the FAK-Src complex promotes binding of ERK and, through its role in enhancing the activation of ERK and JNK, FAK can promote MMP-9 secretion and cell migration (Hauck et al., 2001, Mitra et al., 2005).

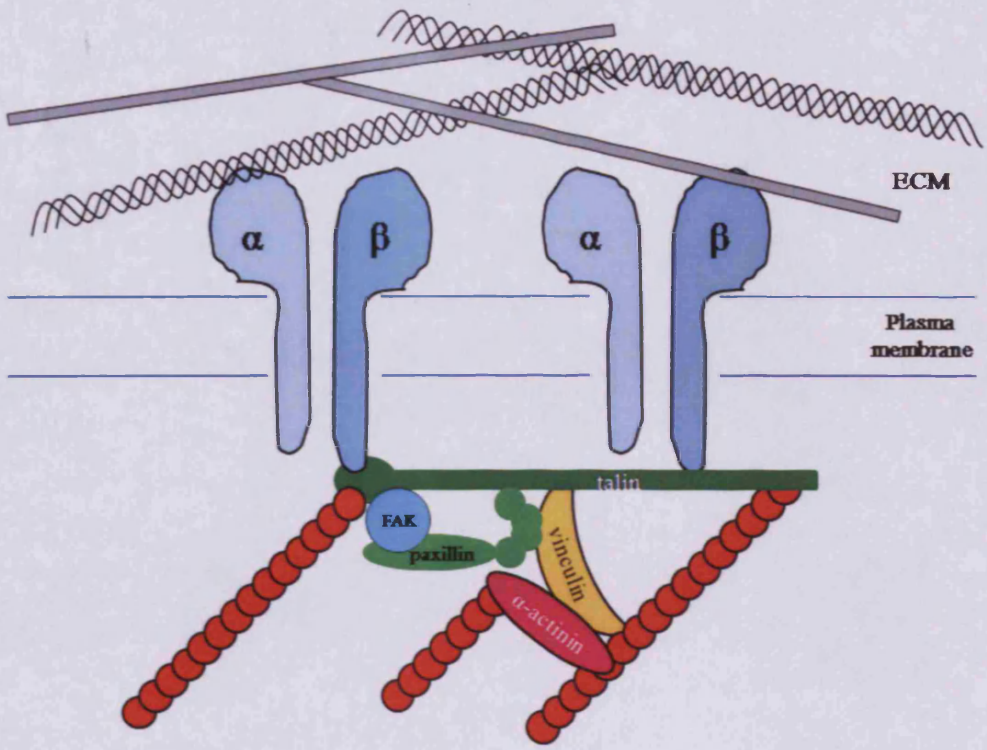

Figure 1.4:- A schematic of select proteins in focal contact links between the extracellular matrix (ECM) and actin cytoskeleton (red). The extracellular domains of integrin αβ heterodimers (blue) bind to ECM molecules. Intracellular proteins bind to the cytoplasmic tails of integrin subunits and associate with each other and with actin microfilaments. FAK- focal adhesion kinase. Adapted from Lo, 2006.

1.1.2.7.2 CD44

CD44 is a single-pass transmembrane glycoprotein expressed by many cell types, including chondrocytes, where it is the primary hyaluronan (HA)-binding receptor (Knudson et al., 1996). As discussed above, in articular cartilage hyaluronan is bound to aggrecan monomers through link protein, forming large proteoglycan aggregates. Therefore, through its binding of HA, CD44 binds and retains the large proteoglycan aggregates that are important to the hydration and mechanical properties of articular cartilage tissue. The binding of HA molecules to the chondrocyte surface through CD44 is independent of collagen and fibronectin molecules and matrices (Knudson and Loeser, 2002). CD44 is also involved in the assembly as well as the retention of the pericellular matrix (Knudson et al., 1996, Nofal and Knudson, 2002); antisense-mediated knockdown of CD44 in cartilage slices resulted in a distinct loss of the proteoglycan-rich matrix (Chow et al., 1998). An increase in the 'NITEGE' neoepitope, which is exposed in aggrecan molecules following cleavage by aggrecanases, was also noted, indicating that the loss of proteoglycan was catabolic as well as passive. In addition to its role in retaining HA and assembling the pericellular matrix, CD44 is also responsible for the internalisation of HA molecules, which are then subsequently degraded. Treatment with IL-1α, a cytokine often used to induce a catabolic phenotype in chondrocytes, increases CD44 expression along with internalisation and catabolism of HA in human articular chondrocytes and cartilage slices (Chow et al., 1995, Nishida et al., 2000).

The cytoplasmic domain of CD44 has the potential for signal transduction, with serine residues (Ser336 and Ser337) that are subject to differential phosphorylation (Knudson and Loeser, 2002), and interactions between the cytoplasmic domain and actin-binding proteins including ankyrin and ezrin (Ponta et al., 2003, Legg et al., 2002). Changes in the interaction of CD44 with the actin cytoskeleton can modulate HA binding (Lokeshwar et al., 1994, Knudson and Loeser, 2002).

In cultured cartilage slices, both actin cytoskeletal disruption and CD44 knockdown cause similar changes in cultured cartilage slices; treatments resulted in a loss of proteoglycan and an increase in the appearance of the NITEGE aggrecan neoepitope (Chow et al., 1998, Nofal and Knudson, 2002). This demonstrates a clear link between CD44 and the cytoskeleton. Changes in the cytoskeleton, or removal of the ankyrin-

binding domain modulates CD44–HA binding, demonstrating an 'inside-out' signalling mechanism through CD44.

1.1.2.7.3 Syndecan Proteoglycans

Syndecans are type I transmembrane heparan sulphate proteoglycans (Okina et al., 2009). There are four syndecans in mammals and they exhibit different tissue distribution. Syndecan-1 is expressed primarily in epithelial cells, syndecan-2 in mesenchymal cells including endothelia, syndecan-3 in neuronal cells whilst syndecan-4 is detected in most tissues (Kim et al., 1994); expression of syndecan-1, -2 and -4 has been detected in cultured rat condyle chondrocytes (Molteni et al., 1999). All syndecans have an N-terminal extracellular domain, a transmembrane domain through which they form homodimers, and a short cytoplasmic domain at their C-terminus (Okina et al., 2009). Heparan sulphate glycosaminoglycans are covalently linked to conserved Ser–Gly motifs surrounded by acidic residues in syndecan extracellular domains (Zhang and Esko, 1994). Through these heparan sulphate chains, syndecans can interact with ECM molecules, growth factors and cytokines (Okina et al., 2009). Intact syndecan extracellular domains are shed from the cell surface by MMPs including MMP-2, MMP-9 (Brule et al., 2006, Fears et al., 2006), MMP-7 (Li et al., 2002) and MMP-14 (Endo et al., 2003). Shedding of syndecan ectodomains can be inhibited by TIMP-2 (Endo et al., 2003) and TIMP-3 (Fitzgerald et al., 2000). This is relevant to the function of syndecans, as soluble ectodomains can compete for cell surface binding and therefore inhibit downstream intracellular signalling.

The cytoplasmic domain of syndecans interacts with the actin cytoskeleton through binding to actin-associated proteins. The cytoplasmic domain of syndecan-2 interacts with ezrin (Granes et al., 2003), a protein that cross-links the actin cytoskeleton to the plasma membrane and binds regulators of actin microfilament assembly (Niggli and Rossy, 2008). The actin-bundling protein α-actinin binds to the cytoplasmic domain of syndecan-4 (Greene et al., 2003). Furthermore, syndecan-4 is enriched in focal adhesions and its overexpression increases focal adhesion formation (Woods and Couchman, 1994, Longley et al., 1999); this is suggested to be mediated by the extracellular domain and ligation of heparan sulphate chains (Okina et al., 2009). Syndecan-4 activates RhoA via PKCα and this is required for focal adhesion formation and maintenance of actin stress fibres in fibroblasts (Dovas et al., 2006).

Of particular relevance to this project, recent research has begun to identify roles for syndecan-4 in both mechanotransduction and osteoarthritis. Mechanical stretching of fibroblasts through syndecan-4-specific cellular attachments activates ERK through a mechanism dependent upon an intact actin cytoskeleton (Bellin et al., 2009), indicating mechanotransduction pathways similar to those of integrins (see section 1.4.2.1.2). Syndecan-4 expression is elevated in human OA cartilage when compared with normal tissue and syndecan-4-knockout mice were protected against surgically-induced OA (Echtermeyer et al., 2009). In wild-type mice, intra-articular injection of syndecan-4 blocking antibodies prevented surgically-induced OA-like changes in the cartilage. Loss of syndecan-4 reduced ERK1/2 phosphorylation, MMP-3 release and aggrecanase (ADAMTS5) activity, suggesting that activation of syndecan-4 promotes MMP-3-mediated activation of ADAMTS5. Furthermore, a recent study has demonstrated that syndecan-4 interacts with the C-terminal domain of MMP-13 (Zhang et al., 2010).

The importance of the ECM receptors in cartilage is highlighted by the studies described above, all showing that uncoupling the chondrocyte cytoskeleton from the matrix, either through modulation of the cytoskeleton, the receptor–cytoskeleton interaction, receptor expression or receptor–ligand binding results in detrimental changes in the cartilage/chondrocyte matrix in a manner similar to that which occurs in OA.

1.2 The Cytoskeleton

All cells possess a three-dimensional (3D) cytoskeleton consisting of networks of actin microfilaments, tubulin microtubules and intermediate filaments. These networks are highly organised and function in diverse cellular processes.

1.2.1 Actin Microfilaments

Actin proteins are highly conserved and ubiquitously expressed in all eukaryotic cells. There are six actin genes in humans (Vandekerckhove and Weber, 1978a, Miwa et al., 1991). β- and γ-actin are known as cytoplasmic actins; their sequence is least similar to muscle (α-)actins and they lack the N-terminal cysteine residue found in α-actins (Vandekerckhove and Weber, 1978b, Gunning et al., 1983). α-actins are expressed in muscle cells, with isoforms specific for skeletal muscle, cardiac muscle, aortic smooth

muscle and enteric smooth muscle (Vandekerckhove and Weber, 1978a, Miwa et al., 1991). Monomeric actin has two major domains or lobes that can each be further divided into two subdomains (domains I to IV; Fig 1.5A) (Kabsch et al., 1990, Schutt et al., 1993). Between the lobes lies a cleft that binds ATP/ADP and a magnesium ion (Fig 1.5A). The globular actin monomers (G-actin) associate and form filaments (F-actin) with a diameter of 7–9 nm; each monomer can associate with four others and they polymerise to produce filaments forming a two-stranded helix (Holmes et al., 1990, Schmid et al., 1994). All monomers face the same direction in actin filaments providing polarity, with a barbed (or plus) end and a pointed (or minus) end at which the ATP-binding cleft of monomers is exposed (Fig 1.5B). Actin monomers can be added and lost at both ends of actin filaments in a process termed 'treadmilling', although the rate of polymerisation and depolymerisation is greater at the barbed end (Woodrum et al., 1975, Cooper and Schafer, 2000). Following the incorporation of ATP-bound actin monomers into filament ends, ATP is hydrolysed to ADP as the filament develops (Cooper and Schafer, 2000, Blain, 2009).

Regulation of actin filament polymerisation is complex and cyclical, involving a large number of proteins, only some of which are discussed below (Table 1.4). Filament disassembly is required to increase the availability of free actin monomers for polymerisation whilst capping proteins, nucleating proteins, sequestering proteins and their upstream regulators spatially and temporally control polymerisation. Cross-linking proteins then determine the 3D organisation and mechanical properties of filament networks. The complex interactions, along with suggested feedback and feed-forward loops, mean that the application of simple linear signalling pathways may be inappropriate or misleading when studying actin cytoskeletal dynamics (Insall and Machesky, 2009).

1.2.1.1 Actin Binding Proteins

Numerous actin binding proteins have been detected *in vivo* and co-ordinate to control actin filament polymerisation, depolymerisation and 3D organisation. Whilst filaments can elongate without assistance, actin-binding proteins assist and regulate polymerisation by promoting nucleation of filaments, binding and 'capping' filament ends, or sequestering monomers (Fig 1.5C). In general, capping proteins bind to the ends of filaments and therefore direct G-actin monomers and filament polymerisation to the

free filament ends (Cooper and Schafer, 2000). The kinetic barrier to nucleation, or initiation, of new filaments observed *in vitro* is overcome *in vivo* by actin-binding proteins that promote nucleation of actin filaments, or proteins which generate free barbed ends by severing existing actin filaments. Using purified proteins *in vitro* to reconstitute sustained movement of *Listeria*, which utilise actin filament dynamics to move around the cytoplasm of living cells, Loisel *et al.* demonstrated that, in addition to G-actin monomers, the inclusion of activated actin related protein 2/3 complex (Arp2/3), capping protein and actin depolymerising factor (ADF) was sufficient for actin polymerisation and bacterial motility; removal of any of these proteins abrogated motility (Loisel et al., 1999).

Actin Binding Protein	**Function**
Capping protein	Capping (+)
Gelsolin	Filament severing, capping (+)
Arp2/3 complex	Nucleation, filament branching, capping (-)
Formins	Nucleation, processive capping (+)
Cofilin/Destrin	Filament depolymerising, filament severing
Thymosin β4	Actin sequestering, inhibits growth at (+) and (-) ends
Profilin	Actin sequestering, promotes growth at (+) end in the presence of thymosin β4 or FH1-containing formins
Filamin	Actin cross-linking, 3D network, scaffold for signalling proteins
α-actinin	Actin bundling

Table 1.4:- Table summarising the actin binding proteins discussed and their functions. (+)/(-) indicate whether the protein performs the function at the barbed/pointed end of the actin microfilament. FH1- formin homology 1 domain.

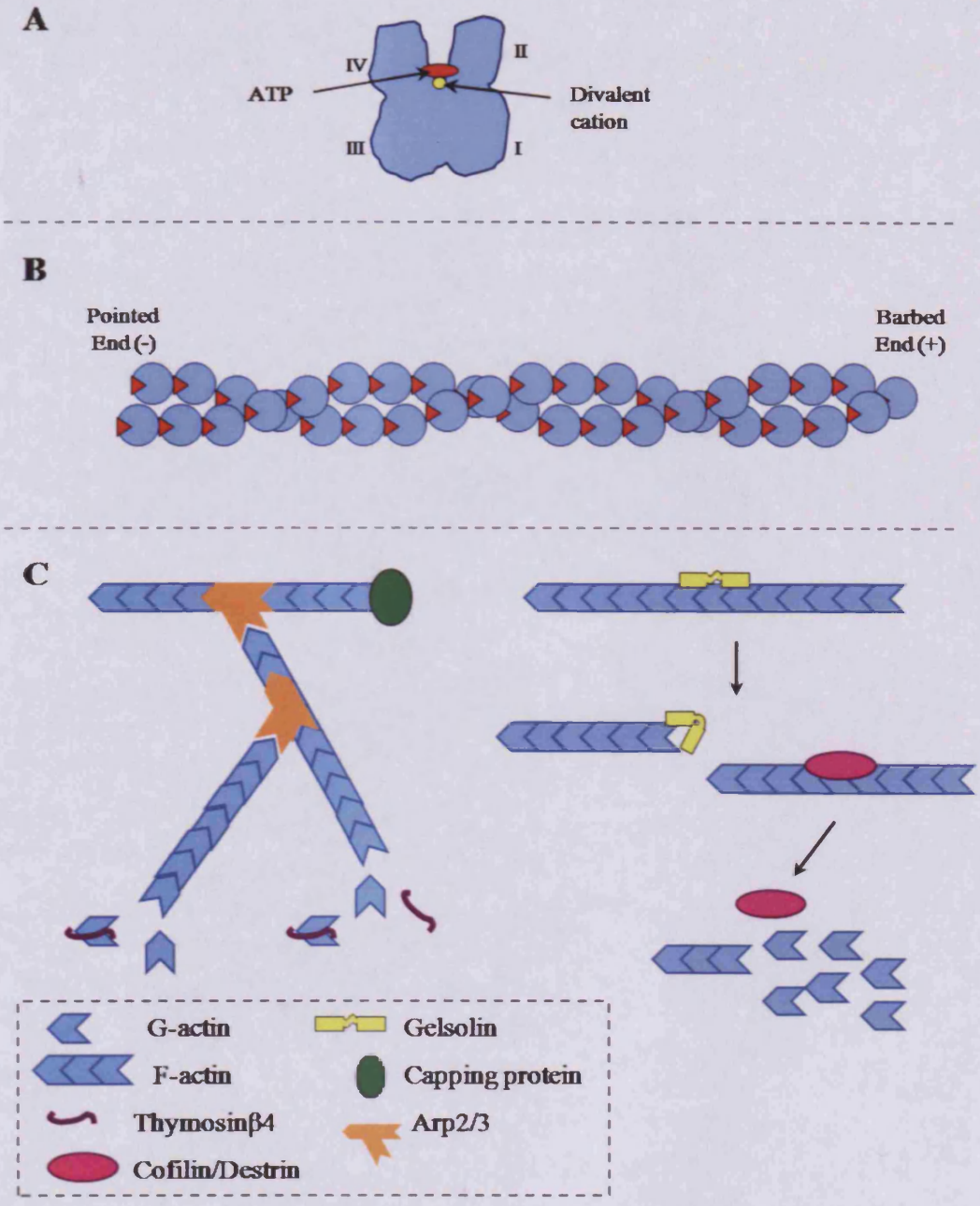

Figure 1.5:- A schematic of actin monomer and microfilament structure and assembly dynamics. **A**- The 3-dimensional structure of an actin monomer indicating the subdomains in roman numerals and the nucleotide (ATP) binding site. **B**- The orientation of actin monomers within actin microfilaments produces a polarised filament with the ATP binding cleft exposed in subunits at the pointed end and subdomains 1 and 3 exposed at the barbed end. **C**- Actin binding proteins regulate filament assembly and disassembly. See text for details.

1.2.1.1.1 Capping Proteins

Capping protein is a heterodimer of α and β subunits that binds to and caps the barbed ends of actin filaments (Cooper and Sept, 2008, Isenberg et al., 1980). Binding of capping protein prevents both the addition and loss of actin subunits from barbed ends and thus prevents both filament growth and depolymerisation. Capping protein is required for actin polymerisation *in vitro* (Loisel et al., 1999) and is suggested to 'funnel' actin polymerisation to required regions in cells by preventing polymerisation at all filament ends. In support of this, knockdown of capping protein by RNA interference resulted in loss of lamellipodia from motile murine melanoma cells and the induction of vasodilator-stimulated phosphoprotein (VASP)-dependent filopodia formation (Mejillano et al., 2004). The capping protein subunit β2 isoform predominates in non-muscle tissue and is a component of cell-cell contacts, whilst the β1 isoform is the predominant form in muscle. The capping activity of capping protein is inhibited by phosphoinositide 4,5-bisphosphate (PIP_2) (Heiss and Cooper, 1991) which binds directly to capping protein near the actin-binding site (Kim et al., 2007). PIP_2 can also remove capping protein that is bound to actin filament barbed ends; this uncapping converts actin filaments from a non-growing to a growing state. Capping protein activity is also regulated by proteins including CARMIL, CKIP-1 and casein kinase 2, and CD2-associated protein (Cooper and Sept, 2008). Microfilament elongation factors including formins and VASP proteins can indirectly regulate capping protein by preventing its binding at barbed ends.

Gelsolin protein structure consists of two homologous halves connected by a long linker (Sun et al., 1999). Gelsolin binds to the side of an actin filament, bridging two longitudinally associated actin subunits, to induce a large conformational change and kink in the filament to sever it (McGough et al., 1998). After severing, gelsolin remains bound to the newly formed barbed end of one of the new shorter filaments, acting as a cap to prevent filaments re-annealing and inhibit growth at the barbed end (Sun et al., 1999). Uncapping of gelsolin could therefore promote actin polymerisation as it increases the number of filaments and free barbed ends. Full-length gelsolin is activated by calcium, which induces a conformational change in the protein. In the inactive form the C-terminal tail inhibits actin binding by the N-terminal domain whilst calcium binding exposes the actin binding site; deletion of the C-terminal tail results in loss of the calcium requirement for gelsolin severing activity and actin-binding (Kwiatkowski et

al., 1989). The C-terminal domain binds actin in a calcium-dependent manner whilst the N-terminal domain binds, severs and caps actin filaments independently of calcium (Kothakota et al., 1997, Sun et al., 1999). Caspase-3 cleaves gelsolin in the linker region and therefore generates a calcium-independent form of gelsolin (Kothakota et al., 1997, Kamada et al., 1998). A decrease in pH (i.e. increase in hydrogen ion concentration) reduces the calcium requirement for gelsolin severing activity (Lamb et al., 1993, Lin et al., 1997). In addition to calcium and hydrogen ions, gelsolin activity is regulated by PIP_2 (Janmey and Stossel, 1987). PIP_2 binds to the N-terminal domain of gelsolin and, as for F-actin subunits, binding is enhanced by calcium (Lin et al., 1997). Phosphotidylinositol monophosphate and PIP_2 bind to gelsolin and inhibit its filament severing activity (Janmey and Stossel, 1987, Janmey et al., 1987). Polyphosphoinositides also dissociate gelsolin–actin complexes and can therefore uncap gelsolin from filament ends to promote filament growth.

In addition to its role in regulation of actin dynamics and therefore the associated processes (section 1.2.1.2), gelsolin also functions in apoptosis (Silacci et al., 2004). Gelsolin acts as a mediator of actin remodelling following cleavage by caspase-3, but is also suggested to act as an inhibitor of apoptosis; over-expression of gelsolin reduces caspase-3 activation and increases resistance to apoptosis (Ohtsu et al., 1997). In addition to the cytoplasmic isoform, a secreted plasma isoform of gelsolin is also expressed which is generated by alternative splicing (Silacci et al., 2004). Plasma gelsolin is suggested to have a prognostic and therapeutic use in a number of medical conditions including sepsis and major trauma (Bucki et al., 2008). Structural similarities and functions of other members of the gelsolin superfamily, including villin, advillin, supervillin, capG and adserervin are reviewed by Silacci *et al*, 2004.

Tropomodulins cap the pointed (slow-growing) end of actin filaments and are regulated by their interaction with tropomyosins, which bind along the side of the actin filament (Kostyukova, 2008). These proteins are not discussed here but have been reviewed by Kostyukova, 2008.

1.2.1.1.2 Arp2/3 Complex Promotes Filament Nucleation

The Arp2/3 complex consists of seven subunits; Arp2 and Arp3 are similar to actin in structure and sequence and the other five subunits (ARPC1–5) are unique and highly conserved throughout evolution (Machesky et al., 1997, Welch et al., 1997). As mentioned above, Arp2/3 is required for actin polymerisation *in vitro* (Loisel et al., 1999). Arp2/3 nucleates and therefore promotes the formation of actin filaments that elongate from their barbed ends (Mullins et al., 1998). The complex binds to and caps the pointed ends of preformed actin filaments but also binds to the sides of actin filaments. Through binding to the sides of filaments, Arp2/3 nucleates the formation of side branches at an angle of 70° from the mother filament, producing a network of branching actin filaments that elongate at their barbed ends (Mullins et al., 1998). As Arp2/3 binds with a higher affinity to ATP- than to ADP-actin filaments, phosphate dissociation in actin filament subunits leads to loss of Arp2/3 binding, debranching and depolymerisation of actin filament networks (Blanchoin et al., 2000). Arp2/3 is activated following interaction with an actin filament and the C-terminus of WASP family proteins (Rohatgi et al., 1999, Insall and Machesky, 2009); PIP_2 activates WASP and actin nucleation by Arp2/3 (Higgs and Pollard, 2000). In humans, the WASP family includes WASP (Wiskott-Aldrich syndrome protein), which is restricted to haematopoietic cells, N-WASP, which is ubiquitously expressed, and four SCAR/WAVE isoforms (Wear et al., 2000). WASP proteins have no effect on actin polymerisation alone, but bind to and activate Arp2/3 to promote nucleation (Machesky et al., 1999).

Formins nucleate actin filaments from free actin monomers; the formin homology 2 (FH2) domains of formins form dimers and stabilise an actin dimer, which then acts as a nucleus for elongation (Insall and Machesky, 2009, Paul and Pollard, 2009, Xu et al., 2004). Dimers form a doughnut-like structure encircling the barbed ends of actin filaments and binding to F-actin subunits. The association of formins with barbed ends protects them from capping proteins, whilst allowing elongation (Zigmond et al., 2003), termed 'processive capping'. FH1-containing formins bind to profilin and concentrate profilin–actin at the barbed ends to accelerate filament growth (Insall and Machesky, 2009, Paul and Pollard, 2009).

Other less-widely studied actin filament nucleation factors, such as Spire, Cobl and VopL/VopF, are not discussed but have been reviewed recently (Dominguez, 2009).

1.2.1.1.3 ADF/Cofilin family

Proteins of the ADF/cofilin family include ADF (known as destrin in mammals and referred to as this from here on), cofilin and actophorin and these mediate actin filament disassembly. As discussed above, destrin was required for reconstitution of actin filament dynamics *in vitro*; disassembly of older filaments is required to generate G-actin for the assembly of new filaments and prevent exhaustion of the free actin monomer pool (Loisel et al., 1999). Destrin/cofilin family proteins bind cooperatively to the side of actin filaments, bridging two longitudinally associated actin subunits (McGough et al., 1997). Binding of destrin/cofilin changes the orientation of actin subunits within the filament and changes the filament twist; this reduces the interactions between actin subunits within filaments, which is suggested to increase the chance that the filament will break and that subunits will dissociate (McGough and Chiu, 1999, Galkin et al., 2001). Destrin/cofilin proteins promote filament assembly both through increasing the rate of subunit dissociation from pointed ends (Carlier et al., 1997) and through filament severing (Maciver et al., 1998). Nucleotide exchange in actin subunits is inhibited by binding of destrin/cofilin proteins, which induce a conformational change in actin so that the ATP-binding cleft is in a 'closed' state (Paavilainen et al., 2008). In direct contrast to the Arp2/3 complex, the affinity of destrin/cofilin for ADP-bound G- and F-actin is higher than its affinity for ATP-bound forms (Carlier et al., 1997). Phosphate dissociation in actin filament subunits therefore leads to increased destrin/cofilin binding and enhanced disassembly of older filament networks (Insall and Machesky, 2009).

The F-actin binding and depolymerising activities of destrin and cofilin are inhibited by the phosphoinositides phosphatidylinositol, PIP and PIP_2 which bind directly to the proteins (Yonezawa et al., 1990). Destrin/cofilin proteins are also negatively regulated by phosphorylation; phosphorylation of serine-3 inhibits the actin-binding and F-actin-depolymerising activities of destrin/cofilin (Morgan et al., 1993, Agnew et al., 1995, Moriyama et al., 1996).

1.2.1.1.4 Actin Sequestering Proteins

Actin sequestering proteins bind to G-actin to decrease the pool of free actin and regulate actin filament polymerisation. Thymosin β4 binds to and sequesters monomeric actin to inhibit polymerisation at the barbed and pointed ends of filaments (Weber et al., 1992, Yu et al., 1993). It does not suppress actin nucleation and does not bind to the ends or sides of actin filaments (Weber et al., 1992). Thymosin β4 forms a 1:1 complex with G-actin and the binding affinity for ATP-actin is 50-fold higher than for ADP-actin (Carlier et al., 1993). Furthermore, thymosin β4 binding inhibits nucleotide exchange in actin monomers (Goldschmidt-Clermont et al., 1992). Thymosin β4 is a small protein of 43 amino acids and, when in aqueous solution is predominantly unstructured (Czisch et al., 1993, Domanski et al., 2004). Folding of thymosin β4 is coupled to its binding to G-actin; upon binding an N-terminal helix contacts actin subdomain 2 and is stabilised, a C-terminal helix is formed and binds to actin subdomain 1, and the thymosin β4 central segment forms an extended interface with actin (Domanski et al., 2004, Dedova et al., 2006); thymosin β4 therefore binds to both the pointed and barbed ends of an actin monomer which explains why polymerisation is inhibited at both ends of actin filaments. No post-translational regulatory mechanism has been identified for thymosin β4 and desequestration of actin from the thymosin β4–actin complex occurs in response to changes in the free G-actin pool, i.e. thymosin β4 functions as a 'G-actin buffer' (Mannherz and Hannappel, 2009). Actin is released from the thymosin β4–actin complex in response to an increase in the number of filament barbed ends, which reduces the critical concentration of actin polymerisation (Nachmias et al., 1993). Desequestration of actin from thymosin β4 can therefore be triggered by uncapping of barbed ends, filament severing or filament nucleation by proteins such as Arp2/3, all of which increase the number of free barbed ends (Mannherz and Hannappel, 2009).

Another G-actin sequestering protein, profilin, competes with thymosin β4 for actin binding (Goldschmidt-Clermont et al., 1992). In contrast to thymosin β4, profilin promotes nucleotide exchange in actin monomers (Mockrin and Korn, 1980), with low concentrations of profilin able to overcome the inhibitory effects of high thymosin β4 concentrations (Goldschmidt-Clermont et al., 1992). Profilin forms a 1:1 complex with G-actin and binding results in moderate opening of the nucleotide cleft (Schutt et al., 1993, Baek et al., 2008). Profilin inhibits actin nucleation and filament growth at pointed

ends but, in the presence of thymosin β4, promotes elongation at barbed ends (Pantaloni and Carlier, 1993, Kang et al., 1999, Dominguez, 2009). As mentioned above, profilin cooperates with formins to enhance filament growth at barbed ends. This is due to the fact that profilin can simultaneously bind to actin and proline-rich sequences (Ferron et al., 2007). Through this binding, processive barbed end elongation factors such as FH1-containing formins and VASP recruit the profilin–actin complex to enhance monomer addition and filament growth. Disruption of the phosphoinositide cycle inhibits actin polymerisation (Lassing and Lindberg, 1988) as PIP_2 and PIP_3 bind to profilin and can dissociate the profilin–actin complex to inhibit the effect of profilin (Lassing and Lindberg, 1985, Goldschmidt-Clermont et al., 1991, Lu et al., 1996).

1.2.1.1.5 Actin Cross-linking Proteins

Actin cross-linking proteins determine the 3D organisation of actin filaments and can contribute to the mechanical properties of the networks. One family of actin cross-linking proteins are filamins. Humans express three filamins, filamin-A, -B and -C (Chakarova et al., 2000); filamin C is specific to skeletal muscle (Thompson et al., 2000) whilst filamin A and B are ubiquitously expressed. Filamin A consists of an N-terminal actin-binding domain followed by 24 tandem immunoglobulin (Ig) repeats with two hinge regions and a C-terminus (Gorlin et al., 1990). Ig repeats 9–15 can bind F-actin (Nakamura et al., 2007) and the actin-binding domain binds F-actin at a ratio of 1:13.5 actin monomers (Gorlin et al., 1990). Filamin A is dissociated from F-actin by the calcium-calmodulin complex (Nakamura et al., 2005). Filamin A monomers dimerise through their C-terminus and Ig repeat 24 to form a homodimer with a V-like shape (Gorlin et al., 1990). Dimerisation provides filamin A with the ability to form cross-links between actin filaments. Filamin A organises actin filaments into flexible 3D orthogonal networks and localises to filament intersections, which form X-, T- or Y-shaped junctions in the actin network (Hartwig et al., 1980, Hartwig and Shevlin, 1986); the first hinge region in filamin A, between Ig repeats 15 and 16, is required to maintain the viscoelastic properties of actin networks (Gardel et al., 2006). Ig repeats 16–24 in filamin A do not bind F-actin but are involved in protein-protein interactions with filamin A binding partners (Nakamura et al., 2007). Filamin A binds numerous cellular components including membrane receptors such as β integrins, ion channels, signalling intermediates such as TRAF2 and Smads, and transcription factors (Stossel et al., 2001, Feng and Walsh, 2004, Popowicz et al., 2006). Filamin A can therefore act as a scaffold

for membrane-receptor-associated signalling proteins. A mechanoprotective role for filamin A was also identified when it was shown that filamin A prevented membrane depolarisation and apoptosis in fibroblasts subjected to integrin-mediated tensile force (Kainulainen et al., 2002). This was later shown to be due to the interaction between filamin A and a GTPase-activating protein (GAP) termed FilGAP; deletion of the filamin A binding site in FilGAP increased force-induced apoptosis in cells (Shifrin et al., 2009). FilGAP is phosphorylated by the Rho effector ROCK which stimulates its Rac-specific GAP activity and inhibits Rac-mediated lamella formation (Ohta et al., 2006).

Other actin cross-linking proteins such as α-actinin and fascin are not discussed. Both α-actinin and fascin are actin-bundling proteins but they produce actin networks with different mechanical properties (Tseng et al., 2001).

1.2.1.1.6 Upstream Regulation of Actin Dynamics: Rho GTPases

The mammalian family of Rho GTPases consists of 20 proteins which function as upstream regulators of the actin cytoskeleton (Heasman and Ridley, 2008). Rho GTPases cycle between an active GTP-bound form and an inactive GDP-bound form and are themselves regulated by factors which affect guanine nucleotide cycling termed guanine exchange factors (GEFs) and GTPase activating proteins (GAPs).

Rho stimulates actin stress fibre formation and assembly of focal adhesions, Rac1 stimulates lamellipodia formation and membrane ruffling, whilst Cdc42 induces filopodia formation at the leading edge of migrating cells. Cdc42 stimulates the formation of unbranched filaments and networks through activation of the formin mDia2 (Peng et al., 2003). Cdc42 can also enhance the activity of N-WASP and WASP which activate Arp2/3 nucleation of actin filaments and formation of branched networks (Rohatgi et al., 1999, Tomasevic et al., 2007). Rac1 activates N-WASP or WAVE to promote Arp2/3-mediated actin nucleation, but has no effect on WASP (Heasman and Ridley, 2008, Tomasevic et al., 2007). Furthermore, Rac activation induces the dissociation of gelsolin–actin complexes and therefore uncaps filaments (Arcaro, 1998) which could promote polymerisation.

The small GTPases Rho, Rac and Cdc42 can also regulate actin cytoskeletal dynamics through destrin/cofilin proteins (Cooper and Schafer, 2000). LIM kinase (LIMK) phosphorylates cofilin at serine-3 and therefore inhibits its activity and hence actin depolymerisation (Moriyama et al., 1996, Yang et al., 1998). The Rho effector ROCK phosphorylates and activates LIMK and increases cofilin phosphorylation (Maekawa et al., 1999). LIMK is also activated downstream of Rac or Cdc42 via the serine/threonine kinase PAK1, which directly phosphorylates LIMK and increases cofilin phosphorylation (Edwards et al., 1999).

Rac, Rho and Cdc42 also bind to filamin A independently of their GTP-binding (Ohta et al., 1999) and the filamin A–FilGAP interaction mediates RhoA antagonism of Rac to suppress leading edge protrusion (Ohta et al., 2006).

1.2.1.2 Functions of Microfilaments

Microfilaments are involved in many diverse cellular processes including cell migration (Insall and Machesky, 2009), changes in cell shape (Sims et al., 1992), cytokinesis and therefore proliferation (Glotzer, 2005, Piekny et al., 2005), endocytosis and vesicle translocation (Girao et al., 2008), and extracellular matrix assembly (Hayes et al., 1999). The actin cytoskeleton is also involved in cell adhesion to ECM components through focal adhesions (Lo, 2006). As they are connected to the ECM through transmembrane receptors, actin microfilaments are ideally situated to transduce signals from the ECM to the cell nucleus. Their role in mechanotransduction in chondrocytes is discussed in section 1.4.3.3.

1.2.2 Microtubules

Tubulin proteins are ubiquitously expressed in eukaryotes and monomers consist of approximately 450 amino acids. Tubulins are divided into three main types termed α-, β- and γ-tubulin, with a number of isoforms identified for each. α-, β- and γ-tubulin have almost identical structures; each has an N-terminal domain containing a nucleotide-binding site, an intermediate domain containing the taxol-binding site and a C-terminal domain (Nogales et al., 1998, Aldaz et al., 2005). α- and β-tubulin monomers associate to form a stable heterodimer in which the N-terminal domain of α-tubulin is at the intradimer interface (Fig 1.6A), explaining why the GTP bound to α-tubulin is non-exchangeable (Nogales et al., 1998). The GTP-binding site in β-tubulin is exchangeable

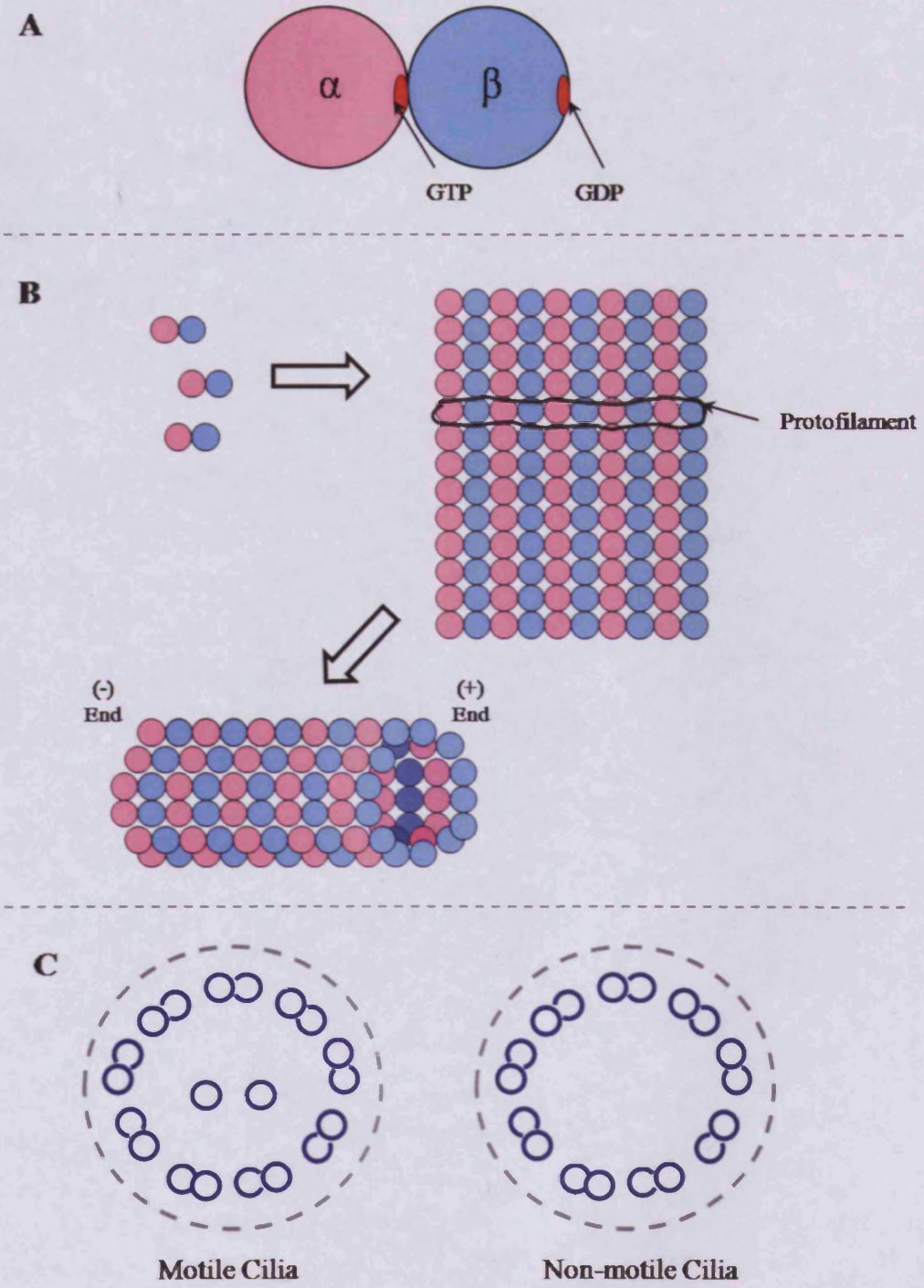

Figure 1.6:- A schematic of the tubulin heterodimer and microtubule structure and assembly. **A**- α-tubulin and β-tubulin associate to form the tubulin heterodimer. **B**- Heterodimers associate longitudinally to form protofilaments, 13 of which associate laterally to form a 2-dimensional sheet which then forms the hollow cylindrical microtubule. **C**- The axoneme of motile cilia consist of nine microtubule doublets and a central pair of microtubules (9 +2); non-motile cilia lack the central pair (9 + 0). Adapted from Lodish et al, Molecular Cell Biology. 4th Ed.

and partially exposed in the heterodimer, but buried and non-exchangeable in the microtubule. The β-tubulin-bound GTP is required for microtubule assembly and is hydrolysed to GDP following addition of the dimer to the microtubule end, therefore β-tubulin within microtubules is GDP-bound (Valiron et al., 2001). αβ dimers associate head-to-tail to form protofilaments (Fig 1.6B). Protofilaments associate laterally to form a sheet which closes to form a 24 nm diameter hollow cylindrical microtubule consisting of 13 protofilaments. Subsequently, αβ dimers are added to and lost from microtubule ends; during growth, dimers add to the ends of two-dimensional sheets which close continuously to form the cylinder (Chretien et al., 1995), whilst during shrinkage/disassembly protofilaments lose lateral associations and curl into rings (Wade and Hyman, 1997). Microtubules do not reach equilibrium *in vivo*. They undergo both 'treadmilling', where αβ dimers are added to the plus end and lost from the minus end with no change in microtubule length, and 'dynamic instability', where microtubules convert between phases of assembly and rapid disassembly with no maintenance of length (Valiron et al., 2001).

In a similar manner to actin in microfilaments, αβ tubulin dimers have a uniform orientation within microtubules which provides them with polarity; β-tubulin is at the fast-growing plus end and α-tubulin at the slower-growing minus end (Figure 1.6B). The minus end is predominantly associated with the centrosome (microtubule organising centre (MTOC)) *in vivo*. The MTOC organises microtubule nucleation and contains the γ-tubulin ring complex, which consists of 13 molecules of γ-tubulin (Zheng et al., 1991, Wiese and Zheng, 2006). Lateral associations formed by GTP-bound γ-tubulin are stronger than those formed by GDP-bound αβ tubulin dimers in microtubules, perhaps explaining how γ-tubulin helps to nucleate and promote microtubule formation (Aldaz et al., 2005).

As discussed for actin microfilaments, microtubule dynamics can be regulated by microtubule-associated proteins (MAPs) *in vivo*, a number of which are themselves regulated by phosphorylation or calcium (for example through interactions with calmodulin) (Valiron et al., 2001). Microtubule-stabilising proteins include the neuron-specific tau and MAP1B, along with the more widely expressed MAP6 and MAP4, the latter of which also promotes tubulin polymerisation (Katsuki et al., 1999, Valiron et al.,

2001). Other proteins such as stathmin (Steinmetz et al., 2000) and the neuron-specific stathmin-2 destabilise microtubules (Valiron et al., 2001).

Other key proteins associated with microtubules are kinesin and dynein families of motor proteins. These use the energy from ATP to move cargo along microtubules in a direction determined by the microtubule polarity and motor protein; most kinesin family proteins move towards the plus end and therefore transport cargo towards the cell periphery, whilst dynein family proteins move towards the minus end and therefore the centre of the cell (Mallik and Gross, 2004).

1.2.2.1 Functions of Microtubules

Microtubules are involved in many cellular processes including protein trafficking and vesicular transport during endo- and exocytosis (Hehnly and Stamnes, 2007). They form the mitotic spindle and are therefore required for cell division and proliferation (Mitchison et al., 1986). Microtubules also form the specialised cell structures cilia and flagella and therefore function in cell motility (Mitchell, 2007). Motile cilia and flagella contain a central bundle of microtubules, called the axoneme, which consists of a central pair of single microtubules surrounded by nine microtubule doublets ('9 + 2'; Figure 1.6C).

1.2.2.1.1 Primary Cilia

Distinct from the motile cilia on mammalian multiciliated epithelial cells, single non-motile primary cilia are present on both epithelial and non-epithelial cell types; these primary cilia lack the central pair of microtubules in their axoneme ('9 + 0'; Figure 1.6C). The primary cilia on renal epithelial cells function as flow sensors; cilia bend passively with fluid flow and cause an increase in intracellular calcium concentration (Praetorius and Spring, 2001, Praetorius and Spring, 2003). Flow-induced calcium transients are reduced in ORPK (Oak Ridge Polycystic Kidney) mice, which lack the polaris protein required for cilia assembly (Liu et al., 2005). Endothelial cells lacking polycystin-2 in their primary cilium are unable to respond to increases in fluid shear stress (AbouAlaiwi et al., 2009), as are wild-type endothelial cells treated with colchicine to disrupt the connection of the cilium to the cytoplasm (Hierck et al., 2008). In bone cells, primary cilia were required for dynamic flow-induced increases in the osteogenic response of osteoblasts and decreases in the bone resorptive response of osteoclasts (Malone et al., 2007). Primary cilia are therefore suggested to function as

mechanosensory organelles in a number of different tissues. In connective tissues, primary cilia have been observed projecting into the ECM in growth plate cartilage, tendon, ligament, meniscus and annulus fibrosus of the intervertebral disc (Donnelly et al., 2008). Primary cilia are also observed on hyaline cartilage chondrocytes (Kouri et al., 1996, Jensen et al., 2004, Poole et al., 2001). The evidence for a role of the chondrocyte primary cilium in mechanotransduction in cartilage is discussed later (see section 1.4.2.1.5).

1.2.3 Intermediate Filaments

Intermediate filaments are so named because, with a diameter of 10 nm, they are intermediate in diameter between actin microfilaments and tubulin microtubules. Unlike the globular and nucleotide-binding actin and tubulin monomers, intermediate filament monomers are filamentous proteins that do not bind or hydrolyse nucleotides (Chang and Goldman, 2004). Over 70 genes encoding intermediate filament proteins have been identified in humans and these are divided into five classes based on amino acid sequence homology, assembly properties and tissue expression. The acidic and basic keratins, which form heteropolymer filaments in epithelial cells, are the type I and II intermediate filament proteins respectively. Type III intermediate filaments form homopolymer filaments and include vimentin, desmin and glial fibrillary acid protein (GFAP), whilst neurofilament proteins including NF-L, NF-M and NF-H are type IV intermediate filament proteins. Type V intermediate filament proteins are the nuclear lamins, lamin A/C, lamin B1 and lamin B2.

Cytoplasmic intermediate filament proteins have similar secondary structures, with a conserved, largely α-helical central rod domain flanked by non-α-helical N- (head) and C-terminal (tail) domains (Parry et al., 2007); the N- and C-terminal domains exhibit little homology and differ in size between intermediate filaments (Chang and Goldman, 2004). The characteristics of intermediate filament assembly are also conserved for the cytoplasmic intermediate filaments (Parry et al., 2007). The fibrillar monomers assemble in parallel to form a dimer with a 'coiled-coil' rod domain (Fig 1.7); dimers can be homo- or heterodimers depending on the intermediate filament type. Tetramers are formed from half-staggered, anti-parallel dimers and these associate laterally to form 'unit-length' filaments (ULF) with a length of approximately 55 nm. The number of polypeptides/monomers in the ULF varies with intermediate filament type. ULFs anneal

longitudinally in the elongation step to form immature intermediate filaments, which then undergo radial compaction to form mature intermediate filaments.

In contrast to microfilaments and microtubules, which exchange subunits at their ends only, intermediate filaments can exchange subunits or oligomers all along their length, making them highly dynamic in nature. Intermediate filament assembly and disassembly are regulated by phosphorylation and dephosphorylation events. Phosphorylation promotes disassembly of vimentin intermediate filaments into soluble tetramers, but also slows the rate of filament assembly; phosphorylation therefore affects the balance between filaments and disassembled subunits, along with the turnover of subunit exchange (Eriksson et al., 2004). Vimentin is phosphorylated on serine and threonine residues within the N- and C-terminal domains by kinases including PKA, PKC, ROCK (Eriksson et al., 2004) and PAK (Goto et al., 2002). As the N-terminal domain of vimentin intermediate filaments is involved in the interaction of filaments with the plasma membrane (Georgatos et al., 1985) in addition to intermediate filament formation (Beuttenmuller et al., 1994), phosphorylation of the head domain can also affect intermediate filament organisation.

Turnover and cytoplasmic organisation of vimentin filaments is partially dependant on microtubules and, to a lesser extent, actin microfilaments (reviewed by Chang and Goldman, 2004). In fibroblasts, microtubules recruit and co-localise with vimentin intermediate filaments (Gurland and Gundersen, 1995, Liao and Gundersen, 1998, Kreitzer et al., 1999) and expression of constitutively active Cdc42 or Rac1 causes vimentin intermediate filament reorganisation and perinuclear collapse (Meriane et al., 2000). In HeLa cells, Cdc42 induced vimentin filament collapse was associated with increased phosphorylation of vimentin at serine-72 by PAK and p70 S6 kinase (Chan et al., 2002). The association of intermediate filaments with both microfilaments and microtubules places them well to mediate cytoskeletal crosstalk (Chang and Goldman, 2004). For example, the collapse of vimentin intermediate filaments in HeLa cells, induced by microtubule disruption or RhoA/ROCK activation (which results in vimentin phosphorylation), results in the translocation of ROCK to the cell periphery and actin stress fibre formation (Sin et al., 1998).

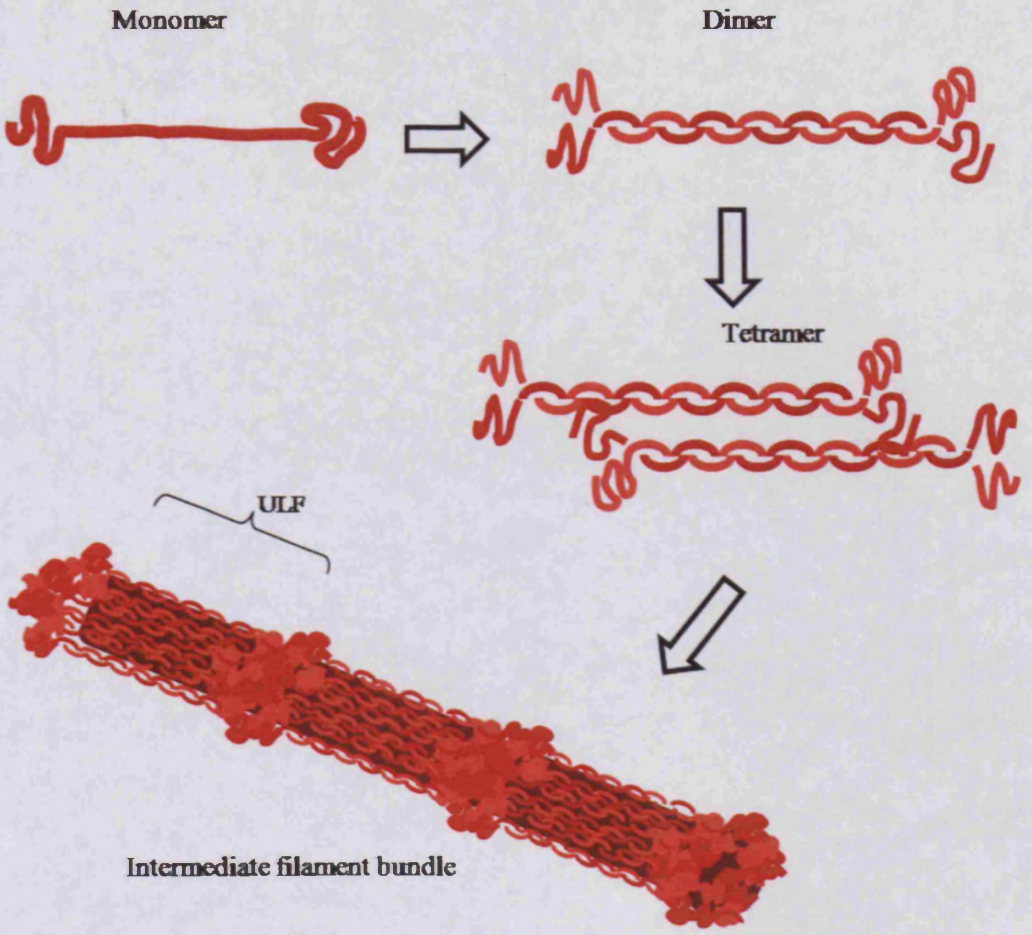

Figure 1.7:- A schematic of intermediate filament structure and assembly. Intermediate filament monomers associate in parallel to form a dimer with a 'coiled-coil' rod domain. Dimers then associate in parallel to form tetramers which associate laterally then longitudinally to form intermediate filaments. ULF- unit length filament. Adapted from Blain, 2009.

1.2.3.1 Functions of Intermediate Filaments

The principal role of intermediate filaments has long been thought to be structural in maintaining the mechanical integrity of cells and tissues (Eckes et al., 1998, Blain, 2009). They have been shown to be particularly important for the mechanical properties of cells under large deformation, increasing in stiffness with increasing strain applied (Wang and Stamenovic, 2000). However, in addition to mediating cytoskeletal crosstalk, intermediate filaments are believed to be important in signal transduction (Perlson et al., 2006). Vimentin is one of the predominant phosphoproteins *in vivo* (Blain, 2009) and intermediate filaments are suggested to function as a phosphate 'sink' or 'sponge' during cell signalling (Kim and Coulombe, 2007). In neurons, soluble vimentin associates with phosphorylated ERK1/2, preventing dephosphorylation i.e. deactivation and enabling translocation towards the nucleus (Perlson et al., 2005, Perlson et al., 2006). In synovial fibroblasts from rheumatoid arthritis patients, vimentin binds directly to p53 (Yang et al., 2005). Caspase-4 mediated cleavage of vimentin released p53 for translocation to the nucleus, where it promoted apoptosis in the fibroblasts.

1.2.4 The Chondrocyte Cytoskeleton

The chondrocyte cytoskeleton consists mainly of actin microfilaments, tubulin microtubules and vimentin intermediate filaments (Benjamin et al., 1994). In addition, some cytokeratins are present along with nuclear lamins.

1.2.4.1 Functions of the Cytoskeleton in Chondrocytes

Mature chondrocytes do not proliferate frequently under physiological conditions and they are trapped within their ECM and cannot migrate. The chondrocyte cytoskeleton therefore functions predominantly in maintaining cell phenotype and mechanical properties, aiding secretion of synthesised matrix molecules, forming cell–matrix interactions and in cell signalling (Blain, 2009). Changes in cytoskeletal organisation and cell shape result in changes in chondrocyte gene expression and the association between the cytoskeleton and phenotype is discussed further in sections 4.1 and 5.1. The Golgi complex interacts with the vimentin (Gao and Sztul, 2001) and tubulin (Vaughan, 2005) networks therefore synthesis and secretion of ECM molecules requires an intact chondrocyte cytoskeleton; disruption of microtubules (Lohmander et al., 1976, Takigawa et al., 1984) or vimentin intermediate filaments (Blain et al., 2006) inhibits the

synthesis and secretion of proteoglycans and collagen in chondrocytes. The cytoskeletal networks also regulate the compressibility and mechanical properties of chondrocytes and this is discussed in section 1.4.3.1. Through their role in cell–matrix interactions, the cytoskeletal elements can regulate the retention of the ECM by regulating the affinity of receptors, such as integrins (Critchley, 2009) and CD44 (Nofal and Knudson, 2002), for their ligands (see section 1.1.2.7). Cytoskeletal elements are also well placed to transduce mechanical signals from the ECM to the chondrocyte nucleus; see section 1.4.2.1.5 and 1.4.3.3 for evidence of a role of the chondrocyte tubulin and actin cytoskeletal networks in mechanotransduction.

1.2.4.2 Structural organisation of the chondrocyte cytoskeleton

Knowledge of the structural organisation of the chondrocyte cytoskeleton has advanced in recent years due to improvements in confocal microscopy and immunofluorescence techniques. The chondrocyte cytoskeleton has been characterised *in situ* in mature bovine articular cartilage, showing actin microfilaments to be predominantly cortical, with dense, punctate staining beneath the plasma membrane (Langelier et al., 2000). Tubulin microtubules and vimentin intermediate filaments have a filamentous structure, with dense networks extending throughout the cytoplasm. As would be expected, tubulin filament bundles appeared thicker than the vimentin filament bundles and exhibited a looser organisation than the tighter vimentin network (Langelier et al., 2000). Organisation of actin and vimentin networks in rat articular cartilage chondrocytes has also been observed *in situ*, with actin again predominantly located at the cell periphery and vimentin exhibiting a complex network throughout the cytoplasm (Durrant et al., 1999). In addition, actin staining at the cell surface was shown to co-localise with vinculin, a protein located in focal adhesions connecting the cells with the matrix. Visualisation of the cytoskeleton of human articular chondrocytes embedded in alginate hydrogel demonstrated a similar actin, tubulin and vimentin organisation to that described above (Trickey et al., 2004).

1.3 Osteoarthritis

Osteoarthritis (OA) is a condition which affects the articular cartilage of the synovial joints, often causing stiffness of the joints and pain. It represents an increasingly large problem to society, with more than one million GP consultations for OA every year (Arthritis Research UK. 2008). More than six million adults in the UK have painful OA in one or both knees and over 650,000 have painful OA in one or both hips. Musculoskeletal conditions including arthritis cost the UK around £5.7 billion per year, with 10 million working days lost in 2006/7 because of the conditions. (Arthritis Research UK. 2008).

1.3.1 Pathophysiology of Osteoarthritis

OA predominantly affects the hip and knee joints, although it is most prevalent in the joints of the hand. Clinically, OA initially presents as joint pain and stiffness, affecting joint mobility. As the disease progresses, symptoms worsen, ultimately resulting in disability, thus requiring the affected joint to be surgically replaced. Over 55,000 hip replacements and 65,000 knee replacements were performed in England and Wales in 2006/7, with a total hip replacement costing on average £7,350 (Arthritis Research UK, 2008). Physiologically, OA is characterised by degradation of the articular cartilage, causing fibrillation of the surface and cartilage thinning. However, OA does not only affect the articular cartilage, it affects the joint as a whole (Fig.1.8). Inflammation of the synovium and the joint capsule is the cause of joint swelling and stiffness, and osteophytes form on the subchondral bone.

1.3.1.1 Osteoarthritic Changes in Articular Cartilage

The changes that occur in osteoarthritic (OA) cartilage have been extensively characterised in the hope that a better understanding of the pathology would lead to identification of targets for therapy. Articular cartilage from human OA and animal models of OA (section 1.3.4) has been thoroughly investigated, from the structural and organisational level, through the biochemical, to the gene expression level.

1.3.1.1.1 Organisational and Extracellular Matrix Changes

Macroscopically, osteoarthritic lesions are evident as interruptions to the smooth, shiny appearance of normal articular cartilage. Lesions occurring at the early stages of the disease are small, increasing in size and depth with disease severity until exposure of the

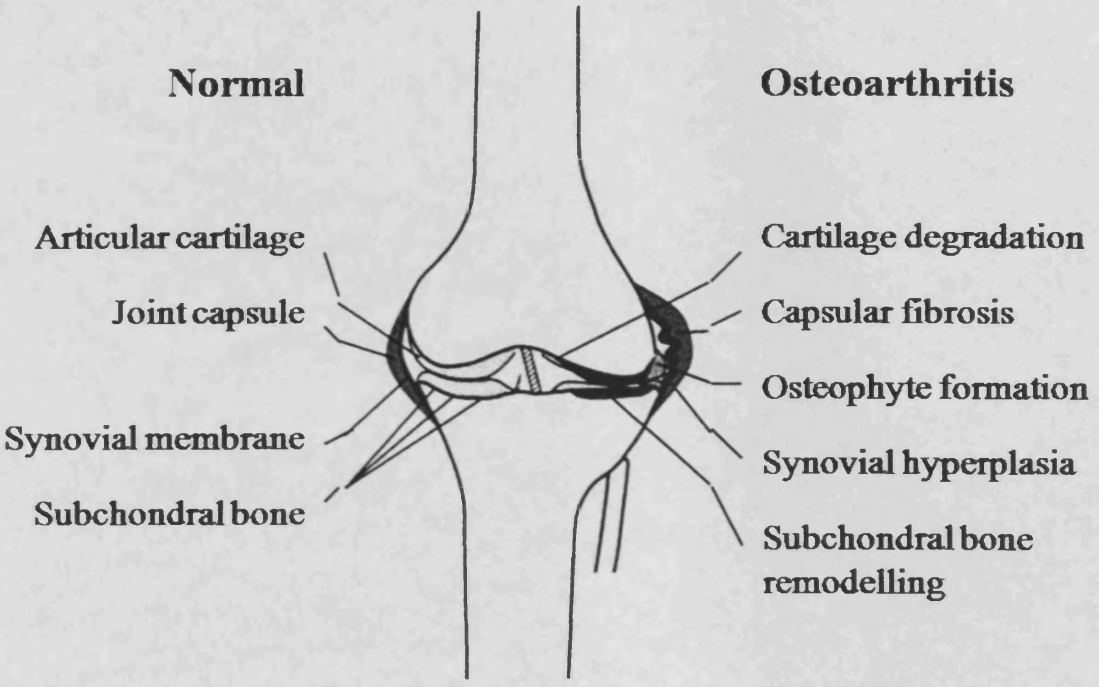

Figure 1.8:- A schematic representation of the main structures of a healthy knee joint and the changes observed in an osteoarthritic joint. Adapted from Aigner *et al.* (2006).

underlying subchondral bone. Systems have long been applied to attempt to quantify or 'grade' the changes occurring in articular cartilage with development of OA, indicating the stage and severity of the disease. In 1971, Mankin *et al* published a grading system of histological changes which correlated with the established biochemical changes; a histologic-histochemical grading system (Mankin et al., 1971). Using human femoral head articular cartilage and histological analysis, they scored regions using four categories and totalled the scores from each. Structure was assessed, ranging from normal (grade 0), through surface irregularities and clefts (also referred to as fissures) extending into the transitional then radial zone, to complete disorganisation (grade 6). The appearance of cells was scored as normal, diffuse hypercellularity, cloning, or hypocellularity. Staining of mucopolysaccarides (proteoglycans) was also scored, ranging from normal, through 'slight', 'moderate' and 'severe reduction', to 'no dye noted'. Finally, the integrity of the tidemark was assessed as either intact or crossed by blood vessels. An increasing severity of OA lesions scored in this way correlated with decreasing proteoglycan content and with increasing rate of proteoglycan and DNA synthesis, as assessed biochemically. The increase in proteoglycan synthesis but reduction in proteoglycan content supports the previously mentioned imbalance between anabolism and catabolism, which is characteristic of osteoarthritis. Mankin *et al* also noted a point in OA progression at which the articular cartilage 'fails'; around grade 10 the rates of proteoglycan and DNA synthesis plateau and begin to decrease, the cartilage no longer showing a 'repair response'.

The heterogeneous nature of OA means that differences in organisation and matrix composition also occur over the surface of a single joint. Comparison of visually intact regions with disrupted regions of OA articular cartilage showed increased fibrillation and decreased glycosaminoglycan content. Chondrocyte 'cloning' (scored using the number of clusters containing more than four cells and their location) was increased in disrupted regions when compared with visually intact regions, although no increase in total cell number was observed (Yagi et al., 2005, Kouri et al., 1996). The concept of increased chondrocyte cloning with OA progression has been questioned recently. As there is no increase in total cell number and many chondrocytes with cilia or filipodia have been observed, it has been proposed that the increase in chondrocyte clusters is due to chondrocyte migration in OA (Kouri et al., 1996, Kouri et al., 1998).

The synthesis, composition, size, and degradation of proteoglycan are altered in osteoarthritis. In the early stages of OA (Mankin grades 2-6) there is a general degradation of proteoglycans combined with replacement with new molecules of altered composition. Molecule size decreases, as does the hyaluronan content of cartilage, and there is an increase in chondroitin-4-sulphate glycosaminoglycan chains and foetal-common epitopes (Rizkalla et al., 1992). There is then extensive replacement of degraded molecules with larger, compositionally different proteoglycans in the later stages of OA (Mankin grades 7-13), as indicated by increased rates of synthesis (Mankin et al., 1971). Hyaluronan content decreases along with chondroitin-6-sulphate and keratan sulphate glycoaminoglycans, whilst chondroitin-4-sulphate and foetal-common epitopes continue to increase (Rizkalla et al., 1992).

Changes in the extracellular matrix with disease progression result in the organisational changes described which contribute to the mechanical failure of the articular cartilage. The orientation and integrity of collagen fibres have been shown to alter in an *in vivo* model of OA (Pond-Nuki dog model of OA- see section 1.3.4), initiating in the pericellular matrix. A decrease in the amount and diameter of collagen fibres was apparent two weeks after induction of OA, along with a change in orientation (Pelletier et al., 1983a). Small angle X-ray scattering showed differences in collagen fibre orientation between normal and OA articular cartilage in naturally occurring equine osteoarthritis. The degree to which normal organisation was disrupted increased with severity of OA lesions (Moger et al., 2007). The same was true of human articular cartilage when analysed using small-angle X-ray diffraction. Collagen fibres of the deeper layers of osteoarthritic tissue were reoriented in regions of cartilage damage, no longer showing the vertical orientation seen in normal cartilage (Mollenhauer et al., 2003). Cleavage of type II collagen is increased in human OA. The pericellular cleavage in the deep zone of normal cartilage is increased in OA cartilage, along with the appearance of both territorial and interteritorial type II collagen cleavage in superficial and mid-zones (Dodge and Poole, 1989). Disruption of the collagen matrix is characteristic of OA and leads to further degeneration of the cartilage and mechanical failure of the tissue, with a reduction in compressive stiffness correlated with extracellular matrix integrity (i.e. a disruption of the collagen network) (Franz et al., 2001).

1.3.1.1.2 Changes in the Chondrocyte Phenotype

Once it was realised that the organisational and biochemical changes described above were predominantly a result of proteins secreted by the chondrocyte rather than proteins from other sources such as the synovial fluid or synovium, investigation of the chondrocyte phenotype became more extensive. The balance of synthesis and degradation of the matrix is controlled by the chondrocyte. This balance is essential in maintaining the function of articular cartilage. An imbalance and shift towards a catabolic phenotype, as occurs in OA (reviewed by (Goldring, 2000)), ultimately results in degradation of the articular cartilage and failure of the joint.

Knowledge of the proteins expressed by normal and osteoarthritic chondrocytes has increased recently with the use of proteomics and mass spectrometry. Osteoarthritic cartilage explants in culture secreted proteins including collagens II, VI and XI, COMP, fibronectin, cartilage glycoprotein 39, MMPs-1, -2, and -3, TIMPs-1 and -2, and CTGF (connective tissue growth factor) (Hermansson et al., 2004, Garcia et al., 2006). Comparison of proteins secreted by normal and osteoarthritic cartilage revealed increased synthesis of type II collagen in OA cartilage. A proteomic profile of osteoarthritic articular cartilage has identified over 100 proteins involved in extracellular matrix organisation, signal transduction and cell communication, immune response and metabolism, although no comparisons were made with normal cartilage (Garcia et al., 2006). Comparisons have been made between proteins expressed by normal and osteoarthritic chondrocytes following isolation from articular cartilage and culture in either monolayer (Ruiz-Romero et al., 2008) or in alginate (Lambrecht et al., 2008). In monolayer cultured primary human chondrocytes, 28 proteins were identified as being differentially regulated in OA; 19 were increased and nine were decreased in OA compared to normal. Proteins involved in the cellular response to stress were increased in OA whilst those involved in glycolysis were decreased (Ruiz-Romero et al., 2008). In alginate, proteins in chondrocytes from visually intact and damaged OA cartilage were compared to each other and to normal chondrocytes, using 2D-electrophoresis and mass spectrometry (Lambrecht et al., 2008). 16 proteins were identified as being increased in OA chondrocytes compared to normal and seven of these were also increased in chondrocytes from visually intact OA cartilage. Eight proteins were identified as being decreased in OA chondrocytes compared to normal and seven of these were also

decreased in chondrocytes from visually intact OA cartilage. In this case, differentially expressed intracellular proteins were involved in metabolic and apoptotic pathways and in the oxidative stress response (Lambrecht et al., 2008).

Gene expression analysis of normal and osteoarthritic chondrocytes has also been extensive, predominantly focusing on expression of genes for extracellular matrix molecules. Type II collagen mRNA expression is often increased in OA cartilage compared to normal (Martin et al., 2001, Gebhard et al., 2003, Aigner et al., 2006a). Other studies have found no significant difference in expression or no correlation with histological or clinical OA grade, due to the large variability associated with human samples (Yagi et al., 2005, Eid et al., 2006). Expression of types V, VI, IX, XI and XV collagen is also increased in OA cartilage compared to normal (Aigner et al., 2006a). The increased expression of types I and III collagen and type X collagen in OA cartilage has been attributed to dedifferentiation and hypertrophy, respectively. This concept has recently been challenged; as ratios of collagens I, III and X expression to that of collagen II showed no difference between normal and OA cartilage, it is argued that the increased expression is due to a general increase in anabolism rather than a shift in chondrocyte phenotype (Gebhard et al., 2003). In contrast, a comparison of normal and OA cartilage, showing increased expression of collagen I and significantly increased expression of collagen II in OA, found that the ratio of collagen II expression to that of collagen I was significantly decreased in OA (Martin et al., 2001).

The expression of non-collagenous matrix molecules has also been shown to change in osteoarthritis. Fibronectin, fibromodulin, tenasin C, CILP and osteonectin expression are increased in OA (Aigner et al., 2006a), as is osteopontin mRNA expression (Yagi et al., 2005, Martin et al., 2001). Results regarding aggrecan expression in OA vary. Intra-joint comparisons have shown decreased expression of aggrecan in advanced OA regions compared to early OA regions of cartilage (Yagi et al., 2005) and an inverse correlation of aggrecan expression with increasing OA severity (Eid et al., 2006). In support of this, another study has shown decreased aggrecan expression in OA cartilage, but with no difference between advanced and minimal OA regions (Brew et al., 2010b). Other comparisons of normal and OA cartilage have shown no difference in aggrecan expression (Aigner et al., 2006a, Martin et al., 2001).

Expression of the transcription factor SOX9, a marker of the chondrocyte phenotype, is decreased in OA cartilage compared to normal (Brew et al., 2010b, Aigner et al., 2003, Aigner et al., 2006a). In support of proteomic studies, discussed above, a comparison of gene expression in normal and OA cartilage using cDNA arrays revealed decreased expression of genes involved in the response to oxidative stress, including superoxide dismutase 2 and thioredoxin-interacting protein (Aigner et al., 2006a).

The importance of the balance between matrix synthesis and degradation is indicated by the imbalance present in OA cartilage. An increase in MMP is observed that is not sufficiently matched by the increase in TIMPs, ultimately resulting in degradation and progression of OA (Dean et al., 1989). In human late stage OA cartilage, expression of the aggrecanases ADAMTS-4 and -5 is increased compared to normal and early stage OA, whilst expression of MMP-3, which also degrades aggrecan, is decreased (Bau et al., 2002). MMP-3 mRNA expression was again shown to be decreased in OA cartilage when compared with normal, and in contrast to the above study, ADAMTS-5 expression was also reduced in OA (Kevorkian et al., 2004). The same study showed decreased expression of MMP-1, TIMP-1 and TIMP-4, but increased expression of MMP-2, -9 and -13 and TIMP-3. Another study has shown no difference in MMP-1 and MMP-14 expression between normal and OA cartilage, but MMP-13 (collagenase 3) expression has been shown to be increased in OA cartilage (Bau et al., 2002, Brew et al., 2010b). Intra-joint comparisons showed no difference in expression of MMP-3, -9, or -13 (Yagi et al., 2005).

1.3.2 Pathogenesis of Osteoarthritis

Degradation and thinning of the articular cartilage observed in OA is brought about by an imbalance in homeostasis, with breakdown of articular cartilage components ultimately exceeding their synthesis. OA is a multi-factorial disorder but can generally be split into two broad classes, primar y OA and secondary OA, depending on the apparent causes.

1.3.2.1 Risk Factors for development of Osteoarthritis

The occurrence of OA increases with age and this late-onset form of the disease is known as primary OA. Age and gender contribute to its development, with knee and hand OA more prevalent in females (Blagojevic et al., 2010). However, OA should not be considered simply a disease of old-age, as not everyone will develop OA as they age.

and function of the articular cartilage. Hyaluronic acid can be administered by intra-articular injection to help restore some of the fluid properties of the cartilage ECM, acting through its role in forming large, hydrophilic aggregates in the cartilage. Intra-articular injections of sodium hyaluronate improve the clinical symptoms of pain and inflammation but have also been shown to reduce levels of MMP-9 in the synovial fluid (Shimizu et al., 2010). The low incidence of adverse side effects is also an advantage over NSAIDs (Brzusek and Petron, 2008). Glucosamine and chondroitin sulphate are used as dietary supplements for some OA sufferers, with glucosamine suggested to stimulate chondrocytes to synthesise proteoglycans and collagen, and chondroitin sulphate able to competitively inhibit degradative enzymes. These have the potential to both increase synthesis of the ECM and reduce its degradation, both of which are key characteristics of OA pathogenesis. Administered in combination, these supplements have been shown to produce a greater improvement in knee pain in sufferers of OA than when used individually (Clegg et al., 2006). Other studies have demonstrated some clinical effectiveness of glucosamine sulphate in the treatment of OA (Black et al., 2009). There is however, controversy over the effectiveness of this 'matrix enhancement therapy'; hence they require further unbiased, large-scale clinical trials of commercially available formulations (Hochberg, 2006). For example, one study has shown that intra-articular injection of sodium hyaluronate demonstrated no advantage over physical exercise in reducing the clinical symptoms of knee OA (Kawasaki et al., 2009).

Non-pharmaceutical interventions include regular exercise and weight loss. As overweight sufferers are continuously subjecting weight-bearing joints such as the hip and the knee to higher mechanical loads than normal, weight loss can reduce the mechanical insult to joints during regular activities, such as walking, and help to improve mobility. Exercise will aid weight loss where it is required, although it has other advantages to OA sufferers; it can develop muscle tone which helps to support the joint, improving joint mobility and controlling the load received by a joint more effectively. One study has shown improvement in pain and physical function in hip or knee OA sufferers following six weeks of treatment with glucosamine sulphate and a further improvement with the introduction of a walking regime (Ng et al., 2010). Regular moderate exercise alone has been shown to improve the glycosaminoglycan (GAG) content of knee articular cartilage in middle-aged people at high risk of developing OA (Roos and Dahlberg, 2005). However, the long-term effects were not studied, nor can

A number of genetic linkage analyses and genome-wide association studies have searched for a genetic susceptibility to OA (Loughlin, 2003, Valdes and Spector, 2010); genes associated with OA include factors involved in the bone morphogenic protein (BMP) or Wnt signalling pathways, apoptotic pathways and inflammation. In addition to age and genetics, there are four main non-heritable risk factors for developing OA; congenital abnormalities, trauma, obesity, and occupation, all four of which are risk factors for development of the other class of OA: secondary OA. Population-based studies have confirmed that the risk of developing knee OA is strongly associated with body mass index (i.e. obesity), previous knee injury or heavy physical stress at work (Blagojevic et al., 2010, Toivanen et al., 2010). Secondary OA tends to develop at a relatively young age, and causes relate to loading of the joint. Increased loading of a joint, whether due to obesity, environmental factors such as an occupation involving a large amount of bending, or impact trauma direct to the cartilage (e.g. sports injuries), can result in the development of OA. Abnormal loading of a joint can also contribute to OA; for example, that caused by congenital defects allowing dislocation, or by impact trauma which disrupts supporting ligaments and results in joint misalignment.

The number of people suffering from OA has increased in the last ten years and will likely continue to do so. This is due to two of its main risk factors- age and obesity. As the population is ageing, more people living over the age of 65 will mean that the occurrence of OA will increase. In addition to this, the prevalence of obesity is increasing in the UK. Besides the other health problems associated with obesity, it is a primary risk factor for development of knee OA. This increase in the number of overweight individuals is likely to result in an increase in the number of young and middle-aged adults suffering from OA. For these reasons, it is becoming increasingly important to find effective treatments for the disease.

1.3.3 Therapeutic Strategies for Osteoarthritis

Currently there is no 'cure' for OA and no disease-modifying drug; current pharmaceutical treatments focus on relieving symptoms such as pain and inflammation. Non-steroidal anti-inflammatory drugs (NSAIDs) can be used to treat the pain and inflammation that often occurs in osteoarthritic joints, but these have no effect on the progression of cartilage degradation. The use of 'chondroprotective' agents has recently emerged and rapidly gained ground due to their potential to improve the composition

the improvements observed be applied to other groups, such as those with early- or late-stage OA (Roos and Dahlberg, 2005).

The treatment of OA symptoms gives some comfort to the sufferer and can moderately and temporarily improve joint function. Nevertheless, as there are no treatments which have been shown to sufficiently repair cartilage defects or alter chondrocyte phenotype, degradation of the cartilage continues, leading to severe disability which can only be treated through surgical replacement of the joint.

Radiography is the technique currently used to determine the presence of OA in a joint (Fig 1.9). The extent of OA in a joint is graded, taking into account the degree of osteophyte formation and joint space narrowing, an indication of thinning of the articular cartilage. The sensitivity of radiography means it is not capable of detecting early OA changes, only detecting changes after the cartilage has thinned and/or osteophytes have formed. The use of magnetic resonance imaging (MRI) is increasing due to its ability to provide clear and detailed imaging of intra-articular structures, including articular cartilage, menisci, and ligaments (Fig 1.10). The more water present in a tissue, the whiter it appears on MRI images. The greater detail of MRI images indicates its potential to detect early-stage OA, thus providing an earlier diagnosis and an opportunity for pharmacological intervention before degradation progresses.

1.3.4 Experimental Models of Osteoarthritis

In vivo studies have shown abnormal loading results in changes to the cartilage similar to those seen in OA. The Pond-Nuki dog model induces OA by producing joint laxity through transection of the anterior cruciate ligament in the knee (Pond and Nuki, 1973) which leads to abnormal loading of the knee as the dog exercises post-surgery. Changes in the joint are indistinguishable from naturally occurring secondary OA (McDevitt et al., 1977), with osteophyte formation just two weeks after the operation and thickening of the joint capsule after three weeks (Pelletier et al., 1983a, McDevitt et al., 1977). Increased thickness and vascularity of the synovial membrane was observed after two weeks and damage to the meniscus, initially surface splitting which progressed to tearing, was also observed, most often on the medial meniscus. Changes in articular cartilage included increased water content accompanied by increased cartilage thickness,

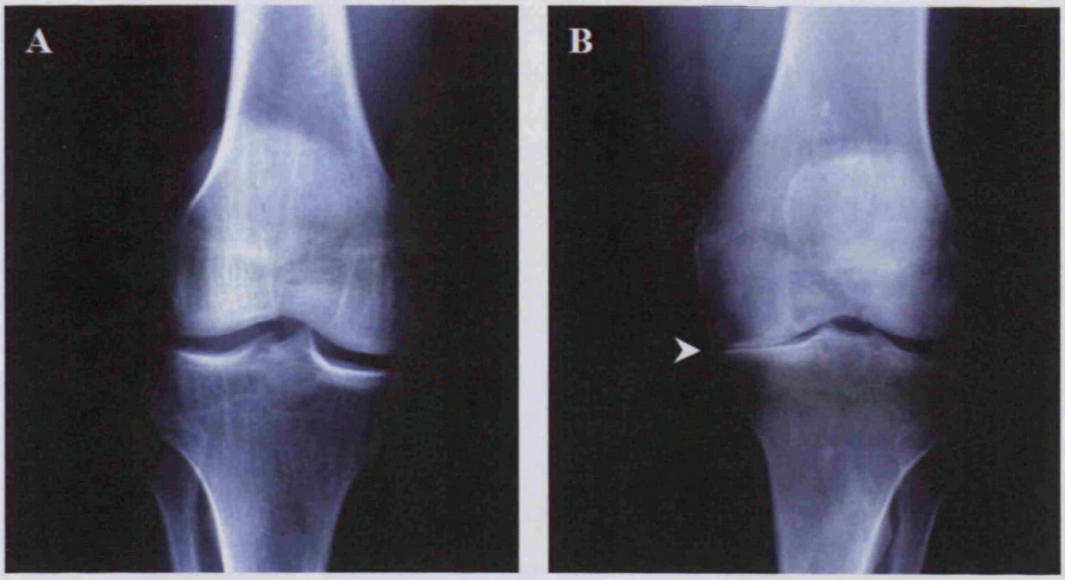

Figure 1.9:- Radiographic images of a normal (A) and an osteoarthritic knee joint requiring total knee replacement surgery (B). Joint space narrowing (white arrow head) indicates a severe loss of articular cartilage. Images are from meded.ucsd.edu/clinicalmed/joints.htm

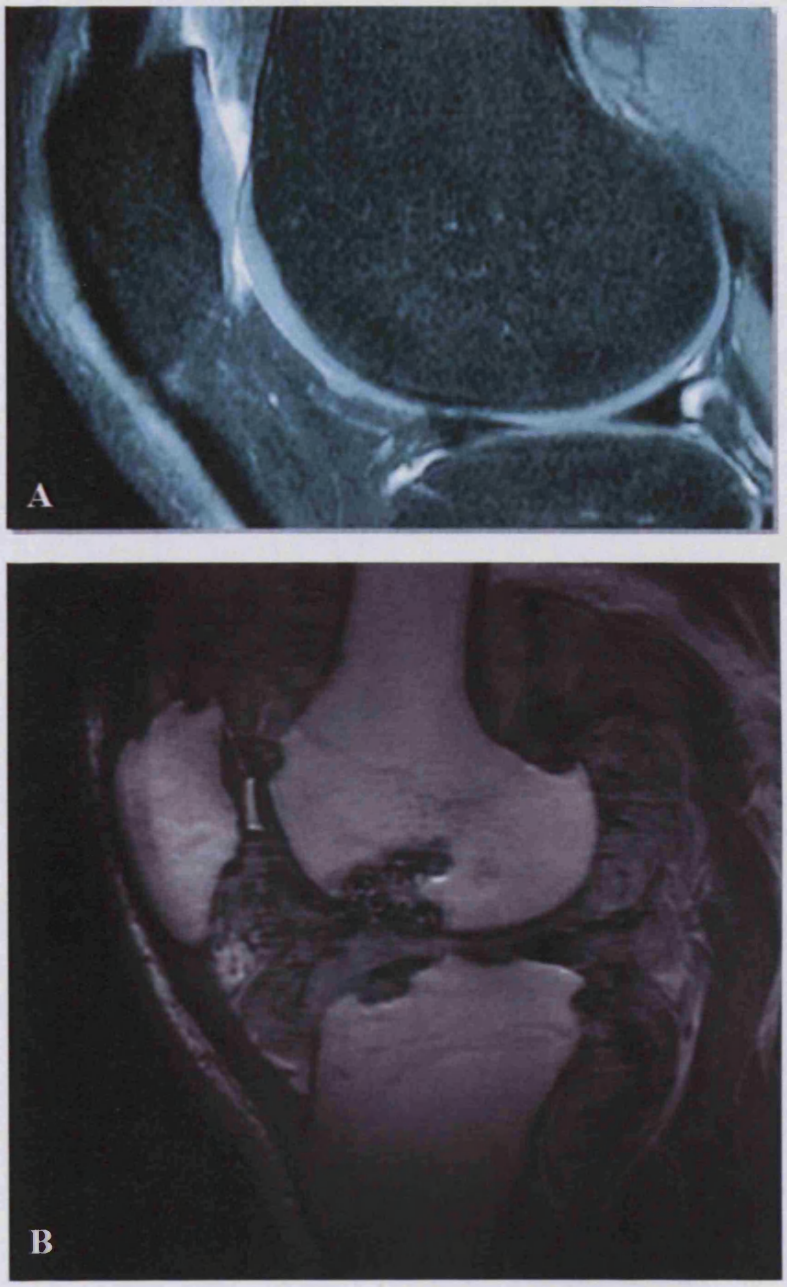

Figure 1.10:- Images of the knee joint, taken using Magnetic Resonance Imaging (MRI). **A**- A healthy knee joint. The articular cartilage can be seen clearly, protecting the ends of the long bones (image from www.kneeclinic.info/knee_imaging.php) **B**- A knee joint requiring total knee replacement due to the severe degradation of the articular cartilage, symptomatic of end-stage osteoarthritis (image used with kind permission of Dr. Hechmi Toumi, Department of Orthopedics, Llandough Hospital, Penlan Road, Llandough. CF64 2XX.).

except in regions of fibrillation (McDevitt and Muir, 1976), and loss of proteoglycans in the superficial zone. Lesions on the cartilage progressed in severity and size with time after surgery, although this was notably more progressive and severe in the region of the medial tibial condyle not covered by the medial meniscus (McDevitt et al., 1977). The same is true for naturally occurring OA, indicating that regions experiencing higher mechanical loads become more severely damaged (Thambyah et al., 2006). Microscopic examination revealed an increase in cell density and number of clones (i.e. lacunae containing two or more nuclei) progressively with time after surgery, again with differences most pronounced in the region experiencing higher mechanical loads (McDevitt et al., 1977, Pelletier et al., 1983a). After 16 weeks, the tissue was microscopically indistinguishable from naturally occurring OA. Collagenolytic activity in articular cartilage also increased in this model, detectable after two weeks and peaking at four weeks post-surgery due to an increase in latent enzyme (Pelletier et al., 1983a). The structure of the collagen network altered after two weeks, with an initial decrease in the number, diameter, and orientation of the fibres which were parallel to the articular surface and no longer to the cell membrane. After eight weeks, fibres were of smaller diameter, fragmented, and orientated parallel to clefts and tears in the cartilage (Pelletier et al., 1983a). Therefore the increased water content observed is likely due to disruption of the collagen network, which becomes less effective in opposing the swelling pressure produced by the proteoglycans (Maroudas, 1976).

Following this early model (Pond and Nuki, 1973), surgical induction of OA through establishment of joint instability has been used in a number of mammalian species to provide models of the disease; joint instability is induced either through transection of the anterior cruciate ligament, as in the Pond-Nuki dog model, or through partial or complete meniscectomy (removal of the meniscus) (van den Berg, 2001, Capin-Gutierrez et al., 2004). Other models include animals that spontaneously develop OA-like cartilage degeneration with ageing, such as the STR/ort mouse (Walton, 1977, Mason et al., 2001), or transgenic models in which expression of cartilage matrix proteins or degrading enzymes are manipulated (van den Berg, 2001). Examples of the latter include mice lacking α1(IX) collagen (Fassler et al., 1994) or α1 integrin (Zemmyo et al., 2003), and mice with hyaline cartilage-specific postnatal expression of constitutively active MMP-13 (Neuhold et al., 2001), all of which develop degenerative joint disease resembling human OA.

1.4 Mechanical Load

Load has long been hypothesised as a key mediator in the development of OA. It is a major element in all of the risk factors associated with the development of secondary OA (section 1.3.2.1). This is supported by observations that regions of fibrillation, known as OA lesions, most often occur at weight-bearing regions of the articular cartilage. In addition to clinical and surgical observations, a number of studies have implicated load as a mediator of cartilage turnover. Changes in joint loading patterns have been induced experimentally, both *in vivo* and *in vitro*, and the results demonstrate a clear role of load in the regulation of chondrocyte phenotype.

1.4.1 Load and Chondrocyte Phenotype

1.4.1.1 In vivo *Studies*

Previous studies have shown that physiological loading of a joint is required for the maintenance of healthy cartilage, as demonstrated by *in vivo* immobilisation studies. Immobilisation of the right hind limb of mature canines (at 90° flexion of hip and knee joints) using a cast resulted in a decrease in proteoglycan synthesis, initially apparent after just six days of joint immobilisation (Palmoski et al., 1979). This was accompanied by an increase in cartilage water content and a decrease in cartilage thickness after three weeks of joint immobilisation. However, the changes were reversible, with proteoglycan synthesis comparable to control levels one week after removal of the cast, water content after two weeks, and cartilage thickness four weeks following removal of the cast (Palmoski et al., 1979). The changes observed were subsequently proven to be due to the absence of normal loading rather than the absence of joint motion (Palmoski et al., 1980). Transection of the ipsilateral paw, preventing loading of a canine knee whilst still allowing for its normal motion, showed changes in cartilage morphology after six weeks without load that were identical to the effects observed after immobilisation: increased water content, decreased cartilage thickness, and decreased proteoglycan synthesis and content (Palmoski et al., 1980). These studies show clearly that load is required to maintain a normal cartilage organisation and therefore function.

However, this applies only to physiological loading of a joint, as other *in vivo* studies have shown abnormal loading results in changes to the cartilage similar to those observed in OA (for changes in the cartilage with OA, see section 1.3.1.1). A number of the animal models of OA described in section 1.3.4 induce abnormal loading of a joint to

promote OA-like phenotypic changes in the cartilage and chondrocytes. The Pond-Nuki dog model induces OA by producing joint laxity through severing of the anterior cruciate ligament (Pond and Nuki, 1973) which leads to abnormal loading of the knee as the dog exercises post-surgery. The subsequent changes in the joint are indistinguishable from naturally occurring secondary OA (McDevitt et al., 1977). Cartilage lesions were notably more progressive and severe in the region of the medial tibial condyle not covered by the medial meniscus. The same is true for naturally occurring OA, indicating that regions experiencing higher mechanical loads become more severely damaged (Thambyah et al., 2006). With regards to a more direct effect of load on chondrocyte phenotype, collagenolytic activity increases in the Pond-Nuki model of OA, detectable after two weeks and peaking at four weeks post-surgery due to an increase in latent enzyme (Pelletier et al., 1983a).

Of note here is a more recent trial investigating the effects of exercise on human knee cartilage, using subjects at risk of OA due to previous meniscectomy (Roos and Dahlberg, 2005). Using delayed gadolinium-enhanced magnetic resonance imaging of cartilage (dGEMRIC) to assess the GAG content of cartilage *in vivo*, the study found that an increase in moderate exercise led to a dose-dependent increase in GAG content as there was a correlation with the self-reported physical activity level. A reduction in pain and improved joint function were also reported.

The complexity of the role of load in articular cartilage turnover is evident. Physiological loading of the joint is required to maintain healthy cartilage, abnormal or over-loading results in cartilage damage and an OA phenotype, whilst moderate exercising of joints at risk of OA prove potentially beneficial. *In vitro* studies have attempted to better characterise the effects of load on articular cartilage.

1.4.1.2 Ex vivo *Cartilage Explants*

Numerous *in vitro* models have been used to monitor the effects of mechanical load on articular cartilage. The different conditions used can make it difficult to directly compare results, as there are variations in the magnitude and frequency of loads applied, including a single impact load (Jeffrey et al., 1997) or compressive loads which are either static (Palmoski and Brandt, 1984) or cyclic (Palmoski and Brandt, 1984, Steinmeyer and Knue, 1997, Blain et al., 2001), each with varying peak loads and

duration. In general, static loads induce catabolic changes whilst cyclic loading is anabolic. As might be expected, increased damage to cartilage correlates with higher peak stress and strain rates, and increasing duration of loading (Kurz et al., 2005); these studies do confirm the ability of load to alter articular cartilage properties and chondrocyte gene expression (reviewed by Kurz et al. 2005).

The mechanical integrity of articular cartilage is disrupted by impact load, as indicated by the significant loss of matrix protein observed over a two week period after a single impact load to articular cartilage (Jeffrey et al., 1997). This was accompanied by a loss of GAG which increased with the severity of impact. Regulation of GAG synthesis and release are also observed following both static and cyclic compressive loading. In adult canine articular cartilage, static compressive loading for two hours suppressed GAG synthesis, as did prolonged cyclic compressive loading (one minute on /one minute off) showing a linear decrease with duration (Palmoski and Brandt, 1984). An increase in the frequency of cyclic loading (four seconds on/11 seconds off) decreased the inhibitory effects of a given load and, at the lower stresses, became stimulatory to increase GAG synthesis (Palmoski and Brandt, 1984). Mature bovine articular cartilage also showed a decrease in proteoglycan synthesis in response to cyclic compressive load (0.1–5.0 MPa) at 1 Hz, with a decrease in frequency of loading inhibiting the decrease in synthesis observed at a given load (Steinmeyer and Knue, 1997). Proteoglycan biosynthesis decreased with increasing load magnitude and duration (one to six days), whilst proteoglycan release increased with load magnitude but decreased with increasing duration. Loss of GAGs from articular cartilage will reduce the mechanical integrity of the tissue and an initial release is suggested to be due to direct mechanical damage rather than an increase in proteolysis (Kurz et al., 2005). This GAG loss could also be due to damage to the collagen network, allowing tissue swelling and diffuse GAG loss (Kurz et al., 2005). The observation that injurious compression of young bovine articular cartilage causes mechanical failure of the tissue, accompanied by an abrupt decrease in the tensile load-carrying capacity of the collagen matrix implies that certain loads can directly damage collagen networks (Quinn et al., 1998).

The modulation of GAG biosynthesis by load indicates that mechanical stress has an effect on chondrocytes as well as on the matrix. There is much evidence supporting this, with load shown to alter chondrocyte gene expression and morphology. A physiological

level of cyclic compressive load has been shown to increase *COL2A1* and aggrecan mRNA levels (Blain, 2002), along with increasing matrix metalloproteinase expression and activation in bovine articular cartilage explants (Blain et al., 2001). Increases in both latent and active forms of MMP-2 and -9 were detectable after three hours of loading. No change in response to load was detectable in the levels of TIMPs, inferring that load can alter cartilage homeostasis, increasing matrix turnover and possibly shifting it towards a catabolic phenotype.

In addition to phenotypic changes, the ultrastructure of chondrocytes can be altered by mechanical load. In response to continuous high hydrostatic pressure applied for three hours *in vitro*, normal human chondrocyte ultrastructure becomes similar to the morphology of unloaded OA chondrocytes, with a significant reduction in the number of mitochondria and Golgi bodies (Fioravanti et al., 2005). Lower, cyclical hydrostatic pressure applied to the same model failed to alter normal chondrocyte morphology in three hours (Fioravanti et al., 2003). However this loading regime significantly increased the number of mitochondria and Golgi bodies present in OA chondrocytes resulting in a morphology comparable to normal. The effects of load on chondrocyte ultrastructure thus parallel the effects on chondrocyte phenotype and matrix metabolism, with cyclic loads of lower magnitude inducing anabolic changes and high magnitude, static loads inducing catabolic changes.

Of note here is that the age and maturation of cartilage appears to affect the response of the tissue to load. Compared to immature bovine tissue, mature cartilage shows less apoptosis and GAG loss in response to mechanical injury (Kurz et al., 2005). Mechanical injury also has less effect on biosynthetic activity in mature cartilage, although mature cartilage exhibits a stronger response to peak stress. Peak stresses in cartilage during compression increase with tissue maturation (Kurz et al., 2005), therefore the different mechanical properties of young and old cartilage could contribute to the different responses to mechanical load.

1.4.2 Mechanotransduction in Chondrocytes

It is clear from the studies mentioned above, that load can alter gene expression in the chondrocyte. The mechanism(s) by which load is sensed and the signal(s) propagated to

the nucleus, termed "mechanotransduction", has not been fully characterised in chondrocytes but current knowledge is summarised below.

1.4.2.1 Cell Surface Mechanosensors

1.4.2.1.1 Mechanosensitive Ion Channels

Cyclic pressure-induced strain causes membrane hyperpolarisation in human chondrocytes in monolayer (Wright et al., 1996). This strain-induced hyperpolarisation is inhibited by the stretch activated ion channel blockers gadolinium and amiloride, the small conductance calcium-activated potassium channel blocker apamin, or the L-type calcium channel blocker nifedipine. In addition, depletion of extracellular calcium by chelation reduced the hyperpolarisation response to pressure-induced strain (Wright et al., 1996). The potassium channel blocker 4-aminopyridine inhibits dynamic compression-induced increases in sGAG synthesis (Mouw et al., 2007) and apamin inhibits membrane hyperpolarisation in normal human chondrocytes induced by exogenous ATP (Millward-Sadler et al., 2004). Cyclic mechanical stretch-induced increases in chondrocyte proliferation were abrogated by the L-type calcium channel blocker nifedipine, which also prevented stretch-induced up-regulation of cartilage matrix protein expression (Lee et al., 2000). Nifedipine treatment also prevented increased sGAG synthesis induced by dynamic compression of bovine chondrocytes in agarose (Mouw et al., 2007). Tyrosine phosphorylation of FAK, β-catenin and paxillin, up-regulation of aggrecan and down-regulation of MMP-3 expression in response to cyclic pressure-induced strain were inhibited by blocking stretch activated ion channels with gadolinium (Lee et al., 2000, Millward-Sadler et al., 2000a). In addition, gadolinium abolished increases in proliferation in response to cyclic mechanical stretching of chondrocytes in 3D collagen scaffolds (Wu and Chen, 2000). Stretch activated ion channels are also suggested to maintain chondrocyte phenotype independently of mechanical stimulation (Perkins et al., 2005). Gadolinium treatment induced dedifferentiation of rat chondrosarcoma cells and primary human chondrocytes in monolayer, as indicated by increased actin stress fibre formation and type I collagen and fibronectin expression; concomitant decreases in aggrecan and type II collagen expression were also observed. Removal of gadolinium from the culture media reversed the dedifferentiation.

1.4.2.1.2 Integrins

As chondrocytes are surrounded by a pericellular matrix and lack cell-cell contacts in an avascular and aneural tissue, integrins are important for the transduction of signals from the extracellular matrix to effect intracellular changes. As discussed in section 1.1.2.7.1 chondrocytes express a number of different combinations of integrin αβ heterodimers and their expression can alter with development or OA progression. In human articular chondrocytes cultured in monolayer, the extent of membrane hyperpolarisation induced by cyclic pressure-induced strain was reduced by inhibition of α5β1 integrins (Wright et al., 1997). In addition to reducing the electrophysiological response to strain, blocking integrins with RGD-containing peptides inhibited downstream signalling, including strain-induced up-regulation of aggrecan, down-regulation of *MMP3* expression (Millward-Sadler et al., 2000a) and tyrosine phosphorylation of FAK, β-catenin and paxillin (Lee et al., 2000). The integrin associated protein CD47 is expressed by normal and OA chondrocytes and directly binds to α5 integrin (Orazizadeh et al., 2008). Antibodies blocking CD47 function prevented changes in membrane potential, tyrosine phosphorylation and aggrecan expression induced by cyclic mechanical stimulation of chondrocytes (Orazizadeh et al., 2008). Using this model, IL-4 was identified as a soluble mediator released into culture media that signalled through IL-4 receptor-α and was required for strain-induced membrane hyperpolarisation and differential aggrecan and *MMP3* expression (Millward-Sadler et al., 2000a, Millward-Sadler et al., 1999). Blocking of integrins also alters the response of chondrocytes in anchorage-independent culture conditions. The inhibition of nitric oxide release and increase in cell proliferation and sGAG synthesis induced by dynamic compression of bovine chondrocytes in agarose was abolished by blocking integrins with RGD-containing peptides (Chowdhury et al., 2006). In the presence of RGD-containing peptides the up-regulation of aggrecan, *COL2A1* and *MMP3* expression induced by dynamic compression of porcine chondrocytes in agarose was inhibited (Kock et al., 2009). Interestingly, the effects of integrin blocking on long-term sGAG biosynthesis were dependent upon the loading frequency; RGD peptides had no effect on the reduction of sGAG content induced by compression at 0.33 Hz, whilst they inhibited the increase in sGAG content induced by compression at 1 Hz (Kock et al., 2009). This could provide a mechanism underlying the differential effects of different loading frequencies on articular cartilage metabolism. β1 integrin blocking antibodies prevented the dynamic compression-induced up-regulation of *COMP* expression in bovine chondrocytes in agarose and in cartilage explants

(Giannoni et al., 2003). In bovine chondrocytes cultured in agarose, blocking either αVβ3 or β1 integrins prevented dynamic compression-induced increases in sGAG synthesis (Chai et al., 2010). As blocking αVβ3 integrin decreased, but blocking β1 integrin increased sGAG synthesis in unloaded controls, Chai *et al.* suggest these integrins regulate the stimulation of proteoglycan synthesis via separate mechanisms, perhaps sensing different mechanical signals.

1.4.2.1.3 Purinergic Mechanotransduction Pathway: Connexin and P2 Receptors

Extracellular ATP signals to cell through the transmembrane P2 receptors, which are subdivided into the P2X and P2Y families; P2X receptors are ligand-gated ion channels whilst P2Y receptors are G-protein-coupled receptors. P2 receptors expressed by human articular chondrocytes include P2Y1, P2Y2, P2X2, P2X4 and P2X7 (Knight et al., 2009). In addition, P2X1 and P2X3 are expressed by bovine chondrocytes, with extracellular ATP inducing the release of nitric oxide and prostaglandin E2 (Varani et al., 2008).

A purinergic mechanotransduction pathway regulating the response to dynamic compression has been identified in chondrocytes embedded in agarose (Pingguan-Murphy et al., 2006, Chowdhury and Knight, 2006). The increases in proteoglycan synthesis and cell proliferation induced by dynamic compression for 48 hours (15%, 1 Hz) were inhibited by the P2 receptor antagonist suramin or by hydrolysis of extracellular ATP (Chowdhury and Knight, 2006). P2 receptor signalling was also required for the suppression of nitric oxide release by dynamic compression; in the presence of suramin, dynamic compression enhanced nitric oxide release. ATP release was induced by cyclic compression of porcine chondrons in pellet culture (Graff et al., 2000) and dynamic compression of bovine chondrocytes in agarose (Garcia and Knight, 2010). Dynamic compression (10–15%, 1 Hz) increased hemichannel opening in bovine chondrocytes. Load-induced ATP release was inhibited by blocking these hemichannels (Garcia and Knight, 2010), suggesting that load activates ATP release through hemichannels, with the extracellular ATP then activating P2 receptors on the chondrocyte (Pingguan-Murphy et al., 2006). Interestingly, the P2 receptor antagonist suramin reduced basal and load-induced ATP release from chondrocytes (Millward-Sadler et al., 2004, Garcia and Knight, 2010), suggesting the presence of an autocrine positive feedback loop in the purinergic mechanotransduction pathway (Garcia and

Knight, 2010). Human articular chondrocytes *in situ* express the mechanosensitive ATP-release channel connexin 43 as an uncoupled hemichannel, therefore connexin 43 is suggested to be involved in load-induced ATP release (Knight et al., 2009).

1.4.2.1.4 FGF Receptor and Pericellular FGF-2

Basic fibroblast growth factor (FGF-2) is bound to perlecan in the pericellular matrix in articular cartilage (Vincent et al., 2007). Cyclic compression of cartilage explants causes release of FGF-2 which signals through FGF receptor 1 (FGFR1) to activate extracellular signal-regulated kinase (ERK) and induce synthesis of MMP-1, -3 and TIMP-1 (Vincent et al., 2002, Vincent et al., 2004). ERK activation, induced by cyclic compression or FGF-2 treatment of porcine cartilage explants and chondrocytes in alginate, was suppressed by inhibition of FGFR1 tyrosine kinase (Vincent et al., 2004, Vincent et al., 2007). Subsequent studies have shown that FGF-2 inhibits IL-1α-induced *ADAMTS4* and *ADAMTS5* expression in normal human chondrocytes, IL-1α-induced aggrecanase activity in normal human cartilage, and protects against the development of OA in mice (Sawaji et al., 2008, Chia et al., 2009), suggesting a role for FGF-2/FGFR1-mediated mechanotransduction in the maintenance of cartilage integrity.

1.4.2.1.5 Primary Cilia on Chondrocytes

As discussed in section 1.2.2.1.1, primary cilia are suggested to function as mechanosensors in a number of different cell types and have been observed to project into the ECM of various connective tissues (Donnelly et al., 2008). Hyaline cartilage chondrocytes possess primary cilia (Kouri et al., 1996, Jensen et al., 2004) and these are one of the most stable features of the chondrocyte microtubule cytoskeleton, as indicated by the presence of acetylated α-tubulin (Poole et al., 2001). In chick embryonic sternal cartilage one primary cilia per chondrocyte was observed and the cilia length varied between 1–4μm. Chondrocyte cilia are suggested to be required for chondrocyte differentiation and cartilage development as ORPK mice, which lack the polaris protein required for ciliary assembly, exhibit abnormal distribution of type II collagen, proteoglycan and type X collagen in their growth plate and impaired growth of the major long bones (McGlashan et al., 2007). In addition, growth plate chondrocytes exhibited altered cytoskeletal organisation; α-tubulin staining was increased, microtubules appeared as thick bundles and cortical F-actin appeared thicker and denser. Furthermore, as mice lacking one of the ciliary proteins Bbs1, Bbs2 and Bbs6 exhibit OA-like changes in their cartilage, primary cilia are also suggested to be required for the maintenance of

cartilage integrity (Kaushik et al., 2009). In a naturally occurring bovine model of OA, the incidence and length of primary cilia is increased in OA articular cartilage chondrocytes when compared with normal (McGlashan et al., 2008).

Ultrastructural studies of chick embryonic sternal chondrocytes *in situ* showed direct connections between the cilia and ECM collagen fibres and, in support of this, β1 integrin is expressed on chondrocyte primary cilia (Poole et al., 2001, McGlashan et al., 2006). Cilia observed *in situ* were usually bent, whilst they were predominantly straight in chondrocytes isolated from their matrix (Poole et al., 2001, Jensen et al., 2004). As a result of these observations, it is suggested that the observed bending of chondrocyte cilia is a result of passive bending in response to forces exerted by the ECM; via this mechanism, mechanical force applied to collagen is transmitted to the axoneme and the inside of the chondrocyte. Furthermore, connexin 43, which is proposed to mediate the release of ATP in the purinergic mechanotransduction pathway (section 1.4.2.1.3), is expressed on 50% of cilia on bovine articular chondrocytes cultured in agarose hydrogels; a primary cilium was detected on approximately 30% of chondrocytes (Knight et al., 2009).

1.4.2.2 Intracellular Signal Transducers

1.4.2.2.1 Calcium

Both static and dynamic compression induces intracellular calcium signalling in bovine chondrocytes in agarose, as indicated by transient increases in intracellular calcium concentration (Pingguan-Murphy et al., 2005, Roberts et al., 2001). The effect of dynamic compression depends on the frequency; increases in calcium transients were maintained for up to five minutes under compression at 1 Hz, whilst increases were not maintained when compression was at 0.33 Hz (Pingguan-Murphy et al., 2006). By contrast, the duration of loading had no effect on intracellular calcium signalling (Pingguan-Murphy et al., 2005). Inhibition of ATP-dependent calcium pumps with thapsigargin, which increases the intracellular calcium concentration, reduced protein and sGAG synthesis in bovine cartilage explants and prevented the dynamic compression-induced increase in sGAG synthesis in bovine chondrocytes in agarose (Mouw et al., 2007). In support of this, inhibition of P2 receptors or removal of extracellular ATP, which abolished dynamic compression-induced increases in proteoglycan synthesis and cell proliferation (Chowdhury and Knight, 2006), prevented

load-induced increases in intracellular signalling (Pingguan-Murphy et al., 2006). These results suggest a role for intracellular calcium signalling in both purinergic and other mechanotransduction pathways which mediate load-induced anabolic effects in chondrocytes.

Calcium signalling is also an intracellular mediator of other mechanotransduction pathways. Increased intracellular calcium concentration, in response to thapsigargin treatment, resulted in membrane hyperpolarisation in human chondrocytes in monolayer, with further hyperpolarisation in response to pressure-induced strain (Wright et al., 1996). Cyclic pressure-induced membrane depolarisation in human monolayer chondrocytes was abolished by inhibitors of phospholipase C, inositol trisphosphate-mediated release of calcium from endoplasmic reticulum stores, or calmodulin (Wright et al., 1997). Furthermore, inhibition of calcium/calmodulin-dependent protein kinase II abolished membrane hyperpolarisation and prevented increases in aggrecan expression induced by mechanical stimulation of normal human chondrocytes (Shimazaki et al., 2006). Changes in intracellular calcium concentration in response to mechanical stimulation could alter actin cytoskeletal organisation through regulation of gelsolin activity and other actin binding proteins (section 1.2.1.1).

1.4.2.2.2 Mitogen Activated Protein Kinases

A number of studies have demonstrated activation of mitogen activated protein kinases (MAPKs) in response to mechanical stimulation of chondrocytes and their requirement for downstream effects. ERK was activated by single impact load in rat cartilage, with phosphorylation of ERK1/2 evident immediately after loading and maintained for up to one hour (Henson and Vincent, 2008). Static and dynamic loading of cartilage explants also activates ERK in chondrocytes (Fanning et al., 2003, Li et al., 2003, Vincent et al., 2004, Fitzgerald et al., 2008, Ryan et al., 2009), as does dynamic loading of chondrocytes seeded in agarose (Bougault et al., 2008) or calcium polyphosphate scaffolds (De Croos et al., 2006). In bovine cartilage explants, inhibition of ERK phosphorylation prevented the increase in cell proliferation and decrease in proteoglycan synthesis induced by static compression (Ryan et al., 2009). ERK inhibition also partially reversed the down-regulation of *COL2A1* and fibronectin expression caused by static compression of bovine cartilage explants for 24 hours (Fitzgerald et al., 2008). ERK signalling was also required for the anabolic changes induced by dynamic

compression, as ERK inhibition prevented the up-regulation of aggrecan, *COL2A1* and TIMP-1 expression in dynamically compressed cartilage explants (Vincent et al., 2004, Fitzgerald et al., 2008).

Phosphorylation and activation of p38 MAPK is also induced by static and dynamic compression of cartilage explants (Fanning et al., 2003, Fitzgerald et al., 2008) and dynamic compression of chondrocytes in agarose (Bougault et al., 2008). In a similar manner to ERK inhibition, inhibition of p38 MAPK partially reversed static compression-induced down-regulation of *COL2A1* and fibronectin expression and abolished the dynamic compression-induced up-regulation of aggrecan expression (Fitzgerald et al., 2008). In contrast to ERK however, p38 MAPK inhibition had no effect on the up-regulation of *COL2A1* in response to dynamic compression, but did suppress the up-regulation of the mechano-sensitive transcription factors c-fos and c-jun (Fitzgerald et al., 2008). Furthermore, p38 MAPK inhibition prevented the up-regulation of *COL2A1*, *SOX9* and aggrecan expression in response to dynamic compression of rat bone marrow-derived mesenchymal stem cells in alginate, indicating a role for p38 MAPK in mechanically-enhanced chondrogenesis (Li et al., 2009a). In human articular chondrocytes in monolayer, p38 MAPK and c-jun N-terminal kinase (JNK) were activated by pressure-induced strain, with p38 MAPK inhibition abrogating strain-induced JNK1 and JNK2 phosphorylation and proteoglycan synthesis (Zhou et al., 2007). In this model, ERK was not activated by mechanical stimulation and ERK inhibition had no effect on strain-induced proteoglycan synthesis.

The JNK pathway is activated by static compression in cartilage explants (Fanning et al., 2003) and cyclic compression of chondrocytes seeded in calcium polyphosphate scaffolds (De Croos et al., 2006). Inhibition of JNK signalling blocked AP-1 binding and prevented the increased expression of *MMP1*, *MMP13*, *COL2A1* and aggrecan induced by cyclic compression of bovine chondrocytes in 3D scaffolds. Cyclic compression-induced increases in synthesis and accumulation of type II collagen and aggrecan were also abrogated by JNK inhibition.

1.4.3 The Chondrocyte Cytoskeleton and Load

1.4.3.1 The Cytoskeleton Controls the Mechanical Properties of the Chondrocyte

The cytoskeleton is important for maintaining the mechanical integrity of cells and this is also the case in chondrocytes. Disruption of actin and vimentin filaments with cytochalasin D and acrylamide respectively reduced the viscoelasticity of human chondrocytes *in vitro* in a dose dependant manner, whereas disruption of microtubules with colchicine had little effect (Trickey et al., 2004). The compressive properties and recovery behaviour of chondrocytes is also regulated by the cytoskeleton (Ofek et al., 2009). Disruption of the actin cytoskeleton with cytochalasin D reduced cell stiffness. Vimentin intermediate filament disruption with acrylamide reduced chondrocyte compressibility, whilst tubulin disruption with colchicine increased cell compressibility. The recovery of chondrocytes following compression was delayed by disruption of each of the cytoskeletal elements. In addition, colchicine treatment reduced the strain threshold of chondrocytes, which is the point after which the biomechanical behaviour of cells is irreversibly altered (Ofek et al., 2009). As altering the biomechanical properties of the chondrocyte influences cell-matrix interactions (Guilak and Mow, 2000), the evidence supports the role of the cytoskeleton in mechanical signal transduction. Further support for this comes from evidence that pre-stress in the cytoskeleton is required for physiological load to affect the nucleolus, with this effect on intra-nuclear structures showing its potential to propagate external signals to the nucleus, potentially altering gene expression (Hu et al., 2005).

1.4.3.2 Effects of Load on the Chondrocyte Cytoskeleton

The distribution of the cytoskeletal elements in the different articular cartilage zones has been studied and suggests load can alter the chondrocyte cytoskeleton. Whilst the distribution of actin was constant throughout the zones of mature bovine cartilage, Western blots showed higher levels of actin present in the superficial zone; this could possibly be due to higher levels of G-actin available for microfilament remodelling in chondrocytes of the superficial zone (Langelier et al., 2000). β-tubulin and vimentin staining were more intense in the superficial zone and decreased through to the deep zone, although there was little difference between zones in cartilage from load-bearing regions of the joint. Differences in staining intensity between cartilage zones, most significantly in vimentin distribution, were suggested by the authors to be due to the different mechanical conditions experienced by the chondrocytes at different depths

(Langelier et al., 2000), highlighting the connection between the cytoskeleton and mechanical load.

The response of the cytoskeleton to load has also been studied, both *in vitro* and *ex vivo*. In rat articular cartilage explants, actin distribution and organisation showed no change in response to static loads of 0.5–4 MPa, whilst changes were noted in vimentin distribution and organisation (Durrant et al., 1999). Tissue statically loaded (2–4 MPa) for one hour showed more widespread labelling of vimentin through the depth of the tissue with increasing load. However, a load of 1 MPa only showed vimentin staining in cells of the deep zone. A load of 0.5 MPa appeared to allow the tissue to act as if in free swelling culture with loss of vimentin organisation which, after one hour, was re-established (Durrant et al., 1999). Disassembly of the vimentin cytoskeleton is induced by a single impact load (0.16 J) in rat articular cartilage, as indicated by increased vimentin immunofluorescence around the chondrocyte nucleus (Henson and Vincent, 2008). Disassembly peaked two hours after impact loading and then decreased, which the authors suggested was indicative of reassembly. An *in vitro* study using human chondrocytes encapsulated in alginate hydrogel demonstrated that there was no change in either actin or tubulin cytoskeletal organisation in response to physiological cyclic hydrostatic pressure (5 MPa, 0.25 Hz, 3 hours) (Fioravanti et al., 2003). However, continuous high hydrostatic pressure (non-physiological loads; 24 MPa, 3 hours) applied to the same system induced changes in both actin and tubulin organisation (Fioravanti et al., 2005). In contrast to the findings of Durrant et al. (1999) and Fioravanti et al. (2003), the actin cytoskeleton has been shown to reversibly remodel in response to load (Knight et al., 2006). Hydrostatic pressure (5 MPa) or compressive load (15%) applied either statically or cyclically (1 Hz) for two hours induced remodelling of actin microfilaments, with staining becoming significantly more punctate. This remodelling was reversible within one hour of removal of load, with the exception of cyclic hydrostatic pressure (Knight et al., 2006). Increases in punctate F-actin structures and actin remodelling have also been observed in agarose embedded normal human articular chondrocytes subjected to 20 minutes of dynamic compression (15%, 0.5 Hz) (Haudenschild et al., 2008a). Cyclic compression (15%, 1 Hz) for 10 seconds delayed fluorescence recovery after photo bleaching of cortical actin in bovine chondrocytes in agarose (Campbell et al., 2007). As cortical actin intensity decreased 10 minutes post-compression, the authors suggest a net depolymerisation in response to cyclic compression.

The above studies clearly show a link between mechanical conditions and the chondrocyte cytoskeleton. Changes observed in the cytoskeleton in response to load correlate with the altered mechanical properties of the chondrocyte (Trickey et al., 2004, Ofek et al., 2009) and therefore its mechanosensitivity in response to load, as suggested by Knight *et al.* (2006).

In addition to direct regulation of cytoskeletal organisation, mechanical load has been shown to modulate expression of cytoskeletal-associated and -regulatory proteins. Phosphorylation and activation of Rho kinase (ROCK), which promotes actin polymerisation, was increased by dynamic compression of human chondrocytes in agarose (Haudenschild et al., 2008a). In this study, inhibition of ROCK activity prevented the load-induced remodelling of the actin cytoskeleton and suppressed load-induced up-regulation of genes encoding the chemokine CCL20 and inducible nitric oxide synthase (iNOS). Expression of the actin-sequestering protein thymosinβ4 was up-regulated in bovine articular cartilage explants subjected to cyclic compression (0.5 MPa, 1 Hz) for 10 minutes (Blain et al., 2003). However, in bovine chondrocytes encapsulated in agarose thymosin β4 expression was unaffected by cyclic compression (15% strain, 1 Hz) for 10 minutes or six hours (Campbell et al., 2007). In the same model, expression of the actin depolymerising proteins cofilin and destrin were transiently increased in response to 10 minutes of cyclic compression. Both these studies demonstrate that load-induced actin reorganisation is orchestrated by increased expression of actin-depolymerising proteins.

1.4.3.3 The Role of Rho GTPases and the Actin Cytoskeleton in Mechanotransduction in Chondrocytes

As integrins connect the cytoskeleton to extracellular matrix molecules, the actin cytoskeleton has unsurprisingly been shown to mediate some of the downstream effects of mechanical stimulation on integrins. Disruption of the actin cytoskeleton in human chondrocytes in monolayer by cytochalasin D treatment inhibited the integrin- and stretch activated ion channel-dependent membrane hyperpolarisation induced by cyclic pressure-induced strain (Wright et al., 1997). RhoA, ROCK and actin cytoskeletal remodelling was induced by dynamic compression of agarose embedded normal human chondrocytes (Haudenschild et al., 2008a). Dynamic compression-induced actin

reorganisation and up-regulation of *CCL20* and *NOS2A* expression was dependent upon ROCK. ROCK activity was also required for the increase in SOX9 phosphorylation and nuclear localisation in response to dynamic compression of human chondrocytes in agarose (Haudenschild et al., 2010). In addition to Rho, the small GTPases Rac and Cdc42 have been suggested to be involved in the mechanoregulation of chondrocyte gene expression. Shear stress-induced c-Jun activity and *MMP9* expression was abolished by expression of dominant-negative forms of Rac or Cdc42 in rabbit chondrocytes cultured as a monolayer (Jin et al., 2000). Rac, and to a lesser extent Cdc42, are required for the shear stress-induced phosphorylation of c-Jun and COX-2 mRNA expression in human chondrocytic cells (Healy et al., 2008).

1.5 Cytoskeletal Changes in Osteoarthritis

Differences between the cytoskeleton in normal and OA chondrocytes have recently been observed and have begun to be characterised. Human chondrocytes isolated from normal and end-stage osteoarthritic articular cartilage were found to have different viscoelastic properties. OA chondrocytes showed significantly increased elastic and viscous properties compared to normal chondrocytes (Trickey et al., 2000). It was subsequently shown that the chondrocyte actin and vimentin cytoskeleton was responsible for these viscoelastic properties (Trickey et al., 2004), indirectly supporting the hypothesis that differences exist between the cytoskeleton of normal and OA chondrocytes.

The first report of cytoskeletal element disorder in human OA was made by Kouri *et al.* (1998). Microscopic techniques were used to investigate the morphology of chondrocytes *in situ* from fibrillated and adjacent non-fibrillated regions of knee articular cartilage. Differences in labelling for all three cytoskeletal elements were observed between non-clonal and clonal chondrocytes (Kouri et al., 1998). Notable differences in the cytoskeletal organisation and morphology of normal and OA chondrocytes have also been observed in human chondrocytes *in vitro* (Fioravanti et al., 2003) and *in situ* in a dog model of OA (Pelletier et al., 1983a). Normal chondrocytes contained abundant endoplasmic reticulum, Golgi bodies and secretory vesicles, with numerous mitochondria and euchromatic nuclei. Cell membranes were intact and had few cytoplasmic processes. In contrast, human OA chondrocytes contained significantly

less endoplasmic reticulum, Golgi bodies and mitochondria compared to normal chondrocytes, while nuclei appeared partially heterochromatic (Fioravanti et al., 2005). In support of this is the observation that chondrocytes in the Pond-Nuki dog model of OA (see section 1.3.4) contained an extensive rough endoplasmic reticulum, large Golgi apparatus and an increased number of lysosomes, although this was just four weeks after induction of OA and possibly represents an initial repair response (Pelletier et al., 1983a).

In addition to differences in morphology, the distribution of actin and tubulin was observed to differ significantly between normal and OA human chondrocytes in alginate culture. In normal chondrocytes, actin was found to be polarised on the apical sides of the cell, while tubulin was localised at the periphery of the cell (Fioravanti et al., 2003). In OA chondrocytes, the actin signal was diffuse or peripheral, with significantly fewer cells showing the apical localisation of normal chondrocytes. Tubulin staining was absent in 65% of OA chondrocytes and diffuse when detected, with a significant decrease in the number of cells showing the intense peripheral staining observed in normal chondrocytes (Fioravanti et al., 2003). It should be noted here that, whilst the organisation of actin and tubulin in normal chondrocytes is unlike that observed by others (Benjamin et al., 1994, Durrant et al., 1999, Langelier et al., 2000), possibly due to *in vitro* conditions and/or fixatives and buffers used (Blanc et al., 2005), normal and OA chondrocytes in this study were treated identically therefore differences observed represent real differences in the cytoskeletal organisation of normal and OA chondrocytes. Another study comparing normal and OA human chondrocytes in alginate culture found differences in the cytoskeleton (Lambrecht et al., 2008). Proteomics revealed increased vimentin in chondrocytes originally isolated from visually damaged regions of OA cartilage when compared with chondrocytes isolated from normal cartilage. Increased vimentin N-terminal cleavage was also observed in OA; the N-terminal of vimentin is involved in intermediate filament formation (Beuttenmuller et al., 1994) and the interaction of filaments with the plasma membrane (Georgatos et al., 1985). Confocal microscopy revealed a disordered vimentin intermediate filament organisation in OA chondrocytes from both visually intact and damaged OA cartilage, no longer showing the narrow intense zone of fluorescence at the periphery of the cytoplasm observed in normal chondrocytes (Lambrecht et al., 2008). In addition to the differences in the vimentin cytoskeleton, protein levels of the other intermediate filament

present in chondrocytes, lamin A/C, is increased in OA chondrocytes (Ruiz-Romero et al., 2008, Lambrecht et al., 2008). Although no differences in actin organisation were observed, comparison of OA chondrocytes from visually intact and damaged regions of cartilage showed increased cofilin protein levels in OA damaged regions (Lambrecht et al., 2008). Gelsolin, an actin depolymeriser, and vinculin, an actin binding protein in focal adhesions have been reported as being over-expressed in OA chondrocytes, whilst β-actin was decreased when compared with normal chondrocytes (Ruiz-Romero et al., 2008).

In addition to the above reports of altered cytoskeletal organisation in human OA, differences have been reported in a rat model of OA (Capin-Gutierrez et al., 2004). Osteoarthritis was induced by partial menisectomy, and loading of the joint was increased by exercising control and OA-induced animals for 20 minutes a day for 20 days after surgery. Electron microscopy revealed differences in the intermediate filament cytoskeleton of normal and OA chondrocytes *in situ*. In normal chondrocytes, intermediate filaments were uniformly distributed as perinuclear bundles with clear integrity, while in OA chondrocytes, intermediate filaments appeared fragmented and disordered. Differences in the organisation of all three cytoskeletal elements were also observed by immunohistochemistry and fluorescence microscopy. Normal chondrocytes *in situ* displayed the typical labelling patterns, as described previously for actin, tubulin and vimentin (Benjamin et al., 1994, Durrant et al., 1999, Langelier et al., 2000), whilst OA chondrocytes had disordered cytoskeletons. Vimentin labelling was dense and punctate in some OA chondrocytes, whilst actin labelling was absent in some cells and organised normally in others. Tubulin labelling also appeared fragmented in OA chondrocytes. Differences in fluorescent labelling of normal and OA chondrocytes (as quantified by using the pixel intensity of cytoskeletal and nuclear labelling) showed both vimentin and tubulin to be significantly decreased (by 37% and 20% respectively) in OA chondrocytes compared to normal. However, no decrease in actin labelling was observed. In addition to the structural and organisational observations, Western blot analysis also revealed differences in tubulin and vimentin expression between normal and OA cartilage (Capin-Gutierrez et al., 2004).

1.6 Hypothesis

Although differences between the cytoskeletal architecture of normal and OA chondrocytes are becoming more evident, it has not yet been determined whether or not the altered cytoskeleton in OA is:

i. a cause of the disease,
ii. a result of the altered chondrocyte phenotype seen in OA, or
iii. a result of the altered mechanical environment of the chondrocyte, due to degradation of the surrounding matrix.

The clear link between cytoskeletal organisation, load, and chondrocyte phenotype, along with the altered cytoskeleton observed in OA has led us to hypothesise that ***an intact cytoskeleton is essential for transducing mechanical signals within articular cartilage chondrocytes, and that dysregulation of cytoskeletal networks will prevent normal ECM-chondrocyte signalling, promoting an imbalance in cartilage homeostasis and a catabolic phenotype – the hallmark of OA***.

1.7 Aims of PhD

The overall aim of this PhD is to determine the effects of disrupting cytoskeletal components on the overall phenotype of human chondrocytes, with more specific aims including:

1. To characterise the cytoskeletal architecture of human OA chondrocytes and its response to mechanical load.
2. To determine the effect of disrupting the three cytoskeletal elements on chondrocyte matrix biosynthesis.
3. To determine the effect of cytoskeletal disruption on the response of cartilage chondrocytes to mechanical load.

Chapter 2: Materials and Methods

2. MATERIALS AND METHODS

Reagents used were purchased from Sigma-Aldrich, UK, unless otherwise stated and were of analytical grade or above.

2.1 Source of Tissue

Human articular cartilage was obtained, with ethical consent through AstraZeneca (Alderley Edge, Cheshire), from the lateral and medial tibial plateau or femoral condyle. Macroscopically normal samples were obtained post-mortem from donors that had never presented with knee pain, and osteoarthritic samples were obtained from patients undergoing knee-replacement surgery. Articular cartilage was harvested from joints approximately 48 hours after removal from the donors. All cartilage samples were immediately snap frozen in liquid nitrogen and stored at -80°C until required.

2.2 *In situ* Determination of Articular Cartilage Composition

2.2.1 Preparation of Tissue for Histology and Immunohistochemistry

Cartilage was removed from storage at -80°C, mounted unfixed in Tissue-Tek mounting medium, and full-depth sections cut at 10μm and 20μm thickness using a cryostat (Bright, UK). Sections were adhered to Histobond® microscope slides (R.A.Lamb) and stored at -20°C. All frozen sections were equilibriated to room temperature before staining.

2.2.2 Histology

For histology, 10μm frozen sections were brought to room temperature, washed twice in phosphate buffered saline (PBS- 0.14M NaCl, pH 7.4, 2.7mM KCl, 1.8mM KH_2PO_4, 10mM Na_2HPO_4), fixed for 15 minutes in 4% paraformaldehyde in PBS and washed a further three times with PBS.

2.2.2.1 Haematoxylin and Eosin

Tissue integrity was visualised using haematoxylin and eosin staining. Sections were removed from PBS (pH 7.4) and washed in water for 10 seconds. Sections were incubated in 70% alcohol for 2 minutes, washed in running water for 2 minutes then stained in Mayer's haematoxylin (0.1% (w/v) haematoxylin, 5% (w/v) aluminium ammonium sulphate, 0.1% (w/v) citric acid, 5% (w/v) chloral hydrate, 0.02% (w/v)

sodium iodate) for 10 minutes. Sections were then washed for 5 minutes in running water, stained in 1% aqueous eosin for 5 minutes and washed in running water for 20 seconds. Sections were then dehydrated by washing in 70% alcohol for 20 seconds, 95% alcohol for 30 seconds and 100% alcohol for 3 minutes. Sections were washed in xylene for 4 minutes and mounted under a coverslip in DPX mountant.

2.2.2.2 Alcian Blue

Glycosaminoglycans were visualised using alcian blue staining. Sections were removed from PBS, washed in water for 10 seconds and incubated in 70% alcohol for 2 minutes. Sections were washed in running water for 2 minutes, stained in Alcian blue (pH 2.5; 1% (w/v) alcian blue, 3% (v/v) acetic acid) for 20 minutes and washed in running water for 1 minute. Sections were stained in Mayer's haematoxylin (section 2.2.2.1) for 10 minutes, washed for 5 minutes in running water and stained in 1% aqueous eosin for 5 minutes. Following a 20 second wash in running water, sections were dehydrated and mounted as described in section 2.2.2.1.

2.2.2.3 Visualisation of Staining

Tissue staining was visualised using a Leica DMRB light microscope, using 1.6x up to 20x objectives. Scale bars were added (using calibration images) in Adobe Photoshop 6.

2.2.3 Optimisation of Fixation Protocols for Preservation of the Chondrocyte Cytoskeleton

For immunohistochemical localisation and visualisation of cytoskeletal networks in chondrocytes, preservation of the organisation was required. Various fixatives and buffers were tested on frozen sections of seven day old bovine articular cartilage removed from the carpo-metacarpal joint.

2.2.3.1 Paraformaldehyde

For immunohistochemistry, 20μm frozen sections were brought to room temperature, fixed with 4% paraformaldehyde in PBS pH 8 for 15 minutes, washed three times with PBST (PBS with 0.5% Tween-20), then permeabilised with cold 100% methanol for 30 minutes.

2.2.3.2 Fixation Method from Zwicky and Baici. 2000

Sections were fixed according to the method published by Zwicky and Baici (2000). Frozen sections (20μm) were brought to room temperature, and sections to be stained for actin and vimentin were wet in buffer 1 (PBS containing 5.5mM sucrose, 4mM $NaHCO_3$, 2mM $MgCl_2$, 2mM EGTA, 10mM 2-(N-morpholino)ethanesulfonic acid (MES), pH 6.1) and fixed with 4% paraformaldehyde in PBS for 15 minutes. Following washes in buffer 1, sections were permeabilised with 0.2% (v/v) Triton-X 100 in buffer 1. Sections to be stained for tubulin were wet in buffer 2 (60mM PIPES, 25mM HEPES, 10mM EDTA, 2mM $MgCl_2$, pH 6.9) and simultaneously fixed and permeabilised with 0.25% (v/v) glutaraldehyde and 0.5% (v/v) Triton X-100 in buffer 2 for 15 minutes. Following two washes in buffer 2, sections were post-fixed for 20 minutes with 1% (v/v) glutaraldehyde in buffer 2, washed three times, incubated in 0.5 mg/ml $NaBH_4$ in buffer 2 with three replacements of buffer at five minute durations to remove autofluorescence, then washed a further three times with buffer 2.

2.2.3.3 Fixation Method from Blanc et al. *2005*

Sections were fixed according to a method adapted from that published by Blanc et al. (2005). The buffer used in all steps was a modified Hank's balanced salt solution (mHBSS) consisting of: 136.9mM NaCl, 5.36mM KCl, 2mM $MgCl_2$, 0.336mM Na_2HPO_4, 0.44mM KH_2PO_4, 4mM $NaHCO_3$, 2mM EGTA, 5.55mM D-glucose, 0.11% (w/v) MES, pH 6.5. Frozen sections (20μm) were brought to room temperature, washed twice with mHBSS, then simultaneously fixed and permeabilised in 0.6% (v/v) glutaraldehyde and 5% (v/v) Triton X-100 in mHBSS for 45 minutes. Sections were washed three times, incubated in 5 mg/ml $NaBH_4$ in mHBSS twice for 5 minutes to block autofluorescence, then washed a further three times.

Following the results of the optimisation (see section 3.2.4), the cytoskeleton of human articular chondrocytes and cartilage sections were fixed using the Blanc et al. (2005) method.

2.2.4 Staining of Cytoskeletal Elements

Sections were blocked for 30 minutes with 5% goat serum in fixation buffer (section 2.2.3.3), washed with buffer then incubated in primary antibody for 2 hours at room temperature. Actin microfilaments were detected using either Alexa Fluor® 488

phalloidin (Molecular Probes, Invitrogen) at 5 units/ml or FITC-conjugated phalloidin at 50μg/ml in buffer, microtubules with mouse monoclonal anti-β-tubulin (TUB 2.1 clone, Sigma) at a dilution of 1:15, and vimentin intermediate filaments with mouse monoclonal anti-vimentin (V9 clone, Sigma) at a dilution of 1:20 in buffer. Sections were washed three times with buffer and those stained with phalloidin were mounted in Vectorshield containing DAPI (Vector Laboratories) to counter-stain nuclei. Sections incubated with primary antibodies were incubated with TRITC-conjugated goat anti-mouse IgG (1:64 in buffer) for one hour. Following a further three washes with buffer, sections were mounted as above. To assess non-specific binding of the secondary antibody, primary antibody was replaced with buffer (appendix 1).

2.2.4.1 Visualisation of Cytoskeletal Organisation

Fluorescence was viewed on a Leica DM6000 Confocal microscope using a 63x oil immersion objective. DAPI fluorescence was excited using a 405nm laser line and detection was between 430-500nm. Phalloidin fluorescence was excited at 488nm (argon laser) and detection was between 510-600nm. Finally, TRITC fluorescence was excited at 543nm using a helium/neon laser, with detection between 580-650nm. A series of scans were taken through the z-plane of the chondrocytes at 0.4μm increments, and these were used to produce three dimensional (3D) reconstructions using LCS lite (Leica Confocal software). In some cases, the DAPI signal was omitted from the 3D reconstruction to aid visualisation of the cytoskeletal organisation. For chondrocytes *in situ* or in agarose, approximately 25 scans covered the depth of the cells.

2.3 Biochemical Composition of Articular Cartilage

2.3.1 Water Content

Whole tissue was weighed, freeze-dried for 48 hours, re-weighed and wet and dry weights used to determine the approximate water content.

2.3.2 Sulphated Glycosaminoglycan Content

Pre-weighed tissue was incubated at 60°C in 20mM sodium phosphate buffer (20mM NaH_2PO_4, 1mM EDTA, 2mM DTT, pH6.8) containing 300μg/ml papain until all tissue had been digested. Iodoacetamide was added to a final concentration of 10mM to stop the reaction. The sulphated glycosaminoglycan (sGAG) content was determined using the dimethylmethylene blue (DMMB) assay (Farndale et al., 1986). Standards (10-

50µg/ml) were prepared using shark chondroitin-4-sulphate and 40µl applied, along with digested samples, in duplicate on a 96 well microtitre plate. 200µl of DMMB solution (16µg/ml 1,9-dimethylmethylene blue, 1% (v/v) ethanol, 29.5mM NaOH, 0.34% (v/v) formic acid) was added to each well and absorbances read immediately at a wavelength of 525 nm. sGAG concentration in each sample was determined as described below.

2.3.2.1 Determination of Sample Concentrations

Standards prepared for the specific assay were used to produce a calibration curve in Minitab 14. The function of the straight line was used to determine the concentration of the molecule being assayed in all samples. Samples which produced an absorbance outside the range of standards were diluted. Dilutions were then assayed and the results scaled up accordingly.

2.3.3 Collagen Content

As hydroxyproline is mainly found in collagen it can be used as a measure of collagen content. The hydroxyproline content of the tissue was determined following published methodology (Woessner, 1976). Pre-weighed tissue was hydrolysed in 6N hydrochloric acid for 24 hours at 110°C, freeze-dried for 16 hours to remove the acid, and resuspended in 200µl distilled water. 30µl hydroxyproline standards (0.5-10µg/ml) and samples were applied in duplicate to a 96 well microtitre plate. To each well, 70µl of diluent (66.6% (v/v) propan-2-ol) and 50µl oxidant (50mM chloramine T, 83.3% (v/v) stock buffer) (stock buffer- 0.42M sodium acetate trihydrate, 0.13M tri-sodium citrate dihydrate, 26mM citric acid, 4% (v/v) propan-2-ol) was added and incubated on a plate shaker for five minutes at room temperature. 125µl colour reagent (0.68M dimethylamino benzaldehyde, 9.15% (v/v) perchloric acid, 84.7% (v/v) propan-2-ol) was added to each well and plates incubated at 70°C for 10–20 minutes to obtain a colour change. Absorbances were read at a wavelength of 540nm and the hydroxyproline content of samples determined as in section 2.3.2.1. The collagen concentration was determined as seven times that of hydroxyproline (based on 14% hydroxylproline content of collagen (Leach, 1960)).

2.3.4 Protein Extraction from Articular Cartilage

Pre-weighed whole tissue was powdered in chambers cooled in liquid nitrogen, using a Mikro-Dismembrator U (B.Braun Biotech International) at 2,000 rpm for 2 minutes.

Protein was extracted overnight at 4°C in 2x Sample Buffer (0.06M Tris-HCl pH 6.8, 2% (w/v) SDS, 10% (v/v) glycerol) containing phosphatase and protease inhibitors (Table 2.1), in a volume of 1ml per 50mg wet weight tissue. Samples were pelleted by centrifugation for 15 minutes at 4°C and 13,000 rpm to remove insoluble matter and supernatants stored at -20°C.

Name of inhibitor cocktail and supplier	Name of inhibitor	Target of inhibitor	1x conc
Phosphatase Inhibitor cocktail, Set I (Sigma)	Cantharidin	Protein Phosphatase 2A	5μM
	Bromotetramisole	Alkaline Phosphatase	25μM
	Microcystin	Protein Phosphatase type 1 and 2A	5nM
Phosphatase Inhibitor cocktail, Set II (Calbiochem)	Imidazole	Cation Chelator	2mM
	Sodium fluoride	Serine/Threonine Phosphatase	1mM
	Sodium molybdate	Acid and Phosphoprotein Phosphatases	1.15mM
	Sodium orthovanadate	Tyrosine Phosphatases	1mM
	Sodium tartrate dihydrate	Acid Phosphatases	4mM
Protease Inhibitor cocktail, Set I (Calbiochem)	AEBSF	Serine Protease	500μM
	Aprotinin	Serine Protease	150nM
	E-64 protease inhibitor	Cysteine Protease	1μM
	EDTA	Cation Chelator	500μM
	Leupeptin	Serine and Cysteine Proteases	1μM

Table 2.1:- Components of the inhibitor cocktails included in protein extractions, the protease inhibited and their final concentration in extracts.

2.3.4.1 BCA Protein Assay

The protein concentration of each sample was determined using the BCA™ protein assay kit (Pierce). Bovine serum albumin was used to prepare standards (250-2,000 μg/ml) which were assayed in duplicate alongside tissue extracts on 96 well microtitre plates. Standards and samples (25μl) were incubated with BCA™ working reagent (200μl) for 30 minutes at 37°C. Protein concentration was detected by colorimetric change by measuring the absorbance at a wavelength of 575 nm and determined as described in section 2.3.2.1.

2.3.4.2 Sodium Dodecyl Sulphate Polyacrylamide Gel Electrophoresis

Sodium dodecyl sulphate polyacrylamide gel electrophoresis (SDS-PAGE) was used to resolve protein extracts based on molecular size (Laemmli, 1970). The size of the protein(s) of interest determined the concentration of acrylamide used to prepare the resolving gel (Table 2.2). A 4% stacking gel was used in all instances. Gels were polymerised using 10% (w/v) ammonium persulphate and N,N,N',N'-tetramethylethyl-enediamine (TEMED). Aliquots of protein extracts were heat denatured at 60°C for 30 minutes in 1x sample buffer (30mM Tris-HCl, pH 6.8, 1% (w/v) SDS, 5% (v/v) glycerol, 1mg/ml bromophenol blue), with (2.5% (v/v) β-mercaptoethanol) or without reduction. Equivalent amounts of protein samples were resolved on gels in Laemmli electrophoresis buffer (0.025M Tris, 0.19M glycine, 0.1% (w/v) SDS), at 100-140V for between 1-2 hours, until the dye front had reached the bottom of the gel. BenchMark™ pre-stained protein ladder (Invitrogen) was resolved on gels alongside samples to provide molecular weight standards.

Reagents	Resolving Gel				Stacking Gel
	7.5%	10%	12.5%	15%	4%
40% acrylamide/ bisacrylamide	2.72 ml	3.83 ml	4.53 ml	5.51 ml	575 µl
1M Tris HCl, pH 8.8	3.63 ml	3.63 ml	3.63 ml	3.63 ml	-
1M Tris HCl, pH 6.8	-	-	-	-	1.3 ml
10% SDS	100 µl	100 µl	100 µl	100 µl	50 µl
10% APS	75 µl	75 µl	75 µl	75 µl	37.5 µl
dH_2O	8.16 ml	7.05 ml	6.35 ml	5.37 ml	4.075 ml
TEMED	15 µl	15 µl	15 µl	15 µl	7.5 µl

Table 2.2:- Volumes and stock solutions used in the preparation of gels for sodium dodecyl polyacrylamide electrophoresis (SDS-PAGE). The percentage of acrylamide used in the resolving gel is dependent on the molecular weights of the proteins of interest.

2.3.4.2.1 Visualisation of Protein Bands

Gels were stained for 1 hour in Coomassie blue (45% (v/v) methanol, 10% (v/v) glacial acetic acid, 0.25% (w/v) Coomassie Brilliant Blue R250) with agitation and then destained (10% (v/v) methanol, 7.5% (v/v) glacial acetic acid) with agitation to reveal protein bands.

2.3.4.3 Gelatin Zymography

The MMP-2 and MMP-9 content of the tissue samples was determined using gelatin zymography (Blain et al., 2001). Equivalent amounts of non-reduced samples were resolved on 7.5% SDS polyacrylamide gels containing 1mg/ml gelatin (1ml of 15 mg/ml gelatin replaces 1ml of dH_2O in the resolving gel; Table 2.2), using Laemmli electrophoresis buffer; running conditions were as described in section 2.3.4.2. Gels were washed three times, 10 minutes each, in 2.5% (v/v) Triton® X-100 to remove the SDS present in the gel, allowing proteins to refold. Gels were then incubated overnight at 37°C in MMP Proteolysis buffer (50mM Tris-HCl, pH 7.8, 50mM $CaCl_2$, 0.5M NaCl) to activate the MMPs. Gels were stained and destained as described in section 2.3.4.2.1, with destaining revealing clear bands on a blue background corresponding to zones of gelatinolytic activity.

2.3.4.3.1 Densitometric Analysis

Gels were scanned using UMAX software, and bands of interest quantified by densitometry using NIH Image 6.2. Where comparison across different gels was required, a standard was included on all gels for normalisation

2.3.4.4 Reverse Gelatin Zymography

The TIMP content of samples was determined using reverse gelatin zymography (Blain et al., 2001). Equivalent amounts of non-reduced samples were resolved on 12.5% SDS polyacrylamide gels containing 2mg/ml gelatin and conditioned media (1ml of 32.5 mg/ml gelatin and 2ml of conditioned media replaced 3ml of dH_2O in the resolving gel; Table.2.2) using Laemmli electrophoresis buffer; running conditions were as described in section 2.3.4.2. The conditioned media (a source of MMPs) was derived from serum starving bovine foreskin fibroblasts (BOVS-1 cell line, courtesy of Dr. Emma Blain). Gels were washed, incubated (section 2.3.4.3) and stained as described (section 2.3.4.2.1), with destaining revealing dark bands where inhibition of gelatinolytic activity

has occurred. Densitometric quantification was performed as described in section 2.3.4.3.1.

2.3.4.5 Western Blotting

Equivalent amounts of protein samples (± reduction) were resolved on SDS polyacrylamide gels (Table.2.2) in Laemmli electrophoresis buffer (Laemmli, 1970). Proteins were transferred to PVDF membrane (Millipore) in transfer buffer (80% Laemmli buffer, 20% methanol) at 20V for 16 hours (Towbin et al., 1979). BenchMark™ pre-stained protein ladder was used as a molecular weight marker and as an indicator of complete transfer of proteins onto the membrane. Protein extract (3µg) from human immortalised chondrocytes (TC28a2 cell line (Goldring et al., 1994)) was loaded as a positive control. Membranes were blocked for one hour in Tris-buffered saline with Tween-20 (TBST; 20mM Tris-HCl, pH 7.4, 0.9% (w/v) NaCl, 0.3% (v/v) Tween-20) containing 4% (w/v) skimmed milk powder. Membranes were incubated at room temperature for two hours in primary antibody in TBST at the dilutions indicated (Table 2.3). Following three washes in TBST, membranes were incubated, with agitation, in horseradish peroxidase (HRP)-conjugated secondary antibody (Table 2.3) in TBST for one hour at room temperature. Following a further six washes with TBST, protein bands were detected by chemiluminescence using ECL™ Western blotting detection reagents (GE Healthcare) and exposed to Hyperfilm™ (GE Healthcare). Films were developed using an AGFA Curix 60 automatic developer and bands quantified by densitometry as described above (section 2.3.4.3.1.).

Primary Antibody	Primary Antibody dilution	Secondary Antibody	Secondary Antibody dilution
Anti-actin - polyclonal (Cytoskeleton Inc. USA)	1:100	Anti-Rabbit IgG (-HRP; Sigma)	1:20,000
Anti-β-Tubulin – IgG1 (clone TUB 2.1; Sigma)	1:200	Anti-Mouse IgG (-HRP; Sigma)	1:10,000
Anti-Vimentin - IgG1 (clone V9; Sigma)	1:200 – 1:400	Anti-Mouse IgG (-HRP; Sigma)	1:10,000

Table 2.3:- Details of the primary and secondary antibodies used in Western blotting to detect cytoskeletal proteins in articular cartilage extracts.

2.3.4.6 Collagen Protein Extraction

Pre-weighed whole tissue was powdered in chambers cooled in liquid nitrogen, using a Mikro-Dismembrator U (B.Braun Biotech International) at 2,000 rpm for two minutes. Protein was extracted using an adapted method (Vincourt et al., 2006). Powdered cartilage was agitated in cartilage extraction buffer (500mM NaCl, 50mM HEPES, pH 7.2 including protease and phosphatase inhibitors (Table 2.1) for two hours at room temperature, in a volume of 1ml per 100mg wet weight tissue. Samples were then centrifuged for five minutes at 6,000g to separate insoluble matter from the supernatants. Supernatants were incubated with 1% (w/v) cetylpyridinium chloride (CPC) at room temperature for one hour with agitation, allowing CPC and proteoglycans to aggregate, then centrifuged at 6,000g for five minutes. The resulting supernatants were dialysed against distilled water for 20 hours at 4°C using dialysis tubing with a molecular weight cut off of 12-14,000 daltons. Dialysed supernatants were freeze-dried, resuspended in sample buffer and stored at -20°C. Pellets containing matter insoluble in cartilage extraction buffer were subjected to guanidium hydrochloride extraction in order to remove proteoglycans and other non-collagenous proteins. The guanidine-insoluble pellets were digested with pepsin to solubilise the collagen.

2.3.4.6.1 Guanidine-HCl Extraction

Pellets were weighed to determine their approximate wet weight prior to extraction in 1ml 4M guanidium hydrochloride (4M guanidium HCl, pH 6.8, 0.05M sodium acetate, 0.01M Na_2EDTA, 0.1M 6-amino hexanoic acid) per 100mg wet weight of tissue. Extractions were performed at 4°C for 48 hours with agitation. Samples were centrifuged at 14,000rpm and 4°C for 15 minutes and the supernatants dialysed, freeze-dried and resuspended as described in section 2.3.4.6, then stored at -20°C.

2.3.4.6.2 Pepsin Digestion

Guanidine-insoluble pellets were re-weighed, washed twice with 0.5M acetic acid and then resuspended in 1mg/ml pepsin in 0.5M acetic acid (100:1 wet weight to pepsin). Digests were incubated, with agitation, at 4°C for 16 hours and then centrifuged at 13,000rpm and 4°C for 15 minutes. Supernatants were freeze-dried and resuspended in 1x sample buffer. Collagen content of samples was determined using the hydroxyproline assay (section 2.3.3) and protein content determined using the BCA assay (section 2.3.4.1). In order to visualise differences in the collagen types present in normal and OA

tissue, samples with equivalent hydroxyproline amounts were resolved by SDS-PAGE (section 2.3.4.2) and analysed by Western Blotting (section 2.3.4.5), using antibodies raised in-house against specific collagen types (Table 2.4).

Primary Antibody	Primary Antibody dilution	Secondary Antibody	Secondary Antibody dilution
AVT6E3 (anti-type II collagen)	1:5	Anti-Mouse IgG (-HRP; Sigma)	1:10,000
Anti-human type I collagen	1:500	Anti-Goat IgG (-HRP; Sigma)	1:80,000

Table.2.4:- The names and dilutions of the primary and corresponding secondary antibodies used in Western blotting to detect collagen in articular cartilage extracts.

2.4 Analysis of Gene Expression in Articular Cartilage

RNA was extracted from frozen human articular cartilage using RNase (ribonuclease) and DNase (deoxyribonuclease) free plasticware only and molecular biology grade reagents.

2.4.1 Extraction of RNA from Cartilage

Frozen cartilage tissue was powdered in a liquid nitrogen freezer mill (Certi Prep Spex 6850) using a pulverisation protocol of five minutes pre-cool, followed by three cycles of one minute grinding with one minute cooling. Powdered tissue was emptied into 8ml of ice-cold Trizol® reagent (Invitrogen, approx 10ml/g tissue) in Oakridge centrifuge tubes (40 ml capacity) and inverted to create a suspension. Samples were kept on ice for as much of the procedural duration as possible.

2.4.1.1 RNA Isolation and Precipitation

Aqueous and organic phases were separated by adding 0.2 volumes of chloroform to the tissue-Trizol® mixture, incubating at room temperature for five minutes with occasional inversion, followed by centrifugation at 10,000 rpm for 30 minutes at 4°C (Beckman centrifuge, rotor SS-34). The aqueous phase containing the RNA was removed into clean tubes, with care taken to transfer as little of the interphase as possible and an equal

volume of isopropanol added. RNA was precipitated at -20°C for 16 hours and subsequently pelleted by centrifugation at 10,000 rpm for 15 minutes at 4°C (SS-34 Beckman rotor). Pellets were washed with 75% ethanol, centrifuged for seven minutes at 9,000 rpm at 4°C, air dried for 10 minutes at room temperature and resuspended in 500µl RNase free water.

2.4.1.2 Removal of Contaminating Genomic DNA and Salts

Samples were applied to RNeasy® Mini columns (Qiagen), to increase the purity and concentration of the RNA, following the supplied protocol, splitting one sample between two Mini columns. RNA was bound to the silica-gel membrane and an on-column DNase I digestion performed for 15 minutes at room temperature, using 27.3 Kunitz units of DNase I per column. Following ethanol washes, RNA was eluted in 30µl (per Mini column) of RNase-free water.

2.4.1.3 Determination of RNA Quantity and Quality

The concentration of RNA in samples from individual columns was determined using the NanoDrop® ND-1000 Spectrophotometer (with NanoDrop 3.0.1 software). Where samples had previously been split into sub-samples for RNA clean-up, the sub-samples were pooled after each was determined to be of acceptable quality, and the new concentration determined. The RNA concentration was determined by absorbance at 260nm on a spectrophotometer (1 absorbance unit = 40µg/ml RNA). The A260/A280 ratio should be approximately 2.0 with the acceptable range being between 1.8–2.1.

2.4.2 Real Time-PCR

2.4.2.1 Confirmation of Primer Binding and Expected Product Size

2.4.2.1.1 RNA Extraction from Immortalised Human Chondrocytes

RNA was extracted from human chondrocytes for use in optimisation of primers designed for amplification of genes expressed in human articular cartilage. Immortalised human chondrocytes (TC28a2 cell line) derived from primary culture of costal chondrocytes (Goldring et al., 1994), were harvested at passage 16, with $1x10^6$ cells, in duplicate, resuspended in 1ml Trizol® reagent and stored at -80°C until RNA extractions were performed. RNA was isolated as described above (section 2.4.1.1) but RNA pellets were resuspended in 89µl RNase free water. Genomic DNA present in RNA extracts

was removed by digestion with 1 unit RNase-free DNase (deoxyribonuclease) in 1x reaction buffer (40mM Tris-HCl, pH 8.0, 10mM $MgSO_4$, 1mM $CaCl_2$) (Promega). Samples were mixed and the reaction incubated at 37°C for 30 minutes. 0.1 volumes of DNase Inactivation Reagent (DNA-*free*™, Ambion) was immediately added, incubated with agitation at room temperature for two minutes, then DNase enzyme and divalent cations removed by centrifugation at 10,000 rpm for two minutes. RNA (100µl) was removed into clean tubes and stored at -80°C until required.

2.4.2.1.2 cDNA Synthesis

Total RNA was reverse transcribed to produce cDNA for subsequent use in PCR. The mRNA population was enriched by incubating 10µl of total RNA for five minutes at 65°C with 250ng random primers (Promega) and 0.5mM dNTPs (Promega) in a final reaction volume of 20µl. 40 units of recombinant RNasin® RNase inhibitor (Promega) was added in the presence of 1x first-strand buffer (50mM Tris-HCl, pH 8.3, 75mM KCl, 5mM $MgCl_2$) and 10mM DTT, both supplied with SuperScript™ III reverse transcriptase (Invitrogen), of which 200 units was added. Reactions were incubated at 25°C for five minutes, followed by 50°C for 50 minutes, then the reaction inactivated by heating to 70°C for 15 minutes. Samples were held at 4°C before storage at -20°C, until cDNA was required.

2.4.2.1.3 PCR

Genes of interest were amplified from cDNA using primers designed against the known gene sequences (http://www.ncbi.nlm.nih.gov/nucleotide). PCR was performed in total reaction volumes of 10µl containing 1µl of cDNA (or RNase-free water as a control), in a 1x reaction containing 0.55 units of Taq DNA polymerase in 1x PCR buffer (10mM Tris-HCl, pH 9.0, 50mM KCl, 0.1% Triton® X-100), 2.5mM $MgCl_2$ (Promega), and 0.2mM of each dNTP (Promega). Forward and reverse primers (Table 2.5) were added to a final concentration of 0.3µM.

Samples were initially denatured at 95°C for five minutes, followed by 40 cycles of: 95°C denaturation for 30 seconds, primer annealing at 60°C (standard Taqman annealing temperature) for 30 seconds, and 72°C extension for 30 seconds. A final extension at 72°C for 10 minutes was performed and samples held at 4°C before analysis of products by agarose gel electrophoresis.

2.4.2.1.4 Agarose Gel Electrophoresis

PCR products were separated by electrophoresis on 2% agarose gels containing 1ng/ml ethidium bromide. Samples, combined with 6x gel loading dye, were loaded alongside a BenchTop 100bp DNA ladder (Promega) and separated with 60V. RNA or DNA bands were visualised under ultra-violet light and images taken through a Gel Doc 2000 (Bio-Rad). Where products were expected to be more than 500bp, a 1 or 1.5% agarose gel was used rather than a 2% gel.

Gene of Interest	Forward (F) and Reverse (R) primer sequence	Annealing Temp (°C)	Product size (bp)
β-actin	F: 5'-TTCGAGACCTTCAACACCCC-3' R: 5'-GGCCAGAGGCATACAGGGA-3'	60	70
Cofilin	F: 5'-AATGATTTATGCCAGCTCCAAGG-3' R: 5'-CAGGGTGCAGCGGTCCTTGACC-3'	60	106
Destrin	F: 5'-GCATCATTGTAGAAGAAGGCAA-3' R: 5'-CAGGAAGCATTCCCACAAA-3'	58	93
Filamin A	F: 5'-CTTACGGAGCAGGTCTGGA-3' R: 5'-GTGTTCACGACGAACTCAGC-3'	58	61
Gelsolin	F: 5'-TGTGATCGAAGAGGTTCCTG-3' R: 5'-CAGGTGTCCAGAAGCATGAC-3'	60	75
Paxillin	F: 5'-GTGGCATCCTGAGTGCTTT-3' R: 5'-AAGCTGCCGTTCACGAAT-3'	55	60
Thymosin β4	F: 5'-TGCAAAGAGGTTGGATCAAG-3' R: 5'-CCAGACAGACAGATGGGAAA-3'	58	103
Vimentin	F: 5'-AAGAGGAAATCCAGGAGCTG-3' R: 5'-AGGTCAGGCTTGGAAACATC-3'	58	79
Tubulin (β-2a)	F: 5'-GGATGTGGTGAGGAAGGAGT-3' R: 5'-TACTCTTCCCGGATCTTGCT-3'	60	126

Table 2.5:- Primer sequences used in PCRs, shown along with their expected molecular size.

2.4.2.2 Taqman® Q-PCR

Known RNA concentrations were used to dilute an aliquot of the RNA samples to 10ng/μl in RNase-free water. Reactions were performed in a final volume of 25μl, each containing 25ng RNA, 400nM forward and reverse primers, 200nM probe, 12.5μl 2x QuantiTect Probe RT-PCR Master Mix and 0.25μl QuantiTect RT Mix (Qiagen

QuantiTect Probe RT-PCR Master Mix and 0.25µl QuantiTect RT Mix (Qiagen QuantiTect Probe RT-PCR Kit). Fluorescently labelled probes and primers designed to *GAPDH*, *SOX9*, *COL2A1*, *VEGF*, *ADAMTS5*, cofilin (*CFL1*), destrin (*DSTN*), filaminA (*FLNA*), gelsolin (*GSN*), paxillin (*PXN*), thymosin β4 (*TMSB4X*), β-tubulin (*TUBB2A*) and vimentin (*VIM*) were used (see Table 2.6). Plates were covered with ABI Prism™ optical adhesive covers (Applied Biosystems) and centrifuged to collect the reactions at the bottom of the wells. Real-time PCR was carried out on an ABI PRISM™ 7700 Sequence Detection System using SDS.1.9.1 software, with reaction conditions as follows: reverse transcription at 50°C for 30 minutes, reverse transcriptase inactivation and DNA polymerase activation at 95°C for 15 minutes, followed by 40 cycles of 95°C denaturation for 15 seconds and 60°C annealing and extension for one minute.

2.4.2.2.1 Analysis of Differential Gene Expression

The threshold was set manually so that it was in the centre of the logarithmic growth phase of the amplification curve for each gene (Fig 2.1). To allow comparison of samples and genes across plates, *GAPDH* for all samples was included on each plate and used as the endogenous control (Ct values normalised to the *GAPDH* Ct value for each sample, giving a ΔCt value per sample per gene). Relative expression units (REU) were calculated using the following formulae:

$R.E.U. = 2^{(a-\Delta Ct)}$ where a = the highest ΔCt value of all samples and genes to be compared.

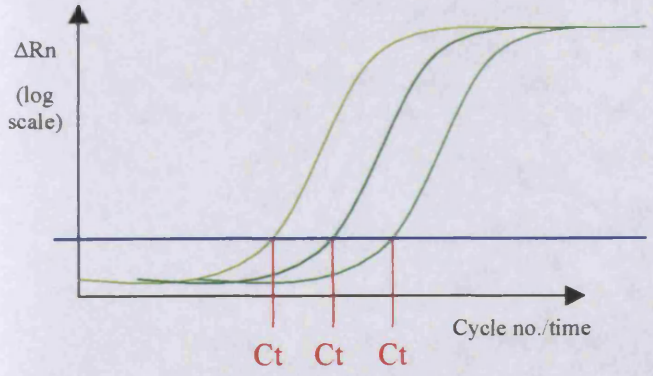

Figure.2.1:- Diagrammatic representation of a Taqman™ amplification curve. The threshold (blue) is set in the logarithmic phase of all curves (green, one per sample). The Ct value is the cycle number at which the curve crosses the threshold.

Gene of Interest	Forward (F) and Reverse (R) primer sequences and probe sequences with modifications as indicated
Cofilin	F: 5'-AATGATTTATGCCAGCTCCAAGG-3' R: 5'-CAGGGTGCAGCGGTCCTTGACC-3' Probe: *Fam* 5'-TGCAATTCATGCTTGATCCCTGTCA-3' *Tamra*
Destrin	F: 5'-GCATCATTGTAGAAGAAGGCAA-3' R: 5'-CAGGAAGCATTCCCACAAA-3' Probe: *Fam* 5'-TGGTTACACCAACATCTCCAACCAA-3' *Tamra*
Filamin A	F: 5'-CTTACGGAGCAGGTCTGGA-3' R: 5'-GTGTTCACGACGAACTCAGC-3' Probe: *Fam* 5'-TGGGTTCCCTGTGACACCGC-3' *Tamra*
Gelsolin	F: 5'-TGTGATCGAAGAGGTTCCTG-3' R: 5'-CAGGTGTCCAGAAGCATGAC-3' Probe: *Fam* 5'-TCCGTTGCCAGGTCTTCCTGC-3' *Tamra*
Paxillin	F: 5'-GTGGCATCCTGAGTGCTTT-3' R: 5'-AAGCTGCCGTTCACGAAT-3' Probe: *Fam* 5'-CGTGAAGCATTCCCGGCACA-3' *Tamra*
Thymosin β4	F: 5'-TGCAAAGAGGTTGGATCAAG-3' R: 5'-CCAGACAGACAGATGGGAAA-3' Probe: *Fam* 5'-CTGACAACGAAGGCCGCGC-3' *Tamra*
Vimentin	F: 5'-AAGAGGAAATCCAGGAGCTG-3' R: 5'-AGGTCAGGCTTGGAAACATC-3' Probe: *Fam* 5'-TCAGGAACAGCATGTCCAAATCGA-3' *Tamra*
Tubulin (β-2a)	F: 5'-GGATGTGGTGAGGAAGGAGT-3' R: 5'-TACTCTTCCCGGATCTTGCT-3' Probe: *Fam* 5'-ATGAGCAGGGTGCCCATCCC-3' *Tamra*
Sox-9	F: 5'-GCCCCAACAGATCGCCTACAG-3' R: 5'-GAGTTCTGGTGGTCGGTGTAGTC-3' Probe: *Fam* 5'-CAGCCCCTCCTACCCGCCCA-3' *Methyl Red*
ADAMTS5	F: 5'-CAGCCACCATCACAGAATTCC-3' R: 5'-TCGTAGGTCTGTCCTGGGAGTT-3' Probe: *Fam* 5'-CATGGTAACTGTTTGCTGGACCTACCACGA-3' *Methyl Red*
VEGF	F: 5'-CGAGGGCCTGGAGTGTGT-3' R: 5'-CGCATAATCTGCATGGTGATG-3' Probe: *Fam* 5'-CCCACTGAGGAGTCC-3' *Methyl Red*

Table 2.6:- Primer and probe sequences used in quantitative Taqman™ PCR. 5' and 3' modifications to probes are shown in italics.

2.5 Disruption of Cytoskeletal Elements in 3D-Cultured Human Articular Chondrocytes

2.5.1 Three-Dimensional Culture of Human Articular Chondrocytes

In order to retain the rounded morphology and phenotype characteristic of chondrocytes in cartilage, isolated chondrocytes were encapsulated and cultured in agarose hydrogels. Basal media used for all cell culture was Dulbecco's Modified Eagle's Medium (DMEM) / F-12 +Glutamax® supplemented with 100 units/ml penicillin, 100μg/ml streptomycin, 292μg/ml L-glutamine, 2.5 μg/ml amphotericin B and 50 μg/ml ascorbate-2-phosphate. All tissue culture reagents were purchased from Invitrogen unless otherwise stated.

2.5.1.1 Monolayer Expansion of Human Articular Chondrocytes

Human chondrocytes were previously isolated by collagenase digestion of articular cartilage removed from the tibial plateau or femoral condyle of donor knees and stored in liquid nitrogen (courtesy of Dr. John Wardale, AstraZeneca). Vials of cells were thawed and seeded into 225cm^2 cell culture flasks in serum-containing media (basal media supplemented with 10% foetal calf serum (FCS)). At confluency, cells were passaged and split in a 1:3 ratio. In order to remove cells that had adhered to the base, flasks were washed twice in 37°C PBS, twice in 37°C 0.05% trypsin-EDTA, then incubated at 37°C for approximately five minutes or until, with a tap, cells no longer adhered to the flask. Cells were rinsed from the base of the flask with media and resuspended in a volume of 15ml media before seeding into clean flasks in a split ratio of 1:3.

2.5.1.1.1 Chondrocyte Culture in Monolayer

Chondrocytes at passage 2 were removed from flasks as described above and counted using a haemocytometer. The cell suspension was then diluted to approximately 5x10^4 cells per ml and plated at a density of 5x10^4 cells per well of a 24-well plate. For immunohistochemistry, cells were plated at 2.5x10^4 cells per well of 8-well chamber slides (Nalge-Nunc International). Following plating out, cells (now at passage 3) were left for four days to adhere before analysis.

2.5.1.1.2 Analysis of Chondrocyte Gene Expression in Monolayer

RNA was extracted from chondrocytes, adding 500µl Trizol® reagent per well of a 24-well plate ($5x10^4$ cells per well) following removal of media, and plates stored at -80°C until required. Plates were thawed at room temperature and lysates removed into labelled tubes, ensuring samples were kept on ice as often as possible. In order to ensure cells were sufficiently lysed and resuspended in Trizol®, pipette tips were thoroughly run over the base area of each well before removal of the reagent. Aqueous and organic phases were separated by adding 0.2 volumes of chloroform to the Trizol®, incubating at room temperature for five minutes with occasional inversion, followed by centrifugation at 12,000 rpm for 15 minutes at 4°C. The aqueous phase was removed into a clean tube and an equal volume of isopropanol added. RNA was precipitated at -20°C for 16 hours and subsequently pelleted by centrifugation at 12,000 rpm for 15 minutes at 4°C. Pellets were washed with 75% ethanol, centrifuged for five minutes at 12,000 rpm at 4°C, air dried for 15 minutes at room temperature, and resuspended in 100µl RNase free water. Resuspended RNA was applied to RNeasy® Micro columns (Qiagen) for purification and concentration, following the manufacturers' protocol. The theory and practise is as described in section 2.4.1.2, although RNA was eluted in 14µl RNase-free water. The concentration and quality of RNA extracts were determined as in section 2.4.1.3. Gene expression was analysed using custom-designed arrays (section 2.5.4.2).

2.5.1.1.3 Visualisation of Cytoskeletal Organisation in Monolayer

Cells were washed once in mHBSS buffer then simultaneously fixed and permeabilised as described in section 2.2.3.3. After a 45 minute fixation, cells were washed twice in mHBSS then stored frozen at -20°C until required. Frozen chamber slides were thawed at room temperature and the cells washed once with mHBSS. An autofluorescence block was performed as described in section 2.2.3.3. The cytoskeletal elements were stained and organisation visualised by confocal microscopy as described in section 2.2.4, with the following modifications: Alexa Fluor® 633 goat anti-mouse IgG (1:100) was used as the secondary antibody and fluorescence was excited at 633nm and detected between 639-660nm. The series of scans taken across the chondrocytes were at 0.3µm increments.

2.5.1.2 Seeding of Human Articular Chondrocytes into Three-Dimensional Culture

Following expansion in monolayer (section 2.5.1.1), human articular chondrocytes at passage 2 were removed from flasks by trypsinisation, counted using a haemocytometer and resuspended to $1x10^6$ cells per ml in serum-containing media. The chondrocyte suspension was added to an equal volume of 6% agarose in Earle's Balanced Salt Solution (EBSS, Sigma) to yield a final concentration of $5x10^5$ cells per ml in 3% agarose. The cell/agarose suspension (12ml) was allowed to solidify in a 60mm diameter Petri dish for 15 minutes at room temperature. Constructs of cells in agarose were removed using a sterile sharp trephine (11mm diameter). Constructs were expelled into individual wells of a 12-well plate and incubated in 2ml serum-containing media for 24hrs at 37°C.

2.5.2 Cytoskeletal Disruption

Serum-containing media was removed from wells and replaced with basal media supplemented with 1x Insulin-Transferrin-Sodium selenite (ITS) media supplement. Cells were allowed to stabilise for 24 hours then ITS-supplemented media was replaced with media containing 1μM cytochalasin D, 1μM colchicine (Tocris), or 2mM acrylamide; untreated cells served as controls. Cells were incubated at 37°C for 6, 12, 24 and 48 hours, with no change of media. Cytochalasin D is a fungal metabolite that inhibits polymerisation of actin microfilaments, sometimes causing depolymerisation, and is used to disrupt structures such as stress fibres (Cooper, 1987). Colchicine is a plant alkaloid that interferes with and disrupts microtubule organisation through distortion of the protein-protein interactions required for polymerisation (Andreu and Timasheff, 1982). The neurotoxin acrylamide selectively disrupts intermediate filaments by an, as yet, unidentified mechanism (Eckert, 1985).

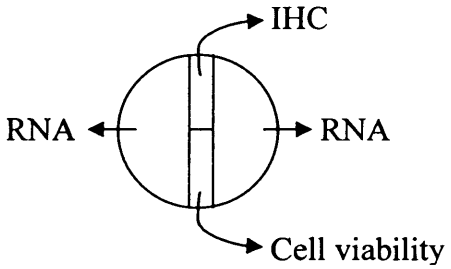

Figure 2.2:- Schematic diagram indicating the processing of cell/agarose constructs for analysis of gene expression (RNA), cytoskeletal organisation (IHC) and cell viability.

At the required time point, a 2mm slice was removed from the centre of each construct and half was used to assay for cell viability (Fig 2.2). The other half was snap frozen for visualisation of cytoskeletal organisation. The remaining portions of the constructs were snap frozen in liquid nitrogen and stored at -80°C until RNA extraction. Media samples were stored at -20°C.

2.5.2.1 Cell Viability Assay

The effects of treatment and the duration of culture on cell viability were determined using the LIVE/DEAD® Viability/Cytotoxicity kit for mammalian cells (Molecular Probes). Cell/agarose plugs were incubated, in the dark, for 45 minutes at 37°C in ITS-supplemented media containing 0.5μM calcein AM and 1μM ethidium homodimer, followed by three 15 minute washes with PBS at 37°C. Staining was viewed through FITC (calcein AM) and TRITC (ethidium homodimer) filters on an inverted fluorescence microscope (Olympus). Images were captured through a camera using SimplePCI software (C.Imaging Systems). Cell viability was calculated by counting the number of red (dead) and green (live) chondrocytes in focus on images, then using the following equation:

$$\text{Cell viability (\%)} = \frac{\text{number of live cells (green)}}{\text{Total number of cells (red + green)}} \times 100$$

2.5.3 Visualisation of Cytoskeletal Disruption in Agarose

A frozen slice from each plug was mounted and sectioned as described in section 2.2.1. Sections were fixed (section 2.2.3.3) and the cytoskeletal elements stained and visualised as described (section 2.2.4), with the following modifications: anti-tubulin and anti-vimentin primary antibodies were used at 1:50 and 1:80 dilutions respectively. At least five cells per test group were viewed and a representative cell scanned by confocal microscopy. Serial scans were taken across chondrocytes at 0.4μm increments and 3D reconstructions performed.

2.5.4 Analysis of Chondrocyte Gene Expression Changes Following Cytoskeletal Disruption

2.5.4.1 Extraction of RNA from Chondrocytes

The depth of agarose plugs was determined to the nearest 0.1mm using a micrometer and values used to calculate plug volumes. RNA was extracted directly from chondrocytes in agarose using RNeasy Mini kits (Qiagen) and following a published method (Mio et al., 2006). Buffer RLT was added to samples at a volume four times that of the agarose plug (4µl RLT per 1µl plug volume) and plugs thawed on ice. Agarose samples were disrupted by drawing up and down through pipette tips and the pH of homogenised samples adjusted using 2M sodium acetate, pH 5.5 (5.05µl per 1ml total volume), then 0.71 volumes (of RLT volume) of 100% ethanol added and samples mixed by pipetting. Samples were loaded onto RNeasy mini columns in 700µl volumes and processed according to the manufacturer's protocol. RNA was eluted in 45µl RNase-free water, then genomic DNA present in RNA extracts was removed by digestion with 2 units recombinant DNase I in 1x DNase I Buffer (10mM Tris-HCl, pH 7.5, 2.5mM $MgSO_4$, 0.5mM $CaCl_2$) (DNA-free™, Ambion). Samples were mixed and the reaction incubated at 37°C for 30 minutes. 0.1 volumes of DNase Inactivation Reagent (DNA-*free*™, Ambion) was immediately added, incubated with agitation at room temperature for 2 minutes, then DNase enzyme and divalent cations removed by centrifugation at 10,000 rpm for 2 minutes. RNA (approximately 50µl) was removed into a clean tube and stored at -80°C until required. The concentration and quality of RNA extracts were determined as in section 2.4.1.3 and concentrations used to dilute samples to 5ng/µl. cDNA was synthesised as described in section 2.4.2.1.2, starting from 50ng of RNA for each sample.

2.5.4.2 Real-Time PCR: Microfluidics TaqMan® Custom Arrays

Applied Biosystems TaqMan® Low Density Custom Array 384 well cards were used to investigate early gene expression changes in human chondrocytes in 3D-culture as a result of 6 hours of cytoskeletal disruption, and to compare gene expression of monolayer- and 3D-cultured human chondrocytes. Cards contained four repeats of 96 gene targets selected by AstraZeneca as targets of interest in osteoarthritis. 200ng of RNA per sample (four samples per card) were loaded onto the 96 wells on cards, in the presence of 206µl QuantiTect Probe RT-PCR Master Mix and 2µl QuantiTect RT Mix

(reagents from the Qiagen QuantiTect™ Probe RT-PCR kit). Plates were centrifuged in custom-made buckets at 1,200 rpm for one minute at room temperature, ensuring a low deceleration, and then sealed. Real-time PCR was carried out on an ABI PRISM™ 7900HT Sequence Detection System using SDS.2.1 software, with reaction conditions as follows: reverse transcription at 50°C for 30 minutes, reverse transcriptase inactivation and DNA polymerase activation at 95°C for 15 minutes, followed by 40 cycles of 95°C for 15 seconds and 60°C for one minutes. Samples from all four treatment groups, from both normal and osteoarthritic donors, from two repeats of the experiment were analysed on array cards (n=2). Results were analysed using a relative quantification study, and the threshold set automatically for each gene. *GAPDH* was set as the endogenous control and a control sample (i.e. untreated) as the exogenous control. Genes and samples with Ct>36 were removed from calculations and the Ct values (Fig.2.1) normalised to the *GAPDH* Ct value for each sample (giving a ΔCt value per sample per gene); amplification curves for housekeeping genes showed the least variability in *GADPH* expression across samples (appendix 2). For normalisation to an exogenous control, a ΔΔCt value was calculated (being the difference between the ΔCt of the test sample and that of the control sample, for each gene of interest). Relative expression units and Relative quantification units were calculated using the following formula (Pfaffl, 2001):

$R.E.U. = 2^{(a-\Delta Ct)}$ where a = the highest ΔCt value of all samples and genes to be compared.

$RQ = 2^{-(\Delta\Delta Ct)}$ A value below 1 represents a negative fold change.

2.5.4.3 Real-Time PCR: SYBR Green

For a more in-depth analysis of gene expression changes over time with cytoskeletal disruption, expression of selected genes of interest was analysed by quantitative PCR in the presence of SYBR green, performed on a Mx3000P™ (Strategene) using MxPro software.

2.5.4.3.1 Primer Design

Forward and reverse primers for use in quantitative PCR were designed for genes of interest. *ACAN*, *SOX9* and *COL1A1* were selected as these are commonly used as markers of chondrocyte phenotype, dedifferentiation or hypertrophy. *MMP13*, *BMF* and *ADAMTS5* were selected from the results of the Taqman array and the cytoskeletal gene *ACTB* selected. Accession numbers for mRNA sequences were obtained from NCBI (www.ncbi.nlm.nih.gov/), and exon boundaries viewed in Ensembl (www.ensembl.org). If variants were found in either NCBI or Ensembl, sequences were aligned using EBI (www.ebi.ac.uk/Tools/clustalw/index.html) and primers designed to regions common to all variants. Primers were designed using Primer3 (http://frodo.wi.mit.edu/) and parameters set as follows; product size between 80 and 220bp, optimum primer melting temperature of 60°C, optimum primer length of 20bp. Primer sequences were then run through a nucleotide BLAST algorithm (www.ncbi.nlm.nih.gov/Blast.cgi) to ensure that they did not cross-react with other genes expressed by chondrocytes. Unmodified oligonucleotides were ordered from Eurofins-MWG and sequences, accession numbers and product sizes are shown in Table 2.7.

Primers shown in Table 2.5 were also used in SYBR green quantitative PCR.

2.5.4.3.2 Generation of Standard Curves

Standard curves were required for each gene in SYBR green quantitative PCR to allow for comparison across plates and experimental repeats and for determination of the reaction efficiency. PCR was performed as described in section 2.4.2.1, using cDNA from TC28a2 immortalised chondrocytes as the template. 5µl of each reaction was analysed by agarose gel electrophoresis (section 2.4.2.1.4) to ensure a single product was present (Fig 2.3 A).

2.5.4.3.2.1 Ligation into pGEM®-T

Following PCR, 1.5µl of the reaction was incubated overnight at 4°C with 25ng pGEM®-T vector (appendix 3) and 1.5 Weiss units T4 DNA Ligase in the presence of 2.5µl 2x Rapid Ligation Buffer (pGEM®-T Vector System, Promega).

Gene of Interest	Forward (F) and Reverse (R) primer sequence	Accession No.	Annealing Temp (°C)	Product size (bp)
ACAN	F: 5'-CCTCTGGACAACCAGGTGTT -3' R: 5'-AAACCAGGTCAGGGACTCCT -3'	NM001135	58	174
SOX9	F: 5'-AATCTCCTGGACCCCTTCAT-3' R: 5'-GTCCTCCTCGCTCTCCTTCT-3'	NM000346	56	198
COL1A1	F: 5'-GTGCTAAAGGTGCCAATGGT-3' R: 5'-CTCCTCGCTTTCCTTCCTCT-3'	NM000088	58	228
MMP13	F: 5'-CCATTACCAGTCTCCGAGGA-3' R: 5'-GGAAGTTCTGGCCAAAATGA-3'	NM002427	58	118
BMF	F: 5'-CAGGGGCTTTCCACTTGAG-3' R: 5'-CCAAGTGGGACCAAGTCAGT-3'	NM033503	58	236
ADAMTS5	F: 5'-GAGGCCAAAAATGGCTATCA -3' R: 5'-ATCGGTCACCTTTGGAGAAA-3'	NM007038	53	159
GAPDH	F:5'GGTATCGTGGAAGGACTCATGA-3' R: 5'-GGGCCATCCACAGTCTTCTG -3'	NM002046	60	68

Table 2.7:- Sequences of primers used in quantitative PCR with SYBR green. Annealing temperatures and product sizes are also shown.

2.5.4.3.2.2 Transformation into highly competent *E. coli* cells

Ligation reactions (2µl) were incubated on ice for 20 minutes with 25µl of JM109 high efficiency competent cells in 14ml culture tubes (BD Biosciences). Cells were heat-shocked at 42°C for 50 seconds and returned to ice for two minutes. Following the addition of 475µl S.O.C. media (Invitrogen), transformations were incubated, with agitation, at 37°C and 210 rpm for 90 minutes.

2.5.4.3.2.3 Blue/White Colony Selection

Transformations (100µl) were plated onto LB agar containing 100µg/ml ampicillin (BioLine), 50µg/ml X-gal (5-bromo-4-chloro-3-indolyl-β-D-galactopyranoside, Promega) and 0.5mM IPTG (isopropyl β-D-1-thiogalactopyranoside) and incubated for 16 hours at 37°C. The pGEMT vector confers ampicillin-resistance therefore only transfected cells will grow on the selection media. The ligation site in the pGEMT vector is within the β-galactosidase gene, therefore vectors containing an insert (PCR product) will not produce functional β-galactosidase and colonies will appear white on the selection media. Vectors that have ligated with no insert synthesise β-galactosidase

(gene transcription induced by IPTG) which acts upon the X-gal substrate in the selection media and appear blue (Biard et al., 1992, Horwitz et al., 1964). White colonies were picked from plates and cultured in 10ml LB broth containing 100µg/ml ampicillin at 37°C for 18 hours, with agitation at 180 rpm.

2.5.4.3.2.4 Plasmid Purification

Cells were pelleted by centrifugation at 2,000g and plasmids extracted from cells using Wizard® Plus SV Miniprep DNA Purification System (Promega), according to the manufacturer's instructions. Following DNA sequencing (Cardiff University DNA Sequencing Core: http://probe.biosi.cf.ac.uk/seq/) of plasmid inserts to confirm ligation and correct sequence of the required PCR product, plasmid DNA was quantified using a NanoDrop® ND-1000 Spectrophotometer (with NanoDrop 3.0.1 software). Concentrations were used to dilute plasmids to 1ng/µl and then a 1:10 dilution series produced standards ranging from 1fg/µl to 1ng/µl.

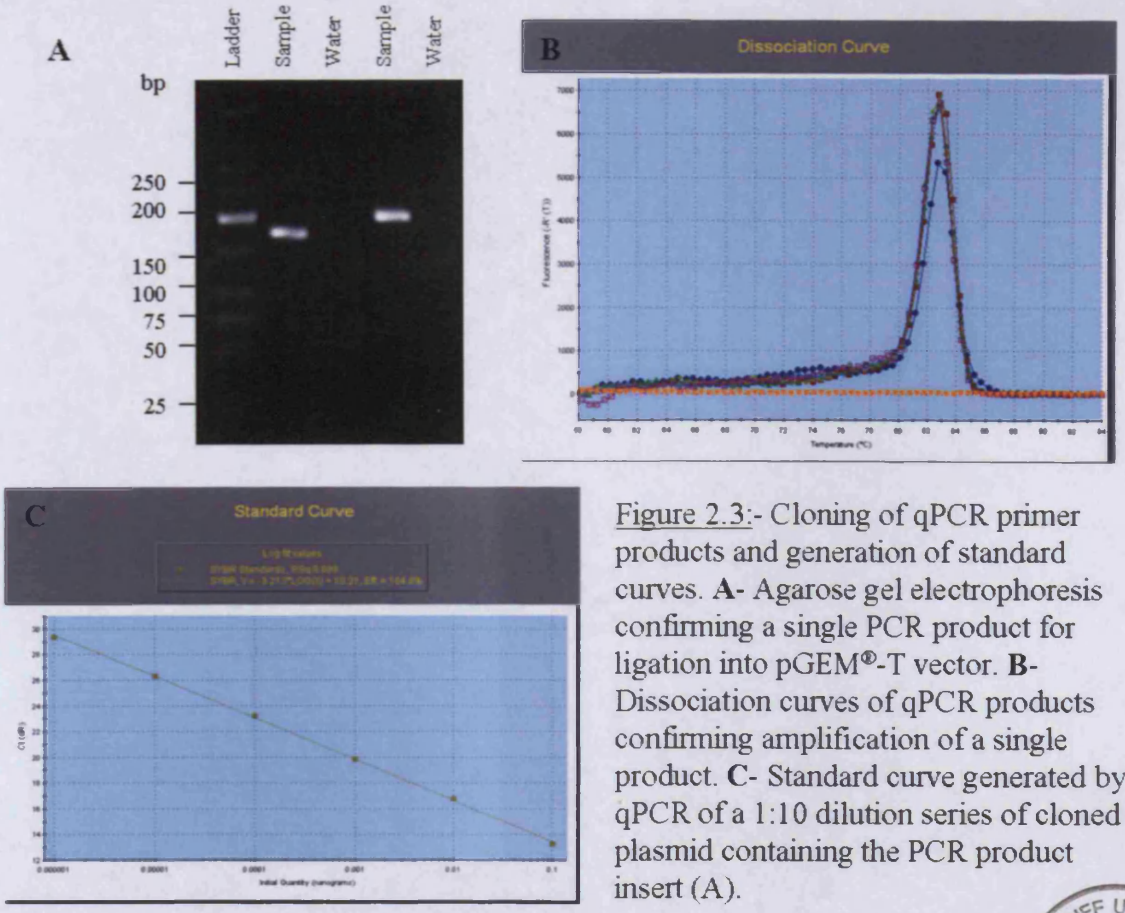

Figure 2.3:- Cloning of qPCR primer products and generation of standard curves. **A-** Agarose gel electrophoresis confirming a single PCR product for ligation into pGEM®-T vector. **B-** Dissociation curves of qPCR products confirming amplification of a single product. **C-** Standard curve generated by qPCR of a 1:10 dilution series of cloned plasmid containing the PCR product insert (A).

2.5.4.3.3 Quantitative PCR

Reactions were performed in 25µl volumes, containing 2µl cDNA and 300nM forward and 300nM reverse primers in the presence of 12.5µl 2x SYBR® Green JumpStart™ Taq ReadyMix™, in 96-well polypropylene plates (Stratagene) and wells sealed with optical caps (Stratagene). Real-time PCR was carried out on a Mx3000P™ using MxPro software, with reaction conditions as follows; DNA polymerase activation and cDNA denaturation at 95°C for 10 minutes, followed by 40 cycles of 95°C for 30 seconds, primer annealing for one minute (for annealing temperatures see Table 2.7) and primer extension at 72°C for 30 seconds. Dissociation curves were generated by an additional cycle of 95°C for one minute, 55°C for 30 seconds and 95°C for 30 seconds. Providing that dissociation curves showed a single product (Fig 2.3 B) and standard curves demonstrated reaction efficiency between 90–110% (Fig 2.3 C), the threshold was set automatically for each gene and results exported. The absolute value, generated using the standard curve, was normalised to that of the endogenous control *GAPDH*, for each sample.

2.6 Compressive Loading of Three Dimensional-Cultured Human Articular Chondrocytes

Human articular chondrocytes from normal and osteoarthritic donors were expanded in monolayer and cultured in agarose as described in section 2.5.1. Following culture for 24 hours in serum-containing media, chondrocyte/agarose constructs were cultured for 24 hours in ITS-supplemented, 'serum-free' media. Prior to loading, constructs were treated for a further 24 hours with cytoskeletal disrupting reagents, as described in section 2.5.2, or left untreated for 24 hours in fresh serum-free media, serving as undisrupted controls. Plugs were subjected to unconfined, uniaxial cyclic compression to a 15% strain at 0.5Hz (one second on / one second off), for 10, 20 or 40 minutes. Samples were processed as described in section 2.5.2 – 2.5.4.

2.6.1 Loading Machine

A custom-made mechanical loading apparatus (Advocet Engineering Services Ltd., UK) was used to load chondrocyte/agarose constructs over short periods of time. The loading apparatus, shown in Figure 2.4, consists of six 25mm diameter aluminium compression plates, controlled by a pneumatic compressor and UDT (universal digital timer), beneath which a 6-well plate can be placed. There is uniform, adjustable displacement across all six wells. Each well contains an individual load sensor with output through a digital transformer. Both compressive force and displacement were visualised and recorded using AcqKnowledge software (both supplied by Biopac, USA). The type of compression cycle and frequency are adjustable and controlled via the UDT on the control panel.

The smallest displacement achievable was 0.75 mm, which equates to a 15% strain as plugs had a depth of 5 mm. A frequency of 0.5 Hz was used for cyclical compressive loading to maintain the integrity of chondrocyte/agarose constructs.
Peak stress was determined for chondrocyte/agarose constructs under a 15% compressive strain; changes in voltage, recorded and visualised using AcqKnowledge software, were converted into force (Newtons) using a calibration curve (see Fig 6.26 A) and force then converted to stress using the equation below.

$$\text{Force (N)} = \text{stress (Pa)} \times \text{cross-sectional area } (m^2)$$

2.6.2 Analysis of Chondrocyte Gene Expression Changes with Cyclic Compressive Load

RNA was extracted as described in section 2.5.4.1 and gene expression analysed by quantitative PCR with SYBR green (section 2.5.4.3.3).

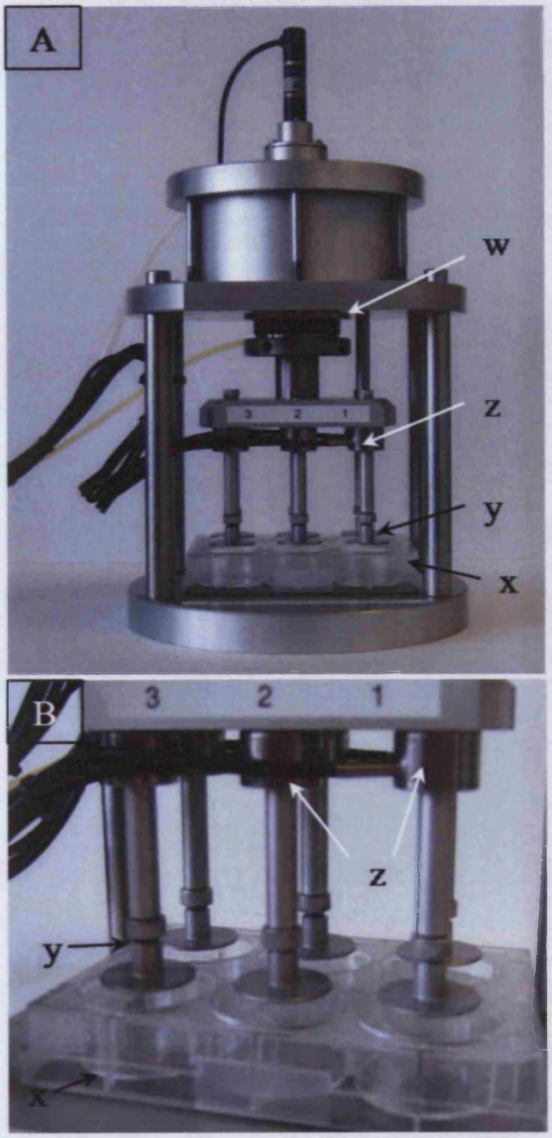

Figure 2.4:- The custom-made mechanical loading apparatus used for cyclic compressive loading of chondrocyte/agarose constructs. Six 25mm diameter aluminium compression plates (y) are controlled by a pneumatic compressor (w) and universal digital timer. A 6-well plate (x) containing chondrocyte/agarose plugs and culture media is placed beneath and compression plate height adjusted (y). Each well contains an individual load sensor (z) with output through a digital transformer.

2.7 Statistical Analyses

All statistical comparisons were performed using Minitab 15 software.

For comparison of normal to osteoarthritic cartilage or chondrocytes, treated to untreated chondrocytes, and loaded to unloaded chondrocytes, the Anderson Darling test for normality was performed for each group of data and the variance ratio (F-test) used to determine the equality of variance. A two-sample t test was used to compare data where both groups were normally distributed and had an equal variance. In the case that a group of data was not normally distributed, data was transformed logarithmically and tests for normality and equal variance were performed as before. If, following transformation, data was not normally distributed, comparisons of the medians of the untransformed data were performed using the non-parametric Mann-Whitney test.

Results are presented graphically as mean ± SEM. The number of samples used to produce data is indicated in the relevant figure legend. Data are significantly different at $p < 0.05$. Due to the higher variability associated with human samples p values < 0.10, although not significant, are included to show trends where an increase in n number could produce statistical significance.

Chapter 3: Characterisation of Normal and Osteoarthritic Cartilage: Cytoskeletal Element Profile and Extracellular Matrix Metabolism

3. CHARACTERISATION OF NORMAL AND OSTEOARTHRITIC CARTILAGE: CYTOSKELETAL ELEMENT PROFILE AND EXTRACELLULAR MATRIX METABOLISM

3.1 INTRODUCTION

As described in section 1.3.1.1.1, cartilage organisation and extracellular matrix (ECM) composition is altered in osteoarthritis (OA). The smooth surface is disrupted and fibrillated, with collagen fibres in the superficial zone significantly less parallel to the surface (Saarakkala et al., 2010). Proteoglycan is lost from the ECM and enzymatic cleavage of both aggrecan and collagen is increased as a result of a shift in the chondrocyte phenotype towards catabolism (section 1.3.1.1.2).

In addition to changes in cartilage organisation, ECM composition and chondrocyte phenotype, differences between the cytoskeletal architecture of normal and OA chondrocytes are becoming more evident. Differences in the cytoskeletal architecture of normal and OA chondrocytes have been observed in human OA (Fioravanti et al., 2003, Lambrecht et al., 2008) and a rat model of OA (Capin-Gutierrez et al., 2004) and the changes are discussed in section 1.5.

Using human normal and OA articular cartilage I sought to:

- Compare the tissue organisation, extracellular matrix composition and gene expression of normal and OA articular cartilage.
- Characterise the cytoskeletal differences between normal and OA chondrocytes, comparing the gene expression, protein expression and organisation of cytoskeletal proteins in normal and OA cartilage.

3.2 RESULTS

3.2.1 Articular Cartilage Organisation

3.2.1.1 Comparison of Normal and Osteoarthritic Cartilage

Normal healthy articular cartilage showed even alcian blue staining indicating that loss of glycosaminoglycan (GAGs) was minimal (Fig 3.1a). The articular surface appeared predominantly intact, although a small amount of disruption to the surface was observed. Chondrocytes were well separated with no signs of clustering. Osteoarthritic articular cartilage showed characteristic features of OA histopathology, with obvious disruption and fibrillation of the articular surface. Chondrocyte clusters were evident throughout the depth of the sample (Fig 3.1b). Loss of alcian blue staining occurred throughout the depth of the section but was most evident in the superficial zone, indicating the loss of GAG that is characteristic of OA. Remaining GAGs in the tissue were localised to the pericellular regions of the cartilage (Fig 3.1b). When examined histologically, normal samples, classed as such because post-mortem donors had no 'overt' symptoms of OA, showed a range of degradative changes (Fig 3.2). Only one sample of the eight normal samples examined histologically had no obvious loss of GAG (Fig 3.2a); two had a small loss in the superficial zone only (Fig 3.2b,c). These three samples had relatively intact surfaces with a small degree of surface disruption. Three samples showed clear loss of GAG from the superficial zone but little from the transitional and radial zones (Fig 3.2d-f). Fibrillation of the articular cartilage surface was also evident. Two samples had more extensive GAG loss, similar to that of the OA samples, with highly fibrillated surfaces, fissures and cell clusters (Fig 3.2g,h). Of note is that the normal and OA tissue sections (Fig 3.1) do not represent the full depth of the cartilage as samples were removed from the joints as shavings parallel to the articular surface. Most lack the calcified cartilage that lies above the subchondral bone and may therefore also lack some of the lower deep zone.

3.2.1.2 Comparison of Fibrillated and Non-fibrillated Regions within One Joint

Human articular cartilage was obtained post-mortem from the lateral tibial plateau of a donor with no 'overt' symptoms of osteoarthritis, i.e. had never presented to a GP with knee pain. However, macroscopically, regions of fibrillation were observed on the tibial plateaus. Therefore full-depth cartilage was sampled from both fibrillated and non-

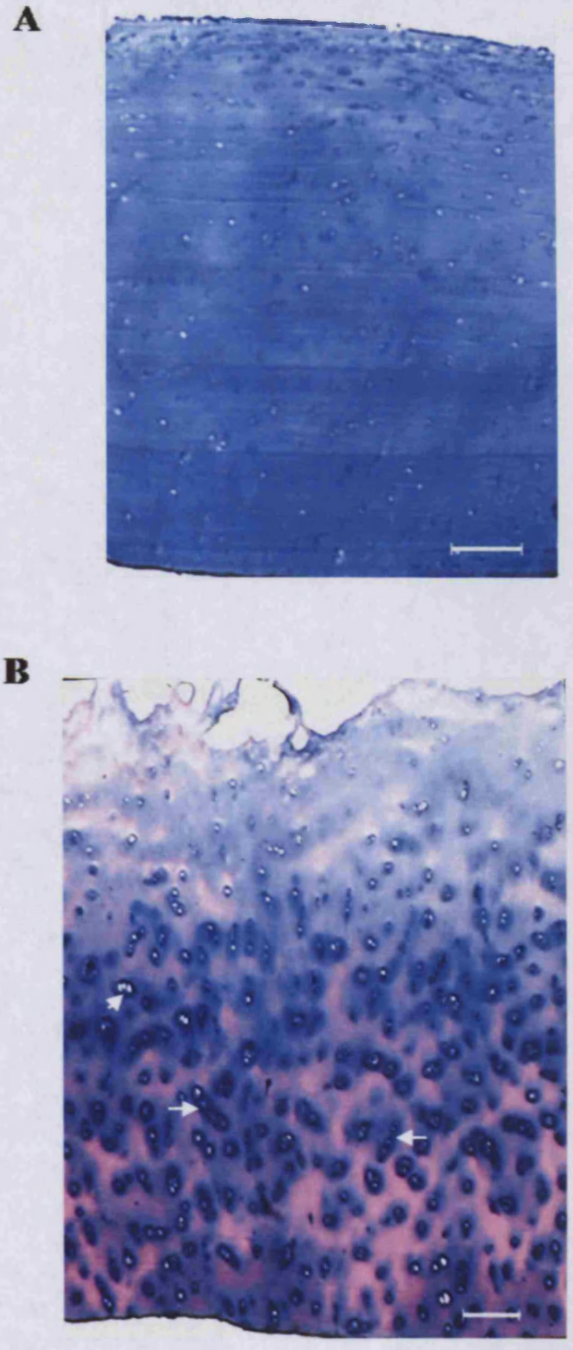

Figure 3.1:- Alcian blue staining of normal and osteoarthritic (OA) human articular cartilage, with tissue samples sectioned perpendicular to the articular surface to allow visualisation of zonal variations (Scale bars = 200μm). Differences in glycosaminoglycan (GAG) content and tissue organisation can be seen between normal and osteoarthritis tissue. **A**- Normal articular cartilage, showing even GAG content throughout and little disruption of the articular surface. **B**- Osteoarthritic articular cartilage, showing loss of GAG throughout, most apparent in the surface zone, with fibrillation of the articular surface and chondrocyte clusters (arrows).

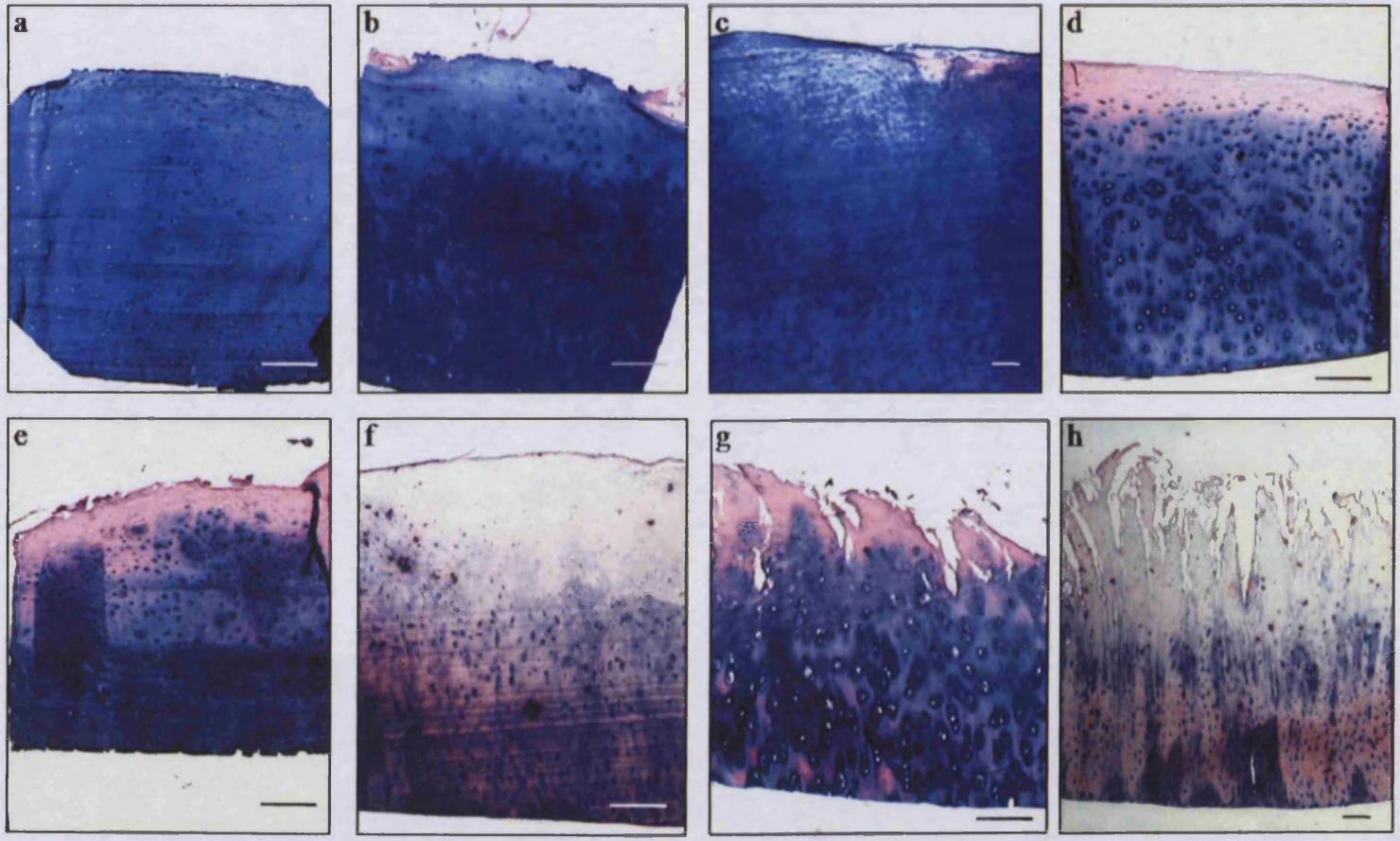

Figure 3.2:- Alcian blue staining of normal human articular cartilage, with tissue samples sectioned perpendicular to the articular surface to allow visualisation of zonal variations (Scale bars = 300μm). Normal samples, from individuals with 'no overt' symptoms of OA, demonstrated varying degrees of degradative changes with differences in glycosaminoglycan (GAG) content, surface fibrillation and tissue organisation.

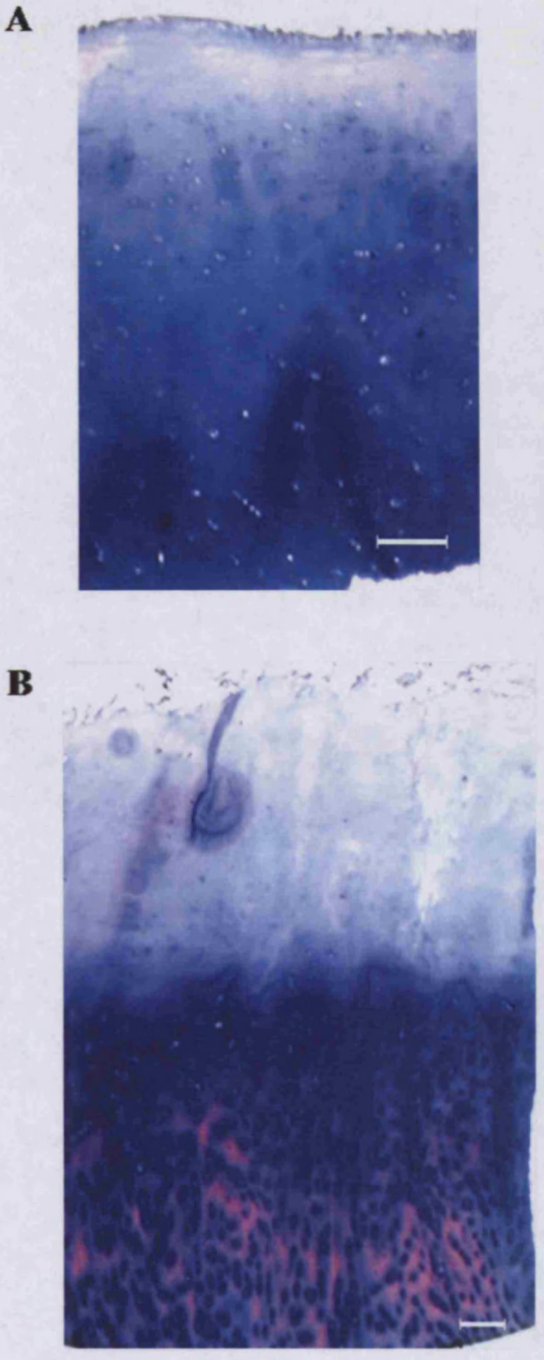

Figure 3.3:- Alcian blue staining of human articular cartilage from a macroscopically non-fibrillated (A) and fibrillated (B) region of a lateral tibial plateau obtained from an individual with no 'overt' symptoms of OA. Tissue samples were sectioned perpendicular to the articular surface to allow visualisation of zonal variations (Scale bars = 200μm). Differences in glycosaminoglycan (GAG) content and tissue organisation can be seen within the same joint.

fibrillated regions of the same lateral tibial plateau. Macroscopically non-fibrillated sections showed a small degree of disruption and fibrillation of the articular surface accompanied by a clear loss of alcian blue staining (i.e. loss of GAG) in the surface zone (Fig 3.3a). There was no loss of staining in the transitional and radial zones, although a small number of chondrocyte clusters were detected in these zones. Sections of fibrillated regions showed complete loss of alcian blue staining of the superficial zone and part of the transitional zone, although loss of staining was evident throughout the tissue depth (Fig 3.3b). As with OA cartilage, GAGs were localised to the pericellular regions and chondrocyte clustering occurred throughout the transitional and radial zones.

3.2.2 Composition of the Extracellular Matrix of Articular Cartilage

3.2.2.1 Water Content

The percentage water content of articular cartilage samples was determined by comparing wet weights to dry weights obtained following freeze-drying of the tissue. Results for normal and OA samples (n=9) were significantly different at the 94% confidence level ($p = 0.056$), with OA tissue containing more water compared to normal (Fig 3.4a).

3.2.2.2 Sulphated-Glycosaminoglycan Content

The sulphated-glycosaminoglycan (sGAG) content of tissue samples was determined using the DMMB assay (Farndale et al., 1986) and results normalised to the dry weight rather than wet weight of the tissue to remove any effect of the difference in water content. OA articular cartilage contained significantly less sGAG ($p = 0.013$, $n = 4$) when compared with normal tissue (Fig 3.4b). As physiologically normal and OA cartilage contain different amounts of water, a comparison of the sGAG content of tissue samples normalised to wet weight was also performed and showed OA cartilage to contain significantly less sGAG compared to normal ($p=0.036$, $n=9$).

3.2.2.3 Collagen Content

Articular cartilage collagen content was determined using an assay of hydroxyproline content, as this rare amino acid is only found in the triple-helical domains of collagen. Amounts of hydroxyproline were multiplied by seven to convert to amounts of collagen, based on an estimation of 14% hydroxyproline content of type II collagen (Leach, 1960). OA cartilage contained significantly more collagen per mg dry weight tissue than normal

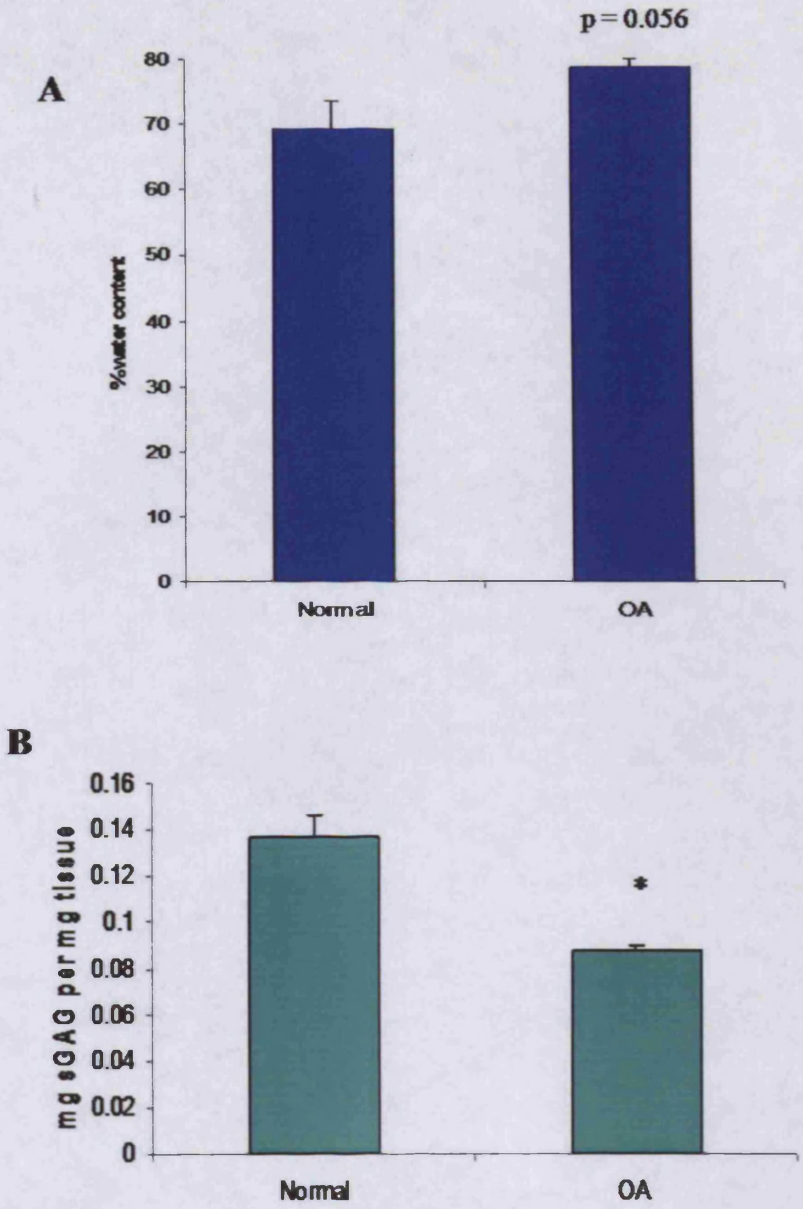

Figure 3.4:- Comparison of the biochemical composition of normal and osteoarthritic (OA) human articular cartilage. A- The percentage water content of normal and osteoarthritic tissue, determined using wet and dry weights (n=9). OA tissue contained more water than normal ($p = 0.056$). B- The amount (mg) of sulphated glycosaminoglycan per mg dry weight of tissue, as quantified by the DMMB assay (n=4). OA tissue contained significantly less sGAG than normal ($p = 0.013$). Data are expressed as mean ± S.E.M, * $p < 0.05$.

cartilage (Fig 3.5a; p=0.030, Mann-Whitney test). However, a comparison of collagen content per mg wet weight tissue revealed no difference between normal and OA articular cartilage (p=0.518).

The levels of type II collagen present in the insoluble portion of normal and osteoarthritic cartilage extracts were detected by Western Blotting. Type I collagen levels were below the limit of detection in most samples, regardless of pathology. There was no difference between the levels of type II collagen detected in normal and OA articular cartilage (Fig 3.5b).

3.2.2.4 Matrix Metalloproteinases and Inhibitors

Articular cartilage protein extracts were assayed for MMPs-2 and -9 content using gelatin zymography. Clear zones of gelatinolytic activity corresponding to both latent and active forms of MMP-2 were observed on gels (Fig 3.6a) and quantified by densitometry using NIH image software. Possible variations due to potential differences in SDS removal and MMP activation between gels was removed by normalising to the pro-MMP-2 standard common to each. Results for normal and OA protein extracts were compared (Fig 3.6b), with no difference found between either pro- (p=0.936) or active-MMP-2 (p=0.395). MMP-9 was not detected in any of the samples, even with increased protein loading.

The levels of TIMPs in protein extracts, quantified using reverse gelatin zymography, also showed little difference between normal and OA samples (Fig 3.7), with no significant difference in levels of TIMP-1 (p=0.801), TIMP-2 (p=0.559) or TIMP-3 (p=0.927).

3.2.3 Gene expression in Articular Cartilage

The expression profile of key genes involved in matrix turnover, previously shown to change in OA, was analysed in chondrocytes in normal and osteoarthritic articular cartilage by quantitative Taqman® PCR or quantitative PCR (qPCR) with SYBR green® (*MMP13*). RNA extracted directly from articular cartilage was used in qPCR reactions with primers and probes designed against genes of interest (Table 2.6, *MMP13* in Table 2.7). *GAPDH* expression showed little variation across samples and was used as an endogenous control. Relative expression units were calculated as described in section

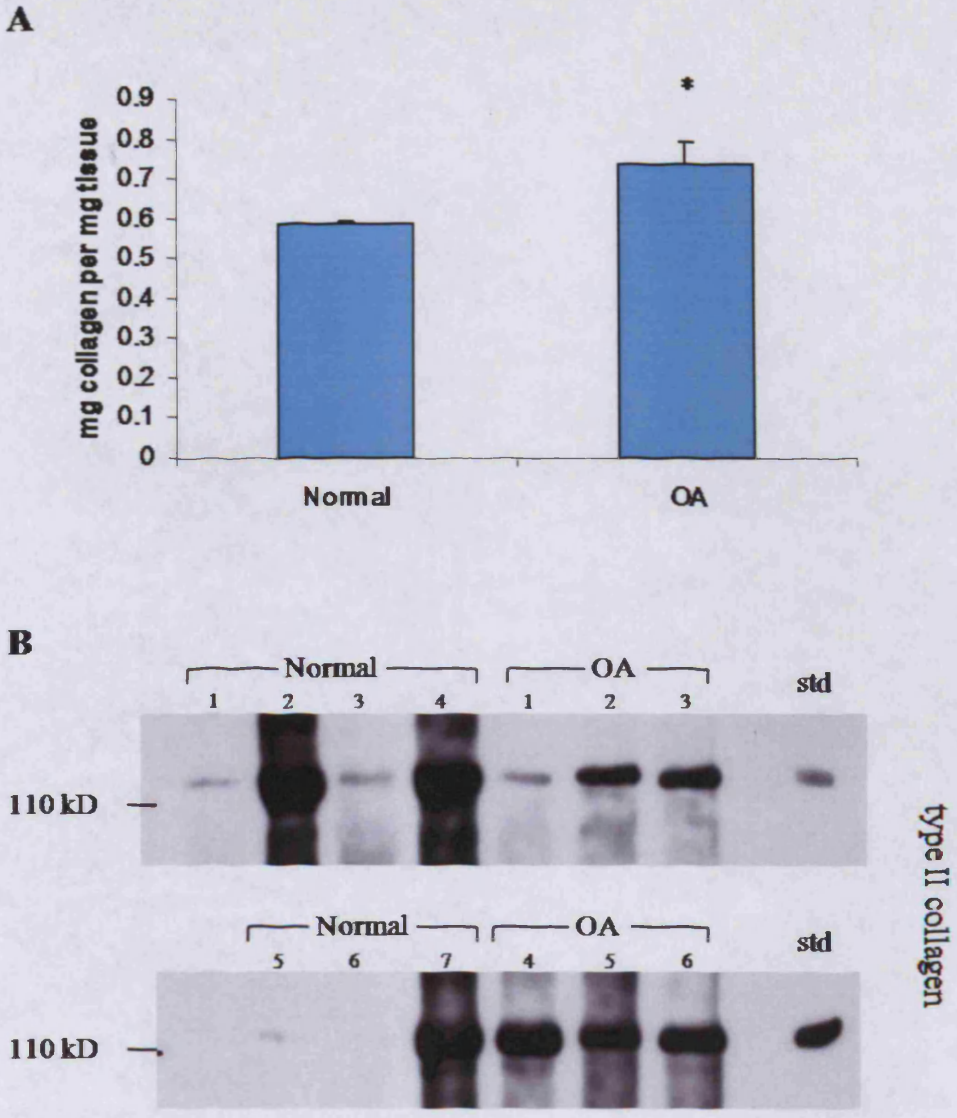

Figure 3.5:- Collagen content of normal and osteoarthritic (OA) human articular cartilage. **A**- The amount of collagen (mg) per mg dry weight of tissue, as determined by assay of hydroxyproline content (n=4), showed an increased collagen content in OA tissue compared to normal ($p = 0.030$, Mann-Whitney test). Data are expressed as mean ± S.E.M, * $p < 0.05$. **B**- Western blots of guanidine-insoluble type II collagen present in normal (n=7) and OA (n=6) human articular cartilage extracts. Equivalent amounts of collagen (2μg of hydroxyproline) were loaded, along with a type II collagen standard (std) and detected using the mouse monoclonal antibody AVT6E3 and a sheep anti-mouse IgG secondary antibody.

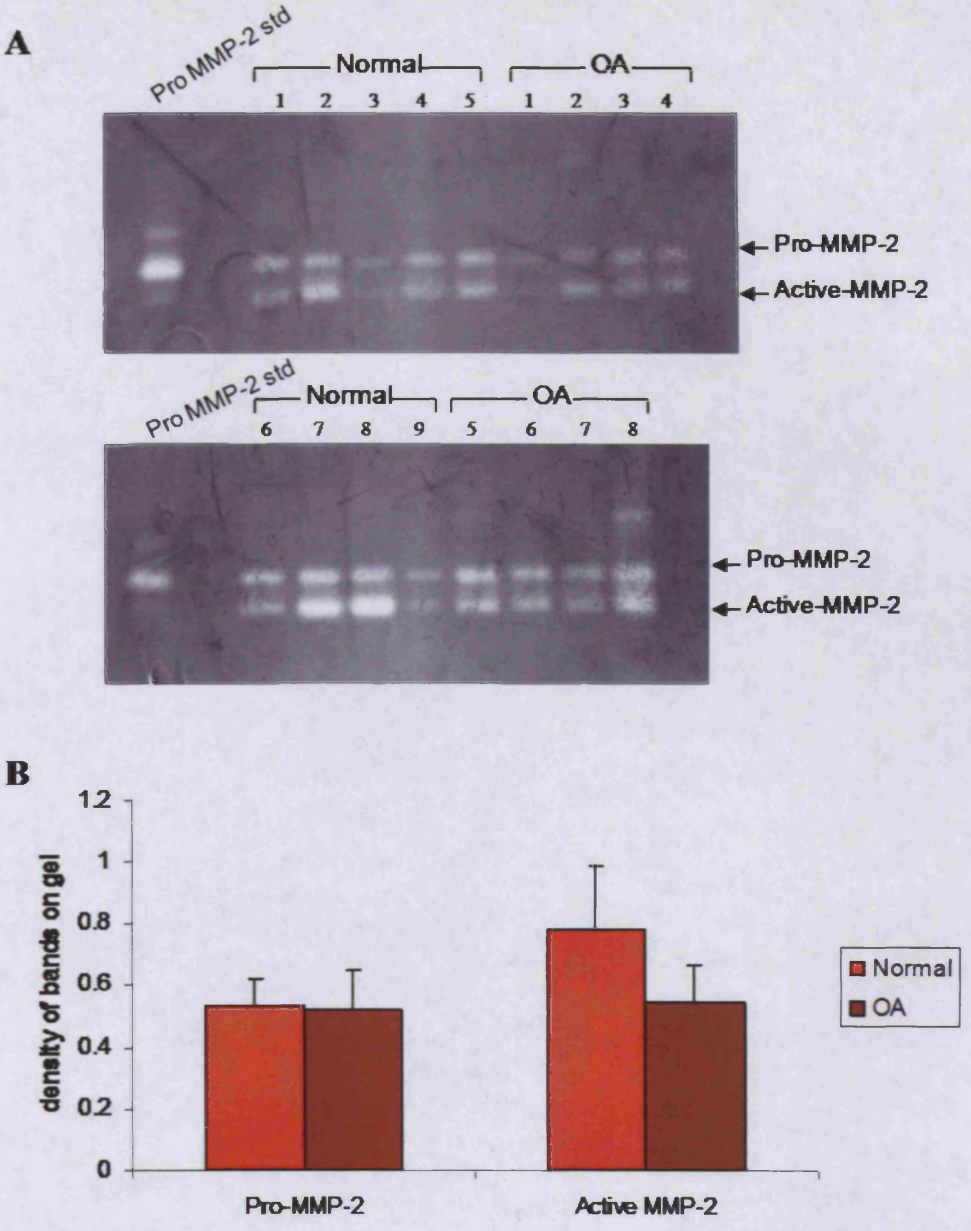

Figure 3.6:- Quantification of the MMP-2 content of normal and osteoarthritic (OA) human articular cartilage (normal, n = 9. OA, n = 8). A- Gelatin substrate zymography was used to detect the latent (72kD) and active (62kD) forms of MMP-2 , with white bands representing zones of gelatinolytic activity. Equivalent amounts of protein (5µg) were loaded. B- Bands from gelatin zymography (A) were quantified by densitometry using NIH image software and values normalised to the pro-MMP-2 standard loaded on the relevant gel. There was no difference in pro- ($p = 0.936$) or active MMP-2 ($p = 0.395$) between normal and OA articular cartilage. MMP-9 was not detected.

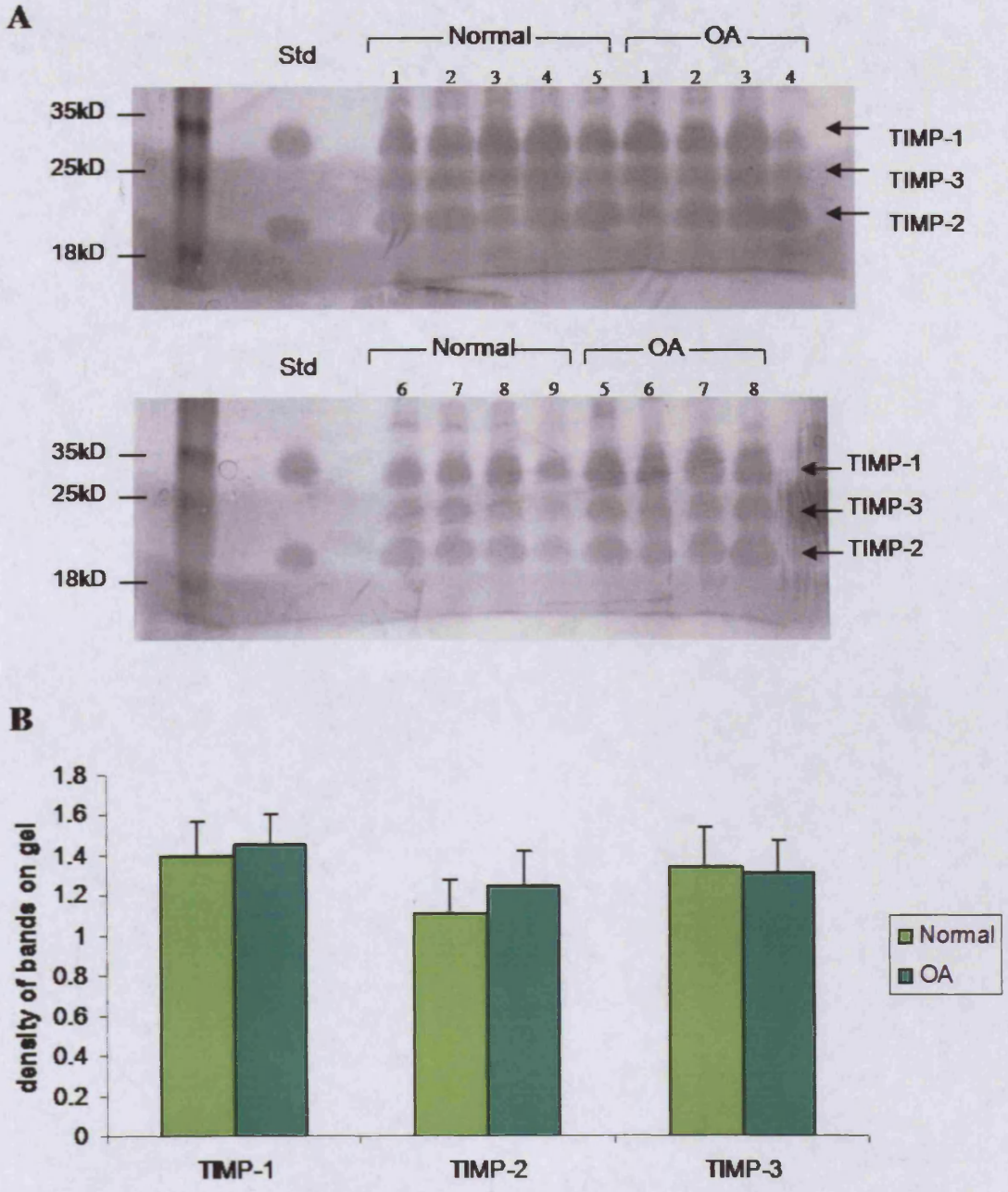

Figure 3.7:- Quantification of the TIMP content of normal and osteoarthritic (OA) human articular cartilage (normal, n = 9. OA, n = 8). A- Gelatin reverse zymography was used to detect TIMPs -1, -2, and -3, with dark bands representing zones of inhibition of gelatinolytic activity. Equivalent amounts of protein (5µg) were loaded. B- Bands from reverse zymography (A) were quantified by densitometry using NIH image software and values normalised to the TIMP-1 standard loaded on the relevant gel. There was no difference in TIMP-1 ($p = 0.801$), TIMP-2 ($p = 0.559$) or TIMP-3 ($p = 0.927$) between normal and OA articular cartilage.

2.4.2.2.1. Expression of *COL2A1* and *MMP13* was significantly higher in OA cartilage compared to normal (Fig 3.8a; $p<0.001$ and $p=0.016$ respectively), while *SOX9* expression was significantly lower in OA cartilage compared to normal ($p=0.001$). The expression of vascular endothelial growth factor (*VEGF*) and the aggrecanase ADAMTS-5 were also significantly decreased in OA cartilage compared to normal ($p=0.005$ and $p=0.037$ respectively) (Fig 3.8b). There was no difference in aggrecan (*ACAN*) expression between normal and OA cartilage ($p=0.293$).

3.2.4 Optimisation of Fixation Protocols

In order to determine the optimal fixation protocol for preservation of all three cytoskeletal elements, four different protocols were tested using frozen immature bovine cartilage sections.

3.2.4.1 Distribution of Cytoskeletal Protein Labelling

Young bovine articular cartilage sections fixed with paraformaldehyde (PFA) and permeabilised with cold methanol, with PBS as the buffer, showed uniform phalloidin fluorescence throughout the tissue zones, whilst vimentin and tubulin staining was brightest around the edges of the sections (data not shown). This was not observed in sections fixed with PFA and permeabilised with Triton® X-100 in the presence of buffer 1 (Zwicky and Baici, 2000) and could therefore simply represent a less effective mode of permeabilisation. Staining of all three cytoskeletal elements was throughout the tissue sections fixed in buffer 1, although tubulin staining was weak which may be due to a lack of microtubule preservation. Sections fixed with glutaraldehyde and permeabilised with Triton® X-100 in buffer 2 (Zwicky and Baici, 2000) or in mHBSS (Blanc et al., 2005) also showed labelling of the cytoskeletal elements throughout the tissue depth, although in sections fixed in mHBSS, tubulin staining in the deep zone was brighter (data not shown).

3.2.4.2 Cytoskeletal Organisation

For determination of the effects of different fixation protocols on cytoskeletal organisation, four chondrocytes from the mid or deep zone were viewed using a confocal microscope and a representative cell scanned for presentation.

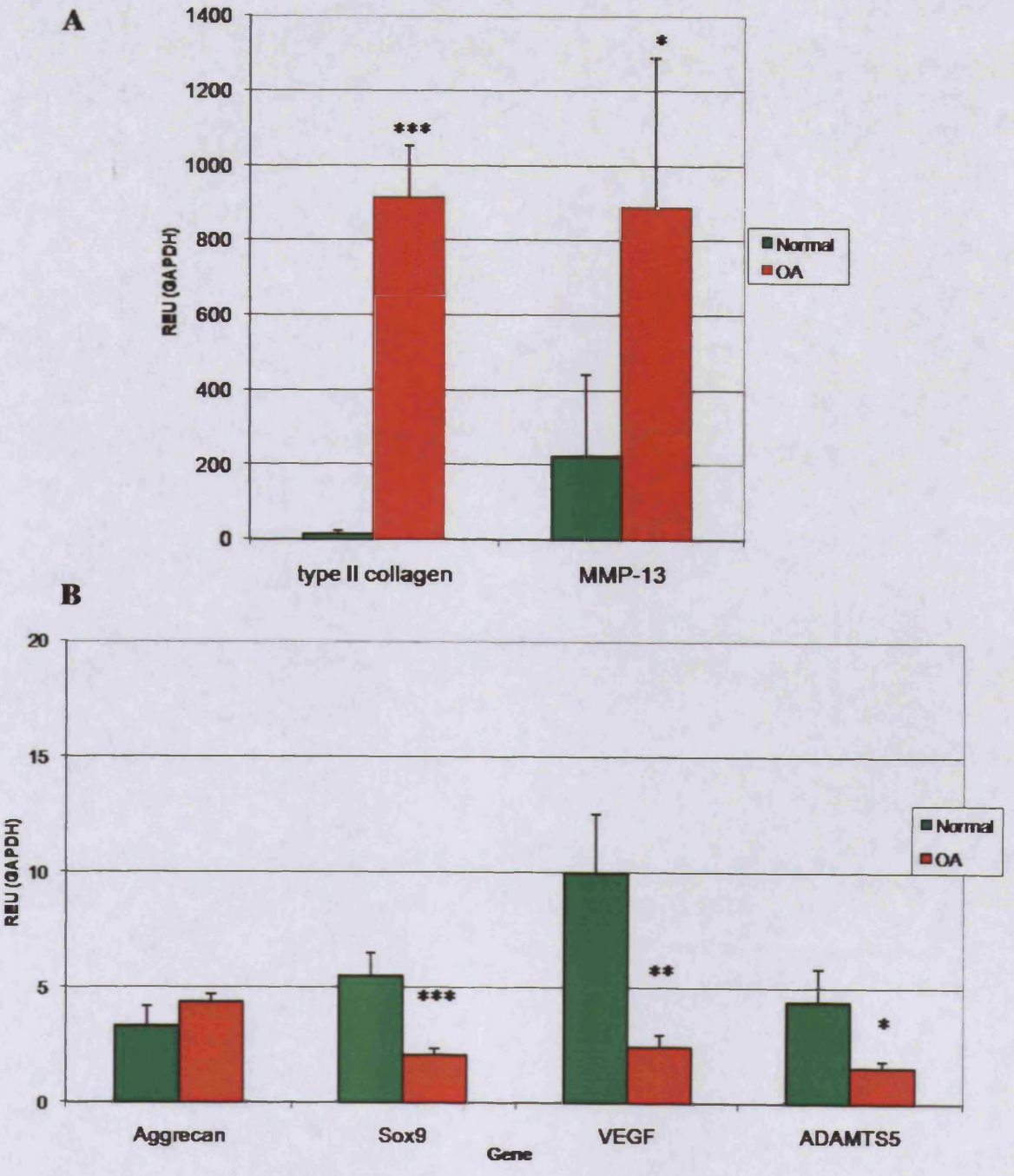

Figure 3.8:- Gene expression in normal (green) and osteoarthritic (red) articular cartilage, determined using quantitative Taqman™ PCR with RNA extracted directly from cartilage tissue (graphs show mean ± S.E.M, n=7, with the exception of n=6 for normal *ADAMTS5*). **A**- *COL2A1* and *MMP13* expression are significantly increased in osteoarthritic articular cartilage compared to normal. **B**- Osteoarthritic articular cartilage expressed significantly less *SOX9*, *VEGF* and *ADAMTS5* compared to normal. There was no difference in aggrecan mRNA expression between normal and osteoarthritic articular cartilage. *$p<0.05$, **$p<0.01$, ***$p<0.001$.

3.2.4.2.1 Actin

Young bovine articular cartilage sections fixed with paraformaldehyde and permeabilised with cold methanol (phosphate buffered saline (PBS) was used as the buffer) showed diffuse staining with some evidence of filament bundles at the periphery of the chondrocyte (Fig 3.9a). Staining appeared close to the nucleus (Fig 3.9b), although it was unclear whether this represented collapse of the microfilaments around the nucleus or diffuse staining extending from the nucleus to the plasma membrane. Chondrocytes in tissue fixed with paraformaldehyde but permeabilised with Triton® X-100 and washed in buffer 1 (Zwicky and Baici, 2000) showed a better preservation of the microfilament network, with staining less condensed around the nucleus and punctate at the cell periphery (Fig 3.9d). Diffuse staining was again observed throughout the cytoplasm, and fluorescence was also closely associated with the nucleus (Fig 3.9e). Preservation of actin microfilaments with glutaraldehyde in buffer 2 (Zwicky and Baici, 2000) was poor, with weak fluorescence that was diffuse and close to the nucleus (Fig 3.9h). However, the use of glutaraldehyde and Triton® X-100 in modified Hank's balanced salt solution (mHBSS) (Blanc et al., 2005) appeared to more effectively preserve the microfilament organisation. Staining was bright and extended throughout the cytoplasm, with a fine punctate appearance at the periphery (Fig 3.9j), and the actin cytoskeleton no longer appeared condensed around the nucleus (Fig 3.9k,l).

3.2.4.2.2 β-tubulin

In young bovine articular cartilage sections fixed with paraformaldehyde and permeabilised with cold methanol in the presence of PBS, microtubules were located close to the nucleus (Fig 3.10b), with a punctate appearance both at the periphery (Fig 3.10a) and throughout the cytoplasm that appeared loosely packed (Fig 3.10c). Microtubule organisation was most poorly preserved by fixation in paraformaldehyde (PFA) and permeabilisation with Triton® X-100 in buffer 1 (Zwicky and Baici, 2000), which resulted in very weak staining with a small number of dense, bright foci of fluorescence (Fig 3.10d-f). Cartilage chondrocytes fixed with glutaraldehyde and permeabilised with Triton® X-100 in the presence of buffer 2 (Zwicky and Baici, 2000) showed a better preservation of the microtubule network, with brighter staining throughout the cytoplasm. There was little evidence of filament bundles, and staining still appeared condensed around the nucleus (Fig 3.10g-i). As with actin microfilaments, simultaneous fixation and permeabilisation with glutaraldehyde and Triton® X-100 but

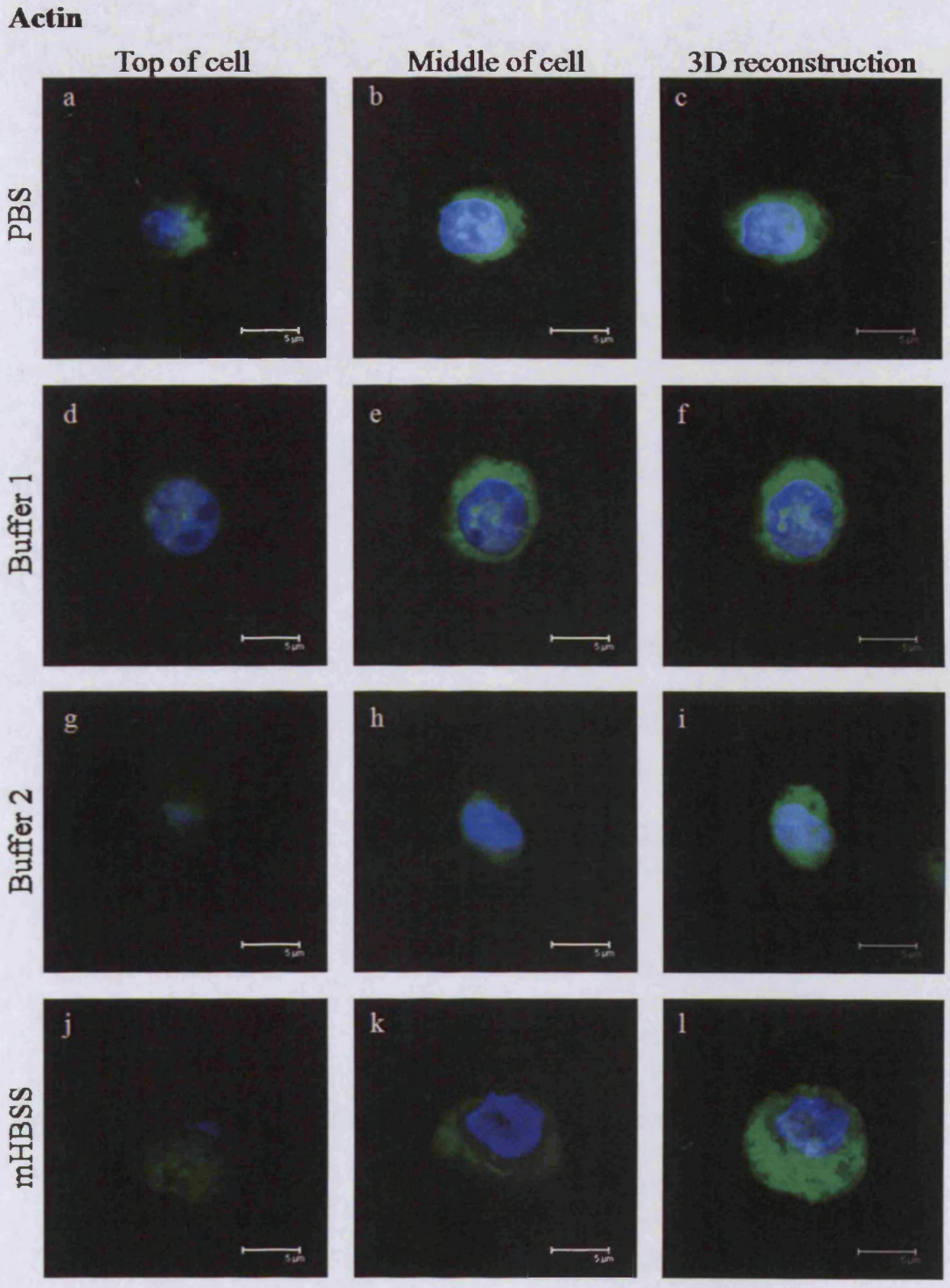

Figure 3.9:- The effect of different fixation protocols on the preservation of the actin cytoskeleton in young bovine articular cartilage chondrocytes *in situ*. Actin microfilaments were visualised using FITC-conjugated phalloidin (green) and nuclei counterstained with DAPI (blue). PBS- paraformaldehyde (PFA) fixed and permeabilised with cold methanol (a-c), Buffer 1- PFA fixed and permeabilised with Triton® X-100 (d-f), Buffer 2 (g-i) and mHBSS (j-l)- glutaraldehyde fixed and permeabilised with Triton® X-100. The mHBSS protocol best preserved actin microfilament organisation.

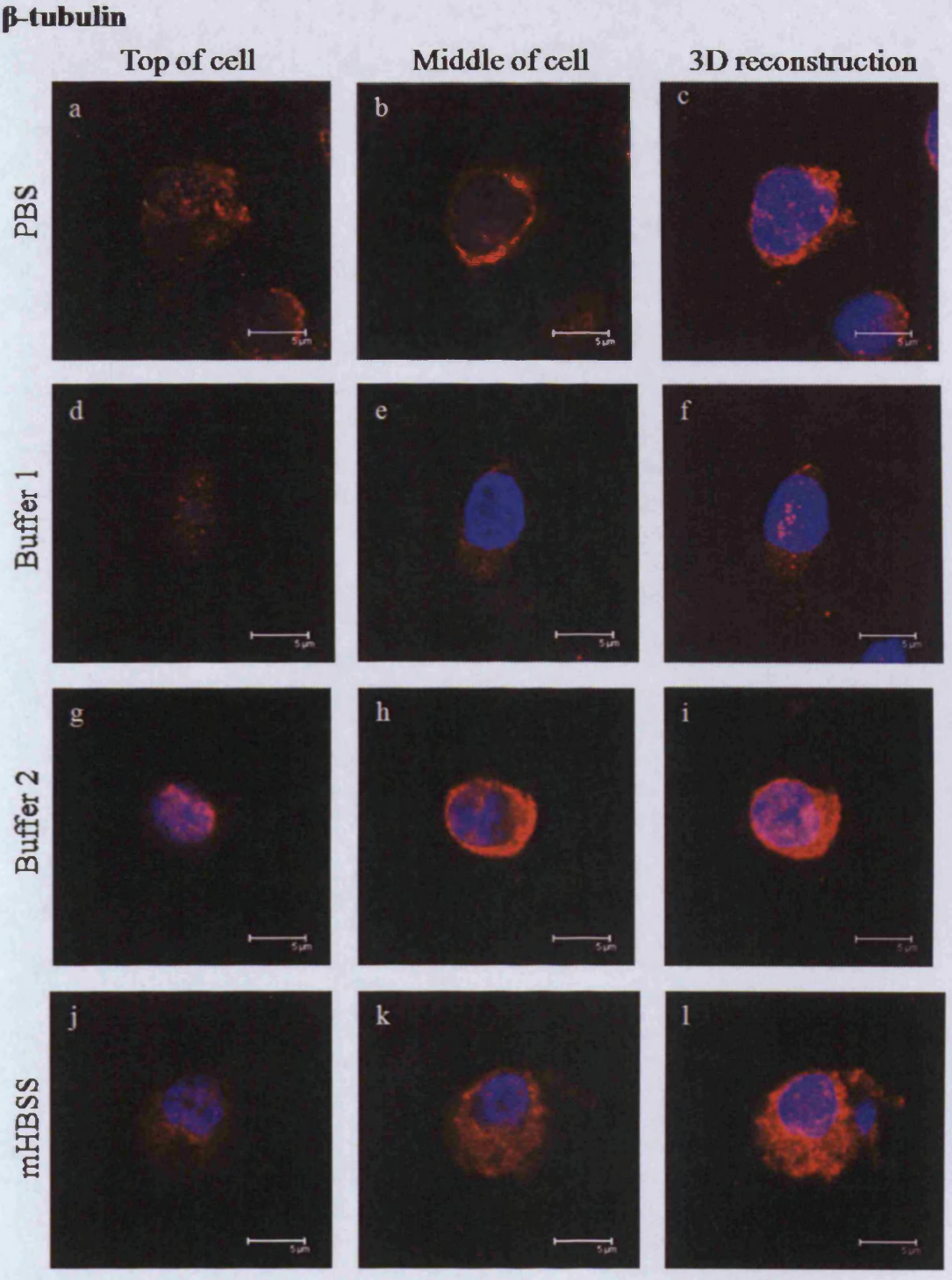

Figure 3.10:- The effect of different fixation protocols on the preservation of the tubulin cytoskeleton in bovine articular cartilage chondrocytes *in situ*. Tubulin microtubules were visualised using anti-β-tubulin primary antibody followed by TRITC-conjugated anti-mouse IgG secondary antibody (red), with nuclei counterstained with DAPI (blue). PBS-paraformaldehyde (PFA) fixed and permeabilised with cold methanol (a-c), Buffer 1- PFA fixed and permeabilised with Triton® X-100 (d-f), Buffer 2 (g-i) and mHBSS (j-l)-glutaraldehyde fixed and permeabilised with Triton ® X-100. The mHBSS protocol best preserved tubulin microtubule organisation.

in the presence of mHBSS as a buffer (Blanc et al., 2005) appeared to best preserve microtubule organisation. Staining was fine and punctate throughout the cytoplasm and, as with actin microfilaments (Fig 3.9j-l), microtubules no longer appeared condensed around the nucleus (Fig 3.10j-l), although there were no obvious filament bundles.

3.2.4.2.3 Vimentin

In young bovine articular cartilage sections, vimentin staining was strong and fluorescence bright with all fixatives and buffers used. Sections fixed with PFA and permeabilised with Triton® X-100 in PBS showed dense staining around the nucleus (Fig 3.11b) with thick, loose filament bundles at the periphery (Fig 3.11a). Chondrocytes in tissue fixed with PFA but permeabilised with Triton® X-100 and in buffer 1 (Zwicky and Baici, 2000) had preserved vimentin intermediate filament bundles that were less condensed around the nucleus than those in PBS (Fig 3.11d-f). Fixation using glutaraldehyde in buffer 2 (Zwicky and Baici, 2000) also preserved the filamentous organisation of the vimentin cytoskeleton, showing a network of filament bundles extending from the nucleus to the plasma membrane (Fig 3.11h). Sections fixed with glutaraldehyde but in mHBSS showed little difference to those fixed in the presence of buffer 2, with a meshwork of filament bundles extending throughout the cytoplasm of the chondrocyte (Fig 3.11j-l).

Collectively, the preservation of all three cytoskeletal elements was best following simultaneous permeabilisation with Triton® X-100 and fixation with glutaraldehyde in mHBSS (Blanc et al., 2005). This protocol was therefore used for subsequent studies.

3.2.5 Cytoskeletal Organisation of Human Chondrocytes *in situ*

3.2.5.1 Comparison of Normal and Osteoarthritic Chondrocytes

Full depth cartilage biopsies were collected from the same region of the tibial plateau of four normal and four osteoarthritic donors. Human articular cartilage sections were simultaneously fixed and permeabilised in glutaraldehyde and Triton® X-100 in mHBSS buffer (Blanc et al., 2005). Three chondrocytes from the superficial, middle and deep zones were scanned from each of the donors. Images were 'blind' scored by two independent individuals. Scores between one and five were assigned to cell images according to the criteria in Figure 3.12. Images used to score each cell were single scans through the edge and centre of the cell, along with 3D reconstructions of the series of

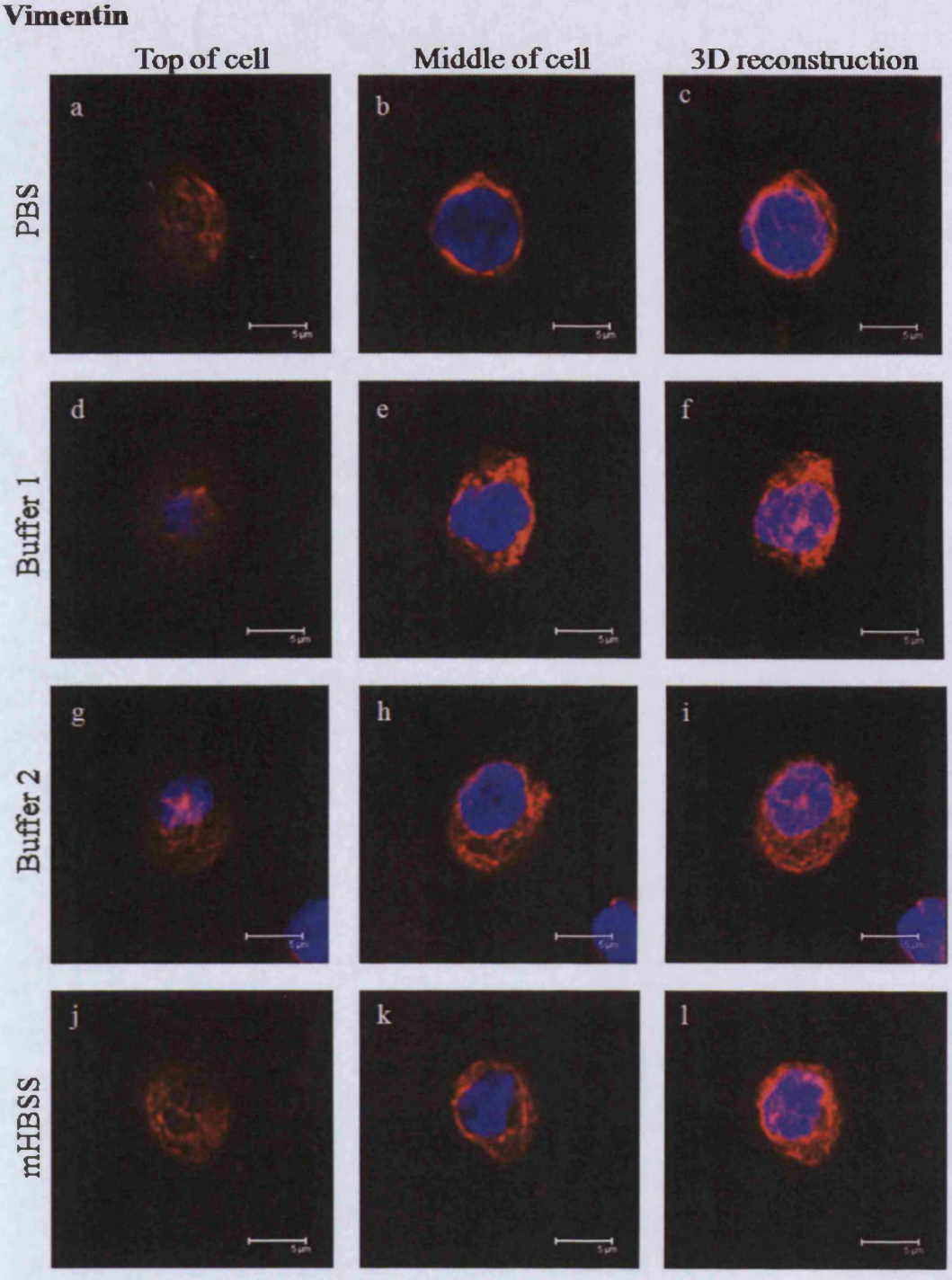

Figure 3.11:- The effect of different fixation protocols on the preservation of the vimentin cytoskeleton in bovine articular cartilage chondrocytes *in situ*. Vimentin intermediate filaments were visualised using anti-vimentin primary antibody followed by TRITC-conjugated anti-mouse IgG secondary antibody (red), with nuclei counterstained with DAPI (blue). PBS-paraformaldehyde (PFA) fixed and permeabilised with cold methanol (a-c), Buffer 1- PFA fixed and permeabilised with Triton® X-100 (d-f), Buffer 2 (g-i) and mHBSS (j-l)- glutaraldehyde fixed and permeabilised with Triton ® X-100. The mHBSS protocol best preserved vimentin intermediate filament organisation.

Figure 3.12:- Images and criteria used to 'blind' score the organisation of the actin (**A**), tubulin (**B**) and vimentin (**C**) elements of the cytoskeleton of human articular chondrocytes *in situ*. A score was assigned to each chondrocyte by two independent individuals using single scans from the edge and centre of cells, along with 3D reconstructions of the series of scans across the depth of the cell.

Actin

Score	3D reconstruction	Centre of cell	Descriptive Criteria
2	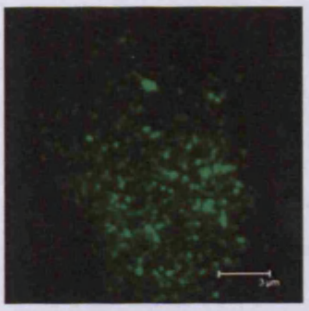	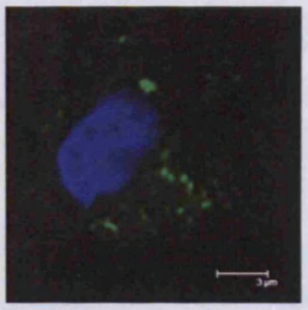	• sharp punctate spots • cytoplasmic localisation • no evidence of peripheral organisation
3	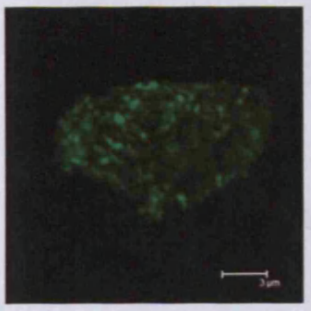	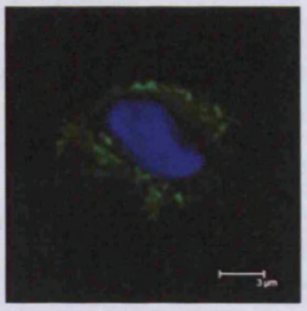	• punctate spots • some cytoplasmic localisation • some evidence of peripheral organisation but not continuous
4	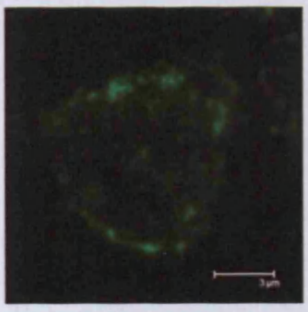	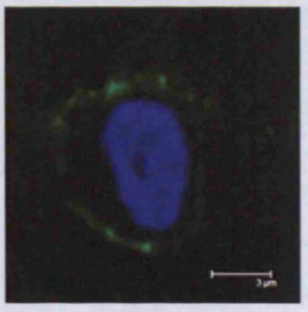	
5	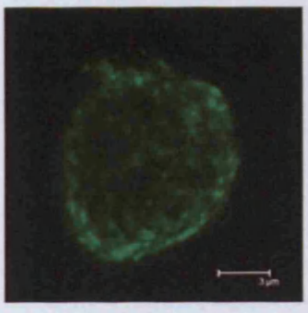	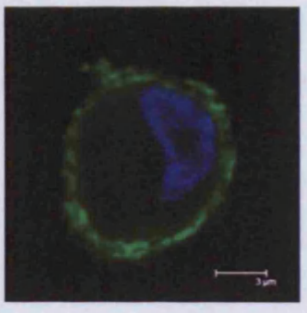	• intense peripheral stain • punctate • continuity of label at the periphery

Tubulin

Score	3D reconstruction	Centre of cell	Descriptive Criteria
1	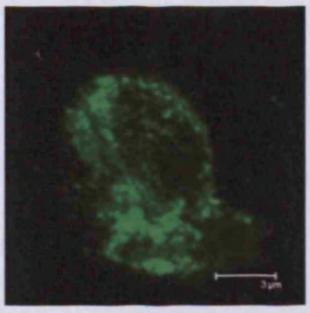	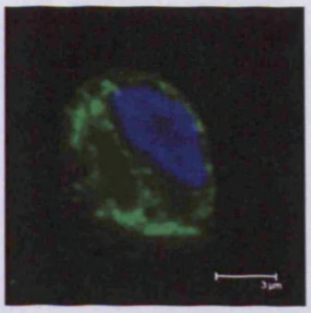	• no visible networks • extensive punctate staining • voids in cytoplasm
2	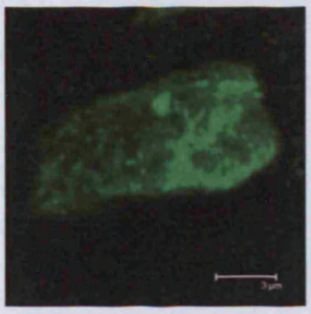	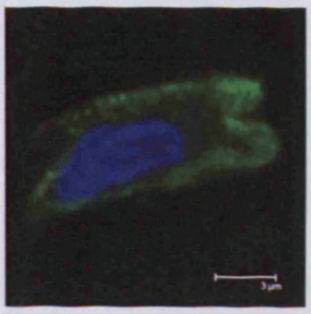	
3	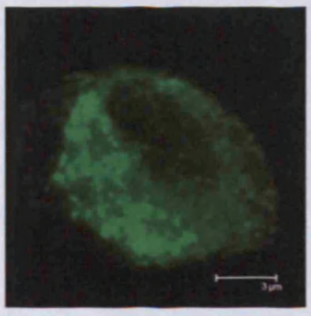	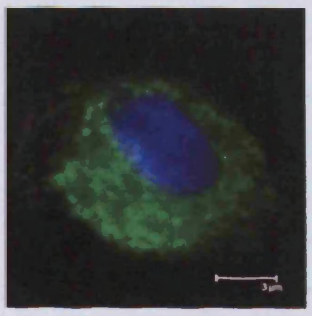	• some networks visible • some punctate staining • voids in cytoplasm
4	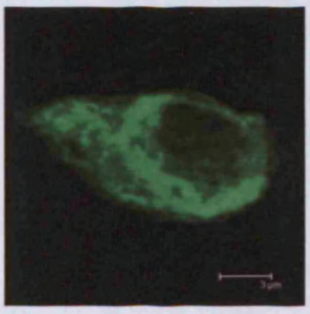	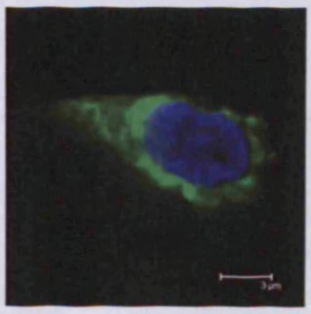	
5	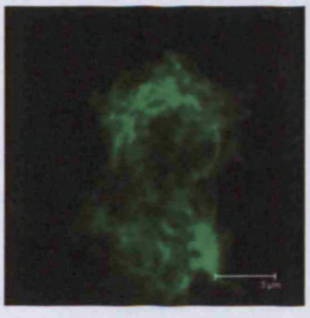	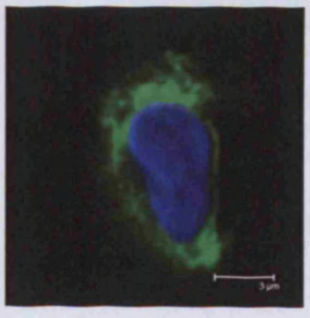	• networks visible and extend through the cytoplasm • no voids

Vimentin

Score	3D reconstruction	Centre of cell	Descriptive Criteria
1	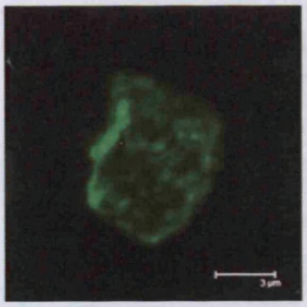	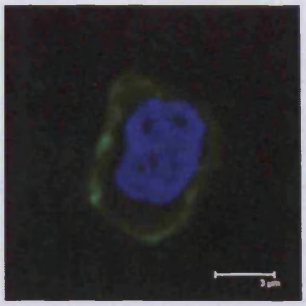	• no obvious filaments • no visible networks
2	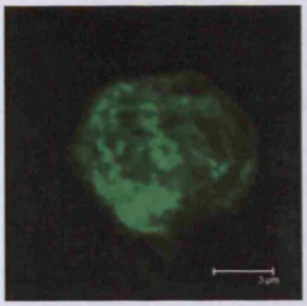	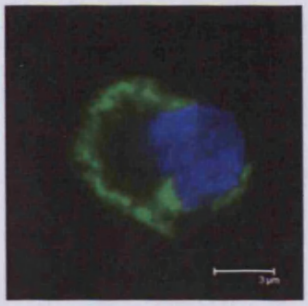	
3	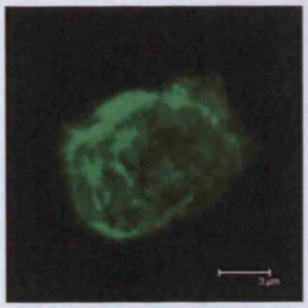	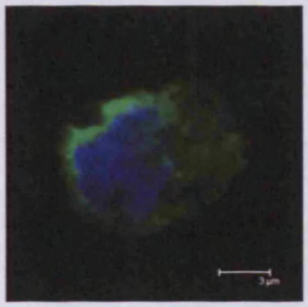	• some filaments visible • some networks visible but not throughout the cytoplasm
4	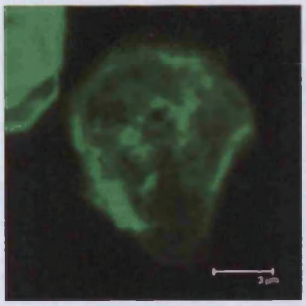	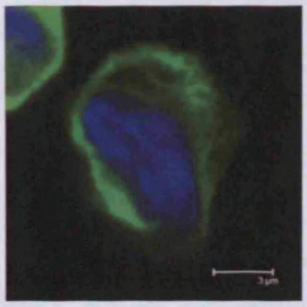	
5	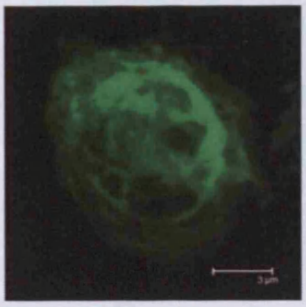	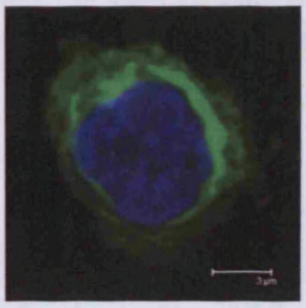	• intact filaments extend throughout the cytoplasm • networks visible

scans across the depth of the chondrocyte.

3.2.5.1.1 Distribution of Labelling in Cartilage Zones

Low power images of normal and osteoarthritic human articular cartilage illustrated the distribution of the fluorescently labelled cytoskeletal elements. Cells throughout the depth of both normal and OA human articular cartilage labelled for actin microfilaments (Fig 3.13a-d). In OA cartilage, actin staining of clustered chondrocytes around surface fibrillations appeared brighter than other cells in OA and normal cartilage (Fig 3.13c). Tubulin staining was fainter but not absent in chondrocytes of the superficial and upper-mid zone of normal cartilage (Fig 3.13e) compared to lower-mid and deep zone chondrocytes (Fig 3.13f). This was not the case in OA cartilage, which showed brighter tubulin labelling in the chondrocytes surrounding surface fibrillations (Fig 3.13g). The superficial and upper-mid zone of normal cartilage also showed fainter vimentin staining, with brighter staining extending into the deep zone (Fig 3.13i). This was not observed in OA cartilage where vimentin labelling was evident throughout the depth of the tissue, although it did appear brighter in the deep zone (Fig 3.13k,l).

3.2.5.1.2 Actin Microfilament Organisation

In mature human normal articular cartilage chondrocytes the actin microfilaments were bright and punctate at the cell periphery (Fig 3.14 a and c). Punctate staining was often observed throughout the cytoplasm, extending from beneath the plasma membrane to the nucleus (Fig 3.14b). The typical organisation of actin microfilaments in osteoarthritic articular cartilage chondrocytes showed less defined punctate spots at the cell periphery (Fig 3.14 d and f) and, unlike that seen more typically in normal chondrocytes, fluorescence was predominantly localised cortically (Fig 3.14e). Scoring of chondrocytes in the superficial, middle and deep zones showed a significant difference in actin microfilament architecture between normal and OA deep zone chondrocytes ($p=0.042$) (Fig 3.14g).

3.2.5.1.3 Tubulin Microtubule Organisation

In normal human articular cartilage chondrocytes typical tubulin staining was visualised as a tightly packed, fine filamentous meshwork of microtubule bundles extending throughout the cytoplasm (Fig 3.15 a-c). In OA chondrocytes microtubule bundles were less clear. Microtubules were observed, but staining was more punctate than that typically observed in normal chondrocytes (Fig 3.15d) and was often more evident in the

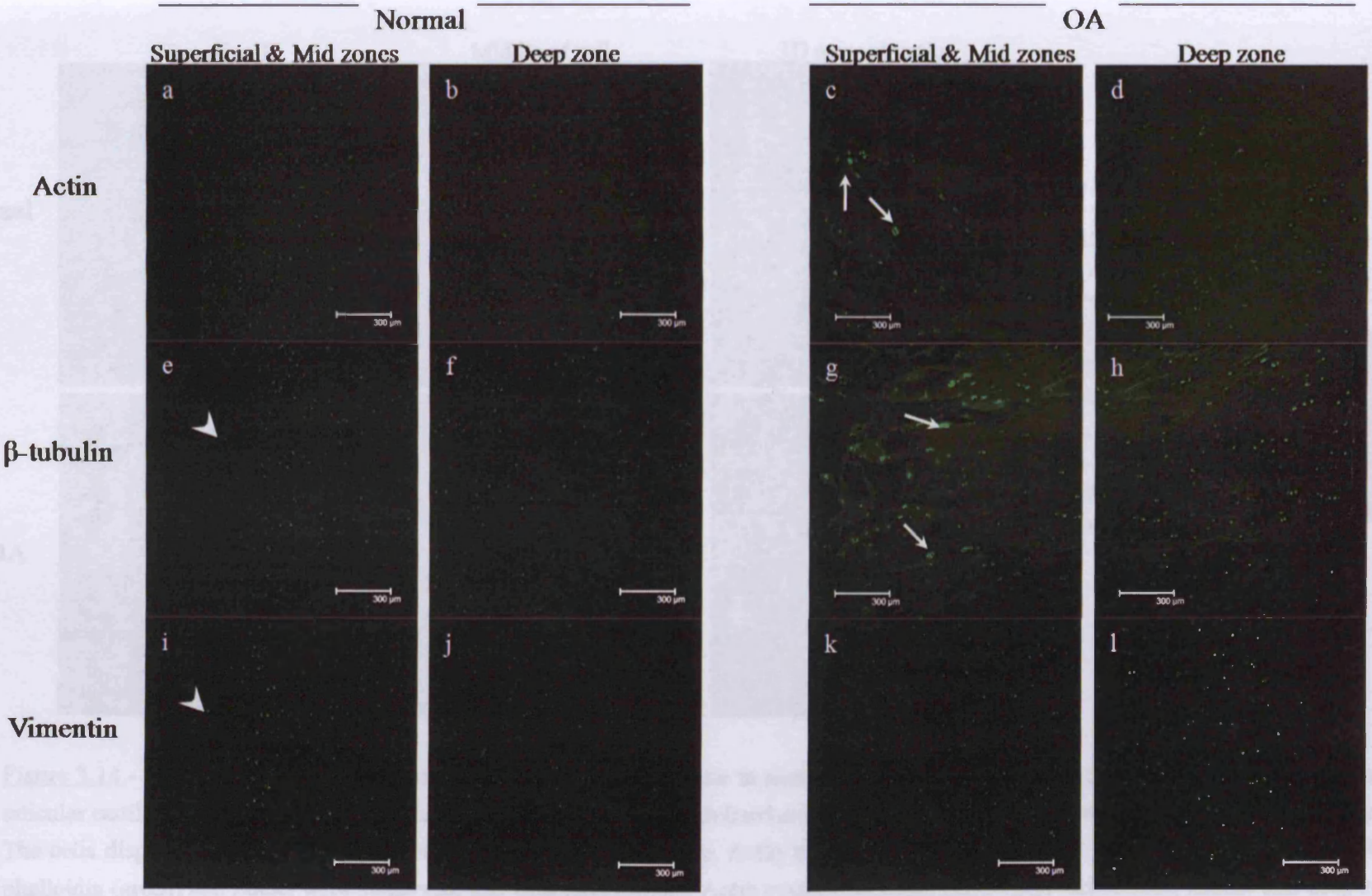

Figure 3.13:- Comparison of the distribution of cytoskeletal elements through the depth of normal and osteoarthritic (OA) human articular cartilage. There was a difference in cytoskeletal labelling intensity in the surface and upper-mid zone chondrocytes (arrow heads) and in chondrocytes surrounding surface fibrillations in OA tissue (arrows). Actin (a-d) was detected with Alexa Fluor 488-phalloidin. Tubulin (e-h) and vimentin (i-l) were detected indirectly with primary antibodies and TRITC-conjugated secondary antibody.

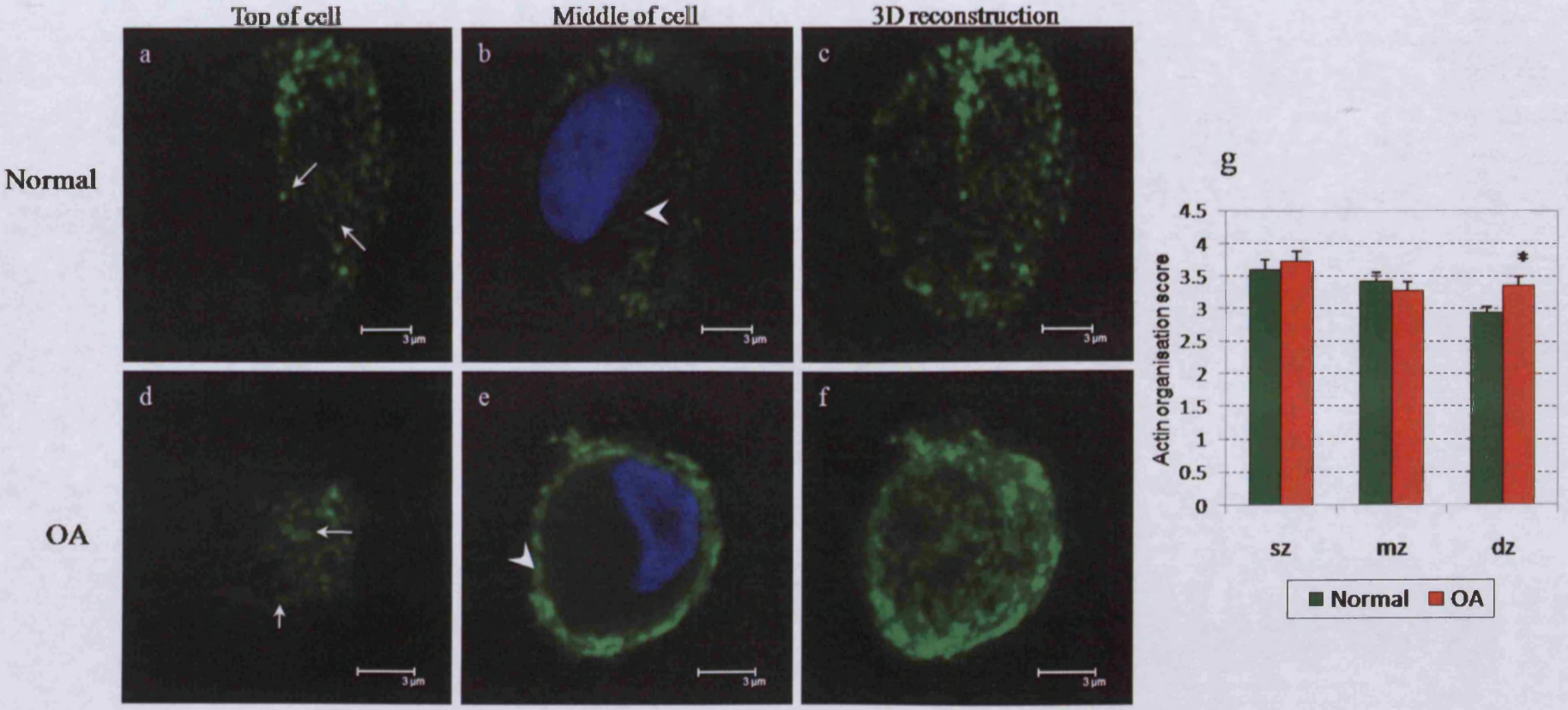

Figure 3.14:- Comparison of the organisation of the actin cytoskeleton in normal (a-c) and osteoarthritic (d-f) chondrocytes from human articular cartilage (20µm sections). Punctate spots (arrows) were less defined and predominantly cortical (arrow heads) in OA chondrocytes. The cells displayed are from the mid (a-c) and superficial (d-f) zone. Actin microfilaments were directly stained with Alexa Fluor 488-phalloidin (green) and nuclei were counterstained with DAPI (blue). Actin organisation was scored and superficial, middle and deep zone normal and OA chondrocyte scores compared to reveal a significant difference between normal and OA in deep zone chondrocytes (g): 3 cells were scored for each zone, from each of the 4 normal and 4 OA donors (n=12). Graphs show mean ± S.E.M. * $p < 0.05$.

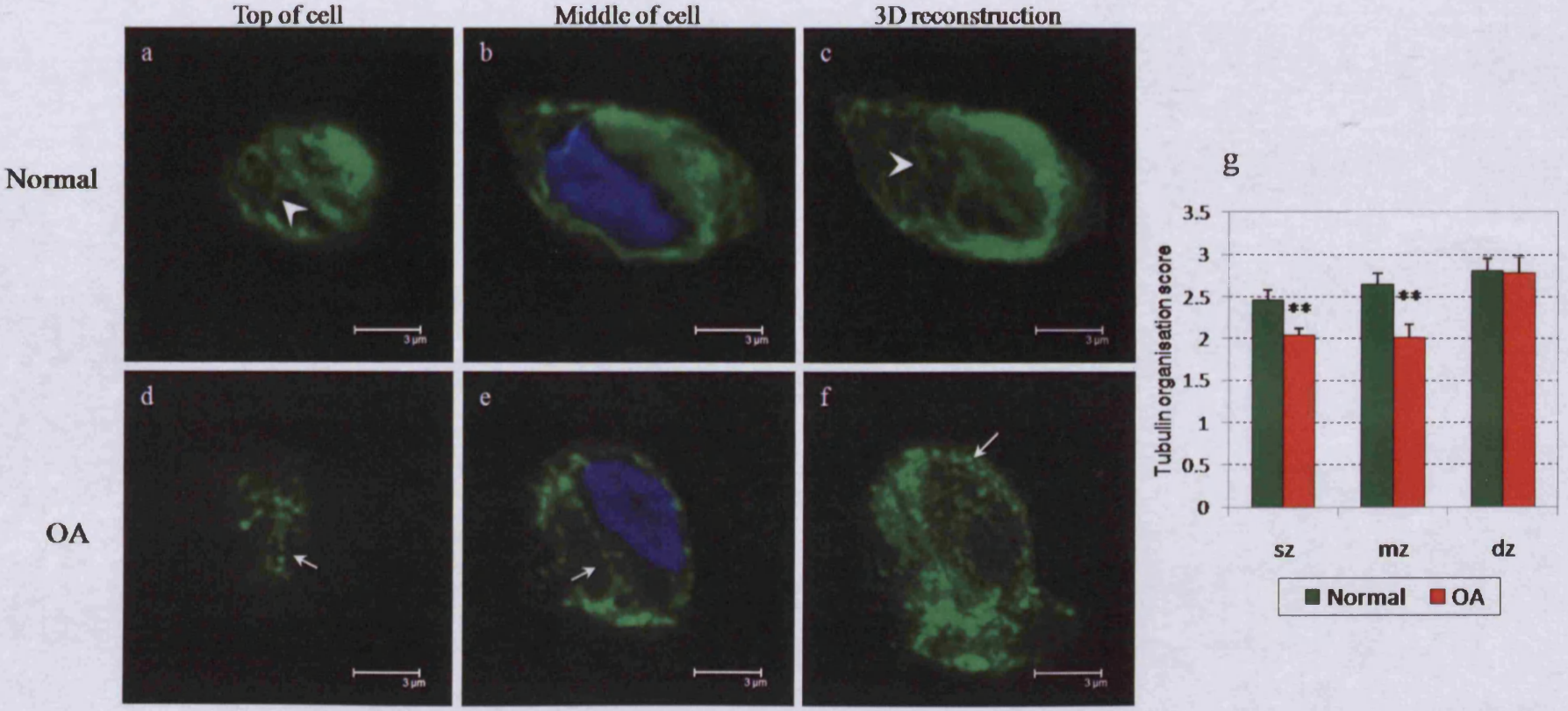

Figure 3.15:- Comparison of the organisation of the tubulin cytoskeleton in normal (a-c) and osteoarthritic (d-f) chondrocytes from human articular cartilage (20µm sections). Microtubule bundles (arrow heads) were less clear and staining was more punctate (arrows) in OA chondrocytes. The cells displayed are from the deep (a-c) and mid (d-f) zone. Tubulin microtubules were detected by indirect immunofluorescence using an anti-β-tubulin primary antibody and a TRITC-conjugated anti-mouse IgG secondary antibody (green). Nuclei were counterstained with DAPI (blue). Tubulin organisation was scored and superficial, middle and deep zone normal and OA chondrocyte scores compared to reveal a significant difference between normal and OA in superficial and mid zone chondrocytes (g): 3 cells were scored for each zone, from each of the 4 normal and 4 OA donors (n=12). Graphs show mean ± S.E.M. ** $p < 0.01$.

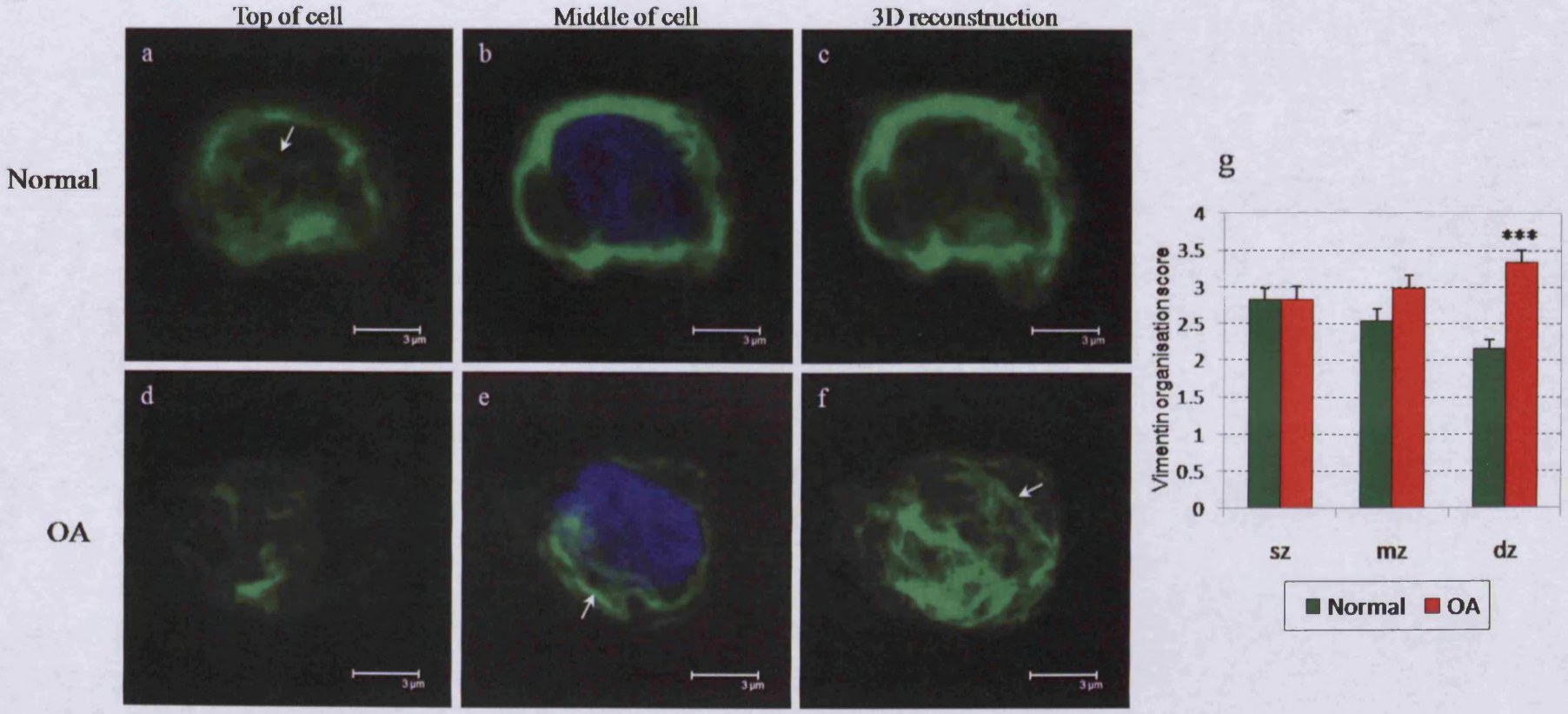

Figure 3.16:- Comparison of the organisation of the vimentin cytoskeleton in normal (a-c) and osteoarthritic (d-f) chondrocytes from human articular cartilage (20µm sections). Intermediate filament bundles (arrows) appeared thicker and more loosely packed in OA chondrocytes. The cells displayed are from the deep (a-c) and mid (d-f) zone. Vimentin intermediate filaments were detected by indirect immunofluorescence using an anti-vimentin primary antibody and a TRITC-conjugated anti-mouse IgG secondary antibody (green). Nuclei were counterstained with DAPI (blue). Vimentin organisation was scored and superficial, middle and deep zone normal and OA chondrocyte scores compared to reveal a significant difference between normal and OA in deep zone chondrocytes (g): 3 cells were scored for each zone, from each of the 4 normal and 4 OA donors (n=12). Graphs show mean ± S.E.M. *** $p < 0.001$.

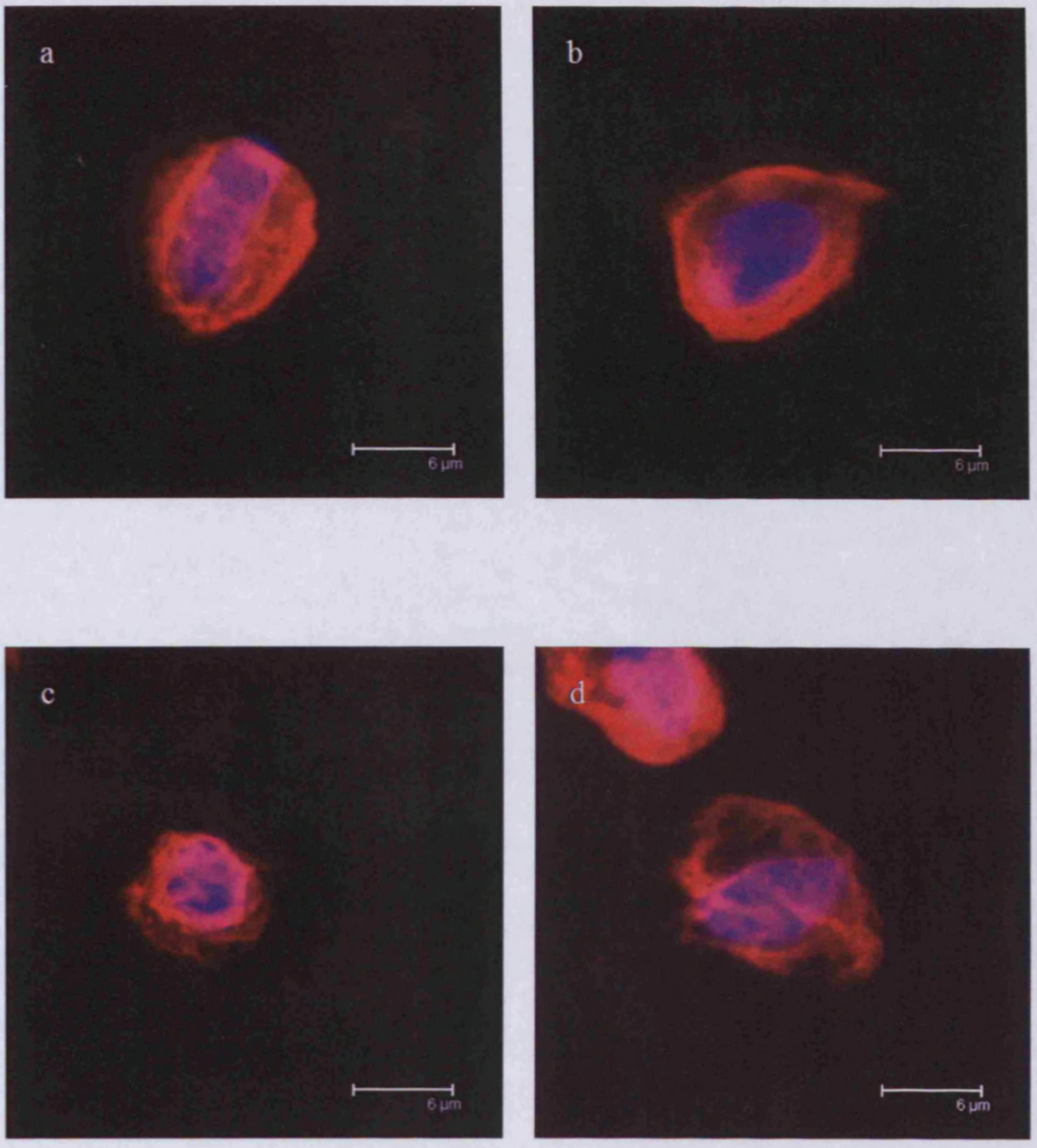

Figure 3.17:- **Comparison of the organisation of the vimentin cytoskeleton in normal (a and b) and osteoarthritic (c and d) chondrocytes within human articular cartilage (20µm sections). Images shown are 3D reconstructions of a series of scans taken at 0.4µm increments across the chondrocyte. Vimentin intermediate filaments were detected by indirect immunofluorescence using anti-vimentin primary antibody and TRITC-conjugated anti-mouse IgG secondary antibody (red). Nuclei are counterstained with DAPI (blue). Vimentin intermediate filaments appear more loosely packed in osteoarthritic chondrocytes compared to normal chondrocytes.**

perinuclear region (Fig 3.15e). Scoring of chondrocytes showed a significant difference in tubulin microtubule architecture between normal and OA chondrocytes in the superficial ($p=0.010$) and mid ($p=0.002$) zones (Fig 3.15g).

3.2.5.1.4 Vimentin Intermediate Filament Organisation

Networks of vimentin filament bundles were observed in both normal and OA human articular cartilage chondrocytes. In normal chondrocytes vimentin filament networks were typically evident at the cell periphery (Fig 3.16a), extending throughout the cell and often appearing as a bright cortical ring (Fig 3.16b). Vimentin tended to appear as fine filamentous networks (Fig 3.17 a and b). In OA chondrocytes vimentin intermediate filament bundles extended from the nucleus to the cell periphery, although networks of intermediate filament bundles were typically more loosely packed and diffuse than those in normal chondrocytes (Fig 3.16 d-f and Fig 3.17 c and d). Scoring of chondrocytes in the superficial, middle and deep zones showed a significant difference in vimentin intermediate filament architecture between normal and OA deep zone chondrocytes ($p<0.001$) (Fig 3.16g).

3.2.5.2 Comparison of Cytoskeletal Organisation in Chondrocytes from Fibrillated and Non-fibrillated Regions within One Joint

The organisation of the chondrocyte cytoskeleton in fibrillated and macroscopically non-fibrillated regions of human articular cartilage taken from the lateral tibial plateau of a donor with no 'overt' symptoms of osteoarthritis was compared. Full-depth tissue sections were fixed and permeabilised according to the (Zwicky and Baici, 2000) method (section 2.2.3.2).

3.2.5.2.1 Actin Microfilaments

Actin staining was observed throughout most cells of the non-fibrillated sections, although fluorescence was not present in all cells. Organisation was punctate and extended throughout the cytoplasm of chondrocytes (Fig 3.18 a and b) and was comparable to the organisation observed in normal articular cartilage chondrocytes (Fig 3.14 b and c). Chondrocytes in fibrillated regions of cartilage also showed punctate actin staining (Fig 3.18d), but in contrast to actin organisation in non-fibrillated regions, this was cortical and did not extend towards the nucleus (Fig 3.18c). This cortical localisation of microfilaments was comparable to that seen in OA articular cartilage

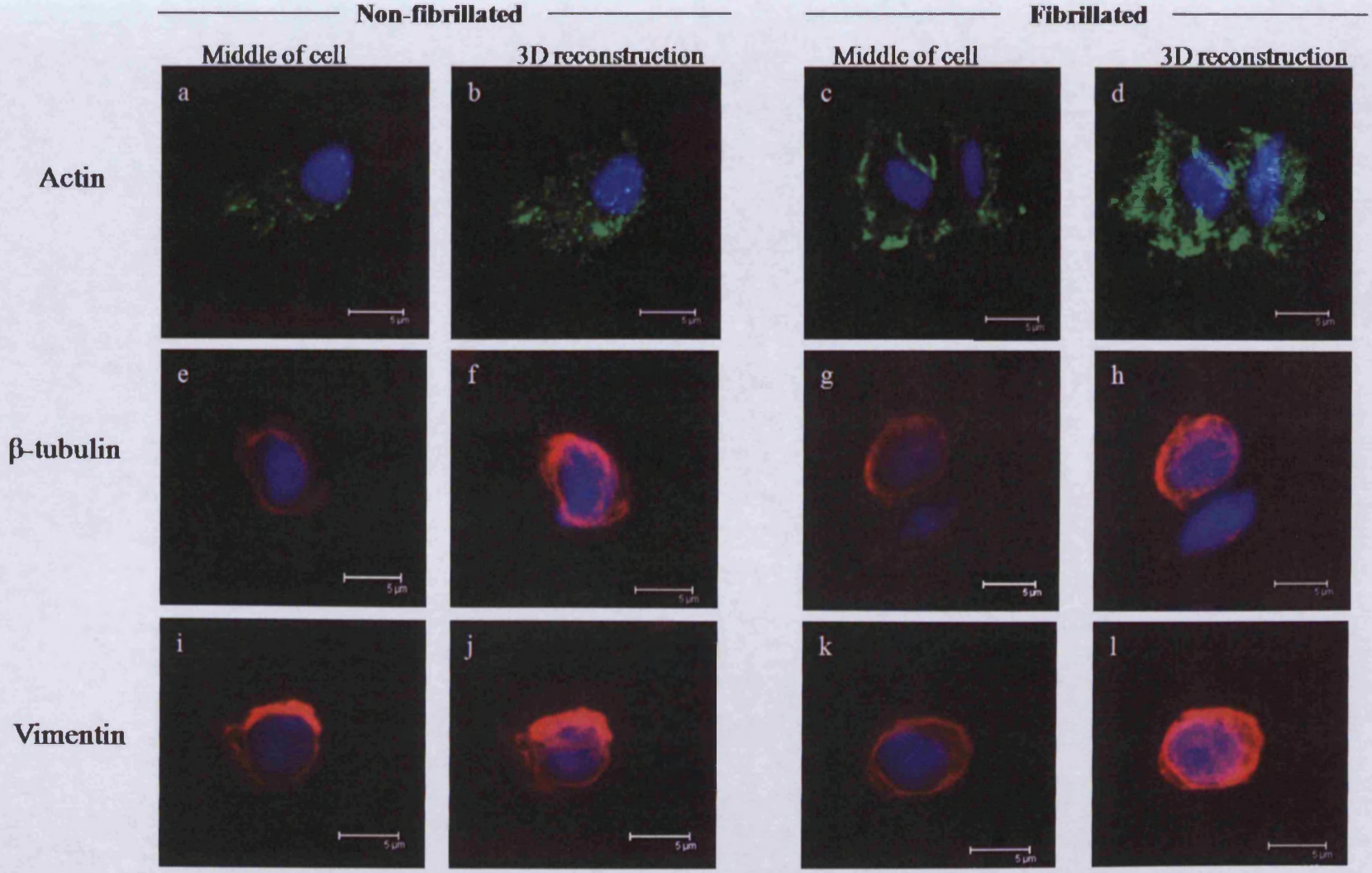

Figure 3.18:- Comparison of the cytoskeletal organisation of human chondrocytes within articular cartilage tissue taken from either a fibrillated or macroscopically non-fibrillated region of the lateral tibial plateau of a post-mortem donor. Articular cartilage sections (20µm) were fixed with either paraformaldehyde (actin and vimentin) or glutaraldehyde (tubulin) and permeabilised with Triton® X-100, in the presence of either buffer 1 (actin and vimentin) or buffer 2 (tubulin). Actin microfilaments were directly stained with Alexa Fluor 488-phalloidin (green), whilst tubulin and vimentin were detected with primary and TRITC-conjugated secondary antibodies (red). Nuclei were counterstained with DAPI (blue).

chondrocytes (Fig 3.14e). Fluorescence was not detected in all cells of the fibrillated tissue, but was most noticeably weak or absent in the superficial zone and adjacent to fibrillation and tears.

3.2.5.2.2 Tubulin Microtubules

In non-fibrillated cartilage chondrocytes, microtubule bundles appeared thick and were condensed around the nucleus, with no visible filamentous network (Fig 3.18 e and f). Microtubule organisation in chondrocytes in fibrillated sections was similar, with dense staining located around the nucleus, although the presence of a filamentous network was more apparent (Fig 3.18h). Whilst the microtubule organisation in chondrocytes was similar between fibrillated and non-fibrillated regions, the distribution of staining differed. Tubulin staining in non-fibrillated sections occurred throughout all cells and cartilage zones, whereas in fibrillated sections staining in the deep zone was poor and was very weak or absent in some cells of the heavily fibrillated superficial zone.

3.2.5.2.3 Vimentin Intermediate Filaments

Vimentin intermediate filament bundles in chondrocytes of non-fibrillated tissue appeared as a thick, filamentous network located close to the nucleus (Fig 3.18 i and j). In fibrillated areas, chondrocytes also contained a filamentous vimentin cytoskeleton. A network of filament bundles extended throughout the chondrocyte cytoplasm, forming a denser network at the cell periphery which extended throughout the cell to the nucleus (Fig 3.18 k and l).

3.2.6 Cytoskeletal Proteins in Articular Cartilage

3.2.6.1 Cytoskeletal Element Protein Expression

Levels of the three main cytoskeletal proteins, actin, β-tubulin and vimentin, were detected by Western blotting and amounts present in normal and osteoarthritic cartilage compared by densitometry. Actin levels appeared to be increased in OA cartilage extracts compared to normal tissue, although this difference was not significant ($p=0.306$). This may be attributed to the fact that actin was not detected in all samples therefore only samples with visible bands at 42 kD were quantified and used in statistical analyses ($n=6$, Fig 3.19a), hence a greater variability. β-tubulin was detected in all samples and showed no difference between normal and OA articular cartilage extracts (Fig 3.19b). Vimentin was also detected in all protein extracts and although there

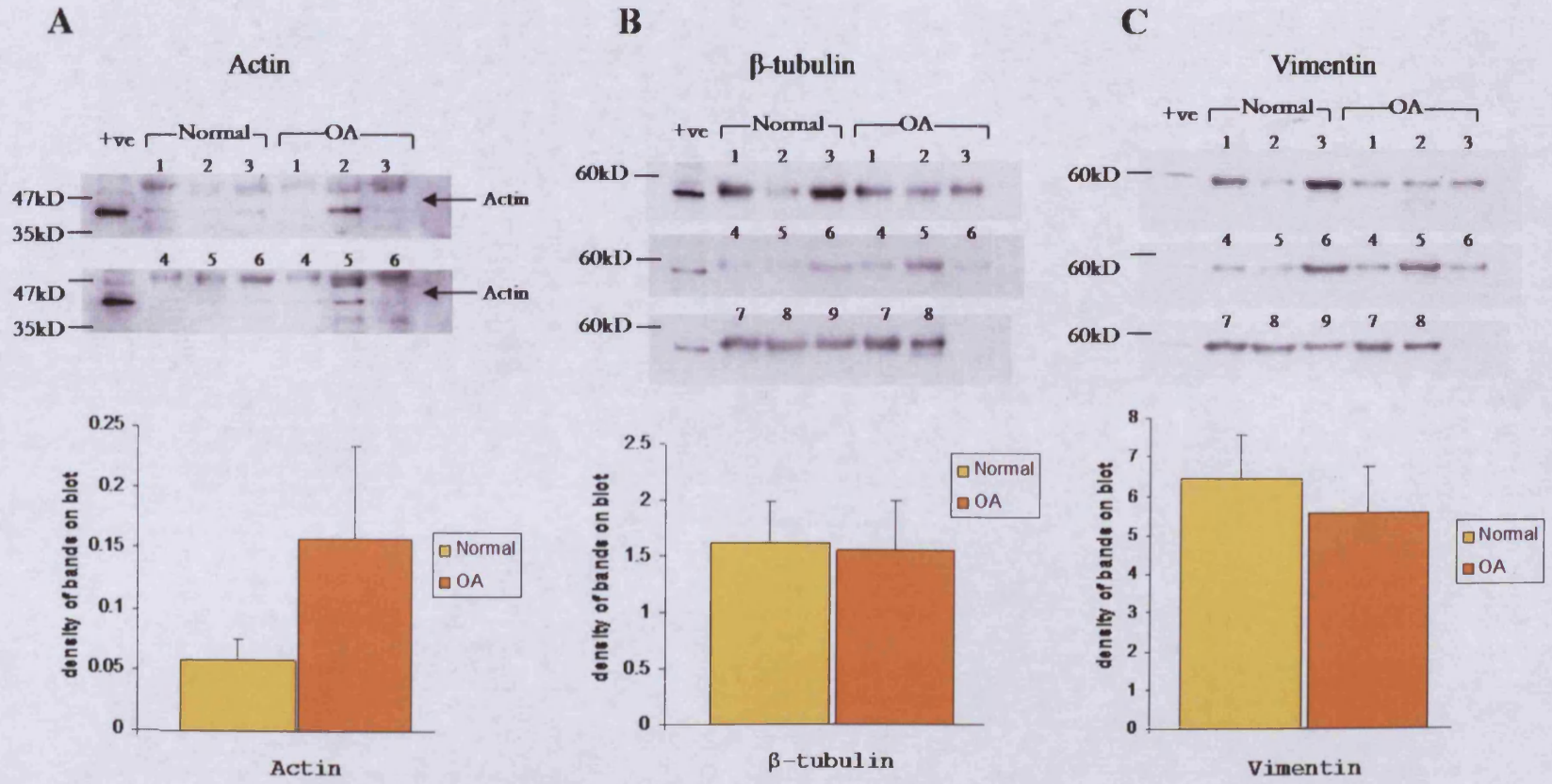

Figure 3.19:- Quantification showed no difference in levels of the cytoskeletal proteins A- actin (42 kD), B- β-tubulin (55 kD) and C- vimentin (58 kD) between normal and osteoarthritic (OA) human articular cartilage (n=9 for normal, n=8 for OA, n=6 for actin). Cytoskeletal proteins were detected by western immunoblot, with equivalent loading of protein (50µg total protein). Bands on immunoblots were quantified by densitometry using NIH image software and normal and osteoarthritic tissue extracts were compared following normalisation to the positive control (+ve) on the relevant gel.

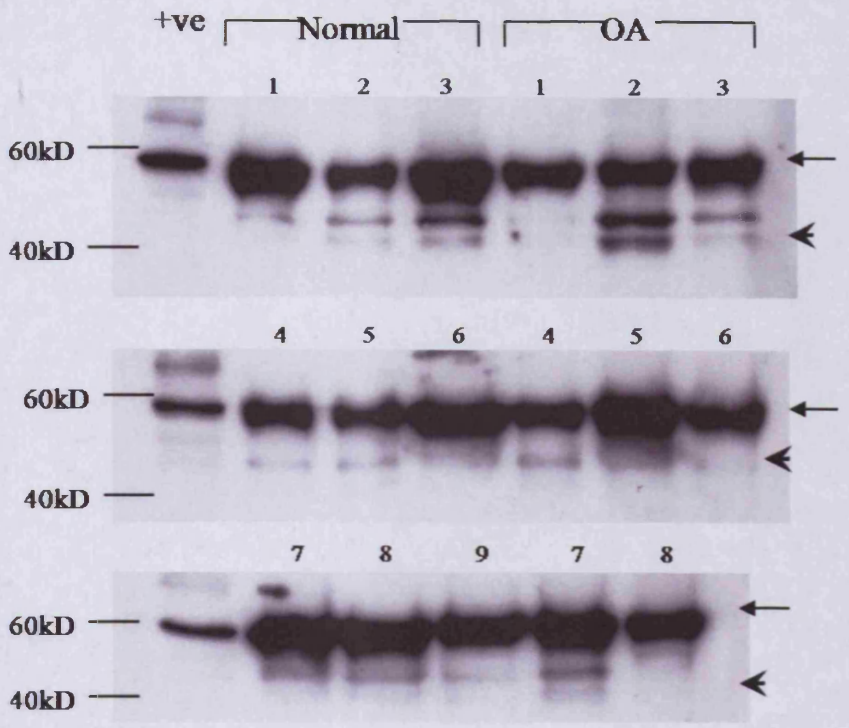

Figure 3.20:- Western blot of sample buffer-soluble vimentin protein present in normal (n=9) and osteoarthritic (n=8) articular cartilage extracts, showing film with a longer exposure to that presented in Figure 3.19c. Following longer exposure, a doublet (arrowheads) around 40–45kD could be detected in most samples below the expected band at 58kD (arrows). Equivalent amounts of protein (50µg) were loaded, and protein extracted from human immortalised chondrocytes (TC28a2 cell line) was loaded as a positive control (3µg, +ve).

appeared to be a decrease in vimentin levels in OA (Fig 3.19c and Fig 3.20), this difference was not statistically significant (p=0.589). Following a longer period of exposure to film than that presented in Figure 3.19c, vimentin blots revealed a doublet around 40–45 kD beneath the expected vimentin protein band of 58 kD (Fig 3.20). This appeared in most of the cartilage extracts and, although these bands have not been characterised, they could represent vimentin degradation products as reported in protein extracts from isolated human normal and OA chondrocytes (Lambrecht et al., 2008). A similar banding pattern on vimentin Western blots was observed and the decreased molecular weight shown to be due to N-terminal vimentin cleavage (Lambrecht et al., 2008).

3.2.6.2 Cytoskeletal Component Gene Expression

Gene expression of the cytoskeletal elements and other cytoskeletal associated proteins was determined using quantitative Taqman™ PCR or quantitative PCR with SYBR green (β-actin). RNA extracted directly from articular cartilage was used in PCR reactions with primers and probes designed against genes of interest (Table 2.6, β-actin in Table 2.5). *GAPDH* was used as an endogenous control and relative expression units calculated for each gene as described in section 2.4.2.2.1. In contrast to Western blotting results, β-tubulin mRNA expression was significantly increased in OA cartilage compared to normal (p=0.031, Fig 3.21). OA cartilage expressed significantly less vimentin when compared with normal cartilage (p=0.007, Fig 3.21). There was no difference in β-actin mRNA expression levels in normal and OA human cartilage (p=0.520). Differences in the mRNA expression of cytoskeletal associated proteins were also observed, with OA cartilage expressing significantly less paxillin mRNA (p=0.007) and significantly more thymosin-β4 mRNA (p=0.018) when compared with normal cartilage (Fig 3.21). There was no difference in mRNA expression levels of filamin A, cofilin, destrin and gelsolin between normal and osteoarthritic cartilage.

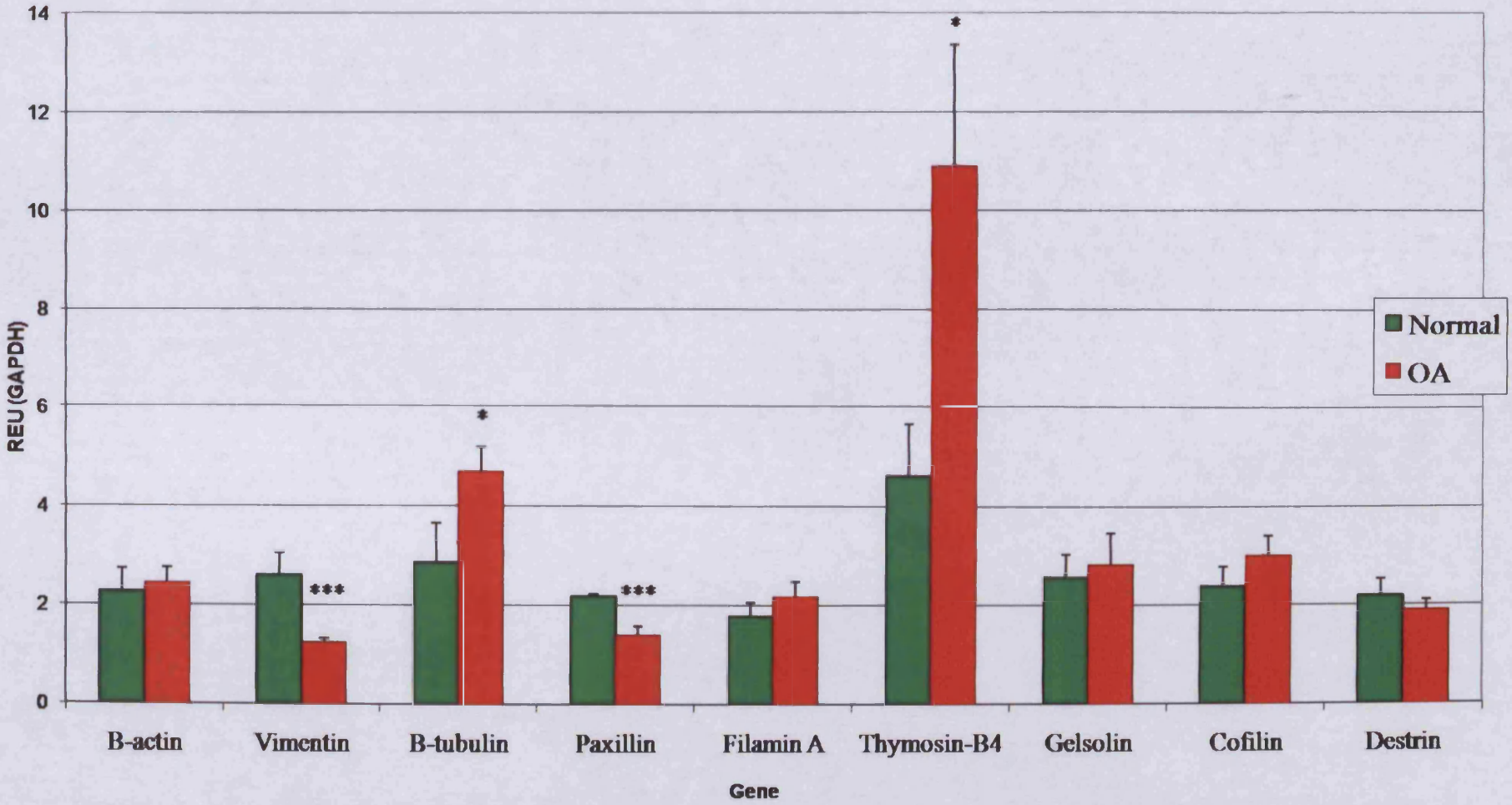

Figure 3.21:- mRNA expression of cytoskeletal genes in normal (green) and osteoarthritic (red) articular cartilage, as determined using quantitative Taqman® PCR on RNA extracted directly from cartilage tissue. Osteoarthritic cartilage expressed significantly more thymosin-β4 and β-tubulin mRNA and significantly less vimentin and paxillin mRNA compared to normal cartilage (n=7, with the exception that n=6 for normal cofilin and destrin and n=5 for normal paxillin following removal of 2 outliers). *$p<0.05$, **$p<0.01$.

3.3 DISCUSSION

Osteoarthritis (OA) is a disease which affects synovial joints and is characterised by degeneration of the articular cartilage. Characterisation of differences that exist between normal and osteoarthritic articular cartilage has led to a better understanding of the disease process, determining how and why degeneration of the tissue progresses and potential targets for therapeutic intervention (Aigner et al., 2006b). However, very little is known about the underlying cellular/molecular mechanisms that propagate such a pathological condition.

3.3.1 Histology of Human Articular Cartilage Samples

Both macroscopic and microscopic differences are apparent between normal articular cartilage and that removed from OA joints. Normal, healthy articular cartilage appears white and shiny with a smooth surface, whilst OA cartilage is yellow with a more 'velvety' appearance, due to disruption of the articular surface. Examination of alcian blue stained sections by light microscopy demonstrated histological differences between normal and OA cartilage. Healthy normal cartilage had a predominantly intact surface accompanied by an apparently intact matrix interspersed with isolated chondrocytes, with no evidence of glycosaminoglycan (GAG) loss. An increased cell density was observed in OA cartilage along with the formation of chondrocyte clusters. Disruption and fibrillation of the articular surface was apparent, and a loss of GAG was observed throughout the tissue. As fibrillation of the articular surface is characteristic of OA, it is not surprising that the morphology of cartilage removed from a fibrillated region of a lateral tibial plateau from an apparently 'clinically normal' joint is comparable to that of OA cartilage. The morphology of adjacent non-fibrillated regions of the same lateral tibial plateau was most comparable to that of normal cartilage, although OA changes could be observed in the form of GAG loss in the superficial zone along with the presence of chondrocyte clusters. These changes would alter the mechanical properties of the cartilage and therefore affect its normal function. A decrease in cartilage compressive stiffness has been shown to correlate with severity of structural alterations of the tissue, such as fibrillation of the articular surface and disruption of the collagen network (Franz et al., 2001). Loss of GAG would reduce the compressive stiffness of the cartilage and also reduce its ability to reform following removal of compressive loads. Disruption and fibrillation of the articular surface, as observed in OA cartilage, would result in altered load and deformation experienced by chondrocytes in the transitional

and radial zones, as collagen networks in the superficial zone would no longer run parallel to the articular surface. In all, the morphological changes observed in OA cartilage will alter the loads experienced by the cartilage chondrocytes and also alter the tissue's response to load.

The differences that are shown to exist between fibrillated and non-fibrillated regions of the same cartilage highlight the potential importance of sampling. Different regions of the lateral and medial tibial plateau experience different load magnitudes during joint articulation, as regions covered by the menisci are exposed to lower forces (Thambyah et al., 2006). Increased load can lead to the development of OA, as shown by *in vivo* models of the disease where induction of OA results from altered and increased loading of joint cartilage (Pond and Nuki, 1973). The severity of the lesions, cartilage damage and biochemical changes that occurred were most severe in regions experiencing higher loads due to lack of protection by the menisci (McDevitt et al., 1977). Important to this study is that the location of the fibrillations were indistinguishable from those observed in naturally occurring OA. Therefore, the regions of both a normal and OA joint from which tissue is removed may need to be taken into account, as different regions will have experienced different load magnitudes. Load has been shown to have different effects on chondrocyte phenotype and matrix turnover *in vivo* (Bayliss et al., 2001, Palmoski et al., 1980, Pelletier et al., 1983a). However, in the Pond-Nuki dog model of OA, the metabolism of articular cartilage chondrocytes as a whole appears to be affected, rather than localised effects in the regions of fibrillation (McDevitt and Muir, 1976). This implies that knowledge of the exact topographical location sampled from within the joint may not be required as this would not affect the significance of any changes detected in the biochemical composition of cartilage, with 'true' OA biochemical and phenotypic changes represented throughout the tissue. Due to the importance of the sampling site and the different load magnitudes across a joint, biopsies from the same region of the tibial plateau were used for the comparison of the cytoskeletal organisation of normal and osteoarthritic chondrocytes *in situ*.

It should be noted that the tissue morphology of 'normal' post-mortem samples varied. This has been observed previously in normal human articular cartilage. When assessed histologically and scored according to the Mankin scale, grossly normal femoral head cartilage ranged from grade one to five (Mankin et al., 1971). Using the same scale,

another study demonstrated grossly normal femoral condyles ranging from grade zero to three (Rizkalla et al., 1992). Mankin grades also varied within donor specimens demonstrating the heterogeneity of osteoarthritis (Mankin et al., 1971, Rizkalla et al., 1992). The comparison of fibrillated and non-fibrillated regions of the same joint in this study also demonstrates this. The range of morphologies of the normal samples could therefore be due to the random selection of a piece of cartilage that was originally located in a weight-bearing region of the joint, or it could be that the donors had early-stage OA. The advancing age of post-mortem donors increases the likeliness of early-OA characteristics appearing, even though donors had never presented to a GP with knee pain; this is possible as there is no correlation between radiographic disease severity scores and clinical pain and function scores (Link et al., 2003). The possibility that some 'normal' samples may in fact be in the early stages of OA could mask the significance of some biochemical and cytoskeletal element differences observed.

3.3.2 Composition of Normal and Osteoarthritic Human Articular Cartilage

3.3.2.1 Biochemical Composition of Normal and Osteoarthritic Articular Cartilage

Analysis of the biochemical composition of normal and OA articular cartilage showed there to be an increased water and collagen content in OA tissue when compared to normal, accompanied by a decrease in the sGAG content. Increased water content in articular cartilage is a characteristic of OA (Martin et al., 2001), and is caused by tissue swelling as a result of disruption of the collagen matrix (Maroudas, 1976). The normal function of collagen is to provide tensile strength and stiffness to the articular cartilage. Where secondary OA arises from joint trauma or impact loading, it is likely that load can directly damage the collagen network, as indicated by the abrupt decrease in the tensile load-bearing capacity of the collagen network following injurious compression (Quinn et al., 1998). The disruption of the collagen network observed in osteoarthritis and models of the disease (Pelletier et al., 1983a, Pelletier et al., 1983b, Dodge and Poole, 1989) reduces the ability of the collagen matrix to resist the swelling pressure caused by the polyanionic proteoglycans, resulting in increased water content (Maroudas, 1976). In normal cartilage this swelling pressure provides the tissue with a compressive stiffness and an ability to reversibly deform in response to compressive loads. The loss of tensile strength caused by disruption of the collagen matrix reduces the compressive stiffness

and therefore the ability of the tissue to recover following deformation. In addition, it reduces the ability of the tissue to resist mechanical compression during joint loading, and ultimately this causes mechanical failure of the cartilage by altering the responsiveness of the tissue to load.

The loss of GAG, indicated by the loss of alcian blue staining in the OA cartilage, was confirmed biochemically by the dimethylmethylene blue (DMMB) assay. The significant loss of GAG content per dry weight of OA cartilage is also characteristic of the pathology and contributes to the mechanical failure of articular cartilage in OA, along with the disruption of the collagen matrix. My results showed no difference in the expression of aggrecan mRNA in normal and OA cartilage, implying that reduced synthesis is not responsible for the loss of proteoglycan in OA. By contrast, a recent study has shown that aggrecan gene expression is reduced in OA cartilage (Brew et al., 2010a). The progressive release of GAG observed in all forms of OA is due to proteoglycan catabolism by matrix metalloproteinases (MMPs) and the 'aggrecanases', ADAMTS-4 and -5 (Caterson et al., 2000). Here, comparison of *ADAMTS5* expression in normal and OA cartilage revealed a significant decrease in mRNA levels in OA cartilage compared to normal, as previously demonstrated in human articular cartilage (Kevorkian et al., 2004). These data are in contrast to other studies showing increased expression of *ADAMTS5* mRNA in human OA cartilage (Bau et al., 2002) and a rat model of OA (Appleton et al., 2007b). Of note though is that mRNA expression levels do not necessarily correlate with protein levels or enzyme activity. However, an immuno-histochemical study of the distribution of the aggrecanase cleavage (NITEGE) neoepitope in human cartilage showed a loss of immunoreactivity in OA cartilage, possibly indicating a decrease in aggrecanase (ADAMTS-4 and -5) activity in OA (Bayliss et al., 2001).

The significant increase in collagen content per dry weight tissue of OA cartilage compared to normal is in contrast to previous evidence of decreased levels of type II collagen protein in OA cartilage (Martin et al., 2001). As type II collagen content is highest in the deep zone of cartilage (Langelier et al., 2000), and OA cartilage often shows a loss in the superficial zone, this observed increase could be due to the increased proportion of deep zone in OA samples compared to normal. In addition, type II pro-collagen synthesis is reported to increase in OA cartilage, particularly in the mid and

deep zones (Nelson et al., 1998). The collagen content was determined using a hydroxyproline assay, which does not distinguish between intact collagen networks and degraded collagen fibrils, nor would it distinguish between cross-linked collagen fibrils and newly synthesised collagen fibrils, or specific collagen types. Therefore it is also possible that the increased collagen content of OA samples is due to a repair response of chondrocytes (Poole et al., 1993), synthesising type II pro-collagen (Nelson et al., 1998) in an attempt to replace damaged networks in the extracellular matrix (ECM). However, it could also simply represent an increased content of collagen that is partially degraded and no longer functional. The highly significant increase in *COL2A1* expression in OA cartilage found here and previously reported in human articular cartilage (Aigner et al., 2003, Martin et al., 2001) supports the former mechanism.

Matrix metalloproteinases (MMPs) are responsible for the progressive degradation of collagen matrices, and a minor proportion of the aggrecan degradation observed in all forms of OA. The balance between the levels of MMPs and their natural inhibitors, the tissue inhibitors of metalloproteinases (TIMPs) is therefore important in articular cartilage, as a shift towards catabolism will ultimately reduce the mechanical integrity of the tissue. This occurs in and is characteristic of OA. In the Pond-Nuki dog model of OA an increase in collagenolytic activity was observed 2-8 weeks following induction of OA (Pelletier et al., 1983a). This collagenolytic activity was also observed in human OA (Pelletier et al., 1983b). Increased levels of a number of the MMPs have been reported in OA cartilage, such as MMP-2, -8, -9, -13 and -14 (membrane-type I MMP) (reviewed in Aigner et al, (2006)). In the present study there was no difference in the levels of latent or active forms of the gelatinase, MMP-2, present in protein extracts of normal and OA cartilage, although this is likely due to its constitutive expression. MMP-9 activity was not detected (even with increased protein loading) by gelatin substrate zymography. Comparison of gene expression in normal and OA articular cartilage showed a significant increase in *MMP13* expression in OA, supporting previous work demonstrating that the collagenase MMP-13 is elevated in OA cartilage (Billinghurst et al., 1997, Dean et al., 1989, Bau et al., 2002, Brew et al., 2010a, Kevorkian et al., 2004). As no difference in the levels of TIMPs-1, -2 or -3 was observed between normal and OA cartilage, any increase in MMP levels observed in OA relative to normal would indicate a characteristic shift towards a catabolic phenotype, as induced by load *in vitro* (Blain et al., 2001) and as occurs in OA (Dean et al., 1989).

3.3.2.2 Gene Expression in Normal and Osteoarthritic Articular Cartilage

In addition to the significant differences in *ADAMTS5*, *MMP13* and *COL2A1* expression between normal and osteoarthritic cartilage discussed above, significant differences in the expression of the transcription factor SOX9 and the angiogen vascular endothelial growth factor (VEGF) were also found. OA cartilage was found to express significantly less *SOX9* mRNA compared to normal, in agreement with previous reports demonstrating a significant loss of *SOX9* mRNA in late stage OA human cartilage (Aigner et al., 2003, Aigner et al., 2006a, Brew et al., 2010a). As SOX9 is known to be required for chondrogenesis and is used commonly as a marker of chondrocyte phenotype, the loss of *SOX9* expression in OA supports the loss of the differentiated phenotype reported to occur in OA. The decrease in *SOX9* mRNA and concomitant increase in *COL2A1* mRNA expression supports previous evidence that there is no correlation in the expression of the two genes in adult human cartilage, suggesting that SOX9 is not the key regulator of *COL2A1* expression in adult human cartilage (Aigner et al., 2003, Yagi et al., 2005). *VEGF* expression was significantly lower in OA cartilage when compared with normal, as demonstrated in a recent study (Brew et al., 2010a). These data however are in contrast to previous studies implying an increased *VEGF* expression in OA, either through an increase in the number of VEGF immunopositive chondrocytes in OA cartilage (Pfander et al., 2001) or a significant increase in VEGF protein extracted from OA cartilage (Enomoto et al., 2003). A positive correlation between VEGF immunoreactivity and OA severity has also been reported (Enomoto et al., 2003). In addition, OA cartilage loses the resistance to vascular invasion exhibited by normal cartilage, with exogenous VEGF enhancing vascular invasion in the same model (Smith et al., 2003), providing indirect evidence for increased VEGF in OA cartilage. Finally, synovial fluid from OA patients reportedly contains significantly higher levels of VEGF protein than that from normal patients (Fay et al., 2006).

3.3.3 Differences in the Profile of Cytoskeletal Elements

Analysis of the three main cytoskeletal proteins in articular cartilage chondrocytes by Western blotting revealed a large degree of variation between samples. An increase in actin protein expression in two of the six OA samples was apparent, but due to high variability in human samples this increase was not significant compared to normal. This is in contrast to a reported decrease in β-actin protein levels in OA chondrocytes,

although in this study primary chondrocytes were isolated from cartilage and cultured in monolayer (Ruiz-Romero et al., 2008). There was no difference in β-actin mRNA levels between normal and OA cartilage. An increase in actin levels has been observed in the superficial zone of mature bovine articular cartilage (Langelier et al., 2000). In this study, Western blotting analysis showed increased levels in the superficial zone compared to the transitional and radial zones and, as this difference was not observed in the levels of F-actin detected by phalloidin, the authors proposed that this represented a higher content of soluble G-actin in the superficial zone, corresponding to an increased requirement for actin microfilament remodelling (Langelier et al., 2000). In agreement with findings using mature bovine articular cartilage, no increase in phalloidin staining was observed in the superficial zone of normal human articular cartilage in the present study. However, chondrocyte clusters surrounding surface fibrillations of OA cartilage sections showed brighter phalloidin staining. It is possible that the altered mechanical properties of OA cartilage (due to the biochemical changes discussed above) results in a greater requirement for remodelling of the chondrocyte actin cytoskeleton as they experience greater loads due to disruption of the articular surface and collagen matrix. The increase in actin observed in OA cartilage may also relate to the increased stiffness of OA chondrocytes (Trickey et al., 2000), as microfilaments have been shown, along with vimentin intermediate filaments, to determine the mechanical properties of chondrocytes (Trickey et al., 2004). To further clarify possible changes in the requirements for actin remodelling, differences in the gene expression of the actin binding proteins thymosin β4, paxillin, filamin, cofilin and gelsolin were determined.

Expression of thymosin β4, a 5 kD actin sequestering protein, has been shown to be mechanically regulated in bovine articular cartilage *in vitro* (Blain et al., 2003). The results presented here showed that, in human articular cartilage, thymosin β4 mRNA is expressed at significantly higher levels in OA cartilage compared to normal. This increase in expression may be due to the increased load experienced by OA cartilage chondrocytes as a result of the altered mechanical properties of the tissue. As thymosin β4 binds G-actin and therefore assists in the regulation of actin filament dynamics, the increased levels of expression observed support the hypothesis that increased actin remodelling is required in OA cartilage in response to the altered mechanical environment of chondrocytes. In addition, cofilin and destrin, both actin depolymerising proteins, have been shown to be mechanically regulated in chondrocytes in culture

(Campbell et al., 2007). No difference in cofilin or gelsolin mRNA expression was observed between normal and OA cartilage in the present study, in contrast to reported increases in protein levels in OA chondrocytes (Ruiz-Romero et al., 2008, Lambrecht et al., 2008). OA cartilage expressed significantly less paxillin mRNA than normal cartilage. As paxillin is an actin-associated protein located in focal adhesions, it is present in the physical link between the actin cytoskeleton and the extracellular matrix. The role of integrin-containing focal adhesions and the actin cytoskeleton in mechanotransduction is emerging, with paxillin phosphorylation a downstream response to mechanical stimulation of α5β1 integrins in human articular chondrocytes (Salter et al., 2001). Therefore the decrease in paxillin expression found here may indicate a decrease in, or a disruption of, one of the mechanical signalling pathways in OA cartilage chondrocytes. Vinculin, another actin-associated protein in focal adhesions, has been reported to be increased in OA chondrocytes (Ruiz-Romero et al., 2008).

Whilst there was no difference in the levels of β-tubulin protein between normal and OA cartilage, as detected by Western Blotting, quantitative PCR demonstrated that OA cartilage expressed significantly more β-tubulin mRNA. In support of this, tubulin staining intensity was decreased in the superficial zone of normal cartilage and increased in the chondrocytes surrounding the surface fibrillations in OA cartilage. These differences between normal and OA cartilage were not observed throughout the depth of the tissue and therefore this could mask differences observed by Western blotting. The lack of correlation of protein with gene expression and immunohistochemical data could be due to difficulties in extraction of intracellular proteins from human articular cartilage. Alternatively, as β-tubulin mRNA levels are auto-regulated, with decreases in the pool of β-tubulin monomers below a critical level releasing β-tubulin mRNA from degradation mechanisms (Cleveland and Havercroft, 1983, Cleveland et al., 1983, Yen et al., 1988), the increase in β-tubulin mRNA levels in human OA cartilage when compared with normal tissue could indicate that the ratio of monomeric to polymerised β-tubulin is decreased in OA cartilage chondrocytes, with total levels of β-tubulin unchanged.

Western blots showed no difference in vimentin levels present in OA cartilage compared to normal, although it should be noted that this only represents the sample buffer-soluble portion of vimentin. A study of cytoskeletal protein expression in mature bovine

cartilage revealed a gradient of RIPA-insoluble vimentin that decreased with depth, which was extracted from insoluble pellets with guanidine-HCl (Langelier et al., 2000). Sample buffer-soluble vimentin blots revealed a doublet around 40–45 kD beneath the expected vimentin protein band of 58 kD. This appeared in most of the cartilage extracts and, although these bands have not been characterised, they could represent vimentin degradation products. Of interest is a change in the banding pattern of vimentin on Western blots that has also been reported in a rat model of OA and in human OA cartilage, with several bands appearing between 55–38 kD, along with the expected 58 kD band for vimentin (Capin-Gutierrez et al., 2004). A recent comparison of vimentin in isolated human normal and OA chondrocytes demonstrated a similar banding pattern on Western blots (Lambrecht et al., 2008). They showed a series of bands migrating below that of the native 58 kD vimentin, with an increased abundance of a lower molecular weight form of vimentin (43 kD) in chondrocytes isolated from OA cartilage. The decreased molecular weight was shown to be due to N-terminal vimentin cleavage (Lambrecht et al., 2008). A single band for native vimentin was present in one normal sample but the other normal samples contained some lower molecular weight bands in addition to the native band (Lambrecht et al., 2008), as did the normal samples in the present study. This implies that N-terminal vimentin cleavage is a normal turnover event in adult human articular cartilage that becomes more pronounced with OA progression. The increased N-terminal vimentin cleavage in OA could reduce the association of vimentin with the plasma membrane (Georgatos et al., 1985) and alter vimentin intermediate filament organisation (Beuttenmuller et al., 1994), the mechanical properties of the chondrocyte (Trickey et al., 2004, Ofek et al., 2009) and chondrocyte mechanotransduction.

The organisation of actin microfilaments, tubulin microtubules and vimentin intermediate filaments in human chondrocytes *in vitro* have been characterised (Trickey et al., 2004), as has the cytoskeletal organisation of osteoarthritic human chondrocytes *in situ* (Kouri et al., 1998). Comparisons have not previously been made between the cytoskeletal organisation of normal and osteoarthritic human chondrocytes *in situ*. Of particular relevance to the aims of this project are that differences in the localisation and fluorescent labelling of the cytoskeleton have been shown to exist between normal and OA human chondrocytes in alginate gels *in vitro* (Lambrecht et al., 2008, Fioravanti et al., 2003) and between normal and OA chondrocytes *in situ* in a rat OA model (Capin-

Gutierrez et al., 2004). In the present study, visualisation of *in situ* chondrocyte cytoskeletal organisation by immunofluorescence and scanning confocal microscopy showed clear differences between normal and osteoarthritic human cartilage chondrocytes. In chondrocytes from normal cartilage, staining of actin microfilaments appeared punctate, as previously described in mature bovine articular cartilage (Langelier et al., 2000), although staining was throughout the cytoplasm rather than localised cortically as previously reported. Microtubule bundles formed a fine filamentous network that extended throughout the cytoplasm, as did vimentin intermediate filament bundles. Chondrocytes in OA cartilage showed an altered cytoskeleton to that observed in normal chondrocytes; scoring of confocal images revealed significant differences in actin and vimentin organisation in deep zone chondrocytes and tubulin organisation in superficial and mid zone chondrocytes. Actin staining remained punctate but was localised to the cell periphery rather than distributed throughout the cytoplasm. A microtubule network was less evident, whilst vimentin filament bundles appeared more diffuse and loosely packed than those in normal chondrocytes. This 'looser' organisation of vimentin intermediate filaments has also been observed in chondrocytes isolated from human OA cartilage cultured in alginate and may be due to the increased N-terminal vimentin cleavage that the same group demonstrated in OA tissue (Lambrecht et al., 2008). The N-terminal of vimentin is involved in intermediate filament formation (Beuttenmuller et al., 1994) and the interaction of filaments with the plasma membrane (Georgatos et al., 1985). Therefore the increased cleavage of this domain is likely to result in a disordered vimentin intermediate filament organisation.

Zonal variations in vimentin have been observed in mature bovine articular cartilage (Langelier et al., 2000), as have changes in vimentin organisation and labelling in response to load (Durrant et al., 1999, Langelier et al., 2000). The observed decrease in vimentin mRNA expression levels in OA cartilage are not reflected in the immunostaining patterns, as vimentin labelling was less intense in the superficial and upper-mid zones of normal cartilage. The vimentin immunostaining results are also in contrast to the increased vimentin signal intensity reported in the superficial zones of mature bovine cartilage (Langelier et al., 2000). Langelier *et al.* showed increased vimentin labelling throughout the depth of the tissue from regions experiencing high loads. As the human cartilage tissues used in the present study were from highly loaded

regions of tibial plateaus, vimentin labelling throughout the depth is as expected. The differences observed in vimentin expression levels may represent a response to the altered mechanical loads experienced by chondrocytes in these regions as a result of extracellular matrix disruption and loss from the tissue. As vimentin has been shown to influence the mechanical properties of the chondrocyte itself (Trickey et al., 2004), the difference in intensity of vimentin staining in some regions could represent a change in the mechanical properties of the chondrocyte. This could potentially result in an altered response to mechanical stimuli and therefore altered synthesis and maintenance of the surrounding matrix. This is supported by a recent study *in vitro*, showing that disruption of vimentin results in a significant decrease in type II collagen, and would therefore contribute to the observed OA phenotype (Blain et al., 2006). Finally, another possible explanation for the loss of staining of cytoskeletal proteins in localised regions of the cartilage zones is the existence of different chondrocyte cell types. Kouri *et al.* demonstrated that chondrocytes which they characterised as 'clonal' or 'secretory' displayed different labelling intensities for the three main cytoskeletal elements (Kouri et al., 1998) and different intermediate filament organisation (Kouri et al., 1996) when compared with other chondrocytes in human OA cartilage.

The ability of load to alter cytoskeletal element organisation (Durrant et al., 1999, Fioravanti et al., 2005, Knight et al., 2006) indicates that the original location of the cartilage specimens in the joint is likely to be important, as the differences in loads experienced by distinct regions of the joint could result in an altered cytoskeletal architecture. This is implied by the alterations in the organisation and distribution of cytoskeletal element labelling observed in the present study, where a comparison of cartilage from different regions of the same joint was performed. Furthermore, observed differences in the distribution of tubulin and vimentin labelling through the depth of mature bovine articular cartilage, existing between peripheral and central load-bearing regions of the same joint surface would support this conclusion (Langelier et al., 2000). For this reason, cartilage sampled from the same region in knee joints was used for the comparison of cytoskeletal organisation. Cartilage was sampled from the highly loaded region of the tibial plateau, unprotected by the meniscus, of normal and OA donors. Therefore the differences in cytoskeletal organisation observed here between normal and OA chondrocytes *in situ* are not due to loading differences over the joint, but are due to pathology or different loading histories of patients. Whether the differences are a result

of the altered mechanical environment and matrix composition of OA or the cause of it remains to be determined.

As discussed above, the appearance of early-OA histological changes were observed in some of the specimens classed as 'normal'. In addition, it has been observed in the Pond-Nuki dog model of OA that changes occur in chondrocyte morphology before any obvious disruption of the articular surface or changes in the cartilage ECM (McDevitt et al., 1977, McDevitt and Muir, 1976). It could therefore be argued that some apparently normal specimens could contain numerous chondrocytes undergoing changes that will ultimately lead to the development of OA. If cytoskeletal dysregulation or reorganisation is an early change in OA, or if indeed it is causal, as we hypothesise, is it possible to be confident that the 'normal' cytoskeletal organisation observed is truly normal? This is compounded by a recent comparison of vimentin protein expression and organisation in human OA chondrocytes (Lambrecht et al., 2008). The greatest difference in vimentin organisation was between chondrocytes isolated from normal cartilage and those isolated from OA cartilage regions with no signs of fibrillation, whilst the greatest difference in abundance of native and N-terminally cleaved vimentin protein was between normal chondrocytes and chondrocytes isolated from visually fibrillated regions of OA cartilage. There was little difference in vimentin content between normal chondrocytes and OA chondrocytes from visually intact regions (Lambrecht et al., 2008). Whilst this raises the problem of the disease state and cytoskeletal organisation of 'normal' samples, it does support our hypothesis that changes to the organisation of the cytoskeleton appear to be an early event in OA, whether causal or not remains to be proven.

3.3.3.1 The Effects of Fixation Protocol on Cytoskeletal Organisation

The fixative, permeabilising agent, and buffer used during fixation of chondrocytes has an effect on the preservation of cytoskeletal architecture, and therefore the structural organisation, shown *in situ* in the present study, and shown previously *in vitro* (Blanc et al., 2005). In addition, a decreased stability of microtubules has been noted in sections stored above -20°C and below room temperature, even following fixation; many reports characterise cytoskeletal organisation following incubation and/or storage of samples at 4°C. These differences in protocol may explain the variations in the reported cytoskeletal organisation of chondrocytes (Benjamin et al., 1994, Capin-Gutierrez et al., 2004, Durrant et al., 1999, Fioravanti et al., 2003, Langelier et al., 2000, Trickey et al., 2004,

Lambrecht et al., 2008). In cases where the cytoskeleton appeared close to the nucleus, it is not certain whether or not this is representative of an *in vivo* collapse of the cytoskeleton, the cytoskeleton extending throughout the cytoplasm which is largely occupied by the nucleus, or a manifestation of the fixation protocol. Blanc et al. (2005) reported that the use of paraformaldehyde in conjunction with Triton® X-100 resulted in shrinkage and distortion of the cytoskeleton (when compared with live chondrocytes) and therefore glutaraldehyde was used in the present study.

In comparing human normal and OA articular cartilage, I have observed that:

- Despite the early OA histological changes observed in the 'normal' articular cartilage samples, biochemical comparisons showed the expected increase in water and collagen content and decreased sGAG content in OA cartilage. In addition, the expected decrease in *SOX9* and increase in *MMP13* mRNA expression was observed. This indicates that significant pathological differences exist between the 'normal' and OA cartilage samples used in the present study.
- Differences exist between the cytoskeleton of normal and OA cartilage chondrocytes. These differences were in network organisation and mRNA expression.

Chapter 4: The Effect of a Three-Dimensional Environment on Chondrocyte Phenotype in Culture

4. THE EFFECT OF A THREE-DIMENSIONAL ENVIRONMENT ON CHONDROCYTE PHENOTYPE IN CULTURE

4.1 INTRODUCTION

Chondrocytes are the cellular component of articular cartilage and are responsible for the synthesis and degradation of the extracellular matrix which gives the articular cartilage its functional properties. Physiological and pathological processes in chondrocytes are often studied using cells isolated from the extracellular matrix of articular cartilage and cultured *in vitro*, which allows the easy manipulation of the chondrocytes and detection of the effects. Isolation of chondrocytes from articular cartilage has been shown to affect chondrocyte gene expression (Benz et al., 2002, Eleswarapu et al., 2007, Hayman et al., 2006). The presence of the pericellular matrix also has an effect on the gene expression of isolated chondrocytes (Zhang et al., 2006b). In addition, the type and concentration of enzymes, and the incubation periods used in the digestion of the cartilage extracellular matrix to release the chondrocytes can have differing effects on subsequent gene expression *in vitro* (Hayman et al., 2006). The *in vitro* system used for the subsequent culture of chondrocytes also affects chondrocyte gene expression and phenotype.

4.1.1 Monolayer Culture of Chondrocytes

When cultured on plastic following their isolation from cartilage, chondrocytes adhere and proliferate. However, this proliferation is accompanied by a steady loss of the differentiated chondrocyte phenotype over the culture period; a phenomenon termed 'dedifferentiation' (Benya et al., 1978). A decrease in the expression and synthesis of type II collagen, the predominant collagen of articular cartilage, is accompanied by an increase in types I and III collagen, collagens which are more typical of fibroblasts (Benya et al., 1977, Benya et al., 1978, Mayne et al., 1976). In addition to changes in the collagen phenotype, proteoglycan synthesis also changes in monolayer culture. Sulphated glycosaminoglycan synthesis decreases with cell-flattening and versican synthesis increases to replace aggrecan (Glowacki et al., 1983). This altered synthesis is reflected in gene expression changes within the monolayer subculture; expression of *COL2A1*, *COL11A1* and aggrecan decrease whilst *COL1A1* and *COL3A1* expression increases (Stokes et al., 2001). In addition to changes in matrix production and gene

expression, cell morphology alters with culture of chondrocytes in monolayer. Chondrocytes lose the round, spherical morphology observed *in situ*, becoming polygonal, then flattened, elongated and fibroblast-like (Stokes et al., 2001). Concomitant with the changes in cell shape is the appearance of actin stress fibres in dedifferentiating chondrocytes (Mallein-Gerin et al., 1991). This actin cytoskeletal organisation is again more typical of fibroblasts. However, the fibroblastic changes in cell shape do not necessarily correlate with the altered matrix production by dedifferentiating chondrocytes in monolayer culture (Mallein-Gerin et al., 1990, von der Mark et al., 1977). Despite this, it has been established that the rounded morphology of chondrocytes plays a crucial role in the maintenance of their differentiated phenotype (Benya and Shaffer, 1982a, Glowacki et al., 1983).

4.1.2 Three-Dimensional Culture of Chondrocytes

The requirement of a rounded morphology for maintenance of the chondrocyte phenotype led to development of culture systems that supported this spherical shape and prevented cell flattening. Often collectively referred to as a 'suspension culture', culture systems used include three-dimensional (3D) encapsulation of the chondrocytes in 'hydrogels' such as agarose (Benya and Shaffer, 1982a) or alginate (Guo et al., 1989), 3D pellet culture (Abbott and Holtzer, 1966), alteration of the adhesiveness of the substratum by coating with poly(2-hydroxyethyl methacrylate) (polyHEMA) (Glowacki et al., 1983) or culture on the surface of a hydrogel (Watt and Dudhia, 1988). In these systems, the chondrocyte phenotype is better maintained; cells have a rounded morphology and synthesise a matrix containing type II collagen and sulphated glycosaminoglycan (Benya and Shaffer, 1982a, Glowacki et al., 1983). Stress fibres do not appear and the actin cytoskeleton maintains a punctate and peripheral localisation (Knight et al., 2006). In these culture conditions the rate of DNA synthesis and proliferation in chondrocytes is reduced when compared with that in monolayer culture (Glowacki et al., 1983, Guo et al., 1989). Therefore, whilst these culture systems prevent the loss of the rounded morphology and chondrocyte phenotype, the very slow proliferation means that cell numbers cannot readily be increased for experimentation.

A number of studies have shown that dedifferentiated chondrocytes cultured in monolayer retain the ability to re-express the differentiated chondrocyte phenotype. Transfer of subcultured chondrocytes from monolayer to suspension culture results in

up-regulation of type II collagen and glycosaminoglycan synthesis, a reduction in cell proliferation and rounding of the chondrocytes; so called 'redifferentiation' (Benya and Shaffer, 1982a). Therefore chondrocyte numbers can be expanded in monolayer culture before being transferred to 3D culture for redifferentiation, a model with particular implications for cartilage tissue engineering. The concept of autologous chondrocyte transplantation (ACT) for treatment of cartilage lesions thus followed, whereby chondrocytes are harvested from small undamaged cartilage regions in the patient, expanded *ex vivo* to obtain sufficient number, then implanted into cartilage lesions where they synthesise a matrix and repair the defect (Grande et al., 1989, Solursh, 1991, Peterson et al., 2000).

The extent to which redifferentiation occurs reduces with increasing number of subcultures and cell divisions (Zaucke et al., 2001). Oxygen tension, cell density and concentration of alginate can influence the redifferentiation of chondrocytes (Domm et al., 2002, Wang et al., 2008a) and application of cyclic hydrostatic pressure to 3D cultures enhances redifferentiation of chondrocytes (Heyland et al., 2006, Kawanishi et al., 2007). The addition of specific growth factors or serum to culture medium during chondrocyte expansion in monolayer influences the extent of redifferentiation when placed in 3D culture, and also the potential for dedifferentiation and proliferation in monolayer (Jakob et al., 2001, Hsieh-Bonassera et al., 2009). For example, the redifferentiation potential of chondrocytes in monolayer is stabilised and extended by treatment with IGF-I, which increases levels of the chondrocyte transcription factor SOX9 and its interaction with phosphorylated ERK1/2 in chondrocyte nuclei (Shakibaei et al., 2006). Transduction of growth factors such as TGFβ1 or IGF-I into chondrocytes has also been shown to increase cartilage matrix synthesis in monolayer and enhance redifferentiation (Shuler et al., 2000, Smith et al., 2000, Sung et al., 2009). The redifferentiation of chondrocytes is also enhanced by transduction with SOX9 which sensitises the cells to growth factors (Li et al., 2004, Tew et al., 2005). Chondrocytes from osteoarthritic cartilage also dedifferentiate in monolayer and these too retain the ability to re-express the chondrocyte phenotype when placed in 3D culture, although redifferentiation of OA cells occurs to a lesser extent than normal chondrocytes (Yang et al., 2006, Tallheden et al., 2005). Transduction of OA chondrocytes with SOX9 enhances redifferentiation, indicating that a pathological background does not permanently compromise the chondrocyte phenotype (Tew et al., 2005). In support of

this, SOX9 transduction of normal and OA chondrocytes in alginate or in native cartilage increases cartilage matrix synthesis; matrix produced by transduced OA chondrocytes reaches levels equal to or above that of non-transduced normal chondrocytes (Cucchiarini et al., 2007).

Considering the aim of tissue engineering, it is unsurprising that the large number of studies on chondrocyte redifferentiation focus on the quantity and quality of matrix produced by chondrocytes. Long time points are studied, often weeks in culture, to allow for completion of redifferentiation and accumulation of matrix. Few studies have assessed the early changes in phenotype that occur during chondrocyte redifferentiation. Benya and Schaffer showed a transient decrease in the rates of collagen, proteoglycan, protein and DNA synthesis when rabbit articular chondrocytes were transferred from monolayer to 3D-agarose culture; the rates of synthesis by fourth passage chondrocytes began to increase after 24–48 hours in agarose culture (Benya and Shaffer, 1982a). More recently, Haudenschild *et al.* used cDNA libraries generated by subtractive hybridisation to analyse differentially regulated genes in chondrocytes, isolated from normal human articular cartilage, either cultured as a monolayer or embedded in an alginate suspension (Haudenschild et al., 2001). Following 48 hours in alginate culture, genes involved in cell growth, extracellular matrix deposition and remodelling, cell adherence and apoptosis were differentially regulated. Expression of genes encoding matrix proteins decreased whilst expression of *MMP1*, *MMP3*, *IL6* and heat shock protein 90 increased. To the best of my knowledge, there has been no comparison of the early gene expression changes between redifferentiating normal and OA chondrocytes.

Custom-designed Taqman arrays (AstraZeneca) were used to compare the gene expression profile of passage three chondrocytes isolated from normal or osteoarthritic articular cartilage, cultured either as a monolayer or after 72 hours in a 3D-agarose environment.

4.2 RESULTS

4.2.1 Changes in Cytoskeletal Organisation

The cytoskeletal organisation of human normal and osteoarthritic chondrocytes cultured either as a monolayer or embedded within a 3D-agarose hydrogel was visualised using immunohistochemistry in conjunction with confocal microscopy. In monolayer, both normal and OA passage three chondrocytes were flat and spread, with processes extending out from the cell (Fig 4.1a-f). Phalloidin staining revealed the presence of stress fibres in monolayer cultured chondrocytes, although OA cells appeared to contain more when compared to normal cells (Fig 4.1 a and d). Microtubule bundle networks were clear and extended throughout the cytoplasm to the cell periphery (Fig 4.1 b and e). Normal and OA monolayer cultured chondrocytes also contained clear networks of vimentin intermediate filament bundles. In normal chondrocytes, intermediate filament networks appeared to be orientated predominantly in a single direction (Fig 4.1c); this was not seen in OA chondrocytes (Fig 4.1f). After 72 hours in agarose culture, passage three normal and OA chondrocytes had regained a rounded morphology (Fig 4.1g-l). Both normal and OA cells were devoid of stress fibres (Fig 4.1 g and j). In normal chondrocytes, actin microfilament staining appeared punctate and was predominantly cortical, with some staining throughout the cell (Fig 4.1g). In OA chondrocytes, staining was localised entirely at the cell periphery, punctate spots appeared larger when compared with normal cells, and networks were evident at the periphery (Fig 4.1j). Microtubule bundle networks were less evident in agarose cultured chondrocytes; tubulin staining was perinuclear in normal chondrocytes (Fig 4.1h) and distributed at the cell periphery in OA chondrocytes (Fig 4.1k). Vimentin intermediate filament bundle networks were apparent in both normal and OA chondrocytes cultured in agarose, extending from the nucleus into a cortical network (Fig 4.1i,l).

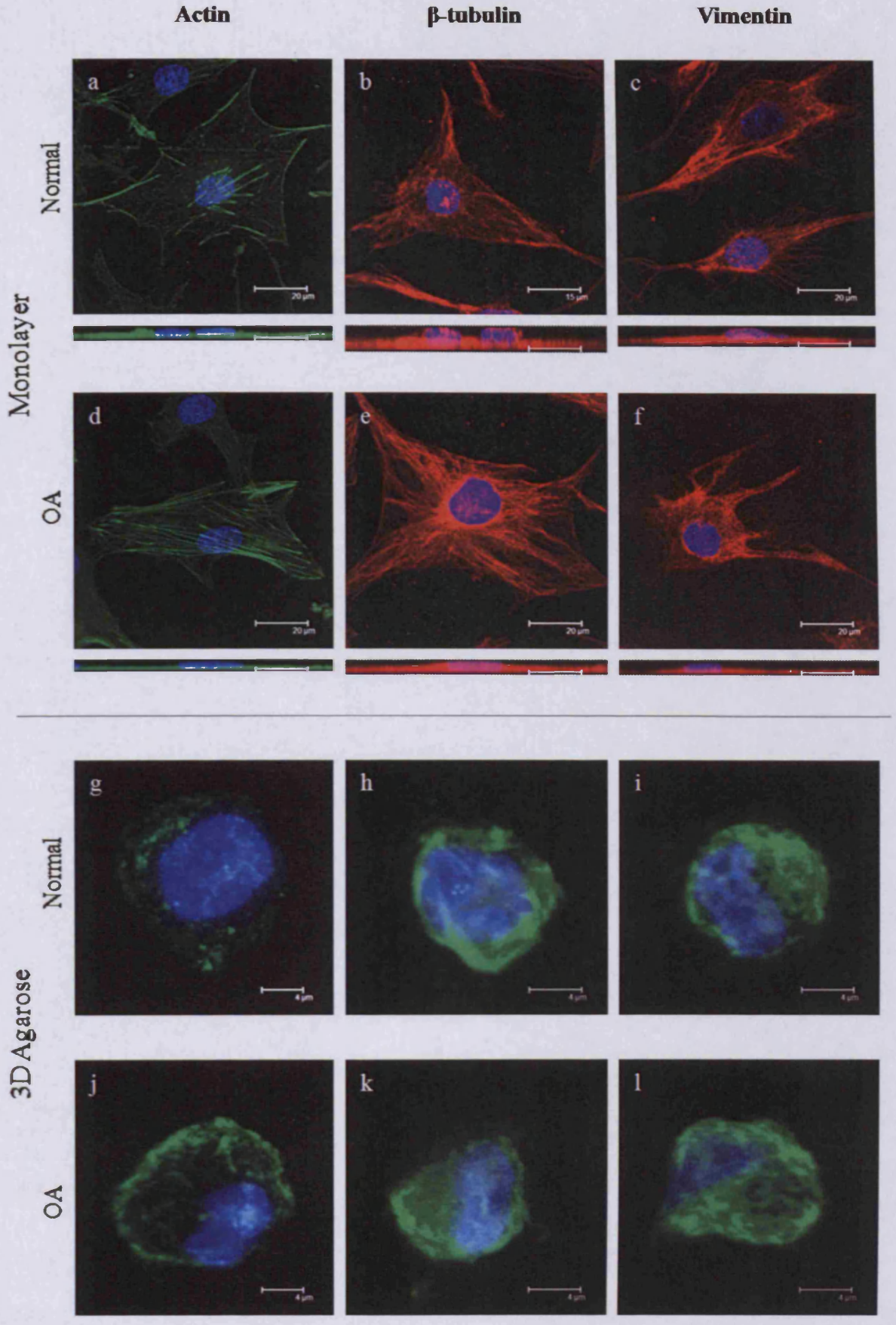
Actin
β-tubulin
Vimentin
Monolayer
Normal
OA
3D Agarose
Normal
OA
a
b
c
d
e
f
g
h
i
j
k
l

4.2.2 Comparison of Gene Expression in Normal and Osteoarthritic Chondrocytes

Analysis of chondrocyte gene expression using custom-designed Taqman arrays revealed differences between normal and OA chondrocytes in both monolayer and 3D agarose culture.

4.2.2.1 Gene Expression Differences in Monolayer Culture

Of the genes detected on the array, three of the four genes involved in angiogenesis (including *VEGF*) and four of the six apoptosis genes (including *GADD45B* and *CASP3*) were expressed at higher levels in OA chondrocytes compared to normal (Fig 4.2). All genes involved in hypertrophy were expressed more highly in OA chondrocytes, as were all genes involved in osteogenesis. β-actin expression was almost three-fold higher in OA chondrocytes compared to normal chondrocytes in monolayer. Expression of the anabolic growth factor TGF-β1 (*TGFB1*) and *FGF2* (basic FGF) was increased and expression of TGF binding protein (*LTBP1*) and *IGF1* decreased in OA chondrocytes. Differences in matrix and degradation gene expression varied. *MMP3* expression was four-fold lower and *MMP13*, *TIMP1* and *FN1* (fibronectin) expression was two-fold lower in OA chondrocytes. *TIMP3* expression was four-fold higher in OA chondrocytes in monolayer compared to normal. *COL2A1* expression was only detected in OA and not in normal monolayer chondrocytes; therefore no fold difference could be calculated. Expression of the common markers of 'dedifferentiation', including *COL1A1* and *COL3A1*, was higher in OA chondrocytes than in normal chondrocytes. However, expression of *SOX9*, a chondrocyte phenotype marker, was also higher in OA chondrocytes. Expression of 'S1', used by AstraZeneca as a marker of non-pathological cartilage, was decreased in OA chondrocytes when compared with normal.

4.2.2.2 Gene Expression Differences in 3D agarose culture

As observed with cells cultured in monolayer, three of the four genes involved in angiogenesis were more highly expressed in OA chondrocytes, although, unlike the monolayer, *VEGF* expression was decreased in OA (Fig 4.3). Expression of 'S1' was decreased in OA chondrocytes when compared with normal. In contrast to the monolayer cells, *COL2A1* expression was detected in normal chondrocytes cultured in 3D agarose hydrogels. In OA chondrocytes, *COL2A1* expression was increased and

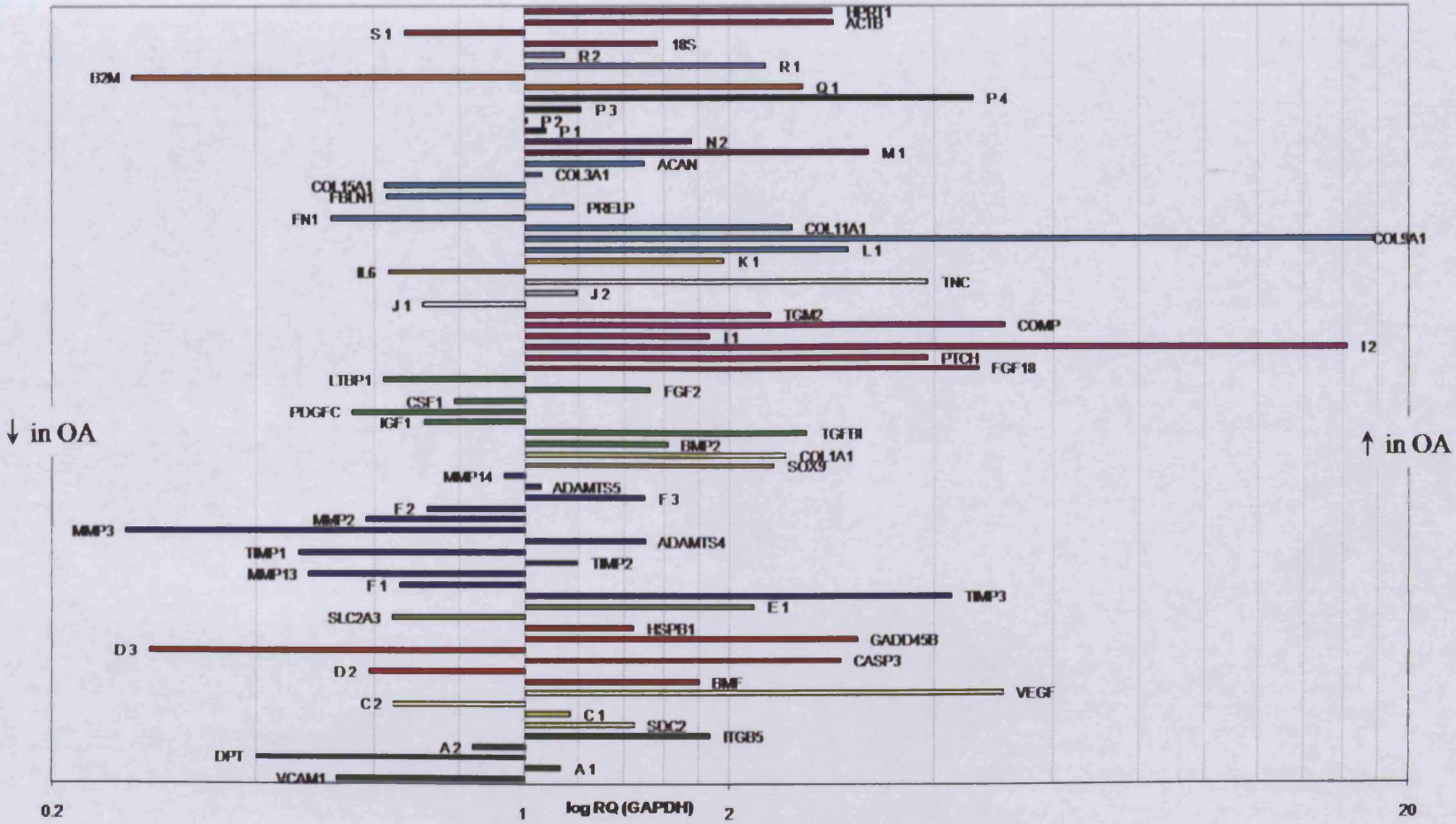

Figure 4.2:- The fold difference in expression of selected genes between chondrocytes isolated from normal and OA cartilage and cultured in monolayer (normalised to the housekeeping gene *GAPDH*). Differences were determined following quantitative PCR using a Taqman custom-designed array (AZ). Gene names are shown, except where confidentiality is required by AZ, in which case a code of one letter and number have been used. Letters (and colours) indicate a process/category which the gene product is involved/belongs; A- adhesion, C- angiogen, D- apoptosis, E- carbohydrate, F- degradation, H- growth factor, I- hypertrophy, J- hypoxia/pH, K- inflammation, L- matrix, M- metabolism, N- neurogen, P- osteogen, Q- proliferation, R- transporter, S- housekeeper. n=1

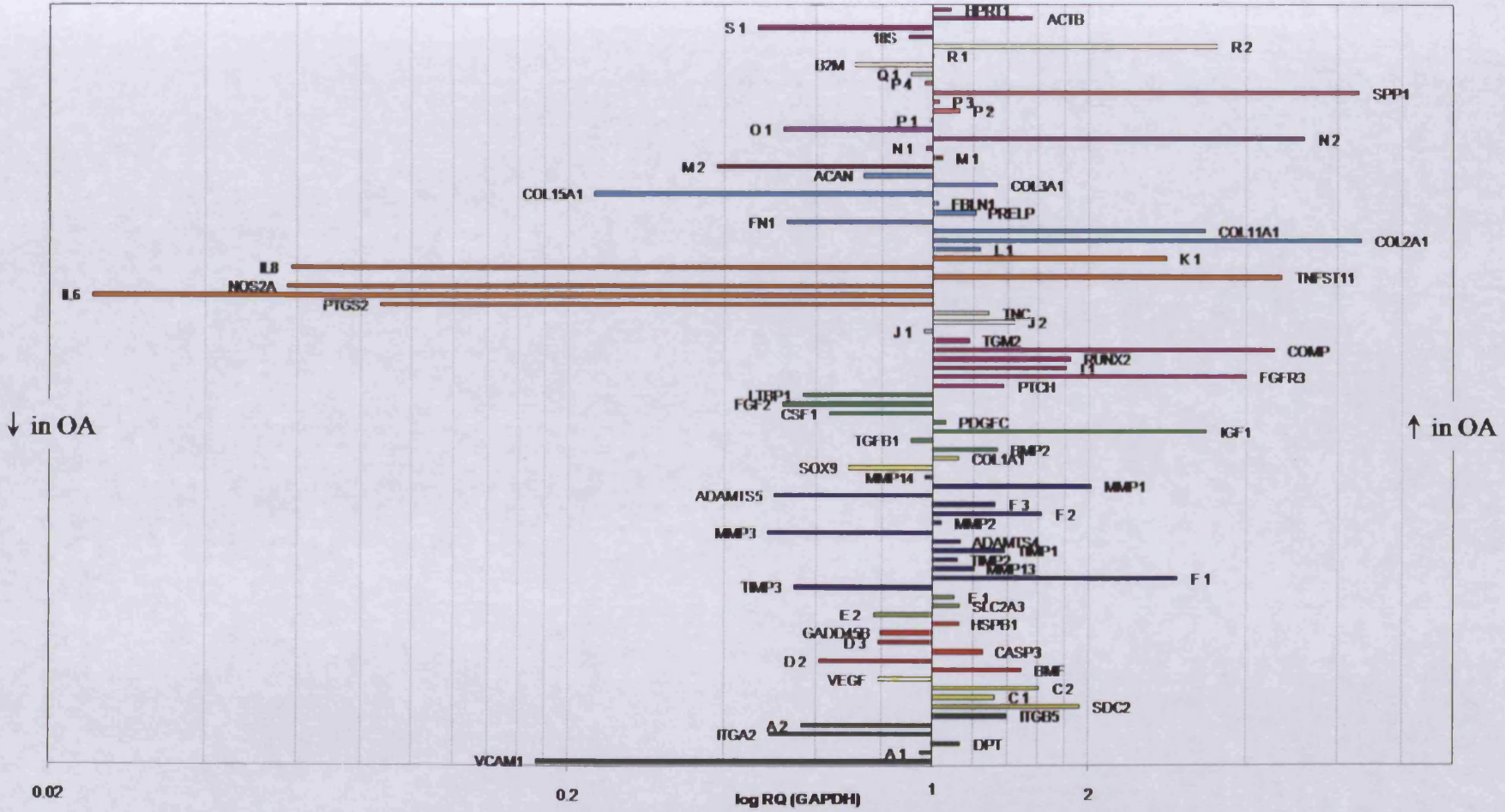

Figure 4.3:- The fold difference in expression of selected genes between chondrocytes isolated from normal and OA cartilage in 3D agarose culture (normalised to the housekeeping gene *GAPDH*). Differences were determined following quantitative PCR using a Taqman custom-designed array (AZ). Gene names are shown, except where confidentiality is required by AZ, in which case a code of one letter and number have been used. Letters (and colours) indicate a process/category which the gene product is involved/belongs; A- adhesion, C- angiogen, D- apoptosis, E- carbohydrate, F- degradation, H- growth factor, I- hypertrophy, J- hypoxia/pH, K- inflammation, L- matrix, M- metabolism, N- neurogen, P- osteogen, Q- proliferation, R- transporter, S- housekeeper. n=2

SOX9 expression decreased compared to normal. Expression of *COL1A1* and *COL3A1* was also higher in OA chondrocytes. As with the cells cultured in monolayer, all genes involved in hypertrophy and osteogenesis were expressed more highly in OA chondrocytes. In contrast to the differences observed in monolayer, expression of *FGF2* (basic FGF) was decreased and expression of *IGF1* increased in OA chondrocytes cultured in 3D agarose hydrogels. Differences in matrix and degradation gene expression varied. *MMP3*, *TIMP3* and *FN1* (fibronectin) expression was over two-fold lower in OA chondrocytes. *COL11A1* and *MMP1* expression was higher in OA chondrocytes embedded in 3D agarose hydrogels when compared with normal chondrocytes. In contrast to the increase observed in OA monolayer chondrocytes (Fig 4.2), *ADAMTS5* expression was decreased in 3D-cultured OA chondrocytes compared to normal (Fig 4.3). A large difference in the gene expression of the pro-inflammatory mediators *NOS2A*, *PTGS2* (encoding COX-2), *IL6* and *IL8* was observed in 3D-cultured OA chondrocytes. It should be noted that expression of these genes in one normal sample (n=2) was much higher than in the other samples and may therefore be skewing the results.

4.2.3 Early Gene Expression Changes with Redifferentiation

Analysis of chondrocyte gene expression using custom-designed Taqman® arrays revealed gene expression changes in monolayer-expanded normal and osteoarthritic chondrocytes following 72 hours culture in a 3D environment.

4.2.3.1 Gene Expression Changes in Normal Chondrocytes

Of the genes detected on the array, four of the five genes involved in adhesion were down-regulated in 3D culture (Fig 4.4). Four of the six apoptosis genes (including *GADD45B* and *HSPB1*, encoding hsp27) were also down-regulated in 3D culture. Of the genes encoding growth factors, five were down-regulated in 3D culture whereas TGF-β1 (*TGFB1*) and TGF binding protein (*LTBP1*) were up-regulated. All genes involved in hypertrophy were down-regulated in 3D culture, as were three of the four detected genes involved in osteogenesis. The genes encoding matrix molecules were down-regulated in 3D culture. *COL2A1* expression was only detected in 3D-cultured normal chondrocytes but not in monolayer-cultured normal chondrocytes, therefore no fold change could be calculated. However, *SOX9* expression increased and *COL1A1* and *COL3A1* expression decreased in 3D culture, indicating the expected shift back towards the chondrocyte

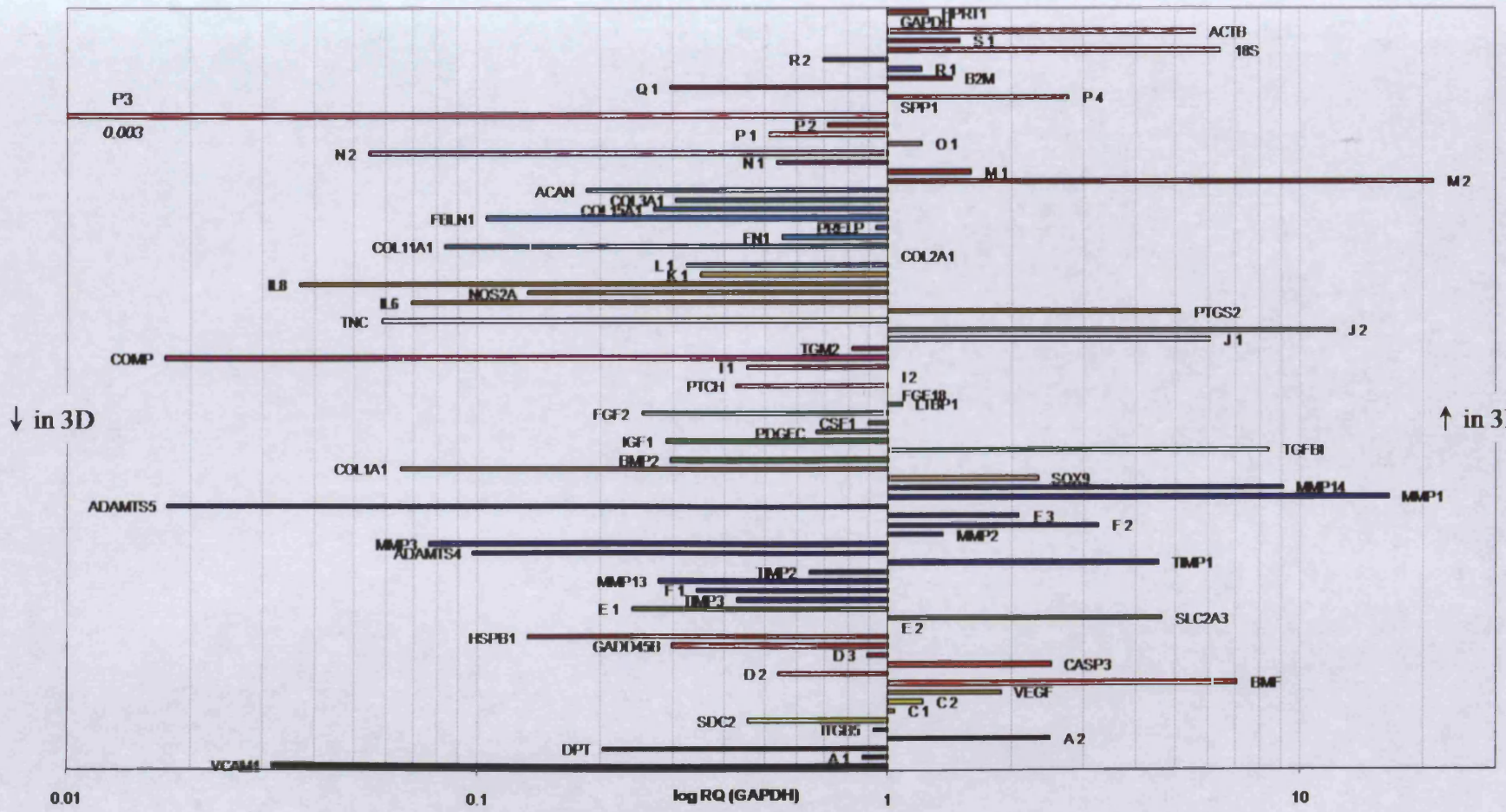

Figure 4.4:- The fold change in expression of selected genes between chondrocytes isolated from normal cartilage and cultured in monolayer or a 3D agarose hydrogel (normalised to the housekeeping gene *GAPDH*). Differences were determined following quantitative PCR using a Taqman custom-designed array (AZ). Gene names are shown, except where confidentiality is required by AZ, in which case a code of one letter and number have been used. Letters (and colours) indicate a process/category which the gene product is involved/belongs; A- adhesion, C- angiogen, D- apoptosis, E- carbohydrate, F- degradation, H- growth factor, I- hypertrophy, J- hypoxia/pH, K- inflammation, L- matrix, M- metabolism, N- neurogen, P- osteogen, Q- proliferation, R- transporter, S- housekeeper. n=1

phenotype. Changes in the expression of degradation genes varied. *MMP1* and *MMP14* expression was increased in 3D culture, whereas *ADAMTS5* expression decreased by over 55-fold. Expression of β-actin mRNA increased 5.6-fold in 3D culture.

4.2.3.2 Gene Expression Changes in Osteoarthritic Chondrocytes

As observed in normal chondrocytes (Fig 4.4), four of the five genes involved in adhesion and four of the six apoptosis genes were down-regulated in OA chondrocytes in 3D culture (Fig 4.5). Four of the seven growth factor genes were up-regulated in 3D culture including *TGFB1* and *IGF1*. All of the genes involved in hypertrophy were down-regulated in OA chondrocytes in 3D culture, as were three of the five detected genes involved in osteogenesis. As for normal chondrocytes, all genes encoding matrix molecules were down-regulated in 3D culture, including a large decrease in *COL2A1* expression (371 fold decrease in 3D). The expected decrease in *COL1A1* and *COL3A1* expression was observed in OA chondrocytes, but, unlike in normal chondrocytes, *SOX9* expression was also decreased in 3D culture. Changes in the expression of degradation genes varied, but *ADAMTS5* mRNA expression was again decreased by over 55-fold. Again, as observed in normal chondrocytes, β-actin mRNA expression increased in the 3D culture of OA chondrocytes (1.6 fold increase).

4.2.3.3 Comparison of the Changes in Normal and Osteoarthritic Chondrocytes

Changes in the expression of many of the genes on the array were similar in the early redifferentiation of both normal and osteoarthritic chondrocytes (Table 4.1). Genes expressing matrix molecules were down-regulated after 72 hours redifferentiation, although the magnitude of *ACAN* and *COL15A1* down-regulation was greater in OA chondrocytes (Fig 4.6A); *ACAN* and *COL15A1* expression was decreased 5.4- and 3.7-fold in 3D normal chondrocytes and 37- and 23-fold in 3D OA chondrocytes. Expression of all of the genes on the array involved in hypertrophy was decreased in redifferentiating normal and OA chondrocytes (Fig 4.6B). Changes in the expression of genes involved in osteogenesis remained the same in both normal and OA chondrocytes (Fig 4.6C). The largest fold change induced by redifferentiation in both normal and OA chondrocytes was seen in the decreased expression of 'P3'. The expected decrease in the expression of the typical 'dedifferentiation' markers *COL1A1* and *COL3A1* was observed, irrespective of pathology (Fig 4.7A). Transcription of *MMP14* increased and *ADAMTS5* decreased in redifferentiating normal and OA chondrocytes (Fig 4.7B). An

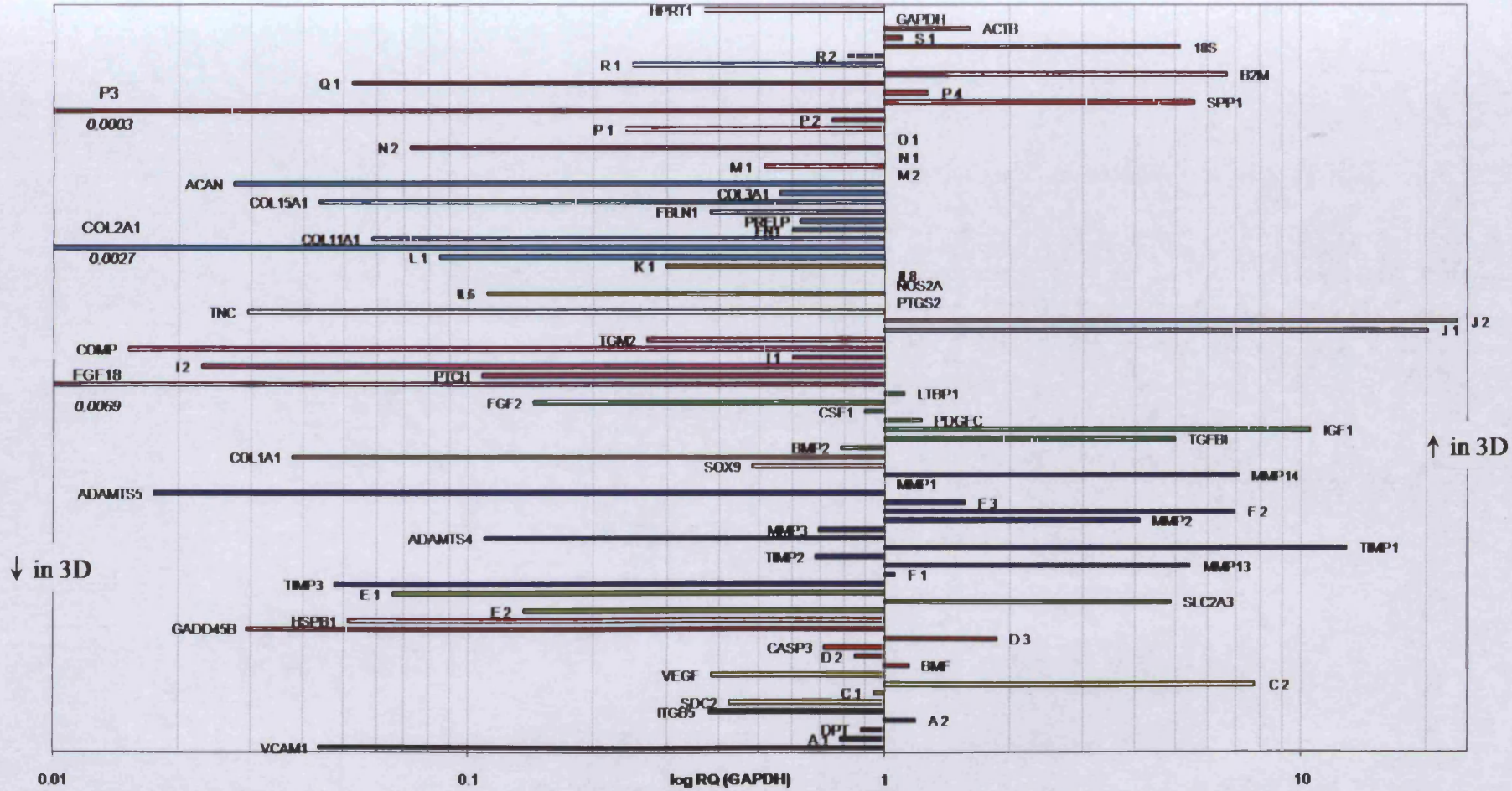

Figure 4.5:- The fold change in expression of selected genes between chondrocytes isolated from OA cartilage cultured in monolayer or a 3D agarose hydrogel (normalised to the housekeeping gene *GAPDH*). Differences were determined following quantitative PCR using a Taqman custom-designed array (AZ). Gene names are shown, except where confidentiality is required by AZ, in which case a code of one letter and number have been used. Letters (and colours) indicate a process/category which the gene product is involved/belongs; A- adhesion, C- angiogen, D- apoptosis, E- carbohydrate, F- degradation, H- growth factor, I- hypertrophy, J- hypoxia/pH, K- inflammation, L- matrix, M- metabolism, N- neurogen, P- osteogen, Q- proliferation, R- transporter, S- housekeeper. n=1

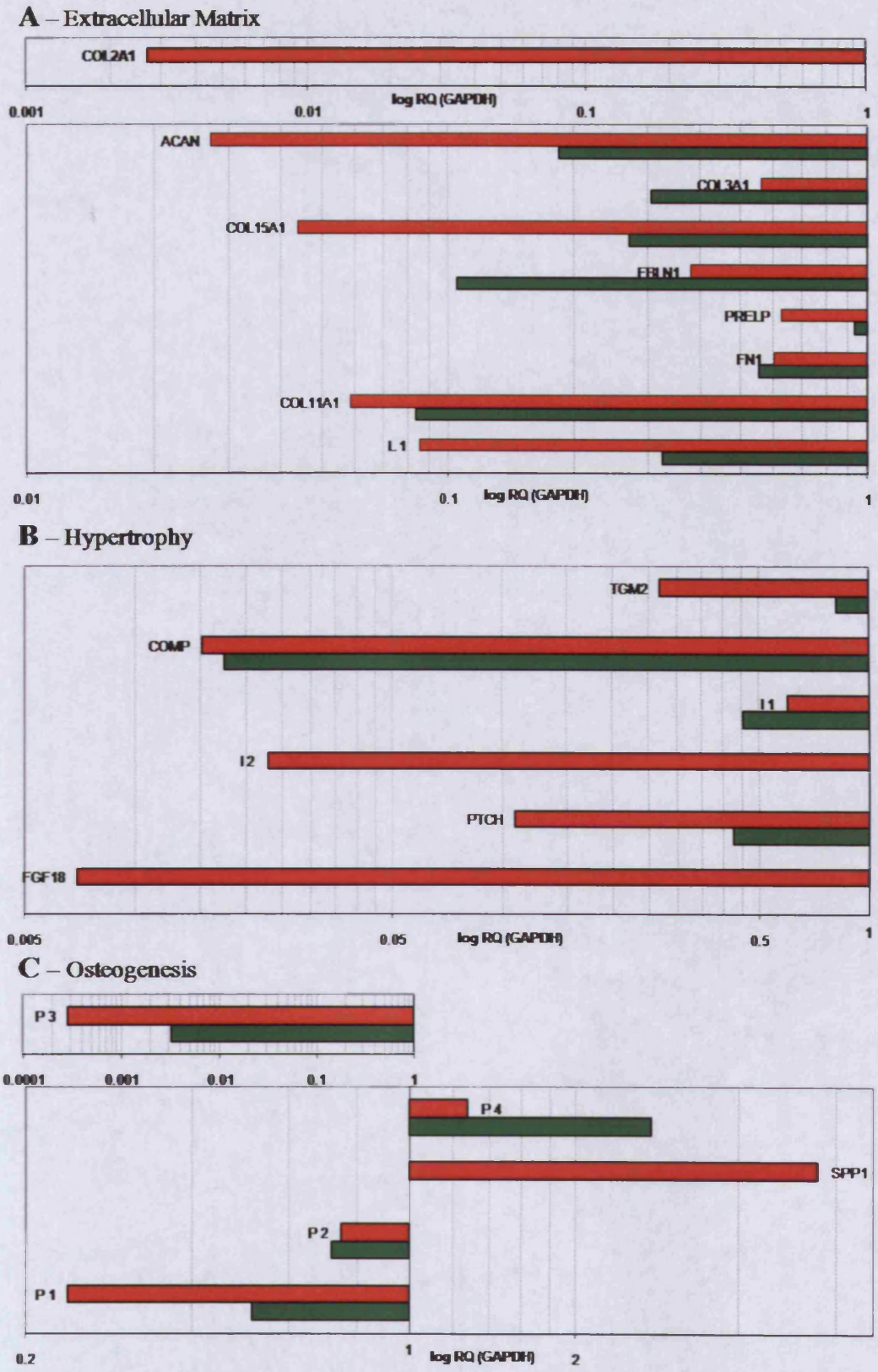

Figure 4.6:- Fold changes in gene expression of normal (green) and osteoarthritic (red) chondrocytes cultured in a 3D agarose hydrogel compared to monolayer culture (n=1). A- Genes encoding extracellular matrix proteins. B- Genes linked with chondrocyte hypertrophy. TGM2 encodes transglutaminase-2 and PTCH encodes patched. C- Genes involved in osteogenesis. SPP1 encodes osteopontin.

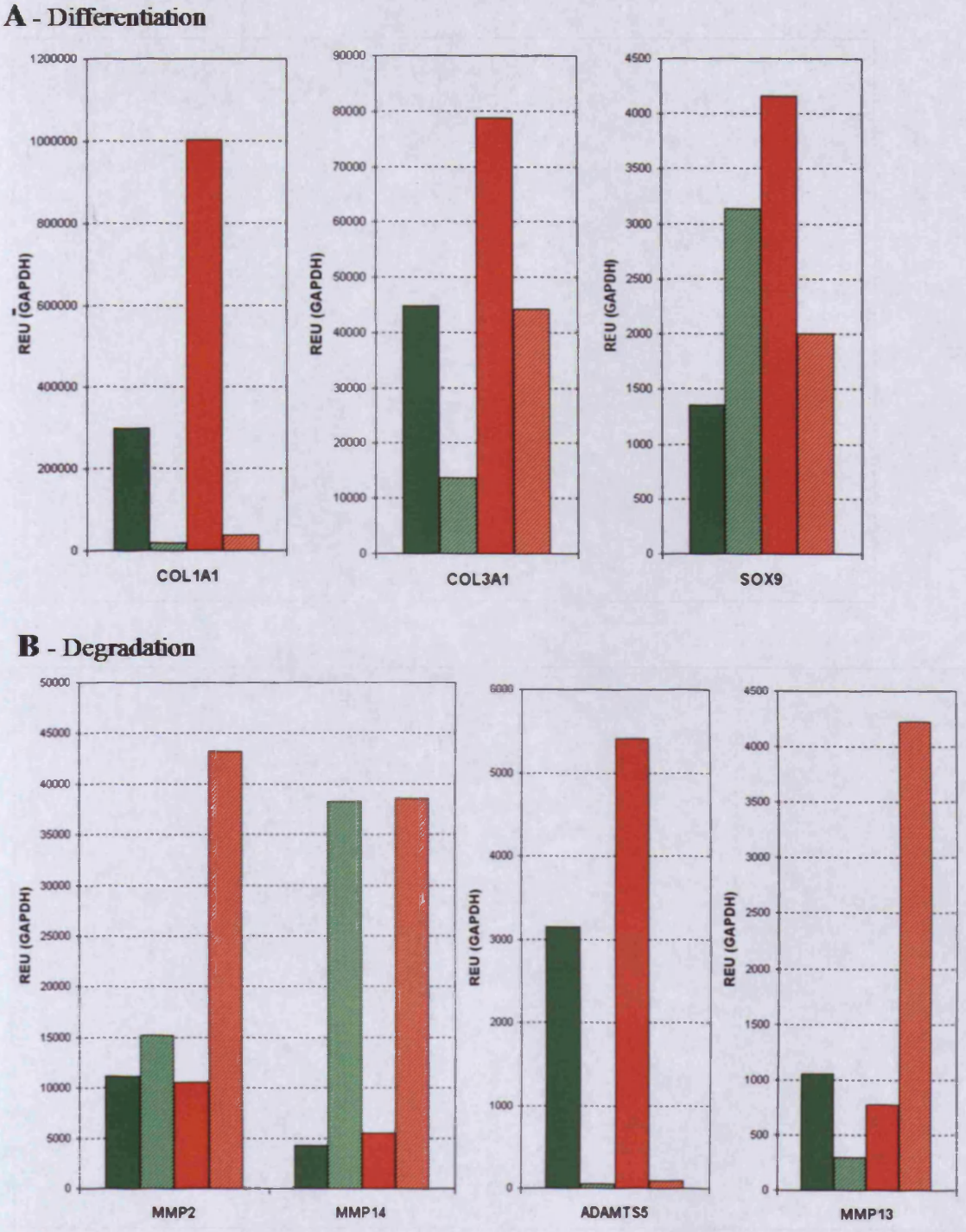

Figure 4.7:- Gene expression in normal and osteoarthritic (OA) chondrocytes cultured in a monolayer or a 3D agarose hydrogel (n=1). A- Typical markers of chondrocyte phenotype (SOX9) and dedifferentiation (COL1A1 and COL3A1). B- Genes encoding matrix degrading enzymes MMP-2, MMP-13, MMP-14, and ADAMTS-5. Normal samples are in green, OA in red. Filled columns are samples cultured in a monolayer and hatched columns are those cultured in a 3D agarose hydrogel.

increase in *TGFB1* mRNA levels and decrease in *FGF2* mRNA expression were also observed in early redifferentiation (Fig 4.8A).

However, differences were observed in gene expression profiles between normal and osteoarthritic chondrocytes during early redifferentiation (Table 4.2). Normal chondrocytes showed the expected increase in *SOX9* expression after 72 hours in 3D agarose culture whilst in OA chondrocytes *SOX9* expression decreased (Fig 4.7A). *MMP13* expression decreased in normal chondrocytes but increased in OA chondrocytes (Fig 4.7B), and the same was true for *IGF1* expression (Fig 4.8A). The change in *CASP3* expression from monolayer to 3D also differed, increasing in normal chondrocytes and decreasing in OA chondrocytes (Fig 4.8B). In addition, although expression of the apoptotic genes *HSPB1* and *GADD45B* decreased in both normal and OA chondrocytes, the decrease was bigger in OA chondrocytes (Fig 4.4 and 4.5).

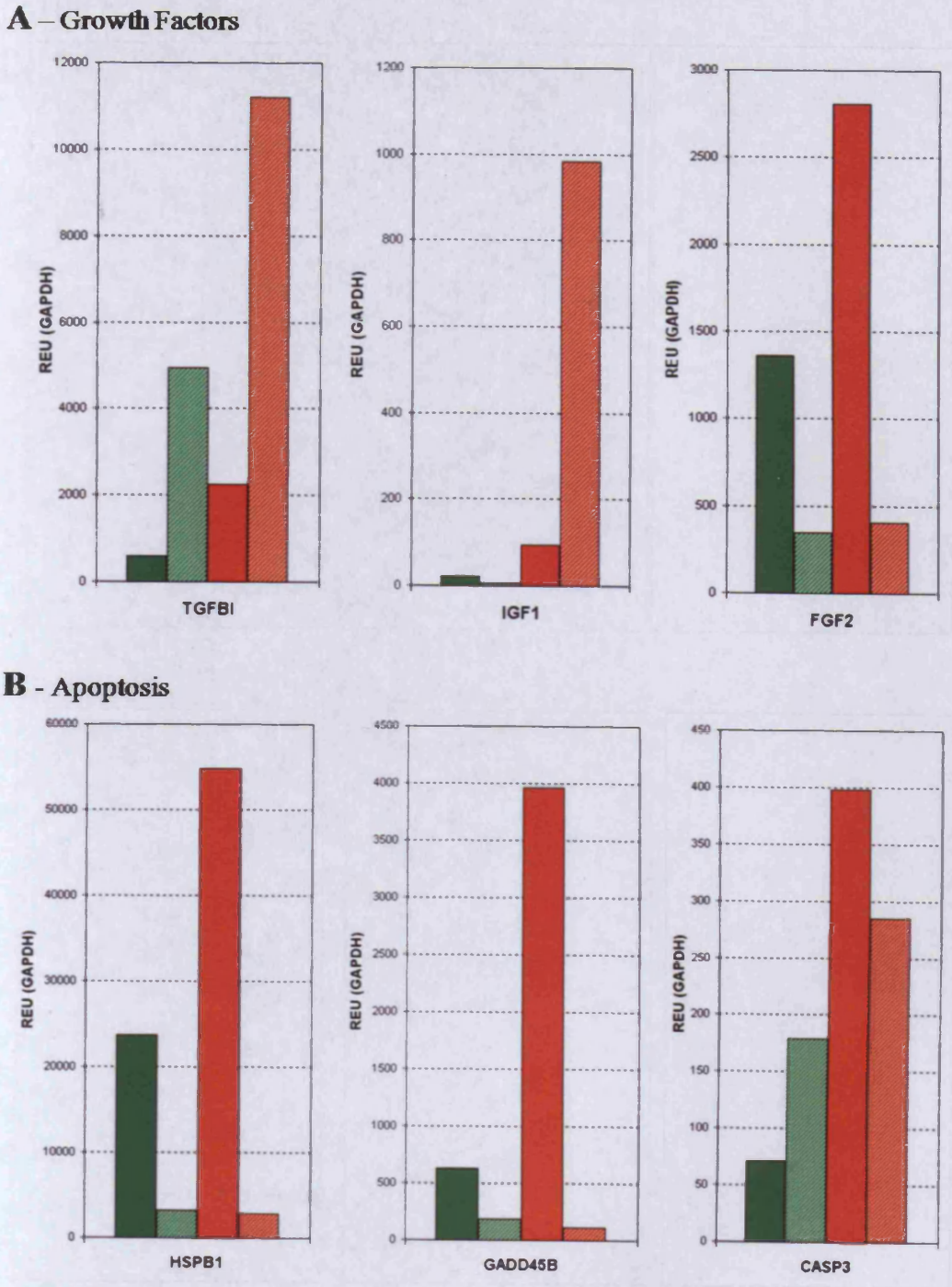

Figure 4.8:- Gene expression in normal and osteoarthritic (OA) chondrocytes cultured in a monolayer or a 3D agarose hydrogel (n=1). A- Genes encoding growth factors TGFβ1, IGF-1 and FGF-2 (bFGF). B- Genes involved in apoptosis (HSPB1 encodes Hsp27). Normal samples are in green, OA in red. Filled columns are samples cultured in a monolayer and hatched columns are those cultured in a 3D agarose hydrogel.

Genes	Change from monolayer to 3D
COL1A1 and *COL3A1*	↓
Matrix	↓
Hypertrophy	↓
'*P3*' (in osteogenesis)	↓
ADAMTS5	↓
MMP14	↑
TGFB1	↑

Table 4.1:- Gene expression changes in chondrocytes cultured in a 3D agarose hydrogel when compared with monolayer culture. Changes were the same in both normal and OA chondrocytes.

Genes	Change in normal chondrocytes	Change in OA chondrocytes
SOX9	↑	↓
MMP13	↓	↑
IGF1	↓	↑
CASP3	↑	↓

Table 4.2:- Gene expression changes in chondrocytes cultured in a 3D agarose hydrogel when compared with monolayer culture. Changes differed between normal and OA chondrocytes.

4.3 DISCUSSION

4.3.1 Differences between Normal and Osteoarthritic Chondrocytes

As in articular cartilage tissue (chapter 3) differences in the cytoskeletal organisation of chondrocytes isolated from human normal and osteoarthritic cartilage were apparent when cultured as either a monolayer or embedded in a 3D agarose hydrogel. In monolayer culture, OA chondrocytes contained more actin stress fibres than normal chondrocytes whereas vimentin intermediate filament bundles had a more clear orientation in normal chondrocytes. Differences in the actin cytoskeleton of normal and OA chondrocytes were still apparent in agarose culture; peripheral spots of actin staining were larger in OA chondrocytes.

In the case of many of the detected genes on the custom array, the difference in expression between normal and osteoarthritic chondrocytes was similar in both culture conditions. The gene 'S1' is used by AstraZeneca as a marker of non-pathological cartilage and has previously been shown to be down-regulated in moderate/severe late-stage OA cartilage (Aigner et al., 2006a). In both monolayer and 3D agarose culture, expression of 'S1' was decreased in OA chondrocytes compared to normal. Genes classed as involved in hypertrophy were expressed more highly in OA chondrocytes in both culture conditions, including *COMP*, *TGM2*, *FGF18* and *FGFR3*. Chondrocyte hypertrophy is characteristic of late-stage OA and genes associated with chondrocyte terminal differentiation have been associated with early focal degeneration in cartilage (Pullig et al., 2000, Tchetina et al., 2005, von der Mark et al., 1992). Cartilage oligomeric protein (COMP) is elevated in OA cartilage and serum levels are associated with cartilage loss (Hunter et al., 2007, Koelling et al., 2006). *TGM2* encodes transglutaminase-2, a protein required for and up-regulated with chondrocyte hypertrophy (Johnson et al., 2003, Johnson and Terkeltaub, 2005). In the Hartley guinea pig model of spontaneous OA, *TGM2* expression increases with OA and serum levels correlate with disease severity (Huebner et al., 2009). FGF18 signals through FGFR3 to regulate chondrocyte proliferation and differentiation and is required for chondrocyte hypertrophy (Davidson et al., 2005, Liu et al., 2007).

In OA chondrocytes in monolayer and agarose culture, expression of *CASP3*, encoding the pro-apoptotic caspase-3, and *HSPB1*, encoding the anti-apoptotic heat shock protein

27 (Hsp27), was higher when compared with normal chondrocytes. *HSPB1* expression has been shown to be up-regulated in human OA articular cartilage, as has expression of caspase-3 (Sharif et al., 2004, Lambrecht et al., 2009, Ijiri et al., 2008). Growth arrest and DNA damage-inducible protein 45β (GADD45β) is also involved in apoptosis. Up-regulation of *GADD45B* by NFκB leads to inhibition of TNFα-induced apoptosis (De Smaele et al., 2001). GADD45β binds to JNK kinase 2 (MAPK kinase 7), inhibiting its catalytic activity and subsequent activation of JNK signalling, thus protecting the cells against apoptosis (Papa et al., 2004). In contrast to this anti-apoptotic role, GADD45β can also be pro-apoptotic; it activates p38 MAPK and promotes TGF-β-induced apoptosis (Yoo et al., 2003). In cartilage chondrocytes, GADD45β has previously been shown to play a cytoprotective role (Ijiri et al., 2008). *GADD45B* expression decreases in both OA bone and articular cartilage (Hopwood et al., 2007, Ijiri et al., 2008). In chondrocyte cultures, *GADD45B* expression was lower in OA chondrocytes cultured in a 3D environment, but higher in OA chondrocytes cultured as a monolayer when compared with the respective normal cells.

In monolayer, expression of the angiogen VEGF was higher in OA chondrocytes compared to normal chondrocytes. This supports work by others indicating an increase in VEGF protein levels in OA cartilage (Pfander et al., 2001, Enomoto et al., 2003). However, comparison of normal and OA cartilage (chapter 3) showed *VEGF* mRNA expression was decreased in OA. This was also the case in the 3D agarose culture, where *VEGF* expression was lower in OA chondrocytes compared to normal. As chondrocytes are reported to be dedifferentiated in OA, the elevated *COL1A1* and *COL3A1* expression in OA chondrocytes in both monolayer and 3D agarose culture is as predicted, and correlates with the observation in OA cartilage (Adam et al., 1984). The expected reduction in *SOX9* expression in OA compared to normal chondrocytes, another indication of loss of the chondrocyte phenotype, was observed in 3D agarose culture but not in monolayer. The proteases MMP-13 and ADAMTS-5, analysed in normal and OA cartilage (chapter 3) also showed different effects of pathology depending on the culture conditions. *MMP13* expression is elevated in OA cartilage (chapter 3; (Bau et al., 2002)) and in OA chondrocytes in 3D culture; however in monolayer culture *MMP13* expression was higher in normal chondrocytes than in OA chondrocytes. *ADAMTS5* expression was higher in OA chondrocytes cultured as a monolayer when compared with normal and this is in support of previous reports indicating elevated *ADAMTS5*

expression in OA (Bau et al., 2002). However, comparison of normal and OA cartilage (chapter 3) revealed decreased *ADAMTS5* expression in OA and this was also observed in 3D agarose culture.

Collectively, these data indicate that the differences in gene expression between chondrocytes in normal and OA cartilage are more accurately reflected when isolated chondrocytes are cultured in a 3D environment i.e. agarose, specifically in the case of *VEGF*, *SOX9*, *MMP13* and *ADAMTS5* expression.

4.3.2 Changes with 'Redifferentiation' in 3D Culture

When cultured in 3D agarose hydrogels, both normal and osteoarthritic chondrocytes regained a morphology and cytoskeletal architecture that is characteristic of a chondrocyte phenotype. Normal and OA chondrocytes became round and actin stress fibres disappeared, with actin staining becoming localised to the cell periphery, as is typical of chondrocytes in articular cartilage (Langelier et al., 2000). In addition, β-actin expression increased in early redifferentiation in both normal and OA chondrocytes, possibly as a result of the cytoskeletal remodelling occurring with the changes in cell shape and chondrocyte phenotype.

Following 72 hours redifferentiation, expression of adhesion genes decreased in both normal and OA chondrocytes. This is as expected as cells have transferred from an anchorage-dependant culture system to a non-adhesive 3D culture system. In support of this, a previous study has shown that *VCAM1* and *ITGB1* (integrin β1) expression was down-regulated following seven and 14 days redifferentiation, respectively, of human articular chondrocytes isolated from non-OA patients undergoing autologous transplantation (ACT) therapy (Tallheden et al., 2004). Expression of the gene '*A2*' increased in 3D culture but, whilst classed by AstraZeneca as a gene encoding an adhesion protein, the 'A2' protein is localised to the plasma membrane rather than playing a more typical role in cell adhesion.

All hypertrophic genes were down-regulated following 72 hours redifferentiation of both normal and OA chondrocytes. *COL10A1*, a marker of chondrocyte hypertrophy, has been shown to be down-regulated in chondrocytes from ACT patients following seven and 14 days of redifferentiation (Tallheden et al., 2004). Although undetected in the

cartilage cDNA samples used in the present study, the decreased *COL10A1* expression shown previously supports the apparent decrease in chondrocyte hypertrophy with redifferentiation. Results from the study of redifferentiation of chondrocytes from ACT patients showed an increase in *COMP* expression at seven and 14 days (Tallheden et al., 2004). In contrast, results presented here indicate in excess of a 50-fold down-regulation of *COMP* expression in both normal and OA chondrocytes. This could be explained by the shorter time point investigated here, where chondrocytes were subject to redifferentiation for three days only, compared to seven and 14 days in the published study.

Changes in the expression of apoptotic genes in early redifferentiation were variable in both normal and OA chondrocytes. *HSPB1* and '*D2*' expression decreased in 3D culture in both normal and OA chondrocytes and these both encode anti-apoptotic proteins. *GADD45B* expression also decreased in 3D culture and, as discussed above, GADD45β can be both pro- and anti-apoptotic (De Smaele et al., 2001, Yoo et al., 2003) but has been shown to be cyto-protective in chondrocytes (Ijiri et al., 2008). In addition, expression of *BMF*, encoding a pro-apoptotic protein not previously described in chondrocytes, increased with redifferentiation. This suggests decreased resistance to apoptosis in early redifferentiation. Changes in expression of '*D3*' and *CASP3* differed between normal and OA chondrocytes. '*D3*' encodes an anti-apoptotic protein and, from monolayer to 3D culture, expression decreased in normal chondrocytes but increased in OA chondrocytes. Caspase-3 is an executioner of apoptosis and, from monolayer to 3D culture, expression increased in normal chondrocytes but decreased in OA chondrocytes. This further suggests a decreased resistance to apoptosis in normal chondrocytes. However this is inconsistent with previous reports of redifferentiation in human normal articular chondrocytes which showed improved resistance to apoptosis and cell survival following 48 hours redifferentiation, and decreased *CASP3* expression after seven days redifferentiation (Haudenschild et al., 2001, Tallheden et al., 2004). The changes in apoptotic gene expression in early redifferentiation of OA chondrocytes is varied, with some gene changes implying decreased resistance to apoptosis and others implying an increased resistance.

Genes encoding extracellular matrix components were down-regulated after 72 hours redifferentiation of normal and OA chondrocytes. This is consistent with previous

reports of decreased matrix synthesis and matrix gene expression in early redifferentiation (Benya and Shaffer, 1982a, Haudenschild et al., 2001). The decrease in *COL1A1* and *COL3A1* expression supports the expected redifferentiation towards a chondrocytic phenotype (Benya and Shaffer, 1982a, Stokes et al., 2001). *COL2A1* expression was detected in normal chondrocytes in 3D agarose but undetected in normal monolayer chondrocytes, implying an up-regulation and redifferentiation of the cartilage collagen phenotype. However, in OA chondrocytes *COL2A1* expression decreased following 72 hours in agarose culture. This could be due to a general decrease in anabolism early in redifferentiation which would be followed by increased matrix synthesis and deposition. Another study has shown that OA chondrocytes, like normal chondrocytes, are able to redifferentiate in 3D culture following monolayer expansion; extracellular type II collagen and glycosaminoglycans were detected at seven days and had increased by 14 days (Tallheden et al., 2005). It is also possible that the decrease in *COL2A1* expression is due to a delayed or slower redifferentiation of OA chondrocytes compared to normal. This is supported by the differential expression of *SOX9* which increased in normal chondrocytes cultured in a 3D agarose hydrogel but decreased in OA chondrocytes. A transient decrease in *SOX9* expression in early redifferentiation has also been observed in ACT chondrocytes, and this was followed by the expected up-regulation with sustained redifferentiation (Tallheden et al., 2004). Previous work has shown that OA chondrocytes retain the ability to redifferentiate, but that their response differs to normal chondrocytes in that they synthesise less total collagen and continue to proliferate after 14 days in 3D pellet culture (Tallheden et al., 2005). The apparent slower redifferentiation of OA chondrocytes is rescued by SOX9 transduction into chondrocytes *in vitro* prior to 3D culture (Tew et al., 2005, Cucchiarini et al., 2007).

Gene expression changes showing the same response of normal and OA chondrocytes to 72 hours culture in 3D agarose supports previous work indicating that a pathological background does not compromise the potential of chondrocytes for redifferentiation (Cucchiarini et al., 2007, Tallheden et al., 2005, Tew et al., 2005). Gene expression changes differing between normal and OA chondrocytes in early redifferentiation, including *SOX9*, *CASP3*, *MMP13* and *IGF1*, suggest that there are inherent differences between normal and OA chondrocytes that are not lost with isolation of chondrocytes from their ECM, or with the transfer of chondrocytes to a culture system more supportive of the chondrocyte phenotype.

- When cultured in 3D agarose hydrogels, chondrocyte phenotype and cytoskeletal organisation resembles that observed in articular cartilage *in situ*.
- The differences in cytoskeletal organisation and gene expression observed between normal and OA cartilage are better represented when chondrocytes are cultured in 3D agarose hydrogels rather than as a monolayer.
- Inherent differences between normal and OA chondrocytes are not lost with isolation from cartilage followed by monolayer culture and embedding in 3D agarose hydrogels.
- During early redifferentiation, genes involved in adhesion and hypertrophy are down-regulated in chondrocytes isolated from both normal and OA cartilage, whilst apoptosis gene regulation varies between normal and OA chondrocytes.
- OA chondrocytes are slower to redifferentiate when compared with normal chondrocytes.

The work discussed in the chapter is preliminary, with repeats of the comparisons using different donors required before firm conclusions can be drawn from the differences observed here.

Chapter 5: Cytoskeleton and Chondrocyte Phenotype

5. CYTOSKELETON AND CHONDROCYTE PHENOTYPE

5.1 INTRODUCTION

Alterations in cell phenotype are linked to changes in the cytoskeleton, whether through direct modification of the cytoskeletal networks or using treatments which alter cytoskeletal organisation.

5.1.1 Direct Modification of the Cytoskeleton Alters Cellular Phenotype

Links between the chondrocyte phenotype and cytoskeletal organisation were discovered following the establishment of the link between phenotype and cell shape (Benya and Shaffer, 1982a). Disruption of actin microfilaments with cytochalasin B/D or microtubules with colchicine inhibited the synthesis and secretion of proteoglycans and collagen in foetal guinea pig epiphyseal chondrocytes (Lohmander et al., 1976, Lohmander et al., 1979). In articular chondrocytes, increased proteoglycan synthesis and secretion was associated with cytochalasin D-induced disruption of the actin cytoskeleton and cell rounding (Newman and Watt, 1988). The recovery of chondrocyte phenotype upon cell rounding, as indicated by increased type II collagen production, was shown to be due to reorganisation of the actin cytoskeleton rather than cell rounding (Benya et al., 1988, Brown and Benya, 1988). Expression of *COL2A1*, aggrecan and *SOX9* is increased in murine chondrocytes in monolayer following disruption of the actin microfilaments with cytochalasin D (Woods and Beier, 2006). Disruption of actin microfilaments in fibroblasts inhibited the synthesis and secretion of GAGs and proteins, and the endocytosis of hyaluronic acid in a dose-dependent manner (Evangelisti et al., 1995). The synthesis and secretion of GAGs and protein synthesis were also inhibited in fibroblasts by disruption of tubulin microtubules, again in a dose-dependent manner (Evangelisti et al., 1995). In rabbit chondrocytes, GAG synthesis was inhibited and chondrocyte phenotype lost following microtubule disruption with colchicine (Takigawa et al., 1984). Collagen synthesis and degradation was decreased following disruption of vimentin intermediate filaments with acrylamide in bovine chondrocytes; mRNA expression of *COL2A1* and aggrecan core protein was also down-regulated with vimentin disruption (Blain et al., 2006).

In addition to modulation of extracellular matrix molecule expression and synthesis, cytoskeletal disruption alters MMP expression. Disruption of actin stress fibres in

cultured rabbit synovial fibroblasts using cytochalasin B caused cells to round, and induced the expression of pro-MMP-1 and pro-MMP-3 (Werb et al., 1986). The presence of actin stress fibres correlated negatively with expression of pro-MMP-1 and -3, indicating that reorganisation of the actin cytoskeleton can induce changes in MMP gene expression (Werb et al., 1986). A further study, using cultured human fibroblasts, showed that disruption of actin stress fibres, again using cytochalasin B, increased MMP-2 and MT1-MMP (MMP-14) mRNA levels (Tomasek et al., 1997). In addition, the disruption of actin stress fibres resulted in a significant increase in the activation of pro-MMP-2 enzyme. Disruption of microtubules with nocodazole demonstrated that the changes in gene expression were due to a specific reorganisation of the actin cytoskeleton and not due to changes in cell shape (Tomasek et al., 1997), as observed in chondrocytes (Brown and Benya, 1988). More recently it has been shown using human fibroblasts cultured in monolayer, that disruption of actin stress fibres also significantly increases the levels of MMP-3, -9, -13 and -14 mRNA (Lambert et al., 2001). This study also indicated that the observed activation of pro-MMP-2 was due to its activation by other MMPs, likely MMP-14. Pro-MMP-2 expression and activation is reduced in bovine chondrocytes following disruption of vimentin intermediate filaments with acrylamide (Blain et al., 2006).

In addition to altering the chondrocyte phenotype in differentiated cells, disruption of the actin, tubulin or vimentin cytoskeleton can also alter chondrogenesis in progenitor cells. Disruption of the actin cytoskeleton with cytochalasin D treatment up-regulates *COL2A1*, *SOX9* and aggrecan expression and enhances chondrogenesis in murine embryonic stem cells cultured in chondrogenic medium (Zhang et al., 2006c). Chondrogenesis in murine mesenchymal limb bud cells is enhanced by cytochalasin D treatment but inhibited by disruption of microtubules with colchicine, as indicated by *SOX9* expression and GAG accumulation (Woods et al., 2005). siRNA knockdown of vimentin reduced the expression of SOX5, SOX6 and SOX9 in human bone marrow-derived multipotent progenitor cells in pellet culture (Bobick et al., 2010). Expression and accumulation of aggrecan and type II collagen was also reduced by vimentin knockdown, which reduced cartilage formation in the model of adult progenitor cell chondrogenesis.

5.1.2 Upstream Regulators of the Actin Cytoskeleton Modulate Chondrocyte Phenotype

The Rho family GTPases regulate actin cytoskeletal dynamics through multiple pathways; downstream kinases such as the LIM kinases and ROCK are activated and these regulate actin-modifying proteins including cofilin, profilin and the Arp2/3 complex. RhoA/ROCK signalling promotes actin stress fibre formation and inhibits *SOX9* expression preventing chondrogenesis (Woods et al., 2005). Conversely, inhibition of ROCK signalling reduces actin stress fibres, induces SOX9 and restores chondrogenesis (Woods et al., 2005, Tew and Hardingham, 2006). Hypertrophic differentiation of chondrocytes is also inhibited by RhoA/ROCK signalling, with downregulation of type X collagen and *MMP13* expression, whilst cyclin D1 expression and chondrocyte proliferation is enhanced (Wang et al., 2004). Overexpression of constitutively active Rho, in articular chondrocytes cultured as a monolayer, increases ROCK-dependent stress fibre formation and upregulates expression of *MMP13* and *COL1A1*, indicating a loss of chondrocyte phenotype (Novakofski et al., 2009). Inhibition of Rho activity with C3 transferase increases *ACAN*, *COL2A1* and *SOX9* expression and reduces *COL1A1*, indicating promotion of the chondrocyte phenotype by Rho inhibition. Furthermore, RhoA protein expression increases with chondrocyte dedifferentiation in monolayer and decreases with redifferentiation in 3D alginate (Kumar and Lassar, 2009).

Activation of the Rho GTPases Rac-1 and Cdc42 is elevated in mature chick embryonic chondrocytes when compared with immature cells implying a role in chondrocyte differentiation (Kerr et al., 2008). Rac-1 increases cortical actin staining when overexpressed in a chondrocyte cell line, with Rac-1 and Cdc42 overexpression inhibiting chondrocyte proliferation whilst promoting *COL10A1* expression and hypertrophic differentiation (Wang and Beier, 2005). In micromass culture both Rac-1 and Cdc42 promote chondrogenesis, up-regulating expression of *SOX9* and type II collagen, and in the case of Rac-1, increasing aggrecan mRNA and GAG synthesis (Woods et al., 2007). By contrast, in equine chondrocytes cultured as a monolayer inhibition of Cdc42 with a dominant-negative mutant increased type II collagen and decreased *MMP3* expression, suggesting Cdc42 inhibits the chondrocyte phenotype in chondrocytes containing actin stress fibres (Fortier et al., 2004).

The effects of the Rho GTPases on chondrocyte differentiation further demonstrate the close link between cytoskeletal organisation and chondrocyte phenotype.

5.1.3 Growth Factors and Cytokines Affect the Cytoskeleton

Cytoskeletal organisation can also be modulated by exogenous growth factors or cytokines. TGFβ1 treatment activates RhoA and Rac1 in retinal epithelial cells, inducing Rho-dependent phosphorylation of LIM kinase and cofilin and rearrangement of the actin cytoskeleton (Lee et al., 2008). In fibroblasts, TGFβ1 activates RhoA and RhoB to induce actin polymerisation and stress fibre formation through ROCK1-mediated phosphorylation of LIM kinase 2 and cofilin (Vardouli et al., 2005). In chondrocytes in 3D culture, TGFβ treatment alters actin cytoskeletal organisation, inducing lamellar ruffling and actin extensions which is indicative of Rac/Cdc42 activation (Haudenschild et al., 2009). TGFβ1 and IGF-I maintain chondrocytes in a round morphology and increase F-actin labelling, resulting in increased cell stiffness (Leipzig et al., 2006). Chondrocyte rounding and cortical actin staining is increased by IGF-I treatment, which reduces Rho activity (Novakofski et al., 2009). IGF-I treatment also reduces Cdc42 activation and decreases actin stress fibres in articular chondrocytes (Fortier et al., 2004). By contrast, TGFα treatment increases actin stress fibre formation in rat chondrocytes (Appleton et al., 2007a).

The pro-inflammatory cytokine TNFα disrupts actin stress fibres in fibroblasts (Gronowicz et al., 1992) and another pro-inflammatory cytokine, IL-1, reorganises the actin cytoskeleton in osteoclasts (Nakamura et al., 2002). In astrocytes, IL-1β treatment results in disruption of actin filaments, aggregation of vimentin networks and down-regulates expression of vimentin and microtubule-associated protein 4 (Liu et al., 1994). In chondrocytes, IL-1α increases Rho activity and stress fibre formation (Novakofski et al., 2009); IL-1β causes cellular contraction indicative of RhoA activation (Haudenschild et al., 2009). In addition, a whole genome array identified a number of cytoskeletal-associated genes regulated in chondrocytes treated with IL-1β (Joos et al., 2008). IL-1β treatment altered actin organisation and down-regulated expression of vimentin, β-tubulin and the actin-associated LIM protein FHL2. IL-1 treatment has also been shown to reduce expression of the cytoskeletal proteins tensin, talin, paxillin and focal adhesion kinase in articular chondrocytes (Vinall et al., 2002).

5.1.4 Growth Factors and Cytokines Modulate Chondrocyte Phenotype

TNFα-induced increases in fibroblast collagenase expression and activity is associated with disruption of actin stress fibres (Gronowicz et al., 1992). In canine chondrocytes cultured in 3D agarose, TNFα reduces GAG content and increases production of nitric oxide and prostaglandin E2 (Kuroki et al., 2005), whilst it promotes MMP-mediated collagen breakdown in bovine cartilage explants (Hui et al., 2001). Loss of the chondrocyte phenotype is induced by IL-1 (Vinall et al., 2002), as IL-1α reduces *COL2A1* expression and up-regulates *MMP13* in articular chondrocytes (Novakofski et al., 2009). IL-1β also down-regulates expression of *COL2A1* and aggrecan whilst up-regulating *MMP13*, *BMP2* and the pro-inflammatory cytokines IL-6 and IL-8 (Sandell et al., 2008). Along with *MMP13* expression, IL-1β increases *TIMP1* and *TIMP2* expression, enhances production of nitric oxide and prostaglandin E2 and decreases GAG content in chondrocytes cultured in 3D agarose hydrogels (Kuroki et al., 2005). Some of the phenotypic changes induced by IL-1 are antagonised by TGFβ1 (Sandell et al., 2008). Conversely, pre-treatment with IL-1β abrogates TGFβ-induced up-regulation of *COL2A1*, aggrecan and *SOX9* expression (Roman-Blas et al., 2007). TGFβ1 or IGF-I can reduce TNFα-induced collagenase expression in bovine cartilage explants (Hui et al., 2001).

TGFβ1 has been shown to both up-regulate and down-regulate type II collagen synthesis in chondrocytes (Galera et al., 1992b, Galera et al., 1992a). TGFβ1 effects are dependent on the differentiation state and cell morphology, inhibiting synthesis in differentiated chondrocytes and promoting synthesis in dedifferentiated cells (Galera et al., 1992a, Ballock et al., 1993). In addition, TGFβ1 increases GAG synthesis in immature, but not mature human articular cartilage where it alters GAG composition to that of more immature cartilage (Hickery et al., 2003). However, TGFβ induces chondrogenic differentiation in bone-marrow derived mesenchymal stem cells encapsulated in alginate (Mehlhorn et al., 2006). TGFα increases chondrocyte proliferation and clustering and up-regulates expression of *MMP13* and cathepsin C (Appleton et al., 2007a). In addition, the expression levels of aggrecan, cartilage link protein, type II collagen and SOX9 are reduced, indicating suppression of the chondrocyte phenotype by TGFα treatment. IGF-I treatment exerts anabolic effects on chondrocyte phenotype, promoting both GAG and type II collagen synthesis (Fortier et al., 2002, Jenniskens et al., 2006). IGF-I up-regulates type II collagen mRNA and protein expression through PI3K signalling, whilst

down-regulating *MMP13* expression and activation via the ERK/MAPK pathway in rat chondrocytes (Zhang et al., 2009).

As growth factors and cytokines can modulate both cytoskeletal organisation and chondrocyte phenotype, it is possible that their effect on gene expression is mediated by the cytoskeleton. In support of this, TNFα-induced increases in fibroblast collagenase expression and activation are associated with disruption of actin stress fibres (Gronowicz et al., 1992), whereas TGFβ1-induced increases in expression of plasminogen activator inhibitor requires an intact actin cytoskeleton (Yang et al., 2007). In addition, Rac1 inhibition or actin disruption prevents TGFβ1-induced biglycan expression (Groth et al., 2005), whilst TGFβ1-stimulated type I collagen expression and accumulation requires Rho/ROCK signalling and an intact actin cytoskeleton in mesangial cells (Hubchak et al., 2003). It has also been suggested that tubulin microtubules act to negatively regulate TGFβ signalling by sequestering Smads (Dong et al., 2000). However it is also possible that the effects on gene expression are mediated by cytoskeletal-independent pathways. Inhibition of Rho with C3 transferase or inhibition of ROCK block the IL-1α-induced increase in actin stress fibre formation but, despite the effects of Rho activation mimicking those of IL-1α, inhibition of Rho or ROCK does not block the effects of IL-1α on chondrocyte gene expression (Novakofski et al., 2009).

The cytoskeletal differences observed between normal and OA chondrocytes (chapter 3), along with the ability of cytoskeletal changes to alter cell phenotype, could suggest that the phenotypic change observed in OA chondrocytes is a result of an altered cytoskeleton. In order to determine whether the cytoskeletal changes are a cause or effect of the OA phenotype, the effects of cytoskeletal disruption on the phenotype of chondrocytes isolated from normal and OA cartilage and cultured in agarose hydrogels were further investigated.

5.2 RESULTS

Normal and osteoarthritic human articular chondrocytes were initially expanded in monolayer. Chondrocytes were taken at passage three, encapsulated in 3% agarose and cultured for 48 hours. Chondrocytes were treated for 6, 12, 24 or 48 hours with either 1μM cytochalasin D to disrupt actin microfilaments, 1μM colchicine to disrupt tubulin microtubules, or 2mM acrylamide to disrupt vimentin intermediate filaments.

5.2.1 The Effect of Cytoskeletal Element Disrupting Treatments on Cell Viability

The viability of normal and osteoarthritic human chondrocytes in agarose culture was determined using the LIVE/DEAD® Viability/Cytotoxicity kit for mammalian cells. In viable chondrocytes the fluorogenic esterase substrate calcein AM is hydrolysed and fluorescence is visible through a FITC (green) filter, whilst dead chondrocytes are visualised with the nucleic acid stain ethidium homodimer-1 and fluorescence detected through a TRITC (red) filter. Normal and OA chondrocytes survived the transition from monolayer to agarose culture and remained viable at 4 days, the latest timepoint assayed (Fig 5.1). Cell death did not increase from the 6 to the 48 hour untreated timepoints in normal chondrocytes in 3D agarose culture (Fig 5.1 A, a,b). However there was a decrease of 13% in the viability in OA chondrocytes (Fig 5.1 B, a,b). There appeared to be an increase in viability of untreated OA chondrocytes (Fig 5.1 B a,b) when compared with normal chondrocytes (Fig 5.1 A a,b). Cytochalasin D treatment did not affect chondrocyte viability after 6 hours (Fig 5.1 A and B, c). At 48 hours, a decrease in cell viability was observed in normal (15%, Fig 5.1 A d) and OA chondrocytes (17%, Fig 5.1 B d) treated with cytochalasin D when compared with untreated controls (Fig 5.1 A and B, b). Colchicine treatment did not affect chondrocyte viability at either 6 or 48 hours and no increase in cell death was evident from 6 hours to 48 hours in colchicine-treated OA chondrocytes (Fig 5.1 B e,f). By contrast, an 11% decrease in cell viability was observed between 6 and 48 hours in colchicine-treated normal chondrocytes (Fig 5.1 A e,f). Acrylamide treatment had no effect on chondrocyte viability at either 6 or 48 hours (Fig 5.1 A and B, g,h).

A – Normal chondrocytes

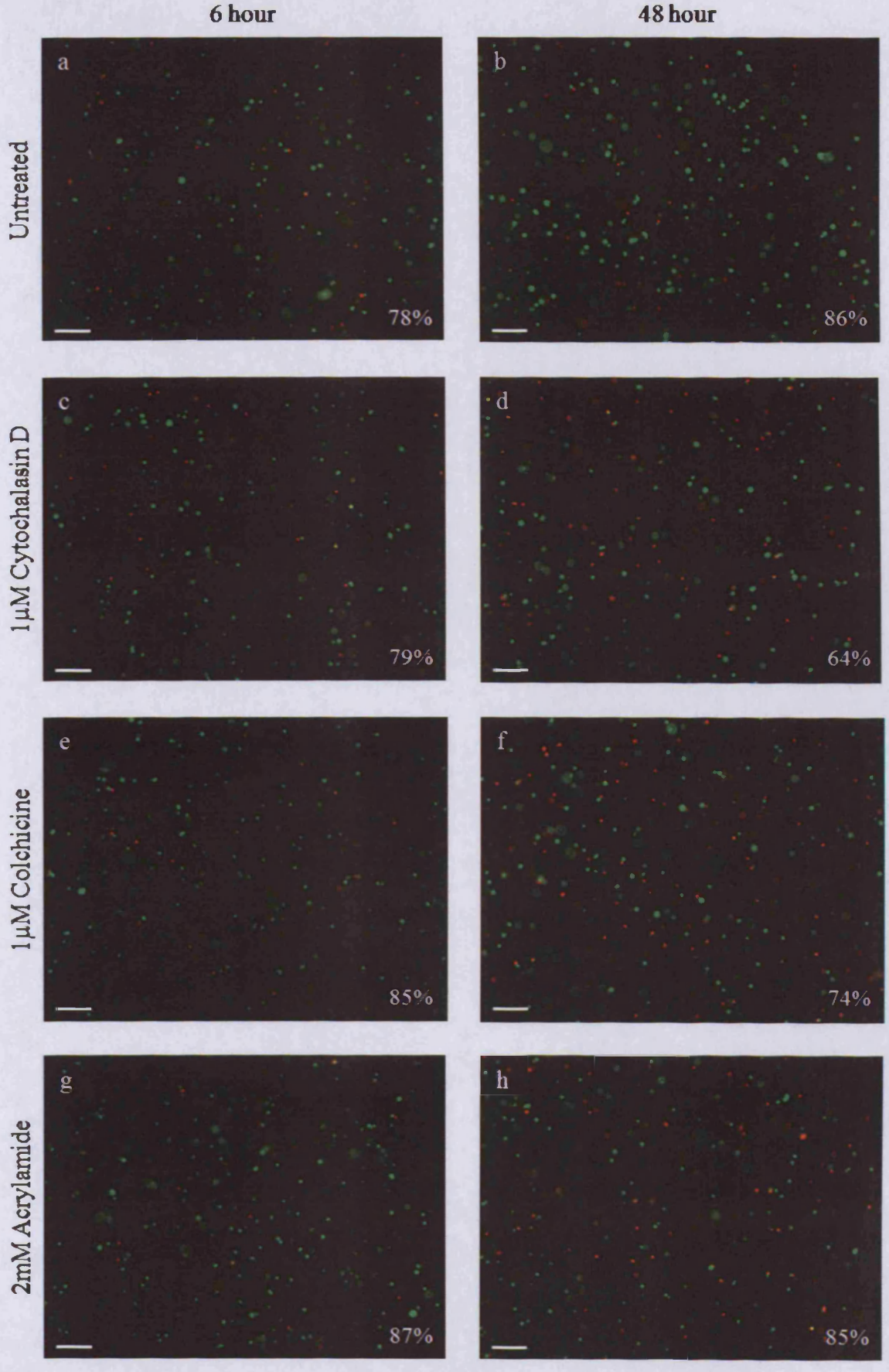

B – Osteoarthritic chondrocytes

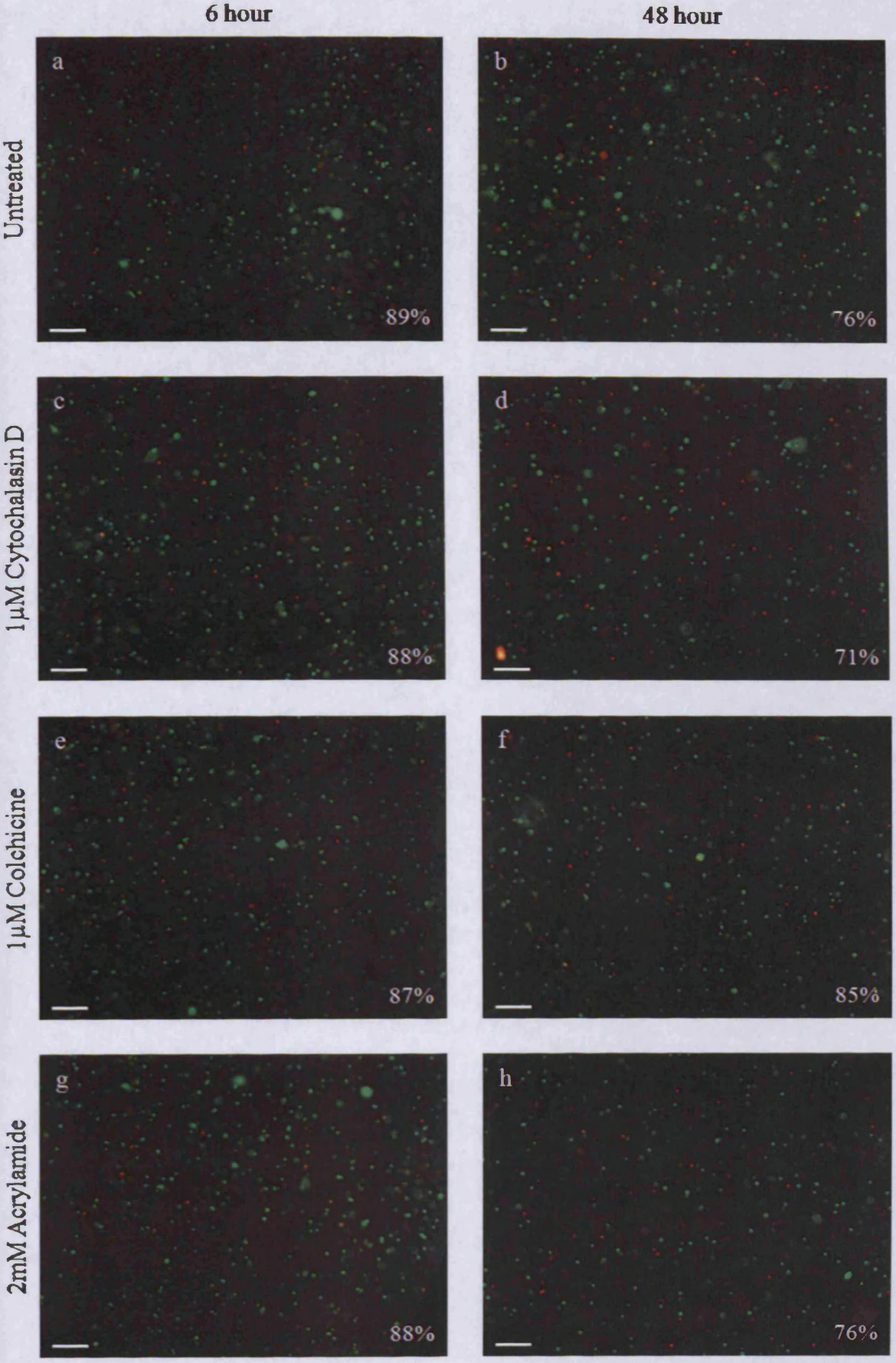

5.2.2 Visualisation and Confirmation of Cytoskeletal Disruption

The cytoskeletal architecture of chondrocytes in agarose culture was visualised by immunofluorescence in conjunction with confocal microscopy.

5.2.2.1 Untreated Chondrocytes

Following expansion in monolayer and transfer into a 3D agarose culture, both normal and OA chondrocytes regained a rounded morphology (section 4.2.1). Actin microfilament staining appeared punctate and was predominantly cortical in untreated normal chondrocytes (Fig 5.2 A and B, a). In untreated OA chondrocytes, actin staining was restricted to the cell periphery, punctuate spots appeared more elongated and networks were visible at the periphery (Fig 5.2 A and B, g). Tubulin microtubule staining appeared diffuse in untreated normal and OA chondrocytes although fine filamentous networks were apparent at the cell periphery (Fig 5.2 A and B, b and h). Untreated normal and OA chondrocytes contained clear vimentin intermediate filament bundle networks, extending throughout the cell from the nucleus to the plasma membrane (Fig 5.2 A and B, c and i).

5.2.2.2 Cytochalasin D-treated Chondrocytes

Treatment of chondrocytes with 1μM cytochalasin D for 24 hours altered the organisation of actin microfilaments. Punctate spots of actin staining appeared larger and less evenly distributed in both normal (Fig 5.2 A and B, d) and OA chondrocytes. Actin staining was also no longer restricted to the periphery of OA cells (Fig 5.2 A and B, j). The tubulin architecture was unaffected by actin microfilament disruption with cytochalasin D treatment (Fig 5.2 A and B, b,e,h and k). Vimentin intermediate filament bundle networks were also unaffected by microfilament disruption in both normal and OA chondrocytes (Fig 5.2 A and B, c,f,i and l).

5.2.2.3 Colchicine-treated Chondrocytes

Treatment of chondrocytes with 1μM colchicine for 24 hours altered the appearance of the tubulin network when compared with untreated controls (Fig 5.3 A and B, a and g). In colchicine-treated normal chondrocytes tubulin microtubule bundles appeared shorter and thicker, with staining less tightly packed around the nucleus (Fig 5.3 A and B, d). In OA chondrocytes microtubule bundles also appeared thicker and more clearly visible following colchicine treatment (Fig 5.3 A and B, j). Tubulin fluorescence was brightest at the cell

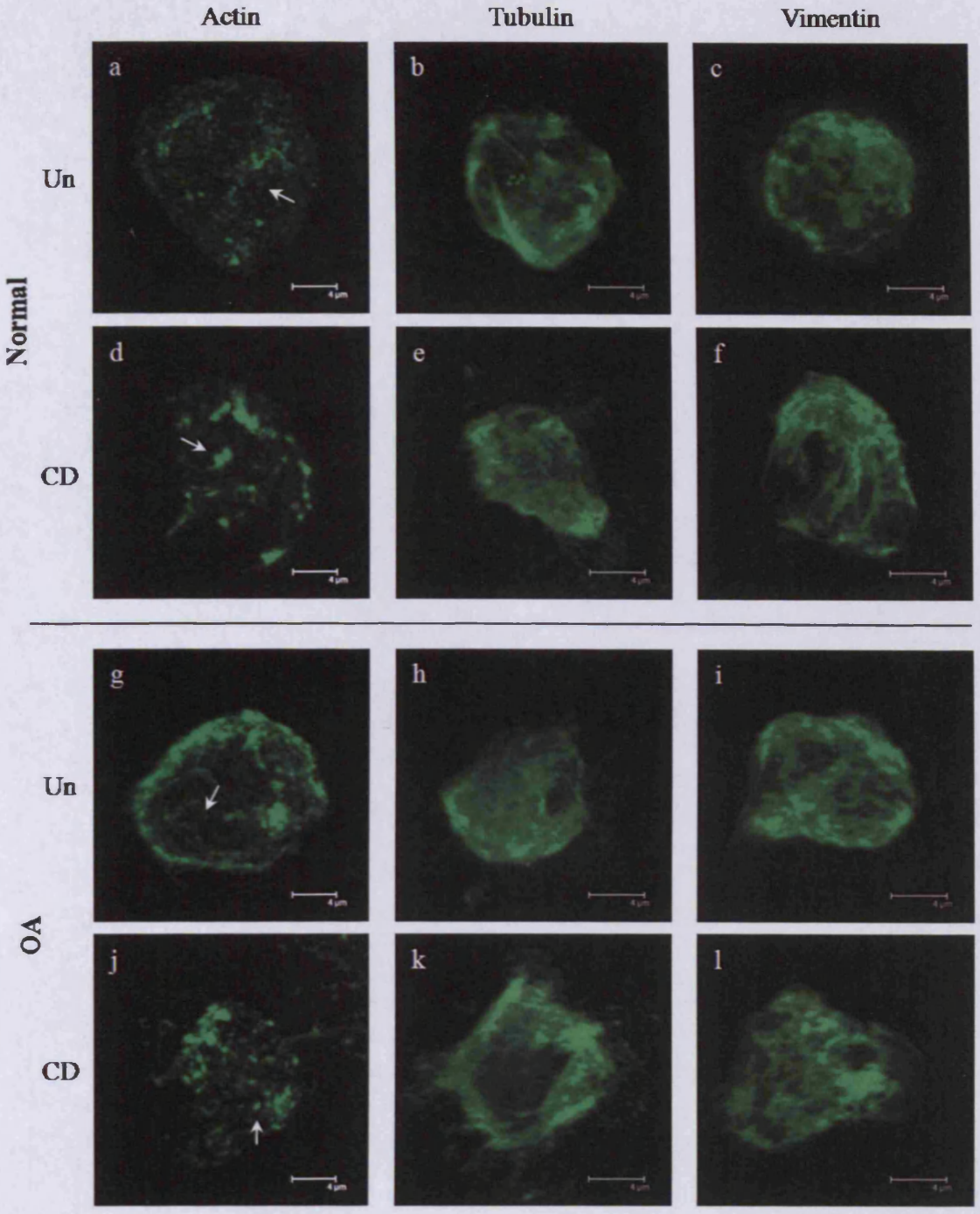

Figure 5.2 A:- ***3D reconstruction*** - Cytoskeletal organisation of normal (a-f) and osteoarthritic (g-l) human articular chondrocytes in 3D agarose culture following disruption of actin microfilaments by treatment with 1μM cytochalasin D for 24 hours. Punctate spots (arrows) appeared larger and less evenly distributed following treatment. Images shown are 3D-reconstructions of a series of scans taken at 0.4μm increments across the chondrocyte. Actin was detected with Alexa fluor 488-phalloidin. Vimentin and tubulin were detected by indirect immunofluorescence using primary antibodies and TRITC-conjugated anti-mouse IgG. 'Un'- untreated chondrocytes, 'CD'- cytochalasin D treated chondrocytes.

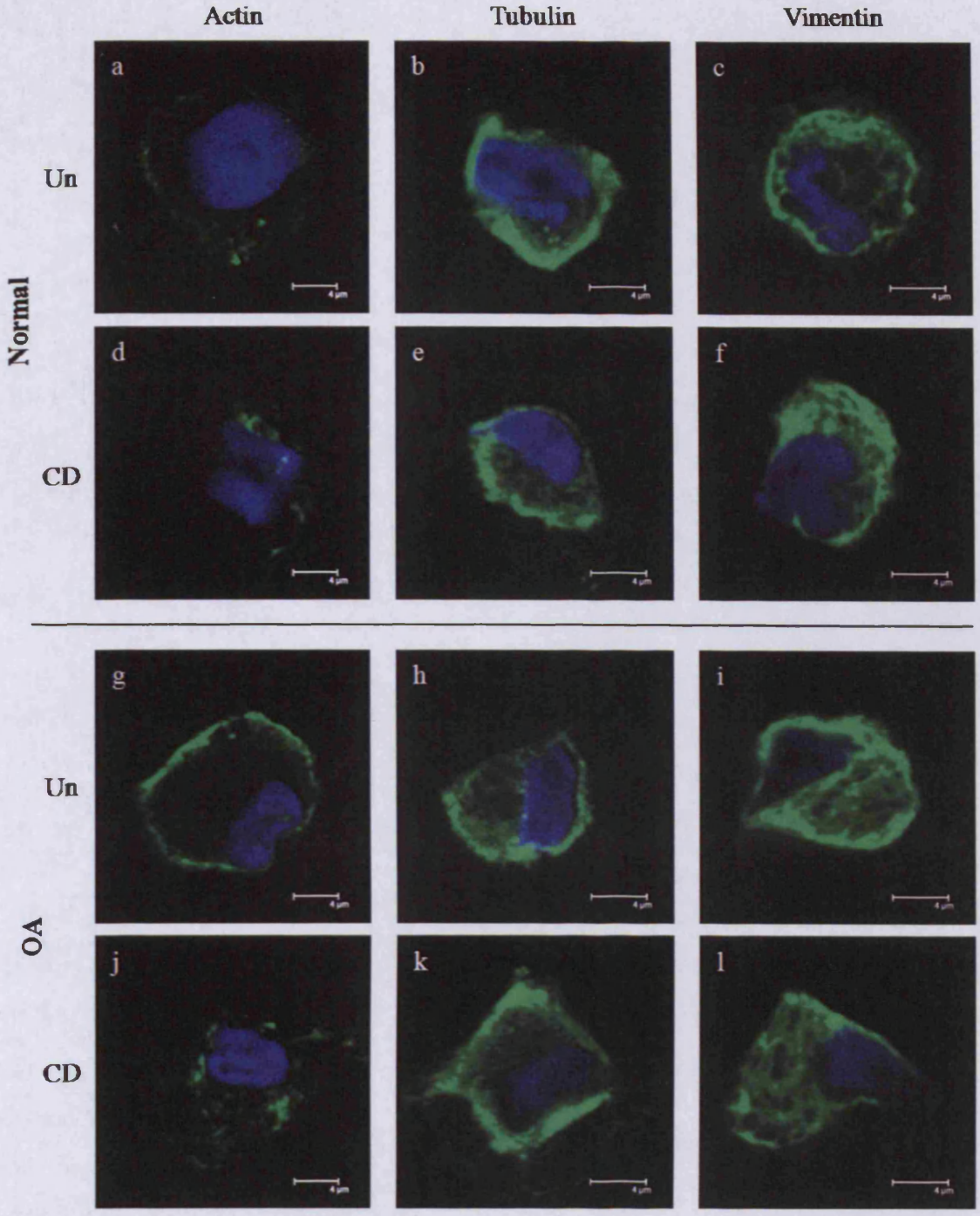

Figure 5.2 B:- ***Single scan*** - Cytoskeletal organisation of normal (a-f) and osteoarthritic (g-l) human articular chondrocytes in 3D agarose culture following disruption of actin microfilaments by treatment with 1μM cytochalasin D for 24 hours. Punctate spots appeared larger and less evenly distributed following treatment. Images shown are a single scan through the centre of the chondrocyte. Actin was detected with Alexa fluor 488-phalloidin. Vimentin and tubulin were detected by indirect immunofluorescence using primary antibodies and TRITC-conjugated anti-mouse IgG. 'Un'- untreated chondrocytes, 'CD'- cytochalasin D treated chondrocytes.

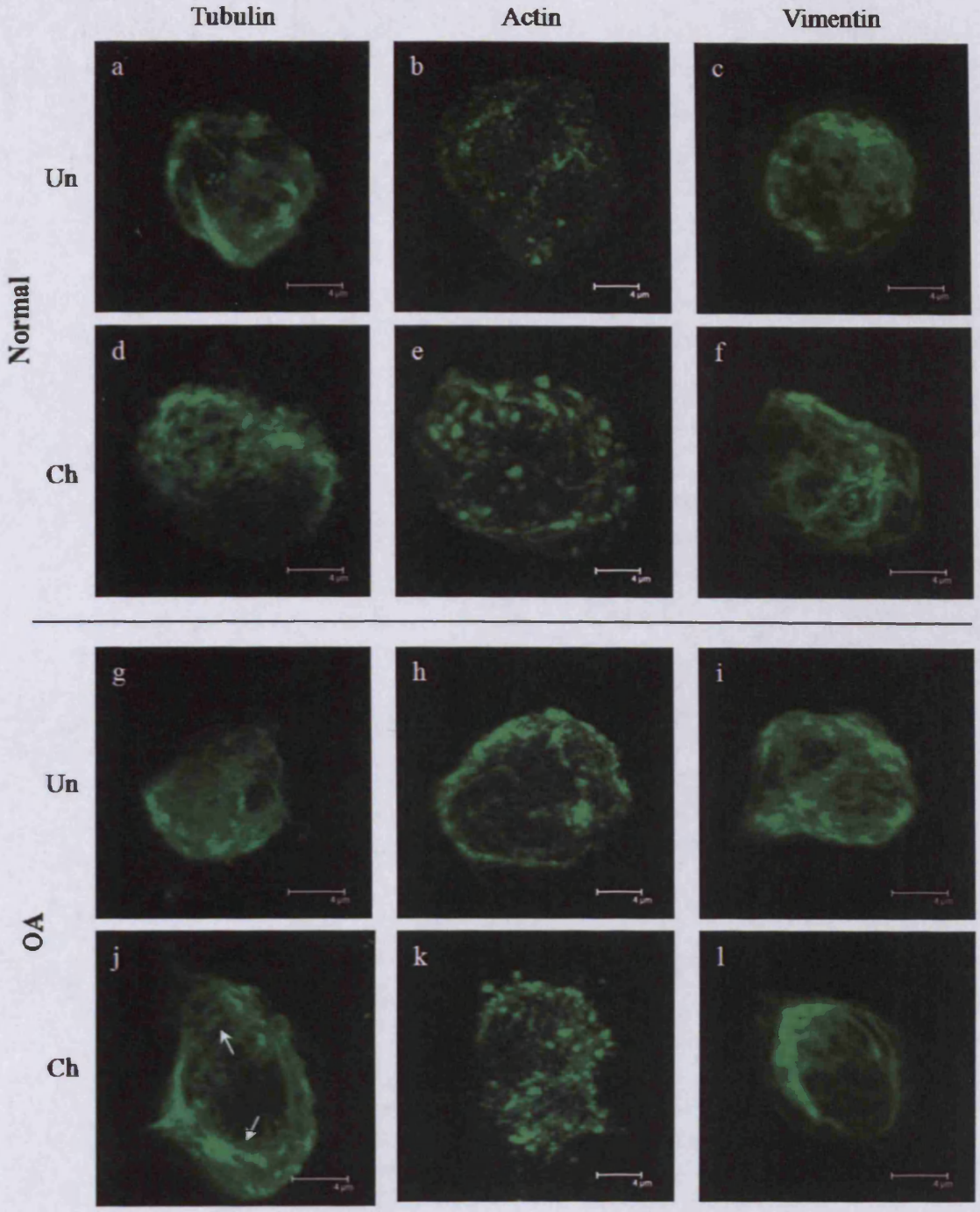

Figure 5.3 A:- ***3D reconstruction*** - Cytoskeletal organisation of normal (a-f) and osteoarthritic (g-l) human articular chondrocytes in 3D agarose culture following disruption of tubulin microtubules by treatment with 1μM colchicine for 24 hours. Microtubule bundles (arrows) appeared thicker and were more clearly visible following treatment. Images shown are 3D-reconstructions of a series of scans taken at 0.4μm increments across the chondrocyte. Vimentin and tubulin were detected by indirect immunofluorescence using primary antibodies and TRITC-conjugated anti-mouse IgG. Actin was detected with Alexa fluor 488-phalloidin. 'Un'- untreated chondrocytes, 'Ch'- colchicine treated chondrocytes.

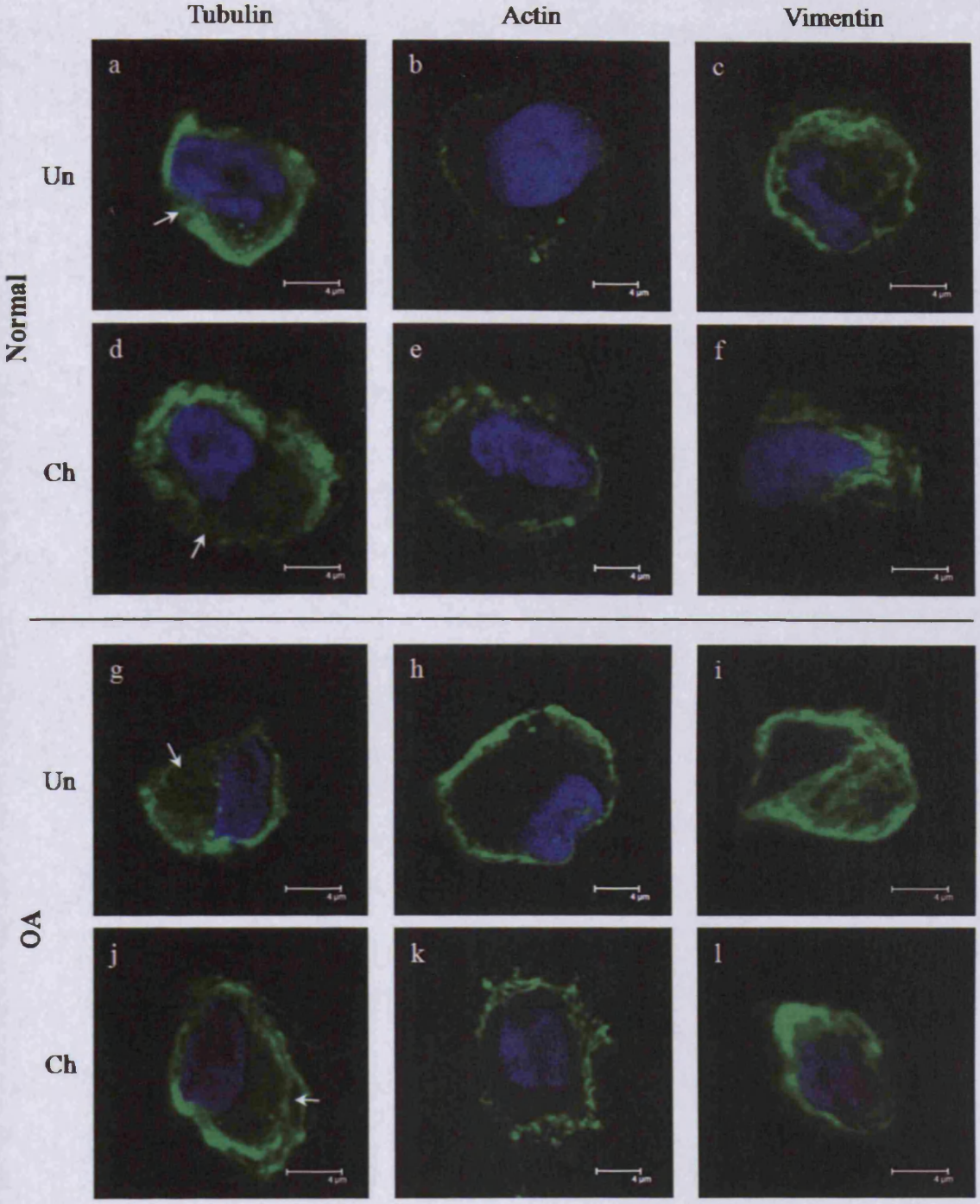

Figure 5.3 B:- ***Single scan*** - Cytoskeletal organisation of normal (a-f) and osteoarthritic (g-l) human articular chondrocytes in 3D agarose culture following disruption of tubulin microtubules by treatment with 1μM colchicine for 24 hours. Microtubule bundles (arrows) appeared thicker and were more clearly visible following treatment. Images shown are a single scan through the centre of the chondrocyte. Vimentin and tubulin were detected by indirect immunofluorescence using primary antibodies and TRITC-conjugated anti-mouse IgG. Actin was detected with Alexa fluor 488-phalloidin. 'Un'- untreated chondrocytes, 'Ch'- colchicine treated chondrocytes.

periphery of both normal and OA colchicine-treated chondrocytes. With colchicine treatment the actin microfilaments of normal chondrocytes became more like those of untreated OA chondrocytes (Fig 5.3 A and B, e and h); punctate spots appeared larger when compared with untreated normal chondrocytes and networks were visible at the cell periphery. Actin staining remained restricted to the cortical region in colchicine-treated normal chondrocytes. Actin microfilaments in OA chondrocytes were unaffected by colchicine treatment (Fig 5.3 A and B, h and k). Vimentin intermediate filament bundle networks were apparent in both untreated and colchicine-treated normal and OA chondrocytes and were unaffected by colchicine treatment (Fig 5.3 A and B, c,f,i and l).

5.2.2.4 Acrylamide-treated Chondrocytes

Treatment of chondrocytes with 2mM acrylamide for 24 hours altered the appearance of vimentin networks (Fig 5.4 A and B). In acrylamide-treated normal chondrocytes vimentin intermediate filaments formed thick bundles and appeared more loosely packed (Fig 5.4 A and B, d). Vimentin filament bundles appeared asymmetrically distributed in both normal and OA chondrocytes following acrylamide treatment, with diffuse or faint intermediate filament bundle networks around the nucleus on one side of the cell and loose networks on the opposing side (Fig 5.4 A and B, d and j). In acrylamide-treated OA chondrocytes vimentin staining was bright at one side of the cell and loosely packed faint intermediate filament bundles surrounded the nucleus (Fig 5.4 A and B, j). Actin microfilaments were unaffected by acrylamide treatment in both normal and OA chondrocytes. In normal chondrocytes, actin staining remained punctate and restricted predominantly to the cell periphery (Fig 5.4 A and B, b and e). In OA chondrocytes, punctate spots of actin staining remained slightly elongated as in untreated controls, but staining was less clearly restricted to the cell periphery (Fig 5.4 A and B, h and k). The appearance of tubulin microtubules in normal and OA chondrocytes was unaffected by acrylamide treatment, with microtubule bundle networks remaining fine and filamentous throughout the cell (Fig 5.4 A and B, c,f,i and l).

Changes in the organisation of the actin (Fig 5.5), tubulin (Fig 5.6) and vimentin (Fig 5.7) cytoskeletal elements are summarised below. In all instances, disruption of a specific cytoskeletal element did not significantly affect the spatial organisation of the other major elements in the chondrocyte after 24 hours of treatment.

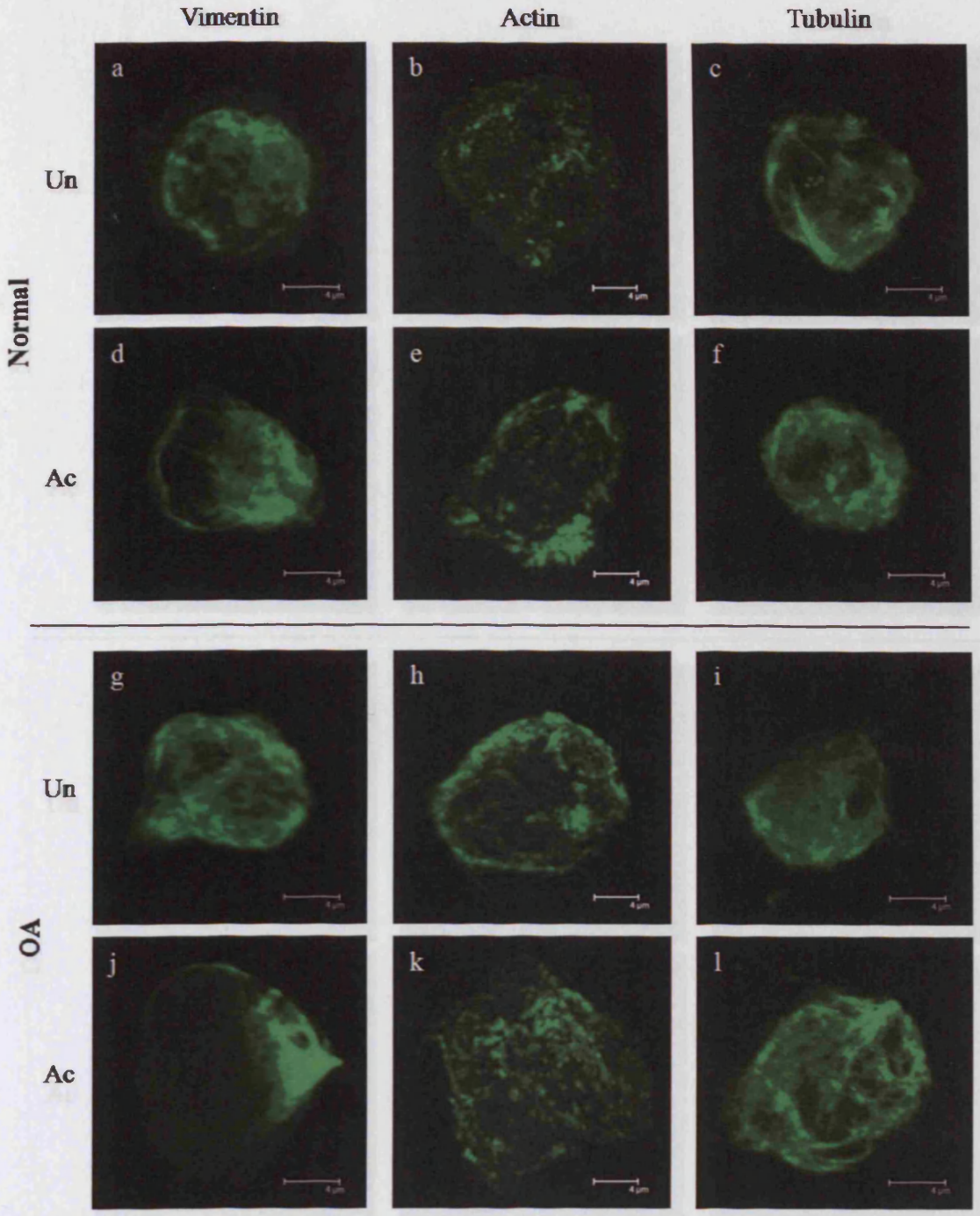

Figure 5.4 A:- ***3D reconstruction*** - Cytoskeletal organisation of normal (a-f) and osteoarthritic (g-l) human articular chondrocytes in 3D agarose culture following disruption of vimentin intermediate filaments by treatment with 2mM acrylamide for 24 hours. Intermediate filament bundles became asymmetrically distributed following treatment. Images shown are 3D-reconstructions of a series of scans taken at 0.4μm increments across the chondrocyte. Vimentin and tubulin were detected by indirect immunofluorescence using primary antibodies and TRITC-conjugated anti-mouse IgG. Actin was detected with Alexa fluor 488-phalloidin. 'Un'- untreated chondrocytes, 'Ac'- acrylamide treated chondrocytes.

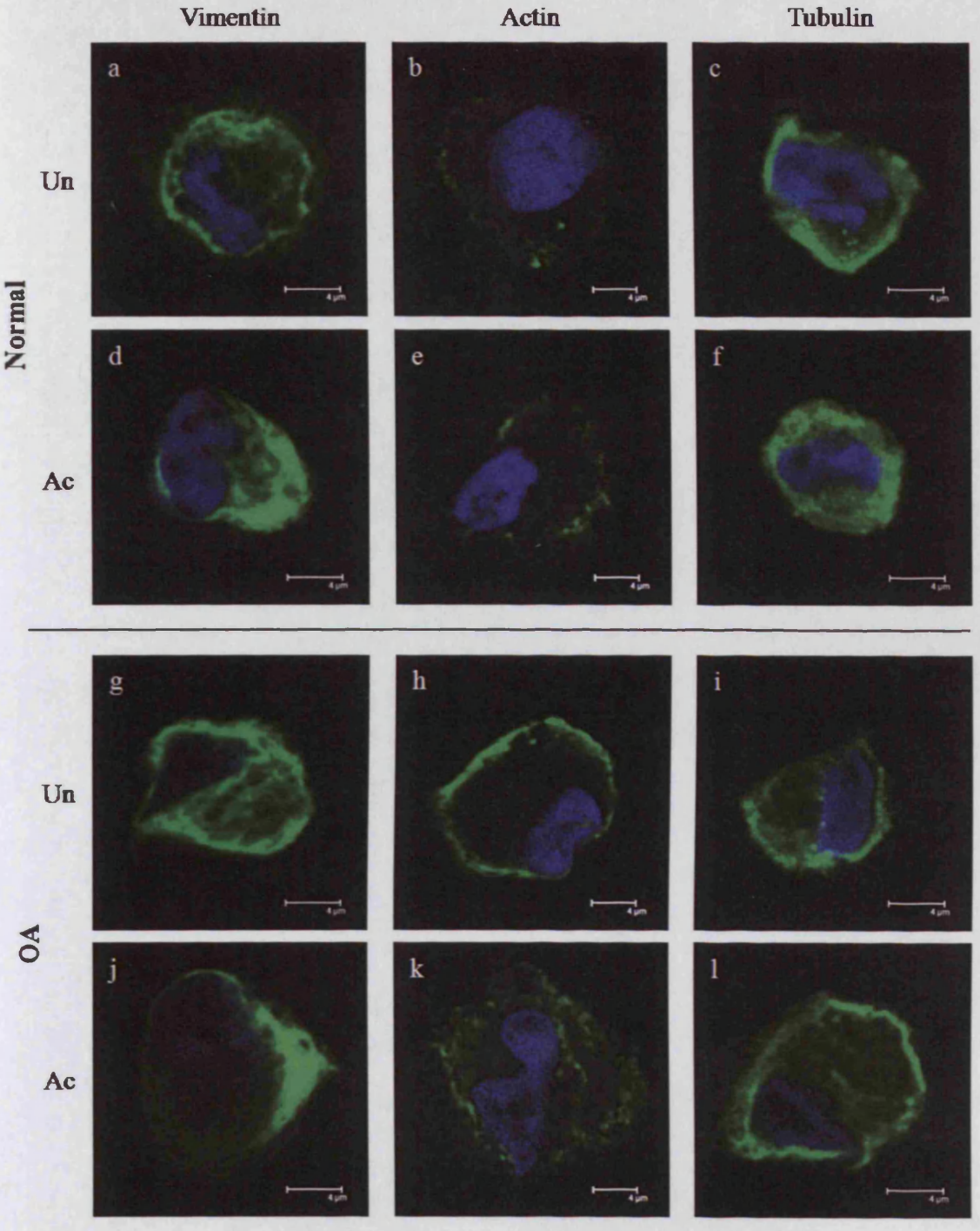

Figure 5.4 B:- ***Single scan*** - Cytoskeletal organisation of normal (a-f) and osteoarthritic (g-l) human articular chondrocytes in 3D agarose culture following disruption of vimentin intermediate filaments by treatment with 2mM acrylamide for 24 hours. Intermediate filament bundles became asymmetrically distributed following treatment. Images shown are a single scan through the centre of the chondrocyte. Vimentin and tubulin were detected by indirect immunofluorescence using primary antibodies and TRITC-conjugated anti-mouse IgG. Actin was detected with Alexa fluor 488-phalloidin. 'Un'- untreated chondrocytes, 'Ac'- acrylamide treated chondrocytes.

Actin
Control
Disruption
Normal
Osteoarthritic
• Sharp punctate spots
• Predominantly cortical
• Larger punctate spots
• Less evenly distributed
• Elongated punctate spots
• Limited to the periphery
• Larger punctate spots
• Less evenly distributed
• Throughout the cell

Tubulin
Control
Disruption
Normal
Osteoarthritic
• Fine tubule bundles
• Packed around nucleus
• Shorter, thicker tubule bundles
• Most dense at periphery
• Fine tubule bundles
• Most dense at periphery
• Thick tubule bundles
• Most dense at periphery

Vimentin

	Control	Disruption
Normal		
	• Fine filament bundles • Networks throughout cell and at cortex	• Thick filament bundles • Loose, asymmetric networks
Osteoarthritic		
	• Thick filament bundles • Loose networks throughout cell	• Faint filament bundles • Loose, asymmetric networks

5.2.3 Gene Expression Changes Following Cytoskeletal Element Disruption

The effect of cytoskeletal disruption on chondrocyte phenotype was analysed using quantitative PCR to determine gene expression changes.

5.2.3.1 Cytoskeletal Associated Genes

There was no difference in β-actin mRNA expression detected between normal and OA chondrocytes at all time points assayed (Fig 5.8). Disruption of actin microfilaments with 1μM cytochalasin D treatment had a significant effect on β-actin mRNA expression in both normal and OA chondrocytes (Fig 5.8). In normal chondrocytes, β-actin expression was increased by cytochalasin D treatment at 12 and 24 hours (5.6 fold; p=0.019 and 4.3 fold; p=0.015 respectively) and remained elevated over controls at 48 hours (4.2 fold; p=0.068). In OA chondrocytes, the increase in β-actin expression at 12 hours (2.5 fold; p=0.037) remained significant at 24 and 48 hours (2.5 fold; p=0.023 and 2.7 fold; p=0.046 respectively). Disruption of tubulin microtubules or vimentin intermediate filaments had no effect on β-actin expression, with the exception of increased expression in normal chondrocytes treated for 12 hours with colchicine (2.1 fold; p=0.049).

Disruption of the actin, tubulin or vimentin cytoskeleton had no significant effect on β-tubulin mRNA expression in normal and OA chondrocytes (Fig 5.9). β-tubulin expression was highly variable, particularly in OA chondrocytes. Vimentin mRNA expression was unaffected by cytoskeletal disruption and no difference was observed between normal and OA chondrocytes (Fig 5.10).

The organisation of actin microfilaments can be regulated by a number of actin-binding proteins. Therefore the effect of cytoskeletal disruption on the expression of a number of actin-binding proteins was investigated. Expression of the actin-depolymerising protein cofilin in normal and OA chondrocytes increased with cytochalasin D treatment at 12 hours and reached significance in normal chondrocytes treated for 24 hours (Fig 5.11; normal 1.9 fold; p=0.013 and OA 1.6 fold; p=0.153). Cofilin expression remained elevated at 48 hours but was no longer significant (1.7 fold; OA p=0.068, data not shown). Cytochalasin D treatment increased destrin expression in normal chondrocytes

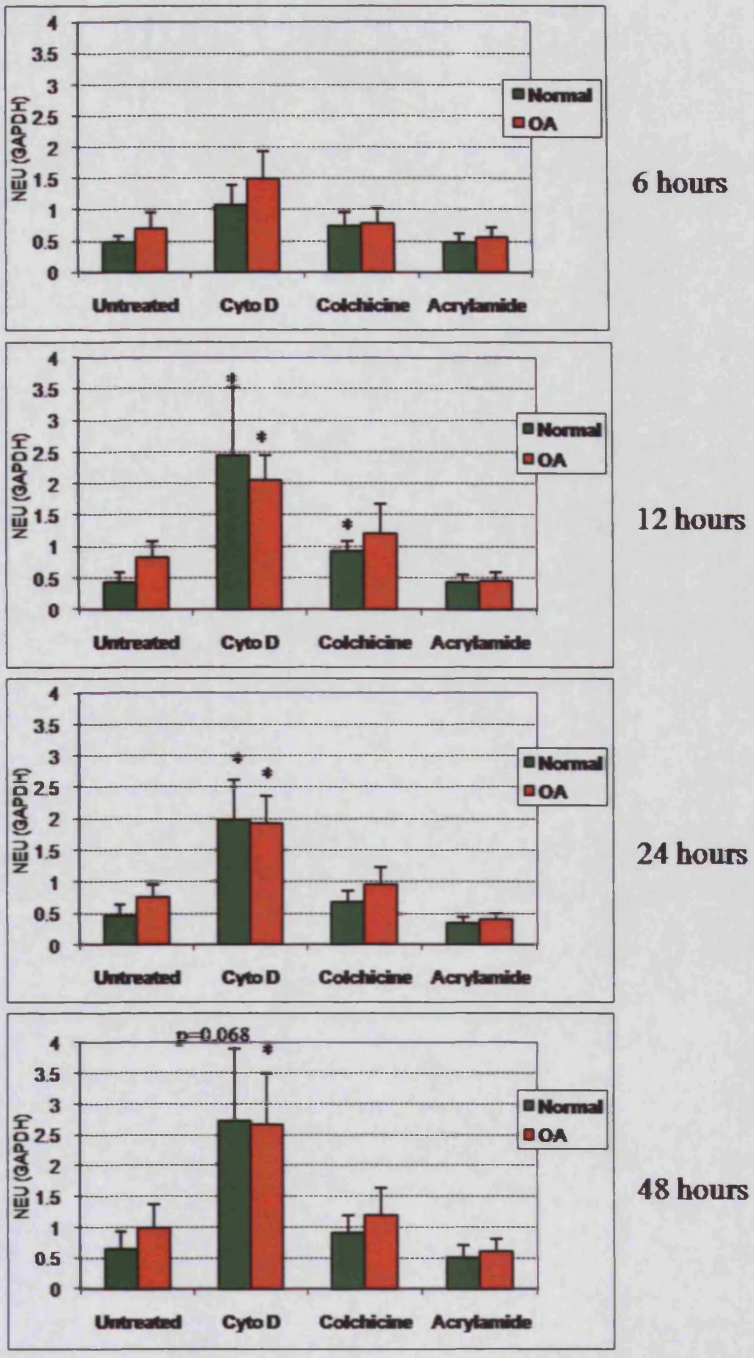

Figure 5.8:- β-actin gene expression changes with cytoskeletal disruption. Absolute mRNA levels were determined using SYBR Green quantitative PCR and normalised to the housekeeping gene GAPDH. Nucleic acids were isolated from chondrocytes from normal and osteoarthritic (OA) cartilage, encapsulated in 3D agarose and cultured without (untreated) or with treatment for 6, 12, 24 or 48 hours – treatments included 1μM cytochalasin D to disrupt actin microfilaments, 1μM colchicine to disrupt tubulin microtubules, or 2 mM acrylamide treatment to disrupt vimentin intermediate filaments. Data are presented as mean ± S.E.M. (n=5). * $p < 0.05$, treatment compared to untreated control.

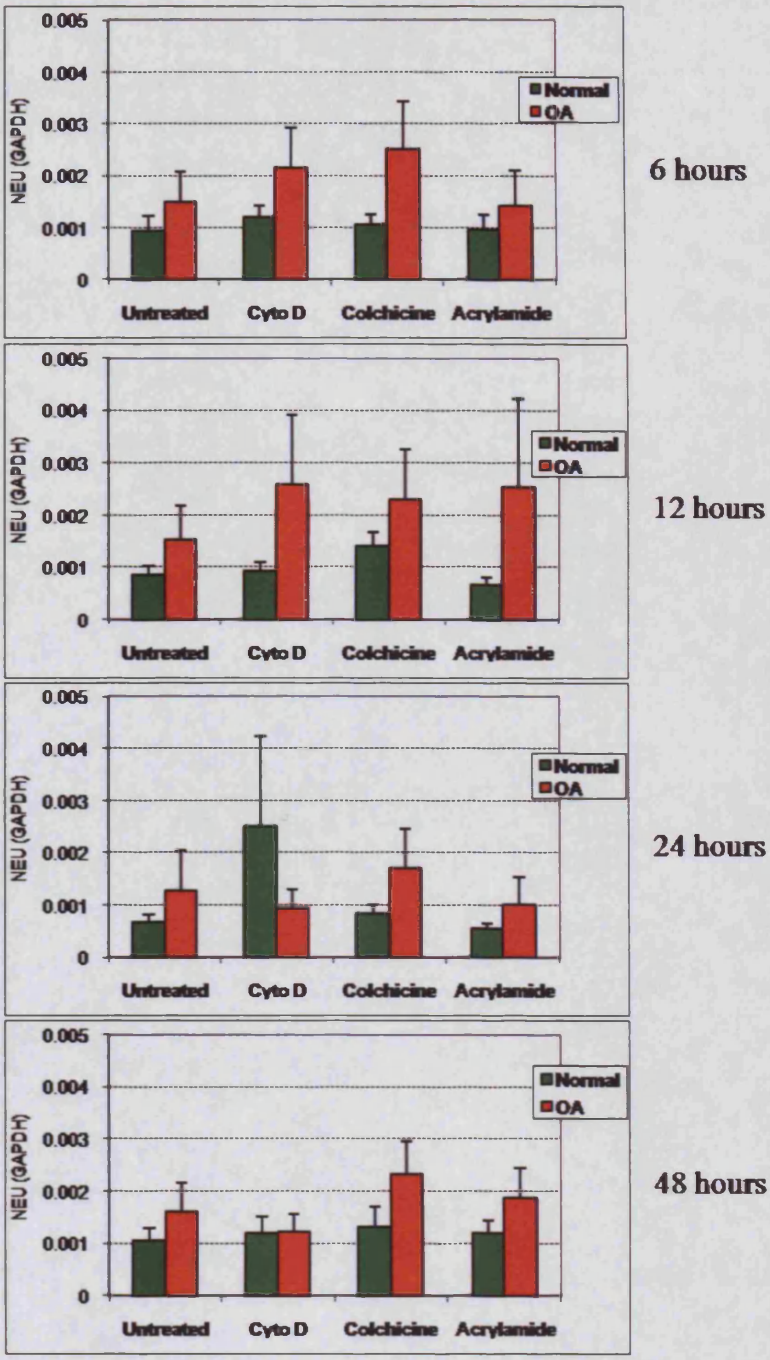

Figure 5.9:- β-tubulin gene expression changes with cytoskeletal disruption. Absolute mRNA levels were determined using SYBR Green quantitative PCR and normalised to the housekeeping gene GAPDH. Nucleic acids were isolated from chondrocytes from normal and osteoarthritic (OA) cartilage, encapsulated in 3D agarose and cultured without (untreated) or with treatment for 6, 12, 24 or 48 hours – treatments included 1μM cytochalasin D to disrupt actin microfilaments, 1μM colchicine to disrupt tubulin microtubules, or 2 mM acrylamide treatment to disrupt vimentin intermediate filaments. Data are presented as mean ± S.E.M. (n=5).

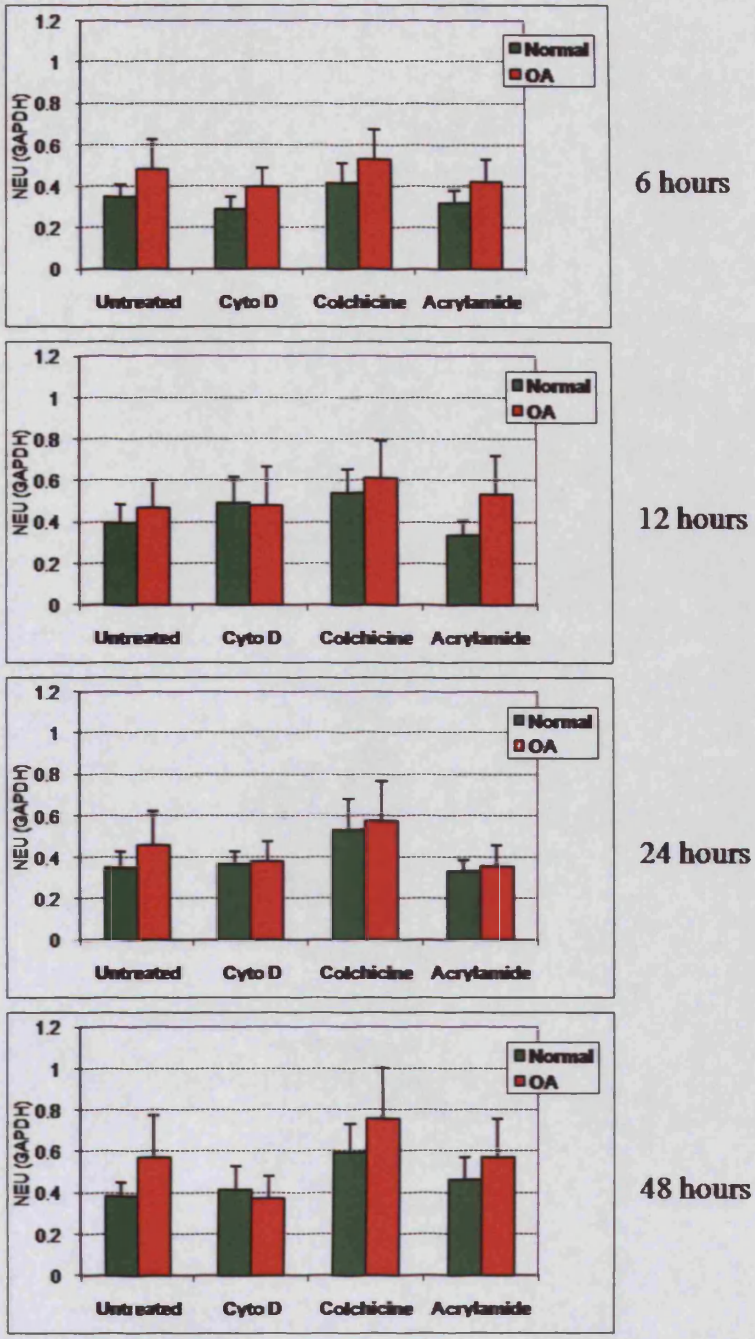

Figure 5.10:- Vimentin gene expression changes with cytoskeletal disruption. Absolute mRNA levels were determined using SYBR Green quantitative PCR and normalised to the housekeeping gene GAPDH. Nucleic acids were isolated from chondrocytes from normal and osteoarthritic (OA) cartilage, encapsulated in 3D agarose and cultured without (untreated) or with treatment for 6, 12, 24 or 48 hours – treatments included 1μM cytochalasin D to disrupt actin microfilaments, 1μM colchicine to disrupt tubulin microtubules, or 2 mM acrylamide treatment to disrupt vimentin intermediate filaments. Data are presented as mean ± S.E.M. (n=5).

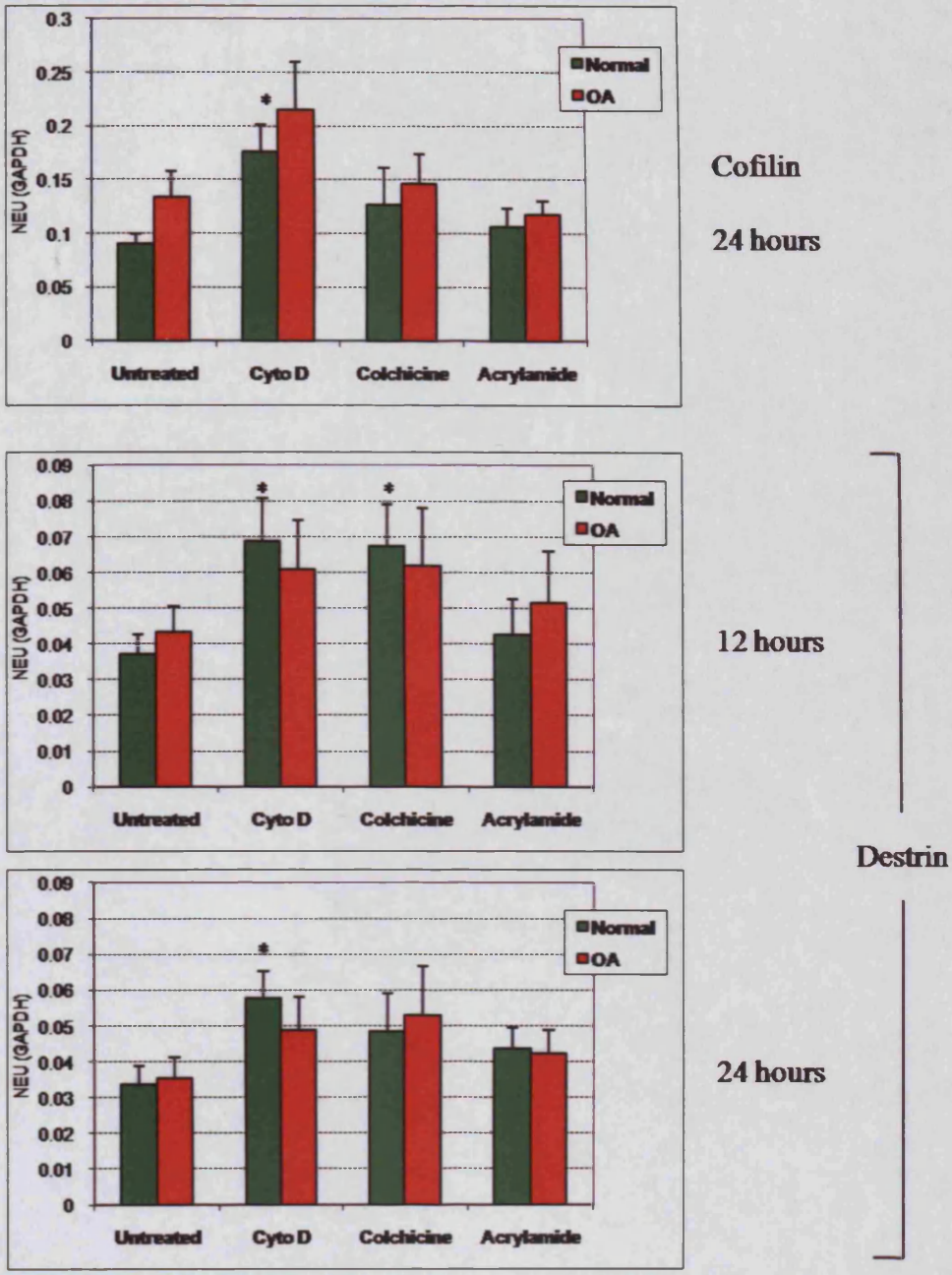

Figure 5.11:- Actin binding protein gene expression changes with cytoskeletal disruption. Absolute mRNA levels were determined using SYBR Green quantitative PCR and normalised to the housekeeping gene GAPDH. Nucleic acids were isolated from chondrocytes from normal and osteoarthritic (OA) cartilage, encapsulated in 3D agarose and cultured without (untreated) or with treatment for 6, 12, 24 or 48 hours – treatments included 1μM cytochalasin D to disrupt actin microfilaments, 1μM colchicine to disrupt tubulin microtubules, or 2mM acrylamide treatment to disrupt vimentin intermediate filaments. Data are presented as mean ± S.E.M. (n=5). * $p < 0.05$, treatment compared to untreated control.

at 12 and 24 hours (Fig 5.11: 1.8 fold; p=0.045 and 1.7 fold; p=0.033, respectively), with expression remaining elevated at 48 hours (1.7 fold; p=0.060, data not shown). Destrin expression in normal chondrocytes was also increased following 12 hours treatment with colchicine (Fig 5.11: 1.8 fold; p=0.046), coinciding with the significant increase in β-actin mRNA levels (Fig 5.8); destrin mRNA levels returned to those of untreated controls by 48 hours treatment (data not shown). Differential regulation of destrin mRNA followed the same trend in OA chondrocytes as normal chondrocytes, although none reached statistical significance. Other cytoskeletal associated genes investigated included thymosin β4, gelsolin and paxillin, none of which showed significant differences between normal and OA chondrocytes or between treated and untreated controls (data not shown).

5.2.3.2 Custom-designed Taqman Array

Custom-designed Taqman® arrays (Applied Biosystems, customised for AstraZeneca) were used to more widely analyse gene expression changes following cytoskeletal disruption in normal and OA cartilage chondrocytes. RNA extracted from chondrocytes treated for 6 hours with a cytoskeletal disrupting agent was used in order to determine early gene expression changes, following normalisation to the housekeeping gene *GAPDH* and then to untreated controls. Fold changes in the expression of selected genes are summarised in Table 5.1.

5.2.3.2.1 Actin Microfilament Disruption

Treatment with 1μM cytochalasin D for 6 hours resulted in up-regulation of β-actin mRNA expression in normal (3 fold) and OA chondrocytes (2.4 fold) (Fig 5.12; ACTB). With regards to the typical markers of chondrocyte phenotype, in normal chondrocytes, early actin microfilament disruption down-regulated *COL1A1* (1.4 fold), up-regulated *SOX9* (1.2 fold), and showed little effect on aggrecan; *COL2A1* was not detected in normal untreated chondrocytes and therefore no fold change could be determined. *COL1A1* and *SOX9* expression was unaffected by 6 hours cytochalasin D treatment in OA chondrocytes, whilst both *COL2A1* (1.9 fold) and *ACAN* (1.2 fold) expression were down-regulated.

The affect of cytochalasin D on *FGFR3* expression differed between normal and OA chondrocytes, with *FGFR3* up-regulated 1.8-fold in normal chondrocytes and down-regulated 1.2-fold in OA chondrocytes. *BMF* mRNA expression was down-regulated in

Actin Disruption (1 µM cytochalasin D)

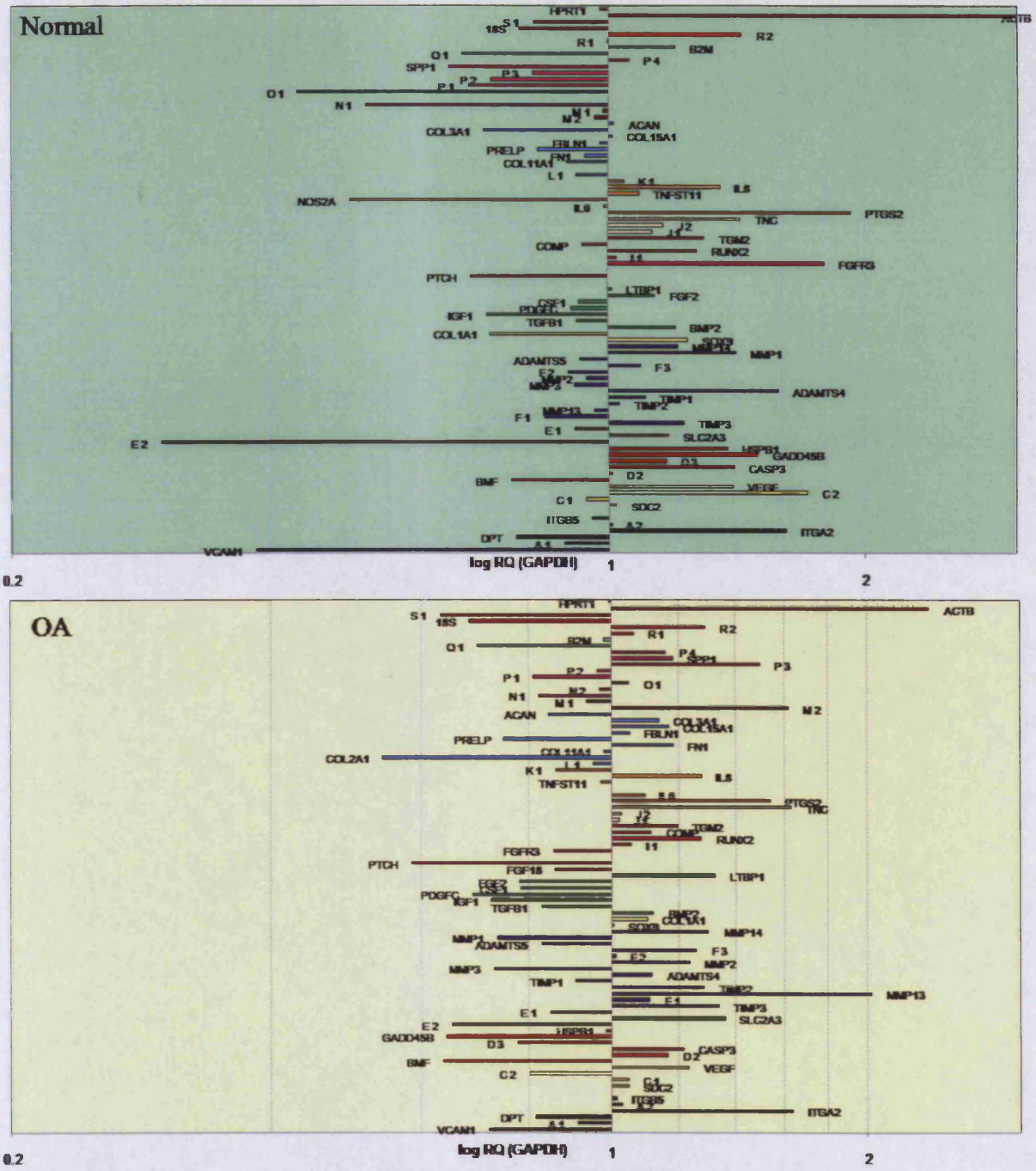

Figure 5.12:- The fold changes of selected genes, expressed by normal and osteoarthritic chondrocytes cultured in 3D agarose, in response to treatment with 1µM cytochalasin D for 6 hours. Changes in response to microfilament disruption were determined relative to untreated controls following quantitative PCR using a Taqman® custom-designed array (AZ) and normalisation to the housekeeping gene GAPDH. Gene names are shown, except where confidentiality is required by AZ, in which case a code of one letter and number have been used. Letters (and colours) indicate a process in / category which the gene product is involved/belongs; A- adhesion, C- angiogen, D- apoptosis, E- carbohydrate, F- degradation, H- growth factor, I- hypertrophy, J- hypoxia/pH, K- inflammation, L- matrix, M- metabolism, N- neurogen, P- osteogen, Q- proliferation, R- transporter, S- housekeeper. n = 2

normal (1.3 fold) and OA chondrocytes (1.6 fold). By contrast, *GADD45B* was up-regulated in normal (1.5 fold) but down-regulated in OA chondrocytes (1.6 fold).

5.2.3.2.2 Tubulin Microtubule Disruption

Following 6 hours treatment with 1μM colchicine to disrupt tubulin microtubules, mRNA expression levels of the chondrocyte phenotype markers *COL1A1* and *SOX9* did not change in normal and OA chondrocytes, whilst *COL2A1* and *AGC* were down-regulated in OA chondrocytes (1.2 fold) (Fig 5.13). *BMF* was down-regulated in normal (1.3 fold) and OA chondrocytes (2 fold). Colchicine treatment appeared to have a greater effect on inflammatory gene expression in OA chondrocytes than in normal chondrocytes; *PTGS2* (encoding COX-2), *IL6* and *IL8* were up-regulated in normal (1.3-, 1.2- and 1.3-fold, respectively) but more extensively elevated in OA chondrocytes (1.7-, 4.4- and 2.4-fold, respectively).

5.2.3.2.3 Vimentin Intermediate Filament Disruption

Treatment for 6 hours with 2mM acrylamide had no effect on the expression of chondrocyte phenotype markers *COL1A1* and *ACAN* in normal and OA chondrocytes (Fig 5.14). *SOX9* expression was down-regulated in normal chondrocytes (1.2 fold) and *COL2A1* expression was down-regulated in OA chondrocytes (1.2 fold). Acrylamide treatment affected growth factor gene expression differently in normal and OA chondrocytes: in OA chondrocytes six of the seven genes were up-regulated, whilst in normal chondrocytes only two of the genes were up-regulated (Fig 5.14). *GADD45B* was down-regulated in normal (1.2 fold) and OA chondrocytes (1.3 fold) whilst *BMF* was up-regulated in normal chondrocytes (1.5 fold) but remained unchanged in OA cells.

Inflammatory genes were altered by 6 hours of treatment with acrylamide. *TNFST11* and *NOS2A* were differentially affected in normal and OA chondrocytes; *TNFST11*, encoding RANK ligand, was up-regulated in normal (2.6 fold) but down-regulated in OA chondrocytes (1.3 fold), whilst *NOS2A*, encoding iNOS, was down-regulated in normal (3.3 fold) but up-regulated in OA chondrocytes (3.9 fold). In addition, although down-regulated in both, expression changes in *IL6*, *IL8* and *PTGS2* were greater in normal chondrocytes when compared with OA chondrocytes.

Tubulin Disruption (1 µM colchicine)

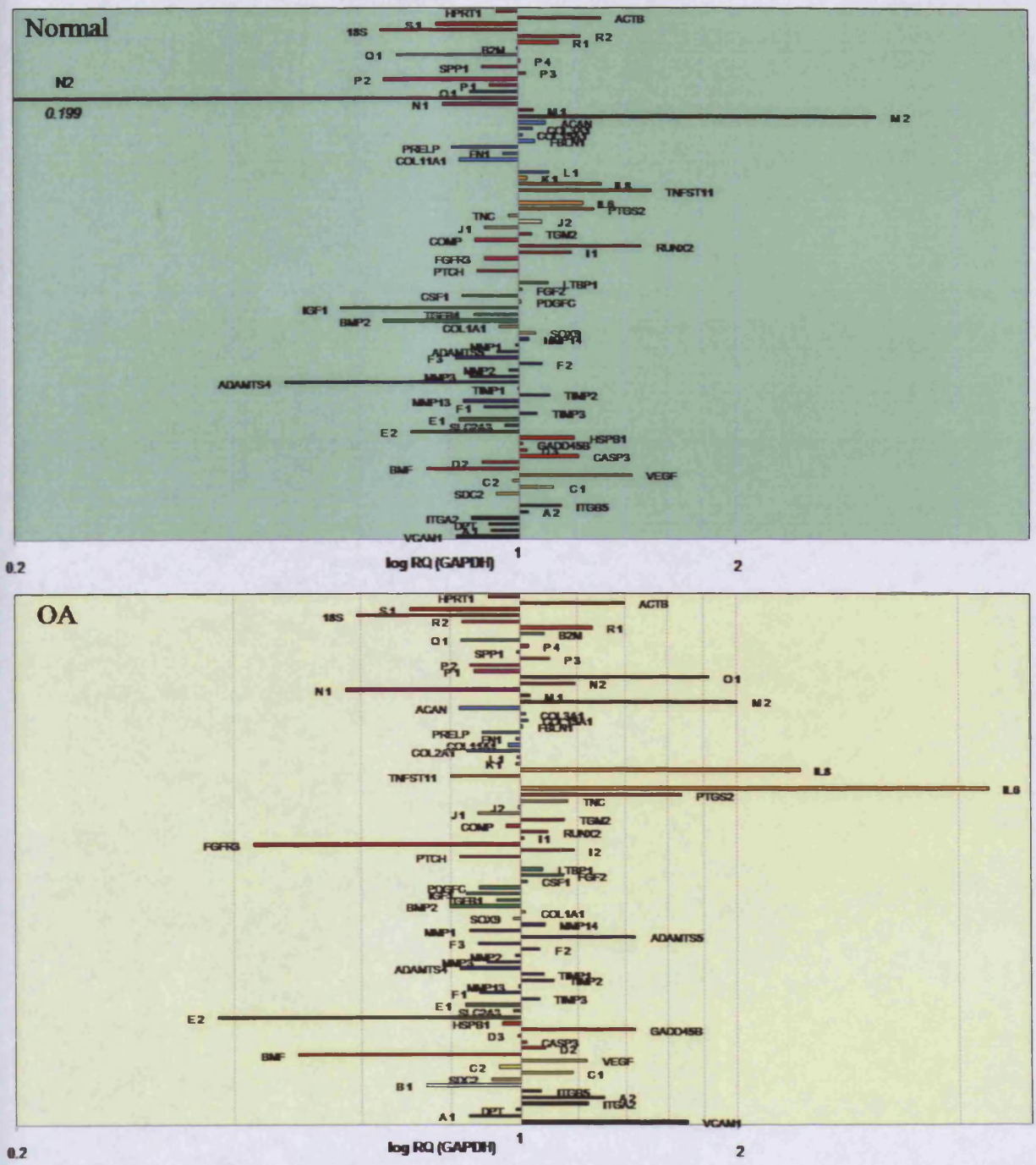

Figure 5.13:- The fold changes of selected genes, expressed by normal and osteoarthritic chondrocytes cultured in 3D agarose, in response to treatment with 1µM colchicine for 6 hours. Changes in response to microtubule disruption were determined relative to untreated controls following quantitative PCR using a Taqman® custom-designed array (AZ) and normalisation to the housekeeping gene GAPDH. Gene names are shown, except where confidentiality is required by AZ, in which case a code of one letter and number have been used. Letters (and colours) indicate a process in / category which the gene product is involved/belongs; A- adhesion, C- angiogen, D- apoptosis, E- carbohydrate, F- degradation, H- growth factor, I- hypertrophy, J- hypoxia/pH, K- inflammation, L- matrix, M- metabolism, N- neurogen, P- osteogen, Q- proliferation, R- transporter, S- housekeeper. n = 2

Vimentin Disruption (2mM acrylamide)

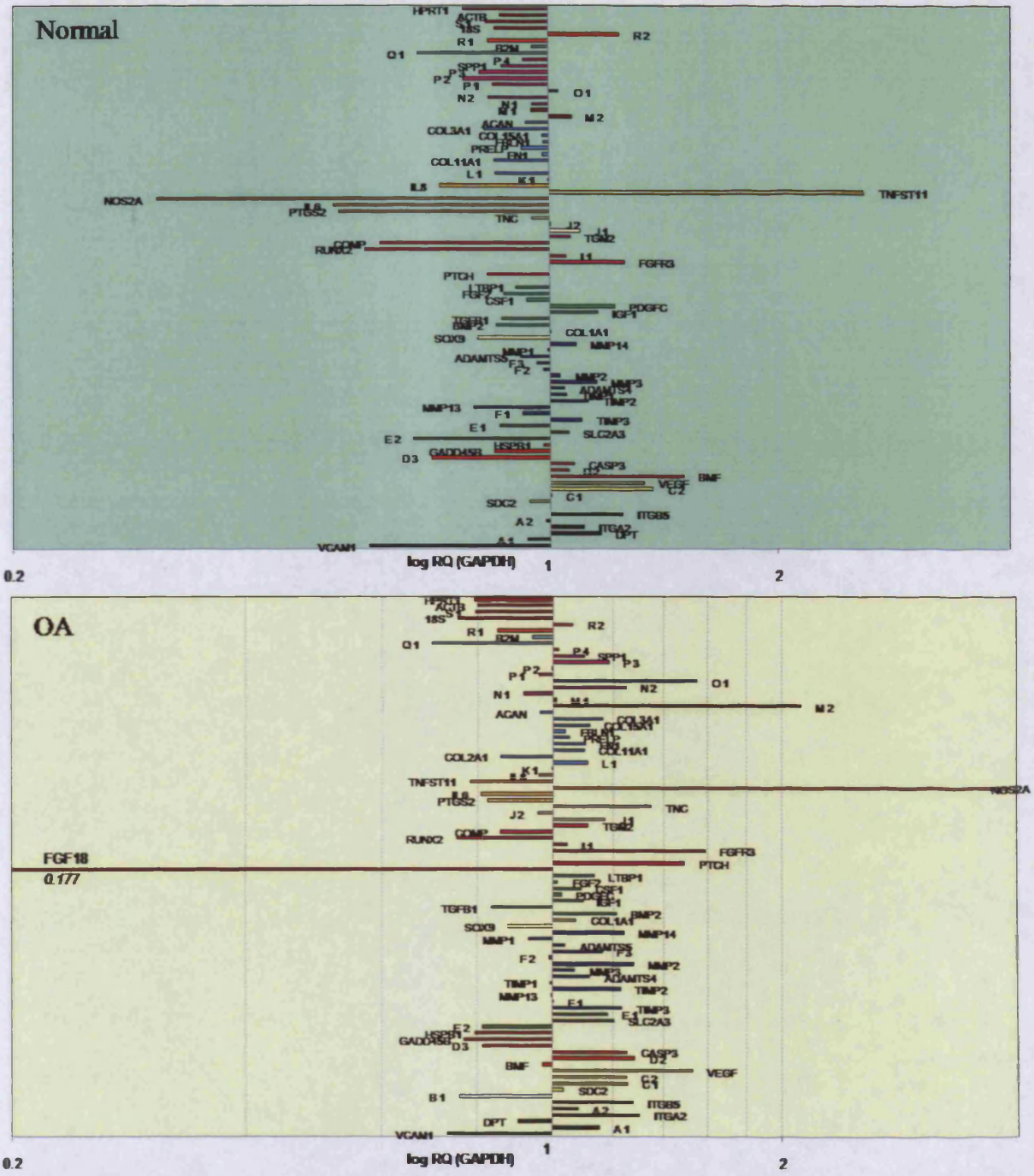

Figure 5.14:- The fold changes of selected genes, expressed by normal and osteoarthritic chondrocytes cultured in 3D agarose, in response to treatment with 2mM acrylamide for 6 hours. Changes in response to vimentin intermediate filament disruption were determined relative to untreated controls following quantitative PCR using a Taqman® custom-designed array (AZ) and normalisation to the housekeeping gene GAPDH. Gene names are shown, except where confidentiality is required by AZ, in which case a code of one letter and number have been used. Letters (and colours) indicate a process in / category which the gene product is involved/belongs; A- adhesion, C- angiogen, D- apoptosis, E- carbohydrate, F- degradation, H- growth factor, I- hypertrophy, J- hypoxia/pH, K- inflammation, L- matrix, M- metabolism, N- neurogen, P- osteogen, Q- proliferation, R- transporter, S- housekeeper. n = 2

Function	Gene	Actin disruption		Tubulin Disruption		Vimentin Disruption	
		Normal	OA	Normal	OA	Normal	OA
β-actin	*ACTB*	+ 3	+ 2.4	+ 1.3	+ 1.4	- 1.2	- 1.2
Phenotype markers	*COL1A1*	- 1.4	=	=	=	=	=
	COL3A1	- 1.4	=	=	=	- 1.2	+ 1.2
	SOX9	+ 1.2	=	=	=	- 1.2	=
	ACAN	=	- 1.2	=	- 1.2	=	=
	COL2A1	nd in Un	- 1.9	nd in Un	- 1.2	nd in Un	- 1.2
Degrad-ation	*ADAMTS5*	=	- 1.2	=	+ 1.4	=	=
	MMP13	=	+ 2	- 1.2	=	- 1.3	=
	MMP14	+ 1.2	+ 1.3	=	=	=	+ 1.2
Growth factors	*FGF2*	=	- 1.3	=	=	=	=
	FGFR3	+ 1.8	- 1.2	=	- 2.3	+ 1.3	+ 1.6
	TGFB1	=	- 1.2	- 1.2	=	- 1.2	- 1.2
	IGF1	- 1.4	- 1.4	- 1.8	- 1.2	+ 1.2	=
Adhesion	*ITGA2*	+ 1.6	+ 1.6	- 1.2	+ 1.2	=	+ 1.3
	ITGB5	=	=	=	=	+ 1.2	+ 1.3
	DPT	- 1.3	- 1.3	=	=	+ 1.2	=
	VCAM1	- 2.6	- 1.4	- 1.2	+ 1.7	- 1.7	- 1.4
Apoptosis	*CASP3*	+ 1.4	+ 1.2	+ 1.2	=	=	+ 1.3
	BMF	- 1.3	- 1.6	- 1.3	- 2	+ 1.5	=
	HSPB1	+ 1.4	=	+ 1.2	=	=	- 1.3
	GADD45B	+ 1.5	- 1.6	=	+ 1.4	- 1.2	- 1.3
Inflammation	*PTGS2*	+ 2	+ 1.5	+ 1.3	+ 1.7	- 1.9	- 1.2
	NOS2A	- 2	nd	nd	nd	- 3.3	+ 3.9
	IL6	=	=	+ 1.2	+ 4.4	- 1.9	- 1.2
	IL8	+ 1.4	+ 1.3	+ 1.3	+ 2.4	- 1.4	=
	TNFSF11	=	=	+ 1.5	- 1.3	+ 2.6	- 1.3

Table 5.1:- Summary of fold changes in expression of selected genes in normal and OA cartilage chondrocytes in response to cytoskeletal disrupting treatments, relative to untreated controls. Gene expression was determined using custom-designed Taqman® arrays. Chondrocytes were cultured in 3D agarose hydrogels and treated for 6 hours with 1μM cytochalasin D to disrupt actin microfilaments, 1μM colchicine to disrupt tubulin microtubules or 2mM acrylamide to disrupt vimentin intermediate filaments. 'nd' is not detected; 'nd in Un' indicates where expression was not detected in untreated controls; = refers to fold changes of magnitude < 1.2.

5.2.3.2.4 Comparison of Gene Changes Across Treatments

Some of the detected fold changes in gene expression in response to cytoskeletal disruption were similar in both normal and osteoarthritic chondrocytes for all treatments (Table 5.2). As the response was consistent in all treatments for both normal and OA cells, these changes could relate to more general effects of cytoskeletal disruption rather than the disruption of specific signalling pathways.

Other genes were similarly regulated in normal and OA chondrocytes, but changes were different depending on the treatment and therefore the cytoskeletal element disrupted (Table 5.3). A difference in response dependent on the disrupted element implies that the change in expression of the gene is not due to general disruption. It could be that transcriptional regulation is a response to altered signalling via pathways involving one or more of the cytoskeletal elements.

A number of genes also demonstrated a differential response to cytoskeletal disruption in OA chondrocytes when compared with normal chondrocytes (Table 5.4). The difference in transcriptional response of diseased cells may be indicative of, or due to, existing alterations in the cytoskeletal elements and pathological changes in OA chondrocytes.

Gene Name	Increased (+) / decreased (-) expression compared to untreated controls
TGFB1	-
VEGF	+
TGM2	+
TIMP2	+
TIMP3	+
MMP14	+
CASP3	+

Table 5.2:- Genes showing similar responses to cytoskeletal disruption in normal and osteoarthritic chondrocytes. Chondrocytes were cultured in 3D agarose and gene changes, following 6 hours of treatment with reagents known to disrupt individual cytoskeletal elements of the cytoskeleton, were determined using a Taqman® custom designed array.

Gene Name	Cytoskeletal element disrupted resulting in **increased** expression	Cytoskeletal element disrupted resulting in **decreased** expression
ADAMTS4	Actin & Vimentin	Tubulin
SOX9	Actin	Vimentin
IGF1	Vimentin	Actin & Tubulin
FGFR3	Vimentin	Tubulin
IL8	Actin & Tubulin	Vimentin
PTGS2	Actin & Tubulin	Vimentin
RUNX2	Actin & Tubulin	Vimentin
GADD45B	Tubulin	Vimentin
BMF	Vimentin	Actin & Tubulin
SLC2A3	Actin & Vimentin	Tubulin
SDC2	Actin	Tubulin

Table 5.3:- Genes showing similar responses in normal and osteoarthritic chondrocytes, but different responses depending on the cytoskeletal element disrupted. Chondrocytes were cultured in 3D agarose and gene changes, following 6 hours of treatment with reagents known to disrupt different cytoskeletal elements, were determined using a Taqman® custom designed array.

Gene Name	Increased(+) / decreased(-) expression		Disrupted Cytoskeletal Element
	Normal	OA	
ADAMTS5	-	+	Tubulin & Vimentin
COMP	-	+	Actin
FGFR3	+	-	Actin
MMP13	-	+	Actin
PTCH	-	+	Vimentin
TNFSF11	+	-	Actin, Tubulin & Vimentin
NOS2A	-	+	Vimentin
VCAM1	-	+	Tubulin
GADD45B	+	-	Actin

Table 5.4:- Genes showing a different response in osteoarthritic chondrocytes compared to normal following the same treatment and therefore disruption of the same cytoskeletal element. Chondrocytes were cultured in 3D agarose and gene changes, following 6 hours of treatment with reagents known to disrupt different cytoskeletal elements, were determined using a Taqman® custom designed array.

5.2.3.3 Other Genes of Interest

From the Taqman® custom-designed array results, genes of interest were selected and the effect of cytoskeletal disruption on mRNA expression levels determined using quantitative PCR with SYBR green.

Unlike gene expression detected in articular cartilage (section 3.2.3), and as implied by differences observed by Taqman® custom designed arrays (section 4.2.2.2), aggrecan gene expression in chondrocytes in 3D agarose culture was significantly affected by pathology (Fig 5.15); expression was decreased in OA chondrocytes when compared with normal chondrocytes at all time points assayed, as determined using a general linear model ($p < 0.0035$ at 6, 12, 24 and 48 hours). In chondrocytes treated for 6 hours with colchicine, aggrecan expression was significantly lower in OA chondrocytes than in normal chondrocytes ($p = 0.043$). Aggrecan expression was also lower than normal in OA chondrocytes treated with cytochalasin D for 6 ($p = 0.055$), 12 ($p = 0.058$) and 24 hours ($p = 0.015$). An effect of vimentin cytoskeletal disruption on aggrecan expression was evident in normal chondrocytes; treatment with acrylamide resulted in downregulation of aggrecan expression, with the decrease reaching significance at 48 hours (Fig 5.15: 4.2 fold; $p = 0.021$).

COL1A1 expression was higher in OA chondrocytes when compared with normal chondrocytes at all time points and in all treatment groups, although a higher degree of variability meant that differences did not reach statistical significance (data not shown). There was no clear effect of cytoskeletal disruption on *COL1A1* expression in normal and OA chondrocytes. As in articular cartilage (section 3.2.3), *SOX9* expression was lower in OA chondrocytes when compared with normal chondrocytes, regardless of treatment or culture period (data not shown). *SOX9* expression in normal and OA chondrocytes was unaffected by cytoskeletal disruption.

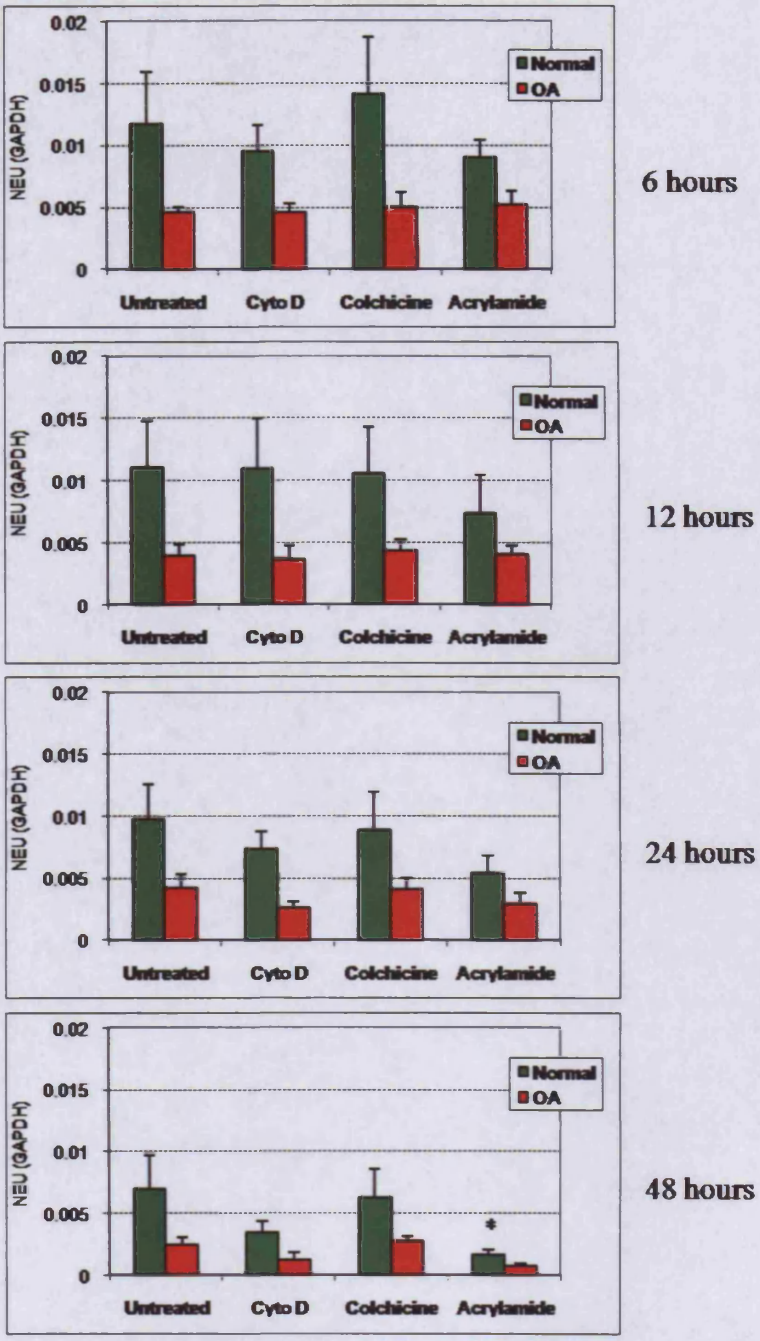

Figure 5.15:- Aggrecan gene expression changes with cytoskeletal disruption. Absolute mRNA levels were determined using SYBR Green quantitative PCR and normalised to the housekeeping gene GAPDH. Nucleic acids were isolated from chondrocytes from normal and osteoarthritic (OA) cartilage, encapsulated in 3D agarose and cultured without (untreated) or with treatment for 6, 12, 24 or 48 hours – treatments included 1μM cytochalasin D to disrupt actin microfilaments, 1μM colchicine to disrupt tubulin microtubules, or 2 mM acrylamide treatment to disrupt vimentin intermediate filaments. Data are presented as mean ± S.E.M. (n=5). * $p < 0.05$, treatment compared to untreated control.

As observed in cartilage (section 3.2.3), *ADAMTS5* expression was significantly lower in untreated OA chondrocytes when compared with untreated normal chondrocytes at all time points assayed (Fig 5.16 A; $p = 0.034$ at 12 hours). In support of changes observed on Taqman® arrays (Fig 5.13), quantitative PCR using SYBR green indicated that colchicine treatment resulted in up-regulation of *ADAMTS5* expression in OA chondrocytes at 6 hours (2.7 fold; $p = 0.012$, Mann Whitney) and 12 hours (2.4 fold; $p = 0.034$); this effect of colchicine on *ADAMTS5* expression was lost following 24 and 48 hours treatment (data not shown). There was no clear effect of cytoskeletal disruption on *ADAMTS5* expression in normal chondrocytes, which showed more varied levels of *ADAMTS5* mRNA (Fig 5.16 A).

At 12 hours *MMP13* mRNA expression was significantly higher in OA chondrocytes when compared with normal chondrocytes in all treatment groups. However, an effect of cytoskeletal disruption on *MMP13* expression was not apparent until 24 hours, when expression in OA chondrocytes was reduced by colchicine (2.2 fold; $p = 0.024$) and acrylamide (2.8 fold; $p = 0.014$) treatment (Fig 5.16 B). At 48 hours the effect of acrylamide treatment on *MMP13* expression in OA chondrocytes remained significant (5.4 fold; $p = 0.015$) whilst the effect of colchicine was no longer significant (2.3 fold; $p = 0.127$). *MMP13* expression in normal chondrocytes followed the same trend as in OA cells, although the effects did not achieve significance.

BMF mRNA expression appeared higher in untreated OA chondrocytes when compared to normal chondrocytes, with the difference increasing over the culture period, but not reaching statistical significance ($p = 0.092$ at 48 hours; Fig 5.16 C). Treatment of OA chondrocytes with cytochalasin D (2.0 fold; $p = 0.069$), colchicine (2.6 fold; $p = 0.022$) or acrylamide (4 fold; $p = 0.010$) for 48 hours reduced *BMF* expression (Fig 5.16 C). There was no significant effect of cytoskeletal disruption on *BMF* mRNA levels in normal chondrocytes.

A - *ADAMTS5* **6 hours** **12 hours**

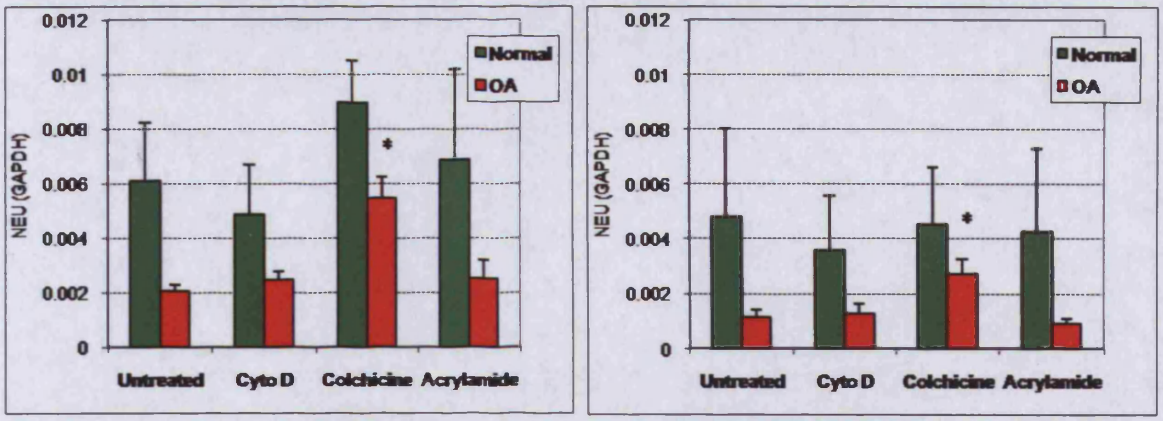

B - *MMP13* **24 hours** **48 hours**

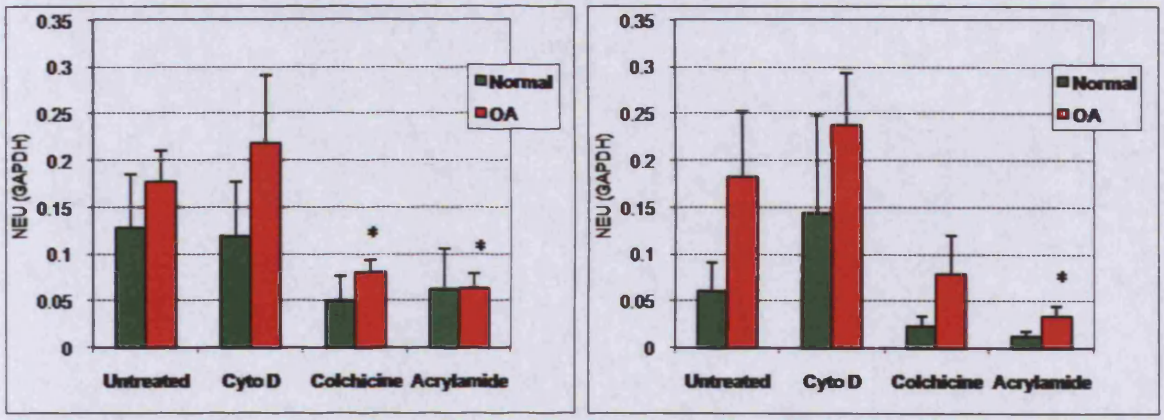

C - *BMF*

48 hours

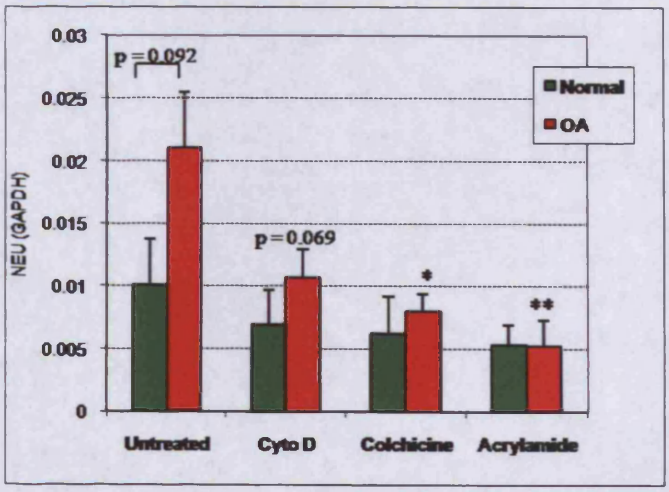

5.2.4 Changes in MMP-2 Expression or Activation Following Cytoskeletal Disruption

Levels of pro-MMP2 released into the media increased over the 48 hour culture period, indicating that both untreated normal and OA chondrocytes were able to synthesise and secrete proteins (Fig 5.17). Active-MMP2 was barely detectable in untreated normal chondrocyte cultures but was evident in culture media from untreated OA chondrocytes, where levels were observed to increase over the culture period. Disruption of actin microfilaments by cytochalasin D treatment increased the activation of MMP-2 in both normal and OA chondrocytes, with active-MMP2 evident after 6 hours of treatment. Levels of active-MMP2 were higher in cytochalasin D-treated OA chondrocytes compared to untreated controls, and active-MMP2 levels increased over those of pro-MMP2 at 24 hours. Disruption of tubulin microtubules with colchicine or vimentin intermediate filaments with acrylamide appeared to have no effect on the levels of pro- and active-MMP2 in normal and OA chondrocyte culture media. MMP-9 was not detected in untreated chondrocyte culture media by gelatin zymography and treatments did not increase MMP-9 expression to the level of detection.

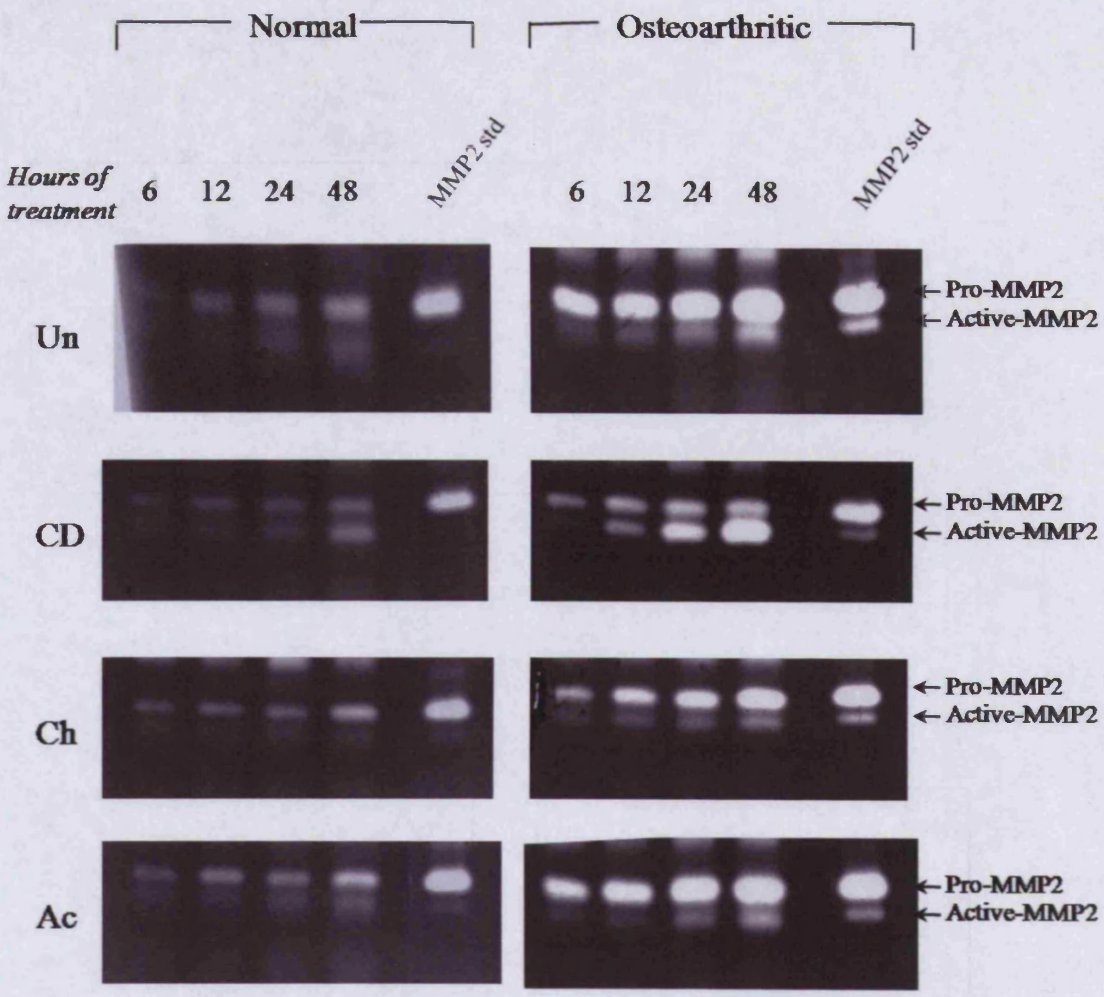

Figure 5.17:- The expression and activation of MMP-2 in chondrocytes isolated from normal and osteoarthritic (OA) cartilage, encapsulated in 3D agarose and cultured with or without treatment for 6, 12, 24 or 48 hours. Gelatin substrate zymography was used to detect the latent (72kD) and active (62kD) forms of MMP-2 with white bands representing zones of gelatinolytic activity. Equivalent volumes of media were loaded. 'Un'- untreated chondrocytes, 'CD'- 1μM cytochalasin D, 'Ch'- 1μM colchicine, 'Ac'- 2 mM acrylamide treated chondrocytes.

5.3 DISCUSSION

Osteoarthritis is characterised by a shift in the balance between anabolism and catabolism in the articular cartilage of synovial joints as a result of an altered chondrocyte phenotype. In addition to an altered phenotype, differences in the chondrocyte cytoskeleton have also been observed in OA chondrocytes (chapter 3). What remains to be determined is whether the changes in the cytoskeleton occur before, alongside or as a result of phenotypic changes in articular chondrocytes.

Numerous studies have highlighted a link between the cytoskeleton and cell phenotype, with changes in cytoskeletal organisation altering gene expression. In chondrocytes, phenotype and cell shape have long been known to be closely associated, with a round morphology associated with a chondrocytic type II collagen phenotype (Benya and Shaffer, 1982b). Alongside changes in chondrocyte phenotype, changes in actin cytoskeletal organisation were also observed (Brown and Benya, 1986), and subsequently shown to be the cause of the phenotypic changes, independent of cell shape perturbations (Benya et al., 1988). Disruption of actin microfilament dynamics promotes hypertrophic differentiation in mouse embryonic tibia chondrocytes (Woods et al., 2009) and increased expression of *SOX9*, a transcription factor required for chondrogenesis and maintenance of the chondrocyte phenotype (Woods et al., 2005). By contrast, *SOX9* expression and GAG synthesis are decreased following microtubule disruption (Woods et al., 2005, Takigawa et al., 1984). Finally, vimentin intermediate filament disruption in chondrocytes results in decreased expression of the chondrocyte phenotype markers *COL2A1* and *ACAN* (type II collagen and aggrecan respectively) (Blain et al., 2006).

Changes in the cytoskeleton have been shown to affect chondrocyte gene expression, and differences in the organisation and expression of cytoskeletal elements are apparent between normal and osteoarthritic human chondrocytes (chapter 3). Therefore the response of human chondrocytes to cytoskeletal disruption has been investigated to determine whether or not the response of OA chondrocytes differs to that of normal chondrocytes. In 3D agarose culture the cytoskeletal organisation and phenotype of chondrocytes resembles that of cartilage chondrocytes *in situ* (chapter 3 and 4). In addition, the differences between normal and OA chondrocyte gene expression in cartilage are more accurately represented in 3D agarose culture (chapter 4);

chondrocytes were therefore cultured and treated with cytoskeletal disrupting agents in a 3D agarose construct.

The concentrations of cytoskeletal disrupting reagents used were based on previous studies on chondrocytes cultured as a monolayer. Treatment with 1μM colchicine effectively disrupts microtubules and reduces *SOX9* expression in chondrocytes (Evangelisti et al., 1995, Woods et al., 2005). My preliminary work on human chondrocytes cultured as a monolayer confirmed disruption of microtubule bundles following 12 hours of treatment with 1μM colchicine (appendix 4). Actin microtubules are disrupted by 1μM cytochalasin B (Evangelisti et al., 1995); cytochalasin D has also been used to disrupt microfilaments at concentrations ranging from 0.4μM (Castilla et al., 2000) to 8μM (Tomasek et al., 1997). In mouse chondrocytes, 3μM cytochalasin D induces up-regulation of *SOX9* expression (Woods et al., 2005), whilst in human chondrocytes, cell rounding is induced in monolayer by 1μM cytochalasin D (Tew and Hardingham, 2006) (appendix 4). In bovine chondrocytes treatment with 5mM acrylamide induces perinuclear collapse of vimentin intermediate filaments (Blain et al., 2006). However vimentin disruption remains effective at 2mM acrylamide with the additional benefit of reduced cytotoxicity (Blain, unpublished observations). Treatment with 2mM acrylamide disrupts vimentin intermediate filament bundles in monolayer human chondrocytes (appendix 4). In all instances disruption of a specific cytoskeletal element was achieved in chondrocytes cultured in 3D agarose, with little or no effect on the organisation of the other major elements after 24 hours of treatment.

5.3.1 Cytoskeletal Elements and Cytoskeletal-associated Proteins

mRNA expression levels of β-actin and the actin-depolymerising proteins cofilin and destrin were increased in response to disruption of actin microfilaments. As cytochalasin D disrupts microfilament dynamics through actin filament capping and cleavage (Urbanik and Ware, 1989) and thus increases the G-actin pool, it is interesting that these F-actin severing proteins are up-regulated. In normal chondrocytes, treatment with colchicine up-regulated β-actin and destrin mRNA expression at 12 hours, perhaps providing an explanation for the small effect of microtubule disruption on actin microfilament organisation observed at 24 hours. Differential regulation of these genes in response to cytoskeletal disruption was primarily observed in chondrocytes isolated from normal cartilage, indicating that these cytoskeletal genes are more sensitive to

cytoskeletal disruption in normal chondrocytes than in OA chondrocytes. Expression of the cytoskeletal and associated proteins that were observed to differ in expression between normal and OA cartilage (chapter 3), including vimentin, β-tubulin, thymosin β4 and paxillin, were unaffected by cytoskeletal disrupting reagents over the 48 hour period studied.

5.3.2 Chondrocyte Phenotype Markers and Matrix Metabolism Genes

With regards to the typical markers of the chondrocyte phenotype, *COL2A1* and *ACAN* were down-regulated in OA chondrocytes with disruption of individual cytoskeletal elements. Reduced expression and synthesis of type II collagen and aggrecan has been demonstrated following vimentin intermediate filament disruption with acrylamide (Blain et al., 2006) and reduced GAG synthesis following microtubule disruption with colchicine suggests a decrease in aggrecan core protein (Takigawa et al., 1984). No significant changes in *SOX9* expression were observed in chondrocyte-agarose constructs over the 48 hours of cytoskeletal disruption. Previous studies have demonstrated down-regulation of *SOX9* with microtubule disruption (Woods et al., 2005) and up-regulation with actin disruption (Woods et al., 2005, Tew and Hardingham, 2006, Zhang et al., 2006c), although these studies focused on the effects of cytoskeletal disruption on chondrogenesis or dedifferentiation/ redifferentiation. For example, Tew and Hardingham, 2006 showed an increase in *SOX9* mRNA expression in mature human chondrocytes after 5 hours of treatment with 1μM cytochalasin D. However, this was observed in monolayer conditions and was associated with a loss of actin stress fibres. Although they demonstrated an up-regulation of *SOX9* expression when monolayer chondrocytes were transferred to alginate culture, the effect of cytochalasin D on *SOX9* expression in chondrocytes cultured in 3D conditions was not investigated (Tew and Hardingham, 2006). The difference in cell morphology and lack of stress fibres could influence the observed effects of treatment, as demonstrated by recent studies in which p38 MAPK stabilised *SOX9* mRNA in human chondrocytes only in the absence of actin stress fibres (Tew and Hardingham, 2006, Tew et al., 2009). Cytoskeletal disruption had little effect on the expression of *COL1A1* and *COL3A1* in 3D agarose culture, with down-regulation observed only in the Taqman® array data and in normal chondrocytes treated with cytochalasin D. As type I and type III collagen are markers of a fibroblastic phenotype, these changes could be an indication of enhanced

redifferentiation with actin disruption in normal chondrocytes; this effect, if any, is small as no significant changes were detected with SYBR® green.

Disruption of actin stress fibres in fibroblasts results in increased expression of pro-MMP1 and -3 (Werb et al., 1986), MMP-2 and MMP-14 (Tomasek et al., 1997), MMP-3, -9, -13 and -14 (Lambert et al., 2001), and increased activation of pro-MMP2 (Lambert et al., 2001, Tomasek et al., 1997). In contrast to reports in fibroblasts, *MMP3* expression was down-regulated following six hours of microfilament disruption in normal and OA chondrocytes. *MMP1* was also down-regulated in OA, but up-regulated in normal chondrocytes. Activation of pro-MMP2 was increased in both normal and OA chondrocytes with actin disruption, and expression of MMP-14 was increased in all treatment and pathology groups. In support of previous work in bovine chondrocytes (Blain et al., 2006), no induction of MMP-2 expression or activation was observed with vimentin disruption. On Taqman® arrays, *MMP13* expression was up-regulated with actin disruption in OA chondrocytes, but no significant differences were observed with SYBR® green using an increased number of samples. By contrast, *MMP13* was down-regulated with disruption of the tubulin or vimentin cytoskeleton in OA chondrocytes. Tubulin disruption also resulted in increased expression of *ADAMTS5* in OA chondrocytes.

Disruption of any of the major cytoskeletal elements in chondrocytes therefore has the potential to affect extracellular matrix composition through the regulation of genes encoding both matrix proteins and matrix-degrading enzymes.

5.3.3 Growth Factor-related Genes

Changes in expression of the growth factor-related genes varied depending on the pathology and the cytoskeletal element disrupted. Expression of *TGFB1* was down-regulated irrespective of the cytoskeletal element disrupted and of pathology. Disruption of microtubule dynamics in bovine chondrocytes with colchicine reduces TGFβ1 secretion but has no effect on *TGFB1* transcription (E.J. Blain, unpublished results). By contrast, cytochalasin B, cytochalasin C and colchicine have been shown to induce increases in TGFβ1 mRNA and protein expression (Varedi et al., 1997, Nahm et al., 2004). It should be noted however that this was observed using fibroblasts, which exhibit a morphology and cytoskeletal organisation closer to that of dedifferentiated

chondrocytes, and distinct from that of differentiated chondrocytes. Whilst TGFβ1 induces chondrogenesis (Mehlhorn et al., 2006) and is anabolic for dedifferentiated chondrocytes, it can also enhance dedifferentiation of mature, differentiated articular (Galera et al., 1992a) and epiphyseal chondrocytes (Ballock et al., 1993) cultured as a monolayer. Up-regulation of Rho GTPase activity and stress fibre formation in chondrocytes by TGFβ1 could also be detrimental to the chondrocyte phenotype (Haudenschild et al., 2009). Therefore down-regulation of *TGFB1* with cytoskeletal disruption does not necessarily imply a reduction in anabolism.

In contrast to *TGFB1*, changes in *IGF1* expression varied according to the cytoskeletal element disrupted; expression was up-regulated with vimentin disruption but down-regulated with actin or tubulin disruption. IGF-I induces anabolic changes in chondrocytes (Fortier et al., 2002, Jenniskens et al., 2006, Zhang et al., 2009) and also promotes a typical chondrocyte morphology and cytoskeletal organisation by reducing Rho and Cdc42 GTPase activity and actin stress fibres (Fortier et al., 2004, Novakofski et al., 2009). Down-regulation of *IGF1* with actin disruption could therefore be a response to altered actin cytoskeletal dynamics and a requirement for Rho GTPase activity. Up-regulation of the anabolic growth factor by vimentin disruption is interesting considering the down-regulation of type II collagen and aggrecan expression observed in the present study and in bovine chondrocytes (Blain et al., 2006).

Changes in *FGFR3* expression varied depending on pathology but were independent of the cytoskeletal element disrupted; expression was up-regulated in normal but down-regulated in OA chondrocytes. FGFR3 and its activation by FGF18 is associated with anabolic effects on articular cartilage and chondrocytes (Ellman et al., 2008). Gain-of-function mutations of FGFR3 are associated with chondrodysplasias and overexpression of constitutively active FGFR3 in foetal chondrocytes is associated with premature hypertrophic differentiation (Legeai-Mallet et al., 2004). FGF18 signals through FGFR3 to suppress mesenchymal cell proliferation and promote chondrogenesis and cartilage matrix synthesis (Davidson et al., 2005). In adult human articular chondrocytes, loss of *FGFR3* expression, along with *COL2A1*, is associated with a reduced capacity to form cartilage *in vivo* (Dell'Accio et al., 2001). In addition, FGFR3-knockout mice exhibit increased expression of *MMP13* and type X collagen along with increased degradation of type II collagen and aggrecan, resulting in cartilage degradation similar to that

observed in OA (Valverde-Franco et al., 2006). In support of this connection with OA, intra-articular injection of FGF18 promotes new cartilage formation and reduces cartilage degeneration in a rat model of OA (Moore et al., 2005). It is interesting therefore that *FGFR3*, which is more highly expressed in OA than in normal chondrocytes (chapter 4), should be down-regulated with cytoskeletal disruption in OA chondrocytes but up-regulated in normal chondrocytes. *FGF18* expression was also down-regulated in OA chondrocytes with disrupted actin and vimentin networks. Differences in *FGF18* expression between normal and OA human chondrocytes and changes in *FGF18* expression with cytoskeletal disruption in normal chondrocytes could not be calculated due to undetected expression in untreated normal chondrocytes; however, detection of expression in treated normal chondrocytes could imply an up-regulation, with *FGF18* changes therefore mirroring those of *FGFR3*. Up-regulation of FGFR3 and FGF18 in OA chondrocytes could be indicative of hypertrophy (Davidson et al., 2005, Liu et al., 2007) or of an anabolic repair response.

Disruption of any of the main elements of the chondrocyte cytoskeleton therefore has the potential to affect chondrocyte phenotype and extracellular matrix composition through the expression of genes encoding growth factors that regulate chondrocyte differentiation, matrix synthesis and matrix degradation.

5.3.4 Inflammation-related Genes

Changes in the expression of *NOS2A*, which encodes inducible nitric oxide synthase (iNOS), and *TNFSF11*, the gene encoding receptor activator of NFκB ligand (RANKL), varied depending on pathology. Vimentin disruption with acrylamide reduced *NOS2A* expression in normal chondrocytes but increased expression in OA chondrocytes. Previous work in neurons has shown increased iNOS expression in response to acrylamide treatment (Kim, 2005). Up-regulation of *NOS2A* was also observed in normal chondrocytes treated with cytochalasin D. In support of this, disruption of actin cytoskeletal dynamics, either by cytochalasin D or inhibition of Rho/ROCK signalling, enhances cytokine-induced iNOS mRNA expression in epithelial cells (Witteck et al., 2003). *NOS2A* expression was undetected in colchicine-treated chondrocytes and therefore no fold-change could be determined. Colchicine decreases iNOS expression in smooth muscle cells (Marczin et al., 1996) and neurons (Gahm et al., 2005), therefore it is possible that down-regulation of *NOS2A* with tubulin disruption resulted in lack of

detection in these samples. Disruption of the tubulin or vimentin cytoskeleton resulted in up-regulation of *TNFSF11* expression in normal but down-regulation in OA chondrocytes. In prostate cancer cells, RANKL is up-regulated during the epithelial to mesenchymal transition and is therefore associated with up-regulation of vimentin (Odero-Marah et al., 2008). RANKL is expressed by osteoblasts and promotes osteoclastogenesis and bone resorption (Bezerra et al., 2005) and its expression is elevated in a subpopulation of OA subchondral bone osteoblasts (Kwan Tat et al., 2008) and late stage OA cartilage (Ijiri et al., 2008). However, whilst RANKL and its receptor, RANK, are expressed in normal and OA cartilage, exogenous RANKL does not activate human articular chondrocytes in culture (Komuro et al., 2001). Down-regulation of RANKL expression in OA chondrocytes could be indicative of the existing difference in expression between OA and normal chondrocytes (chapter 4 and Ijiri et al, 2008); up-regulation in normal chondrocytes would therefore indicate a detrimental response to cytoskeletal disruption.

In contrast to *NOS2A* and *TNFSF11* expression changes, *PTGS2* and *IL8* expression changes were independent of pathology but dependent on the cytoskeletal element disrupted. *PTGS2*, encoding cyclooxygenase-2 (COX-2) was up-regulated with disruption of actin or tubulin but down-regulated with vimentin disruption. In support of this, colchicine or cytochalasin D treatment increases COX-2 protein expression and synthesis of prostaglandin E2 in human endothelial and epithelial cells (Sawyer et al., 2001, Subbaramaiah et al., 2000). In chondrocytes however, disruption of the actin cytoskeleton by cytochalasin D inhibits COX-2 expression and prostaglandin E2 production induced by nitric oxide (NO) (Kim et al., 2003). *IL8* expression was also up-regulated in chondrocytes with actin and tubulin disruption but down-regulated with disruption of vimentin. The effects of cytoskeletal changes on *IL8* expression have not previously been demonstrated in chondrocytes. However, microtubule disruption by colchicine induces *IL8* expression in epithelial cells (Shibata et al., 1996) and cytochalasin D enhances *IL8* expression in monocyte-like cells (Kustermans et al., 2008). IL-8-induced cell migration and phosphorylation of focal adhesion kinase requires an intact actin and tubulin cytoskeleton (Cohen-Hillel et al., 2006), suggesting that cytoskeletal disruption can alter IL-8 signalling as well as expression.

Prostaglandin E2 decreases aggrecan expression, proteoglycan synthesis and type II collagen in human articular chondrocytes (Li et al., 2009b); by contrast, very low concentrations of prostaglandin E2 suppress *MMP13* expression and type II collagen cleavage in OA cartilage (Tchetina et al., 2007). Furthermore, NO suppresses proteoglycan and type II collagen synthesis whilst increasing MMP activity in articular cartilage chondrocytes (Taskiran et al., 1994, Cao et al., 1997, Murrell et al., 1995). Dysregulation of key inflammatory genes in response to disruption of any of the main elements of the chondrocyte cytoskeleton could therefore further affect chondrocyte phenotype and extracellular matrix composition.

5.3.5 Apoptosis-related Genes

Expression of *CASP3*, which encodes pro-apoptotic caspase-3, was up-regulated with cytoskeletal disruption, independently of treatment and pathology. *CASP3* expression is elevated over normal levels in human OA chondrocytes cultured in 3D agarose (chapter 4) and in human OA cartilage (Sharif et al., 2004). Acrylamide increases caspase-3 activity in chondrocytes (Blain et al., 2006), lymphocytes (Blasiak et al., 2004) and neurons (Sumizawa and Igisu, 2007). In chondrocytes, NO-induced caspase-3 activation is suppressed by actin disruption with cytochalasin D (Kim et al., 2003). Actin cytoskeletal disruption with cytochalasin D also prevents caspase-3 activation in a number of other cell types including platelets (Ben Amor et al., 2006), B-cells (Melamed and Gelfand, 1999) and cardiomyocytes (Okada et al., 2005). As cell viability assays showed no significant increase in cell death over 48 hours with each treatment, the up-regulation of *CASP3* expression could have apoptosis-independent consequences. For example, caspase-3 can cleave vimentin at asparagine 85, resulting in disruption of intermediate filament networks in cells (Byun et al., 2001). Modified isoforms of caspase-3-cleaved vimentin are detected in synovial tissue from patients with rheumatoid arthritis (Tilleman et al., 2008). In addition to cleavage of vimentin, caspase-3-mediated cleavage of gelsolin generates a product that severs actin filaments *in vitro* and induces cell rounding (Kothakota et al., 1997). Therefore up-regulation of *CASP3* expression by cytoskeletal disruption in agarose-embedded chondrocytes could result in further modification of cytoskeletal organisation.

GADD45B expression was up-regulated in chondrocytes following tubulin disruption but down-regulated after vimentin disruption. There is little clear evidence linking

GADD45β with the cytoskeleton in any cell type. Differential *GADD45B* expression in actin disassembled chondrocytes was dependent upon pathology; *GADD45B* expression was up-regulated in normal but down-regulated in OA chondrocytes, corroborating the observation of decreased *GADD45B* expression in OA chondrocytes encapsulated in agarose (chapter 4). *GADD45B* expression is reduced in both bone and cartilage in late stage OA (Hopwood et al., 2007, Ijiri et al., 2008). GADD45β can be both pro-and anti-apoptotic, inhibiting TNFα-induced or promoting TGFβ-induced apoptosis (De Smaele et al., 2001, Yoo et al., 2003). In human articular chondrocytes, GADD45β is cytoprotective whilst suppressing *COL2A1* promoter activity and mRNA expression (Ijiri et al., 2008); in murine epiphyseal chondrocytes GADD45β promotes terminal differentiation and stimulates *MMP13* promoter activity (Ijiri et al., 2005). Altered expression of *GADD45B* could therefore affect the chondrocyte phenotype and ultimately the matrix composition of the cartilage tissue.

Taqman® array data revealed down-regulation of *BMF* expression in normal and OA chondrocytes with disruption of actin and tubulin, whilst in acrylamide-treated cells, *BMF* expression was elevated in normal chondrocytes but was unchanged in OA. Further investigation by quantitative PCR demonstrated down-regulation of *BMF* expression after 48 hours of actin, tubulin or vimentin disruption in OA chondrocytes. My results indicated that *BMF* is expressed more highly in agarose-cultured OA chondrocytes when compared with normal cells. *BMF* encodes Bcl2-modifying factor, a Bcl2 family member that promotes apoptosis through binding of pro-survival Bcl2 proteins (Puthalakath et al., 2001). Interestingly, Bcl2 expression is reduced in OA cartilage when compared with normal (Brew et al., 2010a). BMF binds to the dynein light chain 2 (DLC2) component of the myosin V motor complex, which sequesters it to actin microfilaments; cytochalasin D treatment releases BMF from F-actin (Puthalakath et al., 2001). The loss of cell attachment and hence integrin signalling, an apoptotic signal termed "anoikis", releases BMF from DLC2, enabling its interaction with pro-survival Bcl2 proteins (Puthalakath et al., 2001). In mammary epithelial cells, *BMF* expression is elevated following actin disruption or loss of matrix attachment (Schmelzle et al., 2007). This is in contrast with my results in human articular chondrocytes which indicate a down-regulation of BMF with disruption of the actin cytoskeleton, particularly in OA chondrocytes. Down-regulation of *BMF* in response to cytoskeletal disruption in

chondrocytes suggests an anti-apoptotic response; this is in direct contrast to the observed up-regulation of pro-apoptotic *CASP3*.

Whilst the response of normal and osteoarthritic chondrocytes is not straightforward, it is clear that cytoskeletal dysregulation has the ability to alter expression of genes involved in diverse processes. Cytoskeletal disruption affects expression of genes with established roles in chondrocyte metabolism and extracellular matrix turnover (Goldring, 2000), in addition to genes that can further alter cytoskeletal organisation and those not previously associated with chondrocytes or the cytoskeleton. The data demonstrating dysregulation of the cytoskeleton in OA chondrocytes infers that this could contribute to the altered chondrocyte phenotype that is a hallmark of OA.

Chapter 6: The Effect of Load and Cytoskeletal Element Disruption on Chondrocyte Phenotype

6. THE EFFECT OF LOAD AND CYTOSKELETAL ELEMENT DISRUPTION ON CHONDROCYTE PHENOTYPE

6.1 INTRODUCTION

6.1.1 Load and Chondrocyte Phenotype

Load has long been hypothesised as a key mediator in the development of OA. It is a major element in all of the risk factors associated with the development of secondary OA (section 1.3.2.1) and in OA joints regions of fibrillation most often occur at weight-bearing regions of the articular cartilage. A number of studies have implicated load as a mediator of cartilage turnover. As discussed in section 1.4.1, experimental induction of changes in joint loading patterns *in vivo* and mechanical compression of *ex vivo* cartilage explants clearly demonstrates a role of load in the regulation of chondrocyte phenotype. The effect on chondrocyte phenotype depends on the loading regimen used, but in general, static loads induce catabolic changes whilst dynamic/cyclic loading is anabolic, and damage to the cartilage increases with increasing load magnitude and duration (Kurz et al., 2005).

In order to remove variables associated with differences in the mechanical integrity of the cartilage matrix, in addition to enabling easy manipulation of chondrocytes and culture conditions, the effects of load have been studied using chondrocytes isolated from cartilage. As chondrocyte phenotype is lost in monolayer but maintained in 3D agarose culture (section 4.1), chondrocytes embedded in hydrogels have been used to study the effects of mechanical loading regimes on chondrocyte phenotype.

6.1.1.1 Chondrocytes Embedded in Agarose

Chondrocytes embedded in agarose transcribe and synthesise chondrocyte matrix molecules (Buschmann et al., 1995, Knight et al., 1998). Bovine chondrocytes show increases in collagen and sGAG content from day one to day six of culture (Knight et al., 1998). Matrix molecules, including proteoglycans and type VI collagen form a pericellular matrix surrounding the chondrocytes, visible after just 24 hours, that develops and increases over the duration of culture (Buschmann et al., 1995, Dimicco et

al., 2007). Static compression reduces proteoglycan and protein synthesis in chondrocyte/agarose constructs, indicating that the biochemical response of *in situ* cartilage chondrocytes is preserved in agarose culture (Buschmann et al., 1995). Cell proliferation has also been shown to be reduced by static compression of bovine chondrocytes in agarose (Lee and Bader, 1997). By contrast, bovine chondrocytes in agarose subjected to four hours of a 5 MPa static hydrostatic pressure, which does not cause cell deformation, showed increased aggrecan expression and GAG synthesis (Toyoda et al., 2003). As in cartilage, cyclic or dynamic compression of chondrocytes in hydrogel produces anabolic changes including increased proteoglycan synthesis (Buschmann et al., 1995, Chowdhury et al., 2003, Mauck et al., 2003, Mio et al., 2005, Wang et al., 2008b), aggrecan gene transcription (Mio et al., 2005, Mauck et al., 2007) and cell proliferation (Lee and Bader, 1997). Protein synthesis or type II collagen content is increased with dynamic compressive loading after 10 hours (Buschmann et al., 1995), 48 hours (Wang et al., 2008b), 21 and 28 days (Mauck et al., 2003, Chokalingam et al., 2009). *COL2A1* promoter activity and mRNA expression has been shown to be increased by dynamic compression for 24 hours (Mio et al., 2005), seven days and 14 days (Chokalingam et al., 2009), whilst loading for just 30 minutes reduced *COL2A1* promoter activity (Bougault et al., 2008).

The frequency of dynamic compressive loading regimes can influence the response of chondrocytes, as observed for proteoglycan synthesis and release in cartilage explants (section 1.4.2). Stimulation of protein synthesis in dynamically compressed bovine chondrocyte/agarose constructs were increased with increasing frequency, from 0.01 Hz to 1 Hz (Buschmann et al., 1995). Proteoglycan synthesis is inhibited by dynamic compression at 0.3 Hz but stimulated at 1 Hz (Lee and Bader, 1997). In addition, differences are noted between dynamic compression applied continuously or intermittently. Increases in proteoglycan synthesis were greater with intermittent dynamic compression regimes when compared with continuous dynamic compression (Chowdhury et al., 2003), whilst expression of *MMP1* and *MMP3* was increased by intermittent loading but down-regulated by continuous compression (Nicodemus and Bryant, 2010).

With the expanding interest in tissue engineering, chondrocytes have been seeded into and studied in numerous constructs and scaffolds other than hydrogels. These studies

have also demonstrated an enhanced chondrocyte phenotype and synthesis of an articular cartilage-like matrix following the application of dynamic mechanical load (Xie et al., 2006, Fehrenbacher et al., 2006, Schmidt et al., 2006, Waldman et al., 2006, Wang et al., 2009a). In bovine chondrocytes seeded onto calcium polyphosphate substrates, *MMP3* and *MMP13* expression were transiently up-regulated following 30 minutes of cyclic compression, increasing at two hours post-loading and returning to baseline levels at six hours (De Croos et al., 2006). Catabolic increases in MMP-13 activity and release of proteoglycans and collagen at six hours post-compression were also transient and were followed by increases in type II collagen and aggrecan mRNA expression and synthesis at 12 and 24 hours post-compression.

6.1.2 The Chondrocyte Cytoskeleton and Load

In addition to its effect on the chondrocyte phenotype, mechanical load can alter the organisation of the chondrocyte cytoskeleton along with the expression and activity of cytoskeletal -associated and -regulatory proteins (see section 1.4.3.2). Furthermore, the actin (section 1.4.3.3) and tubulin (section 1.4.2.1.5) cytoskeletal networks have been implicated in chondrocyte mechanotransduction pathways.

6.1.3 Mechanotransduction in Osteoarthritic Chondrocytes

Changes in the mechanical integrity of the extracellular matrix, the chondrocyte phenotype, the viscoelasticity of chondrocytes and the chondrocyte cytoskeleton in OA could result in altered mechanotransduction in OA chondrocytes. In support of this, the integrin-, IL-4- and stretch activated ion channel-dependent membrane hyperpolarisation induced in normal human chondrocytes by cyclic pressure-induced strain was not observed in human OA chondrocytes in monolayer (Millward-Sadler et al., 2000b). OA chondrocytes exhibit membrane depolarisation rather than hyperpolarisation, but the depolarisation was dependent on $\alpha 5\beta 1$ integrins, stretch activated ion channels, tyrosine kinases and phospholipase C (Millward-Sadler et al., 2000b) as is the electrophysiological response of normal chondrocytes (Wright et al., 1996, Wright et al., 1997, Lee et al., 2000). In contrast to normal chondrocytes, in which membrane hyperpolarisation was prevented by protein kinase C inhibitors or cytochalasin D (Wright et al., 1997), the actin cytoskeleton and protein kinase C were not required for membrane depolarisation in OA chondrocytes (Millward-Sadler et al., 2000b). Inhibition of PI3 kinase blocked mechanically-induced membrane potential changes in OA

chondrocytes but not normal chondrocytes. In the same model, mechanical stimulation did not alter the expression of aggrecan or *MMP3* in OA chondrocytes, although this regimen up-regulated aggrecan and down-regulated *MMP3* expression in normal chondrocytes (Millward-Sadler et al., 2000a). Collectively these data suggest different or divergent mechanotransduction pathways exist in OA chondrocytes. In support of this, strain-induced depolarisation in OA chondrocytes is mediated by secretion of IL-1β in addition to IL-4 (Salter et al., 2002), whilst only IL-4 is involved in strain-induced hyperpolarisation in normal chondrocytes (Millward-Sadler et al., 1999). Furthermore, in the mechanotransduction pathway discussed, IL-4 is suggested to signal through the type II IL-4 receptor in normal chondrocytes (Millward-Sadler et al., 2000a) but through the type I IL-4 receptor in OA chondrocytes (Salter et al., 2002).

The fact that 1) the chondrocyte cytoskeleton can be altered in response to load and 2) the chondrocyte phenotype is influenced by load or disruption of the cytoskeleton, provides clear evidence for a significant role of the cytoskeleton in chondrocyte mechanotransduction and, hence, modulation of gene expression. Therefore the observed differences in the cytoskeletal organisation of OA chondrocytes could alter the response of chondrocytes to load.

I therefore sought to:

- Characterise changes in the cytoskeletal organisation of normal and OA human chondrocytes in response to cyclic compression.
- Determine changes in the gene expression of cytoskeletal components in response to cyclic compression.
- Determine the effect of cyclic compression on expression of chondrocyte phenotype markers.
- Determine the role of the chondrocyte cytoskeleton in these responses to compression by disrupting the cytoskeleton prior to loading.
- Determine any differences in the response of chondrocytes isolated from normal and OA articular cartilage.

6.2 RESULTS

Normal and osteoarthritic human articular chondrocytes were expanded in monolayer, before passage three chondrocytes were encapsulated in 3% agarose and cultured for 48 hours. Chondrocytes were treated for 24 hours with either 1μM cytochalasin D to disrupt actin microfilaments, 1μM colchicine to disrupt tubulin microtubules, or 2mM acrylamide to disrupt vimentin intermediate filaments. Chondrocyte/agarose constructs were then subjected to a cyclic compressive load of 15% strain at 0.5 Hz for 10, 20 or 40 minutes in the presence of treatments; some samples were loaded for 40 minutes and then allowed to recover for 5 hours.

6.2.1 The Effect of Load and Treatments on Cell Viability

The viability of normal and osteoarthritic human chondrocytes in agarose culture was determined using the LIVE/DEAD® Viability/Cytotoxicity kit for mammalian cells. In viable chondrocytes the fluorogenic esterase substrate calcein AM is hydrolysed and fluorescence is visible with a FITC (green) filter, whilst dead chondrocytes are visualised with the nucleic acid stain ethidium homodimer-1 and fluorescence is detectable with a TRITC (red) filter. The viability of normal and OA chondrocytes was not affected by treatment for 24 hours with 1μM cytochalasin D, 1μM colchicine or 2mM acrylamide (Fig 6.1A and B, a-d). In normal chondrocytes, there was no increase in cell death in all treatment groups loaded for 10 (Fig 6.1A e-h), 20 (Fig 6.1A i-l), and 40 minutes (Fig 6.1A m-p). There appeared to be a reduction in cell viability in constructs left to recover for 5 hours post-load (Fig 6.1A q-t) when compared with those loaded for 40 minutes (Fig 6.1A m-p), particulary in colchicine- and acrylamide-treated samples which showed a 13% decrease in viability over the recovery period. In OA chondrocytes there was no clear decrease in cell viability following 10 (Fig 6.1B e-h), 20 (Fig 6.1B i-l) or 40 minutes load (Fig 6.1B m-p). When compared with unloaded controls there was a decrease in cell viability in samples loaded for 40 minutes and allowed to recover for 5 hours (Fig 6.1B q-t) and the effect was most evident in untreated chondrocytes (15% decrease, Fig 6.1B q).

A – Normal Chondrocytes

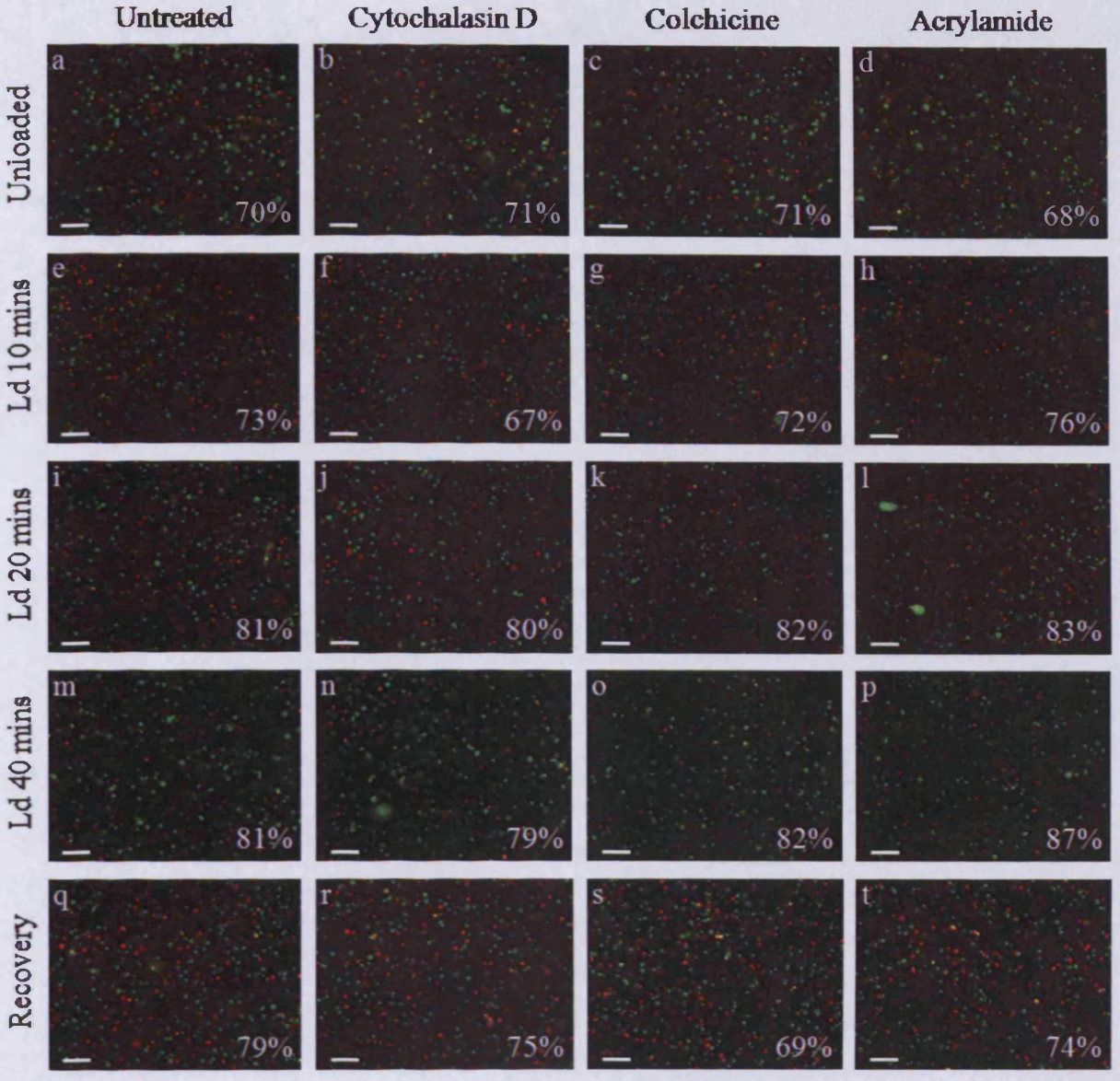

Figure 6.1 A:- **Viability of chondrocytes from normal human articular cartilage, encapsulated in 3D agarose, cultured without or with the indicated treatment, then either unloaded (a-d), loaded (cyclic compression; 15%, 0.5 Hz) for 10 (e-h), 20 (i-l) or 40 (m-p) minutes, or loaded for 40 minutes then left to recover for 5 hours (q-t). Viability was determined using the LIVE/DEAD® Viability/Cytotoxicity kit for mammalian cells (Molecular Probes). Live (green) and dead (red) chondrocytes in slices of agarose constructs were viewed on a fluorescence microscope. Percentages displayed indicate the viability, calculated from chondrocytes in focus. Scale bars = 200μm.**

B – Osteoarthritic Chondrocytes

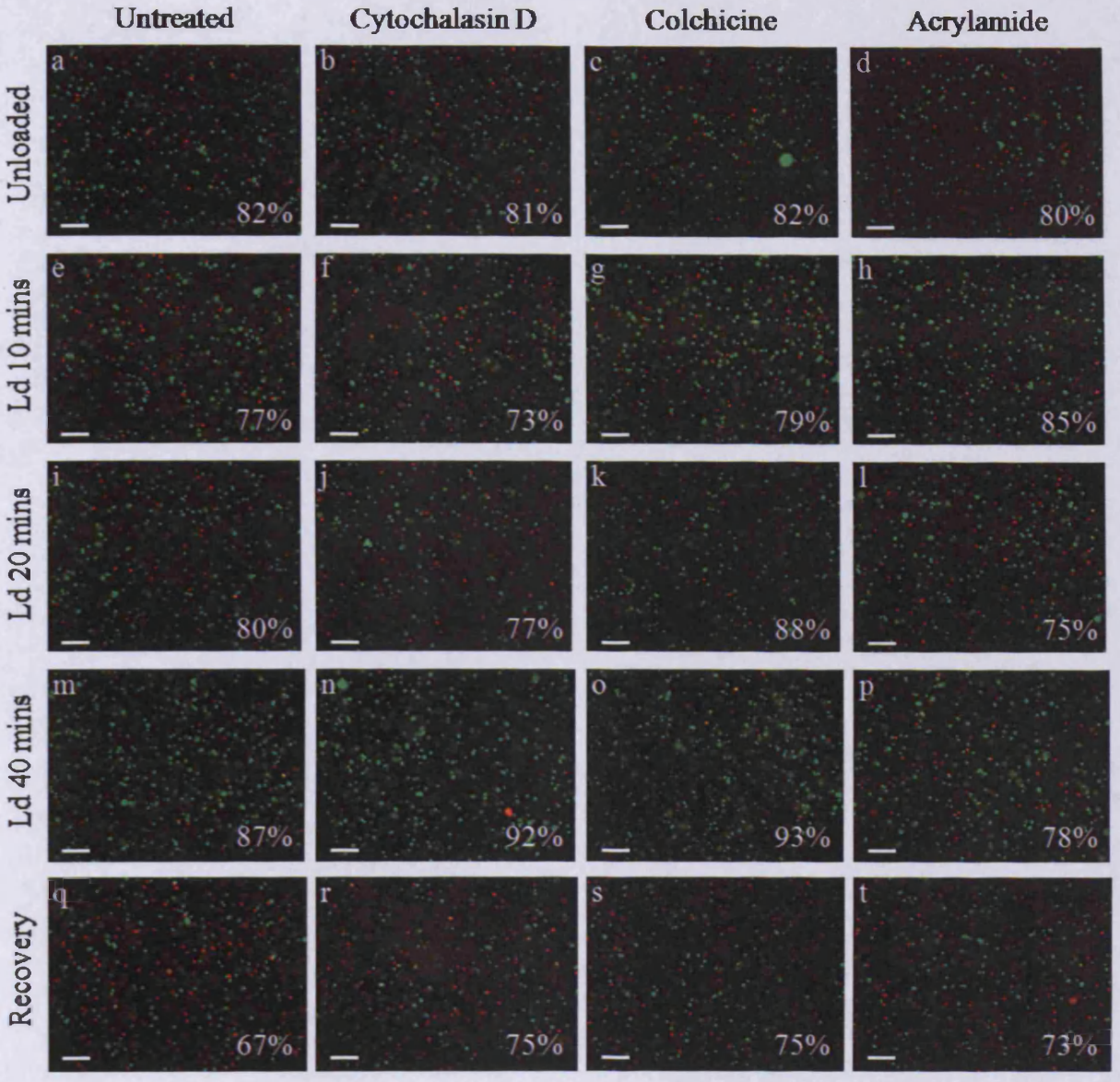

Figure 6.1 B:- **Viability of chondrocytes from osteoarthritic human articular cartilage, encapsulated in 3D agarose, cultured without or with the indicated treatment, then either unloaded (a-d), loaded (cyclic compression was to 15% strain at 0.5 Hz) for 10 (e-h), 20 (i-l) or 40 (m-p) minutes, or loaded for 40 minutes then left to recover for 5 hours (q-t). Viability was determined using the LIVE/DEAD® Viability/Cytotoxicity kit for mammalian cells (Molecular Probes). Live (green) and dead (red) chondrocytes in slices of agarose constructs were viewed on a fluorescence microscope. Percentages displayed indicate the viability, calculated from chondrocytes in focus. Scale bars = 200μm.**

6.2.2 Changes in Cytoskeletal Organisation with Load

The cytoskeletal architecture of chondrocytes in agarose culture that were either subjected to 40 minutes of load or left for a 5 hour recovery post-load was visualised by immunofluorescence in conjunction with confocal microscopy.

6.2.2.1 Untreated Chondrocytes

6.2.2.1.1 Normal Untreated Chondrocytes

Actin Microfilaments: As demonstrated in section 5.2.2.1, untreated and unloaded normal chondrocytes in 3D agarose culture showed punctate, predominantly cortical actin microfilament staining (Fig 6.2A and B a). Following 40 minutes of cyclic compressive loading, actin staining appeared less punctate and more diffuse (Fig 6.2A d), although the localisation remained predominantly at the cell periphery (Fig 6.2B d). At the end of a 5 hour recovery period normal chondrocytes partially regained the punctate appearance of actin staining observed in unloaded controls (Fig 6.2A g), although fluorescence was more cortical and some diffuse actin microfilament staining remained (Fig 6.2A and B g).

Tubulin microtubules: Tubulin staining appeared diffuse throughout untreated and unloaded normal chondrocytes, with some evidence of fine filamentous staining that was denser around the cell periphery (Fig 6.2A and B b). Loading for 40 minutes caused tubulin to become punctate and more dense in the perinuclear region rather than at the periphery (Fig 6.2A and B e). Following a 5 hour recovery period, tubulin lost its punctate appearance and returned to the diffuse staining of unloaded controls, appearing denser at the periphery with some evidence of fine microtubule bundles (Fig 6.2A and B, h).

Vimentin Intermediate Filaments: Unloaded and untreated normal chondrocytes exhibited clear networks of vimentin intermediate filament bundles that extended throughout the cell to a cortical network (Fig 6.2A and B c). Following 40 minutes of loading, the clear cortical network was lost, intermediate filament bundles appeared clearer and more densely packed (Fig 6.2A and B f). Intermediate filament bundles became even more densely packed and appeared thicker after the recovery period (Fig 6.2B f and i). Vimentin intermediate filament organisation did not return to that of unloaded control chondrocytes within the 5 hour recovery period (Fig 6.2A and B i).

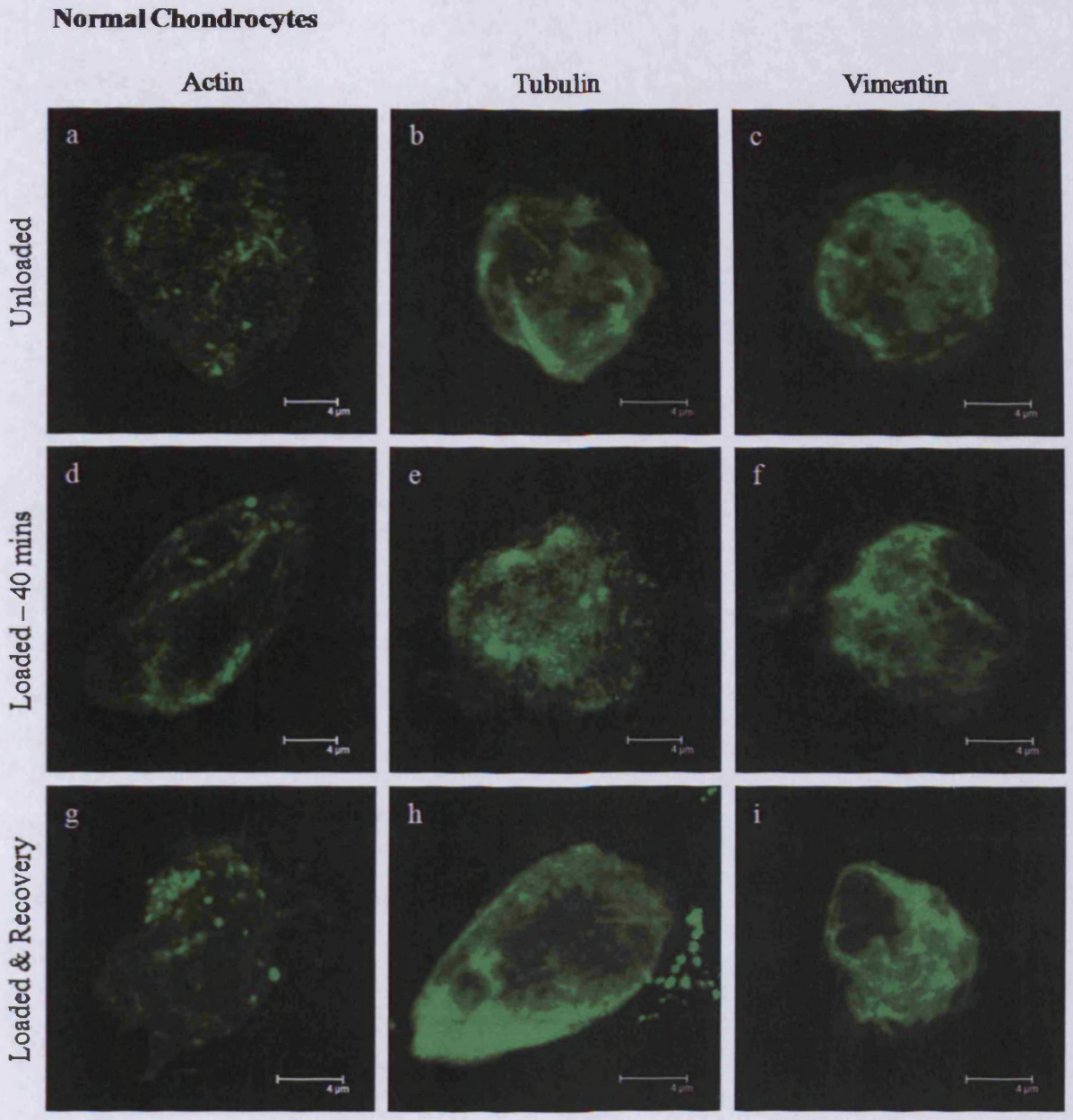

Figure 6.2 A:- ***3D reconstruction*** - The effect of load on the cytoskeletal organisation of normal human articular chondrocytes in 3D agarose culture. Chondrocytes were loaded (cyclic compression; 15%, 0.5 Hz) for 40 minutes (d-f) and recovery was determined five hours after loading (g-i). Unloaded chondrocytes in agarose served as controls (a-c). With recovery post-load actin and tubulin, but not vimentin, organisation returned to that of controls. Images shown are 3D-reconstructions of a series of scans taken at 0.4µm increments across the chondrocyte. Actin was detected with Alexa fluor 488-phalloidin. Vimentin and tubulin were detected by indirect immunofluorescence using primary antibodies and TRITC-conjugated anti-mouse IgG.

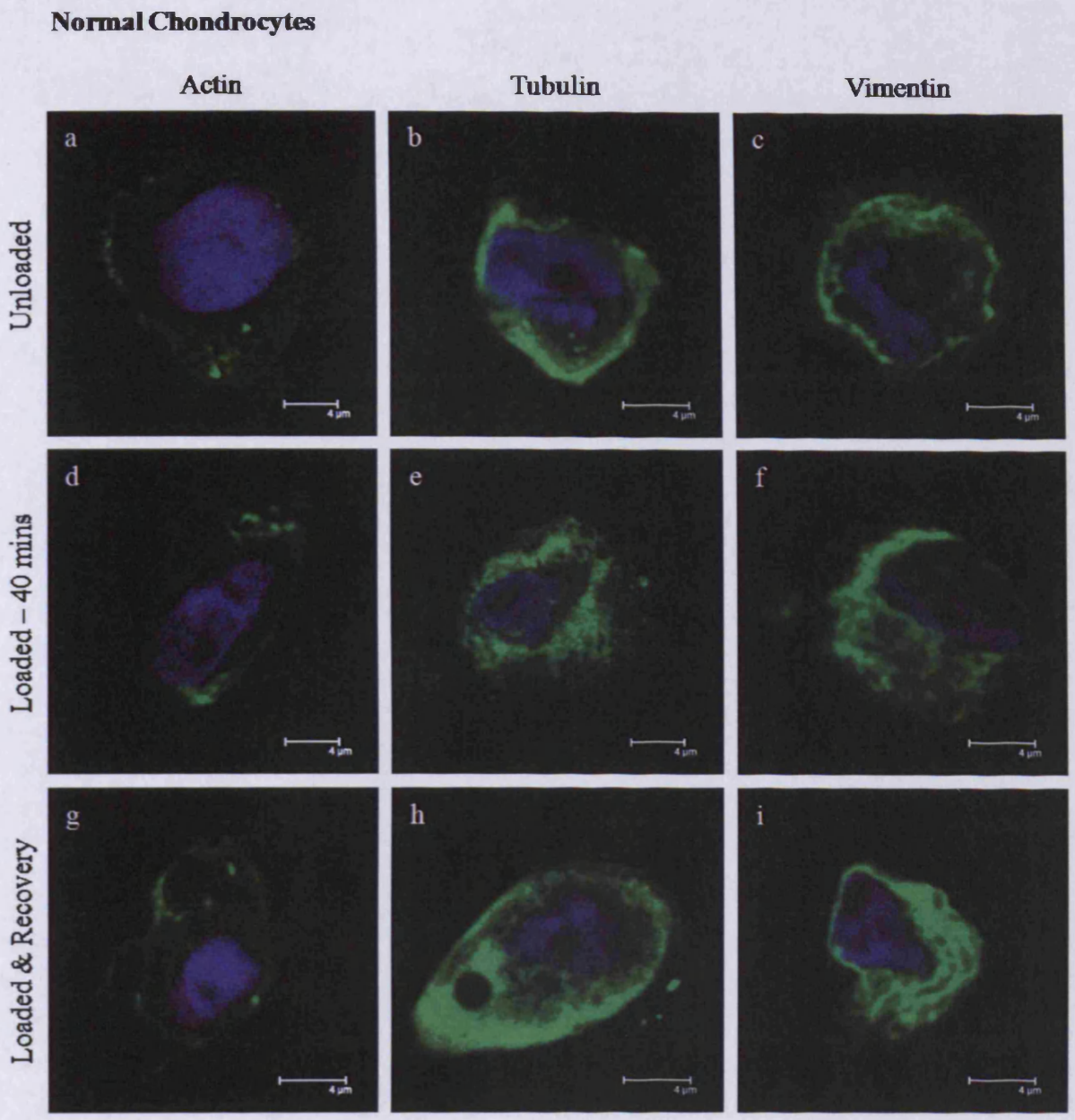

Figure 6.2 B:- ***Single scan*** - The effect of load on the cytoskeletal organisation of normal human articular chondrocytes in 3D agarose culture. Chondrocytes were loaded (cyclic compression; 15%, 0.5 Hz) for 40 minutes (d-f) and recovery was determined five hours after loading (g-i). Unloaded chondrocytes in agarose served as controls (a-c). With recovery post-load actin and tubulin, but not vimentin, organisation returned to that of controls. Images shown are scans through the centre of the cell. Actin was detected with Alexa fluor 488-phalloidin. Vimentin and tubulin were detected by indirect immunofluorescence using primary antibodies and TRITC-conjugated anti-mouse IgG. Nuclei were counterstained with DAPI (blue).

6.2.2.1.2 Osteoarthritic Untreated Chondrocytes

Actin Microfilaments: In unloaded and untreated OA chondrocytes, actin microfilaments appeared as elongated punctate spots in a clear cortical ring (Fig 6.3A and B a), with actin staining in OA cells more restricted to the cell periphery than in normal chondrocytes. Following 40 minutes of cyclic compressive loading, the punctate spots of actin became clearer but less closely packed than in unloaded controls, resulting in an apparent disruption of the cortical ring (Fig 6.3A and B d). Actin staining became more tightly packed following a 5 hour recovery, exhibiting a thick filamentous appearance that was not apparent in unloaded controls (Fig 6.3A and B g).

Tubulin Microtubules: As in normal chondrocytes, tubulin microtubule staining appeared diffuse throughout unloaded and untreated OA chondrocytes, with a dense staining at the cell periphery (Fig 6.3A and B b). Tubulin staining became punctate after 40 minutes of loading and lost the dense peripheral localisation observed in unloaded controls (Fig 6.3A and B e). Following recovery for 5 hours, clear microtubule bundle networks were apparent throughout OA chondrocytes and the bright cortical staining was regained (Fig 6.3A and B h); microtubule bundles appeared more 'organised' in recovery OA cells than in unloaded controls.

Vimentin Intermediate Filaments: Unloaded and untreated OA chondrocytes contained clear vimentin intermediate filament bundle networks that extended throughout the cell, appearing more densely packed when compared with unloaded normal chondrocytes (Fig 6.3A and B c). Following 40 minutes of loading, intermediate filament bundle networks were still evident, but appeared finer (Fig 6.3A and B f). The apparent thickness of chondrocyte vimentin intermediate filament bundles after 5 hours of recovery resembled that of unloaded controls, although they were more loosely packed (Fig 6.3A and B i).

Tubulin microfilament organisation did not differ between unloaded normal and OA chondrocytes, nor did the changes in response to 40 minutes of cyclic compressive load. However, microtubule organisation following a 5 hour recovery period differed significantly between normal and OA chondrocytes, with tubulin staining returning to the profile of that of unloaded controls in normal chondrocytes but forming clear microtubule bundle networks in OA chondrocytes. Actin microfilament organisation also appeared to be enhanced in OA chondrocytes left to recover whilst partially returning to that of unloaded controls in normal samples.

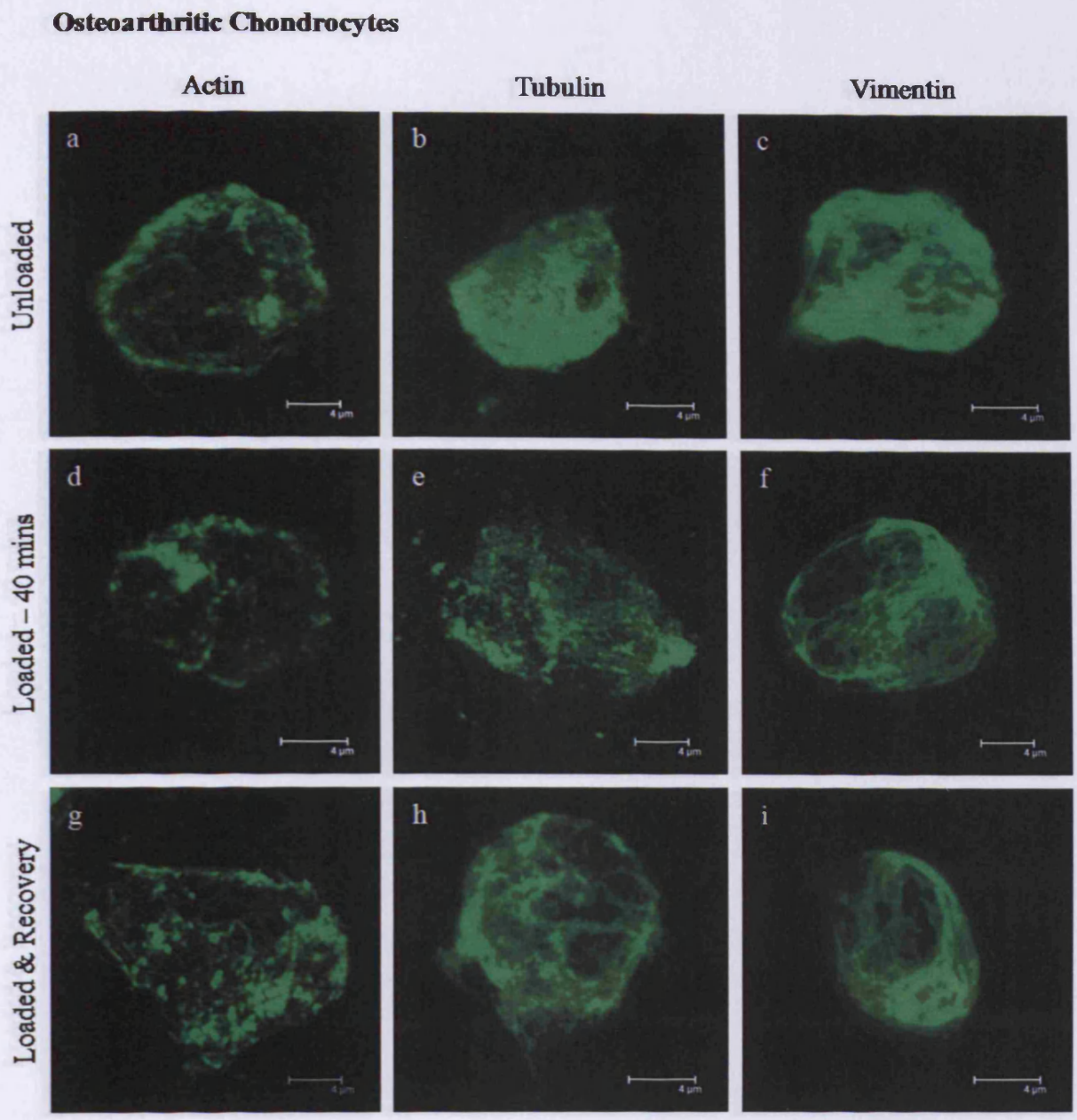

Figure 6.3 A:- ***3D reconstruction*** - The effect of load on the cytoskeletal organisation of osteoarthritic human articular chondrocytes in 3D agarose culture. Chondrocytes were loaded (cyclic compression; 15%, 0.5 Hz) for 40 minutes (d-f) and recovery was determined five hours after loading (g-i). Unloaded chondrocytes in agarose served as controls (a-c). Bundles of actin and tubulin were more clear following recovery post-load, whilst vimentin organisation returned to that of controls. Images shown are 3D-reconstructions of a series of scans taken at 0.4µm increments across the chondrocyte. Actin was detected with Alexa fluor 488-phalloidin. Vimentin and tubulin were detected by indirect immunofluorescence using primary antibodies and TRITC-conjugated anti-mouse IgG.

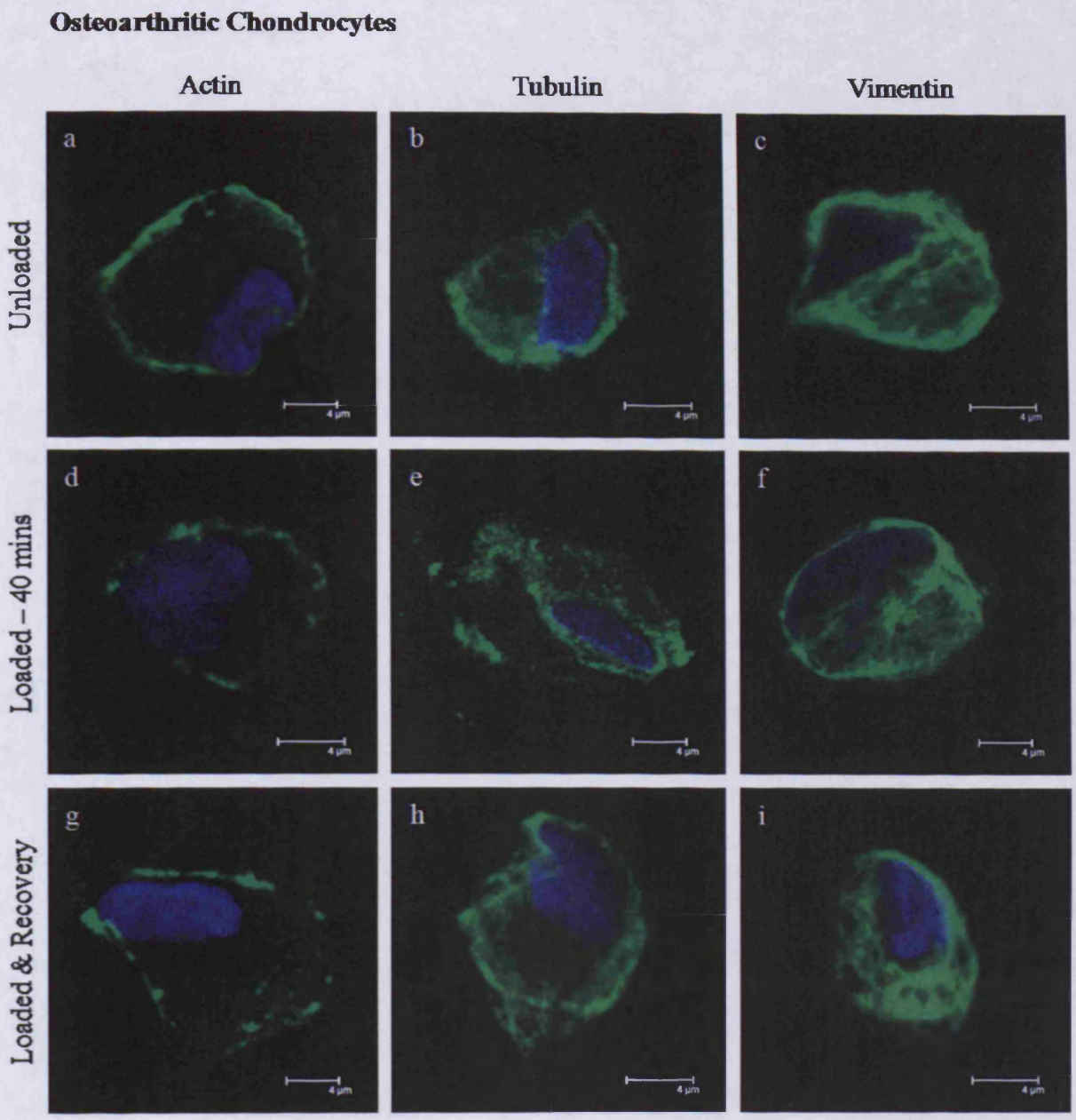

Figure 6.3 B:- ***Single scan*** - The effect of load on the cytoskeletal organisation of osteoarthritic human articular chondrocytes in 3D agarose culture. Chondrocytes were loaded (cyclic compression; 15%, 0.5 Hz) for 40 minutes (d-f) and recovery was determined five hours after loading (g-i). Unloaded chondrocytes in agarose served as controls (a-c). Bundles of actin and tubulin were more clear following recovery post-load, whilst vimentin organisation returned to that of controls. Images shown are scans through the centre of the cell. Actin was detected with Alexa fluor 488-phalloidin. Vimentin and tubulin were detected by indirect immunofluorescence using primary antibodies and TRITC-conjugated anti-mouse IgG. Nuclei were counterstained with DAPI (blue).

Interestingly, normal chondrocytes did not recover their vimentin intermediate filament organisation, with the organisation of normal recovery samples most closely resembling that of unloaded OA chondrocytes.

6.2.2.2 Actin microfilament organisation with cytoskeletal disruption

6.2.2.2.1 Cytochalasin D-treated chondrocytes

As demonstrated in section 5.2.2.2, treatment of normal chondrocytes with 1μM cytochalasin D resulted in disruption of actin microfilament organisation; in unloaded samples, actin localisation in untreated chondrocytes became less evenly distributed and the cortical ring was lost with cytochalasin D treatment (Fig 6.4A and B d). Additional changes in the actin cytoskeleton with 40 minutes of loading in cytochalasin D-treated normal chondrocytes were similar to those in untreated samples, with actin staining becoming less punctate (Fig 6.4A and B e). As in untreated samples, punctate staining reappeared following 5 hours recovery in cytochalasin D-treated normal chondrocytes, although cytochalasin D continued to inhibit the peripheral localisation of actin staining (Fig 6.4A and B f).

In OA chondrocytes cytochalasin D treatment also prevented the cortical localisation of actin microfilament staining (Fig 6.5B d-f). In unloaded OA chondrocytes punctate actin staining became less tightly packed following cytochalasin D treatment (Fig 6.5A d); as a result of this, the reduction in density caused by 40 minutes loading of untreated OA chondrocytes was less evident in those treated with cytochalasin D (Fig 6.5A and B e). The punctate appearance of actin became clearer and there was evidence of microfilament networks following 5 hours recovery comparable with that observed in untreated OA chondrocytes after recovery (Fig 6.5A and B c,f).

In both normal and OA chondrocytes, cytochalasin D treatment resulted in disruption of the actin microfilament organisation, with the most obvious effect on the peripheral distribution of actin. However there did not appear to be an additive effect of cytochalasin D treatment and load on actin cytoskeletal organisation.

6.2.2.2.2 Colchicine-treated chondrocytes

Disruption of tubulin microtubules with 1μM colchicine treatment had little effect on actin microfilaments, although punctate actin spots increased in size in unloaded normal

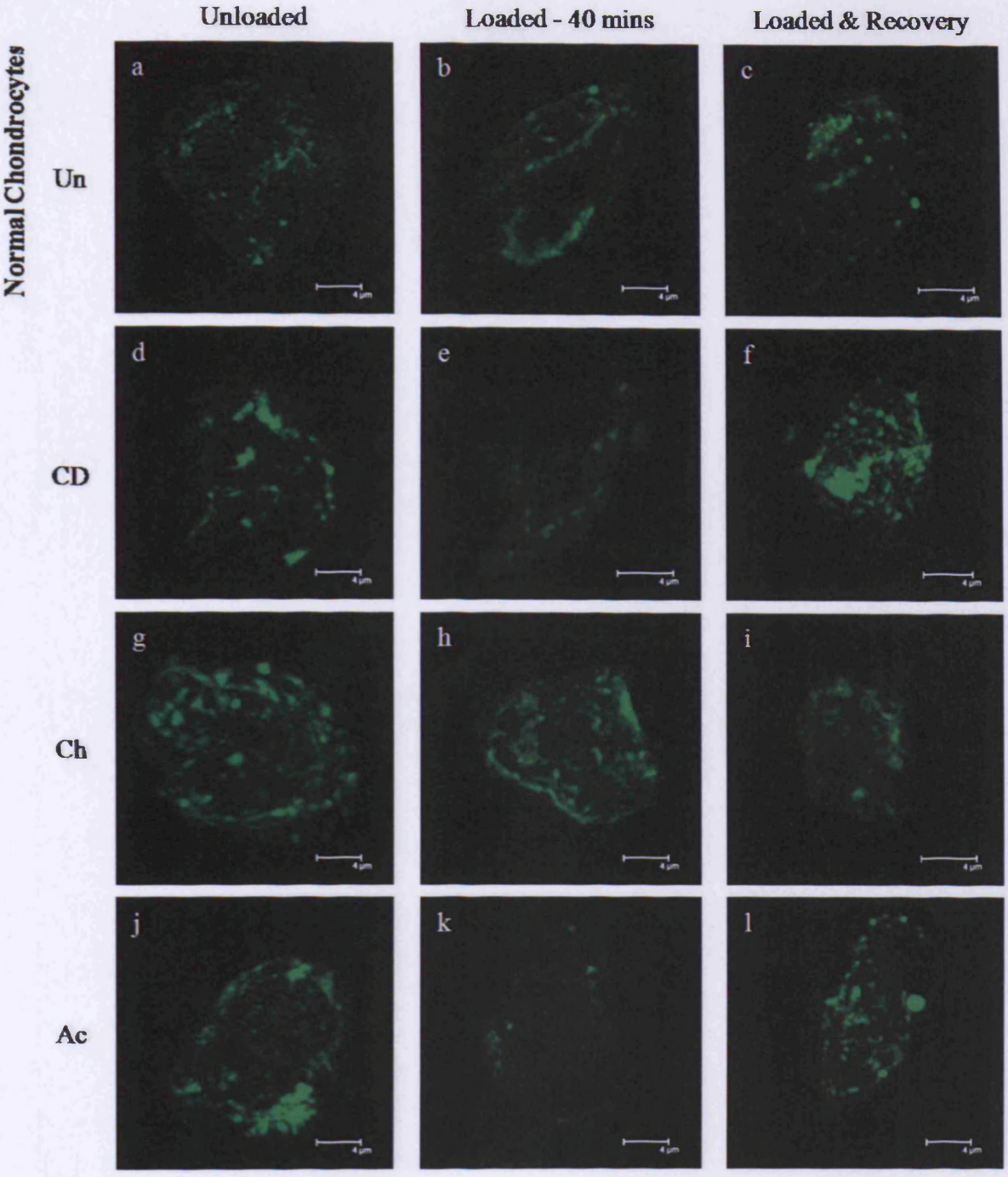

Figure 6.4 A:- *3D reconstruction* - The effect of load on the actin cytoskeleton of normal human articular chondrocytes in 3D agarose culture, in the absence (Un, a-c) or presence of 1μM cytochalasin D (CD, d-f) to disrupt actin microfilaments, 1μM colchicine (Ch, g-i) to disrupt tubulin microtubules, or 2mM acrylamide (Ac, j-l) to disrupt vimentin intermediate filaments. Chondrocytes were loaded (cyclic compression; 15%, 0.5 Hz) for 40 minutes (b,e,h,k) and recovery was determined five hours after loading (c,f,i,l). Unloaded chondrocytes in agarose served as controls (a,d,g,j). The recovery of actin organisation post-load was prevented by colchicine but not cytochalasin D or acrylamide. Images shown are 3D-reconstructions of a series of scans taken at 0.4μm increments across the chondrocyte. Actin was detected with Alexa fluor 488-phalloidin.

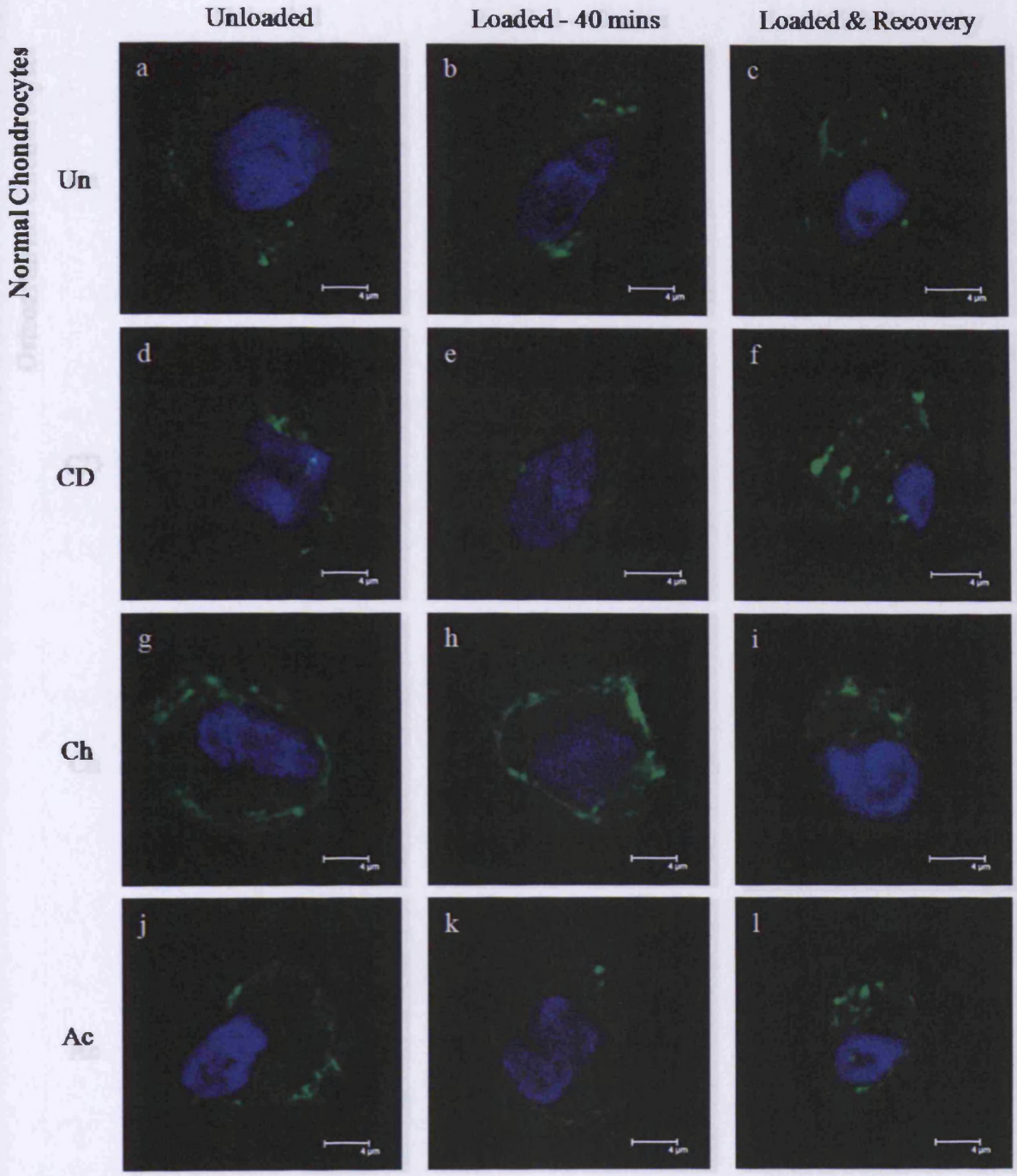

Figure 6.4 B:- ***Single scan*** - The effect of load on the actin cytoskeleton of normal human articular chondrocytes in 3D agarose culture, in the absence (Un, a-c) or presence of 1μM cytochalasin D (CD, d-f) to disrupt actin microfilaments, 1μM colchicine (Ch, g-i) to disrupt tubulin microtubules, or 2mM acrylamide (Ac, j-l) to disrupt vimentin intermediate filaments. Chondrocytes were loaded (cyclic compression; 15%, 0.5 Hz) for 40 minutes (b,e,h,k) and recovery was determined five hours after loading (c,f,i,l). Unloaded chondrocytes in agarose served as controls (a,d,g,j). The recovery of actin organisation post-load was prevented by colchicine but not cytochalasin D or acrylamide. Images shown are scans through the centre of the cell. Actin was detected with Alexa fluor 488-phalloidin. Nuclei were counterstained with DAPI (blue).

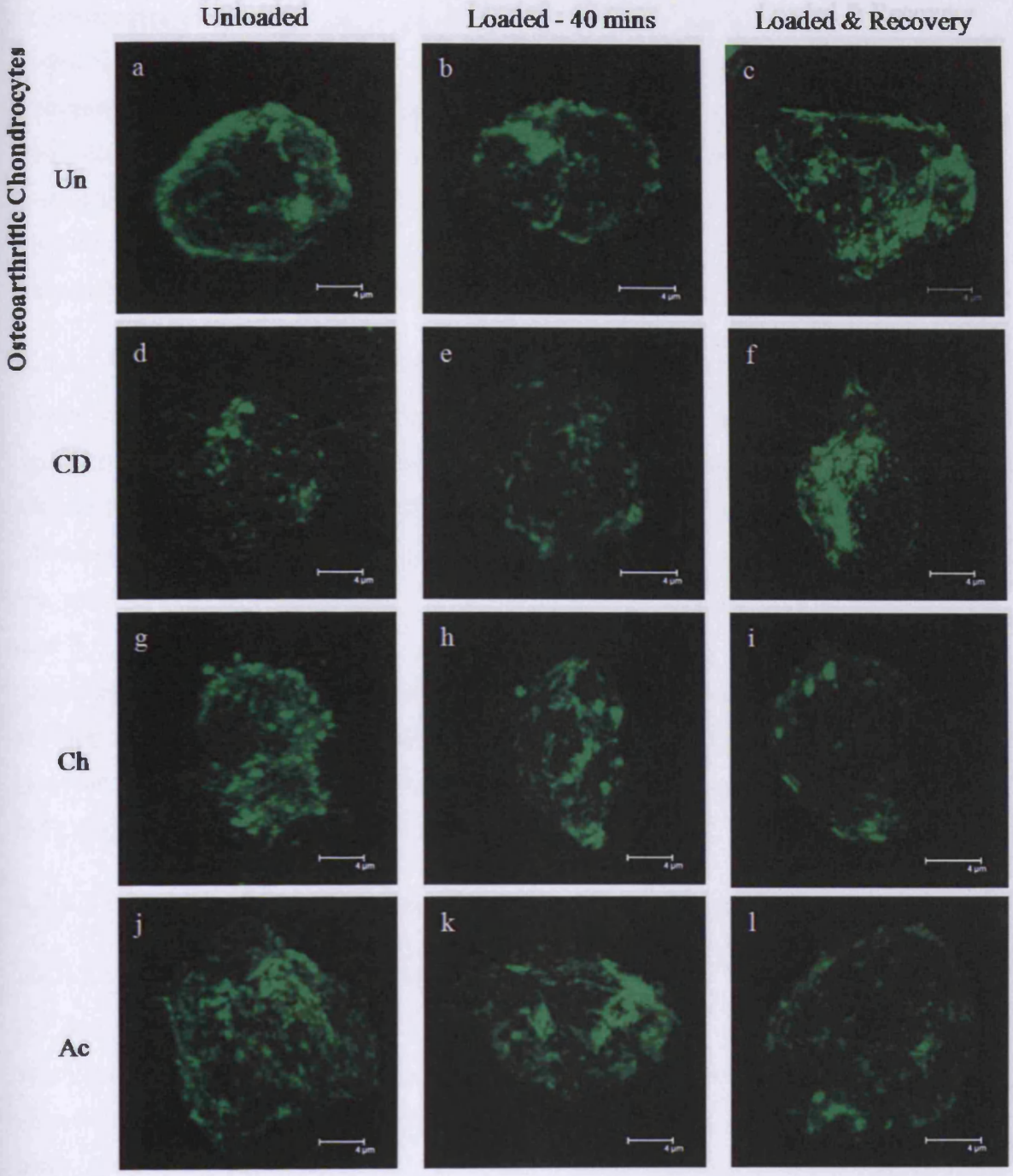

Figure 6.5 A:- ***3D reconstruction*** - The effect of load on the actin cytoskeleton of osteoarthritic human articular chondrocytes in 3D agarose culture, in the absence (Un, a-c, g-i) or presence of 1μM cytochalasin D (CD, d-f, j-l) to disrupt actin microfilaments , 1μM colchicine (Ch, g-i) to disrupt tubulin microtubules, or 2mM acrylamide (Ac, j-l) to disrupt vimentin intermediate filaments. Chondrocytes were loaded (cyclic compression; 15%, 0.5 Hz) for 40 minutes (b,e,h,k) and recovery was determined five hours after loading (c,f,i,l). Unloaded chondrocytes in agarose served as controls (a,d,g,j). Load-induced changes in actin organisation were unaffected by the treatments. Images shown are 3D-reconstructions of a series of scans taken at 0.4μm increments across the chondrocyte. Actin was detected with Alexa fluor 488-phalloidin.

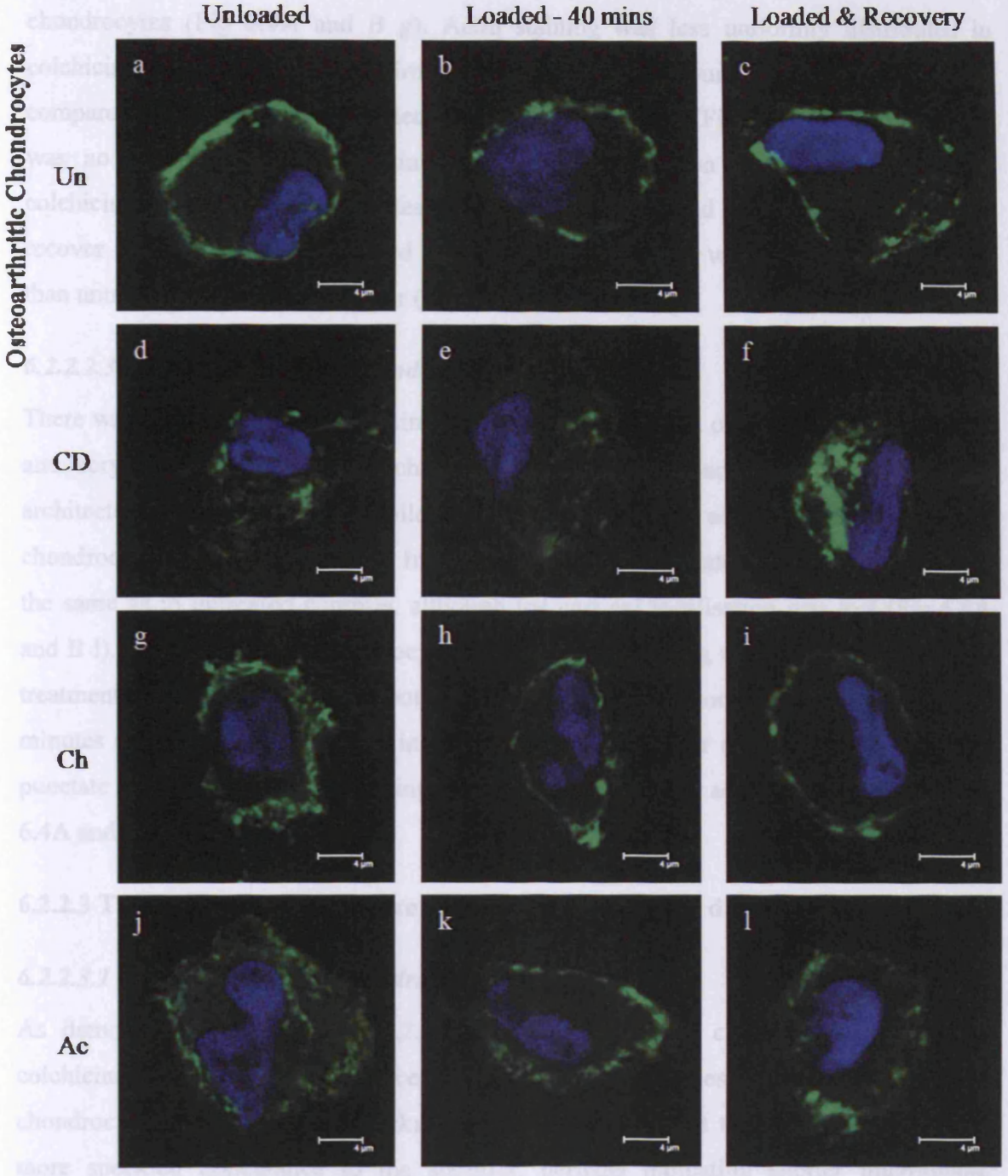

Figure 6.5 B:- ***Single scan*** - The effect of load on the actin cytoskeleton of osteoarthritic human articular chondrocytes in 3D agarose culture, in the absence (Un, a-c, g-i) or presence of 1μM cytochalasin D (CD, d-f, j-l) to disrupt actin microfilaments , 1μM colchicine (Ch, g-i) to disrupt tubulin microtubules, or 2mM acrylamide (Ac, j-l) to disrupt vimentin intermediate filaments. Chondrocytes were loaded (cyclic compression; 15%, 0.5 Hz) for 40 minutes (b,e,h,k) and recovery was determined five hours after loading (c,f,i,l). Unloaded chondrocytes in agarose served as controls (a,d,g,j). Load-induced changes in actin organisation were unaffected by the treatments. Images shown are scans through the centre of the cell. Actin was detected with Alexa fluor 488-phalloidin. Nuclei were counterstained with DAPI (blue).

chondrocytes (Fig 6.4A and B g). Actin staining was less uniformly distributed in colchicine-treated normal chondrocytes following a 5 hour recovery period when compared with unloaded and loaded colchicine-treated cells (Fig 6.4A and B g-i). There was no clear difference in actin cytoskeletal organisation between untreated and colchicine-treated OA chondrocytes whether unloaded, loaded for 40 minutes, or left to recover for 5 hours (Fig 6.5A and B g-i), although staining was perhaps less punctate than untreated controls in the latter (Fig 6.5A and B i).

6.2.2.2.3 Acrylamide-treated chondrocytes

There was no difference in the actin cytoskeletal organisation of unloaded and untreated and acrylamide-treated normal chondrocytes (Fig 6.4A and B j). However, actin architecture appeared to be lost following 40 minutes load in acrylamide-treated normal chondrocytes (Fig 6.4A and B k). In recovery samples, punctate actin staining appeared the same as in untreated controls, although the cortical localisation was lost (Fig 6.4A and B l). In unloaded OA chondrocytes the cortical actin ring was lost with acrylamide treatment (Fig 6.5A and B j), but partially restored in chondrocytes loaded for 40 minutes (Fig 6.5A and B k) and in those allowed to recover (Fig 6.5A and B l). The punctate appearance of actin staining remained unaffected by acrylamide treatment (Fig 6.4A and 6.5A, j-l).

6.2.2.3 Tubulin microtubule organisation with cytoskeletal disruption

6.2.2.3.1 Colchicine-treated chondrocytes

As demonstrated in section 5.2.2.3, treatment of normal chondrocytes with 1μM colchicine altered the appearance of tubulin microtubules. In unloaded normal chondrocytes, microtubule networks were clearer throughout the cell but there was a more speckled appearance to the staining, perhaps indicating shorter microtubule bundles (Fig 6.6A and B d). In both untreated and colchicine-treated normal chondrocytes tubulin staining was brightest at the cell periphery. The punctate appearance of tubulin in untreated loaded chondrocytes was less evident in loaded colchicine-treated normal chondrocytes (Fig 6.6A and B e). In addition, tubulin staining remained brightest at the cell periphery, rather than in the perinuclear region as in untreated controls (Fig 6.6B e). Following 5 hours of recovery in colchicine-treated normal chondrocytes, tubulin microtubule bundles became thicker and were densely packed throughout the cell (Fig 6.6A and B f).

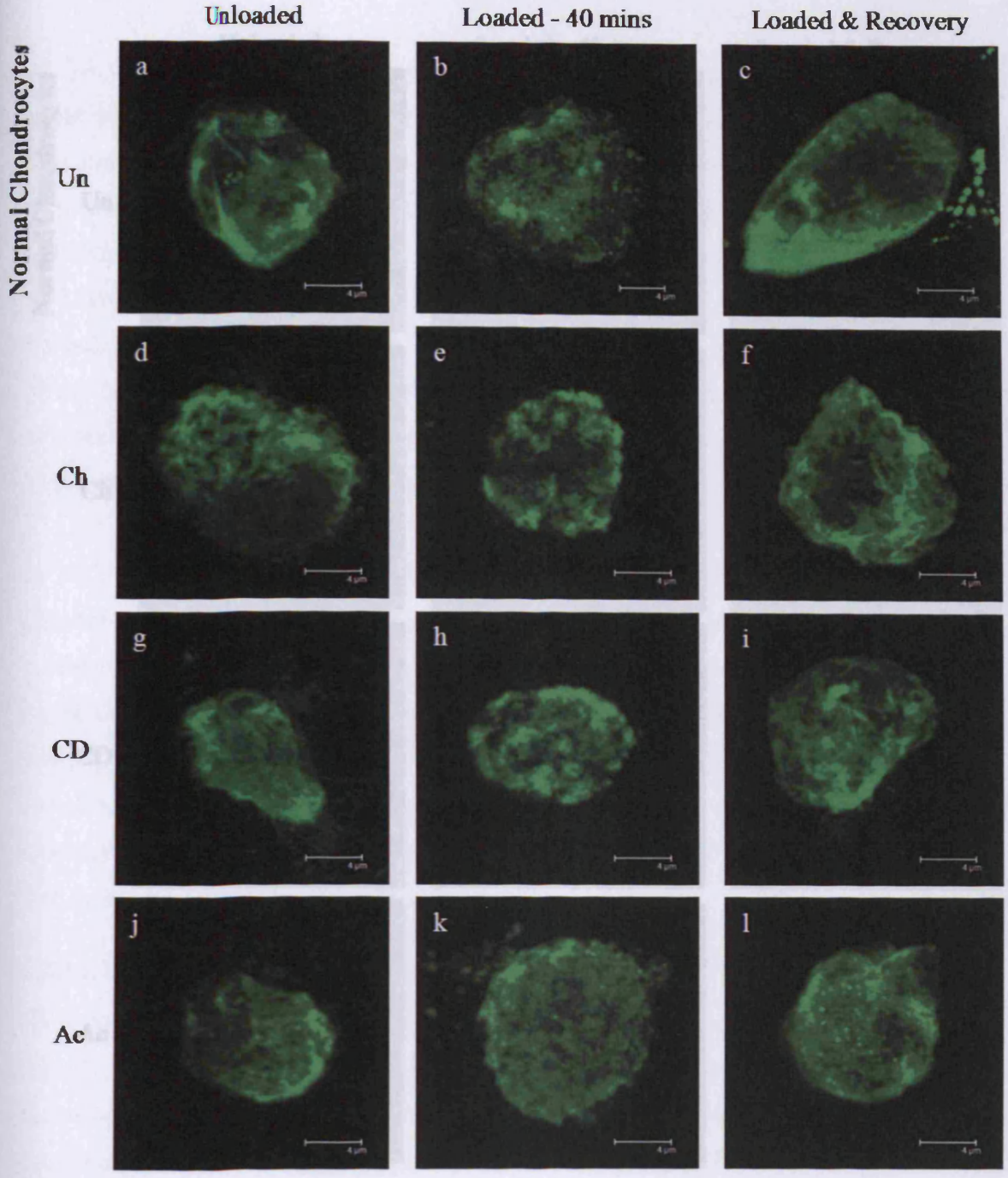

Figure 6.6 A:- ***3D reconstruction*** - The effect of load on the tubulin cytoskeleton of normal human articular chondrocytes in 3D agarose culture, in the absence (Un, a-c) or presence of 1μM colchicine (Ch, d-f) to disrupt tubulin microtubules, 1μM cytochalasin D (CD, g-i) to disrupt actin microfilaments, or 2mM acrylamide (Ac, j-l) to disrupt vimentin intermediate filaments. Chondrocytes were loaded (cyclic compression; 15%, 0.5 Hz) for 40 minutes (b,e,h,k) and recovery was determined five hours after loading (c,f,i,l). Unloaded chondrocytes in agarose served as controls (a,d,g,j). The recovery of tubulin organisation post-load was affected by colchicine but not cytochalasin D or acrylamide. Images shown are 3D-reconstructions of a series of scans taken at 0.4μm increments across the chondrocyte. Tubulin was detected by indirect immunofluorescence using primary antibody and TRITC-conjugated anti-mouse IgG.

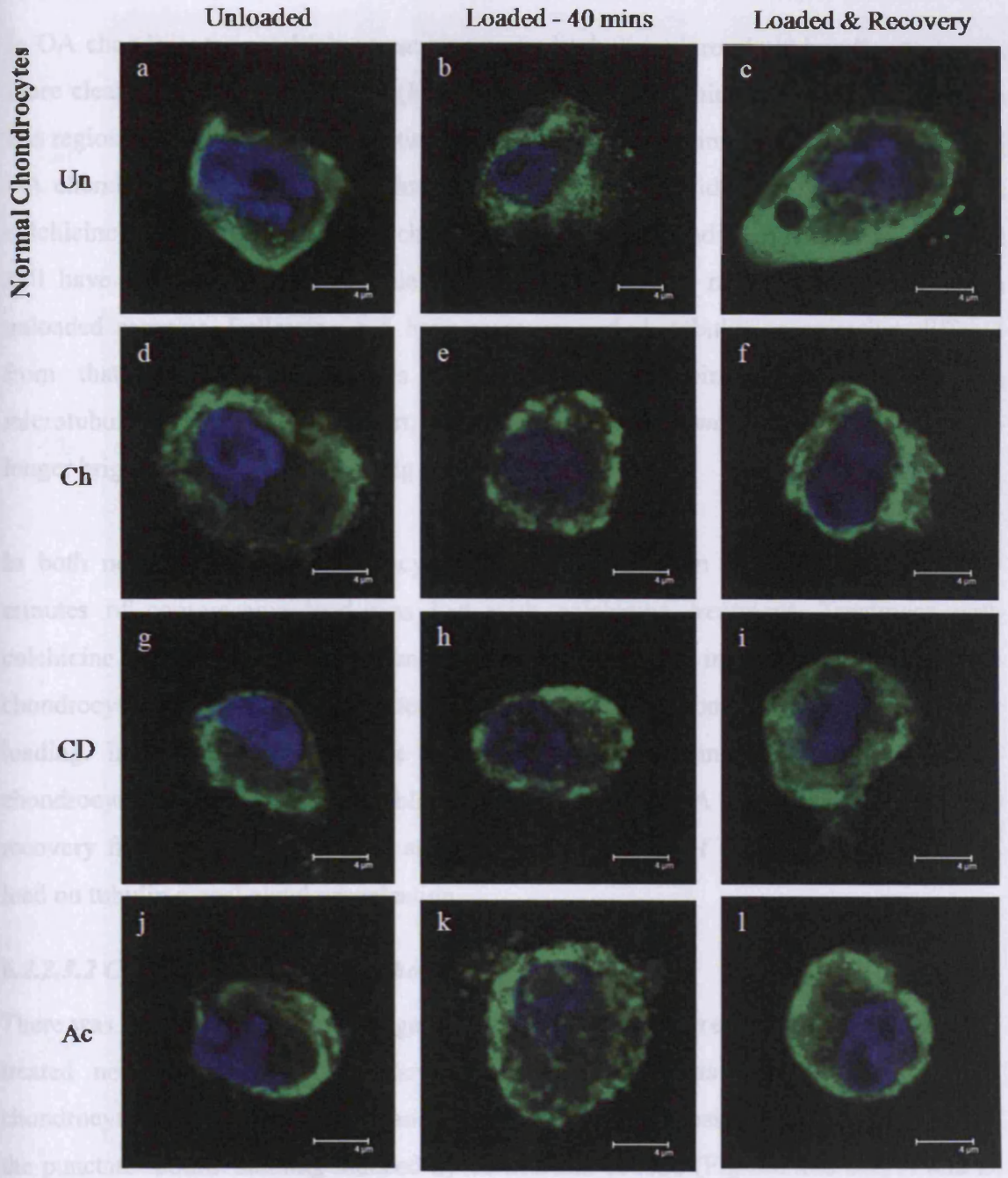

Figure 6.6 B:- ***Single scan*** - The effect of load on the tubulin cytoskeleton of normal human articular chondrocytes in 3D agarose culture, in the absence (Un, a-c) or presence of 1μM colchicine (Ch, d-f) to disrupt tubulin microtubules, 1μM cytochalasin D (CD, g-i) to disrupt actin microfilaments, or 2mM acrylamide (Ac, j-l) to disrupt vimentin intermediate filaments. Chondrocytes were loaded (cyclic compression; 15%, 0.5 Hz) for 40 minutes (b,e,h,k) and recovery was determined five hours after loading (c,f,i,l). Unloaded chondrocytes in agarose served as controls (a,d,g,j). The recovery of tubulin organisation post-load was affected by colchicine but not cytochalasin D or acrylamide. Images shown are scans through the centre of the cell. Tubulin was detected by indirect immunofluorescence using primary antibodies and TRITC-conjugated anti-mouse IgG. Nuclei were counterstained with DAPI (blue).

In OA chondrocytes colchicine treatment caused tubulin microtubule bundles to appear more clearly at the cell periphery (Fig 6.7A d) with the staining remaining brightest in this region (Fig 6.7B d). The induction of punctate tubulin staining observed in untreated OA chondrocytes following 40 minutes loading was less evident in those treated with colchicine, as observed in normal chondrocytes (Fig 6.7A and B e). However, load did still have an effect as microtubule bundle networks were no longer as clear as in unloaded samples. Following a 5 hour recovery period, tubulin organisation differed from that of untreated controls and unloaded colchicine-treated chondrocytes; microtubule bundles appeared short, there were no clear networks and staining was no longer brightest at the periphery (Fig 6.7A and B f).

In both normal and OA chondrocytes the punctate tubulin staining induced by 40 minutes of compressive load was lost with colchicine treatment. Treatment with colchicine caused microtubule bundles to appear thicker in both normal and OA chondrocytes and particularly affected microtubule organisation following recovery after loading. Interestingly, microtubule organisation in colchicine treated unloaded OA chondrocytes most closely resembled that of untreated OA chondrocytes following recovery from load. There was an apparent additive effect of colchicine treatment and load on tubulin cytoskeletal organisation.

6.2.2.3.2 Cytochalasin D-treated chondrocytes

There was little difference in the organisation of tubulin in untreated and cytochalasin D-treated normal and OA chondrocytes. No difference was observed in unloaded chondrocytes (Fig 6.6 and 6.7, A and B, g), whilst cytochalasin D treatment prevented the punctate tubulin staining induced by 40 minutes of load (Fig 6.6 and 6.7, A and B, h). After recovery, the appearance of microtubule bundles in normal chondrocytes was unaffected by cytochalasin D treatment (Fig 6.6A and B i). In OA chondrocytes after recovery from loading, the microtubule bundle networks formed in untreated samples were less clear, but still present, in cytochalasin D-treated cells (Fig 6.7A and B i).

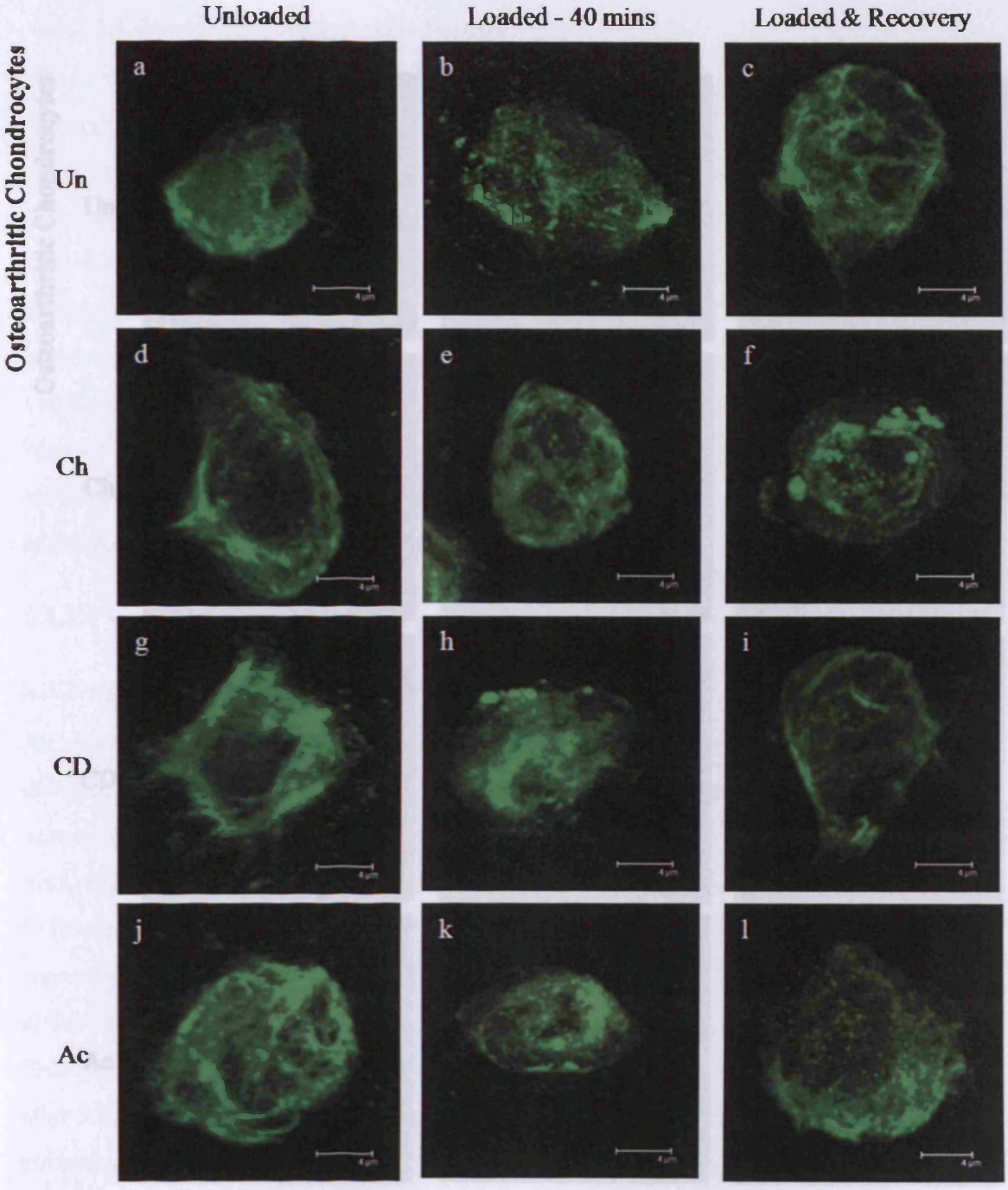

Figure 6.7 A:- ***3D reconstruction*** - The effect of load on the tubulin cytoskeleton of osteoarthritic human articular chondrocytes in 3D agarose culture, in the absence (Un, a-c) or presence of 1μM colchicine (Ch, d-f) to disrupt tubulin microtubules, 1μM cytochalasin D (CD, g-i) to disrupt actin microfilaments , or 2mM acrylamide (Ac, j-l) to disrupt vimentin intermediate filaments. Chondrocytes were loaded (cyclic compression; 15%, 0.5 Hz) for 40 minutes (b,e,h,k) and recovery was determined five hours after loading (c,f,i,l). Unloaded chondrocytes in agarose served as controls (a,d,g,j). The recovery of tubulin organisation post-load was affected by colchicine and acrylamide but not cytochalasin D. Images shown are 3D-reconstructions of a series of scans taken at 0.4μm increments across the chondrocyte. Tubulin was detected by indirect immunofluorescence using primary antibody and TRITC-conjugated anti-mouse IgG.

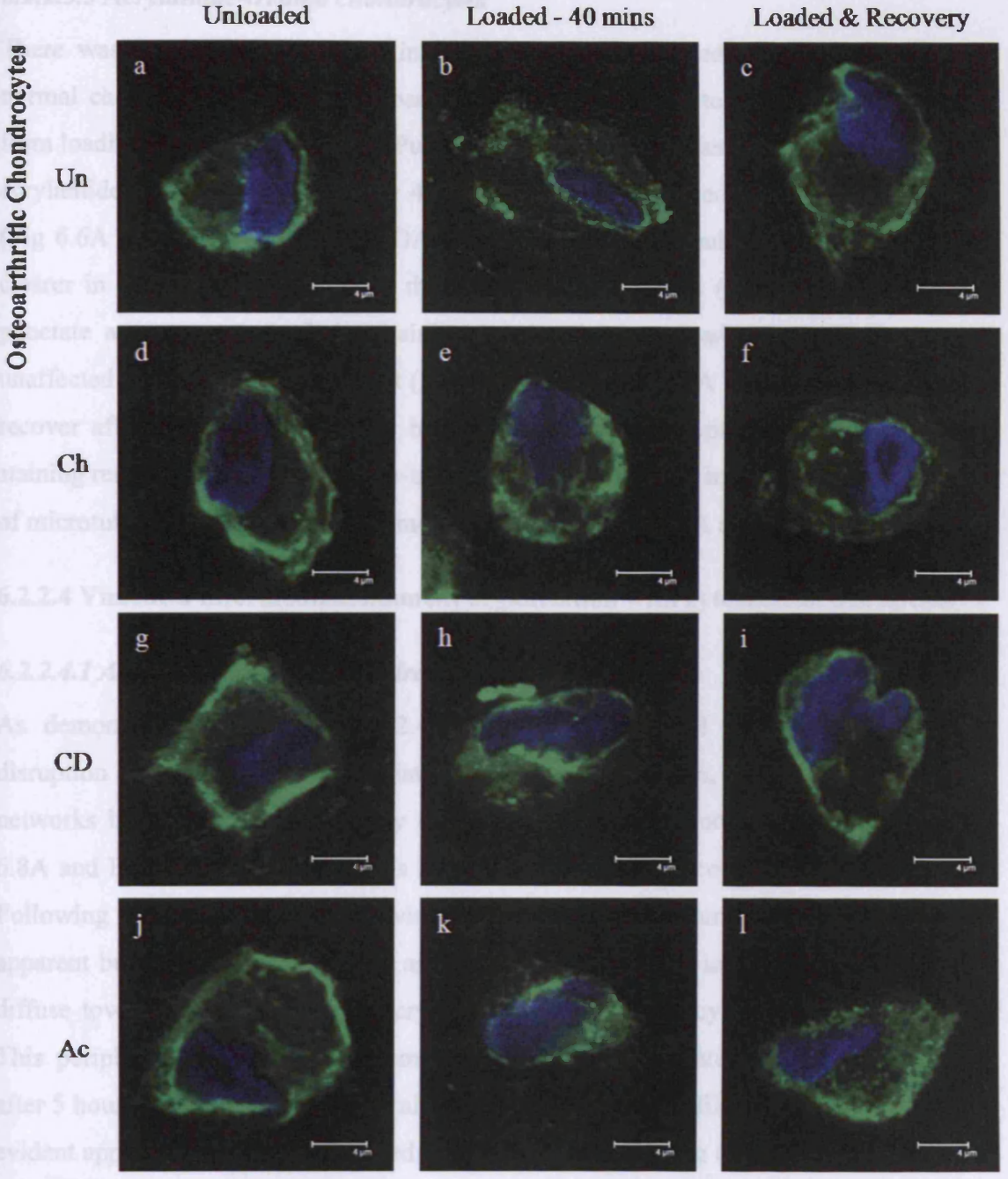

Figure 6.7 B:- ***Single scan*** - The effect of load on the tubulin cytoskeleton of osteoarthritic human articular chondrocytes in 3D agarose culture, in the absence (Un, a-c) or presence of 1μM colchicine (Ch, d-f) to disrupt tubulin microtubules, 1μM cytochalasin D (CD, g-i) to disrupt actin microfilaments , or 2mM acrylamide (Ac, j-l) to disrupt vimentin intermediate filaments. Chondrocytes were loaded (cyclic compression; 15%, 0.5 Hz) for 40 minutes (b,e,h,k) and recovery was determined five hours after loading (c,f,i,l). Unloaded chondrocytes in agarose served as controls (a,d,g,j). The recovery of tubulin organisation post-load was affected by colchicine and acrylamide but not cytochalasin D. Images shown are scans through the centre of the cell. Tubulin was detected by indirect immunofluorescence using primary antibodies and TRITC-conjugated anti-mouse IgG. Nuclei were counterstained with DAPI (blue).

6.2.2.3.3 Acrylamide-treated chondrocytes

There was no difference in tubulin organisation in untreated and acrylamide-treated normal chondrocytes whether unloaded, loaded for 40 minutes, or allowed to recover from loading (Fig 6.6A and B j-l). Punctate tubulin staining was evident but less sharp in acrylamide-treated cells loaded for 40 minutes when compared with untreated controls (Fig 6.6A and B k). In unloaded OA chondrocytes microtubule bundle networks were clearer in acrylamide-treated cells than in untreated controls (Fig 6.7A and B j). The punctate appearance of tubulin staining in chondrocytes loaded for 40 minutes was unaffected by acrylamide treatment (Fig 6.7A and B k). In OA chondrocytes allowed to recover after loading, microtubule bundle networks were apparent but some punctate staining remained in the acrylamide-treated cells, which could indicate a slower recovery of microtubule organisation with vimentin disruption (Fig 6.7A and B l).

6.2.2.4 Vimentin intermediate filament organisation with cytoskeletal disruption

6.2.2.4.1 Acrylamide-treated chondrocytes

As demonstrated in section 5.2.2.4, treatment with 2mM acrylamide resulted in disruption of vimentin intermediate filament organisation, with filament bundle networks becoming asymmetrically distributed in unloaded normal chondrocytes (Fig 6.8A and B d); this asymmetry was lost with loading and recovery (Fig 6.8B e and f). Following 40 minutes of load, vimentin intermediate filament bundles were still apparent but were not as extensive as in untreated controls; vimentin staining appeared diffuse towards the periphery of acrylamide-treated chondrocytes (Fig 6.8A and B e). This peripheral diffuse staining remained in acrylamide-treated normal chondrocytes after 5 hours of recovery post-load, although the intermediate filament bundles that were evident appeared thicker, as observed in untreated controls (Fig 6.8A and B f).

In unloaded OA chondrocytes acrylamide treatment also caused an asymmetric distribution of vimentin intermediate filament staining, with faint intermediate filament bundles evident throughout most of the cell and brighter, denser networks to one side (Fig 6.9A and B d). Unlike in normal chondrocytes, this asymmetry persisted following 40 minutes of load in acrylamide-treated OA chondrocytes (Fig 6.9A and B e). The effect of load observed in untreated controls, causing vimentin intermediate filament bundles to appear finer, was also observed in loaded acrylamide-treated OA chondrocytes (Fig 6.9A and B e),

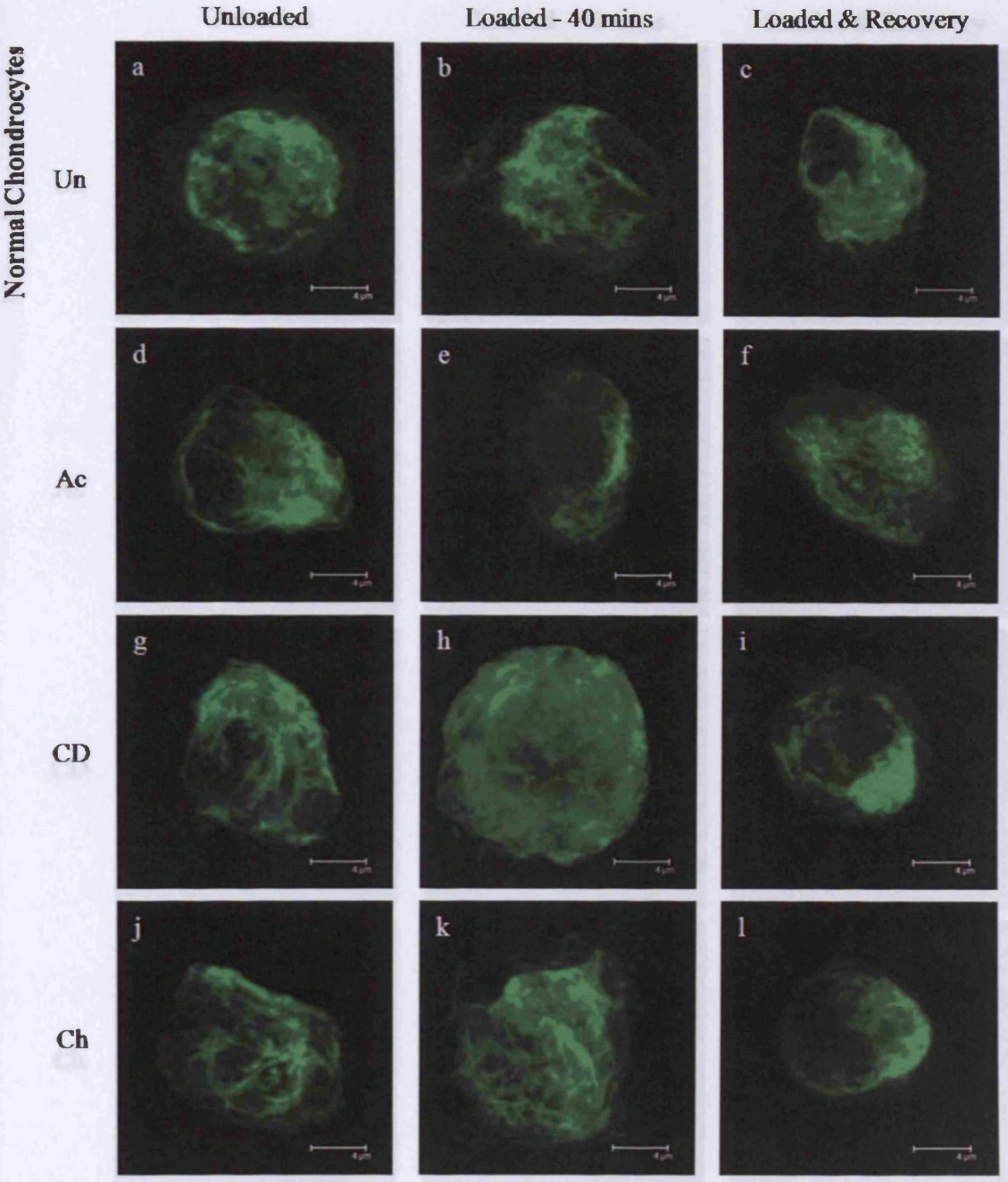

Figure 6.8 A:- ***3D reconstruction*** - The effect of load on the vimentin cytoskeleton of normal human articular chondrocytes in 3D agarose culture, in the absence (Un, a-c) or presence of 2mM acrylamide (Ac, d-f) to disrupt vimentin intermediate filaments, 1μM cytochalasin D (CD, g-i) to disrupt actin microfilaments, or 1μM colchicine (Ch, j-l) to disrupt tubulin microtubules. Chondrocytes were loaded (cyclic compression; 15%, 0.5 Hz) for 40 minutes (b,e,h,k) and recovery was determined five hours after loading (c,f,i,l). Unloaded chondrocytes in agarose served as controls (a,d,g,j). Load-induced changes in vimentin organisation were unaffected by the treatments. Images shown are 3D-reconstructions of a series of scans taken at 0.4μm increments across the chondrocyte. Vimentin was detected by indirect immunofluorescence using primary antibody and TRITC-conjugated anti-mouse IgG.

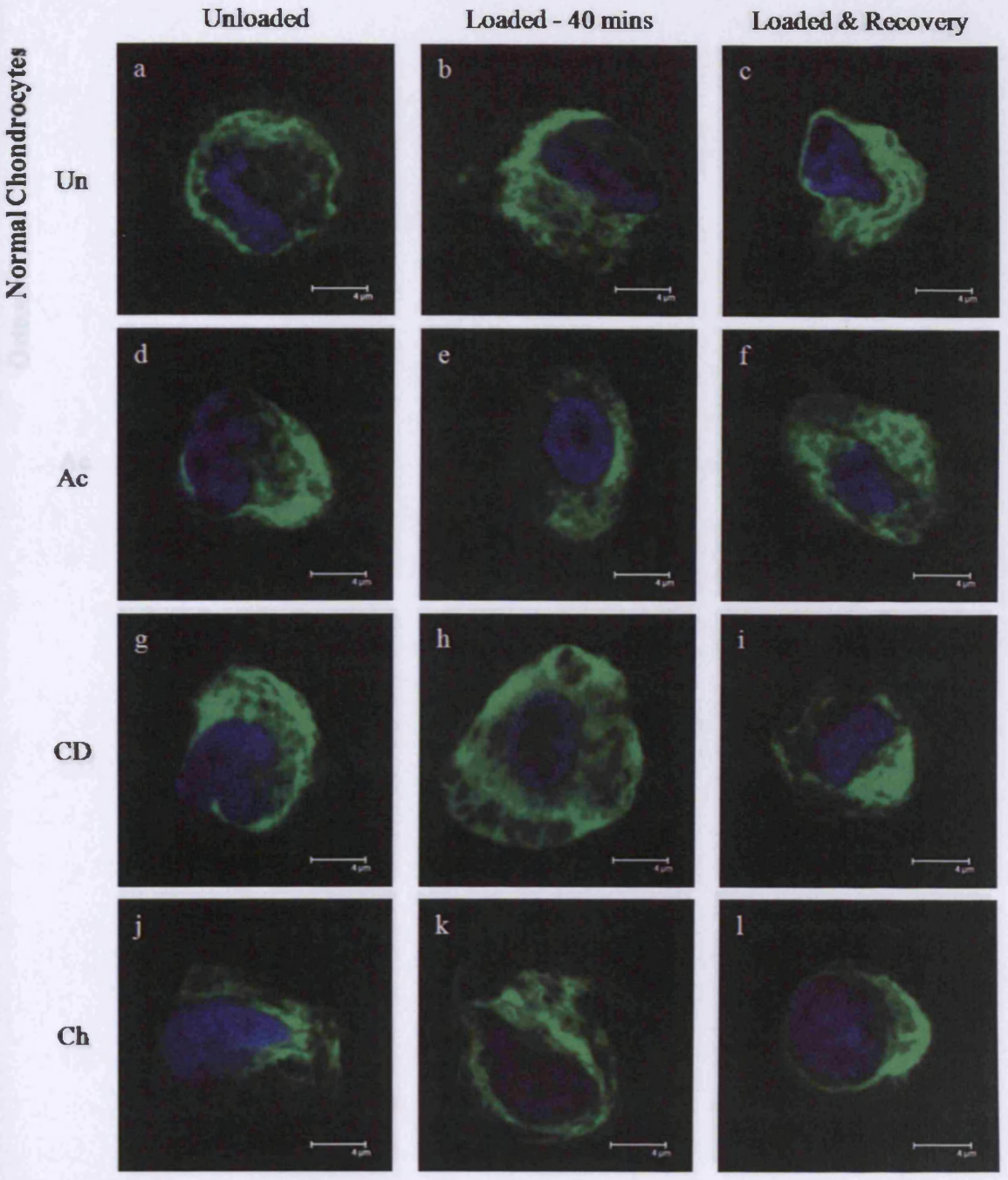

Figure 6.8 B:- ***Single scan*** - The effect of load on the vimentin cytoskeleton of normal human articular chondrocytes in 3D agarose culture, in the absence (Un, a-c) or presence of 2mM acrylamide (Ac, d-f) to disrupt vimentin intermediate filaments, 1μM cytochalasin D (CD, g-i) to disrupt actin microfilaments, or 1μM colchicine (Ch, j-l) to disrupt tubulin microtubules. Chondrocytes were loaded (cyclic compression; 15%, 0.5 Hz) for 40 minutes (b,e,h,k) and recovery was determined five hours after loading (c,f,i,l). Unloaded chondrocytes in agarose served as controls (a,d,g,j). Load-induced changes in vimentin organisation were unaffected by the treatments. Images shown are scans through the centre of the cell. Vimentin was detected by indirect immunofluorescence using primary antibodies and TRITC-conjugated anti-mouse IgG. Nuclei were counterstained with DAPI (blue).

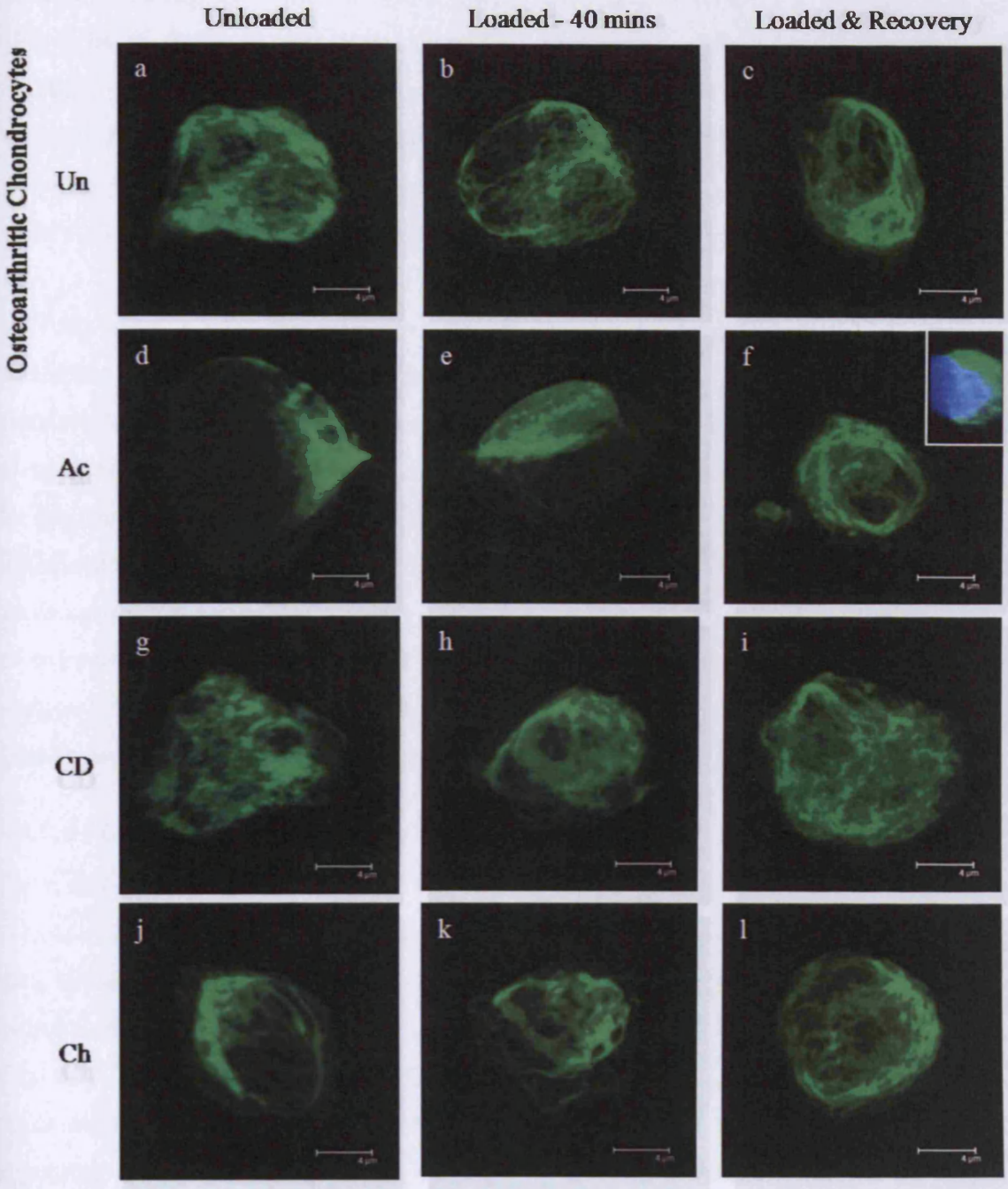

Figure 6.9 A:- ***3D reconstruction*** - The effect of load on the vimentin cytoskeleton of osteoarthritic human articular chondrocytes in 3D agarose culture, in the absence (Un, a-c) or presence of 2mM acrylamide (Ac, d-f) to disrupt vimentin intermediate filaments, 1μM cytochalasin D (CD, g-i) to disrupt actin microfilaments, or 1μM colchicine (Ch, j-l) to disrupt tubulin microtubules. Chondrocytes were loaded (cyclic compression; 15%, 0.5 Hz) for 40 minutes (b,e,h,k) and recovery was determined five hours after loading (c,f,i,l). Unloaded chondrocytes in agarose served as controls (a,d,g,j). Load-induced changes in vimentin organisation were unaffected by the treatments. Images shown are 3D-reconstructions of a series of scans taken at 0.4μm increments across the chondrocyte. f – insert is a 90° rotation of the reconstruction on the y-axis. Vimentin was detected by indirect immunofluorescence using primary antibody and TRITC-conjugated anti-mouse IgG.

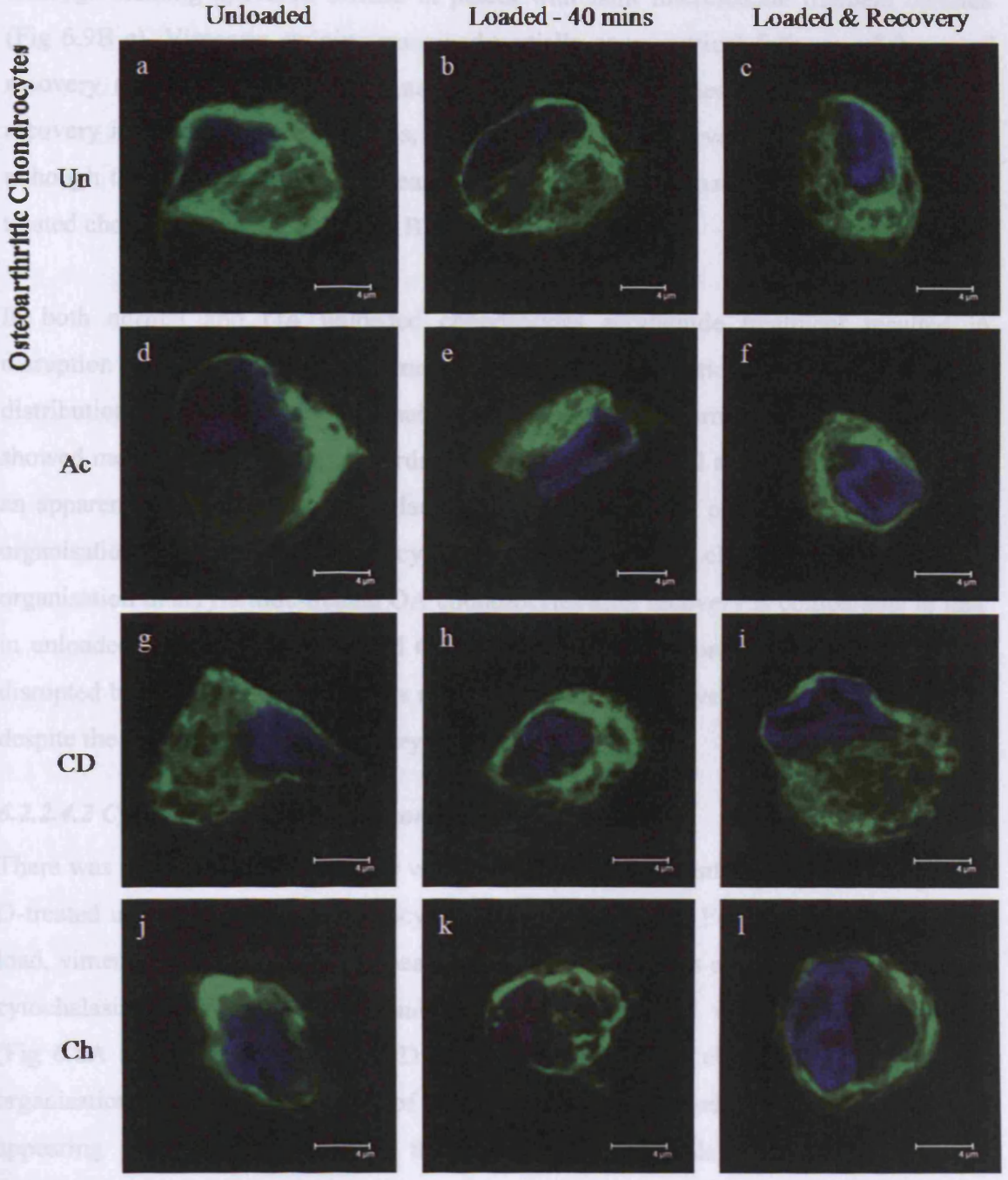

Figure 6.9 B:- ***Single scan*** - The effect of load on the vimentin cytoskeleton of osteoarthritic human articular chondrocytes in 3D agarose culture, in the absence (Un, a-c) or presence of 2mM acrylamide (Ac, d-f) to disrupt vimentin intermediate filaments, 1μM cytochalasin D (CD, g-i) to disrupt actin microfilaments, or 1μM colchicine (Ch, j-l) to disrupt tubulin microtubules. Chondrocytes were loaded (cyclic compression; 15%, 0.5 Hz) for 40 minutes (b,e,h,k) and recovery was determined five hours after loading (c,f,i,l). Unloaded chondrocytes in agarose served as controls (a,d,g,j). Load-induced changes in vimentin organisation were unaffected by the treatments. Images shown are scans through the centre of the cell. Vimentin was detected by indirect immunofluorescence using primary antibodies and TRITC-conjugated anti-mouse IgG. Nuclei were counterstained with DAPI (blue).

although staining appeared diffuse in places with faint intermediate filament bundles (Fig 6.9B e). Vimentin staining remained partially asymmetrical following 5 hours of recovery (Fig 6.9A f – insert). Intermediate filament bundles appeared thicker with recovery in acrylamide-treated cells, comparable to that observed in untreated controls, although the filament bundles appeared to be more densely packed in the acrylamide-treated chondrocytes (Fig 6.9A and B f).

In both normal and OA unloaded chondrocytes acrylamide treatment resulted in disruption of the vimentin intermediate filament organisation and an asymmetric distribution. This asymmetry was maintained in OA but not normal chondrocytes, which showed more diffuse staining towards the periphery of the cell after loading. There was an apparent additive effect of acrylamide treatment and load on vimentin cytoskeletal organisation in normal chondrocytes, but not in OA chondrocytes. Vimentin organisation in acrylamide-treated OA chondrocytes after recovery is comparable to that in unloaded and recovery untreated OA chondrocytes; therefore vimentin organisation disrupted by acrylamide treatment is rescued by load and recovery in OA chondrocytes, despite the continued presence of acrylamide.

6.2.2.4.2 Cytochalasin D-treated chondrocytes

There was no clear difference in the vimentin organisation of untreated and cytochalasin D-treated unloaded normal chondrocytes (Fig 6.8A and B g). Following 40 minutes of load, vimentin filament bundles appeared thicker and were less clear in some regions of cytochalasin D-treated normal chondrocytes when compared with untreated controls (Fig 6.8A and B h). Cytochalasin D treatment showed little clear effect on vimentin organisation following 5 hours of recovery, with intermediate filament bundles appearing perhaps a little shorter than in untreated controls (Fig 6.8A and B i). Cytochalasin D treatment had no effect on vimentin organisation in OA chondrocytes whether unloaded, loaded for 40 minutes, or allowed to recover from loading (Fig 6.9A and B g-i), although vimentin filament bundles appeared thicker than in untreated controls following 40 minutes of compressive load (Fig 6.9A and B h).

6.2.2.4.3 Colchicine-treated chondrocytes

There was no difference in the organisation of the vimentin cytoskeleton in untreated and colchicine-treated normal chondrocytes that were unloaded or loaded for 40 minutes (Fig 6.8A and B j-k). Following a 5 hour recovery from loading, intermediate filament

bundle networks were less evident in colchicine-treated samples (Fig 6.8A and B l). Colchicine treatment had no discernable effect on vimentin organisation in unloaded or post-load recovery OA chondrocytes (Fig 6.9A and B, j and l). However, immediately after loading for 40 minutes vimentin filament bundles appeared thicker in colchicine-treated OA chondrocytes (Fig 6.9A and B k).

Key changes in the organisation of actin (Fig 6.10), tubulin (Fig 6.11) and vimentin (Fig 6.12) cytoskeletal networks with load and post-load recovery are summarised in figures 6.10 to 6.12. Additional effects of cytoskeletal disruption on load-induced organisation changes are also indicated.

6.2.3 Changes in Gene Expression with Load and Cytoskeletal Element Disruption

The effect of cyclic compressive loading on chondrocyte phenotype, along with any additional effect of cytoskeletal disruption, was analysed using quantitative PCR to determine gene expression changes.

6.2.3.1 Cytoskeletal associated genes

6.2.3.1.1 β-actin

β-actin mRNA expression levels showed a trend towards decreasing with loading for 10 and 20 minutes, although no changes reached significance. This trend was the same with load in both normal and OA chondrocytes and was unaffected by treatment with cytochalasin D (Fig 6.13 A), colchicine or acrylamide (data not shown). β-actin mRNA levels appeared to return to those of unloaded controls after 40 minutes of loading in untreated (Fig 6.13 A) and acrylamide-treated (data not shown) normal chondrocytes. Following recovery for 5 hours after loading, β-actin expression remained decreased or further decreased and again this trend was the same across all treatment groups and pathologies, although statistical significance was not reached (Fig 6.13 B and data not shown). As demonstrated in section 5.2.3.1, β-actin expression increased with cytochalasin D treatment (at 24 hours; normal $p = 0.015$, OA $p = 0.023$). β-actin mRNA expression was significantly increased with cytochalasin D treatment in all loading groups in both normal and OA chondrocytes (Fig 6.13).

Actin
Control
Loaded
Recovery
Normal
Sharp punctate spots
Predominantly cortical
Less punctate and more diffuse staining
Predominantly cortical
Punctate spots
Predominantly cortical
Recovery prevented by disruption of tubulin or vimentin cytoskeletal networks
Osteoarthritic
Punctate spots
Tightly packed
Limited to the periphery
Punctate spots
Less tightly packed
Limited to the periphery
Punctate and filamentous
Tightly packed
Limited to the periphery

Tubulin
Control
Loaded
Recovery
Normal
Osteoarthritic
• Fine tubule bundles
• Packed around nucleus
• Punctate
• Predominantly perinuclear
• Fine tubule bundles
• Most dense at cell periphery
• Recovery affected by disruption of tubulin cytoskeletal networks
• Fine tubule bundles
• Most dense at periphery
• Punctate
• Throughout the cell
• Clear microtubule bundles
• Networks throughout cell
• Recovery affected by disruption of tubulin or vimentin cytoskeletal networks

Vimentin
Control
Loaded
Recovery
Normal
Osteoarthritic
• Fine filament bundles
• Networks throughout cell and at cortex
• Fine filament bundles
• Cortical network lost
• Networks more dense
• Thick filament bundles
• Dense networks
• Thick filament bundles
• Loose networks throughout cell
• Fine filament bundles
• Networks throughout cell
• Thick filament bundles
• Loose networks throughout cell

β-actin

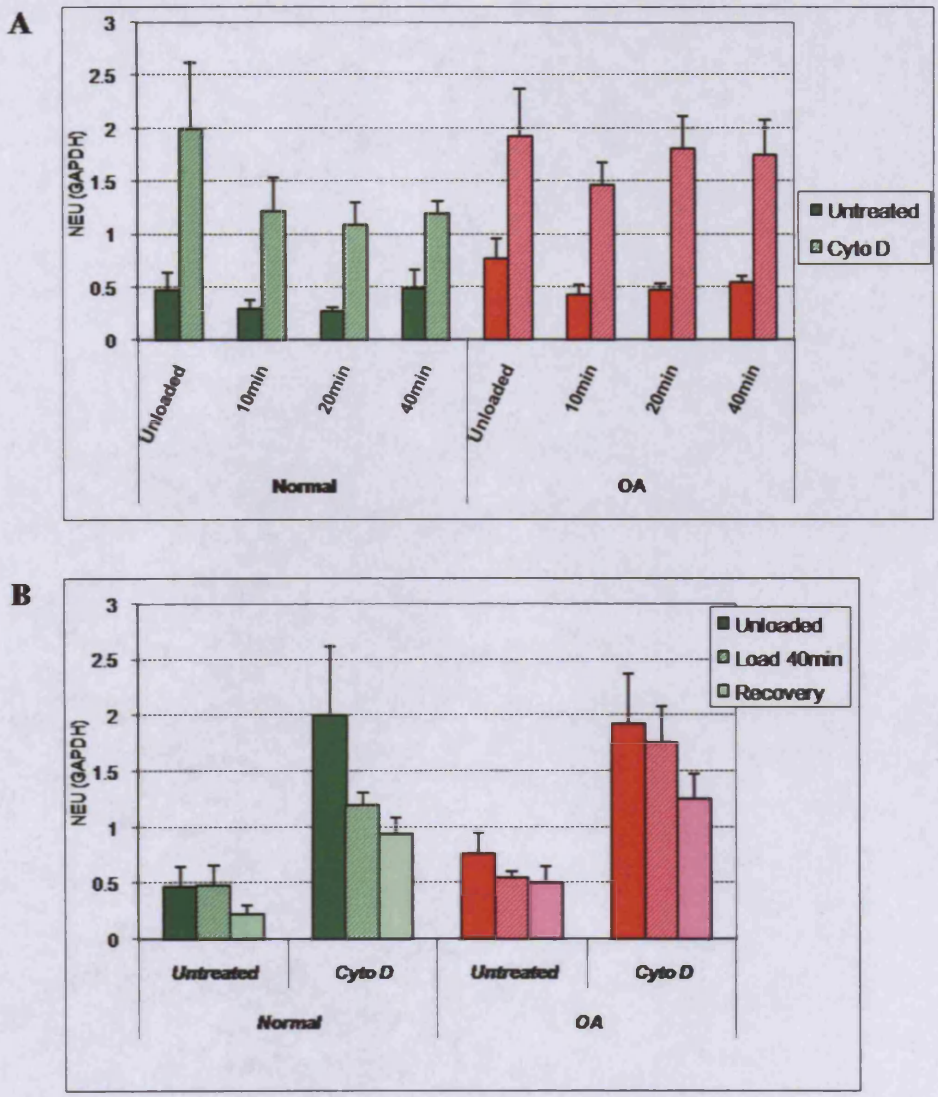

Figure 6.13:- β-actin gene expression changes with compressive load and actin microfilament disruption. Absolute mRNA levels were determined using SYBR Green quantitative PCR and normalised to the housekeeping gene GAPDH. Nucleic acids were isolated from chondrocytes from normal and osteoarthritic (OA) cartilage, encapsulated in 3D agarose and cultured without (untreated) or with 1μM cytochalasin D (Cyto D) for 24 hours before loading. Agarose constructs were loaded for 10, 20 or 40 minutes (A) or loaded for 40 minutes and left to recover for 5 hours (B). Data are presented as mean ± S.E.M. (n=5, n=3 for recovery).

6.2.3.1.2 β-tubulin

In untreated normal chondrocytes β-tubulin mRNA expression increased with loading (Fig 6.14 A) and reached significance after 20 (1.7 fold; p = 0.037) and 40 minutes of load (1.8 fold; p = 0.020). β-tubulin expression was further increased after 5 hours of recovery post-load (Fig 6.14 B) although increased variability meant that the difference did not reach statistical significance (2.7 fold increase over unloaded controls; p=0.073). OA chondrocytes showed a high variability in β-tubulin mRNA expression levels (Fig 6.14). As a result of this, no trends for changes with load were evident.

β-tubulin expression also increased with load in normal chondrocytes treated with colchicine (Fig 6.14 A), which may have been responsible for, or a result of, the altered tubulin microtubule organisation observed (section 6.2.2.3.1). β-tubulin expression was increased 1.6 fold (p = 0.046) after 20 minutes of load in colchicine-treated normal chondrocytes (Fig 6.14 A). There was an additive effect of colchicine treatment on β-tubulin expression after 40 minutes loading, with expression increasing 2.7 fold over unloaded colchicine-treated chondrocytes (p = 0.013); as a result of this, β-tubulin expression was increased significantly over untreated controls loaded for 40 minutes (p = 0.036; Fig 6.14 A). No further increases in β-tubulin expression were observed in colchicine-treated cells allowed to recover for 5 hours post-load (2.9 fold increase over unloaded cells; p = 0.069; Fig 6.14 B). Therefore the additive effect of colchicine with load on tubulin organisation (section 6.2.2.3.1) was also observed at the mRNA expression level. The effect of acrylamide on β-tubulin expression was very similar to that of colchicine. Expression was increased in normal chondrocytes after 20 (2.6 fold; p = 0.007) and 40 minutes of load (4 fold; p = 0.020), indicating an additive effect with load (Fig 6.14 C). There was no further increase in expression with recovery (4 fold higher than unloaded samples; p = 0.012). Like colchicine- and untreated chondrocytes, the load-induced increase in β-tubulin mRNA expression was only observed in normal, not OA chondrocytes. Cytochalasin D treatment had no effect on β-tubulin expression in response to load (data not shown), corroborating the tubulin localisation data (section 6.2.2.3.2).

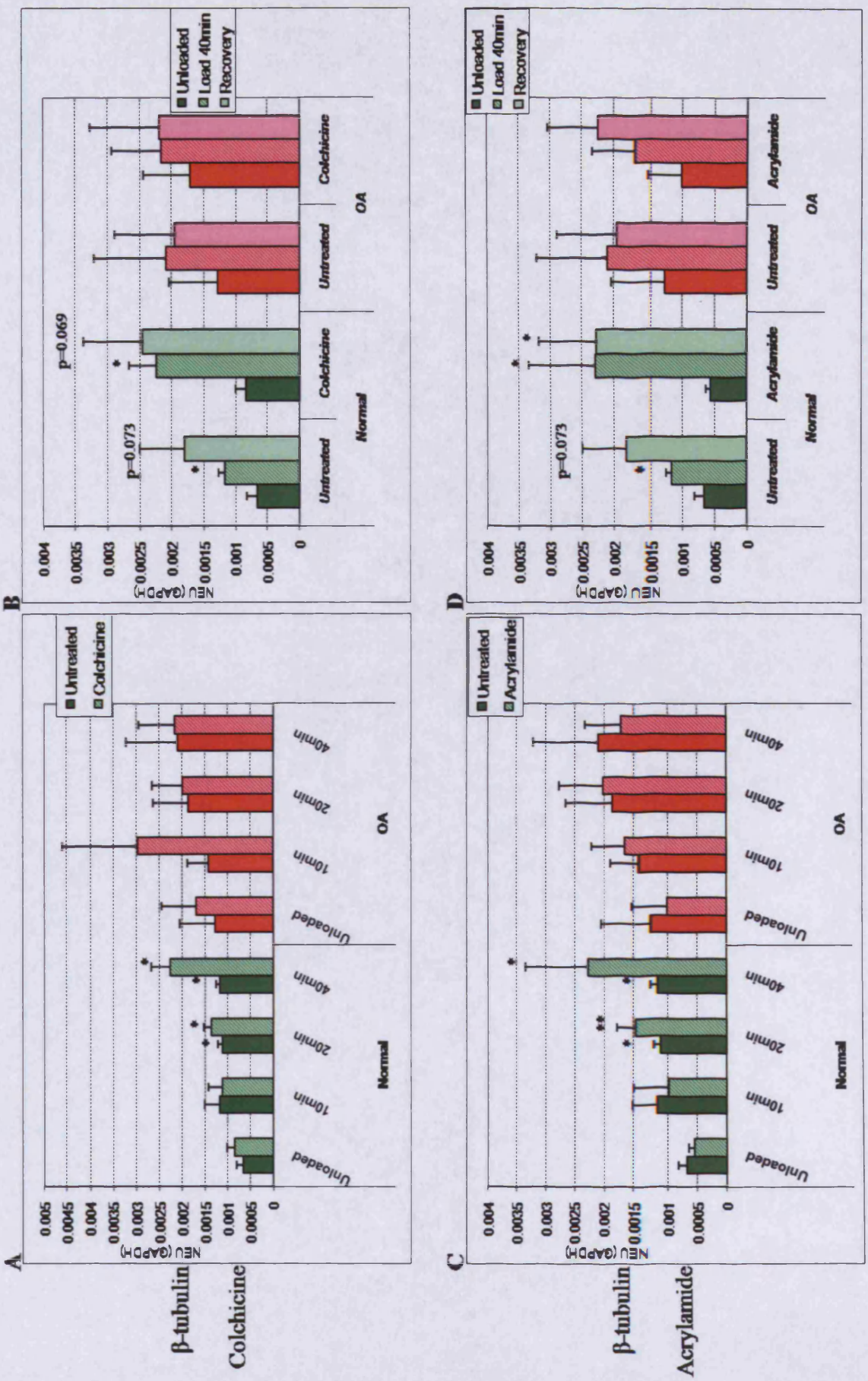
A
B
C
D
β-tubulin
Colchicine
Acrylamide
NEU (GAPDH)
Untreated
Colchicine
Acrylamide
Unloaded
Load 40min
Recovery
Normal
OA
Unloaded
10min
20min
40min
p=0.069
p=0.073

6.2.3.1.3 Vimentin

Vimentin mRNA expression levels did not change significantly with load in untreated normal and OA chondrocytes (Fig 6.15). In normal chondrocytes, vimentin expression levels decreased after 5 hours of recovery post-load (1.6 fold below 40 minutes load, not significant), dropping below those of unloaded controls (1.3 fold), but not significantly (Fig 6.15 B). This effect was also observed in OA chondrocytes, but again differences were not significant (recovery vs. unloaded – 1.9 fold, $p = 0.399$; recovery vs. 40 minutes load – 2.3 fold, $p = 0.286$).

Changes in vimentin mRNA expression with loading followed the same trend in acrylamide-treated chondrocytes as in untreated controls (Fig 6.15 A and B). Following recovery from load, acrylamide treatment resulted in a bigger decrease in vimentin expression in normal chondrocytes (Fig 6.15 B), although this decrease did not reach significance (2.1 fold below unloaded; $p = 0.066$. 2.3 fold below 40 minutes loaded; $p = 0.057$). The decrease in vimentin expression after 5 hours of recovery post-load was enhanced by cytochalasin D treatment of normal (2.1 fold below unloaded; $p = 0.048$) and OA (2.3 fold below unloaded; $p = 0.087$) chondrocytes (Fig 6.15 C). Colchicine treatment had no effect on vimentin mRNA expression under any of the loading conditions in normal and OA chondrocytes (data not shown).

6.2.3.1.4 Cofilin

mRNA expression levels of the actin-depolymerising protein cofilin increased 1.8 fold in normal chondrocytes subjected to 40 minutes of load (Fig 6.16 A), although this increase was not significant ($p = 0.108$). Cofilin mRNA expression did not alter in loaded OA chondrocytes. In both normal and OA chondrocytes cofilin expression levels returned to those of unloaded controls following a 5 hour recovery post-load (Fig 6.16 B).

As described in section 5.2.3.1, cofilin mRNA expression was increased in normal chondrocytes in response to treatment with cytochalasin D for 24 hours (1.9 fold; $p = 0.013$). Cofilin expression also increased with load in cytochalasin D-treated normal chondrocytes (Fig 6.16 A), but the increase was smaller than that in untreated samples (1.3 fold at 40 minutes load). By contrast, load-induced increases in cofilin expression were larger in cytochalasin D-treated OA chondrocytes when compared to untreated controls (1.5 fold increase at 40 minutes load); as a result, cofilin expression was

Vimentin

A

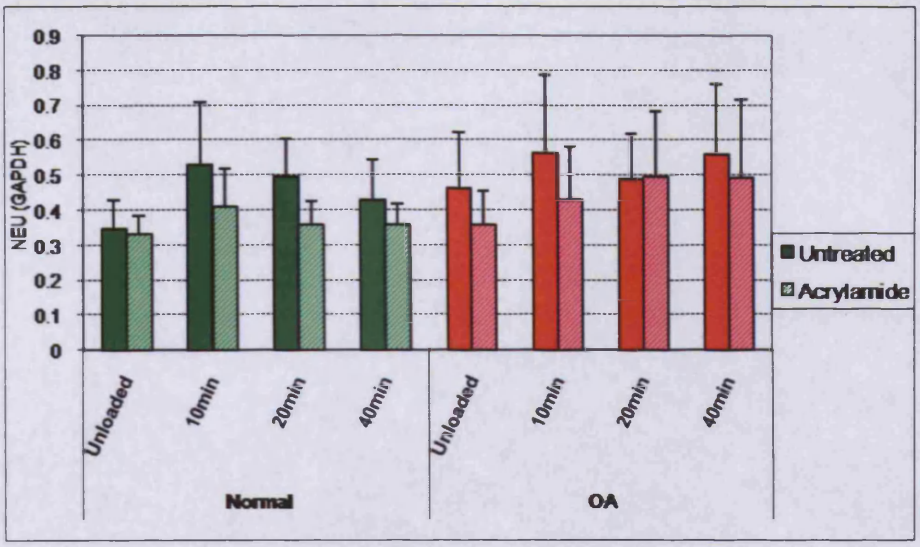

B

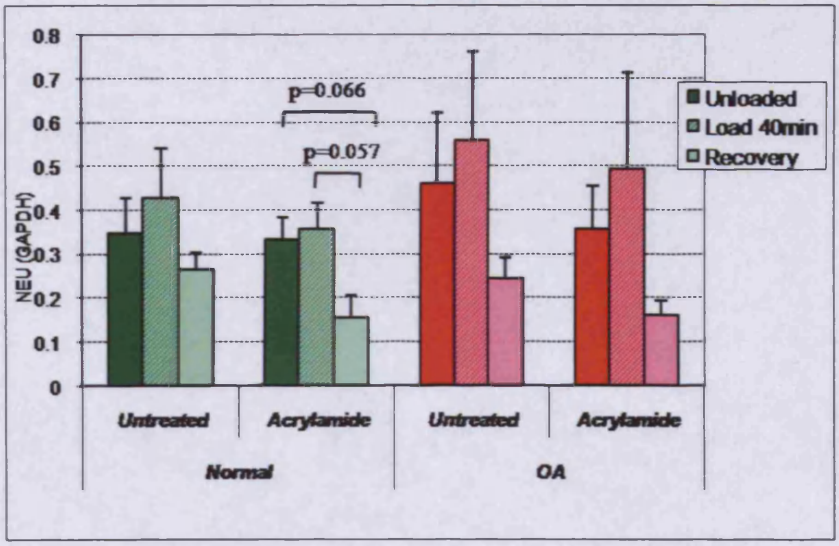

C

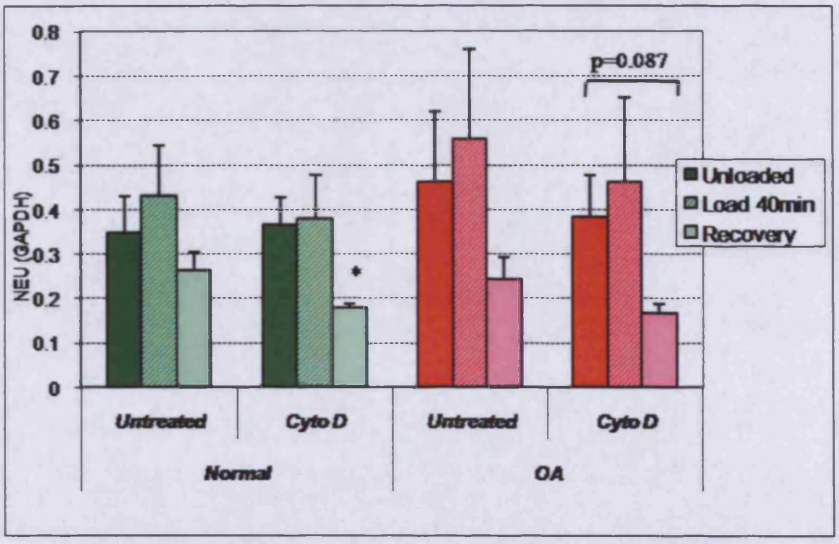

Cofilin

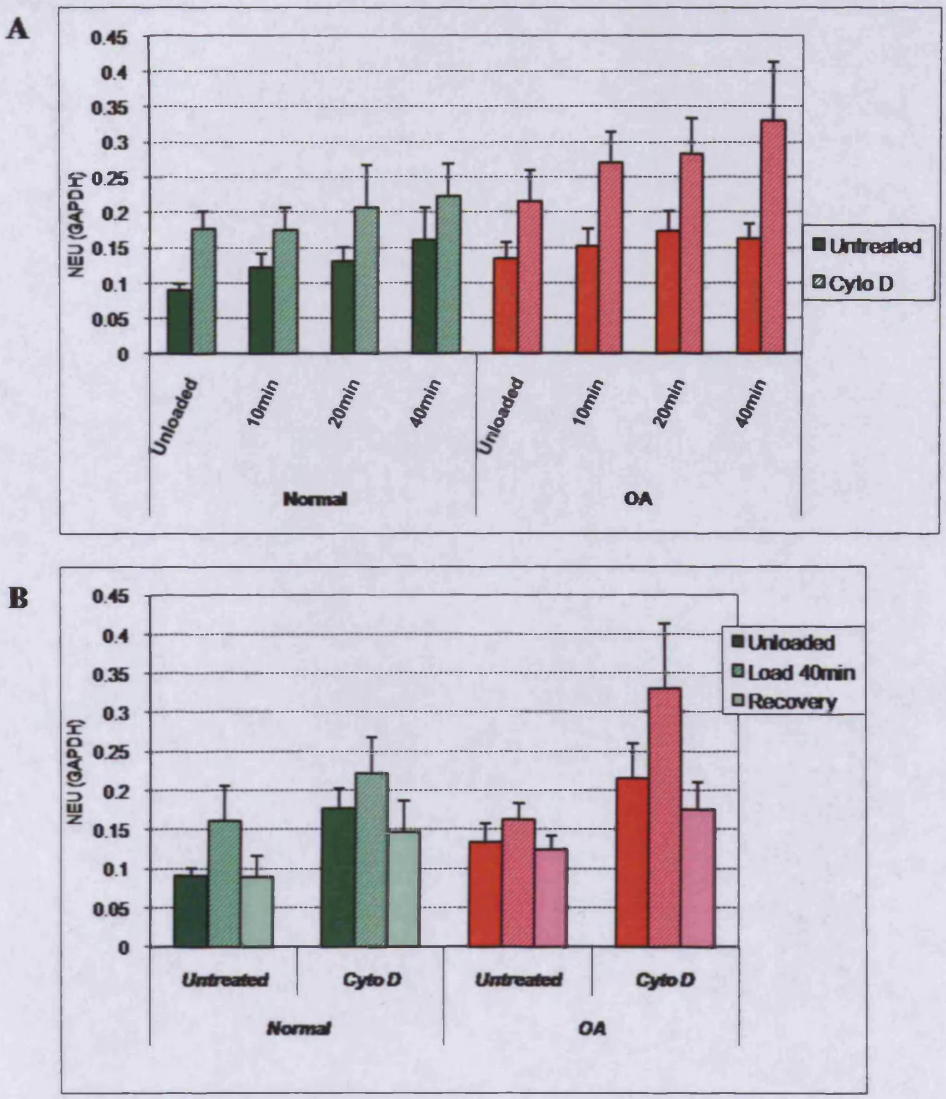

Figure 6.16:- Cofilin gene expression changes with compressive load and actin microfilament disruption. Absolute mRNA levels were determined using SYBR Green quantitative PCR and normalised to the housekeeping gene GAPDH. Nucleic acids were isolated from chondrocytes from normal and osteoarthritic (OA) cartilage, encapsulated in 3D agarose and cultured without (untreated) or with 1μM cytochalasin D (Cyto D) for 24 hours before loading. Agarose constructs were loaded for 10, 20 or 40 minutes (A) or loaded for 40 minutes and left to recover for 5 hours (B). Data are presented as mean ± S.E.M. (n=5, n=3 for recovery).

significantly higher in cytochalasin D-treated OA chondrocytes than untreated controls after 10 ($p = 0.045$) and 40 minutes of load ($p = 0.040$; Fig 6.16 A). There was no additional effect of cytochalasin D treatment on cofilin expression following recovery after loading (Fig 6.16 B). Disruption of vimentin intermediate filaments with acrylamide enhanced the down-regulation of cofilin mRNA with 5 hours recovery post-load in normal (1.8 fold below 40 minutes loaded; $p = 0.206$) and OA (1.7 fold below 40 minutes loaded; $p = 0.046$) chondrocytes (data not shown). Cofilin expression in the presence or absence of load was unaffected by colchicine treatment in normal and OA chondrocytes (data not shown).

6.2.3.1.5 Destrin

In untreated normal chondrocytes, mRNA expression levels of the actin-depolymerising protein destrin was significantly increased after 10 minutes of load (1.6 fold; $p = 0.014$); levels then began to decrease after 20 and 40 minutes of load (Fig 6.17 A). A subtle increase (1.3 fold) in destrin mRNA levels was also observed in OA chondrocytes after 10 minutes of load, although the increase was not significant (Fig 6.17 A). There were no further changes in destrin mRNA levels following a 5 hour recovery period in untreated normal or OA chondrocytes (Fig 6.17 B).

As demonstrated in section 5.2.3.1, destrin expression was significantly increased following treatment of normal chondrocytes with cytochalasin D and was also increased over the untreated controls in all loading groups (Fig 6.17). Destrin mRNA levels also increased (1.3 fold) in cytochalasin D-treated chondrocytes subjected to 10 minutes of load, but due to variability this was not significant (Fig 6.17 A). Destrin mRNA levels returned to baseline expression (i.e. unloaded cells) after 40 minutes of load. However, unlike untreated controls, destrin expression increased 1.4 fold over the 5 hour recovery period (Fig 6.17 B; 40 minutes load vs. recovery; $p = 0.098$) resulting in a significant effect of treatment in recovery cells ($p = 0.021$). Destrin expression increased with load in cytochalasin D-treated OA chondrocytes (1.5 fold increase after 10 minutes; not significant) and remained elevated after 20 and 40 minutes of load (Fig 6.17 A). The additive effect of cytochalasin D treatment and load resulted in an enhanced effect of treatment after 10 ($p = 0.071$), 20 ($p = 0.069$) and 40 minutes ($p = 0.009$) of load. Following 5 hours of recovery from loading, destrin expression remained elevated in cytochalasin D-treated OA chondrocytes, as did the significant effect of treatment ($p =$

0.013; Fig 6.17 B). Acrylamide or colchicine treatment had no effect on destrin expression in the presence or absence of load in normal and OA chondrocytes, with the exception that colchicine treatment resulted in increased destrin expression in OA chondrocytes over the 5 hour recovery period (40 minutes load vs. recovery; $p = 0.017$; data not shown).

6.2.3.1.6 Gelsolin

Expression of another actin-depolymerising factor, gelsolin, was unaffected by loading of normal and OA chondrocytes (data not shown). Treatment of chondrocytes with cytochalasin D, colchicine or acrylamide did not affect gelsolin mRNA expression with loading or recovery; however, a decrease in gelsolin expression following recovery was observed after acrylamide treatment, but this down-regulation did not reach statistical significance in normal (1.7 fold below 40 minutes loaded; $p = 0.060$) or OA chondrocytes (2.2 fold below 40 minutes loaded; $p = 0.072$; data not shown).

6.2.3.1.7 Thymosin β4

Thymosin β4 mRNA expression appeared to be increased after 10 minutes loading in untreated normal chondrocytes (1.7 fold), remaining elevated at 20 minutes but decreasing to unloaded levels after 40 minutes loading; however, expression changes were not significant (Fig 6.18 A). Untreated OA chondrocytes showed no change in thymosin β4 expression with loading. Following a 5 hour recovery from loading there was no further change in thymosin β4 expression in normal or OA chondrocytes (Fig 6.18 B).

Load-induced changes in thymosin β4 expression were unaffected by cytochalasin D treatment in normal chondrocytes (Fig 6.18 A and B). By contrast, the response of OA chondrocytes was influenced by cytochalasin D treatment. Thymosin β4 expression increased gradually in response to load and was elevated 1.6 fold ($p = 0.081$) over unloaded cytochalasin D-treated OA chondrocytes after 40 minutes of load (Fig 6.18 A). The additive effect of cytochalasin D and load resulted in an effect of treatment at 10 ($p = 0.005$), 20 ($p = 0.076$) and 40 minutes ($p = 0.061$) of load. Over the 5 hour recovery period there was a significant decrease in thymosin β4 expression in cytochalasin D-treated OA chondrocytes (2.6 fold below 40 minutes load; $p = 0.042$, Fig 6.18 B). Colchicine treatment also appeared to increase thymosin β4 expression in unloaded normal ($p = 0.085$) and OA chondrocytes (Fig 6.18 C). Colchicine treatment showed no

Destrin

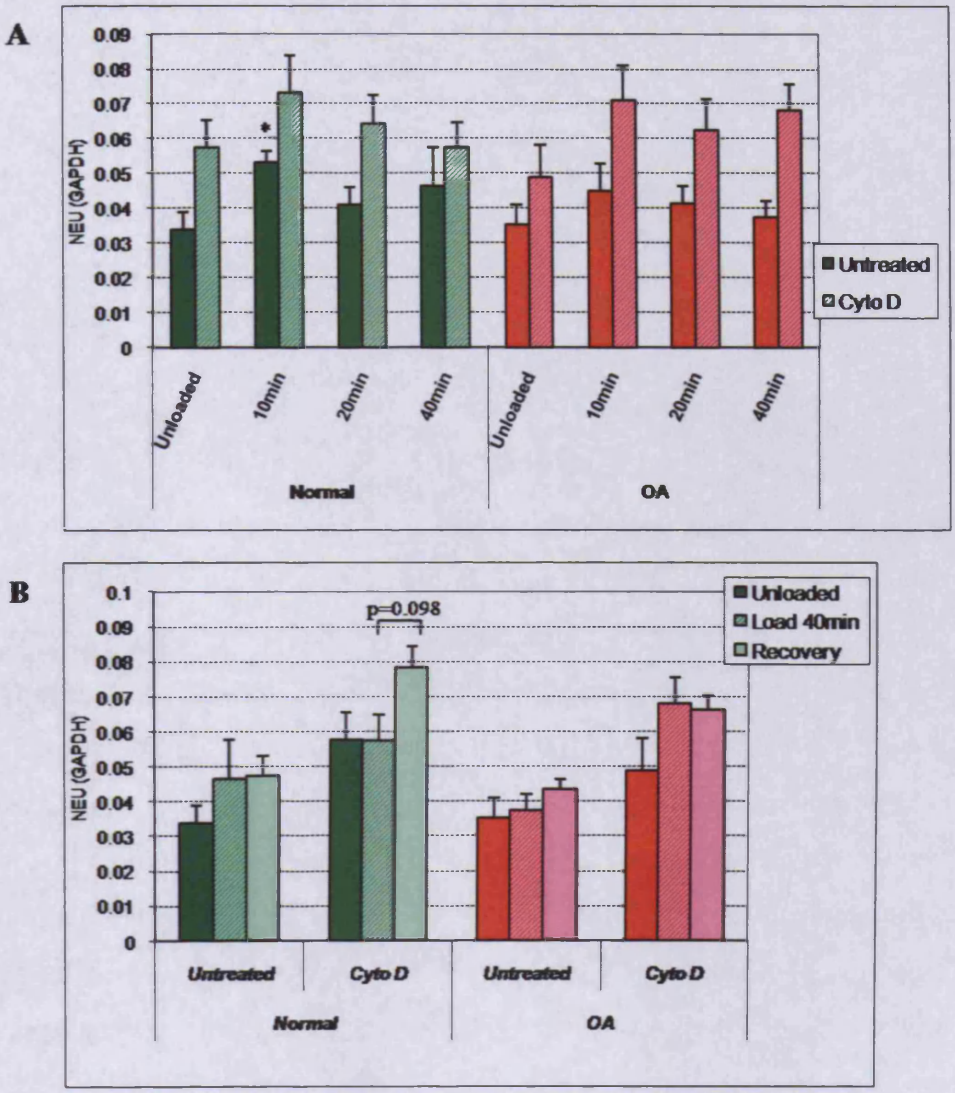

Figure 6.17:- Destrin gene expression changes with compressive load and actin microfilament disruption. Absolute mRNA levels were determined using SYBR Green quantitative PCR and normalised to the housekeeping gene GAPDH. Nucleic acids were isolated from chondrocytes from normal and osteoarthritic (OA) cartilage, encapsulated in 3D agarose and cultured without (untreated) or with 1μM cytochalasin D (Cyto D) for 24 hours before loading. Agarose constructs were loaded for 10, 20 or 40 minutes (A) or loaded for 40 minutes and left to recover for 5 hours (B,C). Data are presented as mean ± S.E.M. (n=5, n=3 for recovery). * $p < 0.05$, loaded compared to unloaded control / loaded with recovery.

Thymosin β4

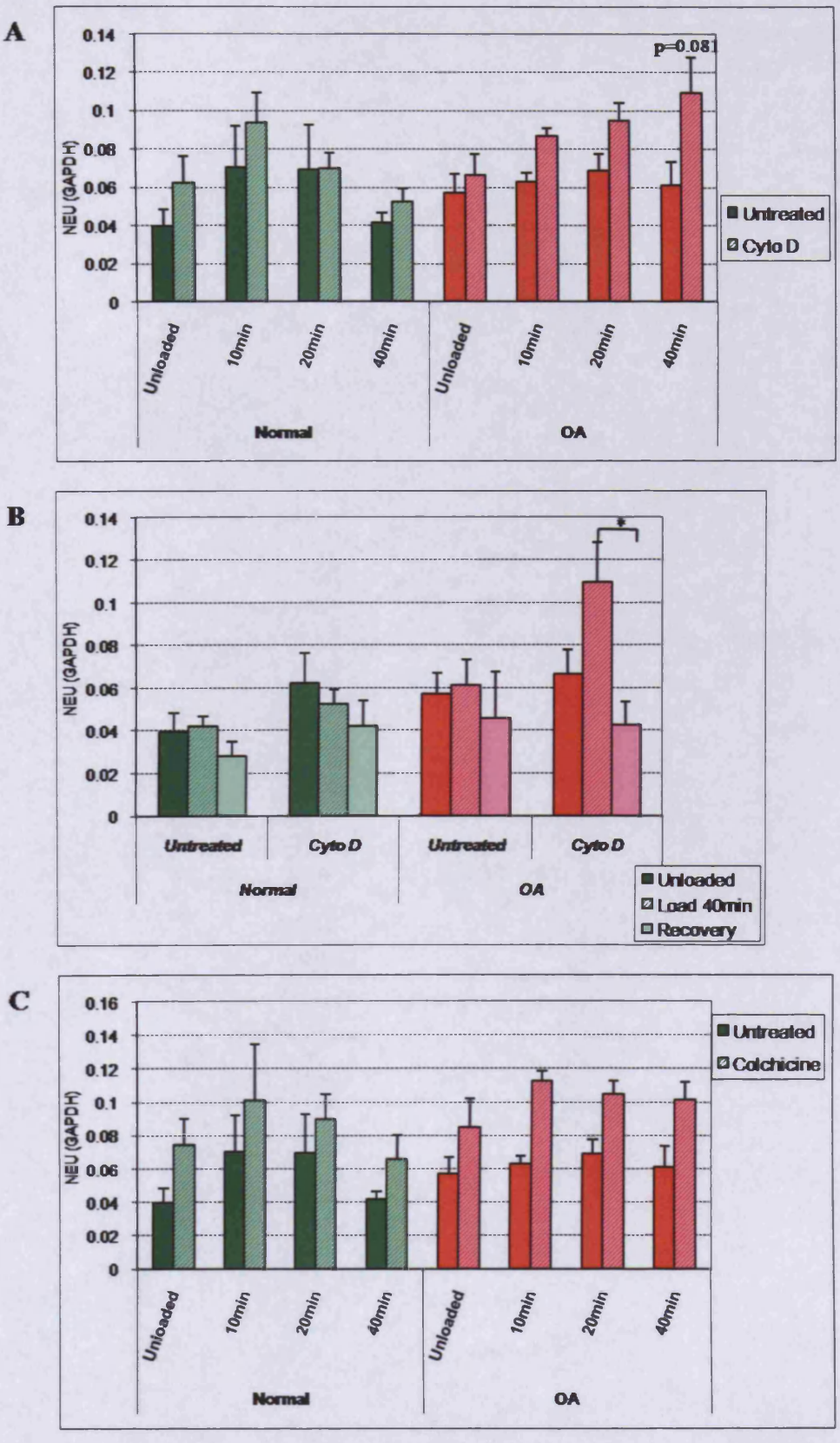
A
p=0.081
NEU (GAPDH)
0.14
0.12
0.1
0.08
0.06
0.04
0.02
0
Unloaded
10min
20min
40min
Normal
OA
Untreated
Cyto D
B
*
Untreated
Cyto D
Normal
OA
Unloaded
Load 40min
Recovery
C
0.16
Colchicine

additional effect on thymosin β4 expression changes with loading in normal chondrocytes. By contrast, colchicine treatment significantly increased thymosin β4 expression in OA chondrocytes subjected to 10 ($p < 0.001$), 20 ($p = 0.016$), and 40 minutes of loading ($p = 0.039$; Fig 6.18 C). Acrylamide had no effect on thymosin β4 expression changes with load.

6.2.3.1.8 Paxillin

In untreated normal and OA chondrocytes paxillin mRNA expression did not respond appreciably to load; however, expression decreased after 40 minutes of load followed by a 5 hour recovery period in normal (1.5 fold decreased below unloaded; $p = 0.087$) and OA chondrocytes (1.9 fold decreased from unloaded; $p = 0.121$; Fig 6.19 A).

Loading for 40 minutes significantly decreased paxillin mRNA expression in colchicine-treated normal chondrocytes when compared with unloaded controls (2.4 fold; $p = 0.029$; Fig 6.19 A). However paxillin mRNA levels returned to those of untreated controls after the 5 hour recovery period. Colchicine treatment did not affect the load-induced changes in paxillin expression in OA chondrocytes; as observed in untreated controls, paxillin expression decreased after 40 minutes loading and further decreased after a 5 hour recovery in colchicine-treated OA chondrocytes (1.8 fold below unloaded; $p = 0.072$; Fig 6.19 A). Acrylamide had no effect on the response of paxillin expression to loading and recovery in normal chondrocytes (Fig 6.19 B). By contrast, acrylamide prevented the decrease in paxillin expression after 40 minutes of load in OA chondrocytes, although a significant reduction in expression following a 5 hour recovery period (2.5 fold below 40 minute loaded; $p = 0.032$) returned paxillin mRNA levels to those of untreated controls (Fig 6.19 B). Cytochalasin D treatment had no effect on paxillin expression changes with loading and recovery.

6.2.3.2 Matrix metabolism genes

6.2.3.2.1 BMF

As described in section 5.2.3.3, mRNA expression of the pro-apoptotic factor BMF was higher in OA chondrocytes cultured in 3D agarose when compared with normal chondrocytes, with the difference becoming more pronounced over the culture period but not reaching statistical significance at 48 hours ($p = 0.092$). *BMF* expression did not alter with loading or recovery in normal and OA chondrocytes (Fig 6.20).

Paxillin

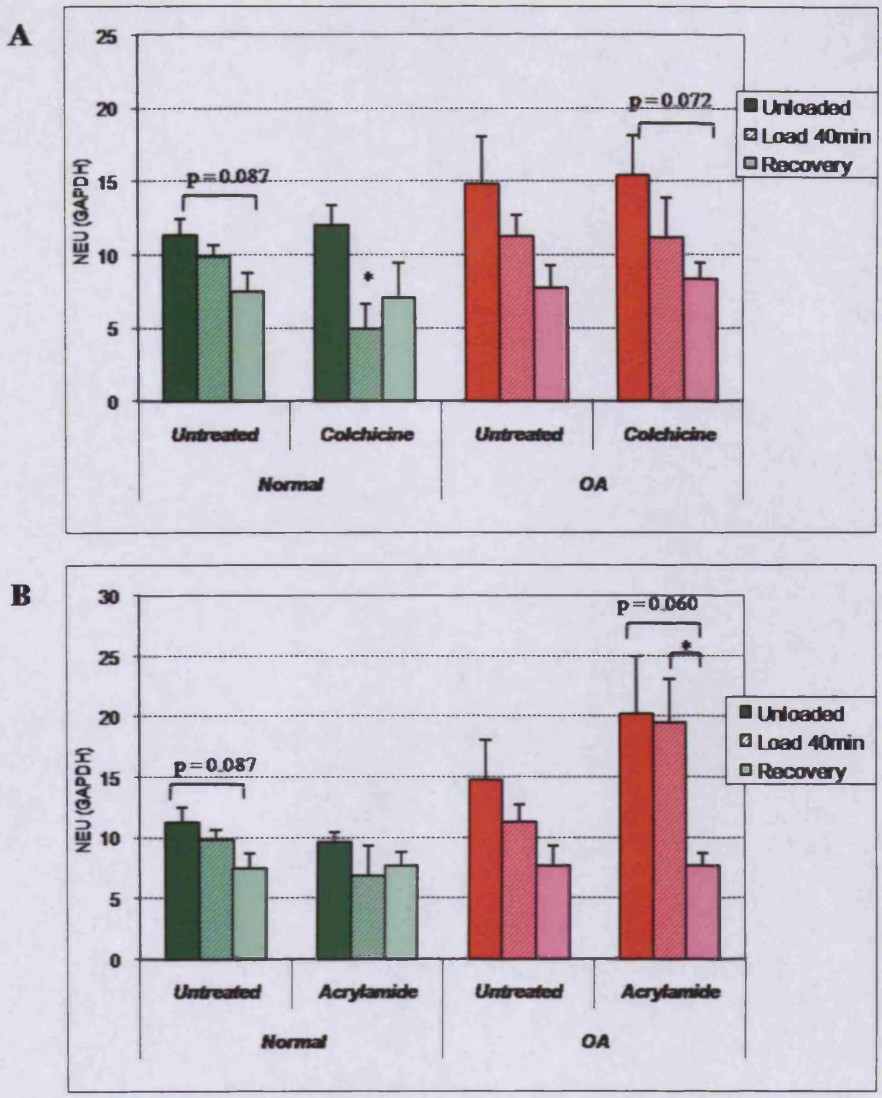

Figure 6.19:- Paxillin gene expression changes with compressive load and cytoskeletal disruption. Absolute mRNA levels were determined using SYBR Green quantitative PCR and normalised to the housekeeping gene GAPDH. Nucleic acids were isolated from chondrocytes from normal and osteoarthritic (OA) cartilage, encapsulated in 3D agarose and cultured without (untreated) or with treatment. Treatments were 1μM colchicine to disrupt tubulin microtubules (A) or 2mM acrylamide to disrupt vimentin intermediate filaments (B). Agarose constructs were loaded for 40 minutes and left to recover for 5 hours. Data are presented as mean ± S.E.M. (n=3). * $p < 0.05$, loaded compared to unloaded control / loaded and recovery.

BMF

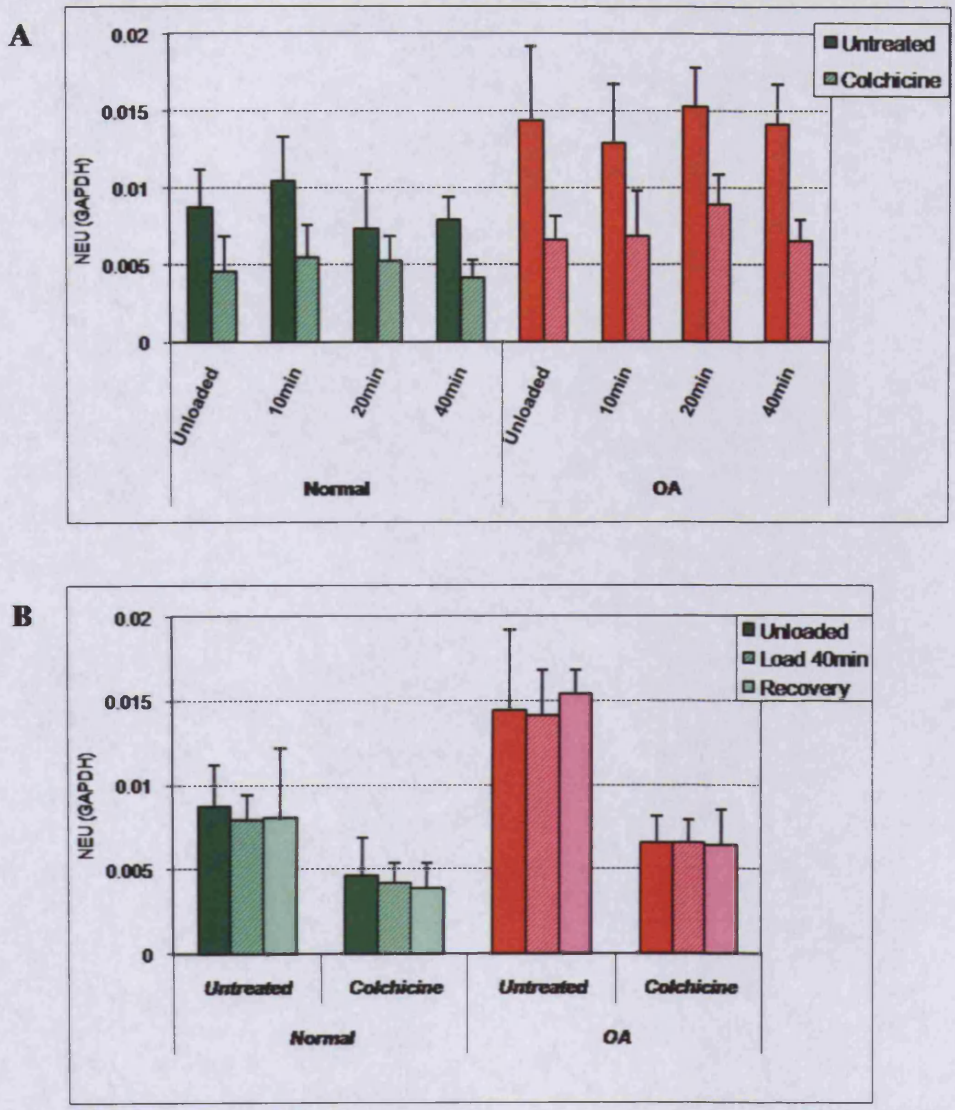

Figure 6.20:- BMF gene expression changes with compressive load and tubulin microtubule disruption. Absolute mRNA levels were determined using SYBR Green quantitative PCR and normalised to the housekeeping gene GAPDH. Nucleic acids were isolated from chondrocytes from normal and osteoarthritic (OA) cartilage, encapsulated in 3D agarose and cultured without (untreated) or with 1μM colchicine. Agarose constructs were loaded for 10, 20 or 40 minutes (A) or loaded for 40 minutes and left to recover for 5 hours (B). Data are presented as mean ± S.E.M. (n=5, n=3 for recovery).

Colchicine treatment reduced *BMF* expression in normal chondrocytes (not significant; at 40 minutes loading, Un vs. Ch $p = 0.081$) but had no effect on expression changes in response to load or recovery (Fig 6.20). *BMF* expression was also reduced by colchicine treatment in OA chondrocytes (section 5.2.3.3; 24 hours $p = 0.162$, 48 hours $p = 0.045$). This effect of colchicine treatment was also observed in loaded OA chondrocytes, with decreased *BMF* expression in OA chondrocytes subjected to 20 ($p = 0.081$) and 40 minutes ($p = 0.037$) of load and after a 5 hour recovery period ($p = 0.025$), when compared with untreated controls (Fig 6.20). Acrylamide also significantly reduced *BMF* expression in OA chondrocytes treated for 48 hours ($p = 0.008$; section 5.2.3.3) but unlike colchicine, a significant effect of acrylamide treatment was only observed in OA chondrocytes after recovery from loading ($p = 0.027$ when compared with untreated recovery; data not shown). Despite these significant effects of treatment, colchicine or acrylamide treatment did not alter *BMF* expression in response to load or recovery, in either normal or OA chondrocytes (Fig 6.20 and data not shown). *BMF* expression was not affected by compression or recovery in cytochalasin D-treated cells (data not shown).

6.2.3.2.2 SOX9

SOX9 mRNA expression was reduced in OA chondrocytes when compared with normal chondrocytes (unloaded $p = 0.098$) and this was observed at all loading time points with the exception of load recovery (Fig 6.21). In normal untreated chondrocytes *SOX9* expression showed a trend to increase with loading and was 1.5 fold higher than in unloaded controls after 40 minutes load, although high variability meant no differences were significant (Fig 6.21 A). *SOX9* expression levels returned to those of unloaded controls after 5 hours of recovery (Fig 6.21B). OA chondrocytes appeared to increase *SOX9* expression in response to load, peaking after 20 minutes (1.8 fold) and returning to the level observed in unloaded controls after 40 minutes of load; however due to sample variability these differences were not significant (Fig 6.21 A). In contrast to the response of normal chondrocytes, *SOX9* expression increased with recovery in OA chondrocytes (2.3 fold increase over unloaded; $p = 0.016$. 2.1 fold increased over 40 minutes of load; $p = 0.052$. Fig 6.21 B).

Cytochalasin D treatment altered the response of normal chondrocytes to load-induced *SOX9* changes, with expression appearing to decrease after 40 minutes of load to levels

SOX9

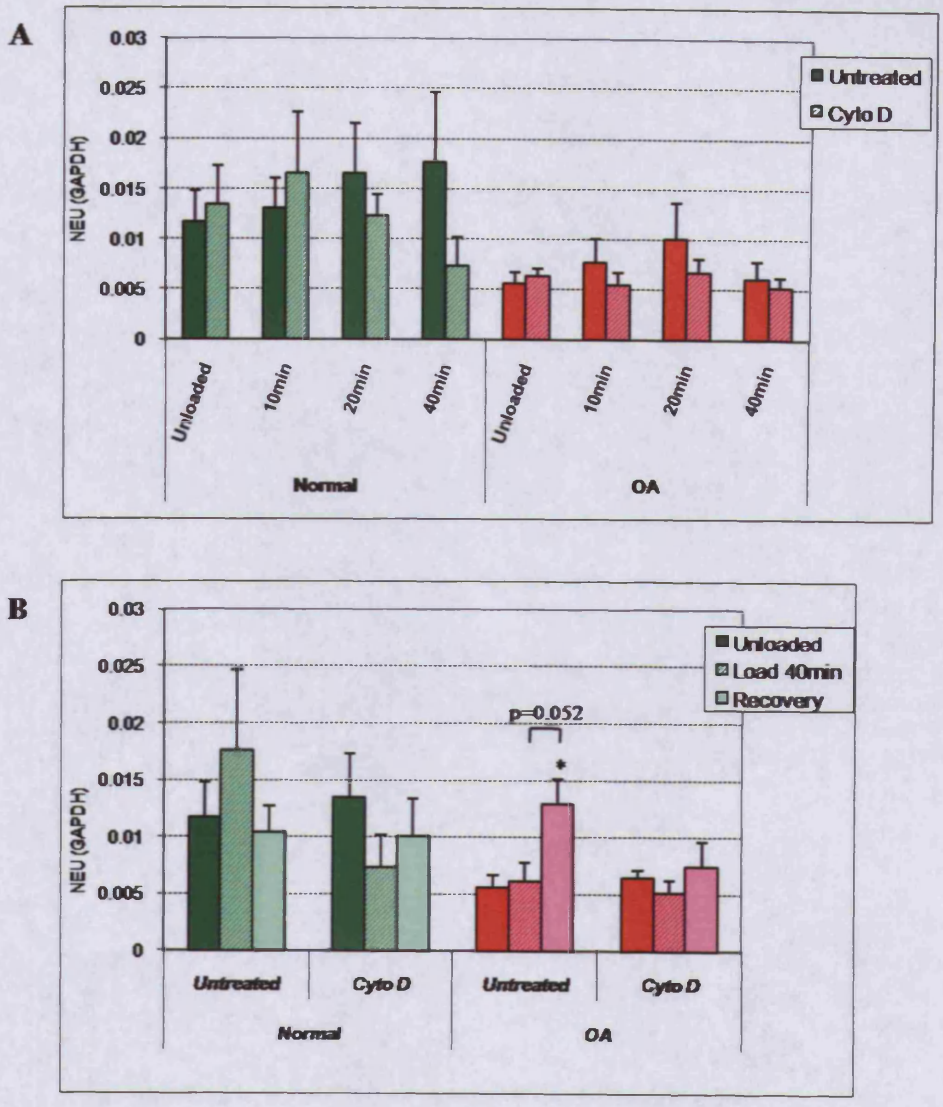

Figure 6.21:- SOX9 gene expression changes with compressive load and actin microfilament disruption. Absolute mRNA levels were determined using SYBR Green quantitative PCR and normalised to the housekeeping gene GAPDH. Nucleic acids were isolated from chondrocytes from normal and osteoarthritic (OA) cartilage, encapsulated in 3D agarose and cultured without (untreated) or with 1μM cytochalasin D. Agarose constructs were loaded for 10, 20 or 40 minutes (A) or loaded for 40 minutes and left to recover for 5 hours (B). Data are presented as mean ± S.E.M. (n=5, n=3 for recovery). * $p < 0.05$, loaded with recovery compared with loaded or unloaded control.

below those of unloaded samples (Fig 6.21 A); no differences were observed between untreated and cytochalasin D-treated normal chondrocytes after recovery (Fig 6.21 B). *SOX9* mRNA levels did not increase in response to load in cytochalasin D-treated OA chondrocytes (Fig 6.21 A) and cytochalasin D treatment prevented the increase in *SOX9* mRNA levels observed in untreated OA chondrocytes 5 hours post-load (Fig 6.21 B). Colchicine and acrylamide treatment had no effect on *SOX9* expression changes in normal and OA chondrocytes subjected to load and/or recovery (data not shown).

6.2.3.2.3 Aggrecan and type II collagen

Aggrecan expression was lower in OA chondrocytes when compared with normal chondrocytes ($p = 0.096$ for unloaded controls; section 5.2.3.3). In addition, aggrecan mRNA levels were reduced in normal and OA chondrocytes subjected to load (Fig 6.22 A); expression was decreased 2.6 fold after 20 minutes of load in normal untreated chondrocytes ($p = 0.078$) and 1.9 fold after 40 minutes of load in OA chondrocytes ($p = 0.155$). Following a 5 hour recovery period post-load, there was a small but non-significant increase in aggrecan expression in normal (1.4 fold increase over 40 minute loaded) and OA chondrocytes (1.6 fold increase over 40 minute loaded), although levels did not return to basal levels (Fig 6.22 B).

As described in section 5.2.3.3 aggrecan mRNA expression was decreased, but not significantly, after treatment of normal chondrocytes with cytochalasin D or acrylamide. However, in normal and OA chondrocytes neither treatment had an effect on the load-induced changes in aggrecan expression, but both treatments prevented the increase in mRNA levels with recovery observed in untreated cells (Fig 6.22 B and data not shown). Colchicine had no effect on aggrecan expression in either cell type in response to load or recovery (data not shown).

COL2A1 mRNA levels were below the level of detection using real time PCR with SYBR® green, therefore differences in expression in response to load and a possible combined effect of load and cytoskeletal disruption could not be determined for type II collagen.

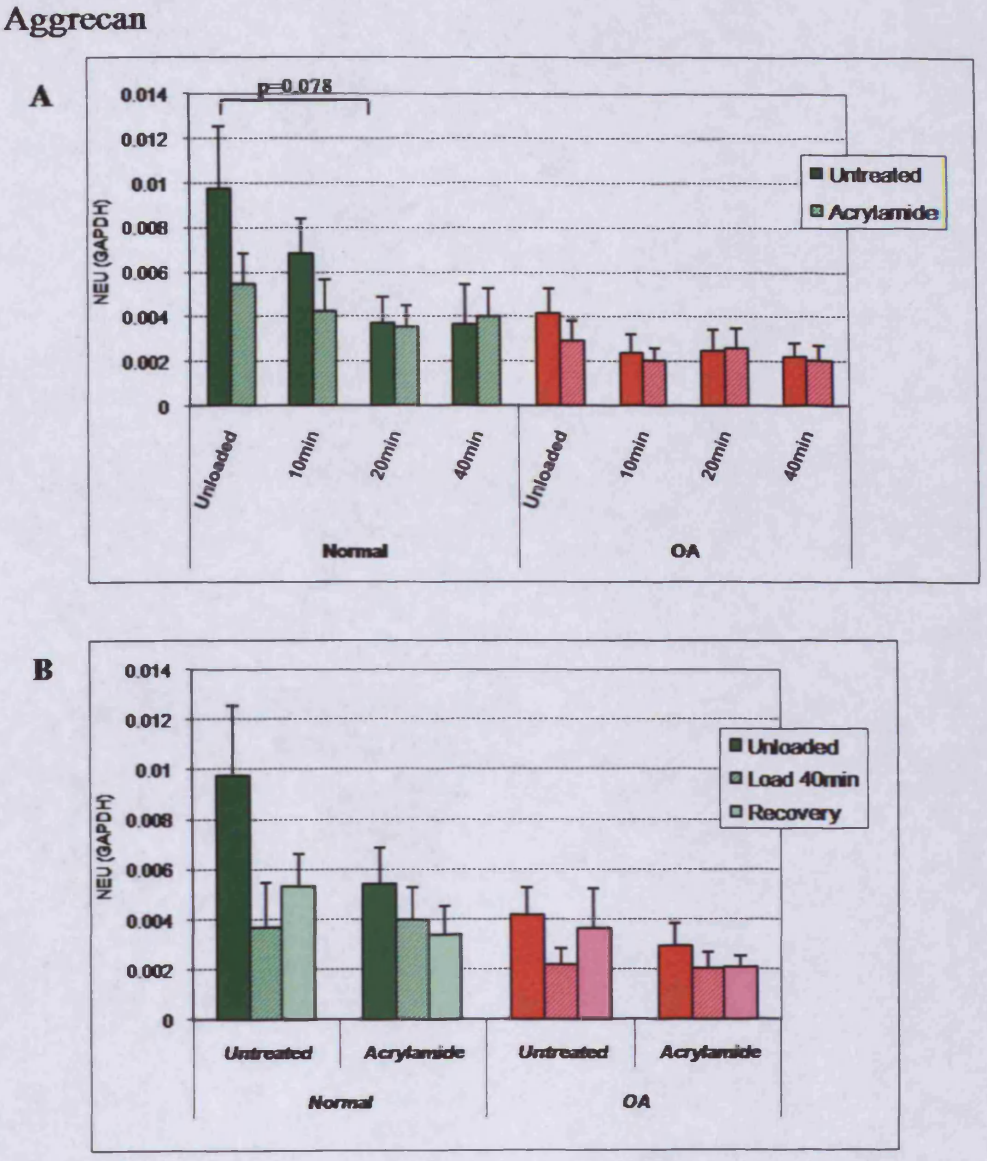

Figure 6.22:- Aggrecan gene expression changes with compressive load and vimentin intermediate filament disruption. Absolute mRNA levels were determined using SYBR Green quantitative PCR and normalised to the housekeeping gene GAPDH. Nucleic acids were isolated from chondrocytes from normal and osteoarthritic (OA) cartilage, encapsulated in 3D agarose and cultured without (untreated) or with 2mM acrylamide. Agarose constructs were loaded for 10, 20 or 40 minutes (A) or loaded for 40 minutes and left to recover for 5 hours (B). Data are presented as mean ± S.E.M. (n=5, n=3 for recovery).

6.2.3.2.4 Type I collagen

In untreated normal chondrocytes, *COL1A1* expression decreased gradually over the loading duration and was 2.3 fold reduced below unloaded controls after 40 minutes of load (not significant; Fig 6.23 A). Following a 5 hour recovery from loading, *COL1A1* expression was further decreased in untreated normal chondrocytes (8.3 fold below unloaded; $p = 0.114$; Fig 6.23 A). In contrast to normal chondrocytes, *COL1A1* expression was unaffected by loading for up to 40 minutes in OA chondrocytes; however mRNA expression levels were reduced 16.8 fold following recovery ($p = 0.023$ for unloaded vs. recovery; Fig 6.23 A). This suggests that physiological load could rescue the chondrocyte collagen phenotype.

There was a trend towards decreased expression of *COL1A1* in both normal and OA chondrocytes following treatment with cytochalasin D. However treatment did not affect the trends in *COL1A1* expression after loading and/or recovery; *COL1A1* mRNA levels were reduced 17.8 fold following recovery of cytochalasin D-treated OA chondrocytes compared with unloaded cells ($p = 0.076$; Fig 6.23 A). The decrease in *COL1A1* expression following 40 minutes of load was enhanced in normal chondrocytes treated with acrylamide (8.1 fold decrease; not significant; Fig 6.23 B). Acrylamide treatment induced a non-significant decrease in *COL1A1* mRNA levels in OA chondrocytes, but had no effect the cells response to load or recovery (Fig 6.23 B), indicating that disruption of vimentin had no effect on the mechanoregulation of *COL1A1* mRNA expression. Colchicine treatment had no effect on *COL1A1* mRNA expression in normal and OA chondrocytes and did not affect the cells responses to load and/or recovery (data not shown).

6.2.3.2.5 MMP-13

Alterations in *MMP13* mRNA expression with loading or recovery mirror *COL1A1* effects in both normal and OA chondrocytes. *MMP13* expression decreased gradually in normal chondrocytes over the loading duration, culminating in a 2.1 fold reduction after 40 minutes of load. *MMP13* mRNA levels further decreased following a 5 hour recovery period (4.2 fold below unloaded levels; $p = 0.262$; Fig 6.24). In OA chondrocytes *MMP13* expression was not mechanically regulated; however transcript levels decreased 2.2 fold following a 5 hour recovery period post-load ($p = 0.090$; Fig 6.24).

COL1A1

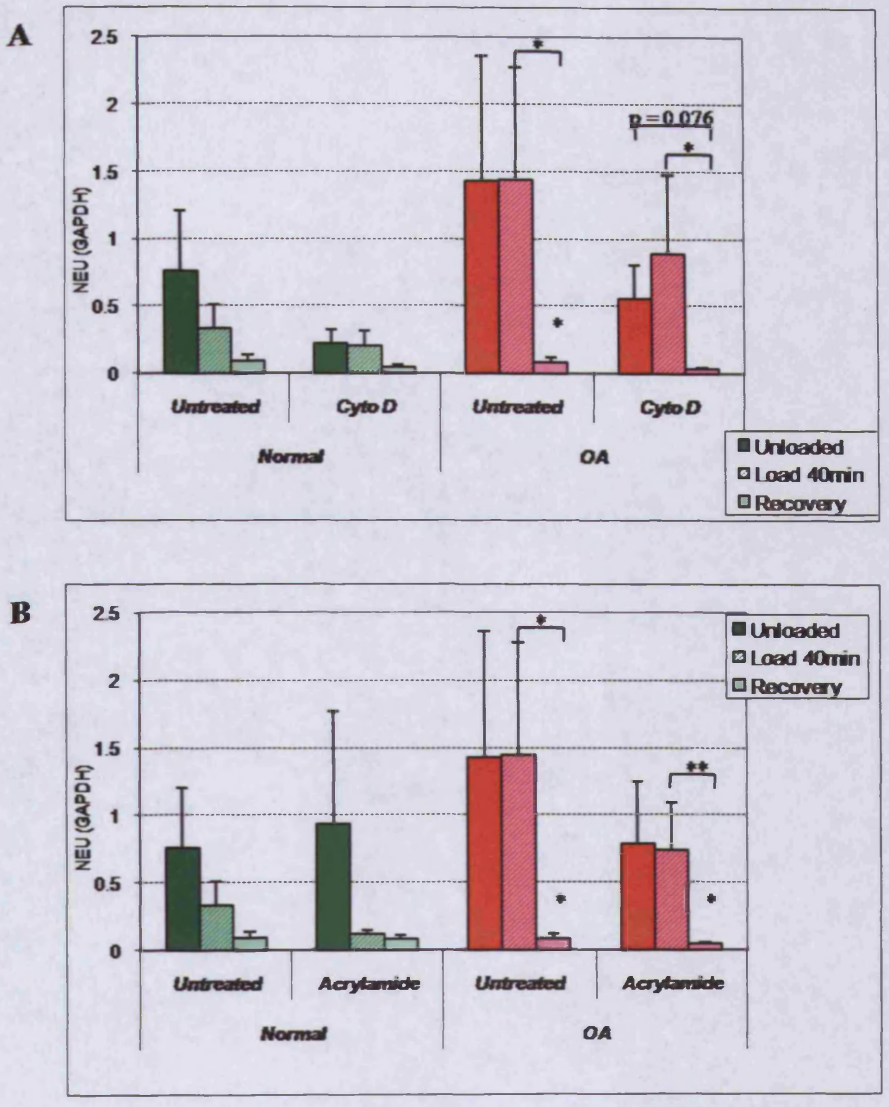

Figure 6.23:- COL1A1 gene expression changes with compressive load and cytoskeletal disruption. Absolute mRNA levels were determined using SYBR Green quantitative PCR and normalised to the housekeeping gene GAPDH. Nucleic acids were isolated from chondrocytes from normal and osteoarthritic (OA) cartilage, encapsulated in 3D agarose and cultured without (untreated) or with treatment for 24 hours before loading. Treatments were 1μM cytochalasin D to disrupt actin microfilaments or 2mM acrylamide to disrupt vimentin intermediate filaments (B). Agarose constructs were loaded for 40 minutes and left to recover for 5 hours. Data are presented as mean ± S.E.M. (n=5, n=3 for recovery). * $p < 0.05$, loaded and recovery compared to loaded or unloaded control.

MMP13

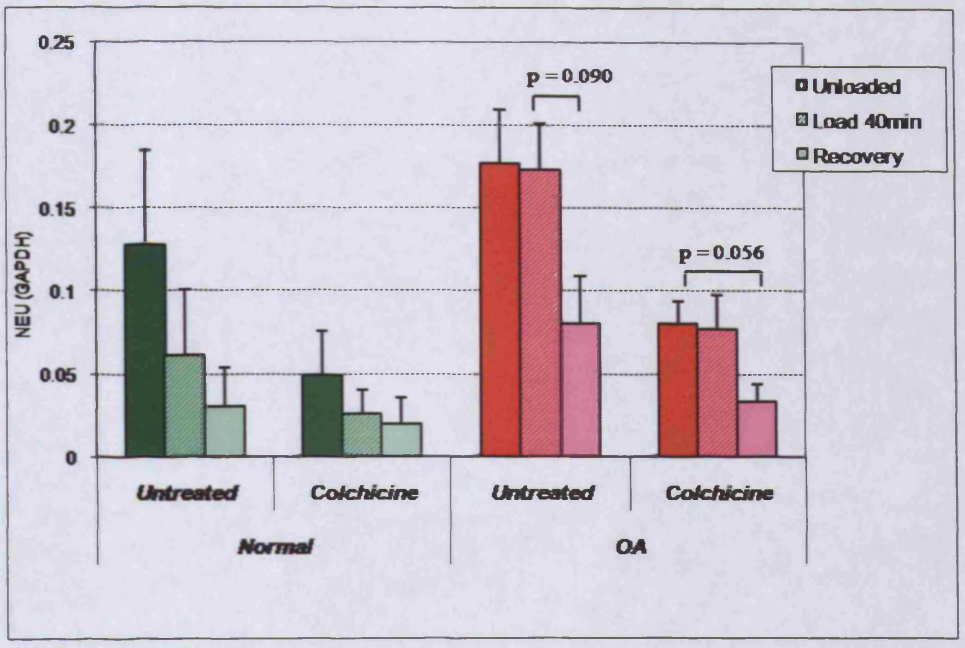

Figure 6.24:- MMP13 gene expression changes with compressive load and tubulin microtubule disruption. Absolute mRNA levels were determined using SYBR Green quantitative PCR and normalised to the housekeeping gene GAPDH. Nucleic acids were isolated from chondrocytes from normal and osteoarthritic (OA) cartilage, encapsulated in 3D agarose and cultured without (untreated) or with 1μM colchicine for 24 hours before loading. Agarose constructs were loaded for 40 minutes and left to recover for 5 hours. Data are presented as mean ± S.E.M. (n=5, n=3 for recovery).

Colchicine treatment significantly reduced *MMP13* mRNA expression in untreated OA chondrocytes ($p = 0.024$; section 5.2.3.3). However, microtubule disruption with colchicine did not further affect the cells response to load and/or recovery, as *MMP13* mRNA levels were consistently decreased in colchicine-treated OA chondrocytes even after recovery from load (2.4 fold; $p = 0.056$, Fig 6.24). The effects of acrylamide on *MMP13* expression were similar to that of colchicine; *MMP13* expression was reduced by acrylamide in normal and OA chondrocytes (unloaded OA cells, $p = 0.014$) but treatment did not alter the load-induced effects on *MMP13* expression in normal and OA chondrocytes (data not shown). Cytochalasin D treatment had no effect on *MMP13* expression or on the cells response to loading and/or recovery in normal and OA chondrocytes.

6.2.3.2.6 ADAMTS5

ADAMTS5 mRNA levels were significantly decreased in OA chondrocytes when compared with normal chondrocytes ($p = 0.048$) as described in section 5.2.3.3. Mechanical load did not affect *ADAMTS5* transcription in the presence or absence of cytochalasin D, colchicine or acrylamide in normal or OA chondrocytes (data not shown).

6.2.4 Changes in MMP-2 with Load and Cytoskeletal Element Disruption

Levels of pro- and active-MMP2 released into the media during loading and recovery of normal and OA chondrocytes were determined using gelatin substrate zymography. As demonstrated in section 5.2.4, levels of pro-MMP2 released into the media were reduced in normal chondrocytes when compared with OA chondrocytes; faint bands of pro-MMP2 were observed in untreated normal chondrocytes cultured for 24 hours whilst active-MMP2 was barely detectable (Fig 6.25, Normal Un UL). There was little pro- and active-MMP2 released into the media by untreated normal chondrocytes over the 10, 20 or 40 minute loading period and there was no clear accumulation of MMP-2 over a further 5 hour recovery period (Fig 6.25, Normal Un). Both pro- and active-MMP2 were detected in unloaded OA chondrocytes cultured for 24 hours (Fig 6.25, OA Un UL). Over the 10 minute loading period sufficient levels of pro-MMP2 were released by

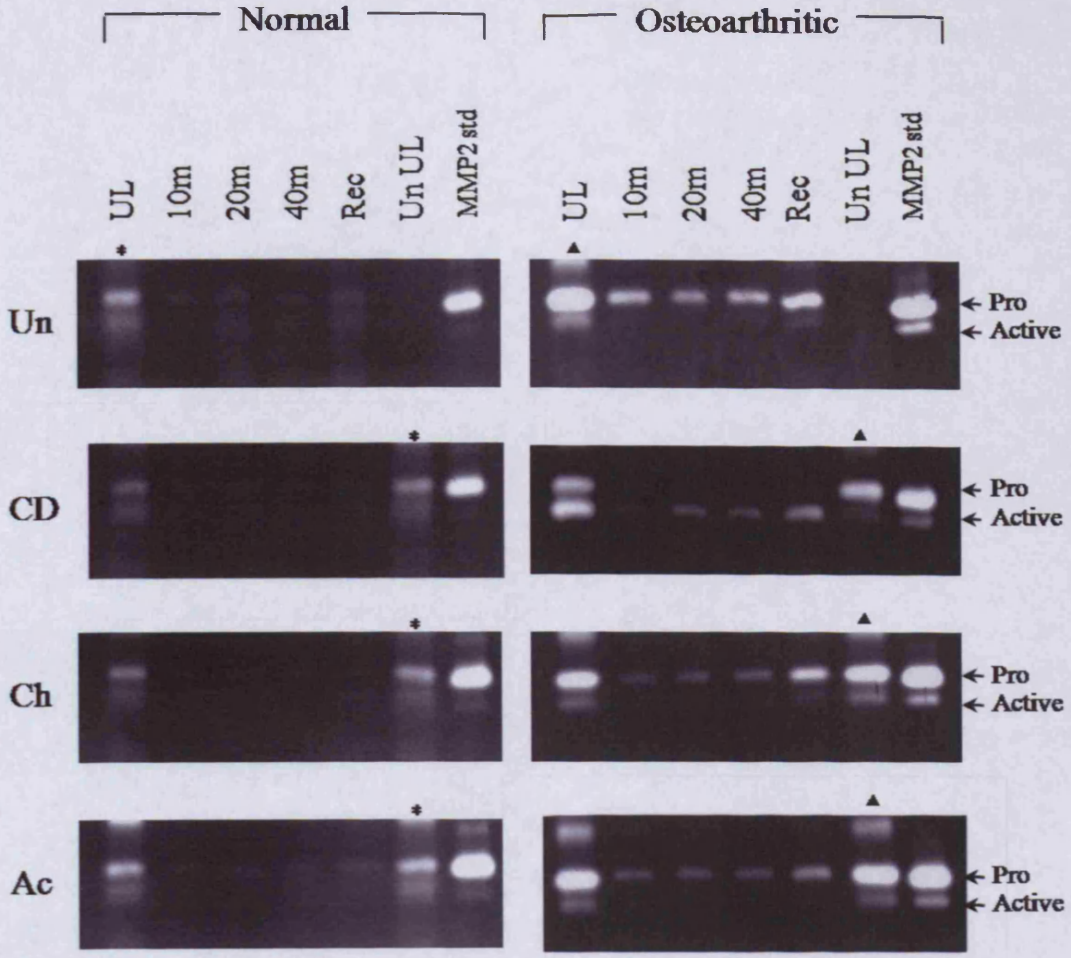

Figure 6.25:- The expression and activation of MMP-2 in chondrocytes isolated from normal and osteoarthritic (OA) cartilage, encapsulated in 3D agarose and cultured with or without treatment for 24 hours (UL). Media was replaced and agarose constructs loaded for 10, 20 or 40 minutes, or loaded for 40 minutes and left to recover for 5 hours (Rec). Gelatin substrate zymography was used to detect the latent (72kD) and active (62kD) forms of MMP-2 with white bands representing zones of gelatinolytic activity. Equivalent volumes of media were loaded. 'Un'- untreated chondrocytes, 'CD'- 1μM cytochalasin D, 'Ch'- 1μM colchicine, 'Ac'- 2 mM acrylamide treated chondrocytes. * or ▲ – same sample; untreated unloaded control for the normal (*) and OA (▲) donor displayed.

untreated OA chondrocytes to allow detection by gelatin zymography. No further increase in pro-MMP2 levels were evident after 20 and 40 minutes of loading, but there was an accumulation over a further 5 hour recovery period, where active-MMP2 was also detected (Fig 6.25, OA Un).

Treatment of normal chondrocytes with cytoskeletal disrupting treatments for 24 hours did not increase pro-MMP2 levels (Fig 6.25, Normal UL), although cytochalasin D increased MMP-2 activation as demonstrated in section 5.2.4. Neither the MMP-2 release induced by compressive loading, nor the accumulation of MMP-2 with recovery, was altered in normal chondrocytes treated with cytochalasin D, colchicine or acrylamide (Fig 6.25). Treatment of OA chondrocytes with cytochalasin D increased MMP2 activation, as demonstrated in section 5.2.4. Pro- and active-MMP2 were detected in the media of cytochalasin D-treated OA chondrocytes loaded for 10 minutes, with levels of active-MMP2 increasing after 20 and 40 minutes of load; a further accumulation of active-MMP2 was observed after a 5 hour recovery period (Fig 6.25, OA CD). Colchicine treatment had no further effect on MMP-2 synthesis and/or activation with load and/or recovery (Fig 6.25, OA Ac). MMP-2 activation was unaffected by acrylamide treatment in OA chondrocytes, but treatment did appear to reduce load-induced pro-MMP2 release and its accumulation over the recovery period (Fig 6.25, OA Ac).

MMP-9 was not detected in untreated normal and OA chondrocyte culture media by gelatin zymography and neither loading nor treatment increased MMP-9 expression to the level of detection (data not shown).

6.2.5 The Effect of Cytoskeletal Element Disruption on Stress under Compressive Load

Peak stress was determined for normal and OA chondrocyte/agarose constructs under a 15% compressive strain; changes in voltage were converted into force using a calibration curve (Fig 6.26 A) and force then converted to stress using the equation below.

$$\text{Stress (Pa)} = \frac{\text{Force (N)}}{9.5033 \times 10^{-5}\ (\text{cross-sectional area } m^2)}$$

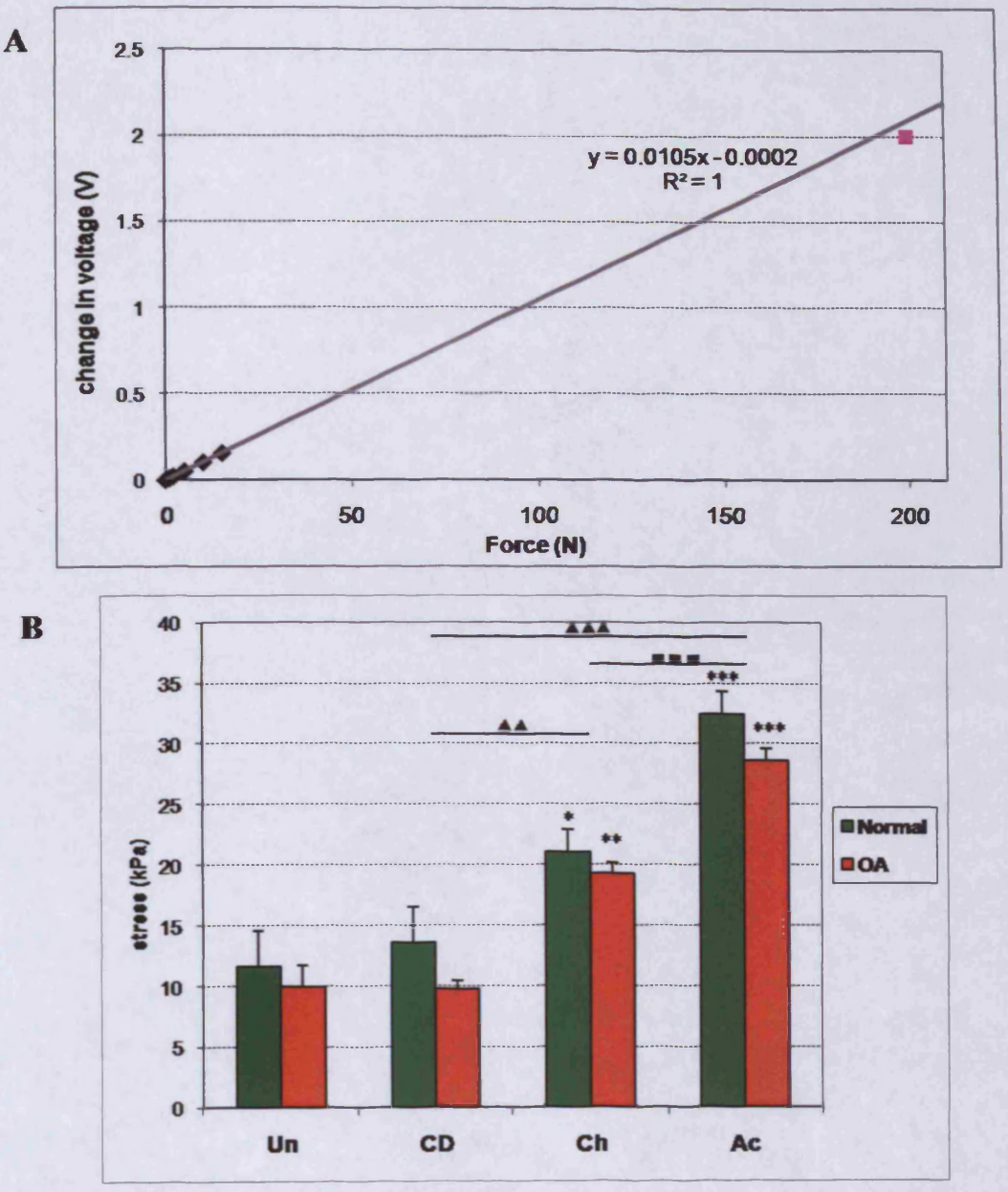

Figure 6.26:- Stresses experienced in chondrocyte-agarose constructs under a 15% strain. Were increased by colchicine and acrylamide treatment. A- Calibration curve for the loading machine. B- Calculated stresses in agarose constructs, under a 15% strain, containing chondrocytes isolated from normal (green) and osteoarthritic (red) cartilage. Constructs were cultured with or without the indicated treatment for 24 hours before loading. Using a calibration curve (A), voltage changes in constructs loaded for 30 seconds, 10 and 40 minutes were converted into force (N) and then stress (kPa). 'Un'- untreated chondrocytes, 'CD'- 1μM cytochalasin D, 'Ch'- 1μM colchicine, 'Ac'- 2 mM acrylamide treated chondrocytes. Graph shows mean of all time points ± SEM. * $p<0.05$, ** $p<0.01$, *** $p<0.001$: * relative to untreated, ▲ relative to CD, ■ relative to Ch.

There was no difference between normal and OA chondrocytes in the stress produced under loading of the chondrocyte/agarose constructs (Fig 6.26 B). Treatment of chondrocytes with cytochalasin D had no effect on the stress produced under loading of normal or OA chondrocytes. A significant increase in the stress in both normal and OA chondrocyte/agarose constructs under load was observed with colchicine (normal: 1.8 fold; $p = 0.050$. OA: 1.9 fold; $p = 0.009$) and acrylamide (normal: 2.8 fold; $p < 0.0001$. OA: 2.9 fold; $p = 0.0001$) treatment (Fig 6.26 B). The stress in colchicine- and acrylamide-treated chondrocyte/agarose constructs was significantly increased over that of the cytochalasin D-treated constructs (CD vs. Ch; $p = 0.002$. CD vs. Ac; $p < 0.001$) and the effect of acrylamide was also significant over that of colchicine ($p = 0.0004$).

	Gene / Cytoskeletal Element	Affected by Cyclic Compression?	Difference between Normal (N) and OA Response to Load?	Additive Effect of Cytoskeletal Element Disruption?
Cytoskeletal Organisation	Actin MFs	Yes – N & OA	Yes, with recovery	Tubulin, N recovery only Vimentin, N only
	Tubulin MTs	Yes – N & OA	Yes, with recovery	Tubulin, N & OA Vimentin, OA recovery only
	Vimentin IFs	Yes – N & OA	No	No
mRNA Levels: Cytoskeletal	β-actin	No	No	No
	Cofilin	ns	No	Actin, reduced response in N Actin, enhanced response in OA Vimentin, OA recovery only
	Destrin	Yes – N only	No (trend in OA)	Actin, N & OA
	Gelsolin	No	No	Vimentin, N & OA recovery
	Thymosin β4	ns	No	Actin, OA only Tubulin, OA only
	Paxillin	ns	No	Tubulin, N & OA Vimentin, OA 40min only
	β-tubulin	Yes – N only	Yes	Tubulin, N only Vimentin, N only
	Vimentin	No	No	Actin, N & OA recovery Vimentin, N recovery only
mRNA Levels: Matrix	BMF	No	No	No
	SOX9	Yes – OA only	Yes	Actin, OA only
	Aggrecan	ns	No	No
	COL1A1	Yes – OA only	Yes	No
	MMP13	ns	No	No
	ADAMTS5	No	No	No

Table 6.1:- Summary of results from loading experiments performed with or without cytoskeletal disruption. 'ns' is used where a trend was clear but changes were not statistically significant.

6.3 DISCUSSION

6.3.1 The Effect of Load on Chondrocyte Phenotype

Physiological load is required for the maintenance of articular cartilage integrity through its influence on the chondrocyte phenotype. Numerous studies both *in vivo* and *in vitro* have shown that load can induce both anabolic and catabolic changes in the chondrocyte phenotype, depending on the loading regime used.

The effect of the loading regime (15%, 0.5 Hz) on the phenotype of human normal and osteoarthritic chondrocytes in agarose was determined by assessing the expression of typical markers of the chondrocyte phenotype. There was a trend towards increased *SOX9* mRNA expression with cyclic compression of normal and OA chondrocytes in agarose, although no differences reached significance. Furthermore, *SOX9* expression was further up-regulated in OA chondrocytes after five hours of recovery post-loading. Dynamic compression of bovine cartilage explants at 0.1 Hz for one hour has been shown to increase *SOX9* expression (Fitzgerald et al., 2008). Other studies using differentiated chondrocytes have shown that dynamic mechanical load has no effect on *SOX9* expression. Cyclic compression (20%, 0.3 Hz) of single bovine chondrocytes or chondrons for 10 minutes had no effect on *SOX9* expression, nor did a recovery period of 18 hours after loading (Wang et al., 2009b, Wang et al., 2010). Cyclic hydrostatic pressure and cyclic tensile strain had no effect on *SOX9* expression in bovine chondrocytes in alginate (Wong et al., 2003). *SOX9* expression was unaffected by dynamically stretching (3%, 0.5 Hz) human chondrocytes in monolayer for three days at two hours per day (Das et al., 2008). By contrast, dynamic and static compression increased *SOX9* expression in rodent chondrocyte precursors encapsulated in hydrogels (Takahashi et al., 1998, Li et al., 2009a). In these studies, dynamic and static compression enhanced chondrogenesis as indicated by up-regulation of aggrecan and *COL2A1* expression in addition to *SOX9*.

The reported effects of mechanical load on aggrecan expression in differentiated chondrocytes are varied. Aggrecan mRNA levels were elevated in bovine chondrocytes in agarose subjected to static hydrostatic pressure for four hours (Toyoda et al., 2003). Cyclic compression (15%) of porcine chondrocytes in agarose at 0.33 Hz or 1 Hz for 12 hours up-regulated aggrecan expression (Kock et al., 2009) as did intermittent dynamic

compression (15%, 1 Hz) of bovine chondrocytes in agarose for 24 hours (Mio et al., 2005). Aggrecan expression is also up-regulated in bovine cartilage explants subjected to dynamic compression at 0.1 Hz (Fitzgerald et al., 2008) and in bovine chondrons dynamically compressed to 20 or 40% strain at 0.3 Hz for 10 minutes (Wang et al., 2009b). In normal human chondrocytes cultured as a monolayer, cyclic pressure-induced strain at 0.33 Hz for 20 minutes up-regulated aggrecan expression (Millward-Sadler et al., 2000a), whilst dynamic stretching (3%) at 0.5 Hz for two hours per day for three days down-regulated aggrecan expression (Das et al., 2008). Another study applying cyclic tensile strain to bovine chondrocytes in alginate showed no change in aggrecan expression with load (Wong et al., 2003). My results showed that, in human normal and OA chondrocytes in agarose, cyclic compression (15%, 0.5 Hz) for 10 to 40 minutes showed a trend towards reducing aggrecan expression, although no changes reached statistical significance and levels began to return to basal levels after a five hour recovery post-load. Differences to other published results are likely due to differences in culture conditions, which would influence the phenotype of control cells, and also to the loading regimes implemented. In addition, the duration of loading used here is relatively short when compared with other studies loading for several hours and focused more towards the improvement of matrix synthesis for tissue engineering strategies.

With regards to chondrocyte phenotype, the trend towards up-regulation of *SOX9* and down-regulation of aggrecan transcription with cyclic compression appears contradictory. These changes could however be transient, with anabolic changes in gene expression occurring at time points later than those studied here. This would be supported by the apparent up-regulation of aggrecan with post-load recovery and by studies of chondrocytes in agarose, subjected to longer periods of dynamic compression or recovery post-load, where increased aggrecan expression and sGAG content have been demonstrated (Buschmann et al., 1995, Chowdhury et al., 2003, Mio et al., 2005, Mauck et al., 2007, Kock et al., 2009). Further work is required to determine *COL2A1* expression levels; this would help to further determine the effects of load on phenotype.

A reduction in *COL1A1* and *MMP13* expression implies that cyclic compression of normal and OA human chondrocytes in agarose positively affects the chondrocyte phenotype. Both *MMP13* and *COL1A1* mRNA expression showed a trend of decreasing with cyclic compression of human normal chondrocytes, with expression further

decreasing after five hours of recovery. In OA chondrocytes, *COL1A1* and *MMP13* expression did not change with cyclic compression but subsequently decreased five hours after compression. In conjunction with the increase in *SOX9* mRNA with recovery post-load, the decrease in *COL1A1* and *MMP13* mRNA expression supports a positive effect of the loading regime on phenotype, particularly in OA chondrocytes. Expression of *MMP13* and *COL1A1* has been shown to be down-regulated in bovine chondrocytes in alginate subjected to cyclic hydrostatic pressure for three hours per day for three days (Wong et al., 2003) and in monolayer cultured human normal chondrocytes subjected to dynamic stretch at 0.5 Hz for two hours per day for three days (Das et al., 2008). By contrast, cyclic tensile strain increased *MMP13* expression in bovine chondrocytes in alginate (Wong et al., 2003). *MMP13* mRNA expression was also increased in bovine cartilage explants subjected to dynamic or static compression (Fitzgerald et al., 2008), and in bovine chondrocytes on calcium polyphosphate scaffolds two hours after cyclic compression (1.4%, 1 Hz, 30 minutes), with MMP-13 protein levels increased six hours post-compression (De Croos et al., 2006). Recent work using the same model separated deep zone and surface-mid zone bovine cartilage chondrocytes and showed that cyclic compression up-regulated *MMP13* expression in surface-mid zone chondrocytes but down-regulated *MMP13* expression in deep zone chondrocytes (Raizman et al., 2009).

Another matrix-degrading protease studied, ADAMTS5, was unaffected by cyclic compression in normal and OA human chondrocytes embedded in agarose. In contrast to these results, other studies have shown an effect of mechanical compression on *ADAMTS5* expression in chondrocytes; in bovine cartilage explants, *ADAMTS5* expression is up-regulated in response to dynamic compression (5%, 0.1 Hz) for one hour (Fitzgerald et al., 2008), static compression (50%) for two to 48 hours (Wheeler et al., 2009) and in response to a single injurious compression (Lee et al., 2005). Differences could be due to the use of human as opposed to bovine chondrocytes, isolated chondrocytes embedded in agarose rather than cartilage explants, or due to the difference in the dynamic compressive loading regime utilised.

Despite being down-regulated by cytoskeletal disruption in OA chondrocytes (chapter 5), mRNA expression of the pro-apoptotic gene *BMF* was unaffected by cyclic compression in normal and OA human chondrocytes embedded in agarose. There are no previous reports of an effect of mechanical stimulation on *BMF* expression. However,

anoikis-induced transcriptional up-regulation of *BMF* expression is inhibited by activation of MEK/ERK signalling (Schmelzle et al., 2007). Activation of ERK by dynamic compression of chondrocytes in agarose (Bougault et al., 2008) could therefore prevent changes in *BMF* expression in response to loading. Phosphorylation of BMF by JNK causes its release from dynein light chain 2 (DLC2) and therefore from the myosin V motor complex which sequesters it to microfilaments (Puthalakath et al., 2001, Lei and Davis, 2003). JNK signalling is activated by cyclic compression of chondrocytes seeded in calcium polyphosphate scaffolds (De Croos et al., 2006) and therefore effects of compression on BMF in human chondrocytes could be mediated post-translationally, i.e. via increased phosphorylation.

6.3.1.1 Additional Effects of Cytoskeletal Disruption with Load on Chondrocyte Phenotype

Disruption of the cytoskeleton in normal and OA chondrocytes embedded in agarose altered the transcriptional response of *SOX9* and aggrecan to cyclic compression. Cytochalasin D treatment, i.e. actin cytoskeletal disruption, appeared to decrease *SOX9* expression in normal chondrocytes subjected to 40 minutes of loading. In OA chondrocytes, disruption of the actin cytoskeleton with cytochalasin D inhibits the increases in *SOX9* expression induced after 20 minutes of cyclic compression and five hours recovery. This suggests that load-induced changes in *SOX9* expression are dependent on the actin cytoskeleton, particularly in OA chondrocytes. Numerous studies have demonstrated a link between *SOX9* expression and changes in actin cytoskeletal organisation, although these are in relation to the role of the actin cytoskeleton in regulation of the chondrocyte phenotype (Woods et al., 2005). In human chondrocytes disruption of actin stress fibres using cytochalasin D, culturing cells in alginate or inhibition of ROCK up-regulates *SOX9* expression (Tew and Hardingham, 2006). Activation of p38 MAPK was shown to stabilise *SOX9* mRNA in human chondrocytes, but only in the absence of actin stress fibres. In support of this, a recent study has shown that osmotic pressure activates p38 MAPK and only up-regulates *SOX9* expression in human articular chondrocytes in the absence of actin stress fibres (Tew et al., 2009). Culture of passaged chondrocytes in alginate or disruption of actin stress fibres by inhibition of ROCK promoted up-regulation of *SOX9* expression in response to hyperosmotic conditions; however, ROCK inhibition had no effect on hyperosmolarity-induced *SOX9* up-regulation in freshly isolated chondrocytes that did not contain actin

stress fibres. p38 MAPK signalling is activated in chondrocytes by dynamic compression (Fitzgerald et al., 2008, Bougault et al., 2008) and hyperosmolarity (Tew et al., 2009); this could stabilise *SOX9* mRNA, providing a mechanism for compression-induced up-regulation of *SOX9* mRNA that is dependent upon actin cytoskeletal organisation. An alternative regulatory mechanism for SOX9 expression and activity that is dependent upon actin could be post-translational phosphorylation. Recent work has shown that dynamic compression (15%, 0.5 Hz) of human primary chondrocytes embedded in agarose for two hours induced a ROCK-dependent increase in the nuclear localisation of SOX9 protein (Haudenschild et al., 2010). Dynamic compression for 16–18 hours increased SOX9 protein levels and phosphorylation. Work in a human chondrosarcoma cell line showed ROCK directly phosphorylates serine-181 in SOX9 which promotes SOX9 nuclear localisation and increases its transcriptional activity. SOX9 can transcriptionally regulate *SOX9* expression via a positive feedback loop (Kumar and Lassar, 2009). Disruption of actin microfilaments with cytochalasin D could alter Rho and therefore ROCK activity, which would subsequently affect the transcriptional activity of SOX9 and *SOX9* mRNA levels.

Whilst disruption of the actin or vimentin cytoskeleton did not affect the trend towards decreased aggrecan expression in response to cyclic compression, disruption of these elements did appear to prevent the increase in aggrecan mRNA expression after five hours of recovery. It is therefore possible that the recovery of aggrecan expression following cyclic compression is mediated by the actin and vimentin cytoskeletal networks. In support of this role for the vimentin cytoskeleton, aggrecan expression is reduced in response to disruption of intermediate filament organisation in bovine chondrocytes (Blain et al., 2006) and in response to siRNA-mediated knockdown of vimentin in human multipotent progenitor cells (Bobick et al., 2010). In contrast to the suggested role for the actin cytoskeleton in mediating the recovery of aggrecan expression post-load, disruption of actin microfilaments with cytochalasin D did not prevent up-regulation of aggrecan expression in murine multipotent progenitor cells induced by cyclic hydrostatic pressure (1 Hz) applied for two hours per day for three days (Shim et al., 2008). Differences to the results presented here could be due to differences in chondrocyte maturity (human mature chondrocytes as opposed to murine mesenchymal stem cells), type of load applied (compressive load as opposed to hydrostatic pressure), load frequency (0.5 Hz rather than 1 Hz), or cellular context

(embedded in agarose as opposed to pellet culture). As for SOX9, a link between aggrecan expression and actin cytoskeletal disruption has been demonstrated in the context of chondrocyte differentiation, with cytochalasin D increasing aggrecan expression and enhancing chondrogenesis in mouse embryonic stem cells cultured in chondrogenic medium (Zhang et al., 2006a). The effect of actin disruption on aggrecan expression however is dependent on cellular context; disruption of actin stress fibres in chondrocytes up-regulates aggrecan expression in monolayer but down-regulates aggrecan expression in 3D micromass culture (Woods et al., 2005); in monolayer, the positive effect of actin disruption on phenotype, i.e. cell rounding, could mask the effect on transcription observed in 3D. In the present study, disruption of tubulin microtubules in human chondrocytes embedded in agarose had no effect on load-induced changes in aggrecan expression. This is in contrast to a previous report showing that disruption of microtubules in monolayer chondrocytes, by treatment with nocodazole, prevents the up-regulation of proteoglycan synthesis in response to cyclic hydrostatic pressure (Jortikka et al., 2000); however, the use of monolayer culture and therefore the altered differentiation status could explain the difference in results.

Disruption of the chondrocyte cytoskeleton had no effect on the load-induced changes in mRNA expression of any other chondrocyte phenotype marker studied, indicating that mechanical regulation of their expression likely occurs independently of the cytoskeleton. That cytoskeletal disruption affects mechano-regulation of these genes at later time points or after longer periods of loading than studied here cannot be excluded.

6.3.2 The Effect of Load on the Chondrocyte Cytoskeleton

Actin Microfilaments

Remodelling of the actin cytoskeleton in response to cyclic compression was evident in both normal and OA human chondrocytes. In normal chondrocytes, cortical F-actin appeared less punctate after 40 minutes of cyclic compression, whilst in OA chondrocytes punctate spots became clearer and less tightly packed. Load-induced changes in actin localisation appeared to be reversible, with staining showing an actin organisation similar to that of unloaded controls after five hours of recovery; in OA chondrocytes actin microfilaments appeared clearer after recovery than in unloaded controls. This is supported by a previous study demonstrating remodelling of the actin cytoskeleton in response to two hours of cyclic compressive loading (15%, 1 Hz) of

bovine chondrocytes in agarose that was reversible within one hour of recovery (Knight et al., 2006). This study showed a more punctate appearance of actin staining immediately after loading. ROCK-dependent increases in punctate F-actin structures have also been observed in normal human chondrocytes embedded in agarose subjected to 20 minutes of dynamic compression (Haudenschild et al., 2008a). Interestingly, in the present study this increase in punctate actin staining was observed in human OA chondrocytes but not in normal chondrocytes, although the loss of punctate staining in normal chondrocytes demonstrated actin remodelling was occurring. It should be noted however that cytoskeletal organisation after 20 minutes of compressive loading was not determined in the present study; therefore reversible increases in punctate actin staining could have occurred earlier than the 40 minute time point assayed. A net cortical actin depolymerisation in response to cyclic compression at 1 Hz for 10 seconds has been shown in bovine chondrocytes in agarose, with cortical actin intensity decreasing after 10 minutes of recovery (Campbell et al., 2007). Actin remodelling appears to be the result of the dynamic changes in chondrocyte shape as there are no changes in actin cytoskeletal organisation in response to static compression of rat articular cartilage (Durrant et al., 1999) or cyclic physiological hydrostatic pressure in human chondrocytes in alginate (Fioravanti et al., 2003).

In addition to altering actin organisation, cyclic compression showed a trend of affecting β-actin mRNA expression in human chondrocytes in agarose. In normal chondrocytes, β-actin expression was transiently down-regulated by 10 and 20 minutes of cyclic compression, increasing to basal levels by 40 minutes of compression but then decreasing after five hours of recovery. β-actin expression also appeared to be down-regulated in OA chondrocytes by cyclic compression, with levels remaining decreased after recovery. This suggests that the recovery of actin organisation is not a result of increases in β-actin transcription. However, altered expression of actin-regulatory proteins in response to cyclic compression could also result in actin remodelling. Consistent with this, mRNA expression of the actin-depolymerising factor destrin was up-regulated in normal human chondrocytes after 10 minutes of cyclic compression. Expression levels then began to decrease with increasing duration of load. Expression of the actin-depolymerising factor cofilin also showed a trend to increase in normal chondrocytes with increasing duration of cyclic compression. Expression of both cofilin and destrin mRNA is up-regulated in response to 10 minutes of dynamic compression

(15%, 1 Hz) in bovine chondrocytes embedded in agarose (Campbell et al., 2007). This study showed no change in expression of the actin-severing factor gelsolin in response to dynamic compression of bovine chondrocytes; this was also observed here in normal and OA human chondrocytes seeded in agarose. Campbell *et al.* 2007 also showed no change in expression of the G-actin sequestering protein thymosin β4 in response to dynamic compression of bovine chondrocytes in agarose. In contrast to this, thymosin β4 expression appeared to be up-regulated in the present study in normal human chondrocytes subjected to 10 and 20 minutes of cyclic compression; expression levels returned to baseline by 40 minutes of load and further decreased following five hours of recovery. Expression of thymosin β4 was up-regulated by 10 minutes of dynamic compression (0.5 MPa, 1 Hz) in bovine cartilage explants (Blain et al., 2003). Cyclic compression had no effect on cofilin, destrin or thymosin β4 expression in OA human chondrocytes, suggesting an effect of pathology on the inability of the cell to respond to mechanical load via the actin cytoskeleton-regulatory proteins.

Expression of paxillin, which associates with actin microfilaments at cell-matrix attachment sites, showed a trend to decrease following five hours of recovery post-load in the present study. Phosphorylation of paxillin is enhanced in human chondrocytes in response to cyclic pressure-induced strain, although this study was performed on chondrocytes in monolayer, an adhesion-dependent culture system promoting the formation of paxillin-containing focal adhesions and actin stress fibres (Lee et al., 2000). Cytoskeletal dynamics in monolayer are therefore likely to differ from those used in this study. However, a decrease in paxillin expression post-load in agarose embedded human chondrocytes could indicate an effect on paxillin-mediated mechanotransduction pathways.

Tubulin Microtubules

Cyclic compression of normal and OA human chondrocytes in agarose induced changes in the organisation of the tubulin cytoskeleton. In both normal and OA chondrocytes, tubulin staining became punctate and the intensity at the cell periphery was lost following 40 minutes of load; in normal chondrocytes tubulin staining became more intense in the perinuclear region. Following five hours of recovery, cortical tubulin staining was regained and microtubule bundles appeared clearer. Interestingly, load and recovery produced a tubulin organisation resembling that of chondrocytes treated with

colchicine. The increased clarity of microtubules following load and recovery or colchicine treatment could therefore be due to: 1) collapse of microtubules into bundles, making them appear thicker and less densely packed, or 2) disruption of a proportion of tubulin microtubules, with the remaining intact tubule bundles then more clearly visible. Interestingly, a recent study has shown that mechanical compression induces reversible widening (i.e. thickening) of mitotic spindles in mammalian cells (Dumont and Mitchison, 2009). A previous study showed no change in tubulin network organisation in human chondrocytes in alginate subjected to physiological cyclic hydrostatic pressure (Fioravanti et al., 2003). However, in the same model, continuous high hydrostatic pressure (non-physiological loads) induced changes in tubulin organisation; the uniform peripheral localisation of microtubules in normal chondrocytes was lost in normal chondrocytes after pressurisation (Fioravanti et al., 2005). In support of the observed remodelling of tubulin microtubules, cyclic compression of normal and OA human chondrocytes in agarose induced up-regulation of β-tubulin mRNA expression. β-tubulin expression was increased in response to loading in normal and OA chondrocytes, although the further increase in expression with recovery was only observed in normal chondrocytes. Load-induced remodelling of the microtubule network could have reduced the pool of β-tubulin monomers in the chondrocytes; reduction below a specific critical level would suppress tubulin auto-regulation via mRNA degradation and therefore increase β-tubulin mRNA levels (Cleveland and Havercroft, 1983, Cleveland et al., 1983, Yen et al., 1988).

Vimentin Intermediate Filaments

Changes in the organisation of the vimentin cytoskeleton were also observed in response to cyclic loading of human chondrocytes in agarose. In normal chondrocytes, vimentin intermediate filament bundles appeared thicker and more densely packed following cyclic compression, and regions of the cortical network were lost. Filament bundle thickening continued throughout the recovery period. As observed with the tubulin network and colchicine, vimentin organisation in recovery cells resembled that of normal chondrocytes treated with acrylamide; increased filament thickness could therefore indicate the formation of bundles and partial collapse of the intermediate filament network. In contrast to normal chondrocytes, vimentin filament bundles in OA chondrocytes appeared finer in response to cyclic compression then appeared thicker and more loosely packed following the recovery period. Changes in vimentin cytoskeletal

organisation have been observed in cartilage explants in response to static compression (Durrant et al., 1999) and a single impact load (Henson and Vincent, 2008). Remodelling of the vimentin cytoskeleton in human chondrocytes in response to cyclic compression was not accompanied by changes in vimentin gene expression.

6.3.2.1 Additional Effects of Cytoskeletal Disruption with Load on Chondrocyte Cytoskeleton

Actin Microfilaments

Disruption of actin microfilaments with cytochalasin D did not prevent remodelling of the actin cytoskeleton in response to cyclic compression, nor did it have any additional effect on changes in β-actin mRNA expression in response to load. However, cytochalasin D treatment did affect load-induced changes in expression of actin associated proteins, although this was not translated into a difference in load-induced F-actin reorganisation. In normal chondrocytes, cytochalasin D reduced the load-induced increase in cofilin expression but caused an increase in destrin expression following recovery that was not observed in untreated chondrocytes. Load-induced up-regulation of thymosin β4 expression was unaffected by cytochalasin D in normal chondrocytes. In contrast, cytochalasin D enhanced load-induced up-regulation of thymosin β4 and destrin expression in OA chondrocytes; thymosin β4 expression decreased following recovery whilst destrin expression remained elevated. Cytochalasin D also enhanced the load-induced up-regulation of cofilin expression in OA chondrocytes. This indicates that the effects of load on cofilin, destrin and thymosin β4 expression are partially mediated by the actin cytoskeleton, which could indicate a feedback loop as these proteins regulate actin microfilament turnover. The role of the actin cytoskeleton in load-induced changes in cofilin and thymosin β4 is altered in OA chondrocytes, with expression in these cells appearing to be more sensitive to cyclic compression in the presence of actin microfilament disruption.

Disruption of tubulin microtubules with colchicine had no effect on load-induced remodelling of the actin cytoskeleton. Changes in β-actin and cofilin expression in response to cyclic compression were also unaffected by colchicine treatment. However, microtubule disruption did alter load-induced changes in destrin and thymosin β4 expression; thymosin β4 expression was up-regulated with cyclic compression whilst destrin expression increased with recovery in colchicine-treated OA chondrocytes. This

effect of colchicine treatment was only observed in OA chondrocytes. A previous study has demonstrated a link between disruption of microtubule dynamics and increases in thymosin β4 expression (Oh et al., 2006). Tubulin disruption enhanced the load-induced reduction in paxillin expression in normal and OA chondrocytes. Paxillin has been shown to bind to α- and γ-tubulin in lymphocytes, co-localising with the microtubule organising centre in both adhesive- and suspension-cultured cells (Herreros et al., 2000). In endothelial cells decreased microtubule stability, induced by co-culture with vascular smooth muscle cells or colchicine treatment, is associated with increased paxillin phosphorylation (Hu et al., 2006, Wang et al., 2009c). The results indicate that the effects of load on destrin, thymosin β4 and paxillin expression are partially mediated by the tubulin cytoskeleton and that, as for actin microfilament-mediated responses, this is altered in OA chondrocytes.

Disruption of vimentin intermediate filaments with acrylamide did not affect actin organisation in loaded human chondrocytes, although treatment did result in loss of cortical actin localisation following recovery in normal chondrocytes. Acrylamide treatment did not alter the load-induced changes in expression of β-actin, destrin or thymosin β4, indicating that mechanical regulation of these genes occurs independently of vimentin intermediate filaments. In the presence of acrylamide, expression of cofilin and gelsolin were down-regulated following five hours of recovery post-load in both normal and OA chondrocytes, indicating that vimentin intermediate filaments could play a role following the removal of compressive load. Acrylamide delayed the load-induced down-regulation of paxillin transcription but did not alter the decrease in levels after recovery of OA chondrocytes; acrylamide did not alter load-induced paxillin mRNA changes observed in normal chondrocytes. As vimentin intermediate filaments play an important role in cell signalling, acting as both a phospho-protein and as a regulator of ERK activation (Perlson et al., 2006, Kim and Coulombe, 2007), they could mediate compression-induced changes in paxillin mRNA expression in OA chondrocytes and recovery of cofilin and gelsolin in normal and OA chondrocytes. In addition to the ability to alter transcription of paxillin demonstrated here, disruption of vimentin intermediate filaments with acrylamide has previously been shown to inhibit tyrosine phosphorylation of paxillin in human colon cancer cells adhered to collagen (Haier and Nicolson, 1999).

Tubulin Microtubules

Disruption of tubulin microtubules with colchicine had an additive effect with load, enhancing changes in tubulin organisation and expression. Colchicine treatment enhanced the up-regulation of β-tubulin expression induced by cyclic compression in normal chondrocytes, with expression remaining elevated following five hours of recovery; no additive effect was observed in OA chondrocytes. In both normal and OA chondrocytes the punctate tubulin staining induced by cyclic compression was lost with colchicine treatment, which caused microtubule bundles to appear thicker. Colchicine particularly affected microtubule organisation following recovery after loading, causing thickening of microtubule bundles in normal chondrocytes but loss of the thick tubule bundles in OA chondrocytes. The additive effect of colchicine and load on tubulin expression and organisation indicates the presence of a regulatory feedback loop between tubulin microtubule dynamics and β-tubulin transcriptional regulation. An auto-regulatory loop exists for β-tubulin, with degradation of ribosome-bound β-tubulin mRNA if the pool of β-tubulin monomers increases above a specific level (Cleveland and Havercroft, 1983, Cleveland et al., 1983, Gay et al., 1987, Pachter et al., 1987). As discussed above, load-induced microtubule remodelling observed in normal human chondrocytes could reduce the β-tubulin monomer pool and increase β-tubulin mRNA levels. The enhanced up-regulation in the presence of colchicine could be due to its suppression of microtubule dynamics (Panda et al., 1995), increasing the demand for β-tubulin monomers and preventing β-tubulin mRNA degradation. The effect of colchicine on load-induced changes in β-tubulin expression in normal chondrocytes was mimicked by disruption of vimentin intermediate filaments with acrylamide. Like colchicine, acrylamide treatment also resulted in a thicker appearance of microtubule bundles in unloaded controls. Whilst acrylamide did not alter load-induced tubulin reorganisation, it did appear to slow the recovery of organisation in both normal and OA chondrocytes, perhaps indicating a role for vimentin intermediate filaments in regulating microtubule dynamics or organisation. There is evidence demonstrating that vimentin intermediate filaments co-localise with detyrosinated microtubules in fibroblasts and that detyrosinated microtubules recruit vimentin intermediate filaments via kinesin (Gurland and Gundersen, 1995, Liao and Gundersen, 1998, Kreitzer et al., 1999). Load-induced changes in the tubulin cytoskeleton most likely occurred independently of the actin cytoskeleton as cytochalasin D treatment had no clear effect on β-tubulin expression or on microtubule organisation.

Vimentin Intermediate Filaments

An additive effect of acrylamide treatment and cyclic compression was less clear for changes in the vimentin cytoskeleton when compared with the microtubule network. In normal chondrocytes treated with acrylamide, load and load with a recovery resulted in regions of diffuse staining and an apparent loss of vimentin intermediate filament bundles towards the cell periphery. However, acrylamide did not affect the thickening of intermediate filament bundles in normal and OA chondrocytes following recovery from load. By contrast, acrylamide treatment enhanced the down-regulation of vimentin expression over the five hour recovery period in normal chondrocytes. Disruption of actin microfilaments with cytochalasin D also enhanced down-regulation of vimentin transcription following recovery from loading. Vimentin gene transcription could be down-regulated in response to load/recovery-induced reorganisation of the actin or vimentin cytoskeleton, perhaps due to interruption of shuttling of transcription factors along F-actin and ERK regulation by vimentin (Perlson et al., 2006); down-regulation of vimentin transcription would therefore be enhanced in the presence of cytochalasin D or acrylamide, as observed in the present study. Cytochalasin D also affected the load-induced reorganisation of the vimentin network, increasing the thickness of intermediate filament bundles in both loaded normal and OA chondrocytes. This could be a structural response to compensate for the loss of actin microfilaments, as both the vimentin and actin cytoskeleton contribute to the viscoelastic properties of chondrocytes (Trickey et al., 2004). Vimentin organisation following recovery was unaffected by cytochalasin D in OA chondrocytes, whilst intermediate filament bundles appeared finer and shorter with cytochalasin D treatment and recovery in normal chondrocytes. Despite showing no effect on load-induced changes in vimentin mRNA expression, disruption of tubulin microtubules with colchicine altered vimentin reorganisation in response to cyclic compression. In normal chondrocytes, colchicine treatment caused intermediate filament bundles to become less clear following recovery from loading, whilst in OA chondrocytes, intermediate filament bundles appeared thicker immediately after compression in the presence of colchicine. The suppression of microtubule dynamics in the presence of colchicine could alter tyrosination of tubulin and therefore the recruitment of vimentin intermediate filaments (Gurland and Gundersen, 1995, Kreitzer et al., 1999).

6.3.2.2 Effects of Load and Cytoskeletal Disruption on Mechanical Properties of Chondrocytes

Disruption of vimentin intermediate filaments appears to affect the recovery of cofilin, gelsolin and vimentin mRNA expression and microtubule organisation following cyclic compression of human chondrocytes. A recent study has shown that cytoskeletal disruption slows the recovery of chondrocytes following mechanical compression (Ofek et al., 2009). Treatment of adult bovine chondrocytes with cytochalasin D, colchicine or acrylamide increased the time taken for recovery of cell height following compression of single cells for 30 seconds. The same study showed that disruption of actin microfilaments decreased bulk cell stiffness, disruption of tubulin microtubules increased cell compressibility, and disruption of vimentin intermediate filaments decreased cell compressibility (Ofek et al., 2009). Human chondrocyte viscoelasticity and cell stiffness is also reduced by actin microfilament disruption (Trickey et al., 2004). In contrast to the results presented by Ofek *et al.* 2009, other studies have shown that vimentin intermediate filament disruption reduces cell stiffness and viscoelasticity (Wang and Stamenovic, 2000, Trickey et al., 2004) whilst microtubule disruption has no effect (Trickey et al., 2004). In the present study, the stress in chondrocyte/agarose constructs under compression was increased by colchicine or acrylamide treatment, suggesting that disruption of the tubulin or vimentin cytoskeleton reduces cell compressibility and therefore increases the force required to produce a 15% strain. The observed effect of vimentin disruption is supported by the results of Ofek *et al.* 2009; the authors suggest that the intermediate filaments function as tensile elements, effectively pulling the cell together (Ofek et al., 2009). Intermediate filaments have been shown to increase in stiffness with increasing stress and this behaviour in cells is not inhibited by acrylamide treatment, nor is it absent from vimentin-deficient fibroblasts (Wang and Stamenovic, 2000). In contrast to the studies mentioned above which were performed using isolated chondrocytes, the chondrocytes studied here were cultured in agarose for three days prior to cyclic compression. Chondrocytes could therefore have begun to synthesise and accumulate a pericellular matrix, the mechanical properties of which could influence the compressibility of chondrocyte/agarose constructs. A previous study showed that bovine chondrocytes exhibit a 'halo' of pericellular matrix after 24 hours in agarose culture, with sGAG and collagen content increasing from day one to day six of culture (Knight et al., 1998). Cell deformation under compressive strain was reduced with increasing pericellular matrix accumulation; at day six the pericellular matrix was

stiffer than the 3% agarose and did not deform during compression. It is also possible therefore that altered pericellular matrix synthesis or retention in response to cytoskeletal disruption could also influence the mechanical properties of chondrocyte/agarose constructs. Cytochalasin D reduces pericellular matrix assembly and retention (Nofal and Knudson, 2002) and acrylamide reduces collagen synthesis in bovine chondrocytes (Blain et al., 2006). Human chondrocytes in the present study were cultured for two days in agarose, then for a further 24 hours with or without cytoskeletal disrupting reagents before compression. As cytochalasin D treatment had no effect on stress under compression, and acrylamide increases rather than reduces stress, it is likely that the effects of cytoskeletal disruption on pericellular matrix synthesis or retention are not significant enough after 24 hours to affect the mechanical properties of the constructs. It is therefore likely that the effects of cytoskeletal disruption on stress under compression are predominantly due to changes in the mechanical properties of the chondrocyte.

6.3.3 The Effect of Pathology on Load-Induced Changes

For a number of the genes studied, load-induced changes in expression differed between normal and OA human chondrocytes. These differences could be indicative of different or divergent mechanotransduction pathways in OA chondrocytes, which has been previously demonstrated in monolayer for the integrin-, stretch-activated ion channel- and IL-4-dependent mechano-transduction pathway (Millward-Sadler et al., 2000b, Salter et al., 2002); see section 6.1.3.

SOX9 mRNA levels increased after five hours of recovery from 40 minutes of cyclic compression in agarose embedded OA human chondrocytes; this response was not observed in normal human chondrocytes. Furthermore, disruption of actin microfilaments with cytochalasin D inhibited the load/recovery-induced increase in *SOX9* mRNA levels in OA chondrocytes, suggesting that load-induced changes in *SOX9* expression are mediated by the actin cytoskeleton. As discussed above (section 6.3.1.1), in the absence of actin stress fibres *SOX9* mRNA is stabilised via p38 MAPK signalling (Tew and Hardingham, 2006, Tew et al., 2009), which can be activated by dynamic compression (Fitzgerald et al., 2008, Bougault et al., 2008). Dynamic compression can also increase *SOX9* mRNA expression through activation of Rho and ROCK, which increases SOX9 transcriptional activity and *SOX9* transcription (Haudenschild et al., 2010, Kumar and Lassar, 2009). Differences between normal and OA human

chondrocytes in load-induced changes in *SOX9* mRNA levels could be due to inherent differences in Rho/ROCK/actin cytoskeleton or in p38 MAPK activation and signalling pathways. It cannot be excluded that increases in *SOX9* mRNA expression occurred with recovery post-load in normal chondrocytes; levels may have increased post-load but returned to baseline by the five hour time point assayed, or they might have increased if the post-load recovery period was extended.

In OA human chondrocytes, *COL1A1* and *MMP13* expression were decreased following a five hour recovery post-load. No significant decrease was observed in normal chondrocytes after the recovery period, although mRNA levels did show a trend of decreasing. The difference in response of normal and OA chondrocytes could therefore be due to the lower basal expression of *COL1A1* and *MMP13* in normal chondrocytes rather than a difference in the mechano-regulation of these genes. Alternatively, the loading regime could have a greater positive effect on the phenotype of OA chondrocytes.

Cyclic compression induced actin cytoskeletal remodelling along with apparently transient decreases in β-actin mRNA expression in both normal and OA human chondrocytes. However, the effect of load on the expression of some of the actin-binding proteins differed between normal and OA human chondrocytes; load increased mRNA expression of destrin, cofilin and thymosin β4 in normal, but not OA human chondrocytes. This could indicate a difference between normal and OA chondrocytes in load-induced actin remodelling, which is supported by the observed differences in actin cytoskeletal reorganisation following 40 minutes of cyclic compression. The additive effect of cytochalasin D treatment with load on mRNA expression of destrin, cofilin and thymosin β4 in both normal and OA human chondrocytes also suggests that mechano-regulation of these genes could be mediated by the actin cytoskeleton. Cytochalasin D treatment up-regulated destrin mRNA expression with recovery post-load in normal chondrocytes and enhanced the load-induced increase in destrin expression in OA chondrocytes; this suggests that the load-induced increase in destrin expression is a response to a requirement for actin cytoskeletal remodelling, with disruption of microfilaments with cytochalasin D enhancing the response. The load-induced increases in cofilin mRNA levels were reduced in normal chondrocytes and enhanced in OA chondrocytes, suggesting that cofilin expression is mechanically regulated in part by the

actin cytoskeleton in normal but not OA chondrocytes; this has been observed for membrane potential changes induced by mechanical strain in human chondrocytes (Wright et al., 1997, Millward-Sadler et al., 2000b). The enhanced load-induced up-regulation of cofilin expression in OA chondrocytes could be a response to an increased requirement for actin remodelling as a result of cytochalasin D treatment. Mechano-regulation of thymosin β4 expression was unaffected by actin microfilament disruption in normal chondrocytes, whilst in OA chondrocytes cytochalasin D treatment induced a thymosin β4 transcriptional response to load. This further suggests differences in actin cytoskeletal remodelling and mechanotransduction pathways between normal and OA human chondrocytes.

Cyclic compression-induced increases in β-tubulin mRNA levels were observed only in normal human chondrocytes and not OA cells. Furthermore, load-induced increases in mRNA levels were enhanced by colchicine or acrylamide treatment in normal chondrocytes, whilst no effect was observed in OA chondrocytes. As discussed above, the increase in β-tubulin mRNA levels could be a result of increased microtubule remodelling in response to cyclic compression, reducing the pool of β-tubulin monomers and relieving auto-regulation and degradation of β-tubulin mRNA (Cleveland and Havercroft, 1983, Cleveland et al., 1983, Yen et al., 1988). The lack of an effect of load on β-tubulin mRNA levels in OA chondrocytes could suggest that load-induced microtubule remodelling does not reduce the β-tubulin monomer pool below the specific level in OA chondrocytes, perhaps due to increased microtubule disassembly in OA, and therefore mRNA levels are unchanged (Cleveland and Havercroft, 1983, Cleveland et al., 1983). This difference in load-induced microtubule remodelling between normal and OA human chondrocytes could be due to the observed differences in basal microtubule organisation or to altered mechano-regulation of microtubule dynamics.

In addition to differential gene expression in response to compression, normal and OA human chondrocytes exhibit differences in the organisation of actin microfilaments and tubulin microtubules after five hours of recovery post-load. Actin and tubulin cytoskeletal organisation returned to that of unloaded controls in normal chondrocytes whilst both microfilaments and microtubule bundles became more evident in OA chondrocytes, suggesting an existing difference in actin and tubulin dynamics.

In summary:

- Cyclic compression induced cytoskeletal remodelling and changes in the expression of β-tubulin, destrin, *SOX9* and *COL1A1* mRNAs in human chondrocytes embedded in agarose.
- Disruption of actin microfilaments affected the load-induced response of cofilin and destrin expression in both normal and OA chondrocytes and the response of thymosin β4 and *SOX9* expression in OA chondrocytes.
- Disruption of vimentin intermediate filaments affected the load-induced response of vimentin and β-tubulin expression and reorganisation of actin cytoskeletal networks in normal chondrocytes, whilst in OA chondrocytes it affected the response of cofilin and paxillin expression and reorganisation of tubulin microtubule networks.
- Disruption of tubulin microtubules affected the load-induced response of paxillin expression in both normal and OA chondrocytes and the recovery of actin microfilament organisation in normal chondrocytes.
- Differences between the effect of cyclic compression on normal and OA human chondrocytes support the existence of different or divergent mechano-transduction pathways. An additive effect of cytoskeletal disruption suggests that these pathways are mediated in part by elements of the chondrocyte cytoskeleton.

Chapter 7: General Discussion

7. GENERAL DISCUSSION

The chondrocyte cytoskeleton comprises three distinct elements, actin microfilaments, tubulin microtubules and vimentin intermediate filaments. The cytoskeleton plays an important role in transducing extracellular signals to the nucleus to modulate chondrocyte gene expression and therefore extracellular matrix (ECM) turnover. It is also important in maintaining the mechanical properties of the chondrocyte (Trickey et al., 2004, Ofek et al., 2009). Changes in chondrocyte phenotype have long been known to be associated with reorganisation of the chondrocyte cytoskeleton (Benya and Shaffer, 1982a, Brown and Benya, 1988). Previous work has shown that disruption of the cytoskeleton alters chondrocyte gene expression (Benya et al., 1988) and that both chondrocyte cytoskeletal organisation (Durrant et al., 1999, Fioravanti et al., 2005, Knight et al., 2006) and matrix molecule gene expression (Blain et al., 2001, Mio et al., 2005) are altered in response to load. Abnormal loading of joints is a major risk factor for the development of osteoarthritis (OA) (Aigner et al., 2006a, Blagojevic et al., 2010) and the cytoskeletal architecture in chondrocytes from both human OA (Fioravanti et al., 2003, Lambrecht et al., 2008) and a rat model of OA (Capin-Gutierrez et al., 2004) has been observed to differ to that of normal chondrocytes. This has led us to hypothesise that dysregulation of cytoskeletal networks prevents normal ECM-chondrocyte signalling and promotes a catabolic phenotype- the hallmark of OA.

7.1 The Implications of Using Human Tissue

Human articular cartilage was used throughout the present study. The use of human material is preferred to that from other mammals as protein–protein interactions and signalling pathways can vary between species. This is particularly relevant when studying pathways and mechanisms relating to human diseases and disorders such as OA. One particular example of this in the OA field is the respective role of ADAMTS4 and ADAMTS5 in disease progression, where the predominant aggrecanase in disease differs between mice and humans: studies in mice have demonstrated that ADAMTS5 knockout alone is sufficient to protect against OA (Glasson et al., 2004, Glasson et al., 2005, Majumdar et al., 2007) and inflammatory arthritis (Stanton et al., 2005) whilst in human articular cartilage explants, siRNA knockdown has demonstrated that both ADAMTS4 and ADAMTS5 mediate aggrecan degradation (Song et al., 2007). The principal disadvantage of using human samples however is the high variability between

donors, resulting in the requirement of a larger number of samples in order for experimental changes to reach statistical significance. However, human material is not as frequently and easily available as that from other species. In particular, the availability of normal human cartilage is limited. The use of human material in the present study resulted in a high degree of variability in most experimental results. When comparing data, this variability results in statistical p values that are not significant at the 95% confidence level. For this reason, changes with p values significant at the 90% confidence level are also discussed based on the assumption that an increased number of samples would likely produce statistical significance.

In addition to that associated with human samples in general, another level of variability is added to the present study by the heterogeneity of OA as a disease (Mankin et al., 1971, Rizkalla et al., 1992). Changes in cartilage organisation and extracellular matrix integrity have been well characterised in OA and used for grading the disease, allowing quantification of severity (Mankin et al., 1971). However, the aetiology of OA is poorly understood and, during the early stages of disease, it is unclear whether changes in the cartilage are widespread or localised to particular regions i.e. whether changes in chondrocytes occur throughout the cartilage (McDevitt and Muir, 1976, Brew et al., 2010b) or only in regions exhibiting surface disruption or fibrillation (Yagi et al., 2005). If the former is true, this raises a potential problem when attempting to determine causal or early disease mechanisms; a visually intact surface does not necessarily mean that the sample is not in the early stages of OA (Mankin et al., 1971, Rizkalla et al., 1992), in which case the early changes will have been missed. Furthermore, the association of cartilage degradation with joint pain has not been determined for OA. In the present study, using human cartilage from AstraZeneca, samples are classified as either 'normal' or 'OA' based on clinical parameters rather than histological grading or even visual analysis of cartilage on the joint; post-mortem samples are classed as 'normal' if the donor had never presented to a GP with knee pain. As there is no correlation between radiographic OA severity and pain (Link et al., 2003), this does not necessarily mean that the cartilage is not in the early or more advanced stages of disease. This problem is enhanced by the advancing age of post-mortem donors, which increases the likelihood that cartilage has begun to exhibit OA-like changes. This is demonstrated in the present study by the varying degrees of degradative changes observed in 'normal' samples; this added variability in 'normal' samples could therefore mask the significance of

differences observed between normal and OA samples. To begin to address this problem, future work would ideally be performed using only post-mortem samples with no macroscopic or histological evidence of cartilage degeneration for normal controls and isolation of chondrocytes; the practicality of this however is unrealistic.

7.2 The Chondrocyte Cytoskeleton is Altered in Osteoarthritis

The present study is the first to characterise and compare the cytoskeletal organisation of normal and OA human chondrocytes *in situ*. Immunofluorescence in conjunction with scanning confocal microscopy showed clear differences between normal and OA human cartilage chondrocyte cytoskeletal architecture. Scoring of confocal images revealed a significant difference in actin and vimentin organisation in deep zone chondrocytes, along with a significant difference in tubulin organisation in superficial and mid zone chondrocytes. ECM organisation and composition vary through the depth of cartilage tissue, along with mechanical forces experienced by chondrocytes. Changes in the ECM alter the strain experienced by chondrocytes in OA cartilage. The fact that significant differences between normal and OA cartilage were observed in the superficial and mid zone for tubulin microtubules but the deep zone for actin and vimentin cytoskeletal networks could be due to their different roles in regulating the biomechanical properties of chondrocytes (Trickey et al., 2004, Ofek et al., 2009). No differences in the protein levels of the three main cytoskeletal elements was observed, suggesting that the differences in architecture are due to reorganisation of existing cytoskeletal elements rather than *de novo* protein synthesis.

The observed differences in cytoskeletal organisation between normal and OA cartilage chondrocytes could result in changes to the chondrocyte phenotype and hence ECM composition. This was demonstrated in agarose-embedded normal and OA chondrocytes, where chemical disruption of each of the cytoskeletal elements altered the expression of genes encoding matrix proteins and matrix-degrading enzymes, along with those encoding growth factors and inflammatory mediators that could subsequently affect chondrocyte phenotype. This supports and expands on previous research demonstrating an effect of actin (Benya et al., 1988, Brown and Benya, 1988, Woods and Beier, 2006), tubulin (Takigawa et al., 1984) and vimentin (Blain et al., 2006) cytoskeletal disruption on the expression of matrix proteins and matrix-degrading enzymes in chondrocytes. The present study is the first to demonstrate down-regulation

of *MMP13* mRNA expression with disruption of the tubulin or vimentin chondrocyte cytoskeleton and down-regulation of *ADAMTS5* transcription with microtubule disruption.

Custom-designed Taqman® arrays also indicated a novel effect of cytoskeletal disruption on chondrocyte expression of *FGFR3*; microtubule disruption down-regulated whilst vimentin intermediate filament disruption up-regulated *FGFR3* mRNA expression. Attempts to validate array data for *FGFR3* were unsuccessful due to inefficiency of the quantitative PCR. Future experiments are required to optimise different primer sets and quantitative PCR conditions to allow validation of the effects of cytoskeletal disruption and to determine any effects of cyclic compression on *FGFR3* expression in normal and OA human chondrocytes. A recent study has implied that increased mechanical load can up-regulate *FGFR3* expression in rat condylar chondrocytes (Papadopoulou et al., 2007) whilst another member of the FGFR subfamily, FGFR1, is suggested to function in chondrocyte mechanotransduction (Vincent et al., 2004, Vincent et al., 2007).

In support of previous work in other cell types (Witteck et al., 2003, Kim, 2005), an effect of actin and vimentin cytoskeletal disruption on *NOS2A* (iNOS) expression was observed in chondrocytes for the first time. Of particular interest was the differential response of *NOS2A* transcription to vimentin disruption, which was down-regulated in normal and up-regulated in OA human chondrocytes. As for *FGFR3*, attempts to validate array data for *NOS2A* were unsuccessful due to inefficiency of quantitative PCRs; optimisation of different primer sets would allow validation of the effects of cytoskeletal disruption and determination of any effects of cyclic compression in normal and OA human chondrocytes. Dynamic compression has recently been shown to up-regulate *NOS2A* via an actin- and ROCK-dependent mechanism in agarose embedded normal human chondrocytes (Haudenschild et al., 2008a, Haudenschild et al., 2008b) but no role of the vimentin cytoskeleton has previously been demonstrated. By contrast, dynamic compression can reduce IL-1β-induced *NOS2A* expression mediated by integrins and p38 MAPK in bovine chondrocytes (Chowdhury et al., 2008).

Taqman® array data also indicated an effect of actin, tubulin and vimentin cytoskeletal disruption on mRNA expression of the pro-apoptotic factor BMF. BMF protein is sequestered to actin microfilaments through its interaction with the DLC2 component of

the myosin V motor complex (Puthalakath et al., 2001) but has not previously been linked to microtubules or vimentin intermediate filaments. Furthermore, this is the first time that *BMF* expression has been described in chondrocytes. Results suggest that *BMF* is more highly expressed in OA chondrocytes when compared with normal chondrocytes although changes did not reach statistical significance. Future experiments using an increased number of donors should produce statistically significant results, whilst comparison of *BMF* expression in normal and OA human articular cartilage would indicate if this up-regulation also occurs *in vivo*. This would be interesting as mRNA expression of anti-apoptotic Bcl2 is reduced in human OA cartilage (Brew et al., 2010b). As BMF functions to bind and sequester Bcl2 proteins (Puthalakath et al., 2001), this would suggest an increased sensitivity to apoptosis in OA (Hashimoto et al., 1998).

7.3 Are the Observed Differences in Cytoskeletal Organisation due to the Altered Mechanical Environment in Osteoarthritic Cartilage?

Along with chondrocyte cytoskeletal architecture, cartilage organisation and extracellular matrix composition was disrupted in OA cartilage, which would alter the mechanical load experienced by chondrocytes within the tissue. As load can induce changes in cytoskeletal organisation (Durrant et al., 1999, Fioravanti et al., 2005, Knight et al., 2006) it was unclear whether the observed differences in OA cytoskeletal organisation were due to the altered mechanical environment in OA cartilage or, as hypothesised, the cause of it. Chondrocytes were isolated from normal and OA human cartilage for culture in identical mechanical environments. In order to achieve large enough numbers for experimentation, chondrocytes were expanded in monolayer to passage three. Differences in cytoskeletal organisation between normal and OA chondrocytes were retained in culture, indicating that the *in situ* differences were not entirely due to the altered mechanical environment in OA cartilage. However, the morphology of normal and OA chondrocytes cultured as a monolayer indicated loss of the typical rounded chondrocyte morphology and therefore phenotype (Benya et al., 1978, Benya and Shaffer, 1982a, Brown and Benya, 1988). In order to ensure that expression changes observed with cytoskeletal disruption were not simply due to redifferentiation to a chondrocytic phenotype, chondrocytes were embedded in agarose, a 3D culture condition that allows maintenance of the typical chondrocyte morphology and phenotype. In 3D agarose culture the cytoskeletal architecture of normal and OA chondrocytes more closely resembled that observed *in situ*. The differences in gene

expression between normal and OA cartilage were also better represented when isolated chondrocytes were cultured in 3D agarose, indicating that the culture system was a good model for use in further experiments. Furthermore, agarose embedded normal and OA chondrocytes exhibited differences in gene expression and cytoskeletal organisation demonstrating that these differences are inherent and not simply a result of the altered mechanical and extracellular environment that exists in OA cartilage.

The effect of load on the cytoskeletal elements of normal and OA chondrocytes was determined by subjecting agarose embedded chondrocytes to cyclic compression at 15% strain and 0.5 Hz. Various loading regimes have been used for dynamic compression of chondrocytes embedded in hydrogels. Many have used a 15% strain (Lee and Bader, 1997, Knight et al., 2006, Mio et al., 2005, Kock et al., 2009, Haudenschild et al., 2010) as this lies within the physiological range for cells in intact cartilage subjected to physiological loads (Guilak et al., 1995, Lee and Bader, 1997). The frequency used is more variable, ranging from 0.01 Hz to 3 Hz (Buschmann et al., 1995, Lee and Bader, 1997). A frequency of 0.5 Hz was selected for use as it lies within the physiological range (Lee and Bader, 1997) and allowed maintenance of construct integrity; higher frequencies resulted in the agarose cracking. An identical loading regime of 15% at 0.5 Hz was also used in a recently published study using normal human chondrocytes embedded in agarose (Haudenschild et al., 2010). In the present study, analysis of the expression of chondrocyte phenotype markers demonstrated that the loading regime up-regulated *SOX9* and down-regulated *COL1A1* and *MMP13* mRNA expression in OA chondrocytes, indicating that no catabolic changes were being induced. However an anabolic response was not observed in *ACAN* expression in the loading and recovery durations studied. Further experiments to determine *COL2A1* and *ACAN* expression changes over longer loading durations and increased recovery periods would allow confirmation of the anabolic changes suggested by the up-regulation of *SOX9* and previous studies subjecting bovine (Mio et al., 2005) and porcine (Kock et al., 2009) chondrocytes embedded in agarose to 15% dynamic compression.

Cyclic compression of agarose embedded normal and OA chondrocytes induced reorganisation of the actin, tubulin and vimentin cytoskeletal networks. This is the first demonstration of cyclic compression-induced reorganisation of the tubulin and vimentin cytoskeleton in normal human chondrocytes and confirms that recently demonstrated in

agarose-embedded normal human chondrocytes for the actin cytoskeleton (Haudenschild et al., 2008a). It is also the first to characterise compression-induced cytoskeletal reorganisation in OA human chondrocytes, although the effects of physiological cyclic (Fioravanti et al., 2003) and continuous high (Fioravanti et al., 2005) hydrostatic pressure have been demonstrated for human OA chondrocytes in alginate. Load can therefore induce cytoskeletal reorganisation in chondrocytes isolated from normal and OA human cartilage. The recovery of actin and tubulin cytoskeletal organisation post-load differed between normal and OA chondrocytes, with networks returning to the organisation of unloaded controls in normal chondrocytes but becoming more evident in OA chondrocytes. This suggests that, whilst the differences in cytoskeletal architecture observed between normal and OA cartilage chondrocytes *in situ* could be a result of loading and an altered mechanical environment, there are differences in the dynamics of the actin and tubulin networks between normal and OA chondrocytes that are independent of loading conditions; this supports the hypothesis that changes in the chondrocyte cytoskeleton occur before cartilage degradation in OA. This is further supported by a study comparing vimentin organisation in alginate embedded chondrocytes isolated from normal, macroscopically intact (minimal) OA and fibrillated (advanced) OA human cartilage (Lambrecht et al., 2008). Results demonstrated that the largest difference in vimentin organisation was between normal human chondrocytes and minimal OA chondrocytes rather than between minimal and advanced OA chondrocytes.

7.4 What Role does the Human Chondrocyte Cytoskeleton Play in Mechanotransduction?

The reorganisation of vimentin intermediate filament networks in chondrocytes in response to cyclic compression was not accompanied by changes in vimentin mRNA levels. Load-induced changes in levels of vimentin protein, phosphorylation and N-terminal cleavage were not determined as protein was not successfully extracted from chondrocytes embedded in agarose. Future experiments would replace the agarose hydrogel with alginate, allowing depolymerisation of the gel and release of chondrocytes for extraction of protein following loading periods. This would help to determine the mechanisms leading to vimentin remodelling in response to cyclic compression. Increases in vimentin phosphorylation would alter network organisation by increasing intermediate filament depolymerisation and slowing the rate of polymerisation (Eriksson

et al., 2004). N-terminal cleavage of vimentin would reduce intermediate filament assembly (Beuttenmuller et al., 1994) and the association of filament networks with the plasma membrane (Georgatos et al., 1985), resulting in the 'looser' organisation observed in normal and OA human chondrocytes following recovery post-load. Increased vimentin N-terminal cleavage has been observed in chondrocytes isolated from OA human cartilage when compared with those from normal human cartilage (Lambrecht et al., 2008) and could contribute to the difference in vimentin intermediate filament network organisation observed *in situ* in human OA in the present study and previously in a rat model of OA (Capin-Gutierrez et al., 2004). Whilst load did not produce significant changes in vimentin mRNA expression in untreated controls, disruption of actin microfilament networks enhanced the down-regulation of vimentin expression with recovery post-load in normal and OA chondrocytes. Remodelling of the actin cytoskeleton following removal of cyclic compression could interrupt the shuttling of transcription factors along microfilaments and reduce vimentin transcription, with cytochalasin D further disrupting microfilaments and vimentin transcription to produce a significant decrease in mRNA levels with recovery post-load. Actin cytoskeletal remodelling in response to the removal of load *in vivo* could explain the significant decrease in vimentin mRNA expression observed in OA cartilage, in which loads experienced by chondrocytes are increased due to disruption of cartilage tissue integrity. Disruption of vimentin networks also enhanced down-regulation of vimentin mRNA expression with recovery post-load, but this was only observed in normal chondrocytes. Vimentin intermediate filaments prevent dephosphorylation of phosphorylated ERK (Perlson et al., 2006), maintaining it in an activated state, and are also suggested to function as substrates for phosphorylation signalling in the cytoplasm (Kim and Coulombe, 2007). Through effects on these signalling intermediates and their downstream transcription factor targets, vimentin filament reorganisation in response to the removal of load could reduce vimentin transcription. Further disruption of intermediate filament organisaton by acrylamide would therefore produce a significant decrease in vimentin mRNA levels with recovery post-load. As for actin remodelling, this could provide a mechanism for the down-regulation of vimentin mRNA expression observed in OA cartilage; the lack of effect of acrylamide treatment on loaded OA chondrocytes could be a result of the basal differences in intermediate filament organisation or signalling pathways between these two cell populations.

In order to delineate the roles of the actin and vimentin cytoskeleton in the regulation of vimentin transcription with recovery post-load, future experiments need to be performed altering the conditions under which chondrocytes recover. For instance, chondrocyte/agarose constructs would be allowed to recover after treatment and load in the absence of cytoskeletal disrupting reagents and the data compared to recovery with cytoskeletal disruption. Extraction of protein and analysis of total and phosphorylated ERK levels would also help to further characterise the mechanism regulating decreased vimentin transcription. Indeed, dynamic compression of murine chondrocytes embedded in agarose has recently been shown to activate ERK signalling (Bougault et al., 2008). If differences in phosphorylation were observed in loaded chondrocytes then the addition of an ERK inhibitor immediately after removal of load could further characterise the role of ERK signalling in the regulation of vimentin expression. However, the role of other signalling intermediates including p38 MAPK, JNK, PKA and PKC in load-induced regulation of vimentin dynamics cannot be discounted.

Cyclic compression up-regulated β-tubulin mRNA expression in normal but not OA chondrocytes embedded in agarose. Furthermore, despite having no effect in the absence of load, colchicine and acrylamide enhanced load-induced up-regulation of β-tubulin transcription in normal chondrocytes only. As β-tubulin mRNA levels are auto-regulated depending on the size of the free tubulin pool (Cleveland and Havercroft, 1983, Cleveland et al., 1983, Yen et al., 1988), β-tubulin transcription could be increased as a result of a reduction of the free tubulin pool caused by the observed load-induced microtubule remodelling. Colchicine treatment suppresses microtubule dynamics (Panda et al., 1995) which in the presence of load would increase the demand for remodelling and thus further increase β-tubulin mRNA levels. Perhaps as a result of the close association of intermediate filaments with microtubules (Gurland and Gundersen, 1995), vimentin disruption with acrylamide could also suppress microtubule dynamics. This could result in an increased demand for microtubule reorganisation under load, a reduction of the β-tubulin pool and hence increased β-tubulin mRNA levels. Extraction of protein from chondrocytes post-load would help to determine a difference in the β-tubulin pool between normal and OA chondrocytes and the effect of cyclic compression and recovery on the size of the pool. The lack of an effect of load with or without cytoskeletal disruption on β-tubulin mRNA levels in OA chondrocytes could indicate that the β-tubulin monomer pool is larger in OA chondrocytes and therefore load-

induced remodelling never decreases it below the critical level to release mRNA from degradation. In support of this, *in situ* observations in rat (Capin-Gutierrez et al., 2004) and human (present study) cartilage suggest that the microtubule network is partially disassembled in OA, which could result in a larger monomer pool. However, the observed increase in β-tubulin mRNA in OA cartilage when compared with normal tissue would suggest that the β-tubulin pool is not larger than in normal cells, as this would result in reduced mRNA levels in OA. Alternatively, the increased β-tubulin mRNA in OA cartilage may never be translated to an increase in protein due to the presence of a defective microtubule network. As demonstrated by cyclic compression of chondrocytes embedded in agarose, the elevated β-tubulin mRNA levels in OA cartilage could be due to increased loading as a result of the altered mechanical environment.

Despite inducing remodelling of the actin microfilament networks, cyclic compression has no effect on β-actin mRNA levels. Load did however up-regulate expression of destrin and appeared to up-regulate cofilin and thymosin β4 expression in normal chondrocytes. Cofilin and destrin are actin depolymerising factors and thymosin β4 sequesters G-actin, indicating that load increases microfilament depolymerisation and the G-actin pool for the observed remodelling of the actin network. This could be the cause of the increased thymosin β4 expression detected in OA cartilage. Whilst actin reorganisation in response to load was observed in OA chondrocytes, changes in expression of the actin binding proteins were only observed in normal chondrocytes. Similarly, up-regulation of cofilin, destrin and β-actin mRNA expression in response to disruption of the actin or tubulin cytoskeleton was also observed only in normal chondrocytes. This indicates that these genes are more sensitive in normal chondrocytes to microfilament and microtubule remodelling induced by either cyclic compression alone or chemical disruption of cytoskeletal dynamics alone.

Interestingly, whilst neither load nor cytoskeletal disruption alone had a significant effect on cofilin, destrin and thymosin β4 mRNA expression, load in combination with actin disruption resulted in transcriptional up-regulation of these genes in OA chondrocytes. Furthermore, in the presence of colchicine, load induced up-regulation of thymosin β4 expression in OA chondrocytes. This suggests that, in contrast to normal chondrocytes, these genes are more sensitive in OA chondrocytes to microfilament and microtubule remodelling induced by cyclic compression in combination with chemical

disruption of cytoskeletal dynamics, as opposed to either of these alone. This further supports the existence of differences in the dynamics of actin and tubulin networks between normal and OA chondrocytes implied by the observed difference in recovery of actin and tubulin cytoskeletal organisation post-load. As OA chondrocytes have an altered cytoskeletal network they may utilise different or divergent mechanotransduction pathways.

mRNA levels of the focal adhesion protein paxillin were decreased in OA cartilage. Paxillin interacts with actin microfilaments (Deakin and Turner, 2008) at sites of cell–matrix contact; it is phosphorylated in response to mechanical stimulation of integrins in human chondrocytes cultured as a monolayer (Lee et al., 2000). Reduced expression of paxillin in OA cartilage chondrocytes could alter chondrocyte mechanotransduction mediated by integrins. In support of this the integrin-, IL-4- and stretch activated ion channel-dependent mechanotransduction pathway characterised in normal human chondrocytes cultured as a monolayer (Wright et al., 1996, Wright et al., 1997, Lee et al., 2000, Millward-Sadler et al., 2000a) has been shown to differ in OA chondrocytes (Millward-Sadler et al., 2000b); see section 6.1.3 for details. Paxillin mRNA levels showed a trend to decrease with recovery post-load in normal and OA chondrocytes, suggesting that the altered mechanical environment in OA cartilage could decrease paxillin expression and result in altered mechanotransduction. In the presence of acrylamide or colchicine the decrease in paxillin expression with recovery post-load was enhanced in OA chondrocytes, with colchicine also enhancing the down-regulation of paxillin transcription in normal chondrocytes loaded for 40 minutes. The effects of load on paxillin mRNA levels in chondrocytes and the reduction in OA cartilage could therefore be due to vimentin and/or tubulin cytoskeletal changes. The distribution of the focal contact proteins paxillin, vinculin and talin is irregular in vimentin-deficient fibroblasts, although ECM adhesion is unaffected (Eckes et al., 1998). Vimentin maintains ERK in an activated state (Perlson et al., 2006) and paxillin can also interact with and regulate ERK signalling (Ishibe et al., 2003); disruption or reduction of ERK signalling would have downstream effects on transcription.

Differences exist between the cytoskeleton networks of chondrocytes in normal and osteoarthritic articular cartilage and these appear to be due to a reorganisation of existing cytoskeletal proteins. As cyclic compression can alter the organisation of all three of the

main chondrocyte cytoskeletal elements, the observed difference in OA cytoskeleton could be a result of the altered mechanical environment in diseased cartilage. However, chemically-induced disruption/reorganisation of each of the three main cytoskeletal elements altered the chondrocyte phenotype, inducing differential expression of actin regulatory proteins, matrix molecules, matrix degrading enzymes, growth factors and inflammatory mediators, and therefore could cause the altered mechanical environment in OA cartilage. When cultured *in vitro* in identical mechanical environments, normal and OA chondrocytes exhibited differences in cytoskeletal architecture and responded differently to cytoskeletal disruption, cyclic compression and the two in combination. This demonstrates that cytoskeletal differences observed *in situ* are not simply a result of an altered mechanical environment, but can contribute to disease mechanisms and progression.

It should be noted here that, contrary to the expected effect, the presence of a cytoskeletal disrupting reagent did not prevent the post-load recovery and reassembly of its target cytoskeletal element networks. This would suggest that, contrary to the original hypothesis, OA is not due to disruption of cytoskeletal networks, as reassembly can still occur post-load in the presence of disrupting reagents. Instead, OA could be caused by a lack of the cytoskeletal element monomers, which would result in the observed differences in organisation. Studies showing reduced immunofluorescent labelling of cytoskeletal elements in human OA (Fioravanti et al., 2005) and a rat model of OA (Capin-Gutierrez et al., 2004) suggest that cytoskeletal element protein levels are decreased. This hypothesis is also supported by the observed decrease in vimentin mRNA in OA cartilage and the increase in thymosin β4 expression which, if translated to protein, could indicate an increase in sequestered G-actin and therefore a decrease in free G-actin and the ability to form functional actin cytoskeletal networks.

7.5 Future Directions

As discussed above, further experiments with an increased number of donors could produce statistical significance where near-significant changes in gene expression were observed. Further investigation of cytoskeletal reassembly post-load, where the cytoskeletal disrupting reagent is removed for the recovery period only, could clarify the role of each cytoskeletal element in the post-load recovery of organisation and gene expression changes. Loading experiments could also be repeated in alginate and protein

extracted from chondrocytes to determine if the transcriptional effects are also observed at the protein level. This would allow for the investigation of the effects of load and/or cytoskeletal disruption on the phosphorylation status of vimentin, ERK1/2 and paxillin, which could begin to delineate the signalling pathways involved.

Whilst results obtained in the present study showed that the differences between normal and OA chondrocytes observed in cartilage are maintained *in vitro* in agarose culture, the use of cartilage explants is preferable as they better represent the conditions surrounding chondrocytes *in vivo*. Degradation and compositional changes in the ECM in OA cartilage could result in changes in or loss of cell–matrix interactions, which would have additional effects on mechanotransduction and chondrocyte phenotype. A recent demonstration of this is that mice lacking the ECM receptor syndecan-4 are protected against OA induced by joint instability (Echtermeyer et al., 2009). The use of human cartilage explants for cyclic compression does however present a problem, as surface fibrillation means it can be difficult to find regions with an even surface to allow uniform compression; this would be particularly problematic for OA human cartilage and would prevent comparison with results from compression of normal explants.

Outside of the current experimental set-up, future directions could determine how the present findings may be utilised to produce a disease-modifying therapy for OA. Could the chondrocyte cytoskeleton be manipulated in OA to prevent the loss of organisation and its effect on gene expression in the presence and absence of load? The actin cytoskeleton is required for many fundamental cell processes so it is not surprising that manipulation results in a severe phenotype. Knockout of β-actin in mice is embryonic lethal at day 10.5, with embryos displaying severe growth retardation and cardiovascular defects, although heterozygous knockouts are viable and fertile (Shawlot et al., 1998, Shmerling et al., 2005, Tondeleir et al., 2009). By contrast, transfection of β-actin changes the shape of endothelial and epithelial cells and exogenous β-actin accumulates as large, unpolymerised deposits at the cell periphery (Mounier et al., 1997). Furthermore, disruption of actin microfilament dynamics in cartilage by tissue-specific inactivation of the Rac1 gene results in skeletal deformities, dwarfism and increased lethality (Wang et al., 2007). A β-tubulin knockout mouse has not been reported, although the requirement of microtubules for mitosis strongly suggests that embryos would not develop. Overexpression of β-tubulin in yeast causes cell cycle arrest and cell

death (Burke et al., 1989). However, in mammalian cells, β-tubulin overexpression has little effect on the cell cycle or on microtubule dynamics (Gonzalez-Garay and Cabral, 1995), most likely due to the tubulin auto-regulatory mechanism returning the monomer pool to the critical level; β-tubulin overexpression reduces synthesis of endogenous β-tubulin and steady state levels of total tubulin are only slightly increased. The exogenous β-tubulin is however capable of assembling normally into microtubules (Blade et al., 1999). Vimentin knockout mice have no obvious phenotype and, whilst no compensatory up-regulation of another intermediate filament was detected (Colucci-Guyon et al., 1994), this could be due to functional compensation by basal levels of the proteins. Studies of vimentin-deficient fibroblasts however have shown decreased mechanical stability along with an altered actin cytoskeleton and decreased migration (Eckes et al., 1998). Overexpression of vimentin is associated with lens degradation in transgenic mice (Capetanaki et al., 1989) and with cancer progression in humans, in particular with increased tumour metastasis (Hu et al., 2004, Wei et al., 2008). Direct manipulation of the cytoskeleton, particularly actin microfilaments is therefore not likely to be a candidate therapy for OA.

Could the changes in the chondrocyte cytoskeleton be used as a biomarker for OA? Current serum and urine biomarkers being evaluated for OA are based on providing an indication of the extent of cartilage degradation including, for example, peptides generated by MMP-mediated cleavage of type II collagen (e.g. CTX-II), COMP and cartilage glycoprotein 39 (YKL-40), which increase with increasing tissue damage (Abramson and Krasnokutsky, 2006, Li et al., 2007, Huang and Wu, 2009). If changes in the cytoskeleton are the cause of, or an early event in, OA disease progression, their use as a biomarker could detect OA earlier than cartilage degradation products. Vimentin in particular could be used as a biomarker and is being assessed for use in the diagnosis of rheumatoid arthritis. Vimentin can be post-translationally modified by peptidylarginine deiminases (PAD) during apoptosis and tissue inflammation to produce citrullinated vimentin (Vossenaar et al., 2003, Asaga et al., 1998); citrullination of the vimentin N-terminal head domain by PAD induced disassembly of vimentin intermediate filaments (Inagaki et al., 1989). Auto-antibodies to citrullinated vimentin are a specific and sensitive serum marker for rheumatoid arthritis (Vossenaar et al., 2003, Poulsom and Charles, 2008). If not citrullinated vimentin, then neoepitope peptides generated by N-

terminal cleavage of vimentin (Lambrecht et al., 2008) could be used as a biomarker for OA.

What is the cause of the observed cytoskeletal differences between normal and OA human cartilage? The results of the present study, as discussed above, suggest that the altered cytoskeletal organisation observed in human OA cartilage is not simply a result of the altered mechanical environment of chondrocytes. However, disruption of the articular surface, proteoglycan content and cartilage organisation in OA does result in chondrocytes being subjected to higher strains as the tissue is less effective at dissipating loads (Saarakkala et al., 2010). If there is a mechanical threshold, above which the cytoskeleton cannot reassemble post-load, then this could more easily be reached in OA chondrocytes when compared with normal and could cause the observed differences. Recent evidence in chondrocytes supporting this hypothesis has emerged. A single impact load induced disassembly of vimentin networks in rat cartilage that did not return to that of controls up to 48 hours post-load (Henson and Vincent, 2008). Furthermore, compression of single bovine chondrocytes demonstrated a 'critical strain threshold' at approximately 30% axial strain, after which cells did not fully recover and the biomechanical behaviour of cells was irreversibly changed (Ofek et al., 2009); strains above this critical level induced catabolic changes in chondrocyte phenotype (Leipzig and Athanasiou, 2008) and disruption of actin microfilaments or tubulin microtubules lowered the threshold (Ofek et al., 2009). The presence of a 'critical strain threshold' could be investigated in human chondrocytes and comparison of normal and OA chondrocytes would reveal if a change in this threshold occurs in OA or triggers an OA phenotype.

Alternatively the cytoskeletal changes observed in OA could be due to proteolytic degradation. In addition to the well characterised up-regulation of extracellular proteinases in OA, intracellular proteinases are also dysregulated and exhibit increased expression in human OA cartilage (Swingler et al., 2009). Expression of a number of aspartic proteases, including cathepsin D and β-secretase 1, and cysteine proteases such as cathepsin K, caspase-2 and -8, calpain-1, -2, -5 and -6 was up-regulated in OA. Furthermore, these proteases or family members have been shown to cleave cytoskeletal proteins. For example; calpains have been shown to cleave vimentin, actin, talin, paxillin, vinculin and microtubule-associated protein 2 (MAP2) (Fischer et al., 1986,

Yoshida et al., 1984, Springer et al., 1997, Liu and Schnellmann, 2003); caspases cleave actin, gelsolin, α-tubulin and vimentin (Mashima et al., 1997, Silacci et al., 2004, Klaiman et al., 2008, Yang et al., 2005, Byun et al., 2001). Vimentin is cleaved by cathepsin G (Nakamura et al., 1992) and cathepsin D degrades MAP2 and, to a lesser extent, tubulin (Johnson et al., 1991). The role of these proteinases in the changes in the cytoskeleton could be assessed in animal models of OA using knockouts or specific inhibitors.

In conclusion, this study has shown that changes in the cytoskeleton of OA chondrocytes are not simply a result of the altered mechanical environment in OA articular cartilage and are maintained following isolation and culture. Changes in the cytoskeleton can affect chondrocyte phenotype and the response of chondrocytes to cyclic compression, therefore the observed differences in organisation and expression could result in the altered phenotype of OA chondrocytes. Differences between the effect of cyclic compression on normal and OA chondrocytes support the existence of different or divergent mechanotransduction pathways that are mediated in part by elements of the chondrocyte cytoskeleton.

Bibliography

BIBLIOGRAPHY

ABBOTT, J. & HOLTZER, H. (1966) The loss of phenotypic traits by differentiated cells. 3. The reversible behavior of chondrocytes in primary cultures. *J Cell Biol,* 28, 473-87.

ABOUALAIWI, W. A., TAKAHASHI, M., MELL, B. R., JONES, T. J., RATNAM, S., KOLB, R. J. & NAULI, S. M. (2009) Ciliary polycystin-2 is a mechanosensitive calcium channel involved in nitric oxide signaling cascades. *Circ Res,* 104, 860-9.

ABRAMSON, S. & KRASNOKUTSKY, S. (2006) Biomarkers in osteoarthritis. *Bull NYU Hosp Jt Dis,* 64, 77-81.

ADAM, M., NOVOTNA, J. & DEYL, Z. (1984) Changes in collagen metabolism--another look at osteoarthrosis. *Acta Biol Hung,* 35, 181-7.

AGNEW, B. J., MINAMIDE, L. S. & BAMBURG, J. R. (1995) Reactivation of phosphorylated actin depolymerizing factor and identification of the regulatory site. *J Biol Chem,* 270, 17582-7.

AIGNER, T., FUNDEL, K., SAAS, J., GEBHARD, P. M., HAAG, J., WEISS, T., ZIEN, A., OBERMAYR, F., ZIMMER, R. & BARTNIK, E. (2006a) Large-scale gene expression profiling reveals major pathogenetic pathways of cartilage degeneration in osteoarthritis. *Arthritis Rheum,* 54, 3533-44.

AIGNER, T., GEBHARD, P. M., SCHMID, E., BAU, B., HARLEY, V. & POSCHL, E. (2003) SOX9 expression does not correlate with type II collagen expression in adult articular chondrocytes. *Matrix Biology,* 22, 363-372.

AIGNER, T., SACHSE, A., GEBHARD, P. M. & ROACH, H. I. (2006b) Osteoarthritis: Pathobiology-targets and ways for therapeutic intervention. *Advanced Drug Delivery Reviews,* 58, 128-149.

ALDAZ, H., RICE, L. M., STEARNS, T. & AGARD, D. A. (2005) Insights into microtubule nucleation from the crystal structure of human gamma-tubulin. *Nature,* 435, 523-7.

AMADO, R., WERNER, G. & NEUKOM, H. (1976) Water content of human articular cartilage and its determination by gas chromatography. *Biochem Med,* 16, 169-72.

ANDREU, J. M. & TIMASHEFF, S. N. (1982) Tubulin Bound to Colchicine Forms Polymers Different from Microtubules. *Proceedings of the National Academy of Sciences of the United States of America-Biological Sciences,* 79, 6753-6756.

APPLETON, C. T., USMANI, S. E., BERNIER, S. M., AIGNER, T. & BEIER, F. (2007a) Transforming growth factor alpha suppression of articular chondrocyte phenotype and Sox9 expression in a rat model of osteoarthritis. *Arthritis Rheum,* 56, 3693-705.

APPLETON, C. T. G., PITELKA, V., HENRY, J. & BEIER, F. (2007b) Global analyses of gene expression in early experimental osteoarthritis. *Arthritis and Rheumatism,* 56, 1854-1868.

ARCARO, A. (1998) The small GTP-binding protein Rac promotes the dissociation of gelsolin from actin filaments in neutrophils. *J Biol Chem,* 273, 805-13.

ARIAS-SALGADO, E. G., LIZANO, S., SARKAR, S., BRUGGE, J. S., GINSBERG, M. H. & SHATTIL, S. J. (2003) Src kinase activation by direct interaction with the integrin beta cytoplasmic domain. *Proc Natl Acad Sci U S A,* 100, 13298-302.

ARMSTRONG, C. G. & MOW, V. C. (1982) Variations in the intrinsic mechanical properties of human articular cartilage with age, degeneration, and water content. *J Bone Joint Surg Am,* 64, 88-94.

ASAGA, H., YAMADA, M. & SENSHU, T. (1998) Selective deimination of vimentin in calcium ionophore-induced apoptosis of mouse peritoneal macrophages. *Biochem Biophys Res Commun,* 243, 641-6.

BAEK, K., LIU, X., FERRON, F., SHU, S., KORN, E. D. & DOMINGUEZ, R. (2008) Modulation of actin structure and function by phosphorylation of Tyr-53 and profilin binding. *Proc Natl Acad Sci U S A,* 105, 11748-53.

BALLOCK, R. T., HEYDEMANN, A., WAKEFIELD, L. M., FLANDERS, K. C., ROBERTS, A. B. & SPORN, M. B. (1993) TGF-beta 1 prevents hypertrophy of epiphyseal chondrocytes: regulation of gene expression for cartilage matrix proteins and metalloproteases. *Dev Biol,* 158, 414-29.

BAU, B., GEBHARD, P. M., HAAG, J., KNORR, T., BARTNIK, E. & AIGNER, T. (2002) Relative messenger RNA expression profiling of collagenases and aggrecanases in human articular chondrocytes in vivo and in vitro. *Arthritis and Rheumatism,* 46, 2648-2657.

BAYLISS, M. T., HUTTON, S., HAYWARD, J. & MACIEWICZ, R. A. (2001) Distribution of aggrecanase (ADAMts 4/5) cleavage products in normal and osteoarthritic human articular cartilage: the influence of age, topography and zone of tissue. *Osteoarthritis and Cartilage,* 9, 553-560.

BELLIN, R. M., KUBICEK, J. D., FRIGAULT, M. J., KAMIEN, A. J., STEWARD, R. L., JR., BARNES, H. M., DIGIACOMO, M. B., DUNCAN, L. J., EDGERLY, C. K., MORSE, E. M., PARK, C. Y., FREDBERG, J. J., CHENG, C. M. & LEDUC, P. R. (2009) Defining the role of syndecan-4 in mechanotransduction using surface-modification approaches. *Proc Natl Acad Sci U S A,* 106, 22102-7.

BEN AMOR, N., PARIENTE, J. A., SALIDO, G. M., BARTEGI, A. & ROSADO, J. A. (2006) Caspases 3 and 9 are translocated to the cytoskeleton and activated by thrombin in human platelets. Evidence for the involvement of PKC and the actin filament polymerization. *Cell Signal,* 18, 1252-61.

BENJAMIN, M., ARCHER, C. W. & RALPHS, J. R. (1994) Cytoskeleton of Cartilage Cells. *Microscopy Research and Technique,* 28, 372-377.

BENYA, P. D., BROWN, P. D. & PADILLA, S. R. (1988) Microfilament Modification by Dihydrocytochalasin-B Causes Retinoic Acid-Modulated Chondrocytes to Reexpress the Differentiated Collagen Phenotype without a Change in Shape. *Journal of Cell Biology,* 106, 161-170.

BENYA, P. D., PADILLA, S. R. & NIMNI, M. E. (1977) Progeny of Rabbit Articular Chondrocytes Synthesize Collagen Type-1 and Type-3 and Type-1 Trimer, but

Not Type-2 - Verifications by Cyanogen-Bromide Peptide Analysis. *Biochemistry,* 16, 865-872.

BENYA, P. D., PADILLA, S. R. & NIMNI, M. E. (1978) Independent regulation of collagen types by chondrocytes during the loss of differentiated function in culture. *Cell,* 15, 1313-21.

BENYA, P. D. & SHAFFER, J. D. (1982a) Dedifferentiated chondrocytes reexpress the differentiated collagen phenotype when cultured in agarose gels. *Cell,* 30, 215-24.

BENYA, P. D. & SHAFFER, J. D. (1982b) Dedifferentiated Chondrocytes Reexpress the Differentiated Collagen Phenotype When Cultured in Agarose Gels. *Cell,* 30, 215-224.

BENZ, K., BREIT, S., LUKOSCHEK, M., MAU, H. & RICHTER, W. (2002) Molecular analysis of expansion, differentiation, and growth factor treatment of human chondrocytes identifies differentiation markers and growth-related genes. *Biochem Biophys Res Commun,* 293, 284-92.

BEUTTENMULLER, M., CHEN, M., JANETZKO, A., KUHN, S. & TRAUB, P. (1994) Structural Elements of the Amino-Terminal Head Domain of Vimentin Essential for Intermediate Filament Formation in-Vivo and in-Vitro. *Experimental Cell Research,* 213, 128-142.

BEZERRA, M. C., CARVALHO, J. F., PROKOPOWITSCH, A. S. & PEREIRA, R. M. (2005) RANK, RANKL and osteoprotegerin in arthritic bone loss. *Braz J Med Biol Res,* 38, 161-70.

BIARD, D. S., JAMES, M. R., CORDIER, A. & SARASIN, A. (1992) Regulation of the Escherichia coli lac operon expressed in human cells. *Biochim Biophys Acta,* 1130, 68-74.

BILLINGHURST, R. C., DAHLBERG, L., IONESCU, M., REINER, A., BOURNE, R., RORABECK, C., MITCHELL, P., HAMBOR, J., DIEKMANN, O., TSCHESCHE, H., CHEN, J., VANWART, H. & POOLE, A. R. (1997) Enhanced cleavage of type II collagen by collagenases in osteoarthritic articular cartilage. *Journal of Clinical Investigation,* 99, 1534-1545.

BLACK, C., CLAR, C., HENDERSON, R., MACEACHERN, C., MCNAMEE, P., QUAYYUM, Z., ROYLE, P. & THOMAS, S. (2009) The clinical effectiveness of glucosamine and chondroitin supplements in slowing or arresting progression of osteoarthritis of the knee: a systematic review and economic evaluation. *Health Technol Assess,* 13, 1-148.

BLADE, K., MENICK, D. R. & CABRAL, F. (1999) Overexpression of class I, II or IVb beta-tubulin isotypes in CHO cells is insufficient to confer resistance to paclitaxel. *J Cell Sci,* 112 (Pt 13), 2213-21.

BLAGOJEVIC, M., JINKS, C., JEFFERY, A. & JORDAN, K. P. (2010) Risk factors for onset of osteoarthritis of the knee in older adults: a systematic review and meta-analysis. *Osteoarthritis Cartilage,* 18, 24-33.

BLAIN, E. J. (2002) The identification of mechanically-regulated genes in articular cartilage that affects extracellular matrix turnover. *Bioscience.* Cardiff, Cardiff University.

BLAIN, E. J. (2009) Involvement of the cytoskeletal elements in articular cartilage homeostasis and pathology. *Int J Exp Pathol,* 90, 1-15.

BLAIN, E. J., GILBERT, S. J., HAYES, A. J. & DUANCE, V. C. (2006) Disassembly of the vimentin cytoskeleton disrupts articular cartilage chondrocyte homeostasis. *Matrix Biology,* 25, 398-408.

BLAIN, E. J., GILBERT, S. J., WARDALE, R. J., CAPPER, S. J., MASON, D. J. & DUANCE, V. C. (2001) Up-regulation of matrix metalloproteinase expression and activation following cyclical compressive loading of articular cartilage in vitro. *Archives of Biochemistry and Biophysics,* 396, 49-55.

BLAIN, E. J., MASON, D. J. & DUANCE, V. C. (2003) The effect of cyclical compressive loading on gene expression in articular cartilage. *Biorheology,* 40, 111-117.

BLANC, A., TRAN-KHANH, N., FILION, D. & BUSCHMANN, M. D. (2005) Optimal processing method to obtain four-color confocal fluorescent images of the cytoskeleton and nucleus in three-dimensional chondrocyte cultures. *Journal of Histochemistry & Cytochemistry,* 53, 1171-1175.

BLANCHOIN, L., POLLARD, T. D. & MULLINS, R. D. (2000) Interactions of ADF/cofilin, Arp2/3 complex, capping protein and profilin in remodeling of branched actin filament networks. *Curr Biol,* 10, 1273-82.

BLASIAK, J., GLOC, E., WOZNIAK, K. & CZECHOWSKA, A. (2004) Genotoxicity of acrylamide in human lymphocytes. *Chem Biol Interact,* 149, 137-49.

BOBICK, B. E., TUAN, R. S. & CHEN, F. H. (2010) The intermediate filament vimentin regulates chondrogenesis of adult human bone marrow-derived multipotent progenitor cells. *J Cell Biochem,* 109, 265-76.

BOUGAULT, C., PAUMIER, A., AUBERT-FOUCHER, E. & MALLEIN-GERIN, F. (2008) Molecular analysis of chondrocytes cultured in agarose in response to dynamic compression. *BMC Biotechnol,* 8, 71.

BREW, C. J., CLEGG, P. D., BOOT-HANDFORD, R. P., ANDREW, J. G. & HARDINGHAM, T. (2010a) Gene expression in human chondrocytes in late osteoarthritis is changed in both fibrillated and intact cartilage without evidence of generalised chondrocyte hypertrophy. *Ann Rheum Dis.* 2008/12/24 ed.

BREW, C. J., CLEGG, P. D., BOOT-HANDFORD, R. P., ANDREW, J. G. & HARDINGHAM, T. (2010b) Gene expression in human chondrocytes in late osteoarthritis is changed in both fibrillated and intact cartilage without evidence of generalised chondrocyte hypertrophy. *Ann Rheum Dis,* 69, 234-40.

BROWN, M. C. & TURNER, C. E. (2004) Paxillin: adapting to change. *Physiol Rev,* 84, 1315-39.

BROWN, P. D. & BENYA, P. D. (1986) Dihydrocytochalasin-B Alters Chondrocyte Microfilament Architecture and Induces Phenotypic Reexpression without Causing Cell Rounding. *Journal of Cell Biology,* 103, A393-A393.

BROWN, P. D. & BENYA, P. D. (1988) Alterations in Chondrocyte Cytoskeletal Architecture During Phenotypic Modulation by Retinoic Acid and Dihydrocytochalasin-B Induced Reexpression. *Journal of Cell Biology,* 106, 171-179.

BRULE, S., CHARNAUX, N., SUTTON, A., LEDOUX, D., CHAIGNEAU, T., SAFFAR, L. & GATTEGNO, L. (2006) The shedding of syndecan-4 and syndecan-1 from HeLa cells and human primary macrophages is accelerated by SDF-1/CXCL12 and mediated by the matrix metalloproteinase-9. *Glycobiology,* 16, 488-501.

BRZUSEK, D. & PETRON, D. (2008) Treating knee osteoarthritis with intra-articular hyaluronans. *Curr Med Res Opin,* 24, 3307-22.

BUCKI, R., LEVENTAL, I., KULAKOWSKA, A. & JANMEY, P. A. (2008) Plasma gelsolin: function, prognostic value, and potential therapeutic use. *Curr Protein Pept Sci,* 9, 541-51.

BUCKWALTER, J. A. & MANKIN, H. J. (1998) Articular cartilage: tissue design and chondrocyte-matrix interactions. *Instr Course Lect,* 47, 477-86.

BURKE, D., GASDASKA, P. & HARTWELL, L. (1989) Dominant effects of tubulin overexpression in Saccharomyces cerevisiae. *Mol Cell Biol,* 9, 1049-59.

BUSCHMANN, M. D., GLUZBAND, Y. A., GRODZINSKY, A. J. & HUNZIKER, E. B. (1995) Mechanical compression modulates matrix biosynthesis in chondrocyte/agarose culture. *J Cell Sci,* 108 (Pt 4), 1497-508.

BYUN, Y., CHEN, F., CHANG, R., TRIVEDI, M., GREEN, K. J. & CRYNS, V. L. (2001) Caspase cleavage of vimentin disrupts intermediate filaments and promotes apoptosis. *Cell Death Differ,* 8, 443-50.

CAMPBELL, J. J., BLAIN, E. J., CHOWDHURY, T. T. & KNIGHT, M. M. (2007) Loading alters actin dynamics and up-regulates cofilin gene expression in chondrocytes. *Biochemical and Biophysical Research Communications,* 361, 329-334.

CAMPER, L., HELLMAN, U. & LUNDGREN-AKERLUND, E. (1998) Isolation, cloning, and sequence analysis of the integrin subunit alpha10, a beta1-associated collagen binding integrin expressed on chondrocytes. *J Biol Chem,* 273, 20383-9.

CAO, M., WESTERHAUSEN-LARSON, A., NIYIBIZI, C., KAVALKOVICH, K., GEORGESCU, H. I., RIZZO, C. F., HEBDA, P. A., STEFANOVIC-RACIC, M. & EVANS, C. H. (1997) Nitric oxide inhibits the synthesis of type-II collagen without altering Col2A1 mRNA abundance: prolyl hydroxylase as a possible target. *Biochem J,* 324 (Pt 1), 305-10.

CAPETANAKI, Y., SMITH, S. & HEATH, J. P. (1989) Overexpression of the vimentin gene in transgenic mice inhibits normal lens cell differentiation. *J Cell Biol,* 109, 1653-64.

CAPIN-GUTIERREZ, N., TALAMAS-ROHANA, P., GONZALEZ-ROBLES, A., LAVALLE-MONTALVO, C. & KOURI, J. B. (2004) Cytoskeleton disruption in chondrocytes from a rat osteoarthrosic (OA)-induced model: its potential role in OA pathogenesis. *Histology and Histopathology,* 19, 1125-1132.

CARLIER, M. F., JEAN, C., RIEGER, K. J., LENFANT, M. & PANTALONI, D. (1993) Modulation of the interaction between G-actin and thymosin beta 4 by the ATP/ADP ratio: possible implication in the regulation of actin dynamics. *Proc Natl Acad Sci U S A,* 90, 5034-8.

CARLIER, M. F., LAURENT, V., SANTOLINI, J., MELKI, R., DIDRY, D., XIA, G. X., HONG, Y., CHUA, N. H. & PANTALONI, D. (1997) Actin depolymerizing

factor (ADF/cofilin) enhances the rate of filament turnover: implication in actin-based motility. *J Cell Biol,* 136, 1307-22.

CASTILLA, M. A., CARAMELO, C., GAZAPO, R. M., MARTIN, O., GONZALEZ-PACHECO, F. R., TEJEDOR, A., BRAGADO, R. & ARROYO, M. V. A. (2000) Role of vascular endothelial growth factor (VEGF) in endothelial cell protection against cytotoxic agents. *Life Sciences,* 67, 1003-1013.

CATERSON, B., FLANNERY, C. R., HUGHES, G. E. & LITTLE, C. B. (2000) Mechanisms involved in cartilage proteoglycan catabolism. *Matrix Biology,* 19, 333-344.

CAWSTON, T. E. & WILSON, A. J. (2006) Understanding the role of tissue degrading enzymes and their inhibitors in development and disease. *Best Pract Res Clin Rheumatol,* 20, 983-1002.

CAWSTON, T. E. & YOUNG, D. A. (2010) Proteinases involved in matrix turnover during cartilage and bone breakdown. *Cell Tissue Res,* 339, 221-35.

CHAI, D. H., ARNER, E. C., GRIGGS, D. W. & GRODZINSKY, A. J. (2010) Alphav and beta1 integrins regulate dynamic compression-induced proteoglycan synthesis in 3D gel culture by distinct complementary pathways. *Osteoarthritis Cartilage,* 18, 249-56.

CHAKAROVA, C., WEHNERT, M. S., UHL, K., SAKTHIVEL, S., VOSBERG, H. P., VAN DER VEN, P. F. & FURST, D. O. (2000) Genomic structure and fine mapping of the two human filamin gene paralogues FLNB and FLNC and comparative analysis of the filamin gene family. *Hum Genet,* 107, 597-611.

CHAN, W., KOZMA, R., YASUI, Y., INAGAKI, M., LEUNG, T., MANSER, E. & LIM, L. (2002) Vimentin intermediate filament reorganization by Cdc42: involvement of PAK and p70 S6 kinase. *Eur J Cell Biol,* 81, 692-701.

CHANG, L. & GOLDMAN, R. D. (2004) Intermediate filaments mediate cytoskeletal crosstalk. *Nature Reviews Molecular Cell Biology,* 5, 601-613.

CHIA, S. L., SAWAJI, Y., BURLEIGH, A., MCLEAN, C., INGLIS, J., SAKLATVALA, J. & VINCENT, T. (2009) Fibroblast growth factor 2 is an intrinsic chondroprotective agent that suppresses ADAMTS-5 and delays cartilage degradation in murine osteoarthritis. *Arthritis Rheum,* 60, 2019-27.

CHIQUET, M. (1999) Regulation of extracellular matrix gene expression by mechanical stress. *Matrix Biol,* 18, 417-26.

CHOKALINGAM, K., HUNTER, S., GOOCH, C., FREDE, C., FLORER, J., WENSTRUP, R. & BUTLER, D. (2009) Three-dimensional in vitro effects of compression and time in culture on aggregate modulus and on gene expression and protein content of collagen type II in murine chondrocytes. *Tissue Eng Part A,* 15, 2807-16.

CHOW, G., KNUDSON, C. B., HOMANDBERG, G. & KNUDSON, W. (1995) Increased Expression of Cd44 in Bovine Articular Chondrocytes by Catabolic Cellular Mediators. *Journal of Biological Chemistry,* 270, 27734-27741.

CHOW, G., NIETFELD, J. J., KNUDSON, C. B. & KNUDSON, W. (1998) Antisense inhibition of chondrocyte CD44 expression leading to cartilage chondrolysis. *Arthritis and Rheumatism,* 41, 1411-1419.

CHOWDHURY, T. T., APPLEBY, R. N., SALTER, D. M., BADER, D. A. & LEE, D. A. (2006) Integrin-mediated mechanotransduction in IL-1 beta stimulated chondrocytes. *Biomech Model Mechanobiol,* 5, 192-201.

CHOWDHURY, T. T., BADER, D. L., SHELTON, J. C. & LEE, D. A. (2003) Temporal regulation of chondrocyte metabolism in agarose constructs subjected to dynamic compression. *Arch Biochem Biophys,* 417, 105-11.

CHOWDHURY, T. T. & KNIGHT, M. M. (2006) Purinergic pathway suppresses the release of .NO and stimulates proteoglycan synthesis in chondrocyte/agarose constructs subjected to dynamic compression. *J Cell Physiol,* 209, 845-53.

CHOWDHURY, T. T., SALTER, D. M., BADER, D. L. & LEE, D. A. (2008) Signal transduction pathways involving p38 MAPK, JNK, NFkappaB and AP-1 influences the response of chondrocytes cultured in agarose constructs to IL-1beta and dynamic compression. *Inflamm Res,* 57, 306-13.

CHRETIEN, D., FULLER, S. D. & KARSENTI, E. (1995) Structure of growing microtubule ends: two-dimensional sheets close into tubes at variable rates. *J Cell Biol,* 129, 1311-28.

CLANCY, R. (1999) Nitric oxide alters chondrocyte function by disrupting cytoskeletal signaling complexes. *Osteoarthritis and Cartilage,* 7, 399-400.

CLEGG, D. O., REDA, D. J., HARRIS, C. L., KLEIN, M. A., O'DELL, J. R., HOOPER, M. M., BRADLEY, J. D., BINGHAM, C. O., WEISMAN, M. H., JACKSON, C. G., LANE, N. E., CUSH, J. J., MORELAND, L. W., SCHUMACHER, H. R., ODDIS, C. V., WOLFE, F., MOLITOR, J. A., YOCUM, D. E., SCHNITZER, T. J., FURST, D. E., SAWITZKE, A. D., SHI, H., BRANDT, K. D., MOSKOWITZ, R. W. & WILLIAMS, H. J. (2006) Glucosamine, chondroitin sulfate, and the two in combination for painful knee osteoarthritis. *New England Journal of Medicine,* 354, 795-808.

CLEVELAND, D. W. & HAVERCROFT, J. C. (1983) Is apparent autoregulatory control of tubulin synthesis nontranscriptionally regulated? *J Cell Biol,* 97, 919-24.

CLEVELAND, D. W., PITTENGER, M. F. & FERAMISCO, J. R. (1983) Elevation of tubulin levels by microinjection suppresses new tubulin synthesis. *Nature,* 305, 738-40.

COHEN-HILLEL, E., YRON, I., MESHEL, T., SORIA, G., ATTAL, H. & BEN-BARUCH, A. (2006) CXCL8-induced FAK phosphorylation via CXCR1 and CXCR2: cytoskeleton- and integrin-related mechanisms converge with FAK regulatory pathways in a receptor-specific manner. *Cytokine,* 33, 1-16.

COLUCCI-GUYON, E., PORTIER, M. M., DUNIA, I., PAULIN, D., POURNIN, S. & BABINET, C. (1994) Mice lacking vimentin develop and reproduce without an obvious phenotype. *Cell,* 79, 679-94.

COOPER, J. A. (1987) Effects of Cytochalasin and Phalloidin on Actin. *Journal of Cell Biology,* 105, 1473-1478.

COOPER, J. A. & SCHAFER, D. A. (2000) Control of actin assembly and disassembly at filament ends. *Curr Opin Cell Biol,* 12, 97-103.

COOPER, J. A. & SEPT, D. (2008) New insights into mechanism and regulation of actin capping protein. *Int Rev Cell Mol Biol,* 267, 183-206.

CRITCHLEY, D. R. (2009) Biochemical and structural properties of the integrin-associated cytoskeletal protein talin. *Annu Rev Biophys,* 38, 235-54.

CUCCHIARINI, M., THURN, T., WEIMER, A., KOHN, D., TERWILLIGER, E. F. & MADRY, H. (2007) Restoration of the extracellular matrix in human osteoarthritic articular cartilage by overexpression of the transcription factor SOX9. *Arthritis Rheum,* 56, 158-67.

CZISCH, M., SCHLEICHER, M., HORGER, S., VOELTER, W. & HOLAK, T. A. (1993) Conformation of thymosin beta 4 in water determined by NMR spectroscopy. *Eur J Biochem,* 218, 335-44.

D'ORTHO, M. P., WILL, H., ATKINSON, S., BUTLER, G., MESSENT, A., GAVRILOVIC, J., SMITH, B., TIMPL, R., ZARDI, L. & MURPHY, G. (1997) Membrane-type matrix metalloproteinases 1 and 2 exhibit broad-spectrum proteolytic capacities comparable to many matrix metalloproteinases. *Eur J Biochem,* 250, 751-7.

DAS, R. H., JAHR, H., VERHAAR, J. A., VAN DER LINDEN, J. C., VAN OSCH, G. J. & WEINANS, H. (2008) In vitro expansion affects the response of chondrocytes to mechanical stimulation. *Osteoarthritis Cartilage,* 16, 385-91.

DAVIDSON, D., BLANC, A., FILION, D., WANG, H., PLUT, P., PFEFFER, G., BUSCHMANN, M. D. & HENDERSON, J. E. (2005) Fibroblast growth factor (FGF) 18 signals through FGF receptor 3 to promote chondrogenesis. *J Biol Chem,* 280, 20509-15.

DE CROOS, J. N., DHALIWAL, S. S., GRYNPAS, M. D., PILLIAR, R. M. & KANDEL, R. A. (2006) Cyclic compressive mechanical stimulation induces sequential catabolic and anabolic gene changes in chondrocytes resulting in increased extracellular matrix accumulation. *Matrix Biol,* 25, 323-31.

DE SMAELE, E., ZAZZERONI, F., PAPA, S., NGUYEN, D. U., JIN, R., JONES, J., CONG, R. & FRANZOSO, G. (2001) Induction of gadd45beta by NF-kappaB downregulates pro-apoptotic JNK signalling. *Nature,* 414, 308-13.

DEAKIN, N. O. & TURNER, C. E. (2008) Paxillin comes of age. *J Cell Sci,* 121, 2435-44.

DEAN, D. D., MARTELPELLETIER, J., PELLETIER, J. P., HOWELL, D. S. & WOESSNER, J. F. (1989) Evidence for Metalloproteinase and Metalloproteinase Inhibitor Imbalance in Human Osteoarthritic Cartilage. *Journal of Clinical Investigation,* 84, 678-685.

DEDOVA, I. V., NIKOLAEVA, O. P., SAFER, D., DE LA CRUZ, E. M. & DOS REMEDIOS, C. G. (2006) Thymosin beta4 induces a conformational change in actin monomers. *Biophys J,* 90, 985-92.

DELL'ACCIO, F., DE BARI, C. & LUYTEN, F. P. (2001) Molecular markers predictive of the capacity of expanded human articular chondrocytes to form stable cartilage in vivo. *Arthritis Rheum,* 44, 1608-19.

DIMICCO, M. A., KISIDAY, J. D., GONG, H. & GRODZINSKY, A. J. (2007) Structure of pericellular matrix around agarose-embedded chondrocytes. *Osteoarthritis Cartilage,* 15, 1207-16.

DODGE, G. R. & POOLE, A. R. (1989) Immunohistochemical detection and immunochemical analysis of type II collagen degradation in human normal,

rheumatoid, and osteoarthritic articular cartilages and in explants of bovine articular cartilage cultured with interleukin 1. *J Clin Invest,* 83, 647-61.

DOMANSKI, M., HERTZOG, M., COUTANT, J., GUTSCHE-PERELROIZEN, I., BONTEMS, F., CARLIER, M. F., GUITTET, E. & VAN HEIJENOORT, C. (2004) Coupling of folding and binding of thymosin beta4 upon interaction with monomeric actin monitored by nuclear magnetic resonance. *J Biol Chem,* 279, 23637-45.

DOMINGUEZ, R. (2009) Actin filament nucleation and elongation factors--structure-function relationships. *Crit Rev Biochem Mol Biol,* 44, 351-66.

DOMM, C., SCHUNKE, M., CHRISTESEN, K. & KURZ, B. (2002) Redifferentiation of dedifferentiated bovine articular chondrocytes in alginate culture under low oxygen tension. *Osteoarthritis Cartilage,* 10, 13-22.

DONG, C., LI, Z., ALVAREZ, R., JR., FENG, X. H. & GOLDSCHMIDT-CLERMONT, P. J. (2000) Microtubule binding to Smads may regulate TGF beta activity. *Mol Cell,* 5, 27-34.

DONNELLY, E., WILLIAMS, R. & FARNUM, C. (2008) The primary cilium of connective tissue cells: imaging by multiphoton microscopy. *Anat Rec (Hoboken),* 291, 1062-73.

DOVAS, A., YONEDA, A. & COUCHMAN, J. R. (2006) PKCbeta-dependent activation of RhoA by syndecan-4 during focal adhesion formation. *J Cell Sci,* 119, 2837-46.

DUMBAULD, D. W., SHIN, H., GALLANT, N. D., MICHAEL, K. E., RADHAKRISHNA, H. & GARCIA, A. J. (2010) Contractility modulates cell adhesion strengthening through focal adhesion kinase and assembly of vinculin-containing focal adhesions. *J Cell Physiol.*

DUMONT, S. & MITCHISON, T. J. (2009) Compression regulates mitotic spindle length by a mechanochemical switch at the poles. *Curr Biol,* 19, 1086-95.

DURRANT, L. A., ARCHER, C. W., BENJAMIN, M. & RALPHS, J. R. (1999) Organisation of the chondrocyte cytoskeleton and its response to changing mechanical conditions in organ culture. *Journal of Anatomy,* 194, 343-353.

ECHTERMEYER, F., BERTRAND, J., DREIER, R., MEINECKE, I., NEUGEBAUER, K., FUERST, M., LEE, Y. J., SONG, Y. W., HERZOG, C., THEILMEIER, G. & PAP, T. (2009) Syndecan-4 regulates ADAMTS-5 activation and cartilage breakdown in osteoarthritis. *Nat Med,* 15, 1072-6.

ECKERT, B. S. (1985) Alteration of Intermediate Filament Distribution in Ptk1 Cells by Acrylamide. *European Journal of Cell Biology,* 37, 169-174.

ECKES, B., DOGIC, D., COLUCCI-GUYON, E., WANG, N., MANIOTIS, A., INGBER, D., MERCKLING, A., LANGA, F., AUMAILLEY, M., DELOUVEE, A., KOTELIANSKY, V., BABINET, C. & KRIEG, T. (1998) Impaired mechanical stability, migration and contractile capacity in vimentin-deficient fibroblasts. *J Cell Sci,* 111 (Pt 13), 1897-907.

EDWARDS, D. C., SANDERS, L. C., BOKOCH, G. M. & GILL, G. N. (1999) Activation of LIM-kinase by Pak1 couples Rac/Cdc42 GTPase signalling to actin cytoskeletal dynamics. *Nat Cell Biol,* 1, 253-9.

EID, K., THORNHILL, T. S. & GLOWACKI, J. (2006) Chondrocyte gene expression in osteoarthritis: Correlation with disease severity. *J Orthop Res,* 24, 1062-8.

ELESWARAPU, S. V., LEIPZIG, N. D. & ATHANASIOU, K. A. (2007) Gene expression of single articular chondrocytes. *Cell Tissue Res,* 327, 43-54.

ELLMAN, M. B., AN, H. S., MUDDASANI, P. & IM, H. J. (2008) Biological impact of the fibroblast growth factor family on articular cartilage and intervertebral disc homeostasis. *Gene,* 420, 82-9.

ENDO, K., TAKINO, T., MIYAMORI, H., KINSEN, H., YOSHIZAKI, T., FURUKAWA, M. & SATO, H. (2003) Cleavage of syndecan-1 by membrane type matrix metalloproteinase-1 stimulates cell migration. *J Biol Chem,* 278, 40764-70.

ENOMOTO, H., INOKI, I., KOMIYA, K., SHIOMI, T., IKEDA, E., OBATA, K., MATSUMOTO, H., TOYAMA, Y. & OKADA, Y. (2003) Vascular endothelial growth factor isoforms and their receptors are expressed in human osteoarthritic cartilage. *American Journal of Pathology,* 162, 171-181.

ERIKSSON, J. E., HE, T., TREJO-SKALLI, A. V., HARMALA-BRASKEN, A. S., HELLMAN, J., CHOU, Y. H. & GOLDMAN, R. D. (2004) Specific in vivo phosphorylation sites determine the assembly dynamics of vimentin intermediate filaments. *J Cell Sci,* 117, 919-32.

EVANGELISTI, R., BECCHETTI, E., BARONI, T., ROSSI, L., ARENA, N., VALENO, V., CARINCI, P. & LOCCI, P. (1995) Modulation of Phenotypic-Expression of Fibroblasts by Alteration of the Cytoskeleton. *Cell Biochemistry and Function,* 13, 41-52.

FANNING, P. J., EMKEY, G., SMITH, R. J., GRODZINSKY, A. J., SZASZ, N. & TRIPPEL, S. B. (2003) Mechanical regulation of mitogen-activated protein kinase signaling in articular cartilage. *J Biol Chem,* 278, 50940-8.

FARNDALE, R. W., BUTTLE, D. J. & BARRETT, A. J. (1986) Improved Quantitation and Discrimination of Sulfated Glycosaminoglycans by Use of Dimethylmethylene Blue. *Biochimica Et Biophysica Acta,* 883, 173-177.

FASSLER, R., SCHNEGELSBERG, P. N., DAUSMAN, J., SHINYA, T., MURAGAKI, Y., MCCARTHY, M. T., OLSEN, B. R. & JAENISCH, R. (1994) Mice lacking alpha 1 (IX) collagen develop noninflammatory degenerative joint disease. *Proc Natl Acad Sci U S A,* 91, 5070-4.

FAY, J., VAROGA, D., WRUCK, C. J., KURZ, B., GOLDRING, M. B. & PUFE, T. (2006) Reactive oxygen species induce expression of vascular endothelial growth factor in chondrocytes and human articular cartilage explants. *Arthritis Research & Therapy,* 8.

FEARS, C. Y., GLADSON, C. L. & WOODS, A. (2006) Syndecan-2 is expressed in the microvasculature of gliomas and regulates angiogenic processes in microvascular endothelial cells. *J Biol Chem,* 281, 14533-6.

FEHRENBACHER, A., STECK, E., ROTH, W., PAHMEIER, A. & RICHTER, W. (2006) Long-term mechanical loading of chondrocyte-chitosan biocomposites in vitro enhanced their proteoglycan and collagen content. *Biorheology,* 43, 709-20.

FENG, Y. & WALSH, C. A. (2004) The many faces of filamin: a versatile molecular scaffold for cell motility and signalling. *Nat Cell Biol,* 6, 1034-8.

FERRON, F., REBOWSKI, G., LEE, S. H. & DOMINGUEZ, R. (2007) Structural basis for the recruitment of profilin-actin complexes during filament elongation by Ena/VASP. *EMBO J,* 26, 4597-606.

FIORAVANTI, A., BENETTI, D., COPPOLA, G. & COLLODEL, G. (2005) Effect of continuous high hydrostatic pressure on the morphology and cytoskeleton of normal and osteoarthritic human chondrocytes cultivated in alginate gels. *Clinical and Experimental Rheumatology,* 23, 847-853.

FIORAVANTI, A., NERUCCI, F., ANNEFELD, M., COLLODEL, G. & MARCOLONGO, R. (2003) Morphological and cytoskeletal aspects of cultivated normal and osteoarthritic human articular chondrocytes after cyclical pressure: a pilot study. *Clinical and Experimental Rheumatology,* 21, 739-746.

FISCHER, S., VANDEKERCKHOVE, J., AMPE, C., TRAUB, P. & WEBER, K. (1986) Protein-chemical identification of the major cleavage sites of the Ca2+ proteinase on murine vimentin, the mesenchymal intermediate filament protein. *Biol Chem Hoppe Seyler,* 367, 1147-52.

FITZGERALD, J. B., JIN, M., CHAI, D. H., SIPARSKY, P., FANNING, P. & GRODZINSKY, A. J. (2008) Shear- and compression-induced chondrocyte transcription requires MAPK activation in cartilage explants. *J Biol Chem,* 283, 6735-43.

FITZGERALD, M. L., WANG, Z., PARK, P. W., MURPHY, G. & BERNFIELD, M. (2000) Shedding of syndecan-1 and -4 ectodomains is regulated by multiple signaling pathways and mediated by a TIMP-3-sensitive metalloproteinase. *J Cell Biol,* 148, 811-24.

FLANNERY, C. R., ZENG, W., CORCORAN, C., COLLINS-RACIE, L. A., CHOCKALINGAM, P. S., HEBERT, T., MACKIE, S. A., MCDONAGH, T., CRAWFORD, T. K., TOMKINSON, K. N., LAVALLIE, E. R. & MORRIS, E. A. (2002) Autocatalytic cleavage of ADAMTS-4 (Aggrecanase-1) reveals multiple glycosaminoglycan-binding sites. *J Biol Chem,* 277, 42775-80.

FORTIER, L. A., DEAK, M. M., SEMEVOLOS, S. A. & CERIONE, R. A. (2004) Insulin-like growth factor-I diminishes the activation status and expression of the small GTPase Cdc42 in articular chondrocytes. *J Orthop Res,* 22, 436-45.

FORTIER, L. A., NIXON, A. J. & LUST, G. (2002) Phenotypic expression of equine articular chondrocytes grown in three-dimensional cultures supplemented with supraphysiologic concentrations of insulin-like growth factor-1. *Am J Vet Res,* 63, 301-5.

FOSANG, A. J., ROGERSON, F. M., EAST, C. J. & STANTON, H. (2008) ADAMTS-5: the story so far. *Eur Cell Mater,* 15, 11-26.

FRANZ, T., HASLER, E. M., HAGG, R., WEILER, C., JAKOB, R. P. & MAINIL-VARLET, P. (2001) In situ compressive stiffness, biochemical composition, and structural integrity of articular cartilage of the human knee joint. *Osteoarthritis and Cartilage,* 9, 582-592.

GAHM, C., HOLMIN, S., RUDEHILL, S. & MATHIESEN, T. (2005) Neuronal degeneration and iNOS expression in experimental brain contusion following treatment with colchicine, dexamethasone, tirilazad mesylate and nimodipine. *Acta Neurochir (Wien),* 147, 1071-84; discussion 1084.

GALERA, P., REDINI, F., VIVIEN, D., BONAVENTURE, J., PENFORNIS, H., LOYAU, G. & PUJOL, J. P. (1992a) Effect of transforming growth factor-beta 1 (TGF-beta 1) on matrix synthesis by monolayer cultures of rabbit articular chondrocytes during the dedifferentiation process. *Exp Cell Res,* 200, 379-92.

GALERA, P., VIVIEN, D., PRONOST, S., BONAVENTURE, J., REDINI, F., LOYAU, G. & PUJOL, J. P. (1992b) Transforming growth factor-beta 1 (TGF-beta 1) up-regulation of collagen type II in primary cultures of rabbit articular chondrocytes (RAC) involves increased mRNA levels without affecting mRNA stability and procollagen processing. *J Cell Physiol,* 153, 596-606.

GALKIN, V. E., ORLOVA, A., LUKOYANOVA, N., WRIGGERS, W. & EGELMAN, E. H. (2001) Actin depolymerizing factor stabilizes an existing state of F-actin and can change the tilt of F-actin subunits. *J Cell Biol,* 153, 75-86.

GAO, G., WESTLING, J., THOMPSON, V. P., HOWELL, T. D., GOTTSCHALL, P. E. & SANDY, J. D. (2002) Activation of the proteolytic activity of ADAMTS4 (aggrecanase-1) by C-terminal truncation. *J Biol Chem,* 277, 11034-41.

GAO, Y. & SZTUL, E. (2001) A novel interaction of the Golgi complex with the vimentin intermediate filament cytoskeleton. *J Cell Biol,* 152, 877-94.

GARCIA, B. A., PLATT, M. D., BORN, T. L., SHABANOWITZ, J., MARCUS, N. A. & HUNT, D. F. (2006) Protein profile of osteoarthritic human articular cartilage using tandem mass spectrometry. *Rapid Commun Mass Spectrom,* 20, 2999-3006.

GARCIA, M. & KNIGHT, M. M. (2010) Cyclic loading opens hemichannels to release ATP as part of a chondrocyte mechanotransduction pathway. *J Orthop Res,* 28, 510-5.

GARDEL, M. L., NAKAMURA, F., HARTWIG, J. H., CROCKER, J. C., STOSSEL, T. P. & WEITZ, D. A. (2006) Prestressed F-actin networks cross-linked by hinged filamins replicate mechanical properties of cells. *Proc Natl Acad Sci U S A,* 103, 1762-7.

GAY, D. A., YEN, T. J., LAU, J. T. & CLEVELAND, D. W. (1987) Sequences that confer beta-tubulin autoregulation through modulated mRNA stability reside within exon 1 of a beta-tubulin mRNA. *Cell,* 50, 671-9.

GEBHARD, P. M., GEHRSITZ, A., BAU, B., SODER, S., EGER, W. & AIGNER, T. (2003) Quantification of expression levels of cellular differentiation markers does not support a general shift in the cellular phenotype of osteoarthritic chondrocytes. *J Orthop Res,* 21, 96-101.

GEIGER, B., TOKUYASU, K. T., DUTTON, A. H. & SINGER, S. J. (1980) Vinculin, an intracellular protein localized at specialized sites where microfilament bundles terminate at cell membranes. *Proc Natl Acad Sci U S A,* 77, 4127-31.

GEORGATOS, S. D., WEAVER, D. C. & MARCHESI, V. T. (1985) Site Specificity in Vimentin Membrane Interactions - Intermediate Filament Subunits Associate with the Plasma-Membrane Via Their Head Domains. *Journal of Cell Biology,* 100, 1962-1967.

GIANNONI, P., SIEGRIST, M., HUNZIKER, E. B. & WONG, M. (2003) The mechanosensitivity of cartilage oligomeric matrix protein (COMP). *Biorheology,* 40, 101-9.

GIRAO, H., GELI, M. I. & IDRISSI, F. Z. (2008) Actin in the endocytic pathway: from yeast to mammals. *FEBS Lett,* 582, 2112-9.

GLASSON, S. S., ASKEW, R., SHEPPARD, B., CARITO, B., BLANCHET, T., MA, H. L., FLANNERY, C. R., PELUSO, D., KANKI, K., YANG, Z., MAJUMDAR, M. K. & MORRIS, E. A. (2005) Deletion of active ADAMTS5 prevents cartilage degradation in a murine model of osteoarthritis. *Nature,* 434, 644-8.

GLASSON, S. S., ASKEW, R., SHEPPARD, B., CARITO, B. A., BLANCHET, T., MA, H. L., FLANNERY, C. R., KANKI, K., WANG, E., PELUSO, D., YANG, Z., MAJUMDAR, M. K. & MORRIS, E. A. (2004) Characterization of and osteoarthritis susceptibility in ADAMTS-4-knockout mice. *Arthritis Rheum,* 50, 2547-58.

GLOTZER, M. (2005) The molecular requirements for cytokinesis. *Science,* 307, 1735-9.

GLOWACKI, J., TREPMAN, E. & FOLKMAN, J. (1983) Cell shape and phenotypic expression in chondrocytes. *Proc Soc Exp Biol Med,* 172, 93-8.

GOLDRING, M. B. (2000) The role of the chondrocyte in osteoarthritis. *Arthritis and Rheumatism,* 43, 1916-1926.

GOLDRING, M. B., BIRKHEAD, J. R., SUEN, L. F., YAMIN, R., MIZUNO, S., GLOWACKI, J., ARBISER, J. L. & APPERLEY, J. F. (1994) Interleukin-1-Beta-Modulated Gene-Expression in Immortalized Human Chondrocytes. *Journal of Clinical Investigation,* 94, 2307-2316.

GOLDSCHMIDT-CLERMONT, P. J., FURMAN, M. I., WACHSSTOCK, D., SAFER, D., NACHMIAS, V. T. & POLLARD, T. D. (1992) The control of actin nucleotide exchange by thymosin beta 4 and profilin. A potential regulatory mechanism for actin polymerization in cells. *Mol Biol Cell,* 3, 1015-24.

GOLDSCHMIDT-CLERMONT, P. J., MACHESKY, L. M., DOBERSTEIN, S. K. & POLLARD, T. D. (1991) Mechanism of the interaction of human platelet profilin with actin. *J Cell Biol,* 113, 1081-9.

GONZALEZ-GARAY, M. L. & CABRAL, F. (1995) Overexpression of an epitope-tagged beta-tubulin in Chinese hamster ovary cells causes an increase in endogenous alpha-tubulin synthesis. *Cell Motil Cytoskeleton,* 31, 259-72.

GORLIN, J. B., YAMIN, R., EGAN, S., STEWART, M., STOSSEL, T. P., KWIATKOWSKI, D. J. & HARTWIG, J. H. (1990) Human endothelial actin-binding protein (ABP-280, nonmuscle filamin): a molecular leaf spring. *J Cell Biol,* 111, 1089-105.

GOTO, H., TANABE, K., MANSER, E., LIM, L., YASUI, Y. & INAGAKI, M. (2002) Phosphorylation and reorganization of vimentin by p21-activated kinase (PAK). *Genes Cells,* 7, 91-7.

GRAFF, R. D., LAZAROWSKI, E. R., BANES, A. J. & LEE, G. M. (2000) ATP release by mechanically loaded porcine chondrons in pellet culture. *Arthritis Rheum,* 43, 1571-9.

GRANDE, D. A., PITMAN, M. I., PETERSON, L., MENCHE, D. & KLEIN, M. (1989) The repair of experimentally produced defects in rabbit articular cartilage by autologous chondrocyte transplantation. *J Orthop Res,* 7, 208-18.

GRANES, F., BERNDT, C., ROY, C., MANGEAT, P., REINA, M. & VILARO, S. (2003) Identification of a novel Ezrin-binding site in syndecan-2 cytoplasmic domain. *FEBS Lett,* 547, 212-6.

GREENE, D. K., TUMOVA, S., COUCHMAN, J. R. & WOODS, A. (2003) Syndecan-4 associates with alpha-actinin. *J Biol Chem,* 278, 7617-23.

GRONOWICZ, G., HADJIMICHAEL, J., RICHARDS, D., CERAMI, A. & ROSSOMANDO, E. F. (1992) Correlation between tumor necrosis factor-alpha (TNF-alpha)-induced cytoskeletal changes and human collagenase gene induction. *J Periodontal Res,* 27, 562-8.

GROTH, S., SCHULZE, M., KALTHOFF, H., FANDRICH, F. & UNGEFROREN, H. (2005) Adhesion and Rac1-dependent regulation of biglycan gene expression by transforming growth factor-beta. Evidence for oxidative signaling through NADPH oxidase. *J Biol Chem,* 280, 33190-9.

GUILAK, F. & MOW, V. C. (2000) The mechanical environment of the chondrocyte: a biphasic finite element model of cell-matrix interactions in articular cartilage. *J Biomech,* 33, 1663-73.

GUILAK, F., RATCLIFFE, A. & MOW, V. C. (1995) Chondrocyte deformation and local tissue strain in articular cartilage: a confocal microscopy study. *J Orthop Res,* 13, 410-21.

GUNNING, P., PONTE, P., OKAYAMA, H., ENGEL, J., BLAU, H. & KEDES, L. (1983) Isolation and characterization of full-length cDNA clones for human alpha-, beta-, and gamma-actin mRNAs: skeletal but not cytoplasmic actins have an amino-terminal cysteine that is subsequently removed. *Mol Cell Biol,* 3, 787-95.

GUO, J. F., JOURDIAN, G. W. & MACCALLUM, D. K. (1989) Culture and growth characteristics of chondrocytes encapsulated in alginate beads. *Connect Tissue Res,* 19, 277-97.

GURLAND, G. & GUNDERSEN, G. G. (1995) Stable, detyrosinated microtubules function to localize vimentin intermediate filaments in fibroblasts. *J Cell Biol,* 131, 1275-90.

HAGG, R., BRUCKNER, P. & HEDBOM, E. (1998) Cartilage fibrils of mammals are biochemically heterogeneous: Differential distribution of decorin and collagen IX. *Journal of Cell Biology,* 142, 285-294.

HAIER, J. & NICOLSON, G. L. (1999) Role of the cytoskeleton in adhesion stabilization of human colorectal carcinoma cells to extracellular matrix components under dynamic conditions of laminar flow. *Clin Exp Metastasis,* 17, 713-21.

HARDINGHAM, T. E. & FOSANG, A. J. (1992) Proteoglycans - Many Forms and Many Functions. *Faseb Journal,* 6, 861-870.

HARTWIG, J. H. & SHEVLIN, P. (1986) The architecture of actin filaments and the ultrastructural location of actin-binding protein in the periphery of lung macrophages. *J Cell Biol,* 103, 1007-20.

HARTWIG, J. H., TYLER, J. & STOSSEL, T. P. (1980) Actin-binding protein promotes the bipolar and perpendicular branching of actin filaments. *J Cell Biol,* 87, 841-8.

HASHIMOTO, G., SHIMODA, M. & OKADA, Y. (2004) ADAMTS4 (aggrecanase-1) interaction with the C-terminal domain of fibronectin inhibits proteolysis of aggrecan. *J Biol Chem,* 279, 32483-91.

HASHIMOTO, S., OCHS, R. L., KOMIYA, S. & LOTZ, M. (1998) Linkage of chondrocyte apoptosis and cartilage degradation in human osteoarthritis. *Arthritis Rheum,* 41, 1632-8.

HAUCK, C. R., SIEG, D. J., HSIA, D. A., LOFTUS, J. C., GAARDE, W. A., MONIA, B. P. & SCHLAEPFER, D. D. (2001) Inhibition of focal adhesion kinase expression or activity disrupts epidermal growth factor-stimulated signaling promoting the migration of invasive human carcinoma cells. *Cancer Res,* 61, 7079-90.

HAUDENSCHILD, D. R., CHEN, J., PANG, N., LOTZ, M. K. & D'LIMA, D. D. (2010) Rho kinase-dependent activation of SOX9 in chondrocytes. *Arthritis Rheum,* 62, 191-200.

HAUDENSCHILD, D. R., CHEN, J., STEKLOV, N., LOTZ, M. K. & D'LIMA, D. D. (2009) Characterization of the chondrocyte actin cytoskeleton in living three-dimensional culture: response to anabolic and catabolic stimuli. *Mol Cell Biomech,* 6, 135-44.

HAUDENSCHILD, D. R., D'LIMA, D. D. & LOTZ, M. K. (2008a) Dynamic compression of chondrocytes induces a Rho kinase-dependent reorganization of the actin cytoskeleton. *Biorheology,* 45, 219-28.

HAUDENSCHILD, D. R., MCPHERSON, J. M., TUBO, R. & BINETTE, F. (2001) Differential expression of multiple genes during articular chondrocyte redifferentiation. *Anat Rec,* 263, 91-8.

HAUDENSCHILD, D. R., NGUYEN, B., CHEN, J., D'LIMA, D. D. & LOTZ, M. K. (2008b) Rho kinase-dependent CCL20 induced by dynamic compression of human chondrocytes. *Arthritis Rheum,* 58, 2735-42.

HAYES, A. J., BENJAMIN, M. & RALPHS, J. R. (1999) Role of actin stress fibres in the development of the intervertebral disc: cytoskeletal control of extracellular matrix assembly. *Dev Dyn,* 215, 179-89.

HAYMAN, D. M., BLUMBERG, T. J., SCOTT, C. C. & ATHANASIOU, K. A. (2006) The effects of isolation on chondrocyte gene expression. *Tissue Eng,* 12, 2573-81.

HEALY, Z. R., ZHU, F., STULL, J. D. & KONSTANTOPOULOS, K. (2008) Elucidation of the signaling network of COX-2 induction in sheared chondrocytes: COX-2 is induced via a Rac/MEKK1/MKK7/JNK2/c-Jun-C/EBPbeta-dependent pathway. *Am J Physiol Cell Physiol,* 294, C1146-57.

HEASMAN, S. J. & RIDLEY, A. J. (2008) Mammalian Rho GTPases: new insights into their functions from in vivo studies. *Nat Rev Mol Cell Biol,* 9, 690-701.

HEHNLY, H. & STAMNES, M. (2007) Regulating cytoskeleton-based vesicle motility. *FEBS Lett,* 581, 2112-8.

HEISS, S. G. & COOPER, J. A. (1991) Regulation of CapZ, an actin capping protein of chicken muscle, by anionic phospholipids. *Biochemistry,* 30, 8753-8.

HENSON, F. M. & VINCENT, T. A. (2008) Alterations in the vimentin cytoskeleton in response to single impact load in an in vitro model of cartilage damage in the rat. *BMC Musculoskelet Disord,* 9, 94.

HERMANSSON, M., SAWAJI, Y., BOLTON, M., ALEXANDER, S., WALLACE, A., BEGUM, S., WAIT, R. & SAKLATVALA, J. (2004) Proteomic analysis of articular cartilage shows increased type II collagen synthesis in osteoarthritis and expression of inhibin betaA (activin A), a regulatory molecule for chondrocytes. *J Biol Chem,* 279, 43514-21.

HERREROS, L., RODRIGUEZ-FERNANDEZ, J. L., BROWN, M. C., ALONSO-LEBRERO, J. L., CABANAS, C., SANCHEZ-MADRID, F., LONGO, N., TURNER, C. E. & SANCHEZ-MATEOS, P. (2000) Paxillin localizes to the lymphocyte microtubule organizing center and associates with the microtubule cytoskeleton. *J Biol Chem,* 275, 26436-40.

HEYLAND, J., WIEGANDT, K., GOEPFERT, C., NAGEL-HEYER, S., ILINICH, E., SCHUMACHER, U. & PORTNER, R. (2006) Redifferentiation of chondrocytes and cartilage formation under intermittent hydrostatic pressure. *Biotechnol Lett,* 28, 1641-8.

HICKERY, M. S., BAYLISS, M. T., DUDHIA, J., LEWTHWAITE, J. C., EDWARDS, J. C. & PITSILLIDES, A. A. (2003) Age-related changes in the response of human articular cartilage to IL-1alpha and transforming growth factor-beta (TGF-beta): chondrocytes exhibit a diminished sensitivity to TGF-beta. *J Biol Chem,* 278, 53063-71.

HIERCK, B. P., VAN DER HEIDEN, K., ALKEMADE, F. E., VAN DE PAS, S., VAN THIENEN, J. V., GROENENDIJK, B. C., BAX, W. H., VAN DER LAARSE, A., DERUITER, M. C., HORREVOETS, A. J. & POELMANN, R. E. (2008) Primary cilia sensitize endothelial cells for fluid shear stress. *Dev Dyn,* 237, 725-35.

HIGGS, H. N. & POLLARD, T. D. (2000) Activation by Cdc42 and PIP(2) of Wiskott-Aldrich syndrome protein (WASp) stimulates actin nucleation by Arp2/3 complex. *J Cell Biol,* 150, 1311-20.

HOCHBERG, M. C. (2006) Nutritional supplements for knee osteoarthritis - Still no resolution. *New England Journal of Medicine,* 354, 858-860.

HOLMES, K. C., POPP, D., GEBHARD, W. & KABSCH, W. (1990) Atomic model of the actin filament. *Nature,* 347, 44-9.

HOLMVALL, K., CAMPER, L., JOHANSSON, S., KIMURA, J. H. & LUNDGREN-AKERLUND, E. (1995) Chondrocyte and chondrosarcoma cell integrins with affinity for collagen type II and their response to mechanical stress. *Exp Cell Res,* 221, 496-503.

HOPWOOD, B., TSYKIN, A., FINDLAY, D. M. & FAZZALARI, N. L. (2007) Microarray gene expression profiling of osteoarthritic bone suggests altered bone remodelling, WNT and transforming growth factor-beta/bone morphogenic protein signalling. *Arthritis Res Ther,* 9, R100.

HORWITZ, J. P., CHUA, J., CURBY, R. J., TOMSON, A. J., DAROOGE, M. A., FISHER, B. E., MAURICIO, J. & KLUNDT, I. (1964) SUBSTRATES FOR CYTOCHEMICAL DEMONSTRATION OF ENZYME ACTIVITY. I. SOME

SUBSTITUTED 3-INDOLYL-BETA-D-GLYCOPYRANOSIDES. *J Med Chem,* 7, 574-5.

HSIEH-BONASSERA, N. D., WU, I., LIN, J. K., SCHUMACHER, B. L., CHEN, A. C., MASUDA, K., BUGBEE, W. D. & SAH, R. L. (2009) Expansion and redifferentiation of chondrocytes from osteoarthritic cartilage: cells for human cartilage tissue engineering. *Tissue Eng Part A,* 15, 3513-23.

HU, L., LAU, S. H., TZANG, C. H., WEN, J. M., WANG, W., XIE, D., HUANG, M., WANG, Y., WU, M. C., HUANG, J. F., ZENG, W. F., SHAM, J. S., YANG, M. & GUAN, X. Y. (2004) Association of Vimentin overexpression and hepatocellular carcinoma metastasis. *Oncogene,* 23, 298-302.

HU, S., CHEN, J., BUTLER, J. P. & WANG, N. (2005) Prestress mediates force propagation into the nucleus. *Biochem Biophys Res Commun,* 329, 423-8.

HU, Y. L., HAGA, J. H., MIAO, H., WANG, Y., LI, Y. S. & CHIEN, S. (2006) Roles of microfilaments and microtubules in paxillin dynamics. *Biochem Biophys Res Commun,* 348, 1463-71.

HUANG, K. & WU, L. D. (2009) YKL-40: a potential biomarker for osteoarthritis. *J Int Med Res,* 37, 18-24.

HUBCHAK, S. C., RUNYAN, C. E., KREISBERG, J. I. & SCHNAPER, H. W. (2003) Cytoskeletal rearrangement and signal transduction in TGF-beta1-stimulated mesangial cell collagen accumulation. *J Am Soc Nephrol,* 14, 1969-80.

HUEBNER, J. L., JOHNSON, K. A., KRAUS, V. B. & TERKELTAUB, R. A. (2009) Transglutaminase 2 is a marker of chondrocyte hypertrophy and osteoarthritis severity in the Hartley guinea pig model of knee OA. *Osteoarthritis Cartilage,* 17, 1056-64.

HUI, W., ROWAN, A. D. & CAWSTON, T. (2001) Modulation of the expression of matrix metalloproteinase and tissue inhibitors of metalloproteinases by TGF-beta1 and IGF-1 in primary human articular and bovine nasal chondrocytes stimulated with TNF-alpha. *Cytokine,* 16, 31-5.

HUMPHRIES, J. D., BYRON, A. & HUMPHRIES, M. J. (2006) Integrin ligands at a glance. *J Cell Sci,* 119, 3901-3.

HUNTER, D. J., LI, J., LAVALLEY, M., BAUER, D. C., NEVITT, M., DEGROOT, J., POOLE, R., EYRE, D., GUERMAZI, A., GALE, D. & FELSON, D. T. (2007) Cartilage markers and their association with cartilage loss on magnetic resonance imaging in knee osteoarthritis: the Boston Osteoarthritis Knee Study. *Arthritis Res Ther,* 9, R108.

IJIRI, K., ZERBINI, L. F., PENG, H., CORREA, R. G., LU, B., WALSH, N., ZHAO, Y., TANIGUCHI, N., HUANG, X. L., OTU, H., WANG, H., WANG, J. F., KOMIYA, S., DUCY, P., RAHMAN, M. U., FLAVELL, R. A., GRAVALLESE, E. M., OETTGEN, P., LIBERMANN, T. A. & GOLDRING, M. B. (2005) A novel role for GADD45beta as a mediator of MMP-13 gene expression during chondrocyte terminal differentiation. *J Biol Chem,* 280, 38544-55.

IJIRI, K., ZERBINI, L. F., PENG, H., OTU, H. H., TSUCHIMOCHI, K., OTERO, M., DRAGOMIR, C., WALSH, N., BIERBAUM, B. E., MATTINGLY, D., VAN FLANDERN, G., KOMIYA, S., AIGNER, T., LIBERMANN, T. A. &

GOLDRING, M. B. (2008) Differential expression of GADD45beta in normal and osteoarthritic cartilage: potential role in homeostasis of articular chondrocytes. *Arthritis Rheum,* 58, 2075-87.

INAGAKI, M., TAKAHARA, H., NISHI, Y., SUGAWARA, K. & SATO, C. (1989) Ca2+-dependent deimination-induced disassembly of intermediate filaments involves specific modification of the amino-terminal head domain. *J Biol Chem,* 264, 18119-27.

INSALL, R. H. & MACHESKY, L. M. (2009) Actin dynamics at the leading edge: from simple machinery to complex networks. *Dev Cell,* 17, 310-22.

ISENBERG, G., AEBI, U. & POLLARD, T. D. (1980) An actin-binding protein from Acanthamoeba regulates actin filament polymerization and interactions. *Nature,* 288, 455-9.

ISHIBE, S., JOLY, D., ZHU, X. & CANTLEY, L. G. (2003) Phosphorylation-dependent paxillin-ERK association mediates hepatocyte growth factor-stimulated epithelial morphogenesis. *Mol Cell,* 12, 1275-85.

JAKOB, M., DEMARTEAU, O., SCHAFER, D., HINTERMANN, B., DICK, W., HEBERER, M. & MARTIN, I. (2001) Specific growth factors during the expansion and redifferentiation of adult human articular chondrocytes enhance chondrogenesis and cartilaginous tissue formation in vitro. *J Cell Biochem,* 81, 368-77.

JANMEY, P. A., IIDA, K., YIN, H. L. & STOSSEL, T. P. (1987) Polyphosphoinositide micelles and polyphosphoinositide-containing vesicles dissociate endogenous gelsolin-actin complexes and promote actin assembly from the fast-growing end of actin filaments blocked by gelsolin. *J Biol Chem,* 262, 12228-36.

JANMEY, P. A. & STOSSEL, T. P. (1987) Modulation of gelsolin function by phosphatidylinositol 4,5-bisphosphate. *Nature,* 325, 362-4.

JEFFREY, J. E., THOMSON, L. A. & ASPDEN, R. M. (1997) Matrix loss and synthesis following a single impact load on articular cartilage in vitro. *Biochim Biophys Acta,* 1334, 223-32.

JENNISKENS, Y. M., KOEVOET, W., DE BART, A. C., WEINANS, H., JAHR, H., VERHAAR, J. A., DEGROOT, J. & VAN OSCH, G. J. (2006) Biochemical and functional modulation of the cartilage collagen network by IGF1, TGFbeta2 and FGF2. *Osteoarthritis Cartilage,* 14, 1136-46.

JENSEN, C. G., POOLE, C. A., MCGLASHAN, S. R., MARKO, M., ISSA, Z. I., VUJCICH, K. V. & BOWSER, S. S. (2004) Ultrastructural, tomographic and confocal imaging of the chondrocyte primary cilium in situ. *Cell Biol Int,* 28, 101-10.

JIN, G., SAH, R. L., LI, Y. S., LOTZ, M., SHYY, J. Y. & CHIEN, S. (2000) Biomechanical regulation of matrix metalloproteinase-9 in cultured chondrocytes. *J Orthop Res,* 18, 899-908.

JOHNSON, G. V., LITERSKY, J. M. & WHITAKER, J. N. (1991) Proteolysis of microtubule-associated protein 2 and tubulin by cathepsin D. *J Neurochem,* 57, 1577-83.

JOHNSON, K. A. & TERKELTAUB, R. A. (2005) External GTP-bound transglutaminase 2 is a molecular switch for chondrocyte hypertrophic differentiation and calcification. *J Biol Chem,* 280, 15004-12.

JOHNSON, K. A., VAN ETTEN, D., NANDA, N., GRAHAM, R. M. & TERKELTAUB, R. A. (2003) Distinct transglutaminase 2-independent and transglutaminase 2-dependent pathways mediate articular chondrocyte hypertrophy. *J Biol Chem,* 278, 18824-32.

JOOS, H., ALBRECHT, W., LAUFER, S., REICHEL, H. & BRENNER, R. E. (2008) IL-1beta regulates FHL2 and other cytoskeleton-related genes in human chondrocytes. *Mol Med,* 14, 150-9.

JORTIKKA, M. O., PARKKINEN, J. J., INKINEN, R. I., KARNER, J., JARVELAINEN, H. T., NELIMARKKA, L. O., TAMMI, M. I. & LAMMI, M. J. (2000) The role of microtubules in the regulation of proteoglycan synthesis in chondrocytes under hydrostatic pressure. *Arch Biochem Biophys,* 374, 172-80.

KABSCH, W., MANNHERZ, H. G., SUCK, D., PAI, E. F. & HOLMES, K. C. (1990) Atomic structure of the actin:DNase I complex. *Nature,* 347, 37-44.

KAINULAINEN, T., PENDER, A., D'ADDARIO, M., FENG, Y., LEKIC, P. & MCCULLOCH, C. A. (2002) Cell death and mechanoprotection by filamin a in connective tissues after challenge by applied tensile forces. *J Biol Chem,* 277, 21998-2009.

KAMADA, S., KUSANO, H., FUJITA, H., OHTSU, M., KOYA, R. C., KUZUMAKI, N. & TSUJIMOTO, Y. (1998) A cloning method for caspase substrates that uses the yeast two-hybrid system: cloning of the antiapoptotic gene gelsolin. *Proc Natl Acad Sci U S A,* 95, 8532-7.

KANG, F., PURICH, D. L. & SOUTHWICK, F. S. (1999) Profilin promotes barbed-end actin filament assembly without lowering the critical concentration. *J Biol Chem,* 274, 36963-72.

KASHIWAGI, M., ENGHILD, J. J., GENDRON, C., HUGHES, C., CATERSON, B., ITOH, Y. & NAGASE, H. (2004) Altered proteolytic activities of ADAMTS-4 expressed by C-terminal processing. *J Biol Chem,* 279, 10109-19.

KASHIWAGI, M., TORTORELLA, M., NAGASE, H. & BREW, K. (2001) TIMP-3 is a potent inhibitor of aggrecanase 1 (ADAM-TS4) and aggrecanase 2 (ADAM-TS5). *J Biol Chem,* 276, 12501-4.

KATSUKI, M., TOKURAKU, K., MUROFUSHI, H. & KOTANI, S. (1999) Functional analysis of microtubule-binding domain of bovine MAP4. *Cell Struct Funct,* 24, 337-44.

KAUSHIK, A. P., MARTIN, J. A., ZHANG, Q., SHEFFIELD, V. C. & MORCUENDE, J. A. (2009) Cartilage abnormalities associated with defects of chondrocytic primary cilia in Bardet-Biedl syndrome mutant mice. *J Orthop Res,* 27, 1093-9.

KAWANISHI, M., OURA, A., FURUKAWA, K., FUKUBAYASHI, T., NAKAMURA, K., TATEISHI, T. & USHIDA, T. (2007) Redifferentiation of dedifferentiated bovine articular chondrocytes enhanced by cyclic hydrostatic pressure under a gas-controlled system. *Tissue Eng,* 13, 957-64.

KAWASAKI, T., KUROSAWA, H., IKEDA, H., TAKAZAWA, Y., ISHIJIMA, M., KUBOTA, M., KAJIHARA, H., MARUYAMA, Y., KIM, S. G., KANAZAWA,

H. & DOI, T. (2009) Therapeutic home exercise versus intraarticular hyaluronate injection for osteoarthritis of the knee: 6-month prospective randomized open-labeled trial. *J Orthop Sci,* 14, 182-91.

KERKELA, E., BOHLING, T., HERVA, R., URIA, J. A. & SAARIALHO-KERE, U. (2001) Human macrophage metalloelastase (MMP-12) expression is induced in chondrocytes during fetal development and malignant transformation. *Bone,* 29, 487-93.

KERR, B. A., OTANI, T., KOYAMA, E., FREEMAN, T. A. & ENOMOTO-IWAMOTO, M. (2008) Small GTPase protein Rac-1 is activated with maturation and regulates cell morphology and function in chondrocytes. *Exp Cell Res,* 314, 1301-12.

KEVORKIAN, L., YOUNG, D. A., DARRAH, C., DONELL, S. T., SHEPSTONE, L., PORTER, S., BROCKBANK, S. M., EDWARDS, D. R., PARKER, A. E. & CLARK, I. M. (2004) Expression profiling of metalloproteinases and their inhibitors in cartilage. *Arthritis Rheum,* 50, 131-41.

KIM, C. W., GOLDBERGER, O. A., GALLO, R. L. & BERNFIELD, M. (1994) Members of the syndecan family of heparan sulfate proteoglycans are expressed in distinct cell-, tissue-, and development-specific patterns. *Mol Biol Cell,* 5, 797-805.

KIM, K. (2005) Effect of subchronic acrylamide exposure on the expression of neuronal and inducible nitric oxide synthase in rat brain. *J Biochem Mol Toxicol,* 19, 162-8.

KIM, K., MCCULLY, M. E., BHATTACHARYA, N., BUTLER, B., SEPT, D. & COOPER, J. A. (2007) Structure/function analysis of the interaction of phosphatidylinositol 4,5-bisphosphate with actin-capping protein: implications for how capping protein binds the actin filament. *J Biol Chem,* 282, 5871-9.

KIM, S. & COULOMBE, P. A. (2007) Intermediate filament scaffolds fulfill mechanical, organizational, and signaling functions in the cytoplasm. *Genes Dev,* 21, 1581-97.

KIM, S. J., HWANG, S. G., KIM, I. C. & CHUN, J. S. (2003) Actin cytoskeletal architecture regulates nitric oxide-induced apoptosis, dedifferentiation, and cyclooxygenase-2 expression in articular chondrocytes via mitogen-activated protein kinase and protein kinase C pathways. *J Biol Chem,* 278, 42448-56.

KLAIMAN, G., PETZKE, T. L., HAMMOND, J. & LEBLANC, A. C. (2008) Targets of caspase-6 activity in human neurons and Alzheimer disease. *Mol Cell Proteomics,* 7, 1541-55.

KNAUPER, V., WILL, H., LOPEZ-OTIN, C., SMITH, B., ATKINSON, S. J., STANTON, H., HEMBRY, R. M. & MURPHY, G. (1996) Cellular mechanisms for human procollagenase-3 (MMP-13) activation. Evidence that MT1-MMP (MMP-14) and gelatinase a (MMP-2) are able to generate active enzyme. *J Biol Chem,* 271, 17124-31.

KNIGHT, M. M., LEE, D. A. & BADER, D. L. (1998) The influence of elaborated pericellular matrix on the deformation of isolated articular chondrocytes cultured in agarose. *Biochim Biophys Acta,* 1405, 67-77.

KNIGHT, M. M., MCGLASHAN, S. R., GARCIA, M., JENSEN, C. G. & POOLE, C. A. (2009) Articular chondrocytes express connexin 43 hemichannels and P2 receptors - a putative mechanoreceptor complex involving the primary cilium? *J Anat,* 214, 275-83.

KNIGHT, M. M., TOYODA, T., LEE, D. A. & BADER, D. L. (2006) Mechanical compression and hydrostatic pressure induce reversible changes in actin cytoskeletal organisation in chondrocytes in agarose. *Journal of Biomechanics,* 39, 1547-1551.

KNUDSON, W., AGUIAR, D. J., HUA, Q. & KNUDSON, C. B. (1996) CD44-anchored hyaluronan-rich pericellular matrices: An ultrastructural and biochemical analysis. *Experimental Cell Research,* 228, 216-228.

KNUDSON, W. & LOESER, R. F. (2002) CD44 and integrin matrix receptors participate in cartilage homeostasis. *Cellular and Molecular Life Sciences,* 59, 36-44.

KOCK, L. M., SCHULZ, R. M., VAN DONKELAAR, C. C., THUMMLER, C. B., BADER, A. & ITO, K. (2009) RGD-dependent integrins are mechanotransducers in dynamically compressed tissue-engineered cartilage constructs. *J Biomech,* 42, 2177-82.

KOELLING, S., CLAUDITZ, T. S., KASTE, M. & MIOSGE, N. (2006) Cartilage oligomeric matrix protein is involved in human limb development and in the pathogenesis of osteoarthritis. *Arthritis Res Ther,* 8, R56.

KOMURO, H., OLEE, T., KUHN, K., QUACH, J., BRINSON, D. C., SHIKHMAN, A., VALBRACHT, J., CREIGHTON-ACHERMANN, L. & LOTZ, M. (2001) The osteoprotegerin/receptor activator of nuclear factor kappaB/receptor activator of nuclear factor kappaB ligand system in cartilage. *Arthritis Rheum,* 44, 2768-76.

KOSTYUKOVA, A. S. (2008) Capping complex formation at the slow-growing end of the actin filament. *Biochemistry (Mosc),* 73, 1467-72.

KOTHAKOTA, S., AZUMA, T., REINHARD, C., KLIPPEL, A., TANG, J., CHU, K., MCGARRY, T. J., KIRSCHNER, M. W., KOTHS, K., KWIATKOWSKI, D. J. & WILLIAMS, L. T. (1997) Caspase-3-generated fragment of gelsolin: effector of morphological change in apoptosis. *Science,* 278, 294-8.

KOURI, J. B., ARGUELLO, C., LUNA, J. & MENA, R. (1998) Use of microscopical techniques in the study of human chondrocytes from osteoarthritic cartilage: An overview. *Microscopy Research and Technique,* 40, 22-36.

KOURI, J. B., JIMENEZ, S. A., QUINTERO, M. & CHICO, A. (1996) Ultrastructural study of chondrocytes from fibrillated and non-fibrillated human osteoarthritic cartilage. *Osteoarthritis and Cartilage,* 4, 111-125.

KREITZER, G., LIAO, G. & GUNDERSEN, G. G. (1999) Detyrosination of tubulin regulates the interaction of intermediate filaments with microtubules in vivo via a kinesin-dependent mechanism. *Mol Biol Cell,* 10, 1105-18.

KUMAR, D. & LASSAR, A. B. (2009) The transcriptional activity of Sox9 in chondrocytes is regulated by RhoA signaling and actin polymerization. *Mol Cell Biol,* 29, 4262-73.

KUROKI, K., STOKER, A. M. & COOK, J. L. (2005) Effects of proinflammatory cytokines on canine articular chondrocytes in a three-dimensional culture. *Am J Vet Res,* 66, 1187-96.

KURZ, B., LEMKE, A. K., FAY, J., PUFE, T., GRODZINSKY, A. J. & SCHUNKE, M. (2005) Pathomechanisms of cartilage destruction by mechanical injury. *Annals of Anatomy-Anatomischer Anzeiger,* 187, 473-485.

KUSTERMANS, G., EL MJIYAD, N., HORION, J., JACOBS, N., PIETTE, J. & LEGRAND-POELS, S. (2008) Actin cytoskeleton differentially modulates NF-kappaB-mediated IL-8 expression in myelomonocytic cells. *Biochem Pharmacol,* 76, 1214-28.

KWAN TAT, S., PELLETIER, J. P., LAJEUNESSE, D., FAHMI, H., LAVIGNE, M. & MARTEL-PELLETIER, J. (2008) The differential expression of osteoprotegerin (OPG) and receptor activator of nuclear factor kappaB ligand (RANKL) in human osteoarthritic subchondral bone osteoblasts is an indicator of the metabolic state of these disease cells. *Clin Exp Rheumatol,* 26, 295-304.

KWIATKOWSKI, D. J., JANMEY, P. A. & YIN, H. L. (1989) Identification of critical functional and regulatory domains in gelsolin. *J Cell Biol,* 108, 1717-26.

LAEMMLI, U. K. (1970) Cleavage of Structural Proteins During Assembly of Head of Bacteriophage-T4. *Nature,* 227, 680-&.

LAMB, J. A., ALLEN, P. G., TUAN, B. Y. & JANMEY, P. A. (1993) Modulation of gelsolin function. Activation at low pH overrides Ca2+ requirement. *J Biol Chem,* 268, 8999-9004.

LAMBERT, C. A., COLIGE, A. C., MUNAUT, C., LAPIERE, C. M. & NUSGENS, B. V. (2001) Distinct pathways in the over-expression of matrix metalloproteinases in human fibroblasts by relaxation of mechanical tension. *Matrix Biology,* 20, 397-408.

LAMBRECHT, S., DHAENENS, M., ALMQVIST, F., VERDONK, P., VERBRUGGEN, G., DEFORCE, D. & ELEWAUT, D. (2009) Proteome characterization of human articular chondrocytes leads to novel insights in the function of small heat-shock proteins in chondrocyte homeostasis. *Osteoarthritis Cartilage.*

LAMBRECHT, S., VERBRUGGEN, G., VERDONK, P. C., ELEWAUT, D. & DEFORCE, D. (2008) Differential proteome analysis of normal and osteoarthritic chondrocytes reveals distortion of vimentin network in osteoarthritis. *Osteoarthritis Cartilage,* 16, 163-73.

LANGELIER, E., SUETTERLIN, R., HOEMANN, C. D., AEBI, U. & BUSCHMANN, M. D. (2000) The chondrocyte cytoskeleton in mature articular cartilage: Structure and distribution of actin, tubulin, and vimentin filaments. *Journal of Histochemistry & Cytochemistry,* 48, 1307-1320.

LAPADULA, G., IANNONE, F., ZUCCARO, C., GRATTAGLIANO, V., COVELLI, M., PATELLA, V., LOBIANCO, G. & PIPITONE, V. (1997) Integrin expression on chondrocytes: Correlations with the degree of cartilage damage in human osteoarthritis. *Clinical and Experimental Rheumatology,* 15, 247-254.

LASSING, I. & LINDBERG, U. (1985) Specific interaction between phosphatidylinositol 4,5-bisphosphate and profilactin. *Nature,* 314, 472-4.

LASSING, I. & LINDBERG, U. (1988) Evidence that the phosphatidylinositol cycle is linked to cell motility. *Exp Cell Res,* 174, 1-15.

LEACH, A. A. (1960) A study of the protein impurities in gelatins with ion-exchange resins. *Biochem J,* 74, 61-9.

LEE, D. A. & BADER, D. L. (1997) Compressive strains at physiological frequencies influence the metabolism of chondrocytes seeded in agarose. *J Orthop Res,* 15, 181-8.

LEE, H. S., MILLWARD-SADLER, S. J., WRIGHT, M. O., NUKI, G. & SALTER, D. M. (2000) Integrin and mechanosensitive ion channel-dependent tyrosine phosphorylation of focal adhesion proteins and beta-catenin in human articular chondrocytes after mechanical stimulation. *J Bone Miner Res,* 15, 1501-9.

LEE, J., KO, M. & JOO, C. K. (2008) Rho plays a key role in TGF-beta1-induced cytoskeletal rearrangement in human retinal pigment epithelium. *J Cell Physiol,* 216, 520-6.

LEE, J. H., FITZGERALD, J. B., DIMICCO, M. A. & GRODZINSKY, A. J. (2005) Mechanical injury of cartilage explants causes specific time-dependent changes in chondrocyte gene expression. *Arthritis Rheum,* 52, 2386-95.

LEGEAI-MALLET, L., BENOIST-LASSELIN, C., MUNNICH, A. & BONAVENTURE, J. (2004) Overexpression of FGFR3, Stat1, Stat5 and p21Cip1 correlates with phenotypic severity and defective chondrocyte differentiation in FGFR3-related chondrodysplasias. *Bone,* 34, 26-36.

LEGG, J. W., LEWIS, C. A., PARSONS, M., NG, T. & ISACKE, C. M. (2002) A novel PKC-regulated mechanism controls CD44 ezrin association and directional cell motility. *Nat Cell Biol,* 4, 399-407.

LEI, K. & DAVIS, R. J. (2003) JNK phosphorylation of Bim-related members of the Bcl2 family induces Bax-dependent apoptosis. *Proc Natl Acad Sci U S A,* 100, 2432-7.

LEIPZIG, N. D. & ATHANASIOU, K. A. (2008) Static compression of single chondrocytes catabolically modifies single-cell gene expression. *Biophys J,* 94, 2412-22.

LEIPZIG, N. D., ELESWARAPU, S. V. & ATHANASIOU, K. A. (2006) The effects of TGF-beta1 and IGF-I on the biomechanics and cytoskeleton of single chondrocytes. *Osteoarthritis Cartilage,* 14, 1227-36.

LI, J., ZHAO, Z., YANG, J., LIU, J., WANG, J., LI, X. & LIU, Y. (2009a) p38 MAPK mediated in compressive stress-induced chondrogenesis of rat bone marrow MSCs in 3D alginate scaffolds. *J Cell Physiol,* 221, 609-17.

LI, K. W., WANG, A. S. & SAH, R. L. (2003) Microenvironment regulation of extracellular signal-regulated kinase activity in chondrocytes: effects of culture configuration, interleukin-1, and compressive stress. *Arthritis Rheum,* 48, 689-99.

LI, Q., PARK, P. W., WILSON, C. L. & PARKS, W. C. (2002) Matrilysin shedding of syndecan-1 regulates chemokine mobilization and transepithelial efflux of neutrophils in acute lung injury. *Cell,* 111, 635-46.

LI, W. W., NEMIROVSKIY, O., FOUNTAIN, S., RODNEY MATHEWS, W. & SZEKELY-KLEPSER, G. (2007) Clinical validation of an immunoaffinity LC-MS/MS assay for the quantification of a collagen type II neoepitope peptide: A biomarker of matrix metalloproteinase activity and osteoarthritis in human urine. *Anal Biochem,* 369, 41-53.

LI, X., ELLMAN, M., MUDDASANI, P., WANG, J. H., CS-SZABO, G., VAN WIJNEN, A. J. & IM, H. J. (2009b) Prostaglandin E2 and its cognate EP receptors control human adult articular cartilage homeostasis and are linked to the pathophysiology of osteoarthritis. *Arthritis Rheum,* 60, 513-23.

LI, Y., TEW, S. R., RUSSELL, A. M., GONZALEZ, K. R., HARDINGHAM, T. E. & HAWKINS, R. E. (2004) Transduction of passaged human articular chondrocytes with adenoviral, retroviral, and lentiviral vectors and the effects of enhanced expression of SOX9. *Tissue Eng,* 10, 575-84.

LIAO, G. & GUNDERSEN, G. G. (1998) Kinesin is a candidate for cross-bridging microtubules and intermediate filaments. Selective binding of kinesin to detyrosinated tubulin and vimentin. *J Biol Chem,* 273, 9797-803.

LIN, K. M., WENEGIEME, E., LU, P. J., CHEN, C. S. & YIN, H. L. (1997) Gelsolin binding to phosphatidylinositol 4,5-bisphosphate is modulated by calcium and pH. *J Biol Chem,* 272, 20443-50.

LINK, T. M., STEINBACH, L. S., GHOSH, S., RIES, M., LU, Y., LANE, N. & MAJUMDAR, S. (2003) Osteoarthritis: MR imaging findings in different stages of disease and correlation with clinical findings. *Radiology,* 226, 373-381.

LIU, C. J., KONG, W., ILALOV, K., YU, S., XU, K., PRAZAK, L., FAJARDO, M., SEHGAL, B. & DI CESARE, P. E. (2006a) ADAMTS-7: a metalloproteinase that directly binds to and degrades cartilage oligomeric matrix protein. *FASEB J,* 20, 988-90.

LIU, C. J., KONG, W., XU, K., LUAN, Y., ILALOV, K., SEHGAL, B., YU, S., HOWELL, R. D. & DI CESARE, P. E. (2006b) ADAMTS-12 associates with and degrades cartilage oligomeric matrix protein. *J Biol Chem,* 281, 15800-8.

LIU, W., MURCIA, N. S., DUAN, Y., WEINBAUM, S., YODER, B. K., SCHWIEBERT, E. & SATLIN, L. M. (2005) Mechanoregulation of intracellular Ca2+ concentration is attenuated in collecting duct of monocilium-impaired orpk mice. *Am J Physiol Renal Physiol,* 289, F978-88.

LIU, W., SHAFIT-ZAGARDO, B., AQUINO, D. A., ZHAO, M. L., DICKSON, D. W., BROSNAN, C. F. & LEE, S. C. (1994) Cytoskeletal alterations in human fetal astrocytes induced by interleukin-1 beta. *J Neurochem,* 63, 1625-34.

LIU, X. & SCHNELLMANN, R. G. (2003) Calpain mediates progressive plasma membrane permeability and proteolysis of cytoskeleton-associated paxillin, talin, and vinculin during renal cell death. *J Pharmacol Exp Ther,* 304, 63-70.

LIU, Z., LAVINE, K. J., HUNG, I. H. & ORNITZ, D. M. (2007) FGF18 is required for early chondrocyte proliferation, hypertrophy and vascular invasion of the growth plate. *Dev Biol,* 302, 80-91.

LO, S. H. (2006) Focal adhesions: What's new inside. *Developmental Biology,* 294, 280-291.

LOESER, R. F. (2000) Chondrocyte integrin expression and function. *Biorheology,* 37, 109-16.

LOESER, R. F., CARLSON, C. S. & MCGEE, M. P. (1995) Expression of beta 1 integrins by cultured articular chondrocytes and in osteoarthritic cartilage. *Exp Cell Res,* 217, 248-57.

LOESER, R. F., SADIEV, S., TAN, L. & GOLDRING, M. B. (2000) Integrin expression by primary and immortalized human chondrocytes: evidence of a differential role for alpha 1 beta 1 and alpha 2 beta 1 integrins in mediating chondrocyte adhesion to types II and VI collagen. *Osteoarthritis and Cartilage,* 8, 96-105.

LOHMANDER, S., MADSEN, K. & HINEK, A. (1979) Secretion of proteoglycans by chondrocytes. Influence of colchicine, cytochalasin B, and beta-D-xyloside. *Arch Biochem Biophys,* 192, 148-57.

LOHMANDER, S., MOSKALEWSKI, S., MADSEN, K., THYBERG, J. & FRIBERG, U. (1976) Influence of colchicine on the synthesis and secretion of proteoglycans and collagen by fetal guinea pig chondrocytes. *Exp Cell Res,* 99, 333-45.

LOISEL, T. P., BOUJEMAA, R., PANTALONI, D. & CARLIER, M. F. (1999) Reconstitution of actin-based motility of Listeria and Shigella using pure proteins. *Nature,* 401, 613-6.

LOKESHWAR, V. B., FREGIEN, N. & BOURGUIGNON, L. Y. W. (1994) Ankyrin-Binding Domain of Cd44(Gp85) Is Required for the Expression of Hyaluronic Acid-Mediated Adhesion Function. *Journal of Cell Biology,* 126, 1099-1109.

LONGHURST, C. M. & JENNINGS, L. K. (1998) Integrin-mediated signal transduction. *Cellular and Molecular Life Sciences,* 54, 514-526.

LONGLEY, R. L., WOODS, A., FLEETWOOD, A., COWLING, G. J., GALLAGHER, J. T. & COUCHMAN, J. R. (1999) Control of morphology, cytoskeleton and migration by syndecan-4. *J Cell Sci,* 112 (Pt 20), 3421-31.

LONGPRE, J. M., MCCULLOCH, D. R., KOO, B. H., ALEXANDER, J. P., APTE, S. S. & LEDUC, R. (2009) Characterization of proADAMTS5 processing by proprotein convertases. *Int J Biochem Cell Biol,* 41, 1116-26.

LOUGHLIN, J. (2003) Genetics of osteoarthritis and potential for drug development. *Curr Opin Pharmacol,* 3, 295-9.

LU, P. J., SHIEH, W. R., RHEE, S. G., YIN, H. L. & CHEN, C. S. (1996) Lipid products of phosphoinositide 3-kinase bind human profilin with high affinity. *Biochemistry,* 35, 14027-34.

MACHESKY, L. M., MULLINS, R. D., HIGGS, H. N., KAISER, D. A., BLANCHOIN, L., MAY, R. C., HALL, M. E. & POLLARD, T. D. (1999) Scar, a WASp-related protein, activates nucleation of actin filaments by the Arp2/3 complex. *Proc Natl Acad Sci U S A,* 96, 3739-44.

MACHESKY, L. M., REEVES, E., WIENTJES, F., MATTHEYSE, F. J., GROGAN, A., TOTTY, N. F., BURLINGAME, A. L., HSUAN, J. J. & SEGAL, A. W. (1997) Mammalian actin-related protein 2/3 complex localizes to regions of lamellipodial protrusion and is composed of evolutionarily conserved proteins. *Biochem J,* 328 (Pt 1), 105-12.

MACIVER, S. K., POPE, B. J., WHYTOCK, S. & WEEDS, A. G. (1998) The effect of two actin depolymerizing factors (ADF/cofilins) on actin filament turnover: pH sensitivity of F-actin binding by human ADF, but not of Acanthamoeba actophorin. *Eur J Biochem,* 256, 388-97.

MAEKAWA, M., ISHIZAKI, T., BOKU, S., WATANABE, N., FUJITA, A., IWAMATSU, A., OBINATA, T., OHASHI, K., MIZUNO, K. & NARUMIYA, S. (1999) Signaling from Rho to the actin cytoskeleton through protein kinases ROCK and LIM-kinase. *Science,* 285, 895-8.

MAJUMDAR, M. K., ASKEW, R., SCHELLING, S., STEDMAN, N., BLANCHET, T., HOPKINS, B., MORRIS, E. A. & GLASSON, S. S. (2007) Double-knockout of ADAMTS-4 and ADAMTS-5 in mice results in physiologically normal animals and prevents the progression of osteoarthritis. *Arthritis Rheum,* 56, 3670-4.

MALLEIN-GERIN, F., GARRONE, R. & VAN DER REST, M. (1991) Proteoglycan and collagen synthesis are correlated with actin organization in dedifferentiating chondrocytes. *Eur J Cell Biol,* 56, 364-73.

MALLEIN-GERIN, F., RUGGIERO, F. & GARRONE, R. (1990) Proteoglycan core protein and type II collagen gene expressions are not correlated with cell shape changes during low density chondrocyte cultures. *Differentiation,* 43, 204-11.

MALLIK, R. & GROSS, S. P. (2004) Molecular motors: strategies to get along. *Curr Biol,* 14, R971-82.

MALONE, A. M., ANDERSON, C. T., TUMMALA, P., KWON, R. Y., JOHNSTON, T. R., STEARNS, T. & JACOBS, C. R. (2007) Primary cilia mediate mechanosensing in bone cells by a calcium-independent mechanism. *Proc Natl Acad Sci U S A,* 104, 13325-30.

MANKIN, H. J., DORFMAN, H., LIPPIELLO, L. & ZARINS, A. (1971) Biochemical and metabolic abnormalities in articular cartilage from osteo-arthritic human hips. II. Correlation of morphology with biochemical and metabolic data. *J Bone Joint Surg Am,* 53, 523-37.

MANKIN, H. J. & THRASHER, A. Z. (1975) Water content and binding in normal and osteoarthritic human cartilage. *J Bone Joint Surg Am,* 57, 76-80.

MANNHERZ, H. G. & HANNAPPEL, E. (2009) The beta-thymosins: intracellular and extracellular activities of a versatile actin binding protein family. *Cell Motil Cytoskeleton,* 66, 839-51.

MARCZIN, N., JILLING, T., PAPAPETROPOULOS, A., GO, C. & CATRAVAS, J. D. (1996) Cytoskeleton-dependent activation of the inducible nitric oxide synthase in cultured aortic smooth muscle cells. *Br J Pharmacol,* 118, 1085-94.

MAROUDAS, A. (1976) Balance between Swelling Pressure and Collagen Tension in Normal and Degenerate Cartilage. *Nature,* 260, 808-809.

MAROUDAS, A., EVANS, H. & ALMEIDA, L. (1973) Cartilage of the hip joint. Topographical variation of glycosaminoglycan content in normal and fibrillated tissue. *Ann Rheum Dis,* 32, 1-9.

MARTIN, I., JAKOB, M., SCHAFER, D., DICK, W., SPAGNOLI, G. & HEBERER, M. (2001) Quantitative analysis of gene expression in human articular cartilage from normal and osteoarthritic joints. *Osteoarthritis Cartilage,* 9, 112-8.

MASHIMA, T., NAITO, M., NOGUCHI, K., MILLER, D. K., NICHOLSON, D. W. & TSURUO, T. (1997) Actin cleavage by CPP-32/apopain during the development of apoptosis. *Oncogene,* 14, 1007-12.

MASON, R. M., CHAMBERS, M. G., FLANNELLY, J., GAFFEN, J. D., DUDHIA, J. & BAYLISS, M. T. (2001) The STR/ort mouse and its use as a model of osteoarthritis. *Osteoarthritis Cartilage,* 9, 85-91.

MAUCK, R. L., BYERS, B. A., YUAN, X. & TUAN, R. S. (2007) Regulation of cartilaginous ECM gene transcription by chondrocytes and MSCs in 3D culture in response to dynamic loading. *Biomech Model Mechanobiol,* 6, 113-25.

MAUCK, R. L., NICOLL, S. B., SEYHAN, S. L., ATESHIAN, G. A. & HUNG, C. T. (2003) Synergistic action of growth factors and dynamic loading for articular cartilage tissue engineering. *Tissue Eng,* 9, 597-611.

MAYNE, R., VAIL, M. S., MAYNE, P. M. & MILLER, E. J. (1976) Changes in type of collagen synthesized as clones of chick chondrocytes grow and eventually lose division capacity. *Proc Natl Acad Sci U S A,* 73, 1674-8.

MCDEVITT, C., GILBERTSON, E. & MUIR, H. (1977) Experimental-Model of Osteoarthritis - Early Morphological and Biochemical Changes. *Journal of Bone and Joint Surgery-British Volume,* 59, 24-35.

MCDEVITT, C. A. & MUIR, H. (1976) Biochemical Changes in Cartilage of Knee in Experimental and Natural Osteoarthritis in Dog. *Journal of Bone and Joint Surgery-British Volume,* 58, 94-101.

MCGLASHAN, S. R., CLUETT, E. C., JENSEN, C. G. & POOLE, C. A. (2008) Primary cilia in osteoarthritic chondrocytes: from chondrons to clusters. *Dev Dyn,* 237, 2013-20.

MCGLASHAN, S. R., HAYCRAFT, C. J., JENSEN, C. G., YODER, B. K. & POOLE, C. A. (2007) Articular cartilage and growth plate defects are associated with chondrocyte cytoskeletal abnormalities in Tg737orpk mice lacking the primary cilia protein polaris. *Matrix Biol,* 26, 234-46.

MCGLASHAN, S. R., JENSEN, C. G. & POOLE, C. A. (2006) Localization of extracellular matrix receptors on the chondrocyte primary cilium. *J Histochem Cytochem,* 54, 1005-14.

MCGOUGH, A. & CHIU, W. (1999) ADF/cofilin weakens lateral contacts in the actin filament. *J Mol Biol,* 291, 513-9.

MCGOUGH, A., CHIU, W. & WAY, M. (1998) Determination of the gelsolin binding site on F-actin: implications for severing and capping. *Biophys J,* 74, 764-72.

MCGOUGH, A., POPE, B., CHIU, W. & WEEDS, A. (1997) Cofilin changes the twist of F-actin: implications for actin filament dynamics and cellular function. *J Cell Biol,* 138, 771-81.

MEHLHORN, A. T., SCHMAL, H., KAISER, S., LEPSKI, G., FINKENZELLER, G., STARK, G. B. & SUDKAMP, N. P. (2006) Mesenchymal stem cells maintain TGF-beta-mediated chondrogenic phenotype in alginate bead culture. *Tissue Eng,* 12, 1393-403.

MEJILLANO, M. R., KOJIMA, S., APPLEWHITE, D. A., GERTLER, F. B., SVITKINA, T. M. & BORISY, G. G. (2004) Lamellipodial versus filopodial

mode of the actin nanomachinery: pivotal role of the filament barbed end. *Cell,* 118, 363-73.

MELAMED, I. & GELFAND, E. W. (1999) Microfilament assembly is involved in B-cell apoptosis. *Cell Immunol,* 194, 136-42.

MERIANE, M., MARY, S., COMUNALE, F., VIGNAL, E., FORT, P. & GAUTHIER-ROUVIERE, C. (2000) Cdc42Hs and Rac1 GTPases induce the collapse of the vimentin intermediate filament network. *J Biol Chem,* 275, 33046-52.

MILLWARD-SADLER, S. J., WRIGHT, M. O., DAVIES, L. W., NUKI, G. & SALTER, D. M. (2000a) Mechanotransduction via integrins and interleukin-4 results in altered aggrecan and matrix metalloproteinase 3 gene expression in normal, but not osteoarthritic, human articular chondrocytes. *Arthritis Rheum,* 43, 2091-9.

MILLWARD-SADLER, S. J., WRIGHT, M. O., FLATMAN, P. W. & SALTER, D. M. (2004) ATP in the mechanotransduction pathway of normal human chondrocytes. *Biorheology,* 41, 567-75.

MILLWARD-SADLER, S. J., WRIGHT, M. O., LEE, H., CALDWELL, H., NUKI, G. & SALTER, D. M. (2000b) Altered electrophysiological responses to mechanical stimulation and abnormal signalling through alpha5beta1 integrin in chondrocytes from osteoarthritic cartilage. *Osteoarthritis Cartilage,* 8, 272-8.

MILLWARD-SADLER, S. J., WRIGHT, M. O., LEE, H., NISHIDA, K., CALDWELL, H., NUKI, G. & SALTER, D. M. (1999) Integrin-regulated secretion of interleukin 4: A novel pathway of mechanotransduction in human articular chondrocytes. *J Cell Biol,* 145, 183-9.

MIO, K., KIRKHAM, J. & BONASS, W. A. (2006) Tips for extracting total RNA from chondrocytes cultured in agarose gel using a silica-based membrane kit. *Anal Biochem,* 351, 314-6.

MIO, K., SAITO, S., TOMATSU, T. & TOYAMA, Y. (2005) Intermittent compressive strain may reduce aggrecanase expression in cartilage: a study of chondrocytes in agarose gel. *Clin Orthop Relat Res,* 225-32.

MITCHELL, D. R. (2007) The evolution of eukaryotic cilia and flagella as motile and sensory organelles. *Adv Exp Med Biol,* 607, 130-40.

MITCHISON, T., EVANS, L., SCHULZE, E. & KIRSCHNER, M. (1986) Sites of microtubule assembly and disassembly in the mitotic spindle. *Cell,* 45, 515-27.

MITRA, S. K., HANSON, D. A. & SCHLAEPFER, D. D. (2005) Focal adhesion kinase: in command and control of cell motility. *Nat Rev Mol Cell Biol,* 6, 56-68.

MIWA, T., MANABE, Y., KUROKAWA, K., KAMADA, S., KANDA, N., BRUNS, G., UEYAMA, H. & KAKUNAGA, T. (1991) Structure, chromosome location, and expression of the human smooth muscle (enteric type) gamma-actin gene: evolution of six human actin genes. *Mol Cell Biol,* 11, 3296-306.

MOCKRIN, S. C. & KORN, E. D. (1980) Acanthamoeba profilin interacts with G-actin to increase the rate of exchange of actin-bound adenosine 5'-triphosphate. *Biochemistry,* 19, 5359-62.

MOGER, C. J., BARRETT, R., BLEUET, P., BRADLEY, D. A., ELLIS, R. E., GREEN, E. M., KNAPP, K. M., MUTHUVELU, P. & WINLOVE, C. P. (2007)

Regional variations of collagen orientation in normal and diseased articular cartilage and subchondral bone determined using small angle X-ray scattering (SAXS). *Osteoarthritis Cartilage,* 15, 682-7.

MOLLENHAUER, J., AURICH, M., MUEHLEMAN, C., KHELASHVILLI, G. & IRVING, T. C. (2003) X-ray diffraction of the molecular substructure of human articular cartilage. *Connect Tissue Res,* 44, 201-7.

MOLTENI, A., MODROWSKI, D., HOTT, M. & MARIE, P. J. (1999) Differential expression of fibroblast growth factor receptor-1, -2, and -3 and syndecan-1, -2, and -4 in neonatal rat mandibular condyle and calvaria during osteogenic differentiation in vitro. *Bone,* 24, 337-47.

MOORE, E. E., BENDELE, A. M., THOMPSON, D. L., LITTAU, A., WAGGIE, K. S., REARDON, B. & ELLSWORTH, J. L. (2005) Fibroblast growth factor-18 stimulates chondrogenesis and cartilage repair in a rat model of injury-induced osteoarthritis. *Osteoarthritis Cartilage,* 13, 623-31.

MORGAN, T. E., LOCKERBIE, R. O., MINAMIDE, L. S., BROWNING, M. D. & BAMBURG, J. R. (1993) Isolation and characterization of a regulated form of actin depolymerizing factor. *J Cell Biol,* 122, 623-33.

MORIYAMA, K., IIDA, K. & YAHARA, I. (1996) Phosphorylation of Ser-3 of cofilin regulates its essential function on actin. *Genes Cells,* 1, 73-86.

MOUNIER, N., PERRIARD, J. C., GABBIANI, G. & CHAPONNIER, C. (1997) Transfected muscle and non-muscle actins are differentially sorted by cultured smooth muscle and non-muscle cells. *J Cell Sci,* 110 (Pt 7), 839-46.

MOUW, J. K., IMLER, S. M. & LEVENSTON, M. E. (2007) Ion-channel regulation of chondrocyte matrix synthesis in 3D culture under static and dynamic compression. *Biomech Model Mechanobiol,* 6, 33-41.

MULLINS, R. D., HEUSER, J. A. & POLLARD, T. D. (1998) The interaction of Arp2/3 complex with actin: nucleation, high affinity pointed end capping, and formation of branching networks of filaments. *Proc Natl Acad Sci U S A,* 95, 6181-6.

MURPHY, G. & NAGASE, H. (2008) Progress in matrix metalloproteinase research. *Mol Aspects Med,* 29, 290-308.

MURRELL, G. A., JANG, D. & WILLIAMS, R. J. (1995) Nitric oxide activates metalloprotease enzymes in articular cartilage. *Biochem Biophys Res Commun,* 206, 15-21.

NACHMIAS, V. T., CASSIMERIS, L., GOLLA, R. & SAFER, D. (1993) Thymosin beta 4 (T beta 4) in activated platelets. *Eur J Cell Biol,* 61, 314-20.

NAGASE, H., VISSE, R. & MURPHY, G. (2006) Structure and function of matrix metalloproteinases and TIMPs. *Cardiovasc Res,* 69, 562-73.

NAHM, D. S., KIM, H. J., MAH, J. & BAEK, S. H. (2004) In vitro expression of matrix metalloproteinase-1, tissue inhibitor of metalloproteinase-1 and transforming growth factor-beta1 in human periodontal ligament fibroblasts. *Eur J Orthod,* 26, 129-35.

NAKAMURA, F., HARTWIG, J. H., STOSSEL, T. P. & SZYMANSKI, P. T. (2005) Ca2+ and calmodulin regulate the binding of filamin A to actin filaments. *J Biol Chem,* 280, 32426-33.

NAKAMURA, F., OSBORN, T. M., HARTEMINK, C. A., HARTWIG, J. H. & STOSSEL, T. P. (2007) Structural basis of filamin A functions. *J Cell Biol,* 179, 1011-25.

NAKAMURA, I., KADONO, Y., TAKAYANAGI, H., JIMI, E., MIYAZAKI, T., ODA, H., NAKAMURA, K., TANAKA, S., RODAN, G. A. & DUONG LE, T. (2002) IL-1 regulates cytoskeletal organization in osteoclasts via TNF receptor-associated factor 6/c-Src complex. *J Immunol,* 168, 5103-9.

NAKAMURA, N., TSURU, A., HIRAYOSHI, K. & NAGATA, K. (1992) Purification and characterization of a vimentin-specific protease in mouse myeloid leukemia cells. Regulation during differentiation and identity with cathepsin G. *Eur J Biochem,* 205, 947-54.

NELSON, F., DAHLBERG, L., LAVERTY, S., REINER, A., PIDOUX, I., IONESCU, M., FRASER, G. L., BROOKS, E., TANZER, M., ROSENBERG, L. C., DIEPPE, P. & ROBIN POOLE, A. (1998) Evidence for altered synthesis of type II collagen in patients with osteoarthritis. *J Clin Invest,* 102, 2115-25.

NEUHOLD, L. A., KILLAR, L., ZHAO, W., SUNG, M. L., WARNER, L., KULIK, J., TURNER, J., WU, W., BILLINGHURST, C., MEIJERS, T., POOLE, A. R., BABIJ, P. & DEGENNARO, L. J. (2001) Postnatal expression in hyaline cartilage of constitutively active human collagenase-3 (MMP-13) induces osteoarthritis in mice. *J Clin Invest,* 107, 35-44.

NEWMAN, P. & WATT, F. M. (1988) Influence of cytochalasin D-induced changes in cell shape on proteoglycan synthesis by cultured articular chondrocytes. *Exp Cell Res,* 178, 199-210.

NG, N. T., HEESCH, K. C. & BROWN, W. J. (2010) Efficacy of a progressive walking program and glucosamine sulphate supplementation on osteoarthritic symptoms of the hip and knee: a feasibility trial. *Arthritis Res Ther,* 12, R25.

NICODEMUS, G. D. & BRYANT, S. J. (2010) Mechanical loading regimes affect the anabolic and catabolic activities by chondrocytes encapsulated in PEG hydrogels. *Osteoarthritis Cartilage,* 18, 126-37.

NIGGLI, V. & ROSSY, J. (2008) Ezrin/radixin/moesin: versatile controllers of signaling molecules and of the cortical cytoskeleton. *Int J Biochem Cell Biol,* 40, 344-9.

NISHIDA, Y., D'SOUZA, A. L., THONAR, E. & KNUDSON, W. (2000) Stimulation of hyaluronan metabolism by interleukin-1 alpha in human articular cartilage. *Arthritis and Rheumatism,* 43, 1315-1326.

NOFAL, G. A. & KNUDSON, C. B. (2002) Latrunculin and cytochalasin decrease chondrocyte matrix retention. *Journal of Histochemistry & Cytochemistry,* 50, 1313-1323.

NOGALES, E., WOLF, S. G. & DOWNING, K. H. (1998) Structure of the alpha beta tubulin dimer by electron crystallography. *Nature,* 391, 199-203.

NOVAKOFSKI, K., BOEHM, A. & FORTIER, L. (2009) The small GTPase Rho mediates articular chondrocyte phenotype and morphology in response to interleukin-1alpha and insulin-like growth factor-I. *J Orthop Res,* 27, 58-64.

ODERO-MARAH, V. A., WANG, R., CHU, G., ZAYZAFOON, M., XU, J., SHI, C., MARSHALL, F. F., ZHAU, H. E. & CHUNG, L. W. (2008) Receptor activator of NF-kappaB Ligand (RANKL) expression is associated with epithelial to mesenchymal transition in human prostate cancer cells. *Cell Res,* 18, 858-70.

OFEK, G., WILTZ, D. C. & ATHANASIOU, K. A. (2009) Contribution of the cytoskeleton to the compressive properties and recovery behavior of single cells. *Biophys J,* 97, 1873-82.

OH, S. Y., SONG, J. H., GIL, J. E., KIM, J. H., YEOM, Y. I. & MOON, E. Y. (2006) ERK activation by thymosin-beta-4 (TB4) overexpression induces paclitaxel-resistance. *Exp Cell Res,* 312, 1651-7.

OHTA, Y., HARTWIG, J. H. & STOSSEL, T. P. (2006) FilGAP, a Rho- and ROCK-regulated GAP for Rac binds filamin A to control actin remodelling. *Nat Cell Biol,* 8, 803-14.

OHTA, Y., SUZUKI, N., NAKAMURA, S., HARTWIG, J. H. & STOSSEL, T. P. (1999) The small GTPase RalA targets filamin to induce filopodia. *Proc Natl Acad Sci U S A,* 96, 2122-8.

OHTSU, M., SAKAI, N., FUJITA, H., KASHIWAGI, M., GASA, S., SHIMIZU, S., EGUCHI, Y., TSUJIMOTO, Y., SAKIYAMA, Y., KOBAYASHI, K. & KUZUMAKI, N. (1997) Inhibition of apoptosis by the actin-regulatory protein gelsolin. *EMBO J,* 16, 4650-6.

OHUCHI, E., IMAI, K., FUJII, Y., SATO, H., SEIKI, M. & OKADA, Y. (1997) Membrane type 1 matrix metalloproteinase digests interstitial collagens and other extracellular matrix macromolecules. *J Biol Chem,* 272, 2446-51.

OKADA, T., OTANI, H., WU, Y., KYOI, S., ENOKI, C., FUJIWARA, H., SUMIDA, T., HATTORI, R. & IMAMURA, H. (2005) Role of F-actin organization in p38 MAP kinase-mediated apoptosis and necrosis in neonatal rat cardiomyocytes subjected to simulated ischemia and reoxygenation. *Am J Physiol Heart Circ Physiol,* 289, H2310-8.

OKINA, E., MANON-JENSEN, T., WHITEFORD, J. R. & COUCHMAN, J. R. (2009) Syndecan proteoglycan contributions to cytoskeletal organization and contractility. *Scand J Med Sci Sports,* 19, 479-89.

ORAZIZADEH, M., LEE, H. S., GROENENDIJK, B., SADLER, S. J., WRIGHT, M. O., LINDBERG, F. P. & SALTER, D. M. (2008) CD47 associates with alpha 5 integrin and regulates responses of human articular chondrocytes to mechanical stimulation in an in vitro model. *Arthritis Res Ther,* 10, R4.

OSTERGAARD, K., SALTER, D. M., PETERSEN, J., BENDTZEN, K., HVOLRIS, J. & ANDERSEN, C. B. (1998) Expression of alpha and beta subunits of the integrin superfamily in articular cartilage from macroscopically normal and osteoarthritic human femoral heads. *Annals of the Rheumatic Diseases,* 57, 303-308.

PAAVILAINEN, V. O., OKSANEN, E., GOLDMAN, A. & LAPPALAINEN, P. (2008) Structure of the actin-depolymerizing factor homology domain in complex with actin. *J Cell Biol,* 182, 51-9.

PACHTER, J. S., YEN, T. J. & CLEVELAND, D. W. (1987) Autoregulation of tubulin expression is achieved through specific degradation of polysomal tubulin mRNAs. *Cell,* 51, 283-92.

PALMOSKI, M., PERRICONE, E. & BRANDT, K. D. (1979) Development and Reversal of a Proteoglycan Aggregation Defect in Normal Canine Knee Cartilage after Immobilization. *Arthritis and Rheumatism,* 22, 508-517.

PALMOSKI, M. J. & BRANDT, K. D. (1984) Effects of static and cyclic compressive loading on articular cartilage plugs in vitro. *Arthritis Rheum,* 27, 675-81.

PALMOSKI, M. J., COLYER, R. A. & BRANDT, K. D. (1980) Joint Motion in the Absence of Normal Loading Does Not Maintain Normal Articular-Cartilage. *Arthritis and Rheumatism,* 23, 325-334.

PANDA, D., DAIJO, J. E., JORDAN, M. A. & WILSON, L. (1995) Kinetic stabilization of microtubule dynamics at steady state in vitro by substoichiometric concentrations of tubulin-colchicine complex. *Biochemistry,* 34, 9921-9.

PANTALONI, D. & CARLIER, M. F. (1993) How profilin promotes actin filament assembly in the presence of thymosin beta 4. *Cell,* 75, 1007-14.

PAPA, S., ZAZZERONI, F., BUBICI, C., JAYAWARDENA, S., ALVAREZ, K., MATSUDA, S., NGUYEN, D. U., PHAM, C. G., NELSBACH, A. H., MELIS, T., DE SMAELE, E., TANG, W. J., D'ADAMIO, L. & FRANZOSO, G. (2004) Gadd45 beta mediates the NF-kappa B suppression of JNK signalling by targeting MKK7/JNKK2. *Nat Cell Biol,* 6, 146-53.

PAPADOPOULOU, A. K., PAPACHRISTOU, D. J., CHATZOPOULOS, S. A., PIRTTINIEMI, P., PAPAVASSILIOU, A. G. & BASDRA, E. K. (2007) Load application induces changes in the expression levels of Sox-9, FGFR-3 and VEGF in condylar chondrocytes. *FEBS Lett,* 581, 2041-6.

PARRY, D. A., STRELKOV, S. V., BURKHARD, P., AEBI, U. & HERRMANN, H. (2007) Towards a molecular description of intermediate filament structure and assembly. *Exp Cell Res,* 313, 2204-16.

PAUL, A. S. & POLLARD, T. D. (2009) Review of the mechanism of processive actin filament elongation by formins. *Cell Motil Cytoskeleton,* 66, 606-17.

PELLETIER, J. P., MARTELPELLETIER, J., ALTMAN, R. D., GHANDURMNAYMNEH, L., HOWELL, D. S. & WOESSNER, J. F. (1983a) Collagenolytic Activity and Collagen Matrix Breakdown of the Articular-Cartilage in the Pond-Nuki Dog-Model of Osteoarthritis. *Arthritis and Rheumatism,* 26, 866-874.

PELLETIER, J. P., MARTELPELLETIER, J., HOWELL, D. S., GHANDURMNAYMNEH, L., ENIS, J. E. & WOESSNER, J. F. (1983b) Collagenase and Collagenolytic Activity in Human Osteoarthritic Cartilage. *Arthritis and Rheumatism,* 26, 63-68.

PENG, J., WALLAR, B. J., FLANDERS, A., SWIATEK, P. J. & ALBERTS, A. S. (2003) Disruption of the Diaphanous-related formin Drf1 gene encoding mDia1 reveals a role for Drf3 as an effector for Cdc42. *Curr Biol,* 13, 534-45.

PERKINS, G. L., DERFOUL, A., AST, A. & HALL, D. J. (2005) An inhibitor of the stretch-activated cation receptor exerts a potent effect on chondrocyte phenotype. *Differentiation,* 73, 199-211.

PERLSON, E., HANZ, S., BEN-YAAKOV, K., SEGAL-RUDER, Y., SEGER, R. & FAINZILBER, M. (2005) Vimentin-dependent spatial translocation of an activated MAP kinase in injured nerve. *Neuron,* 45, 715-26.

PERLSON, E., MICHAELEVSKI, I., KOWALSMAN, N., BEN-YAAKOV, K., SHAKED, M., SEGER, R., EISENSTEIN, M. & FAINZILBER, M. (2006) Vimentin binding to phosphorylated Erk sterically hinders enzymatic dephosphorylation of the kinase. *J Mol Biol,* 364, 938-44.

PETERSON, L., MINAS, T., BRITTBERG, M., NILSSON, A., SJOGREN-JANSSON, E. & LINDAHL, A. (2000) Two- to 9-year outcome after autologous chondrocyte transplantation of the knee. *Clin Orthop Relat Res,* 212-34.

PFAFFL, M. W. (2001) A new mathematical model for relative quantification in real-time RT-PCR. *Nucleic Acids Res,* 29, e45.

PFANDER, D., KORTJE, D., ZIMMERMANN, R., WESELOH, G., KIRSCH, T., GESSLEIN, M., CRAMER, T. & SWOBODA, B. (2001) Vascular endothelial growth factor in articular cartilage of healthy and osteoarthritic human knee joints. *Annals of the Rheumatic Diseases,* 60, 1070-1073.

PIEKNY, A., WERNER, M. & GLOTZER, M. (2005) Cytokinesis: welcome to the Rho zone. *Trends Cell Biol,* 15, 651-8.

PINGGUAN-MURPHY, B., EL-AZZEH, M., BADER, D. L. & KNIGHT, M. M. (2006) Cyclic compression of chondrocytes modulates a purinergic calcium signalling pathway in a strain rate- and frequency-dependent manner. *J Cell Physiol,* 209, 389-97.

PINGGUAN-MURPHY, B., LEE, D. A., BADER, D. L. & KNIGHT, M. M. (2005) Activation of chondrocytes calcium signalling by dynamic compression is independent of number of cycles. *Arch Biochem Biophys,* 444, 45-51.

POND, M. J. & NUKI, G. (1973) Experimentally-induced osteoarthritis in the dog. *Ann Rheum Dis,* 32, 387-8.

PONTA, H., SHERMAN, L. & HERRLICH, P. A. (2003) CD44: from adhesion molecules to signalling regulators. *Nat Rev Mol Cell Biol,* 4, 33-45.

POOLE, A. R., RIZKALLA, G., IONESCU, M., REINER, A., BROOKS, E., RORABECK, C., BOURNE, R. & BOGOCH, E. (1993) Osteoarthritis in the human knee: a dynamic process of cartilage matrix degradation, synthesis and reorganization. *Agents Actions Suppl,* 39, 3-13.

POOLE, C. A. (1997) Articular cartilage chondrons: Form, function and failure. *Journal of Anatomy,* 191, 1-13.

POOLE, C. A., ZHANG, Z. J. & ROSS, J. M. (2001) The differential distribution of acetylated and detyrosinated alpha-tubulin in the microtubular cytoskeleton and primary cilia of hyaline cartilage chondrocytes. *J Anat,* 199, 393-405.

POPOWICZ, G. M., SCHLEICHER, M., NOEGEL, A. A. & HOLAK, T. A. (2006) Filamins: promiscuous organizers of the cytoskeleton. *Trends Biochem Sci,* 31, 411-9.

PORTER, S., CLARK, I. M., KEVORKIAN, L. & EDWARDS, D. R. (2005) The ADAMTS metalloproteinases. *Biochem J,* 386, 15-27.

POULSOM, H. & CHARLES, P. J. (2008) Antibodies to citrullinated vimentin are a specific and sensitive marker for the diagnosis of rheumatoid arthritis. *Clin Rev Allergy Immunol,* 34, 4-10.

PRAETORIUS, H. A. & SPRING, K. R. (2001) Bending the MDCK cell primary cilium increases intracellular calcium. *J Membr Biol,* 184, 71-9.

PRAETORIUS, H. A. & SPRING, K. R. (2003) The renal cell primary cilium functions as a flow sensor. *Curr Opin Nephrol Hypertens,* 12, 517-20.

PULLIG, O., WESELOH, G., RONNEBERGER, D. L., KAKONEN, S. M. & SWOBODA, B. (2000) Chondrocyte differentiation in human osteoarthritis: Expression of osteocalcin in normal and osteoarthritic cartilage and bone. *Calcified Tissue International,* 67, 230-240.

PUTHALAKATH, H., VILLUNGER, A., O'REILLY, L. A., BEAUMONT, J. G., COULTAS, L., CHENEY, R. E., HUANG, D. C. & STRASSER, A. (2001) Bmf: a proapoptotic BH3-only protein regulated by interaction with the myosin V actin motor complex, activated by anoikis. *Science,* 293, 1829-32.

QUINN, T. M., GRODZINSKY, A. J., HUNZIKER, E. B. & SANDY, J. D. (1998) Effects of injurious compression on matrix turnover around individual cells in calf articular cartilage explants. *Journal of Orthopaedic Research,* 16, 490-499.

RAIZMAN, I., DE CROOS, J. N., ST-PIERRE, J. P., PILLIAR, R. M. & KANDEL, R. A. (2009) Articular cartilage subpopulations respond differently to cyclic compression in vitro. *Tissue Eng Part A,* 15, 3789-98.

RIZKALLA, G., REINER, A., BOGOCH, E. & POOLE, A. R. (1992) Studies of the articular cartilage proteoglycan aggrecan in health and osteoarthritis. Evidence for molecular heterogeneity and extensive molecular changes in disease. *J Clin Invest,* 90, 2268-77.

ROBERTS, S. R., KNIGHT, M. M., LEE, D. A. & BADER, D. L. (2001) Mechanical compression influences intracellular Ca2+ signaling in chondrocytes seeded in agarose constructs. *J Appl Physiol,* 90, 1385-91.

ROHATGI, R., MA, L., MIKI, H., LOPEZ, M., KIRCHHAUSEN, T., TAKENAWA, T. & KIRSCHNER, M. W. (1999) The interaction between N-WASP and the Arp2/3 complex links Cdc42-dependent signals to actin assembly. *Cell,* 97, 221-31.

ROMAN-BLAS, J. A., STOKES, D. G. & JIMENEZ, S. A. (2007) Modulation of TGF-beta signaling by proinflammatory cytokines in articular chondrocytes. *Osteoarthritis Cartilage,* 15, 1367-77.

ROOS, E. M. & DAHLBERG, L. (2005) Positive effects of moderate exercise on glycosaminoglycan content in knee cartilage - A four-month, randomized controlled trial in patients at risk of osteoarthritis. *Arthritis and Rheumatism,* 52, 3507-3514.

RUIZ-ROMERO, C., CARREIRA, V., REGO, I., REMESEIRO, S., LOPEZ-ARMADA, M. J. & BLANCO, F. J. (2008) Proteomic analysis of human osteoarthritic chondrocytes reveals protein changes in stress and glycolysis. *Proteomics,* 8, 495-507.

RYAN, J. A., EISNER, E. A., DURAINE, G., YOU, Z. & REDDI, A. H. (2009) Mechanical compression of articular cartilage induces chondrocyte proliferation

and inhibits proteoglycan synthesis by activation of the ERK pathway: implications for tissue engineering and regenerative medicine. *J Tissue Eng Regen Med,* 3, 107-16.

SAARAKKALA, S., JULKUNEN, P., KIVIRANTA, P., MAKITALO, J., JURVELIN, J. S. & KORHONEN, R. K. (2010) Depth-wise progression of osteoarthritis in human articular cartilage: investigation of composition, structure and biomechanics. *Osteoarthritis Cartilage,* 18, 73-81.

SALTER, D. M., GODOLPHIN, J. L. & GOURLAY, M. S. (1995) Chondrocyte heterogeneity: immunohistologically defined variation of integrin expression at different sites in human fetal knees. *J Histochem Cytochem,* 43, 447-57.

SALTER, D. M., HUGHES, D. E., SIMPSON, R. & GARDNER, D. L. (1992) Integrin Expression by Human Articular Chondrocytes. *British Journal of Rheumatology,* 31, 231-234.

SALTER, D. M., MILLWARD-SADLER, S. J., NUKI, G. & WRIGHT, M. O. (2001) Integrin-interleukin-4 mechanotransduction pathways in human chondrocytes. *Clinical Orthopaedics and Related Research,* S49-S60.

SALTER, D. M., MILLWARD-SADLER, S. J., NUKI, G. & WRIGHT, M. O. (2002) Differential responses of chondrocytes from normal and osteoarthritic human articular cartilage to mechanical stimulation. *Biorheology,* 39, 97-108.

SANDELL, L. J., XING, X., FRANZ, C., DAVIES, S., CHANG, L. W. & PATRA, D. (2008) Exuberant expression of chemokine genes by adult human articular chondrocytes in response to IL-1beta. *Osteoarthritis Cartilage,* 16, 1560-71.

SAWAJI, Y., HYNES, J., VINCENT, T. & SAKLATVALA, J. (2008) Fibroblast growth factor 2 inhibits induction of aggrecanase activity in human articular cartilage. *Arthritis Rheum,* 58, 3498-509.

SAWYER, S. J., NORVELL, S. M., PONIK, S. M. & PAVALKO, F. M. (2001) Regulation of PGE(2) and PGI(2) release from human umbilical vein endothelial cells by actin cytoskeleton. *Am J Physiol Cell Physiol,* 281, C1038-45.

SCHMELZLE, T., MAILLEUX, A. A., OVERHOLTZER, M., CARROLL, J. S., SOLIMINI, N. L., LIGHTCAP, E. S., VEIBY, O. P. & BRUGGE, J. S. (2007) Functional role and oncogene-regulated expression of the BH3-only factor Bmf in mammary epithelial anoikis and morphogenesis. *Proc Natl Acad Sci U S A,* 104, 3787-92.

SCHMID, M. F., AGRIS, J. M., JAKANA, J., MATSUDAIRA, P. & CHIU, W. (1994) Three-dimensional structure of a single filament in the Limulus acrosomal bundle: scruin binds to homologous helix-loop-beta motifs in actin. *J Cell Biol,* 124, 341-50.

SCHMIDT, O., MIZRAHI, J., ELISSEEFF, J. & SELIKTAR, D. (2006) Immobilized fibrinogen in PEG hydrogels does not improve chondrocyte-mediated matrix deposition in response to mechanical stimulation. *Biotechnol Bioeng,* 95, 1061-9.

SCHUTT, C. E., MYSLIK, J. C., ROZYCKI, M. D., GOONESEKERE, N. C. & LINDBERG, U. (1993) The structure of crystalline profilin-beta-actin. *Nature,* 365, 810-6.

SHAKIBAEI, M., SEIFARTH, C., JOHN, T., RAHMANZADEH, M. & MOBASHERI, A. (2006) Igf-I extends the chondrogenic potential of human articular

chondrocytes in vitro: molecular association between Sox9 and Erk1/2. *Biochem Pharmacol,* 72, 1382-95.

SHARIF, M., WHITEHOUSE, A., SHARMAN, P., PERRY, M. & ADAMS, M. (2004) Increased apoptosis in human osteoarthritic cartilage corresponds to reduced cell density and expression of caspase-3. *Arthritis Rheum,* 50, 507-15.

SHAWLOT, W., DENG, J. M., FOHN, L. E. & BEHRINGER, R. R. (1998) Restricted beta-galactosidase expression of a hygromycin-lacZ gene targeted to the beta-actin locus and embryonic lethality of beta-actin mutant mice. *Transgenic Res,* 7, 95-103.

SHIBATA, Y., NAKAMURA, H., KATO, S. & TOMOIKE, H. (1996) Cellular detachment and deformation induce IL-8 gene expression in human bronchial epithelial cells. *J Immunol,* 156, 772-7.

SHIFRIN, Y., ARORA, P. D., OHTA, Y., CALDERWOOD, D. A. & MCCULLOCH, C. A. (2009) The role of FilGAP-filamin A interactions in mechanoprotection. *Mol Biol Cell,* 20, 1269-79.

SHIM, J. W., WISE, D. A. & ELDER, S. H. (2008) Effect of Cytoskeletal Disruption on Mechanotransduction of Hydrostatic Pressure by C3H10T1/2 Murine Fibroblasts. *Open Orthop J,* 2, 155-62.

SHIMAZAKI, A., WRIGHT, M. O., ELLIOT, K., SALTER, D. M. & MILLWARD-SADLER, S. J. (2006) Calcium/calmodulin-dependent protein kinase II in human articular chondrocytes. *Biorheology,* 43, 223-33.

SHIMIZU, M., HIGUCHI, H., TAKAGISHI, K., SHINOZAKI, T. & KOBAYASHI, T. (2010) Clinical and biochemical characteristics after intra-articular injection for the treatment of osteoarthritis of the knee: prospective randomized study of sodium hyaluronate and corticosteroid. *J Orthop Sci,* 15, 51-6.

SHMERLING, D., DANZER, C. P., MAO, X., BOISCLAIR, J., HAFFNER, M., LEMAISTRE, M., SCHULER, V., KAESLIN, E., KORN, R., BURKI, K., LEDERMANN, B., KINZEL, B. & MULLER, M. (2005) Strong and ubiquitous expression of transgenes targeted into the beta-actin locus by Cre/lox cassette replacement. *Genesis,* 42, 229-35.

SHULER, F. D., GEORGESCU, H. I., NIYIBIZI, C., STUDER, R. K., MI, Z., JOHNSTONE, B., ROBBINS, R. D. & EVANS, C. H. (2000) Increased matrix synthesis following adenoviral transfer of a transforming growth factor beta1 gene into articular chondrocytes. *J Orthop Res,* 18, 585-92.

SILACCI, P., MAZZOLAI, L., GAUCI, C., STERGIOPULOS, N., YIN, H. L. & HAYOZ, D. (2004) Gelsolin superfamily proteins: key regulators of cellular functions. *Cell Mol Life Sci,* 61, 2614-23.

SILVER, F. H. & GLASGOLD, A. I. (1995) Cartilage wound healing. An overview. *Otolaryngol Clin North Am,* 28, 847-64.

SIMS, J. R., KARP, S. & INGBER, D. E. (1992) Altering the cellular mechanical force balance results in integrated changes in cell, cytoskeletal and nuclear shape. *J Cell Sci,* 103 (Pt 4), 1215-22.

SIN, W. C., CHEN, X. Q., LEUNG, T. & LIM, L. (1998) RhoA-binding kinase alpha translocation is facilitated by the collapse of the vimentin intermediate filament network. *Mol Cell Biol,* 18, 6325-39.

SMITH, J. O., OREFFO, R. O., CLARKE, N. M. & ROACH, H. I. (2003) Changes in the antiangiogenic properties of articular cartilage in osteoarthritis. *J Orthop Sci,* 8, 849-57.

SMITH, P., SHULER, F. D., GEORGESCU, H. I., GHIVIZZANI, S. C., JOHNSTONE, B., NIYIBIZI, C., ROBBINS, P. D. & EVANS, C. H. (2000) Genetic enhancement of matrix synthesis by articular chondrocytes: comparison of different growth factor genes in the presence and absence of interleukin-1. *Arthritis Rheum,* 43, 1156-64.

SOLURSH, M. (1991) Formation of cartilage tissue in vitro. *J Cell Biochem,* 45, 258-60.

SONG, R. H., TORTORELLA, M. D., MALFAIT, A. M., ALSTON, J. T., YANG, Z., ARNER, E. C. & GRIGGS, D. W. (2007) Aggrecan degradation in human articular cartilage explants is mediated by both ADAMTS-4 and ADAMTS-5. *Arthritis Rheum,* 56, 575-85.

SPRINGER, J. E., AZBILL, R. D., KENNEDY, S. E., GEORGE, J. & GEDDES, J. W. (1997) Rapid calpain I activation and cytoskeletal protein degradation following traumatic spinal cord injury: attenuation with riluzole pretreatment. *J Neurochem,* 69, 1592-600.

STANTON, H., ROGERSON, F. M., EAST, C. J., GOLUB, S. B., LAWLOR, K. E., MEEKER, C. T., LITTLE, C. B., LAST, K., FARMER, P. J., CAMPBELL, I. K., FOURIE, A. M. & FOSANG, A. J. (2005) ADAMTS5 is the major aggrecanase in mouse cartilage in vivo and in vitro. *Nature,* 434, 648-52.

STEINMETZ, M. O., KAMMERER, R. A., JAHNKE, W., GOLDIE, K. N., LUSTIG, A. & VAN OOSTRUM, J. (2000) Op18/stathmin caps a kinked protofilament-like tubulin tetramer. *EMBO J,* 19, 572-80.

STEINMEYER, J. & KNUE, S. (1997) The proteoglycan metabolism of mature bovine articular cartilage explants superimposed to continuously applied cyclic mechanical loading. *Biochemical and Biophysical Research Communications,* 240, 216-221.

STOKES, D. G., LIU, G., DHARMAVARAM, R., HAWKINS, D., PIERA-VELAZQUEZ, S. & JIMENEZ, S. A. (2001) Regulation of type-II collagen gene expression during human chondrocyte de-differentiation and recovery of chondrocyte-specific phenotype in culture involves Sry-type high-mobility-group box (SOX) transcription factors. *Biochem J,* 360, 461-70.

STOSSEL, T. P., CONDEELIS, J., COOLEY, L., HARTWIG, J. H., NOEGEL, A., SCHLEICHER, M. & SHAPIRO, S. S. (2001) Filamins as integrators of cell mechanics and signalling. *Nat Rev Mol Cell Biol,* 2, 138-45.

SUBBARAMAIAH, K., HART, J. C., NORTON, L. & DANNENBERG, A. J. (2000) Microtubule-interfering agents stimulate the transcription of cyclooxygenase-2. Evidence for involvement of ERK1/2 AND p38 mitogen-activated protein kinase pathways. *J Biol Chem,* 275, 14838-45.

SUMIZAWA, T. & IGISU, H. (2007) Apoptosis induced by acrylamide in SH-SY5Y cells. *Arch Toxicol,* 81, 279-82.

SUN, H. Q., YAMAMOTO, M., MEJILLANO, M. & YIN, H. L. (1999) Gelsolin, a multifunctional actin regulatory protein. *J Biol Chem,* 274, 33179-82.

SUNG, L. Y., CHIU, H. Y., CHEN, H. C., CHEN, Y. L., CHUANG, C. K. & HU, Y. C. (2009) Baculovirus-mediated growth factor expression in dedifferentiated chondrocytes accelerates redifferentiation: effects of combinational transduction. *Tissue Eng Part A,* 15, 1353-62.

SWINGLER, T. E., WATERS, J. G., DAVIDSON, R. K., PENNINGTON, C. J., PUENTE, X. S., DARRAH, C., COOPER, A., DONELL, S. T., GUILE, G. R., WANG, W. & CLARK, I. M. (2009) Degradome expression profiling in human articular cartilage. *Arthritis Res Ther,* 11, R96.

TAKAHASHI, I., NUCKOLLS, G. H., TAKAHASHI, K., TANAKA, O., SEMBA, I., DASHNER, R., SHUM, L. & SLAVKIN, H. C. (1998) Compressive force promotes sox9, type II collagen and aggrecan and inhibits IL-1beta expression resulting in chondrogenesis in mouse embryonic limb bud mesenchymal cells. *J Cell Sci,* 111 (Pt 14), 2067-76.

TAKIGAWA, M., TAKANO, T., SHIRAI, E. & SUZUKI, F. (1984) Cytoskeleton and differentiation: effects of cytochalasin B and colchicine on expression of the differentiated phenotype of rabbit costal chondrocytes in culture. *Cell Differ,* 14, 197-204.

TALLHEDEN, T., BENGTSSON, C., BRANTSING, C., SJOGREN-JANSSON, E., CARLSSON, L., PETERSON, L., BRITTBERG, M. & LINDAHL, A. (2005) Proliferation and differentiation potential of chondrocytes from osteoarthritic patients. *Arthritis Res Ther,* 7, R560-8.

TALLHEDEN, T., KARLSSON, C., BRUNNER, A., VAN DER LEE, J., HAGG, R., TOMMASINI, R. & LINDAHL, A. (2004) Gene expression during redifferentiation of human articular chondrocytes. *Osteoarthritis Cartilage,* 12, 525-35.

TASKIRAN, D., STEFANOVIC-RACIC, M., GEORGESCU, H. & EVANS, C. (1994) Nitric oxide mediates suppression of cartilage proteoglycan synthesis by interleukin-1. *Biochem Biophys Res Commun,* 200, 142-8.

TCHETINA, E. V., DI BATTISTA, J. A., ZUKOR, D. J., ANTONIOU, J. & POOLE, A. R. (2007) Prostaglandin PGE2 at very low concentrations suppresses collagen cleavage in cultured human osteoarthritic articular cartilage: this involves a decrease in expression of proinflammatory genes, collagenases and COL10A1, a gene linked to chondrocyte hypertrophy. *Arthritis Res Ther,* 9, R75.

TCHETINA, E. V., SQUIRES, G. & POOLE, A. R. (2005) Increased type II collagen degradation and very early focal cartilage degeneration is associated with upregulation of chondrocyte differentiation related genes in early human articular cartilage lesions. *Journal of Rheumatology,* 32, 876-886.

TEW, S. R. & HARDINGHAM, T. E. (2006) Regulation of SOX9 mRNA in human articular chondrocytes involving p38 MAPK activation and mRNA stabilization. *J Biol Chem,* 281, 39471-9.

TEW, S. R., LI, Y., POTHACHAROEN, P., TWEATS, L. M., HAWKINS, R. E. & HARDINGHAM, T. E. (2005) Retroviral transduction with SOX9 enhances re-expression of the chondrocyte phenotype in passaged osteoarthritic human articular chondrocytes. *Osteoarthritis Cartilage,* 13, 80-9.

TEW, S. R., PEFFERS, M. J., MCKAY, T. R., LOWE, E. T., KHAN, W. S., HARDINGHAM, T. E. & CLEGG, P. D. (2009) Hyperosmolarity regulates SOX9 mRNA posttranscriptionally in human articular chondrocytes. *Am J Physiol Cell Physiol,* 297, C898-906.

THAMBYAH, A., NATHER, A. & GOH, J. (2006) Mechanical properties of articular cartilage covered by the meniscus. *Osteoarthritis and Cartilage,* 14, 580-588.

THOMPSON, T. G., CHAN, Y. M., HACK, A. A., BROSIUS, M., RAJALA, M., LIDOV, H. G., MCNALLY, E. M., WATKINS, S. & KUNKEL, L. M. (2000) Filamin 2 (FLN2): A muscle-specific sarcoglycan interacting protein. *J Cell Biol,* 148, 115-26.

TILLEMAN, K., VAN STEENDAM, K., CANTAERT, T., DE KEYSER, F., ELEWAUT, D. & DEFORCE, D. (2008) Synovial detection and autoantibody reactivity of processed citrullinated isoforms of vimentin in inflammatory arthritides. *Rheumatology (Oxford),* 47, 597-604.

TOIVANEN, A. T., HELIOVAARA, M., IMPIVAARA, O., AROKOSKI, J. P., KNEKT, P., LAUREN, H. & KROGER, H. (2010) Obesity, physically demanding work and traumatic knee injury are major risk factors for knee osteoarthritis--a population-based study with a follow-up of 22 years. *Rheumatology (Oxford),* 49, 308-14.

TOMASEK, J. J., HALLIDAY, N. L., UPDIKE, D. L., AHERNMOORE, J. S., VU, T. K. H., LIU, R. W. & HOWARD, E. W. (1997) Gelatinase A activation is regulated by the organization of the polymerized actin cytoskeleton. *Journal of Biological Chemistry,* 272, 7482-7487.

TOMASEVIC, N., JIA, Z., RUSSELL, A., FUJII, T., HARTMAN, J. J., CLANCY, S., WANG, M., BERAUD, C., WOOD, K. W. & SAKOWICZ, R. (2007) Differential regulation of WASP and N-WASP by Cdc42, Rac1, Nck, and PI(4,5)P2. *Biochemistry,* 46, 3494-502.

TONDELEIR, D., VANDAMME, D., VANDEKERCKHOVE, J., AMPE, C. & LAMBRECHTS, A. (2009) Actin isoform expression patterns during mammalian development and in pathology: insights from mouse models. *Cell Motil Cytoskeleton,* 66, 798-815.

TOWBIN, H., STAEHELIN, T. & GORDON, J. (1979) Electrophoretic Transfer of Proteins from Polyacrylamide Gels to Nitrocellulose Sheets - Procedure and Some Applications. *Proceedings of the National Academy of Sciences of the United States of America,* 76, 4350-4354.

TOYODA, T., SEEDHOM, B. B., YAO, J. Q., KIRKHAM, J., BROOKES, S. & BONASS, W. A. (2003) Hydrostatic pressure modulates proteoglycan metabolism in chondrocytes seeded in agarose. *Arthritis Rheum,* 48, 2865-72.

TRICKEY, W. R., LEE, G. M. & GUILAK, F. (2000) Viscoelastic properties of chondrocytes from normal and osteoarthritic human cartilage. *Journal of Orthopaedic Research,* 18, 891-898.

TRICKEY, W. R., VAIL, T. P. & GUILAK, F. (2004) The role of the cytoskeleton in the viscoelastic properties of human articular chondrocytes. *Journal of Orthopaedic Research,* 22, 131-139.

TSENG, Y., FEDOROV, E., MCCAFFERY, J. M., ALMO, S. C. & WIRTZ, D. (2001) Micromechanics and ultrastructure of actin filament networks crosslinked by human fascin: a comparison with alpha-actinin. *J Mol Biol,* 310, 351-66.

TURNER, C. E., GLENNEY, J. R., JR. & BURRIDGE, K. (1990) Paxillin: a new vinculin-binding protein present in focal adhesions. *J Cell Biol,* 111, 1059-68.

URBANIK, E. & WARE, B. R. (1989) Actin filament capping and cleaving activity of cytochalasins B, D, E, and H. *Arch Biochem Biophys,* 269, 181-7.

VALDES, A. M. & SPECTOR, T. D. (2010) The genetic epidemiology of osteoarthritis. *Curr Opin Rheumatol,* 22, 139-43.

VALIRON, O., CAUDRON, N. & JOB, D. (2001) Microtubule dynamics. *Cell Mol Life Sci,* 58, 2069-84.

VALVERDE-FRANCO, G., BINETTE, J. S., LI, W., WANG, H., CHAI, S., LAFLAMME, F., TRAN-KHANH, N., QUENNEVILLE, E., MEIJERS, T., POOLE, A. R., MORT, J. S., BUSCHMANN, M. D. & HENDERSON, J. E. (2006) Defects in articular cartilage metabolism and early arthritis in fibroblast growth factor receptor 3 deficient mice. *Hum Mol Genet,* 15, 1783-92.

VAN DEN BERG, W. B. (2001) Lessons from animal models of osteoarthritis. *Curr Opin Rheumatol,* 13, 452-6.

VANDEKERCKHOVE, J. & WEBER, K. (1978a) At least six different actins are expressed in a higher mammal: an analysis based on the amino acid sequence of the amino-terminal tryptic peptide. *J Mol Biol,* 126, 783-802.

VANDEKERCKHOVE, J. & WEBER, K. (1978b) Mammalian cytoplasmic actins are the products of at least two genes and differ in primary structure in at least 25 identified positions from skeletal muscle actins. *Proc Natl Acad Sci U S A,* 75, 1106-10.

VARANI, K., DE MATTEI, M., VINCENZI, F., TOSI, A., GESSI, S., MERIGHI, S., PELLATI, A., MASIERI, F., ONGARO, A. & BOREA, P. A. (2008) Pharmacological characterization of P2X1 and P2X3 purinergic receptors in bovine chondrocytes. *Osteoarthritis Cartilage,* 16, 1421-9.

VARDOULI, L., MOUSTAKAS, A. & STOURNARAS, C. (2005) LIM-kinase 2 and cofilin phosphorylation mediate actin cytoskeleton reorganization induced by transforming growth factor-beta. *J Biol Chem,* 280, 11448-57.

VAREDI, M., GHAHARY, A., SCOTT, P. G. & TREDGET, E. E. (1997) Cytoskeleton regulates expression of genes for transforming growth factor-beta 1 and extracellular matrix proteins in dermal fibroblasts. *J Cell Physiol,* 172, 192-9.

VAUGHAN, K. T. (2005) Microtubule plus ends, motors, and traffic of Golgi membranes. *Biochim Biophys Acta,* 1744, 316-24.

VINALL, R. L., LO, S. H. & REDDI, A. H. (2002) Regulation of articular chondrocyte phenotype by bone morphogenetic protein 7, interleukin 1, and cellular context is dependent on the cytoskeleton. *Exp Cell Res,* 272, 32-44.

VINCENT, T., HERMANSSON, M., BOLTON, M., WAIT, R. & SAKLATVALA, J. (2002) Basic FGF mediates an immediate response of articular cartilage to mechanical injury. *Proc Natl Acad Sci U S A,* 99, 8259-64.

VINCENT, T. L., HERMANSSON, M. A., HANSEN, U. N., AMIS, A. A. & SAKLATVALA, J. (2004) Basic fibroblast growth factor mediates transduction of mechanical signals when articular cartilage is loaded. *Arthritis Rheum,* 50, 526-33.

VINCENT, T. L., MCLEAN, C. J., FULL, L. E., PESTON, D. & SAKLATVALA, J. (2007) FGF-2 is bound to perlecan in the pericellular matrix of articular cartilage, where it acts as a chondrocyte mechanotransducer. *Osteoarthritis Cartilage,* 15, 752-63.

VINCOURT, J. B., LIONNETON, F., KRATASSIOUK, G., GUILLEMIN, F., NETTER, P., MAINARD, D. & MAGDALOU, J. (2006) Establishment of a reliable method for direct proteome characterization of human articular cartilage. *Molecular & Cellular Proteomics,* 5, 1984-1995.

VON DER MARK, K., GAUSS, V., VON DER MARK, H. & MULLER, P. (1977) Relationship between cell shape and type of collagen synthesised as chondrocytes lose their cartilage phenotype in culture. *Nature,* 267, 531-2.

VON DER MARK, K., KIRSCH, T., NERLICH, A., KUSS, A., WESELOH, G., GLUCKERT, K. & STOSS, H. (1992) Type-X Collagen-Synthesis in Human Osteoarthritic Cartilage - Indication of Chondrocyte Hypertrophy. *Arthritis and Rheumatism,* 35, 806-811.

VOSSENAAR, E. R., ZENDMAN, A. J., VAN VENROOIJ, W. J. & PRUIJN, G. J. (2003) PAD, a growing family of citrullinating enzymes: genes, features and involvement in disease. *Bioessays,* 25, 1106-18.

WADE, R. H. & HYMAN, A. A. (1997) Microtubule structure and dynamics. *Curr Opin Cell Biol,* 9, 12-7.

WALDMAN, S. D., COUTO, D. C., GRYNPAS, M. D., PILLIAR, R. M. & KANDEL, R. A. (2006) A single application of cyclic loading can accelerate matrix deposition and enhance the properties of tissue-engineered cartilage. *Osteoarthritis Cartilage,* 14, 323-30.

WALTON, M. (1977) Studies of degenerative joint disease in the mouse knee joint; scanning electron microscopy. *J Pathol,* 123, 211-7.

WANG, G. & BEIER, F. (2005) Rac1/Cdc42 and RhoA GTPases antagonistically regulate chondrocyte proliferation, hypertrophy, and apoptosis. *J Bone Miner Res,* 20, 1022-31.

WANG, G., WOODS, A., AGOSTON, H., ULICI, V., GLOGAUER, M. & BEIER, F. (2007) Genetic ablation of Rac1 in cartilage results in chondrodysplasia. *Dev Biol,* 306, 612-23.

WANG, G., WOODS, A., SABARI, S., PAGNOTTA, L., STANTON, L. A. & BEIER, F. (2004) RhoA/ROCK signaling suppresses hypertrophic chondrocyte differentiation. *J Biol Chem,* 279, 13205-14.

WANG, N. & STAMENOVIC, D. (2000) Contribution of intermediate filaments to cell stiffness, stiffening, and growth. *Am J Physiol Cell Physiol,* 279, C188-94.

WANG, P. Y., CHOW, H. H., TSAI, W. B. & FANG, H. W. (2009a) Modulation of gene expression of rabbit chondrocytes by dynamic compression in polyurethane scaffolds with collagen gel encapsulation. *J Biomater Appl,* 23, 347-66.

WANG, Q. G., MAGNAY, J. L., NGUYEN, B., THOMAS, C. R., ZHANG, Z., EL HAJ, A. J. & KUIPER, N. J. (2009b) Gene expression profiles of dynamically compressed single chondrocytes and chondrons. *Biochem Biophys Res Commun,* 379, 738-42.

WANG, Q. G., NGUYEN, B., THOMAS, C. R., ZHANG, Z., EL HAJ, A. J. & KUIPER, N. J. (2010) Molecular profiling of single cells in response to mechanical force: comparison of chondrocytes, chondrons and encapsulated chondrocytes. *Biomaterials,* 31, 1619-25.

WANG, Y., DE ISLA, N., DECOT, V., MARCHAL, L., CAUCHOIS, G., HUSELSTEIN, C., MULLER, S., WANG, B. H., NETTER, P. & STOLTZ, J. F. (2008a) Influences of construct properties on the proliferation and matrix synthesis of dedifferentiated chondrocytes cultured in alginate gel. *Biorheology,* 45, 527-38.

WANG, Y., DE ISLA, N., HUSELSTEIN, C., WANG, B., NETTER, P., STOLTZ, J. F. & MULLER, S. (2008b) Effect of alginate culture and mechanical stimulation on cartilaginous matrix synthesis of rat dedifferentiated chondrocytes. *Biomed Mater Eng,* 18, S47-54.

WANG, Y. H., YAN, Z. Q., SHEN, B. R., ZHANG, L., ZHANG, P. & JIANG, Z. L. (2009c) Vascular smooth muscle cells promote endothelial cell adhesion via microtubule dynamics and activation of paxillin and the extracellular signal-regulated kinase (ERK) pathway in a co-culture system. *Eur J Cell Biol,* 88, 701-9.

WATT, F. M. & DUDHIA, J. (1988) Prolonged expression of differentiated phenotype by chondrocytes cultured at low density on a composite substrate of collagen and agarose that restricts cell spreading. *Differentiation,* 38, 140-7.

WEAR, M. A., SCHAFER, D. A. & COOPER, J. A. (2000) Actin dynamics: assembly and disassembly of actin networks. *Curr Biol,* 10, R891-5.

WEBER, A., NACHMIAS, V. T., PENNISE, C. R., PRING, M. & SAFER, D. (1992) Interaction of thymosin beta 4 with muscle and platelet actin: implications for actin sequestration in resting platelets. *Biochemistry,* 31, 6179-85.

WEI, J., XU, G., WU, M., ZHANG, Y., LI, Q., LIU, P., ZHU, T., SONG, A., ZHAO, L., HAN, Z., CHEN, G., WANG, S., MENG, L., ZHOU, J., LU, Y. & MA, D. (2008) Overexpression of vimentin contributes to prostate cancer invasion and metastasis via src regulation. *Anticancer Res,* 28, 327-34.

WELCH, M. D., DEPACE, A. H., VERMA, S., IWAMATSU, A. & MITCHISON, T. J. (1997) The human Arp2/3 complex is composed of evolutionarily conserved subunits and is localized to cellular regions of dynamic actin filament assembly. *J Cell Biol,* 138, 375-84.

WERB, Z., HEMBRY, R. M., MURPHY, G. & AGGELER, J. (1986) Commitment to Expression of the Metalloendopeptidases, Collagenase and Stromelysin - Relationship of Inducing Events to Changes in Cytoskeletal Architecture. *Journal of Cell Biology,* 102, 697-702.

WHEELER, C. A., JAFARZADEH, S. R., ROCKE, D. M. & GRODZINSKY, A. J. (2009) IGF-1 does not moderate the time-dependent transcriptional patterns of

key homeostatic genes induced by sustained compression of bovine cartilage. *Osteoarthritis Cartilage,* 17, 944-52.

WIESE, C. & ZHENG, Y. (2006) Microtubule nucleation: gamma-tubulin and beyond. *J Cell Sci,* 119, 4143-53.

WITTECK, A., YAO, Y., FECHIR, M., FORSTERMANN, U. & KLEINERT, H. (2003) Rho protein-mediated changes in the structure of the actin cytoskeleton regulate human inducible NO synthase gene expression. *Exp Cell Res,* 287, 106-15.

WOESSNER, J. F. (1976) Determination of Hydroxyproline in Connective Tissues. IN HALL, D. A. (Ed.) *The Methodology of Connective Tissue Research.* Oxford, Joynson-Bruvvers Ltd.

WOESSNER, J. F. (1991) Matrix Metalloproteinases and Their Inhibitors in Connective-Tissue Remodeling. *Faseb Journal,* 5, 2145-2154.

WONG, M., SIEGRIST, M. & GOODWIN, K. (2003) Cyclic tensile strain and cyclic hydrostatic pressure differentially regulate expression of hypertrophic markers in primary chondrocytes. *Bone,* 33, 685-93.

WOODRUM, D. T., RICH, S. A. & POLLARD, T. D. (1975) Evidence for biased bidirectional polymerization of actin filaments using heavy meromyosin prepared by an improved method. *J Cell Biol,* 67, 231-7.

WOODS, A. & BEIER, F. (2006) RhoA/ROCK signaling regulates chondrogenesis in a context-dependent manner. *J Biol Chem,* 281, 13134-40.

WOODS, A. & COUCHMAN, J. R. (1994) Syndecan 4 heparan sulfate proteoglycan is a selectively enriched and widespread focal adhesion component. *Mol Biol Cell,* 5, 183-92.

WOODS, A., JAMES, C. G., WANG, G., DUPUIS, H. & BEIER, F. (2009) Control of Chondrocyte Gene Expression by Actin Dynamics: A Novel Role of Cholesterol/Roralpha Signaling in Endochondral Bone Growth. *J Cell Mol Med.*

WOODS, A., WANG, G., DUPUIS, H., SHAO, Z. & BEIER, F. (2007) Rac1 signaling stimulates N-cadherin expression, mesenchymal condensation, and chondrogenesis. *J Biol Chem,* 282, 23500-8.

WOODS, A., WANG, G. Y. & BEIER, F. (2005) RhoA/ROCK signaling regulates Sox9 expression and actin organization during chondrogenesis. *Journal of Biological Chemistry,* 280, 11626-11634.

WOODS, V. L., SCHRECK, P. J., GESINK, D. S., PACHECO, H. O., AMIEL, D., AKESON, W. H. & LOTZ, M. (1994) Integrin Expression by Human Articular Chondrocytes. *Arthritis and Rheumatism,* 37, 537-544.

WOZNIAK, M. A., DESAI, R., SOLSKI, P. A., DER, C. J. & KEELY, P. J. (2003) ROCK-generated contractility regulates breast epithelial cell differentiation in response to the physical properties of a three-dimensional collagen matrix. *J Cell Biol,* 163, 583-95.

WRIGHT, M., JOBANPUTRA, P., BAVINGTON, C., SALTER, D. M. & NUKI, G. (1996) Effects of intermittent pressure-induced strain on the electrophysiology of cultured human chondrocytes: evidence for the presence of stretch-activated membrane ion channels. *Clin Sci (Lond),* 90, 61-71.

WRIGHT, M. O., NISHIDA, K., BAVINGTON, C., GODOLPHIN, J. L., DUNNE, E., WALMSLEY, S., JOBANPUTRA, P., NUKI, G. & SALTER, D. M. (1997) Hyperpolarisation of cultured human chondrocytes following cyclical pressure-induced strain: evidence of a role for alpha 5 beta 1 integrin as a chondrocyte mechanoreceptor. *J Orthop Res,* 15, 742-7.

WU, Q. Q. & CHEN, Q. (2000) Mechanoregulation of chondrocyte proliferation, maturation, and hypertrophy: ion-channel dependent transduction of matrix deformation signals. *Exp Cell Res,* 256, 383-91.

XIE, J., HAN, Z. Y. & MATSUDA, T. (2006) Mechanical compressive loading stimulates the activity of proximal region of human COL2A1 gene promoter in transfected chondrocytes. *Biochem Biophys Res Commun,* 344, 1192-9.

XU, Y., MOSELEY, J. B., SAGOT, I., POY, F., PELLMAN, D., GOODE, B. L. & ECK, M. J. (2004) Crystal structures of a Formin Homology-2 domain reveal a tethered dimer architecture. *Cell,* 116, 711-23.

YAGI, R., MCBURNEY, D., LAVERTY, D., WEINER, S. & HORTON, W. E., JR. (2005) Intrajoint comparisons of gene expression patterns in human osteoarthritis suggest a change in chondrocyte phenotype. *J Orthop Res,* 23, 1128-38.

YANG, C., PATEL, K., HARDING, P., SOROKIN, A. & GLASS, W. F., 2ND (2007) Regulation of TGF-beta1/MAPK-mediated PAI-1 gene expression by the actin cytoskeleton in human mesangial cells. *Exp Cell Res,* 313, 1240-50.

YANG, K. G., SARIS, D. B., GEUZE, R. E., VAN RIJEN, M. H., VAN DER HELM, Y. J., VERBOUT, A. J., CREEMERS, L. B. & DHERT, W. J. (2006) Altered in vitro chondrogenic properties of chondrocytes harvested from unaffected cartilage in osteoarthritic joints. *Osteoarthritis Cartilage,* 14, 561-70.

YANG, N., HIGUCHI, O., OHASHI, K., NAGATA, K., WADA, A., KANGAWA, K., NISHIDA, E. & MIZUNO, K. (1998) Cofilin phosphorylation by LIM-kinase 1 and its role in Rac-mediated actin reorganization. *Nature,* 393, 809-12.

YANG, X., WANG, J., LIU, C., GRIZZLE, W. E., YU, S., ZHANG, S., BARNES, S., KOOPMAN, W. J., MOUNTZ, J. D., KIMBERLY, R. P. & ZHANG, H. G. (2005) Cleavage of p53-vimentin complex enhances tumor necrosis factor-related apoptosis-inducing ligand-mediated apoptosis of rheumatoid arthritis synovial fibroblasts. *Am J Pathol,* 167, 705-19.

YEN, T. J., GAY, D. A., PACHTER, J. S. & CLEVELAND, D. W. (1988) Autoregulated changes in stability of polyribosome-bound beta-tubulin mRNAs are specified by the first 13 translated nucleotides. *Mol Cell Biol,* 8, 1224-35.

YONEZAWA, N., NISHIDA, E., IIDA, K., YAHARA, I. & SAKAI, H. (1990) Inhibition of the interactions of cofilin, destrin, and deoxyribonuclease I with actin by phosphoinositides. *J Biol Chem,* 265, 8382-6.

YOO, J., GHIASSI, M., JIRMANOVA, L., BALLIET, A. G., HOFFMAN, B., FORNACE, A. J., JR., LIEBERMANN, D. A., BOTTINGER, E. P. & ROBERTS, A. B. (2003) Transforming growth factor-beta-induced apoptosis is mediated by Smad-dependent expression of GADD45b through p38 activation. *J Biol Chem,* 278, 43001-7.

YOSHIDA, H., MURACHI, T. & TSUKAHARA, I. (1984) Degradation of actin and vimentin by calpain II, a Ca2+-dependent cysteine proteinase, in bovine lens. *FEBS Lett,* 170, 259-62.

YU, F. X., LIN, S. C., MORRISON-BOGORAD, M., ATKINSON, M. A. & YIN, H. L. (1993) Thymosin beta 10 and thymosin beta 4 are both actin monomer sequestering proteins. *J Biol Chem,* 268, 502-9.

ZAIDEL-BAR, R., BALLESTREM, C., KAM, Z. & GEIGER, B. (2003) Early molecular events in the assembly of matrix adhesions at the leading edge of migrating cells. *J Cell Sci,* 116, 4605-13.

ZAUCKE, F., DINSER, R., MAURER, P. & PAULSSON, M. (2001) Cartilage oligomeric matrix protein (COMP) and collagen IX are sensitive markers for the differentiation state of articular primary chondrocytes. *Biochem J,* 358, 17-24.

ZEMMYO, M., MEHARRA, E. J., KUHN, K., CREIGHTON-ACHERMANN, L. & LOTZ, M. (2003) Accelerated, aging-dependent development of osteoarthritis in alpha1 integrin-deficient mice. *Arthritis Rheum,* 48, 2873-80.

ZENG, W., CORCORAN, C., COLLINS-RACIE, L. A., LAVALLIE, E. R., MORRIS, E. A. & FLANNERY, C. R. (2006) Glycosaminoglycan-binding properties and aggrecanase activities of truncated ADAMTSs: comparative analyses with ADAMTS-5, -9, -16 and -18. *Biochim Biophys Acta,* 1760, 517-24.

ZHANG, L. & ESKO, J. D. (1994) Amino acid determinants that drive heparan sulfate assembly in a proteoglycan. *J Biol Chem,* 269, 19295-9.

ZHANG, L., YANG, M., YANG, D., CAVEY, G., DAVIDSON, P. & GIBSON, G. (2010) Molecular Interactions of MMP-13 C-Terminal Domain with Chondrocyte Proteins. *Connect Tissue Res.*

ZHANG, M., WANG, J. J. & CHEN, Y. J. (2006a) Effects of mechanical pressure on intracellular calcium release channel and cytoskeletal structure in rabbit mandibular condylar chondrocytes. *Life Sciences,* 78, 2480-2487.

ZHANG, M., ZHOU, Q., LIANG, Q. Q., LI, C. G., HOLZ, J. D., TANG, D., SHEU, T. J., LI, T. F., SHI, Q. & WANG, Y. J. (2009) IGF-1 regulation of type II collagen and MMP-13 expression in rat endplate chondrocytes via distinct signaling pathways. *Osteoarthritis Cartilage,* 17, 100-6.

ZHANG, Z., FAN, J., BECKER, K. G., GRAFF, R. D., LEE, G. M. & FRANCOMANO, C. A. (2006b) Comparison of gene expression profile between human chondrons and chondrocytes: a cDNA microarray study. *Osteoarthritis Cartilage,* 14, 449-59.

ZHANG, Z., MESSANA, J., HWANG, N. S. & ELISSEEFF, J. H. (2006c) Reorganization of actin filaments enhances chondrogenic differentiation of cells derived from murine embryonic stem cells. *Biochem Biophys Res Commun,* 348, 421-7.

ZHENG, Y., JUNG, M. K. & OAKLEY, B. R. (1991) Gamma-tubulin is present in Drosophila melanogaster and Homo sapiens and is associated with the centrosome. *Cell,* 65, 817-23.

ZHOU, Y., MILLWARD-SADLER, S. J., LIN, H., ROBINSON, H., GOLDRING, M., SALTER, D. M. & NUKI, G. (2007) Evidence for JNK-dependent up-regulation of proteoglycan synthesis and for activation of JNK1 following cyclical

mechanical stimulation in a human chondrocyte culture model. *Osteoarthritis Cartilage,* 15, 884-93.

ZIEGLER, W. H., LIDDINGTON, R. C. & CRITCHLEY, D. R. (2006) The structure and regulation of vinculin. *Trends Cell Biol,* 16, 453-60.

ZIGMOND, S. H., EVANGELISTA, M., BOONE, C., YANG, C., DAR, A. C., SICHERI, F., FORKEY, J. & PRING, M. (2003) Formin leaky cap allows elongation in the presence of tight capping proteins. *Curr Biol,* 13, 1820-3.

ZWICKY, R. & BAICI, A. (2000) Cytoskeletal architecture and cathepsin B trafficking in human articular chondrocytes. *Histochemistry and Cell Biology,* 114, 363-372.

Appendices

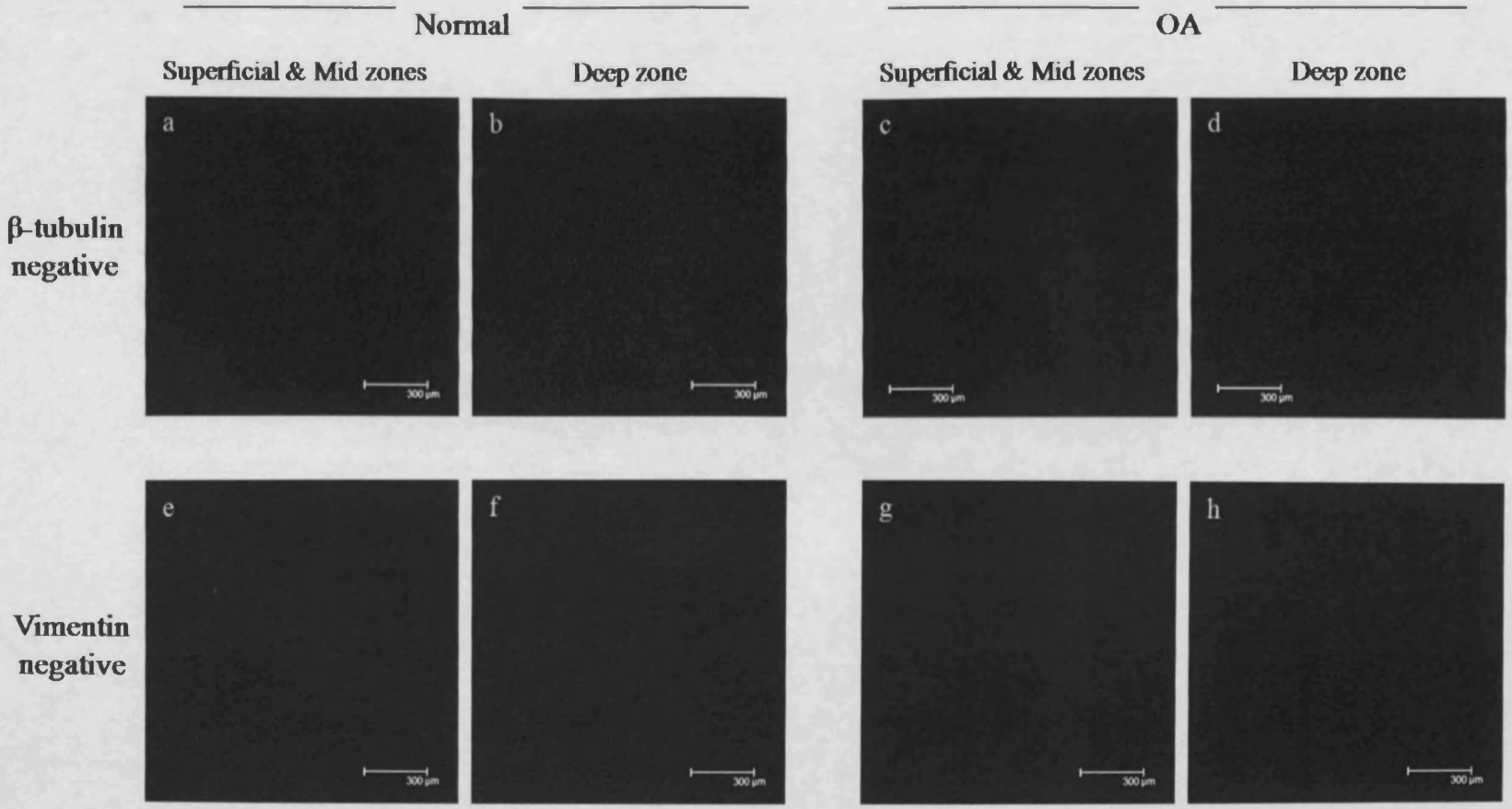

Appendix 1:- Immunohistochemical controls demonstrating the non-specific binding of the TRITC-conjugated secondary antibody through the depth of normal and osteoarthritic (OA) human articular cartilage sections (20µm). Representative primary-negative controls displayed correspond to sections displayed in Fig 3.13.

A

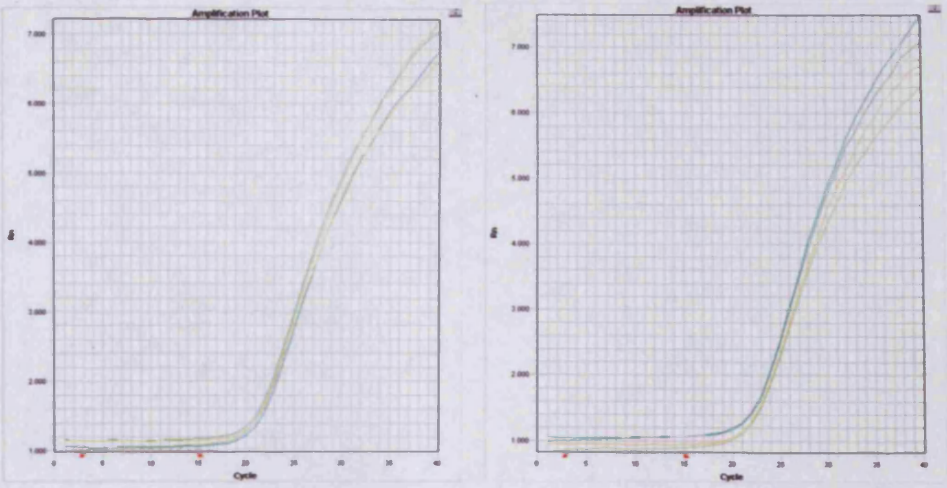

B

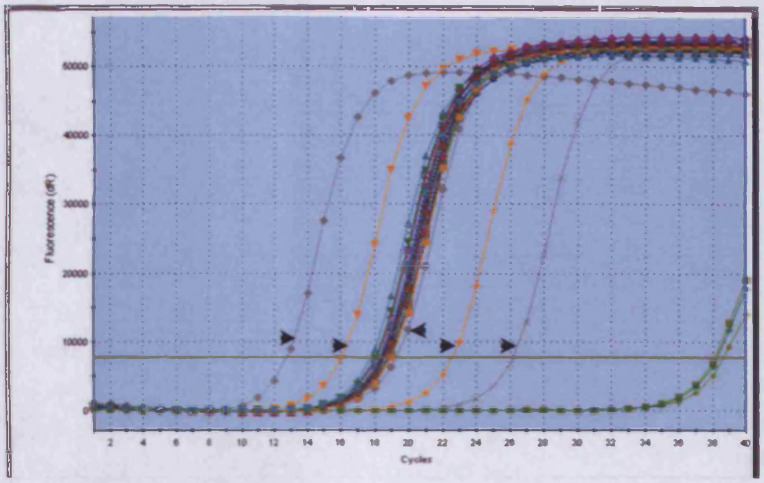

Appendix 2:- GAPDH amplification curves from Taqman (A) and SYBR Green (B) quantitative PCR. The variation of Ct values across samples was low and therefore GAPDH was selected for use as the housekeeping gene for normalisation of all quantitative PCR data (standards included in the SYBR Green quantitative PCR are indicated with black arrowheads).

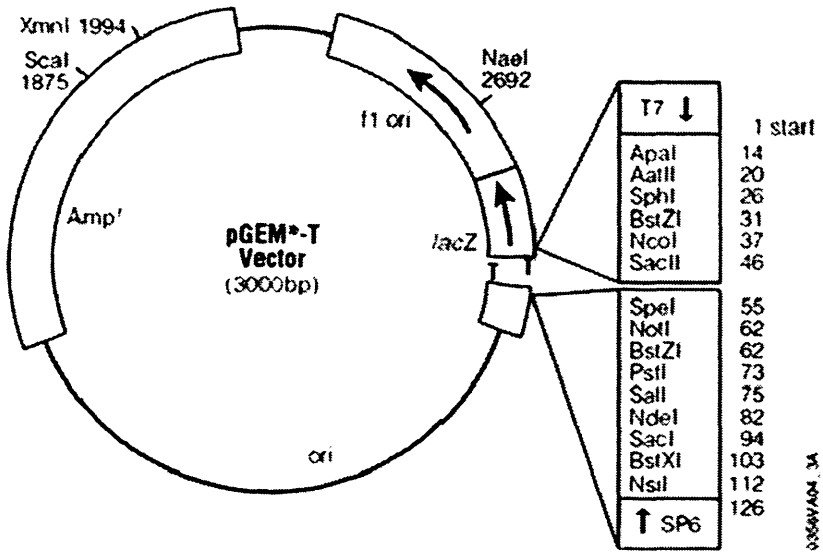

Appendix 3:- Map of the pGEM®-T Vector (Promega) used for the cloning of PCR products. Ligated vectors with inserts were then transfected into JM109 high efficiency competent *E. coli* cells, cloned and plasmids purified for use as standards in SYBR Green® quantitative PCR. The vectors contain T7 and SP6 RNA polymerase promoters flanking a multiple cloning region within the α-peptide coding region of the enzyme β-galactosidase (lacZ). Insertional inactivation of the α-peptide allows recombinant clones to be directly identified by blue/white screening on indicator plates.

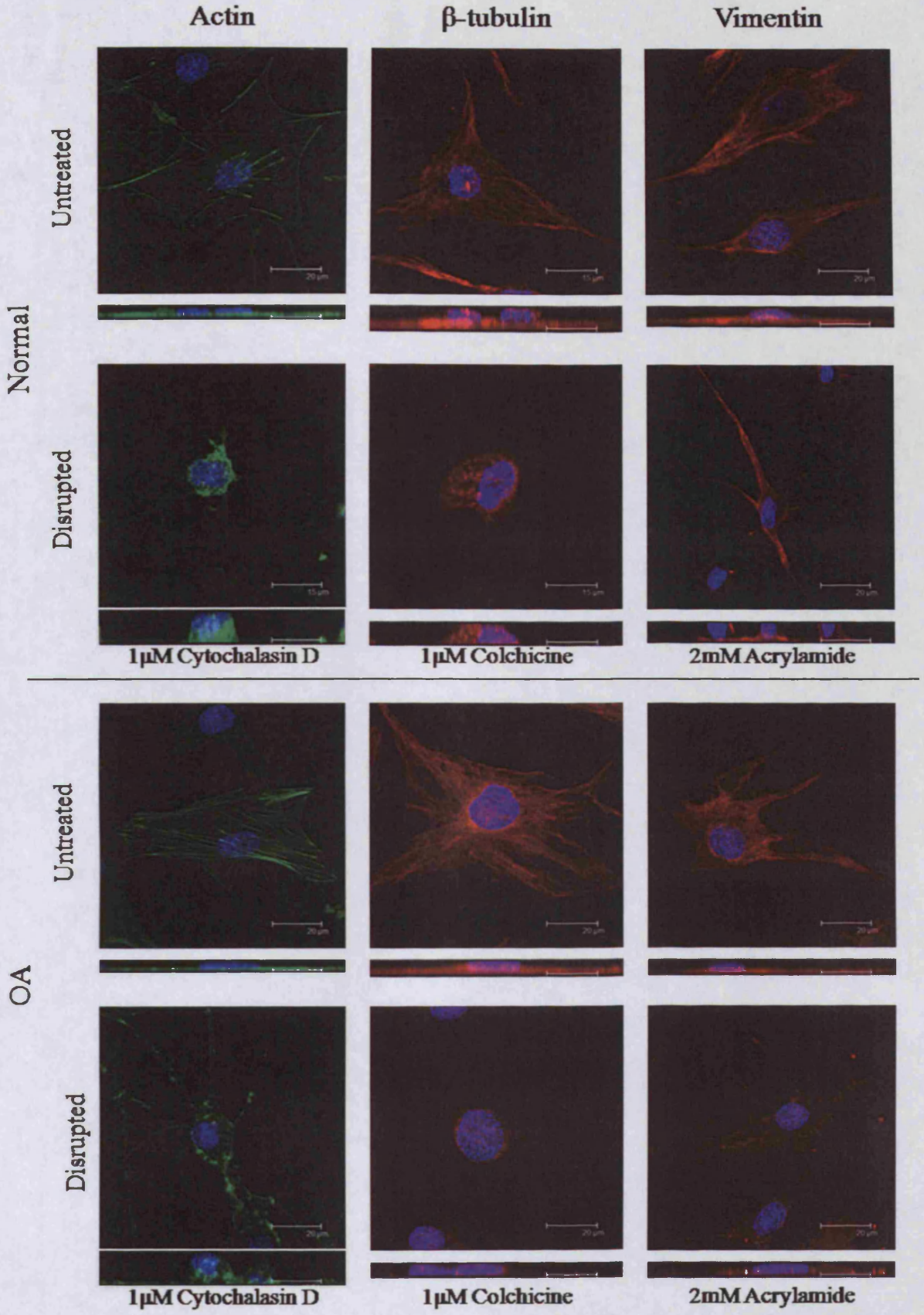
Actin
β-tubulin
Vimentin
Normal
Untreated
Disrupted
1µM Cytochalasin D
1µM Colchicine
2mM Acrylamide
OA
Untreated
Disrupted
1µM Cytochalasin D
1µM Colchicine
2mM Acrylamide

PRESENTATIONS

INVITED TALKS

- April 2008, British Society of Matrix Biology (BSMB) Conference in York, UK. Invited to present a talk entitled "Gene Expression of Human Chondrocytes: 3D Culture vs. Monolayer".
- September 2007, British Society of Matrix Biology (BSMB) Conference in Keele, UK. Invited to present a talk entitled "The Chondrocyte Cytoskeleton and its Role in the Regulation of Phenotype".

POSTER PRIZES

- July 2006, Federation of European Connective Tissue Societies (FECTS) Conference in Oulu, Finland. Title: "Comparison of the Cytoskeletal Organisation of Human Normal and Osteoarthritic Chondrocytes".

CONFERENCE ABSTRACTS & POSTERS

- July 2008, Federation of European Connective Tissue Societies (FECTS) Conference in Marseille, France. Title: "Involvement of the Cytoskeleton in the Regulation of Articular Chondrocyte Phenotype in 3D Culture".
- Harrison R.J, Blain E.J, Wardale R.J and Duance V.C. (2009) Involvement of the cytoskeleton in the regulation of articular chondrocyte phenotype in 3D culture. Int. J. Exp. Pathol. 90: A112.
- Harrison R.J, Blain E.J, Wardale R.J and Duance V.C. (2009) Comparison of gene expression of human chondrocytes in monolayer and 3D-culture. Int. J. Exp. Pathol. 90: A66.
- Harrison R.J, Blain E.J, Wardale R.J and Duance V.C. (2008) The chondrocyte cytoskeleton and its role in the regulation of phenotype. Int. J. Exp. Pathol. 89: A11.
- Harrison R.J, Blain E.J, Wardale R.J and Duance V.C. (2007) Differences in cytoskeletal protein organisation in normal and osteoarthritic chondrocytes. Int. J. Exp. Pathol. 88: A63.
- Harrison R.J, Blain E.J, Wardale R.J and Duance V.C. (2007) Comparison of the cytoskeletal organisation of human normal and osteoarthritic chondrocytes. Int. J. Exp. Pathol. 88: A15.